FLOOD PLAN
COORDINATION
ORGANIZATION
(FPCO)

KREDITANSTALT FÜR
WIEDERAUFBAU (KfW)

CAISSE FRANCAISE
DE DEVELOPPEMENT (CFD)

Call - 795
FAP-21/22

BANK PROTECTION AND RIVER TRAINING (AFPM) PILOT PROJECT FAP 21/22

(18)

DRAFT FINAL REPORT PLANNING STUDY

BN-648
A-795(2)

VOLUME VI

W.A.R.P.O. LIBRARY. DHAKA

ANNEX 11: Remote Sensing Study of Morphological Processes
ANNEX 12: Surveys
ANNEX 13: Subsoil Investigations
ANNEX 14: Physical Model Tests

JANUARY 1993

CONSULTING CONSORTIUM FAP 21/22

RHEIN-RUHR ING.-GES.MBH, DORTMUND/GERMANY

COMPAGNIE NATIONALE DU RHONE, LYON/FRANCE
PROF.DR. LACKNER&PARTNERS, BREMEN/GERMANY
DELFT HYDRAULICS, DELFT/NETHERLANDS

In association with:

BANGLADESH ENGINEERING &
TECHNOLOGICAL SERVICES LTD.(BETS)
DESH UPODESH LIMITED (DUL)

BANK PROTECTION AND RIVER TRAINING (AFPM) PILOT PROJECT FAP 21/22

DRAFT FINAL REPORT PLANNING STUDY

VOLUME VI

ANNEX 11: Remote Sensing Study of Morphological Processes
ANNEX 12: Surveys
ANNEX 13: Subsoil Investigations
ANNEX 14: Physical Model Tests

JANUARY 1993

CONTENTS OF DRAFT FINAL REPORT

Volume 0	Executive Summary	
Volume I A	Main Report FAP 21	
Volume I B*	Main Report FAP 22	
Volume II*	Annex 1	River Training and Morphological Response
	Annex 2	River Morphology
Volume III*	Annex 3	Surface Screens
	Annex 4	Simplified Mathematical Models for Investigation of Recurrent AFPM Measures
	Annex 6	Mathematical Model Tests (Part A)
Volume IV*	Annex 7	Socio-Economic and Administrative Assessment (Part A, B)
	Annex 9	Economic Assessment
	Annex 10	Navigation Study
Volume V	Annex 5	Hydrologic Data
	Annex 6	Mathematical Model Tests (Part B)
	Annex 7	Socio-Economic and Administrative Assessment (Part C)
	Annex 8	Ecological Assessment
Volume VI	Annex 11	Remote Sensing Study of Morphological Processes
	Annex 12	Surveys
	Annex 13	Subsoil Investigations
	Annex 14	Physical Model Tests
Volume VII	Annex 15	Special Scour Investigations
	Annex 16	Design of Cover Layers of Revetment
	Annex 17	Design of Filter Layers of Revetment
	Annex 18	Dimensioning of Groynes
	Annex 19	Constructional Aspects
	Annex 20	Study of Alternative Design Solutions
	Annex 21	Preliminary Design of Test Structures
	Annex 22	Financial Analysis

*) Submitted with the FAP 22 Draft Final Report

BANK PROTECTION AND RIVER TRAINING
(AFPM) PILOT PROJECT
FAP 21/22

DRAFT FINAL REPORT

ANNEX 11

REMOTE SENSING STUDY OF MORPHOLOGICAL PROCESSES

JANUARY 1993

ANNEX 11

REMOTE SENSING STUDY OF MORPHOLOGICAL PROCESSES

Table of Contents

		Page
1	**GENERAL**	1
2	**AVAILABLE DATA**	
2.1	General	4
2.2	Satellite Images	
2.2.1	Selection	4
2.2.2	Processing	7
2.2.3	Results	9
2.3	BWDB Cross-sections	
2.3.1	Introduction	9
2.3.2	Available Data	9
2.3.3	Processing	12
2.3.4	Analysis	12
2.4	BIWTA Soundings	14
2.5	Other Data	15
3	**PLANFORM CHANGES**	
3.1	General	16
3.2	Analysis of Bank Erosion Rates	
3.2.1	Introduction	16
3.2.2	Selection of Data for Inclusion of Width/Depth Ratio	17
3.2.3	Analysis of Influence of Width/Depth Ratio	18
3.2.4	Methodology for Inclusion of Upstream Channel Curvature	20
3.2.5	Results of Inclusion of Upstream Channel Curvature	27
3.2.6	Discussion of Improved Reductions Method for Bank Erosion Rates	31

		Page
3.3	Bifurcation Analysis	
3.3.1	Introduction	32
3.3.2	Abandonment of Bifurcated Channels	33
3.3.3	Influence of Bifurcations Asymmetry	37
3.3.4	Influence of Bifurcations Position	40
3.3.5	Migration of Bifurcations	43
3.3.6	Conclusions of Bifurcation Analysis	44
3.4	Width Changes of Bifurcated Channels	45
3.5	Multiple Year Composites	
3.5.1	Introduction	49
3.5.2	Number of Water Occurrences	49
3.5.3	Successive River Courses	49
3.6	Towards a Predictive Model	51
4	**STUDY OF TEST AREAS**	
4.1	Test Areas	54
4.2	Approach	55
4.3	Analysis	
4.3.1	General	56
4.3.2	Kamarjani	56
4.3.3	Bahadurabad	59
4.3.4	Chandanbaisa	61
4.3.5	Nakalia	63
4.3.6	Other Possible Areas	65
4.4	Conclusion and Recommendations	66
5	**CONCLUSIONS**	67

LIST OF FIGURES

Fig. 1-1:	Location map	3
Fig. 2.2-1:	Coverage of satellite images	6
Fig. 2.3-1:	Cross-sections measured by BWDB in the period 1966-1990	10

		Page
Fig. 2.3-2:	Example of cross-section measured in the Jamuna river	11
Fig. 2.3-3:	Example of cyclic behaviour	13
Fig. 2.3-4:	Phase as a function of the chainage	14
Fig. 2.4-1:	BIWTA soundings available for the present study	15
Fig. 3.2-1:	Relative bank erosion rate versus relative radius of curvature	17
Fig. 3.2-2:	Relative erosion versus curvature, labelled for width/depth ratio	18
Fig. 3.2-3:	Width versus radius of curvature	18
Fig. 3.2-4:	Relative erosion versus curvature, labelled for water depth	19
Fig. 3.2-5:	Relative erosion versus relative radius of curvature	20
Fig. 3.2-6:	Example of encountered difficulties when defining channel centre line	21
Fig. 3.2-7:	Selected bends for study of inclusion of upstream curvature	22
Fig. 3.2-8:	Yearly planform changes of bend 1	23
Fig. 3.2-9:	Yearly planform changes of bend 2	24
Fig. 3.2-10:	Changes in planform of bend 1 in period 1989-1992	26
Fig. 3.2-11:	Changes in planform of bend 2 in period 1976-1980	26
Fig. 3.2-12:	Effective radius of curvature and migration relation through time, for co-ordinate pairs 3 to 6	28
Fig. 3.2-13:	Effective of curvature and migration relation through time, for co-ordinate pairs 7 to 10	28
Fig. 3.2-14:	Migration through time, for the co-ordinate pairs 3 to 10	29
Fig. 3.2-15:	Effective radius of curvature and through time, for co-ordinate pairs 3 to 10	30
Fig. 3.2-16:	Change in migration versus change in effective radius of curvature, over two subsequent one year periods	30
Fig. 3.2-17:	Effective radius of curvature versus migration, for reaches 1 to 5, migration relation related to first year planform	31
Fig. 3.2-18:	Effective radius of curvature versus migration, reach 1 to 5, migration related to second year planform	32
Fig. 3.3-1:	Terminology used for bifurcation study	34
Fig. 3.3-2:	Sinuosity versus deviation angle, labelled for abandonment	35
Fig. 3.3-3:	Relative length versus deviation angle, labelled for abandonment	35
Fig. 3.3-4:	Frequency of abandonment for different angle classes	36
Fig. 3.3-5:	Probability of abandonment for different angle classes	37
Fig. 3.3-6:	Diagram of investigated bifurcations, abandonment and symmetric behaviour through time	38
Fig. 3.3-7:	Degree of angle asymmetry versus degree of width asymmetry, within the lower left box the symmetry requirements are met	38

Page

Fig. 3.3-8:	Degree of angle asymmetry versus deviation angle, labelled for abandonment	39
Fig. 3.3-9:	Deviation angle, channel 1 versus channel 2, labelled for abandonment, shaded area meets angle symmetry requirement	39
Fig. 3.3-10:	Positions of the maintained bifurcated channels	40
Fig. 3.3-11:	Positions of the abandoned bifurcated channels	40
Fig. 3.3-12:	Positions of the maintained bifurcated channels, differentiated for deviation angle class	41
Fig. 3.3-13:	Positions of the abandoned bifurcated channels, differentiated for deviation angle class	42
Fig. 3.3-14:	Sketch showing pattern of flow in meanders	42
Fig. 3.3-15:	Migration of symmetric and asymmetric bifurcations	43
Fig. 3.3-16:	Bifurcation migration versus angle asymmetry, labelled for width asymmetry	44
Fig. 3.4-1:	Frequency distribution of the change in width data	45
Fig. 3.4-2:	Relative change in width versus various planform parameters	46
Fig. 3.4-3:	Relative change in width versus change in angle	47
Fig. 3.4-4:	Absolute change in width versus change in angle	47
Fig. 3.4-5:	Relative change in width, channel 1 versus channel 2	48
Fig. 3.5-1:	Multi-year composites of low-flow satellite images of the deep channels of the Jamuna river	50
Fig. 4.3-1:	Possible future development of Kamarjani test area	58
Fig. 4.3-2:	Possible future development of Bahadurabad test area	60
Fig. 4.3-3:	Possible future development of Chandanbaisa test area	62
Fig. 4.3-4:	Possible future development of Nakalia test area	64
Fig. Ap.4-1:	Improved bank erosion analysis migration-effective radius of curvature graphs	82
Fig. Ap.4-2:	Improved bank erosion analysis migration-effective radius of curvature graphs	83
Fig. Ap.4-3:	Improved bank erosion analysis migration-effective radius of curvature graphs	84
Fig. Ap.4-4:	Improved bank erosion analysis migration-effective radius of curvature graphs	85
Fig. Ap.4-5:	Improved bank erosion analysis migration-effective radius of curvature graphs	86
Fig. Ap.4-6:	Improved bank erosion analysis migration-effective radius of curvature graphs	87
Fig. Ap.4-7:	Improved bank erosion analysis migration-effective radius of curvature graphs	88

Page

LIST OF TABLES

Table 2.2-1: Overview of images used in the present study 5
Table 2.2-2: Water levels at the dates of acquiring the satellite images 7
Table 2.2-3: Applied colouring code for multi-temporal images 8

Table Ap.2-1: Image processing procedure with error values 75
Table Ap.5-1: Comprehensive description of bifurcation studied 88

REFERENCES 69

APPENDICES

Appendix 1: List of Available Material 71
Appendix 2: Accuracy of Satellite Image Study 74
Appendix 3: Determination of Channel Centre Co-ordinates 79
Appendix 4: Inclusion of Influence of Upstream Curvature 80
Appendix 5: Comprehensive Description of Bifurcations Studied 88

1 GENERAL

In the present Project an extensive study component is included that uses satellite images to improve the understanding of morphological processes in braided rivers with fine sand as bed and bank material. This study serves two purposes:

(1) to provide the best possible predictions of where the test structures to be built under FAP 21 have to be sited, and

(2) to improve the prediction methods for expected bank erosion area, as the basis for decisions as to where protective measures may be needed.

The location map of the rivers of Bangladesh is presented in Fig. 1-1. Some background for the present study is provided hereafter.

Within the framework of FAP 21 bank protection works will be built along the Jamuna river. These protection works should also have to be "tested" by the river, hence they have to be built at sites where over the coming years the river will attack its banks. So for the selection of the sites of the test structures it is required to identify the locations with the maximum probability of serious bank erosion over the coming years.

In fully meandering rivers the location of bank erosion can fairly well be predicted at this moment, and using a sequence of maps or satellite images also the celerity of bank erosion can be deduced. Recently this has resulted in the development of numerical models for the prediction of changes in planform of meandering rivers (Johannessen and Parker, 1985; Crosato, 1991). In addition methods have been developed to predict the occurrence of cut-offs in meandering rivers (Klaassen and van Zanten, 1989). Although the reliability of the predictions with these tools is still fairly limited, they represent a major step forward as far as the planning of bank protection works along meandering rivers is concerned. The development of these tools has been possible because of the improved understanding of processes active in meandering rivers.

For braiding rivers like the Jamuna river the insight into the controlling processes has not yet reached such a level that predictive models can be developed. What is lacking to start with, is a full understanding of the processes that are active in such a braided river with fine sand as bed and bank material. Processes that could have been identified are for example: (i) bank erosion along curved reaches, (ii) cut-offs that seem to be controlled by the cut-off ratio and the geometry of the bifurcation and (iii) a number of other items (see Klaassen and Masselink, 1992) and the Brahmaputra River Training Studies, FAP 1, Draft Final Report, ANNEX 4.

Hence, bits and pieces of the complete understanding are gradually being assembled like relations for bank erosion as a function of the channel characteristics and the factors governing natural cut-offs under the Jamuna Bridge Project (Klaassen and Masselink, 1992),

the notion of stable and moving chars and the life-time of very aggressive curved channel reaches under the Brahmaputra River Training Studies.

Improved understanding of the controlling processes in this type of braided rivers is also very much needed for the FAP 22 component of the Project. It is felt that Active Flood Plain Management can only be feasible if the strategy is to strengthen favourable developments and AFPM measures are selected that are working in conjunction with the riverine forces and not against them. Hence they should be used at times and at places where enforcement of natural tendencies leads to a favourable development. To identify the preferable locations and the appropriate times a good insight in the morphological processes is needed too.

The above is the rationale for carrying out a fairly extensive analysis of a sequence of satellite images, aiming at improving the insight into channel processes and their importance for bank erosion processes.

Broadly speaking the present study can be divided in two parts, notably:

(i) one part dealing with the identification of the best sites for constructing the test structures, and

(ii) another part dealing with processes in Jamuna type of rivers, under which for example the following topics are being studied:
- the celerity of bank erosion in relation to channel characteristics (as a continuation of the work carried out within the framework of the Jamuna Bridge Project and Brahmaputra River Training Studies), and
- the occurrence of cut-offs, in relation to the cut-off ratio and the geometry of the bifurcation.

Discussion on approach followed and results obtained are presented in this ANNEX. The study of the processes active in a braided river with fine sand as bed and bank material had to be limited to the most important processes and even now the data are still being elaborated. The results still to be obtained, partly related to the importance of tectonics and partly related to the importance of the yearly hydrograph can be used in later stages of FAP 21/22.

In the following, first the available data on which the further analysis is based are described briefly. Next the results of the analysis of morphological processes in the Jamuna river are presented. Finally an analysis is made of the recent river morphological processes near the pre-selected sites for the test structures. The emphasis is on the probability that in the near future the test structures would be "tested" and the predictability of the future conditions. Furthermore recent developments in the river are reviewed to verify whether other test areas can be identified that are also promising in this respect.

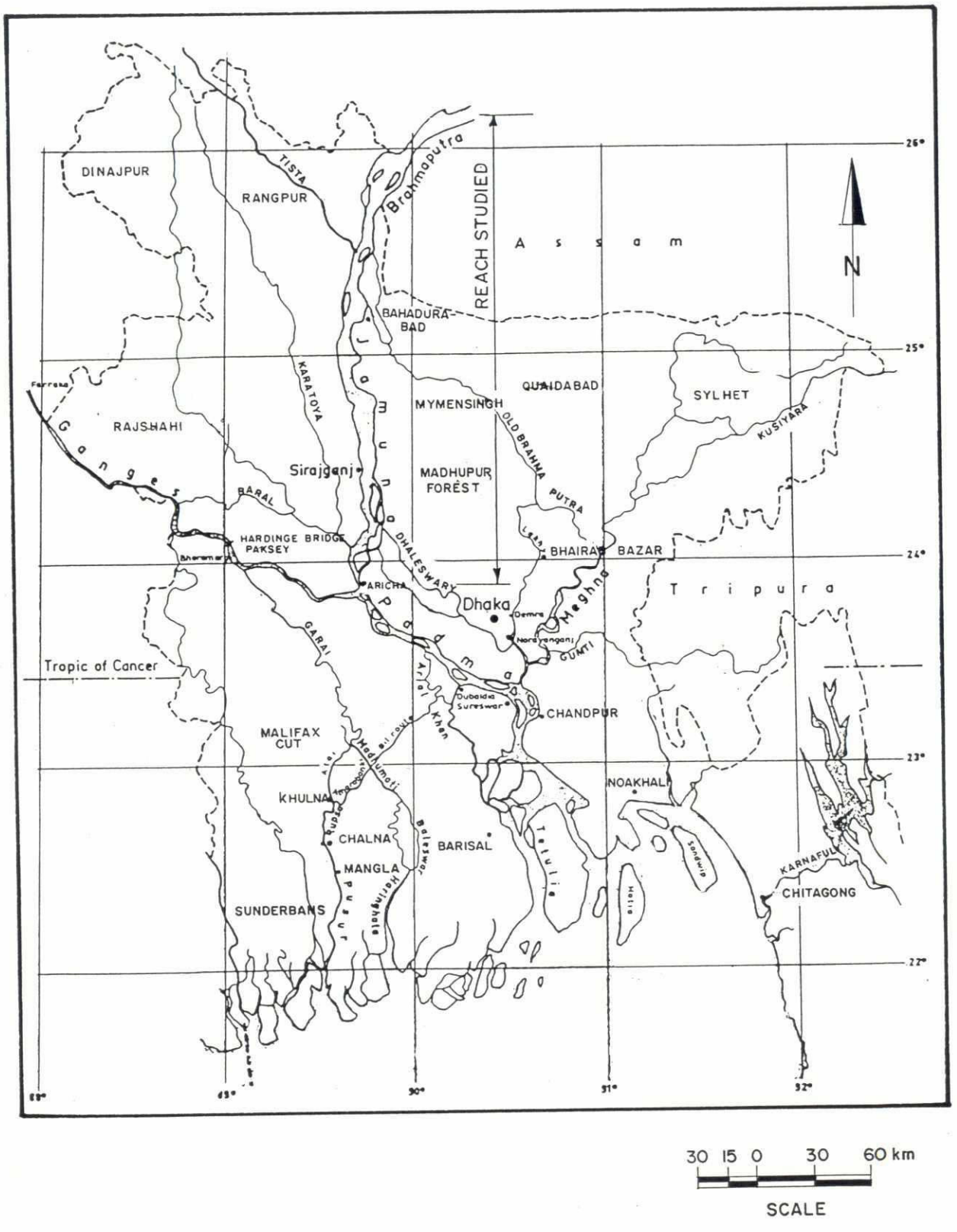


Fig. 1-1: Location map

(Source: Thijsse, 1964)

2 AVAILABLE DATA

2.1 GENERAL

For the present study mainly satellite images are being used. In addition, however, also cross-sections measured by Bangladesh Water Development Board (BWDB) were processed. Furthermore some sounding charts as prepared by Bangladesh Inland Water Transport Authority (BIWTA) are being used. In the following sections these data are described.

2.2 SATELLITE IMAGES

2.2.1 Selection

The study discussed here, based on the comparison of satellite images of the Jamuna river for successive years for the period 1973-1992, is essentially the same as the approach used in the Jamuna Bridge Project and later in the Brahmaputra River Training Studies.

For the analysis mostly Landsat images were selected. Partly these images are (older) MSS images (with resolution of 80 x 80 m) and partly the more recent TM images (with a resolution of 30 x 30 m). The origin of the data is diverse: part had already been acquired under the Jamuna Bridge Project, some processed tapes were provided by FINMAP, other processed data were obtained from FAP 19 and finally a number of tapes with the digital material was bought from either EOSAT in the USA or the National Remote Sensing Center in Thailand. In addition a number of MOS images from Japan were acquired.

An overview of the images used and their origin is provided in Table 2.2-1. In total 35 images were selected (including the ones already processed under the Jamuna Bridge Project) and if required CCT's (Computer Compatible Tapes) were purchased. The images relate to both the lower reach of the Jamuna river (148(138)/43, downstream of Bahadurabad) and the more upstream reach (148(138)/42). The coverage of the different images is presented in Fig. 2.2-1.

In line with the Jamuna Bridge Project here, apart from the "normal" criteria for the selection of an image (good quality, no cloud cover), an additional criterion was used. By preference images were selected in which, the stage at Sirajganj was around 6.50 m + PWD on the date of the image being acquired. This was done to clearly isolate the changes in channel location due to bank erosion and not to mix it up with changes in channel width for different stages. It should be stated here that the objective in this respect could not be reached fully because of the limited availability of the image. Overviewing the images available it can be stated that out of a period of 20 low water level seasons (1972/73 through 1991/92) 15 images became available, including three periods with fairly long records of 4 to 5 years:

- 1972/73;
- 1975/76 through 1979/80 (5 consecutive low water level seasons);
- 1982/83 through 1986/87 (5 consecutive low water level seasons), and
- 1988/89 through 1991/92 (4 consecutive low water level seasons).

For two intervals no images were available (1973/74 through 1974/75 and 1980/81 through 1981/82), while the images of 1987/88 were finally not purchased for budget constrain to allow for the processing of the latest years.

Year	Date	Satellite	Scene	Status and remarks
72/73	21-02-73	MSS USA	138-42	Completed
	21-02-73	MSS USA	138-43	Completed
73/74	------	MSS USA	138-42	Not available
	------	MSS USA	138-43	Not available
74/75	------	MSS USA	138-42	Not available
	------	MSS USA	138-43	Not available
75/76	10-01-76	MSS USA	138-42	Completed
	10-01-76	MSS USA	138-43	Completed
76/77	09-02-77	MSS USA	138-42	Completed
	09-02-77	MSS USA	138-43	Completed
77/78	22-02-78	MSS USA	138-42	Completed
	22-02-78	MSS USA	138-43	Completed
78/79	26-02-79	MSS USA	138-42	Completed
	25-12-78	MSS USA	138-43	Completed
79/80	16-01-80	MSS USA	138-42	Completed
	16-01-80	MSS USA	138-43	Completed
80/81	------	MSS Tha	138-42	Not available
	------	MSS Tha	138-43	Not available
81/82	------	MSS Tha	138-42	Not available
	------	MSS Tha	138-43	Not available
82/83	05-02-83	MSS Tha	138-42	Completed
	05-02-83	MSS Tha	138-43	Completed
83/84	23-02-84	MSS Tha	138-42	Completed
	23-02-84	MSS Tha	138-43	Completed
84/85	25-02-85	MSS Tha	138-42	Completed
	25-02-85	MSS Tha	138-43	Completed
85/86	20-02-86	MSS Tha	138-42	Completed
	20-02-86	MSS Tha	138-43	Completed
86/87	07-02-87	MSS Tha	138-42	Completed
	07-02-87	MSS Tha	138-43	Completed
87/88	10-02-88	TM Tha	148-42	Cancelled
	10-02-88	TM Tha	148-43	Cancelled
88/89	03-03-89	MOS Jap	51.84W	Completed
	03-03-89	MOS Jap	51.85W	Completed
	11-01-89	MOS Jap	51.85E	Completed
	11-01-89	MOS Jap	51.86E	Completed
89/90	06-02-90	MOS Jap	51.84W	Completed
	06-02-90	MOS Jap	51.85W	Completed
	30-01-90	TM Tha	148-43	Completed
90/91	------	MOS Jap	51.84W	Completed
	24-04-91	MOS Jap	51.85W	Completed
	21-03-91	TM Tha	148-43	Completed
91/92	08-03-92	TM Tha	148-42	Completed
	08-03-92	TM Tha	148-43	Completed

Table 2.2-1: Overview of images used in the present study

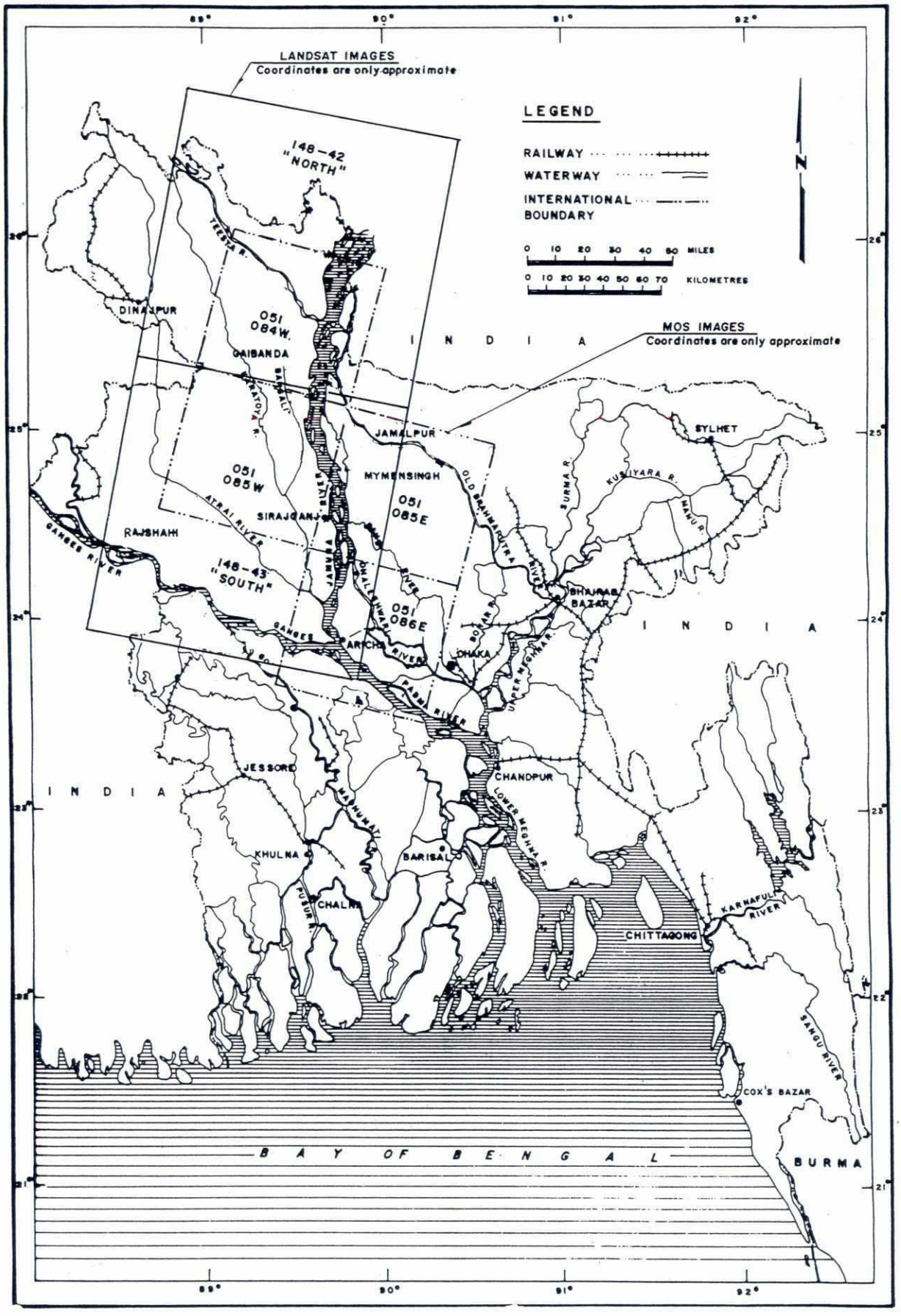


Fig. 2.2-1: Coverage of satellite images

Table 2.2-2 provides an overview of the water levels at the stations Bahadurabad, Sirajganj and Baruria Transit (confluence with the Ganges river) for the selected images. The average water level at Sirajganj is almost 7.00 m, and varies between 6.16 and 7.68 m + PWD.

		Water Level (m+PWD)		
Low Water Level Season	Date	Bahadurabad	Sirajganj	Baruria (91.9L)
72/73	21-02-73	13.09	6.64	2.51
75/76	10-01-76	13.54	7.14	2.63
76/77	09-02-77	13.09	6.62	1.99
77/78	22-02-78	13.07	6.46	1.96
78/79	25-12-78	13.99	7.24	2.64
	26-02-79	13.11	6.20	1.86
79/80	16-01-80	13.78	6.96	2.14
82/83	05-02-83	13.23	7.00	1.80
83/84	23-02-84	13.12	6.16	1.88
84/85	25-02-85	13.49	6.72	1.78
85/86	20-02-86	13.38	7.04	2.12
86/87	07-02-87	13.30	6.94	2.24
87/88	10-02-88	13.44	7.10	2.25
88/89	11-01-89	14.01	7.84	2.68
	03-03-89	13.94	7.69	2.31
89/90	30-01-90	13.69	7.66	2.23
	06-02-90	13.75	7.65	2.04
90/91	21-03-91	13.70	7.96	2.09
	24-04-91	15.07	9.34	3.19
91/92	08-03-92	13.76	7.58	2.00
Average		13.58	7.20	2.22

Table 2.2-2: Water levels at the dates acquiring the satellite images

2.2.2 Processing

The processing of the CCT's with digital information was done by the National Aerospace Laboratory (NLR) in The Netherlands by means of the Reseda processing system. The tapes were read and data were subsequently geometrically corrected and resampled. In doing so the original pixel size of either 80 or 30 m was corrected to about 50 m. The geometrical correction was done on the basis of some ten points which could be identified on the image of the year 1977 and from which the coordinates could be obtained from topographical maps. The accuracy of this correction was evaluated and the inaccuracy is not greater than the size

of the pixels after resampling. All the other images were corrected using the 1977 image as a "base map".

The next step in the analysis is the classification. Conform the Jamuna Bridge Project, for the present study four classes were distinguished: water, bare soil, sand and vegetation. The classification was done as the basis of band 5 and band 7. The classification diagram used is different from the diagrams for the different years, but the shape of the diagram is similar. The following colour code is used:

- blue : water
- grey : bare soil
- orange : sand
- green : vegetation

In earlier studies (Roque, 1983) the class "bare soil" was not identified separately and it may be argued that this class can be mixed up with wet sand or charland under cultivation. It was found, however, that deleting this class resulted in substantial loss of information on geomorphological features.

Changes over the years in water and land distributions are obtained by comparing the classification for different years. In total 16 possibilities are present, based on the four identified classes. Compared to the Jamuna Bridge study a slightly different code was used to indicate changes. The applied code is indicated in Table 2.2-3.

An example how to read this table is given: if in a previous image a certain pixel was identified as vegetated land and in the next image as water then on the figure showing the differences, this pixel is shown with a red colour. Water that has remained surface water is indicated as dark blue. "No changes" are in Table 2.2-3 "on the diagonal".

		1992			
		Water	Sand	Bare Soil	Vegetated Soil
1989	Water	Blue	Light yellow	Very light grey	Pale green
	Sand	Pink	Yellow	Light grey	Light green
	Bare soil	Salmon rose	Brownish yellow	Grey	Green
	Vegetated soil	Red	Brown	Dark grey	Dark green

Table 2.2-3: Applied colouring code for multi-temporal images

It is important to have an insight into the accuracy of the full procedure used here to obtain changes in land and water distribution. Within the framework of the Jamuna Bridge Study these inaccuracies were analyzed and it was found that differences are anyhow significant when they are larger than about 200 m. This figure was obtained after analyzing all errors

involved. A value of 200 m corresponds to 0.8 mm on scale 1:250,000. More informations on the accuracy of the full procedure is provided in Appendix 2.

2.2.3 Results

Primary results of the present remote sensing study are geometrically corrected and the classified images of the Jamuna river for particular years were presented. In total 30 of these images were produced, 15 for the south and 15 for the north image respectively. From these images "difference-images" can be prepared conforming to the method described in the preceeding section. In total 22 of these multi-temporal images were prepared. In addition some special products were prepared, notably (i) an image where all the channels were plotted over the period 1973-1992, giving all channels different colours and (ii) an image where the probability of occurrence of a major channel in the period 1973-1992 is indicated.

In a further step the primary results, as laid down in the products described above, were analyzed, conforming to what is indicated in Chapter 1. Results of this analysis are discussed in the following chapters.

2.3 BWDB CROSS-SECTIONS

2.3.1 Introduction

Apart from planform data, also cross sectional characteristics of the Jamuna river were studied. This was done on the basis of soundings which have been measured by the Bangladesh Water Development Board (BWDB) since 1965/66. The analysis carried out was mainly aiming at the identification of any consistent changes in channel location, notably a cyclicity (see Technical Report No.2, FAP 21/22) and as such is an extension of the work by Masselink (1989) for Jamuna Bridge Project.

The present analysis expands also on the work by Ullah (1987), who compared soundings of 1965/66 with more recent ones from 1983/84, and the work carried out under the Jamuna Bridge Project, where the complete series of soundings were analyzed over the period 1965/66 through 1985/86. By including all available soundings over the whole period (and not just one in the beginning and one in the end of the considered period), a better insight is obtained into the fluctuations over the years in relation to any trends in bed levels and channel locations. In this analysis also the most recent years until 1990 are included.

2.3.2 Available Data

Initially BWDB measurements were done every year, but they were interrupted in 1970 due to the Independence War. In 1975/76 the soundings were taken up again, although the Jamuna river was not included in the countrywide morphological measurements every year.

In the period between 1965/66 and 1989/90 for most of the cross-sections in total some 12 soundings are available for analysis.

The soundings had been carried out during the low water level season. Both the submerged areas and the dry islands (locally called chars) in between the braids were sounded. The bed levels are related to the PWD. The horizontal distance was measured from monuments. Sometimes the monuments got lost either by bank erosion or by other causes. Consequently for a number of cross-sections it is not possible to make a quantitative comparison of channel location in the horizontal direction. Gauge histories were studied to identify cross-sections that could be included in the analysis.

Initially the distance between the cross-sections was 7 km, but gradually more cross-sections have been introduced over the years. Fig. 2.3-1 provides an overview of the sounded cross-sections. In the present study twelve cross-sections were selected for detailed analysis. An example of some measured cross-sections is given in Fig. 2.3-2.

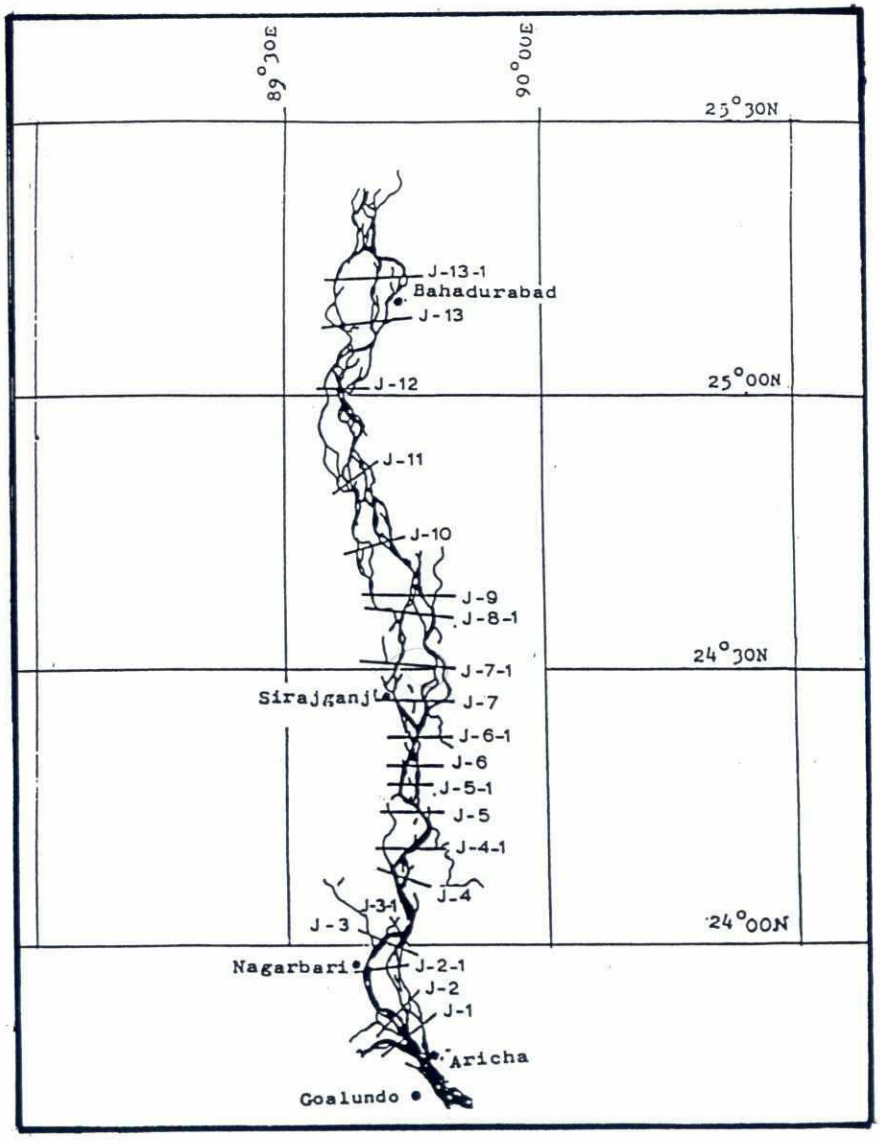


Fig. 2.3-1: Cross-sections measured by BWDB in the period 1966 to 1990

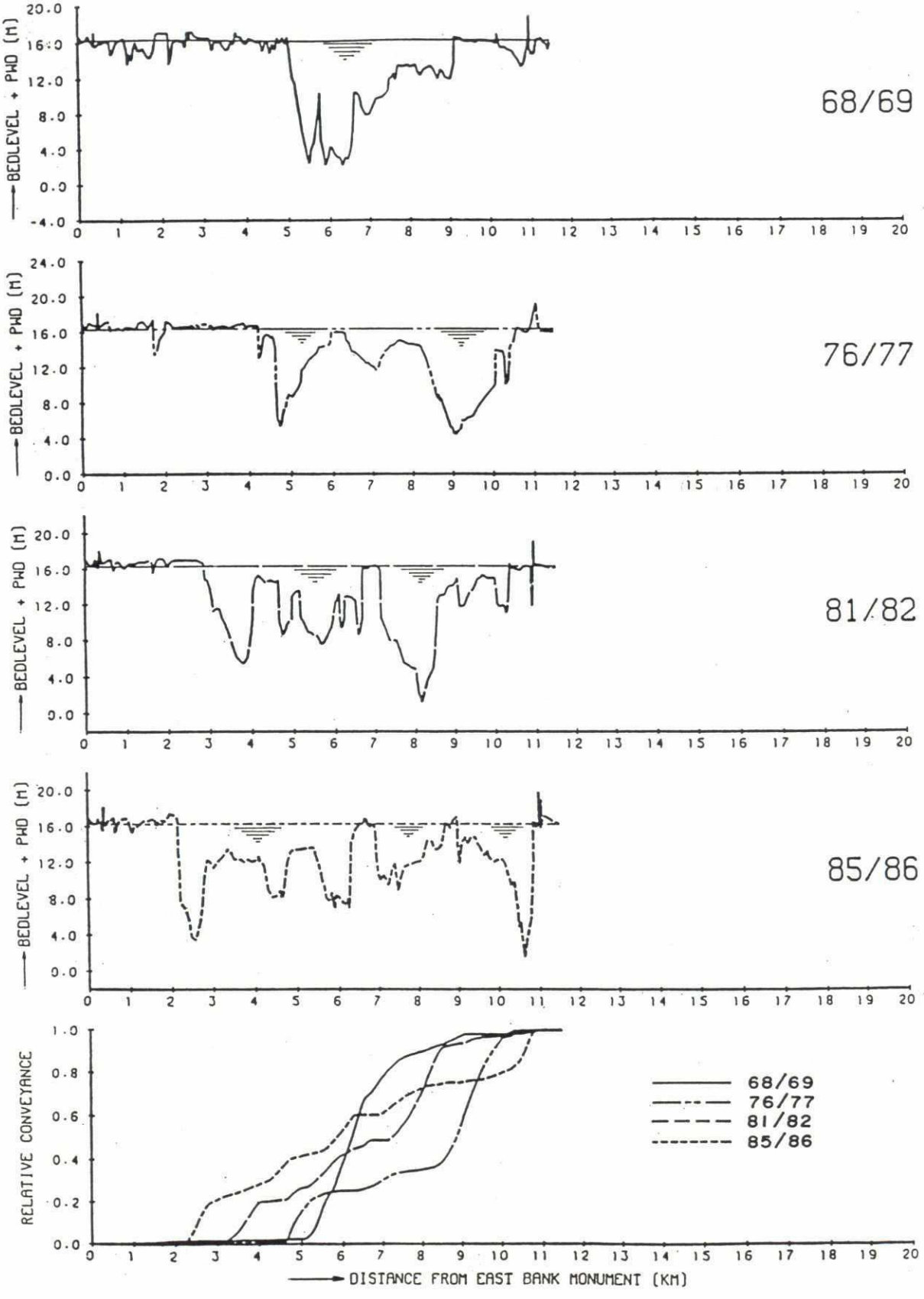


Fig. 2.3-2: Example of cross-sections measured in the Jamuna river

2.3.3 Processing

For the study of any cyclicity in the behaviour of the river system, a computer program was used that was developed for the study of cross-sections of the Jamuna river within the framework of the Jamuna Bridge Project. This program uses the sounded data as input, and subsequently the following processing is being done per cross-section:

- stages are plotted in the sounded cross-sections, and channels and sand bars (chars) are differentiated for three discharge levels, notably for: (i) 44,000 m^3/s (bankfull stage), (ii) 12,000 m^3/s (intermediate), (iii) 4,000 m^3/s (average low water level);
- the total wet area for each of the three discharge levels is computed;
- going from the left (eastern) bank to the right (western) bank monument the cumulative conveyance is computed as a function of the distance to the left bank monument; in a second step this relationship is made dimensionless by dividing it by the total conveyance for that particular cross-section and stage (for an example of the result see Fig. 2.3-2), and
- the width and the average levels of the individual channel in each cross-section is determined, together with the average char level, the average channel level averaged over all channels, and finally the average bed level of the whole sounded cross-section, including both the parts above the water and the submerged parts.

2.3.4 Analysis

The analysis of the cross sectional data is based on equation (2.3-1) to the location of the 50 % conveyance points in a cross-section in different years:

$$Y = Y_{avg} + C_1 \cdot \sin [\, C_2 \cdot (T_2 - T_0) + C_2 \cdot (T_0 - T_1) \,] \qquad (2.3\text{-}1)$$

in which

Y	=	distance of the 50 % conveyance point	(m)
Y_{avg}	=	the average distance of the 50 % conveyance points with respect to a selected reference year	(m)
C_1	=	amplitude	(m)
C_2	=	celerity defined in $2\,\pi/T$	(per year)
T	=	period	(year)
T_0	=	reference year	(year)
T_1	=	start sinus function	(year)
T_2	=	year of the prediction of the 50 % conveyance point	(year)

After selection of Y_{avg} and C_1, the value of C_2 has been determined by a minimization procedure. The minimization parameter for the iterative parameters fitting A is defined as:

$$A_i = \sum_{i=1}^{N} [\, Y_{i,observed} - Y_{i,calculated} \,]^2 \qquad (2.3\text{-}2)$$

The average migration, Y_{avg}, with respect to the migration in the selected reference year was first estimated as the average of the given data points. For a good curve fitting it was necessary to multiply Y_{avg} with a coefficient, if the given data points did not cover one complete cycle with a minimum and a maximum value of the 50 % conveyance point; consequently also the value of the average migration had to be adjusted. This coefficient varied between 0.6 and 2.4, but in all cross-sections minus the cross-sections with these extreme values between a narrow range of 1.0 to 1.4.

Next the amplitude C_1 in the formula 2.3-1 was estimated as the difference between the maximum migration minus the minimum migration in the points, which are given in the graphs for different years.

First this curve fitting procedure was applied to each cross-section separately. From these data an average period was estimated at 22.8 years. Next this procedure was repeated with a constant period for all cross-sections, see example in Fig. 2.3-3.

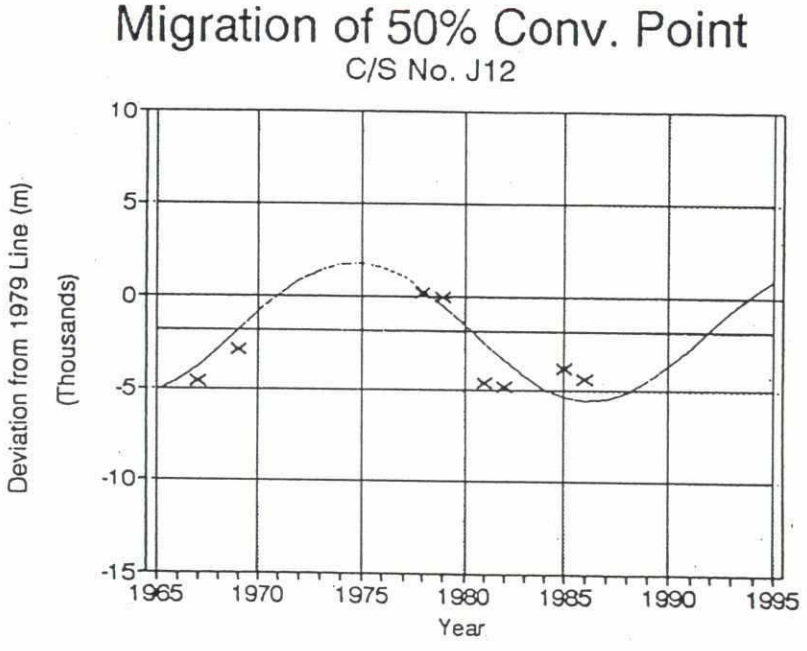


Fig. 2.3-3: Example of cyclic behaviour

The amplitude of the cyclic behaviour was found not to be constant in the various cross-sections : the minimum amplitude is about 1000 m and the maximum almost 6000 m. In cross-sections J-6 and in J-11 the amplitude is so small that the cyclic behaviour becomes obscured by the scatter in the data points.

If an average period of 22.8 years is assumed, then in the next step the phase of the sine function in the subsequent cross-sections is evaluated. By adding and subtracting a whole cycle in some cross-sections an increasing or decreasing sequence of phase values in subsequent cross-sections is obtained. This means that the available data is not sufficient to

determine if this assumed cyclic behaviour propagates in upstream or downstream direction, see Fig. 2.3-4.

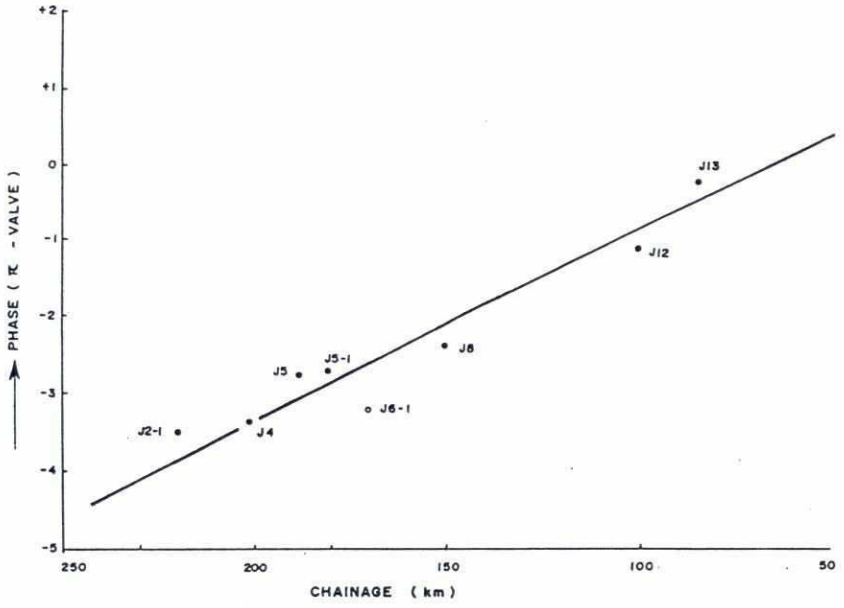


Fig. 2.3-4: Phase as a function of the chainage

Assuming a downstream propogation, the cyclic behaviour has the following tentative characteristics: a period of about 22.8 years, a wave length of about 80 km and a downstream propagation velocity of 3.5 km per year.

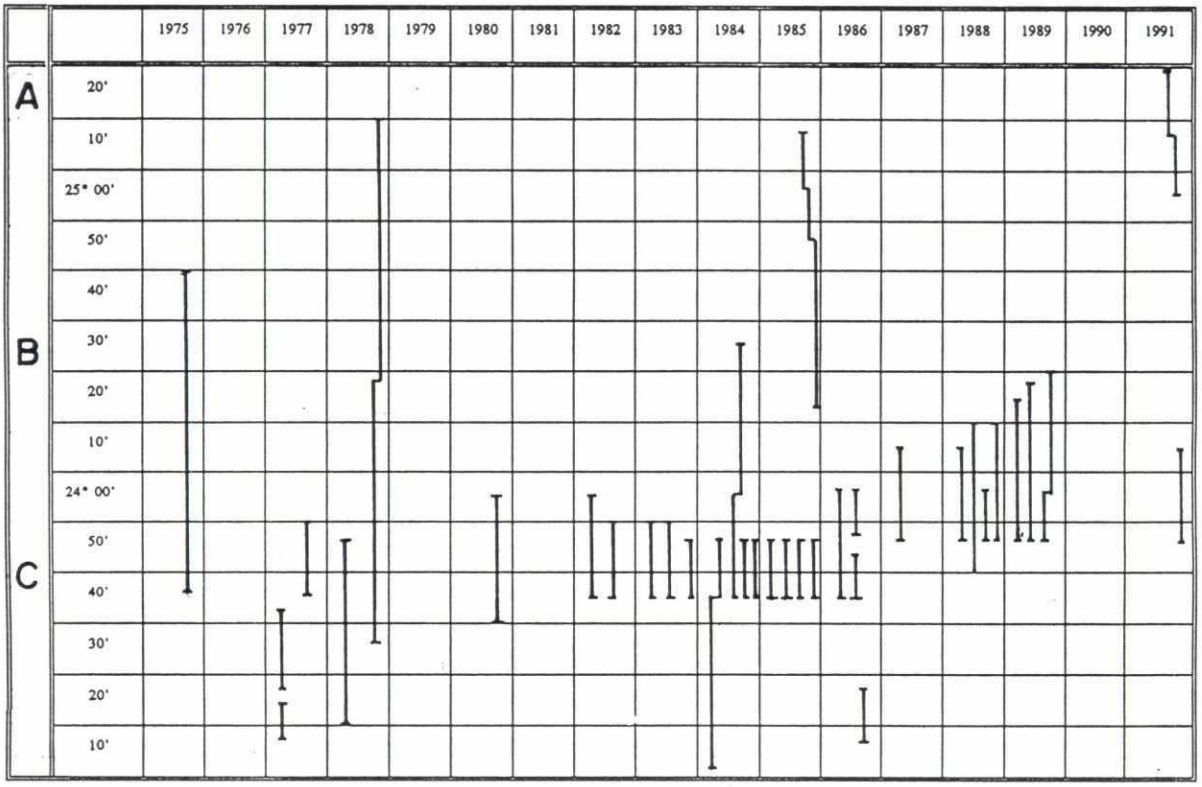
The general conclusion is, however, that not sufficient data of cross-sections of the Jamuna river is available for this very special analysis of the assumed cyclic behaviour of the 50 % conveyance point. For this analysis the distance between the cross-sections should be smaller than the distance of the available cross-sections.

Therefore it can not be proved with this analysis that this cyclic behaviour really exists. If the results of this analysis are combined with the results of the analysis of the satellite images, then the conclusion is that for the time being a cyclic behaviour of the conveyance points in the cross-sections cannot be proven and hence cannot be used for the selection of test areas.

2.4 BIWTA SOUNDINGS

In addition to the BWDB, soundings of the Bangladesh Inland Water Transport Authority (BIWTA) were used. These soundings provide a more complete coverage of the deeper channels of the Jamuna river, but their frequency is much lower. See Fig. 2.4-1, where an overview is given of the available BIWTA soundings. The surveys are carried out to produce navigational charts. The surveys are made with echo-sounding equipment and a Decca main chain positioning system. Survey charts are usually plotted on scale 1:25,000 or 1:50,000 and lanes are plotted at 250 m distances. Only three full coverage of the Jamuna river are

available and two more partial ones. Especially the soundings in the years 1978 and 1985 are very useful for the satellite study of the river processes.



Legend:
A - Bahadurabad
B - Sirajganj
C - Aricha

Fig. 2.4-1: BIWTA soundings available for the present study

2.5 OTHER DATA

Within the framework of the present study also a number of other data were used either explicitly or implicitly. These data can be found in the various reports that have been published over the last years. Data on bed material, sediment transport and resistance to flow were found in the various reports of the Jamuna Bridge Project, Phase I and Phase II. Also data on bank material and sediment transport were found in the various reports published as part of the Brahmaputra River Training Studies. For a description of these data, and a summary of the characteristics of the Brahmaputra/Jamuna river systems reference is made to ANNEX 2.

3 PLANFORM CHANGES

3.1 GENERAL

In this chapter the results of an analysis of the available data on the planform and on planform changes of the Jamuna river are presented, in particular of the satellite images. The emphasis is on bank erosion rates and bifurcations. Other phenomena like the rapid narrowing or widening that can be observed in the Jamuna river have only been studied briefly. The same holds for the influence of the yearly hydrograph. To develop a descriptive model of these changes in planform, ultimately all processes that are active in the Jamuna river should be identified, investigated and understood. The results presented here are followed by some remarks relating to the development of a predictive model of the processes in a braided sand-bed river like the Jamuna river.

3.2 ANALYSIS OF BANK EROSION RATES

3.2.1 Introduction

The aim of the analysis of bank erosion rates is to develop a relation between bank erosion and relevant channel characteristics, that can be used for predictional purposes. The analysis is actually a continuation of the work carried out within the framework of the Jamuna Bridge Project and later research carried out at Delft Hydraulics (see Masselink, 1989 and Klaassen and Masselink, 1992). These studies have yielded a relation between the relative erosion rate E/W and the relative radius of curvature:

$$\frac{E}{W} - f\left(\frac{R}{W}\right) \qquad (3.2\text{-}1)$$

in which

E	=	yearly erosion	(m)
W	=	channel width	(m)
R	=	radius of curvature	(m)

The relation proposed by Klaassen and Masselink (1992) is enclosed here as Fig. 3.2-1. It can be observed that in this figure the scatter is substantial.

In the present study it was attempted to reduce the scatter by including more parameters that may be of importance, notably the depth of the channel and the upstream curvature of the channel. The rationale for including the water depth is that it is felt that there may be a difference in behaviour of recent channels and channels that have been present for quite some time. Recent channels seem to be characterized by small width/depth ratios, because they are still in the process of adapting to the local conditions. Inclusion of the effects of the upstream radii of curvature is a way to take into account the retarded adaptation of the flow in bends.

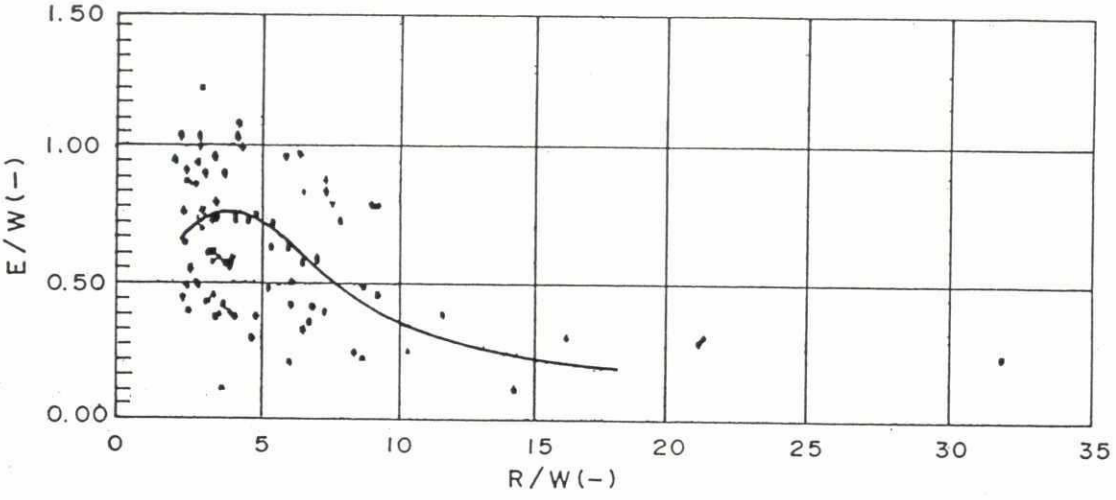


Fig. 3.2-1: Relative bank erosion rate versus relative radius of curvature
(Source: Klaassen and Masselink, 1992).

3.2.2 Selection of Data for Inclusion of Width/Depth Ratio

For selection of data for inclusion of width/depth ratio, two conditions had to be fulfilled to include change-detection images in the present analysis:

(i) change-detection images of two consecutive years should be available to enable the determination of the bank erosion rate;

(ii) soundings should be available of the same reach, to allow for the determination of the depth of the channel.

During the time of the analysis only two change-detection images were available that fulfilled both conditions, notably 1977/78S and 1986/87S. Note that these images were also used by Masselink (1989). Regarding the availability of sounding data still the following can be stated: these sounding data were taken from the cross-sections which quite often did not correspond with the exact bend location. When a considerable difference existed between the width in the cross-section and the width at the bend locations (as measured from the satellite image) a correction was made. The width was corrected in such a way that the real flow area was kept constant. In some cases however, this procedure could not be applied because of different planform.

From the above mentioned years bends were selected adopting the following criteria:

- only migrating bends, no shifting bends;
- no bifurcations or confluences in the vicinity of the bend, these were supposed to have an important influence on the planform changes and were studied lateron in more detail;
- no widening or narrowing on both sides of the channel. The fact is that the same process (erosion or sedimentation) acted on both sides of the channel assumed to be

caused by a large change in discharge. The bends were therefore no longer considered comparable;

- minimum width should be 0.5 mm on the satellite image prints, 125 m in reality, this is the smallest distance one can measure with reasonable accuracy, and
- depth data should be available.

3.2.3 Analysis of Influence of Width/Depth Ratio

From the selected 16 bends the width and radius of curvature were obtained from both consecutive single-year classified images, and the depth was obtained from the soundings. The erosion was derived from the change-detection image. These data were plotted in several graphs to investigate possible relationships. Results are presented in Figs. 3.2-2 through 3.2-4. These figures are discussed hereafter.

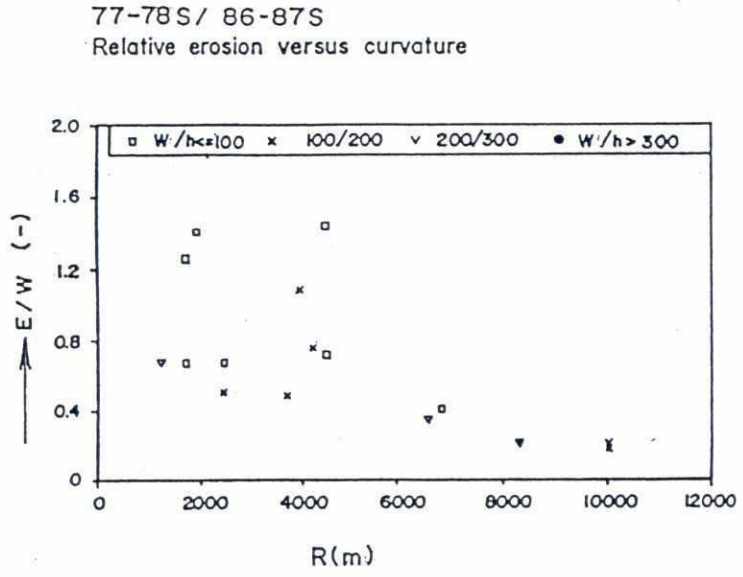


Fig. 3.2-2: Relative erosion versus curvature, labelled for width/depth ratio

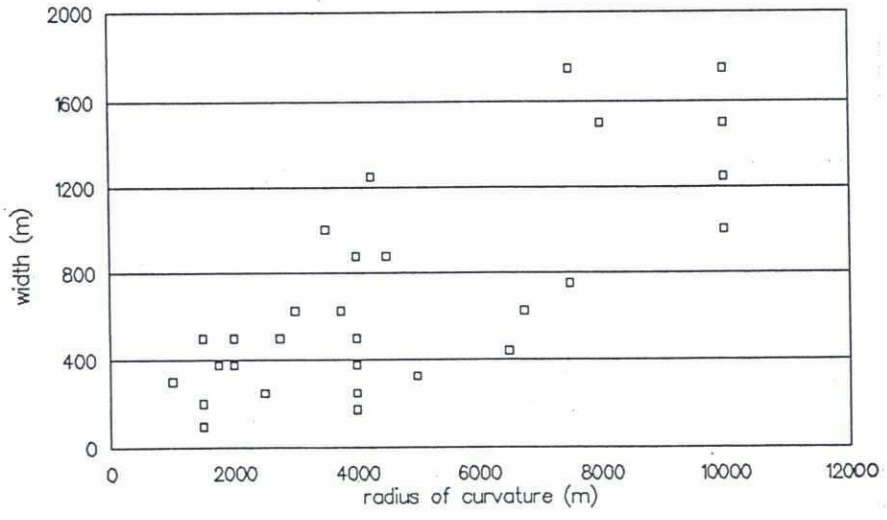


Fig. 3.2-3: Width versus radius of curvature

In Fig. 3.2-2 the relative erosion E/W is plotted versus the radius of curvature R, where the labels added to the data points refer to the width/ water depth (W/h) ratio of the channel considered. At first sight this figure looks very promising and three trends are visible:

- a larger radius of curvature gives relatively a low erosion rate;
- width-depth ratio increases with increasing radius of curvature, and
- width-depth ratio increases with decreasing relative erosions.

The first trend observed is mainly caused by the width/radius relation, see Fig. 3.2-3.

For this figure use has been made of all the studied bends. With increasing radius of curvature, width increases as well. So a third parameter, which is divided by width, is expected to decrease with increasing radius of curvature. The negative correlation of the width-depth ratio and the radius of curvature is again caused by the width-curvature relation mentioned above. The separation in vertical direction is caused by the use of width in both rations. A large width value will cause low relative erosion (E/W) and a large width-depth ratio (W/h). So the observed trend does probably not indicate an independent, but a spurious relation of the type which has been discussed by Benson (1965). However, that only width causes the trend in the W/h labelling can be seen from Fig. 3.2-4. This figure is same as Fig. 3.2-2, but labelled for depth instead of width-depth ratio. No trend can be observed in this graph.

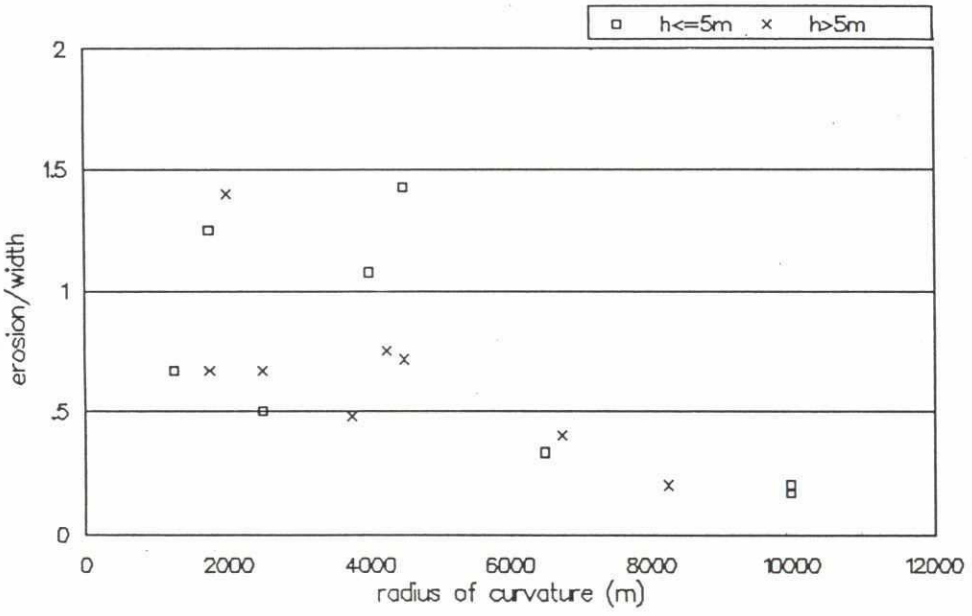


Fig. 3.2-4: Relative erosion versus curvature, labelled for water-depth

In previous investigations, e.g. Nanson and Hickin (1983) and Masselink (1989), the relation between relative erosion and relative curvature proved to be very important. Most striking in these studies is the decrease in relative erosion with an increase in relative curvature, but in the present analysis a similar relation was not found, see Fig. 3.2-5. The opposite trend seems even visible, increase in relative erosion with an increase in relative curvature.

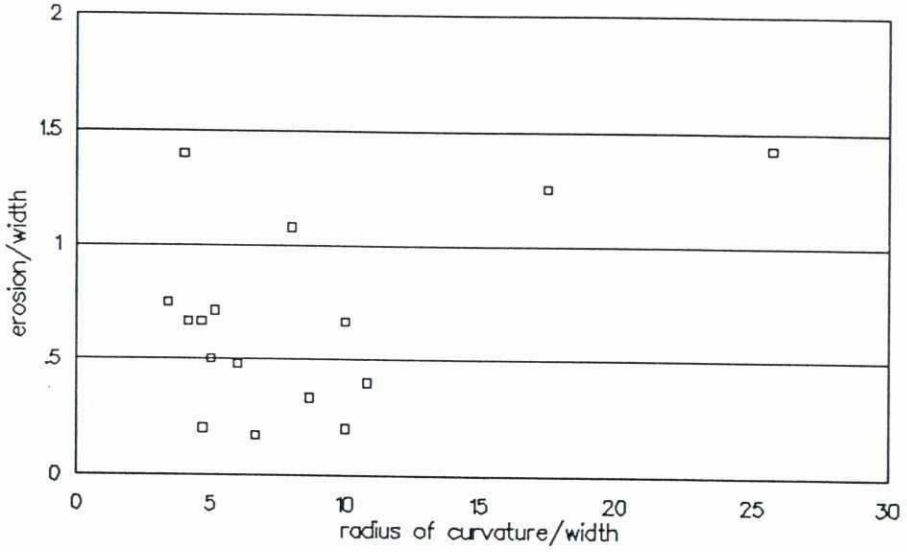


Fig. 3.2-5: Relative erosion versus relative radius of curvature

Probable explanations for the different results could be:

- The small number of locations used in this investigation. Only the two points that demonstrate the opposite trend are taken from the same, relatively small and deep channel, so the significance can be doubted. Adding new data to the investigation could perhaps clarify this point;
- The trend observed here is the trend one might expect to find when using width in both ratios. Again the relation might be considered as spurious;
- Masselink used a two year average R/W. No average was taken when in one year R/W was greater than 5 and in the other it was smaller than 5. In that case the latter was selected. In this analysis the first year R/W was chosen, because that was the initial situation from which the erosion started. If one wants to make predictions, one is also forced to start from this situation, and
- Subjective criteria in obtaining the parameters could also play a role.

The conclusion from the above analysis is that inclusion of the depth or the width/depth ratio does not improve the predictive method prepared by Klaassen and Masselink (1992).

3.2.4 Methodology for Inclusion of Upstream Channel Curvature

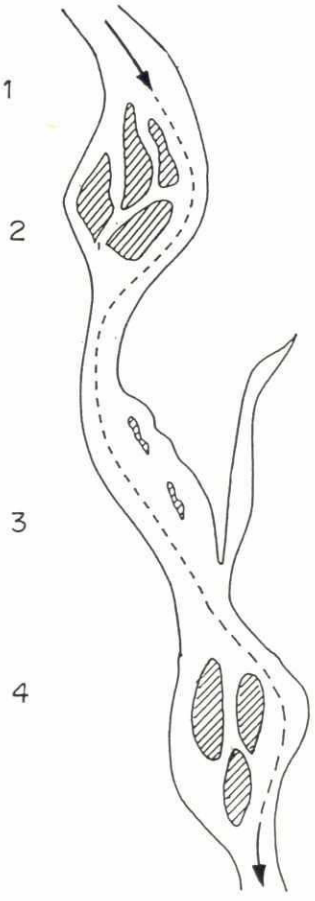
Since the results of the former bank erosion analysis were not satisfactory, an alternative approach was attempted. Improvements were made into the way the radius of curvature was included in the analysis. In previous studies the local bank erosion was linked to the local radius of curvature. The variation of the radius through the bend upstream of the reach for which the erosion was studied is thought to be an important omission in former studies. So this was included in subsequent new more detailed investigation.

Some large bends that showed a similar planform and clear migration over a number of years were selected. A strongly different planform was thought to be caused by other processes

than migration alone; like avulsion or change in discharge. Migration is normally an extension process. For the Jamuna, however, translation was found to be an important process, that strongly influenced the planform changes. The effect of translation is discussed in Subsection 3.2.6.

Migration corresponds to erosion, based on an assumption that channel width does not change considerably from year to year. So the results of this analysis can be compared to the earlier bank erosion studies.

After selecting the bend, sample points were taken at approximately every 600 m from the smoothed channel centre line. Normally the geometric centre was taken, but when the centre of the hydraulic conveyance was thought to deviate substantially the latter was chosen as explained in Fig. 3.2-6.



NOTE:

1. Small chars were ignored
2. Southernmost channel was chosen because it is the only channel that also existed during the last year
3. Centre of hydraulic conveyance was expected to be west of gemetric centre
4. Average of the two bifurcated channels was chosen

Fig. 3.2-6: Example of encountered difficulties when defining channel centre line

Coordinates for the centre line points were obtained from the data files of the single-year classified images. For this procedure the Reseda system at the NLR was used, a description of the methodology can be found in Appendix 3. The coordinates were inserted in a spreadsheet (Supercalc 5). Since all images were corrected to the same coordinate system, it was possible to compare consecutive years from the coordinates alone. The location of the studied bends is presented in Fig. 3.2-7.

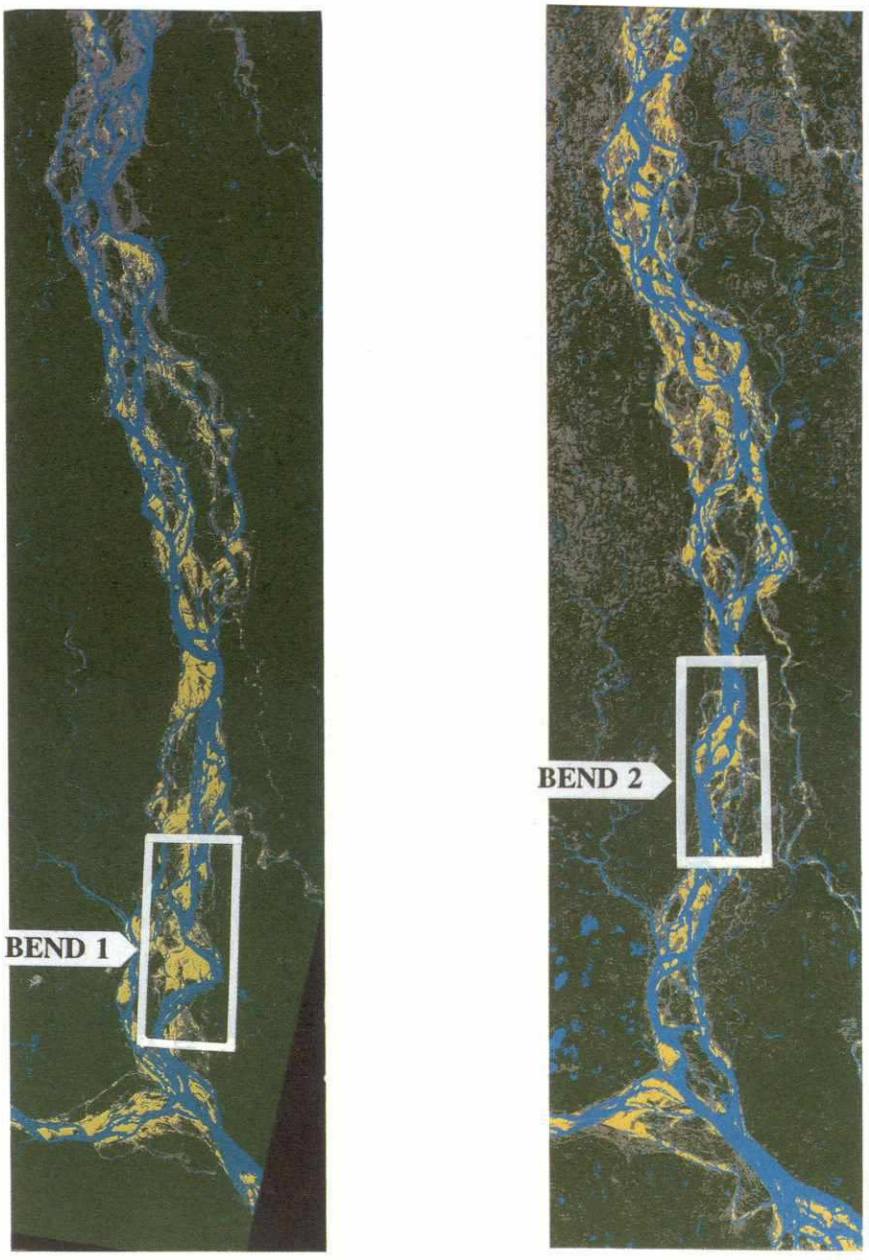
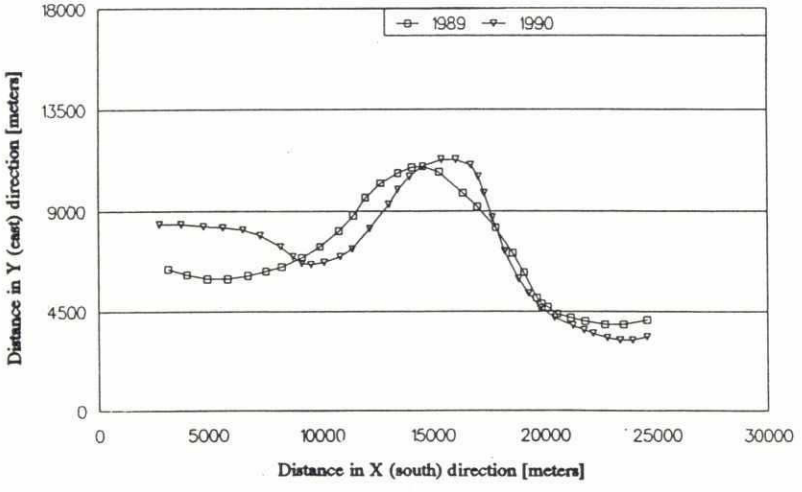
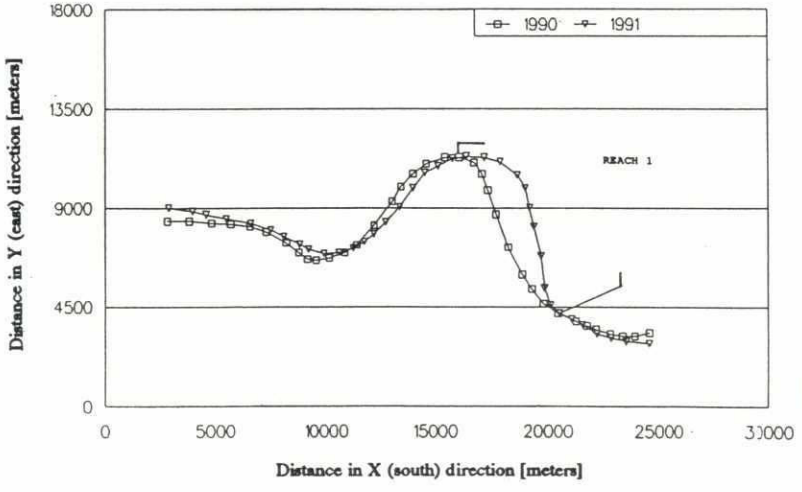


Fig. 3.2-7: Selected bends for study of inclusion of upstream curvature

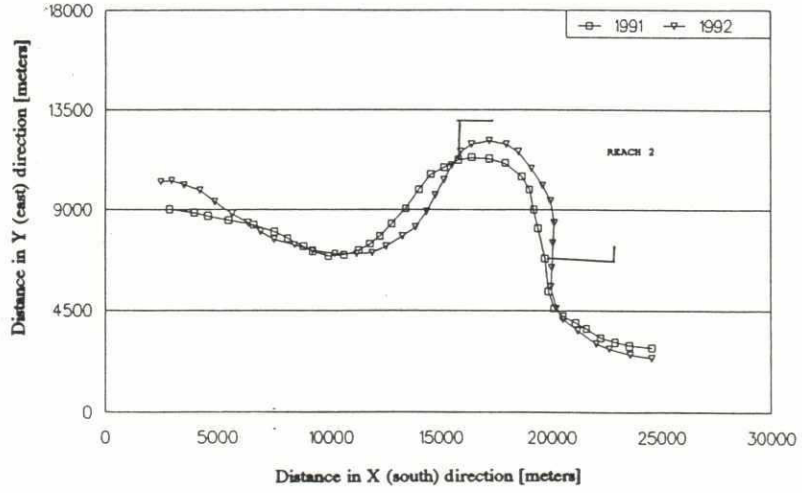
In Figs. 3.2-8 through 3.2-11 the planform changes of the two selected bends are depicted, as year-to-year changes as well as changes during the whole period.



(a) 1989-1990



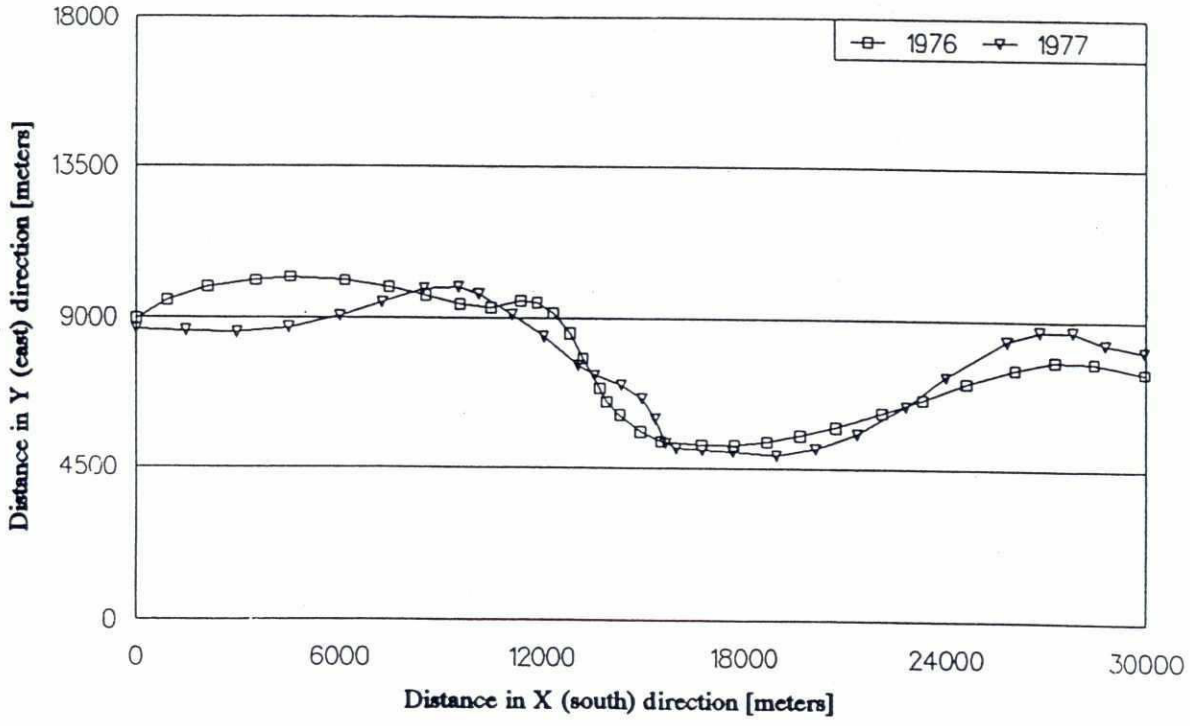
(b) 1990-1991



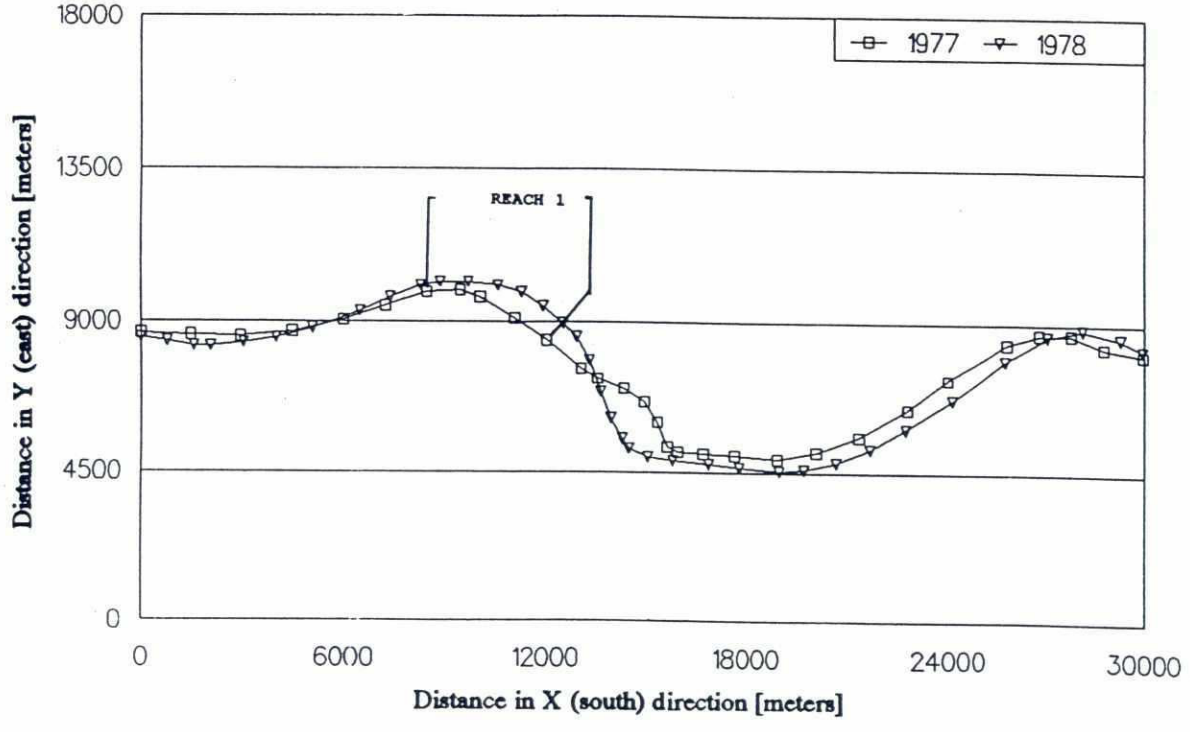
(c) 1991-92

Fig. 3.2-8: Yearly planform changes of bend 1

W A R P O
LIBRARY
DHAKA

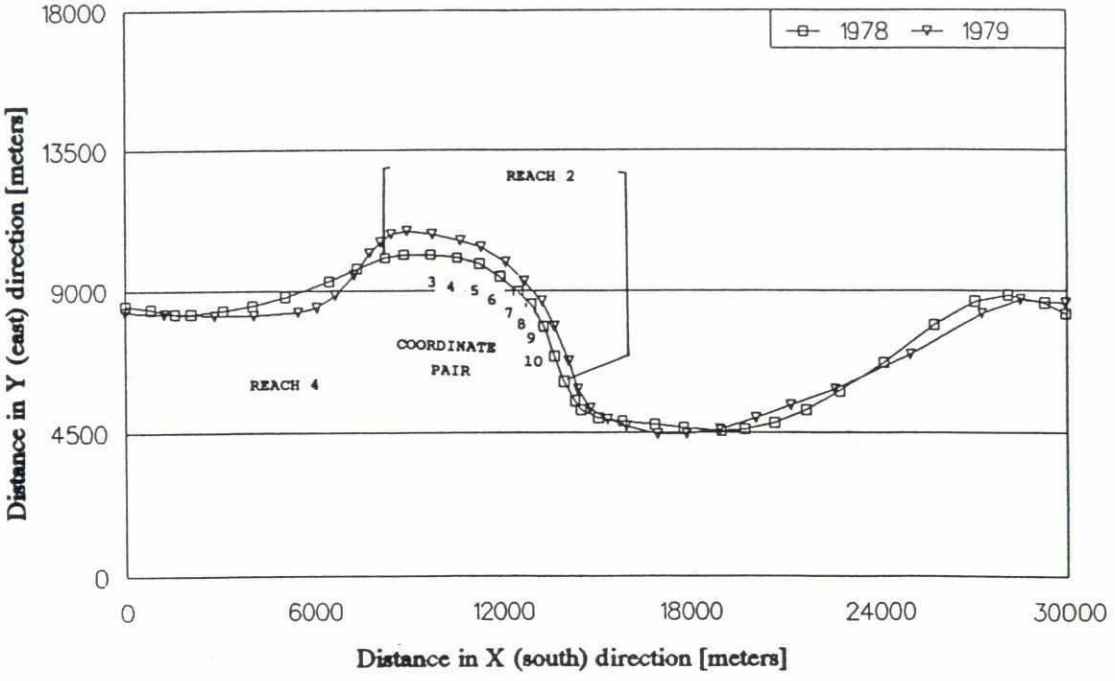


(a) 1976-1977

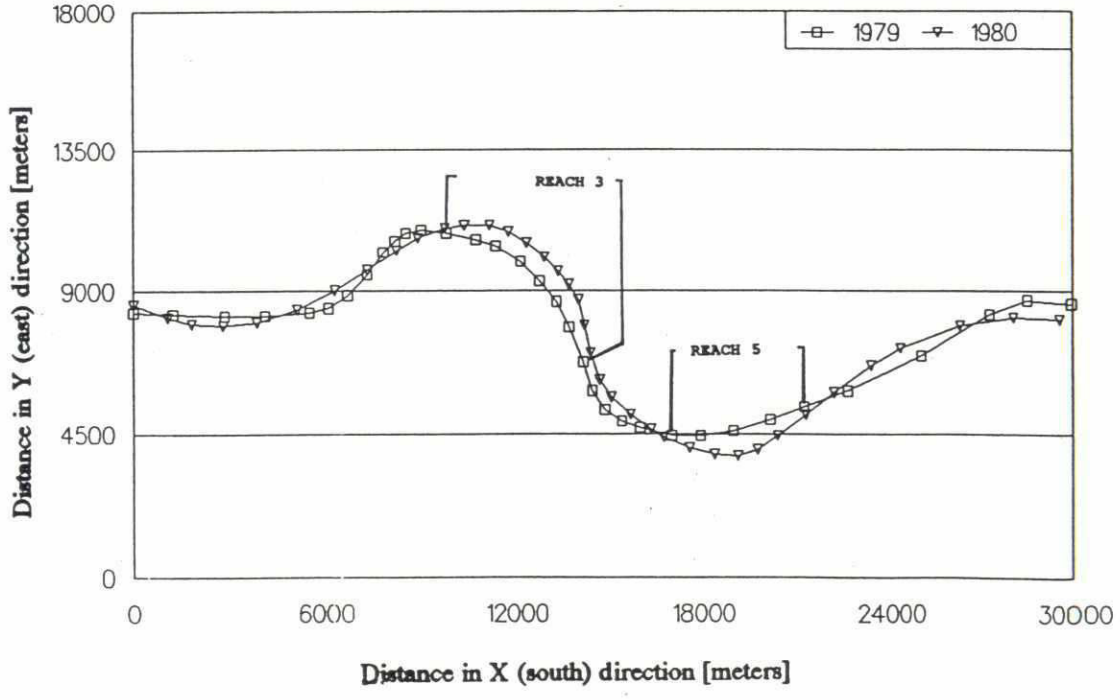


(b) 1977-1978

Fig. 3.2-9: Yearly planform changes of bend 2



(c) 1978-1979



(d) 1979-1980

Fig. 3.2-9 (continued): Yearly planform changes of bend 2

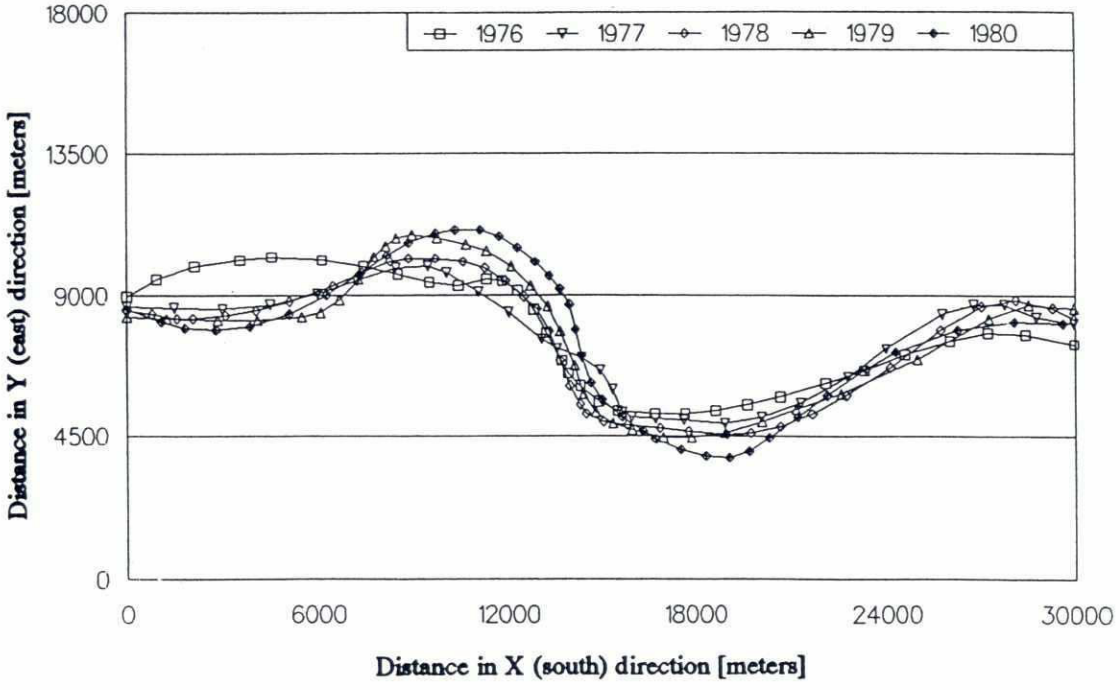


Fig. 3.2-10: Changes in planform of bend 1 in period 1989-1992

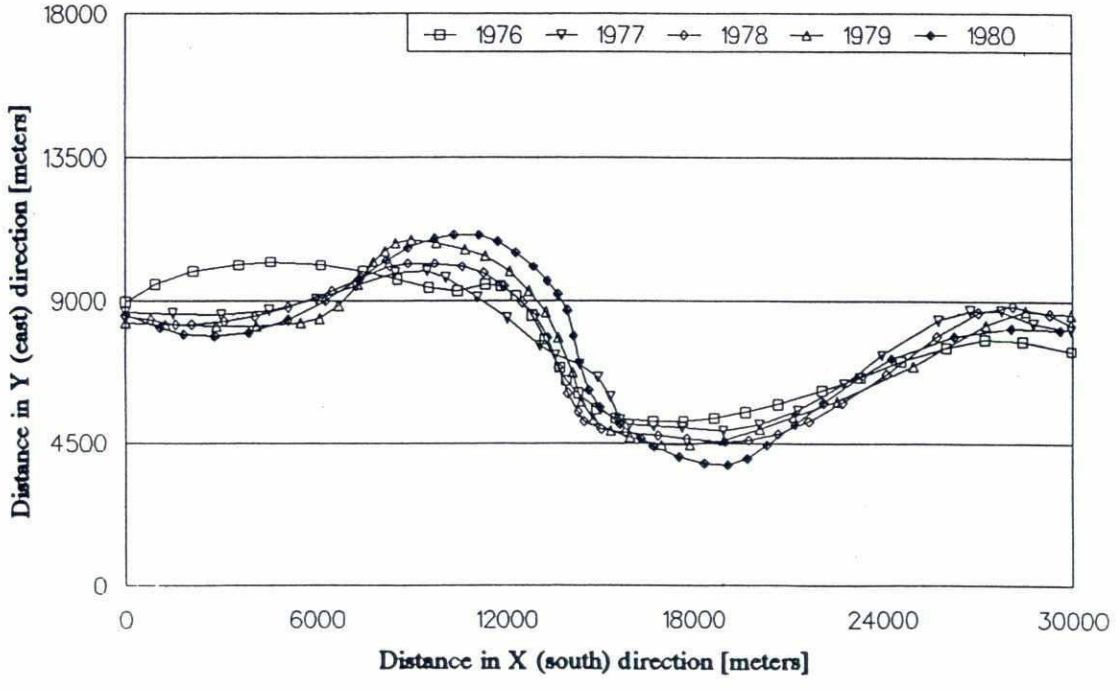


Fig. 3.2-11: Changes in planform of bend 2 in period 1976-1980

From printouts at scale 1:150,000 the year-to-year migration was obtained. It was interpreted in two ways; related to the first (initial) year and related to the second year planform. The migration was measured as the distance perpendicular to either one of the before mentioned planforms. In a dynamic river like the Jamuna considerable changes in river planform between two years exist. It was expected that the observed migration was some times more related to the recent radius of curvature than to the initial one. A simple computer program of Delft Hydraulics was used to calculate an effective local radius of curvature of the sample points. This is a weighted average of local and upstream curvatures, using a procedure suggested by Howard and Kmudson (1984). The weighting factor depends on a user-defined adaptation length. The effect of this adaptation length is discussed in Appendix 4.

The effective local radius of curvature was then compared to the migration (bank erosion) in graphs, in which migration was plotted against radius. Both parameters are divided by width to facilitate a comparison with earlier investigations. The width for both bends was kept constant at a definite average; 1200 m for bend 1 and 1500 m for bend 2. This was done not to introduce so many variables. The graphs that were constructed in this way are given in Appendix 4. In total seven reaches (of two different bends) were studied. These reaches are shown in the Fig. 3.2-8 and 3.2-9. Graphs were constructed with the migration related to both the first and second year planform. These different migration values were related to the effective radius of curvature of the corresponding year (see Subsection 3.2-5).

3.2.5 Results of Inclusion of Upstream Channel Curvature

The graphs, using a 5000 m adaptation length, that show migration related to the first year effective radius of curvature, all have an approximately similar shape. It is a curve with low migration values for both low and high radii. The highest migration values can be found for value of relative, effective, radius of curvature values of 3 to 5. These graphs are similar to the ones of Nanson and Hickin (1983). So the erosion-curvature relation that was found by them seems valid for individual bends in the Jamuna river as well, contrary to the results presented earlier.

When examining the graphs that use the migration related to the second year effective radius of curvature, a different general shape is apparent. These graphs show an approximate straight line with a negative direction coefficient. Closer study reveals that the highest migration values have moved to the left, i.e. they are related now to lower effective radii. Locations that had a strong migration showed a decrease in relative, effective radius from moderate to low. This process can for example be seen in Appendix 4, reach 2 of bend 1.

Another effect of relating migration to the second year planform is that, for some bends, more coordinates could be included in the analysis. The opposite signs of migration and effective radius of curvature had disappeared in some cases. So, as was intended, relating migration to the second year planform indeed improved the migration-radius of curvature relation for some locations.

The changes in effective radius of curvature and migration over time can be seen in Figs. 3.2-12 and 3.2-13. For eight coordinate pairs from bend 2 present in the subsequent reaches 1 to 3, the effective radius and its migration are given. The subsequent moments in time are connected by lines.

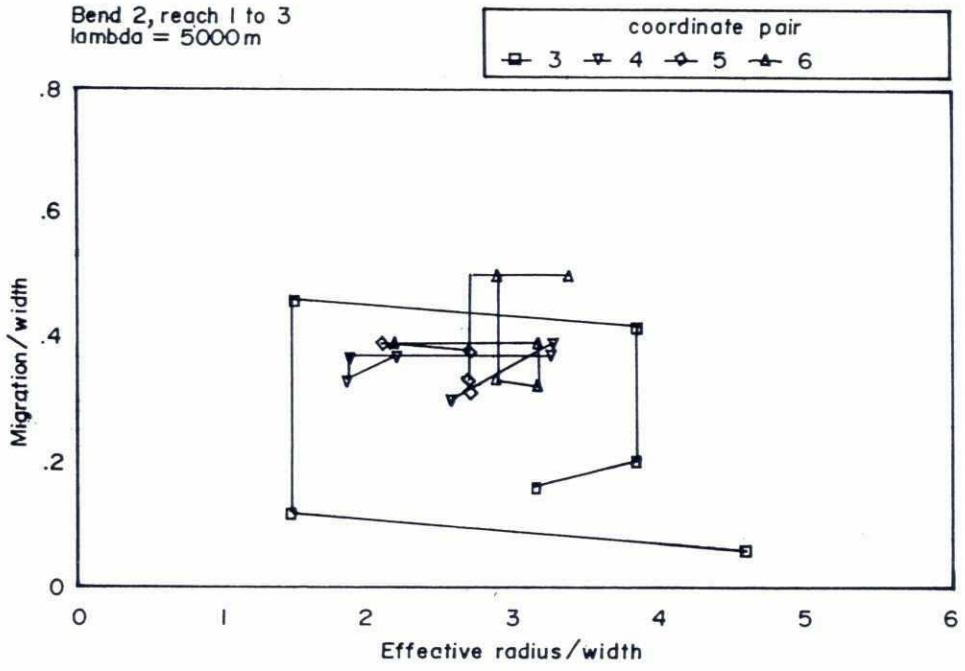


Fig. 3.2-12: Effective radius of curvature and migration relation through time, for coordinate pairs 3 to 6

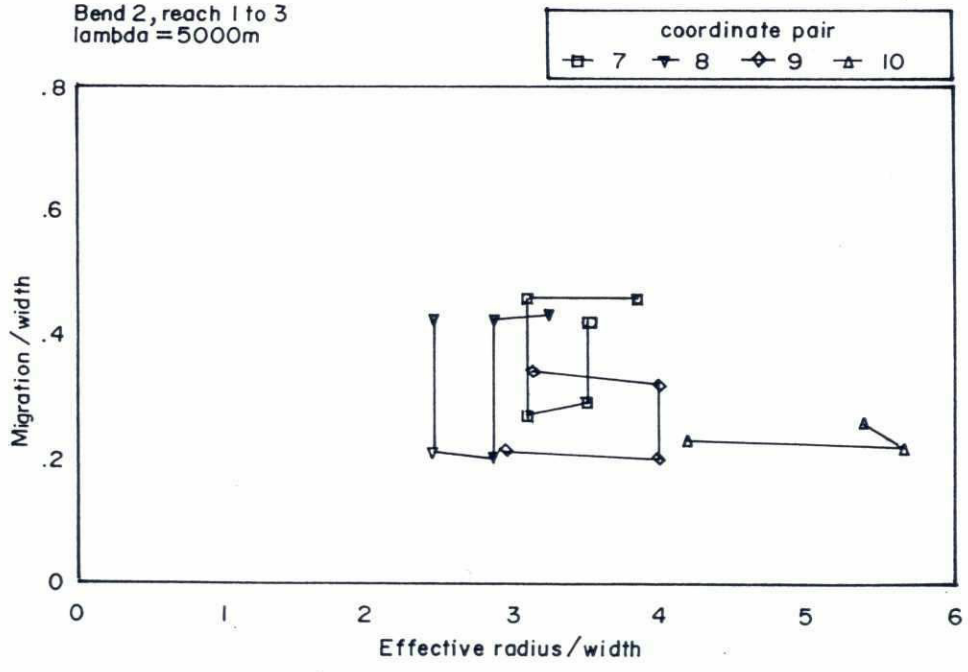


Fig. 3.2-13: Effective radius of curvature and migration relation through time, for coordinate pairs 7 to 10

The first point for a certain coordinate pair gives the migration that took place from 1977 to 1978, related to the effective radius of curvature in 1977. The following point gives the migration of the same period related to the 1978 effective radius. The third point gives the 1978 to 1979 migration for the 1978 effective radius. These graphs show that, for most coordinate pairs, a kind of cyclic behaviour occurred in bend 2. Low migration over a one year period normally combines with an increase in effective radius of curvature from the initial to the second year. This increased radius normally meets an increased migration in the following period. At the end of this period the radius decreases again and the cycle starts again. Especially coordinate pairs 3,4,7 and 9 show this trend. The absolute values connected with this trend differ substantially, but the values 2 and 4 for the effective radius, and the values 0.2 and 0.5 for the migration seem to be the common upper and lower extremes for the cycle.

The cyclic behaviour can also be illustrated with Fig. 3.2-14 and 3.2-15. These show the separate relations of migration and effective radius of curvature over time. For both the migration and the radius of curvature the values that were related to the first year planform were taken. If the migration is then compared to the effective radius, it seems that the two parameters are positively correlated. An increase in effective radius corresponds with an increased migration. This can also be seen from Fig. 3.2-16, in which the absolute change in effective radius is plotted against the absolute change in migration.

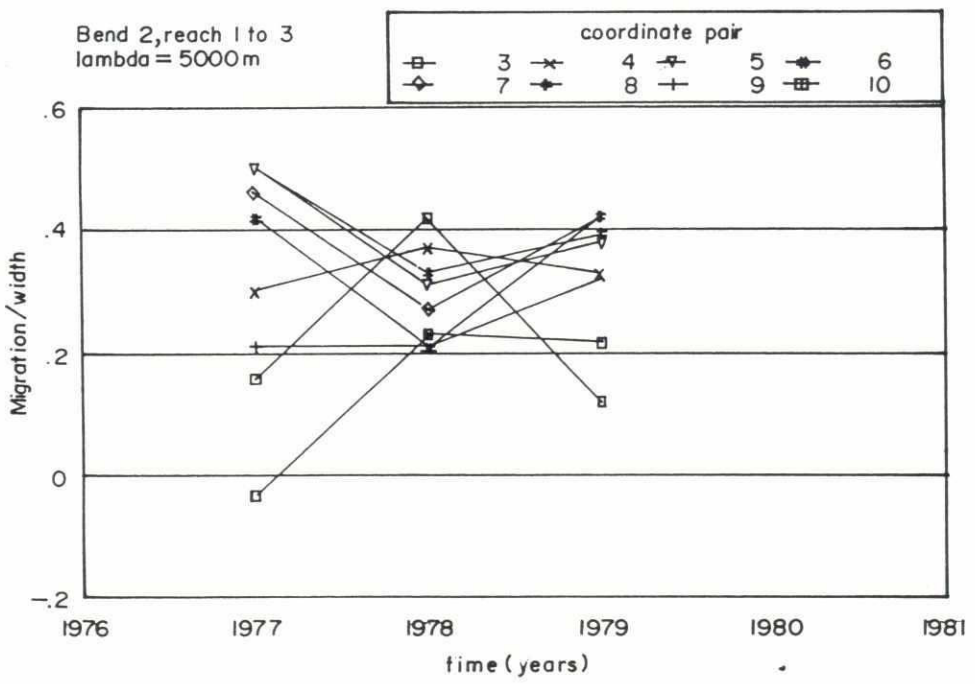


Fig. 3.2-14: Migration through time, for the coordinate pairs 3 to 10

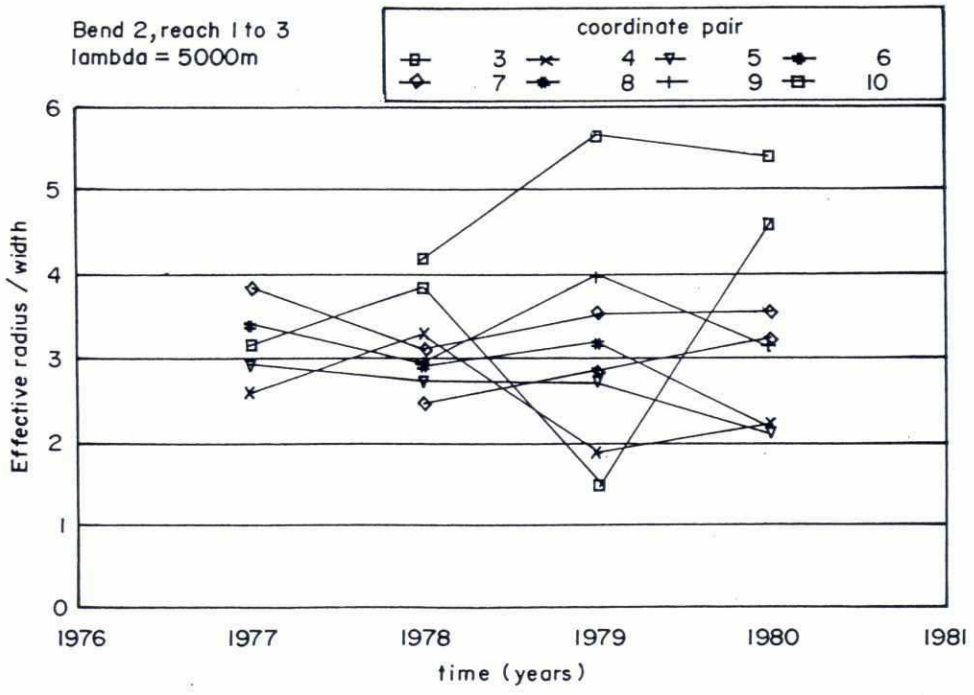


Fig. 3.2-15: Effective radius of curvature through time, for coordinate pairs 3 to 10

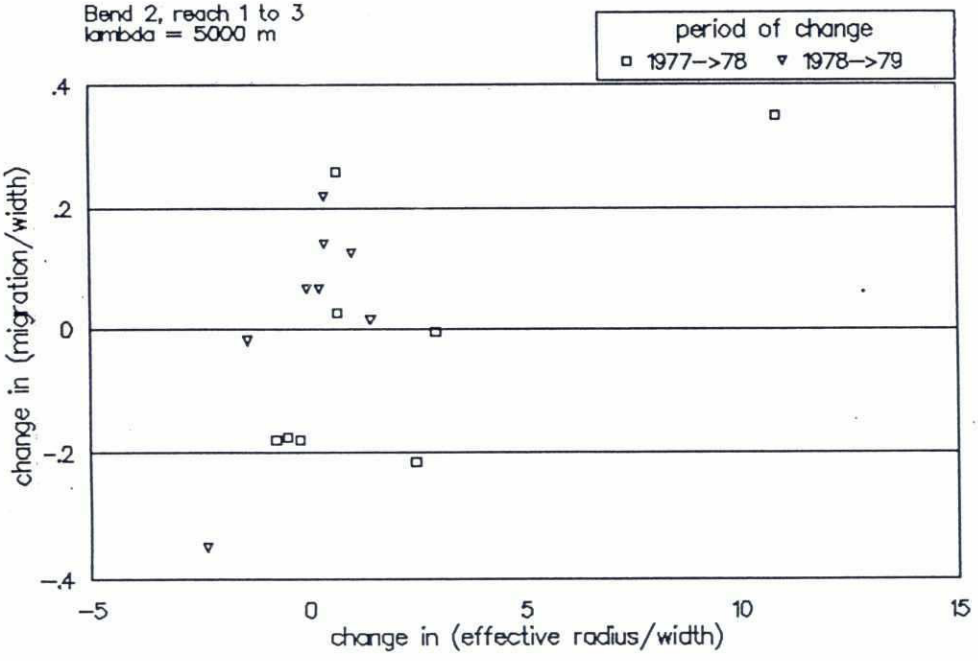


Fig. 3.2-16: Change in migration versus change in effective radius of curvature, over two subsequent one year periods

3.2.6 Discussion of Improved Reduction Method for Bank Erosion Rates

The study presented in above subsections does have some limitations given here in:

- The derivation of the channel centre line is somewhat subjective. This inaccuracy is expected to be less than two pixels (100 m);
- The assumption that width does not change considerably from year to year does not hold good for the dynamic Jamuna river. So bend migration is not necessarily equal to bank erosion;
- The width of a bend can also change considerably, thus affecting the relative migration and relative radius of curvature;
- Both the radius of curvature and the migration differ greatly over short distances. Especially in the almost straight reaches of the bends the calculated radius may differ extremely (100 to 500 %) over 600 m or so. So possible trends can easily be obscured. Probably a better measure would be the curvature, which is the reciprocal of the radius of curvature. The large percentual differences will be insignificant in this way. This measure has not been used here, though, in order to keep the results comparable to the work of Nanson and Hickin (1983), Masselink (1989), Klaassen and Masselink (1992).

However, the studied locations have been carefully selected on the basis of limitations stated above.

The careful selection limits the validity of the observations. The individual character of graphs further limits the validity. The latter can be illustrated with the Figs. 3.2-17 and 3.2-18 in which the individual graphs are combined. These combination plots show a less clear relationship than the individual plots. It seems that for a general erosion-curvature relation, additional information is required.

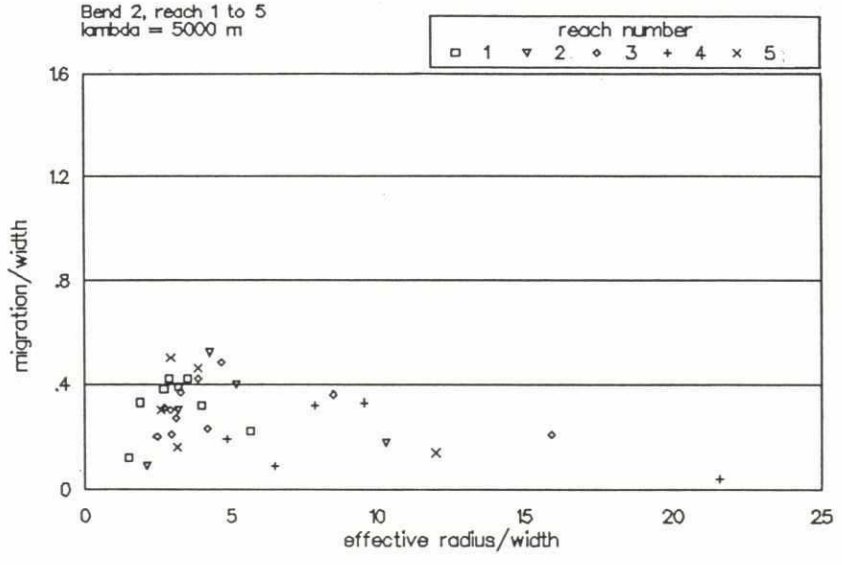


Fig. 3.2-17: Effective radius of curvature versus migration, for reaches 1 to 5, migration related to first year planform

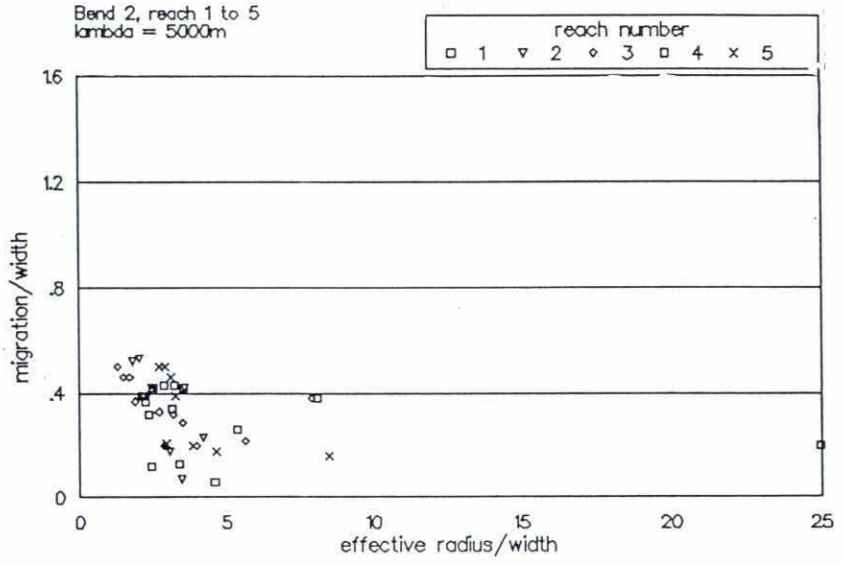


Fig. 3.2-18: Effective radius of curvature versus migration, reach 1 to 5, migration related to second year planform

Figs. 3.2-12 and 3.2-13 can be used to help predicting migration. Locations with a high (3 to 4) effective radius of curvature and a low (0.2 to 0.3) migration in the previous period, are expected to show increased migration (0.4) in the following period. Locations with a low effective radius, that had high migration in the previous year, are supposed to have less migration in the following year. It should be noted that the relation, as seen in Figs. 3.2-12 and 3.2-13, is only based on the study of one bend over a four year period. More research, preferably over a longer period, should be done to test the validity of the present observations.

The present study supports that, at least for some bends, a relation between migration (erosion) and radius of curvature exists. The use of this relation in a general erosion prediction model however, still seems very limited. Additional studies will be required for such general predictions.

3.3 BIFURCATION ANALYSIS

3.3.1 Introduction

Braided rivers, such as the Jamuna river, are characterized by a large number of bifurcations. These bifurcations are important locations in the river where water and sediment are divided. A large part of the present study deals with the analysis of these bifurcations. Two processes acting at the bifurcations were studied in detail; abandonment and migration. Both are dealt with in separate subsections.

Bifurcations were only studied when they met the following conditions:

- They should have two downstream channels. Bifurcations that have three (or more) channels are fairly complex and are not included in this analysis, and
- The inter-channel char should be of considerable size, more than 5 sq.km and preferably classified as bare soil with (some) vegetation.

In total 19 bifurcations, from the period 1976-1992 were studied. See Appendix 5 for a comprehensive description of the investigated bifurcations. Some of the bifurcations existed for 17 years whilst others disappeared within 2 years. The average life-time was 3.25 years. Only three of the selected bifurcations were located on the northern satellite images. This can be explained from the fact that the northern part of the Jamuna river is more dynamic. This dynamic behaviour results in more complex bifurcations that do not meet the requirements for selection.

3.3.2 Abandonment of Bifurcated Channels

(i) General

The main objective of the abandonment analysis is to gain insight into the apparently erratic process of channel abandonment. Abandonment in this analysis is defined as the abandoning of one channel in favour of the other, as a result of which the bifurcation disappears. A shift of one or two of the bifurcated channels to a new course (avulsion) was not considered to be an abandonment, because the bifurcation itself remains.

(ii) Bifurcation geometry

It was assumed that the geometry of the bifurcation is an important factor in the process of abandonment, because it affects the distribution of sediment. Therefore the bifurcation geometry, as well as different spatial properties of the bifurcated channels were studied.

After selecting the bifurcation, the deviation angles of the bifurcated channel centre lines with the upstream channel direction were determined. Channels deviating to the right hand side of the upstream direction were defined to have a positive angle, the channels deviating to the left thus having a negative angle. The determination of the exact bifurcation location and the upstream and bifurcated channel centre lines is subject to some personal independent; the derived parameters are thus no real objective parameters.

Besides the deviation angles (α_1, α_2) the following parameters were determined from the satellite image prints, (see Fig. 3.3-1 for a depiction of these parameters):

The following terminologies were used for bifurcation study:

α_1, α_2 = Deviation angle of the bifurcated channels with the upstream channel direction
L_1, L_2 = Length of the individual bifurcated channels
D = Direct distance from bifurcation to confluence point

The numbers in subscript indicate whether the left ($_1$) or right ($_2$) channel is concerned (looking downstream).

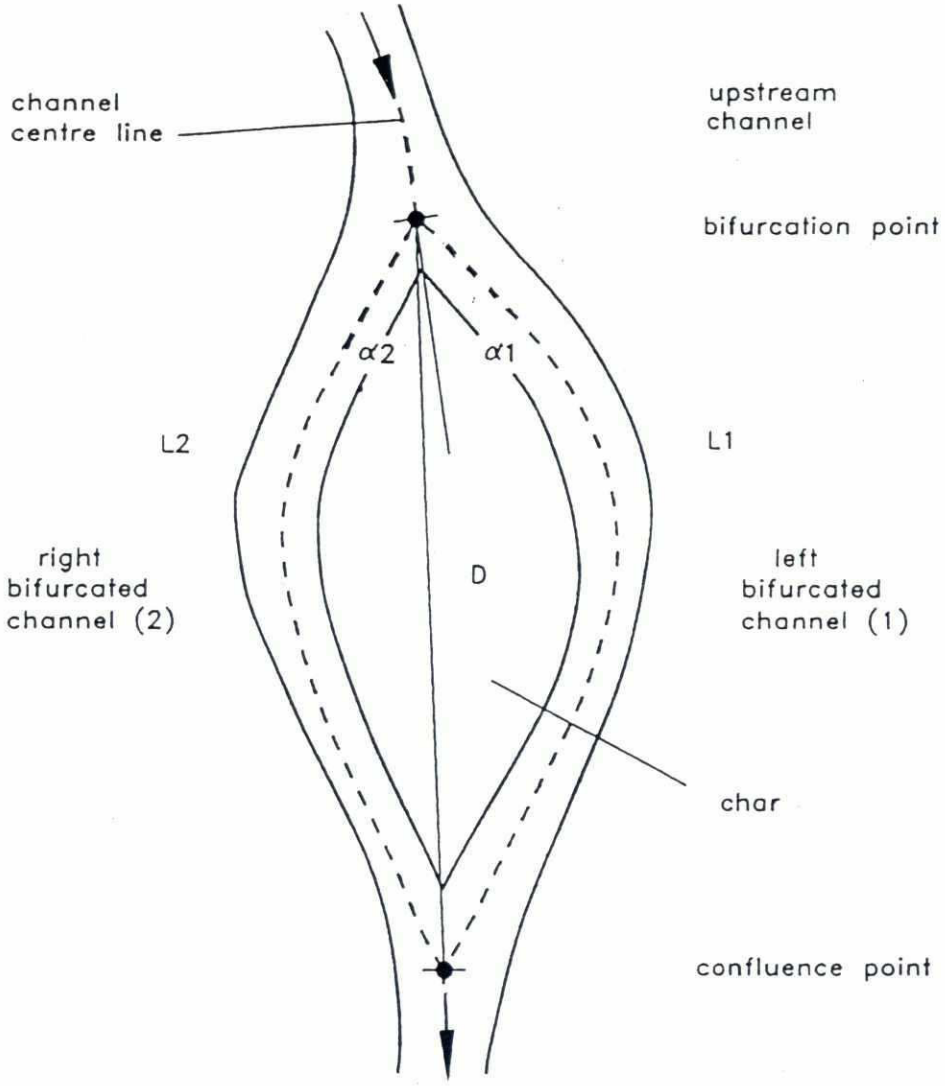


Fig. 3.3-1: Terminology used for bifurcation study

Three parameters were considered to greatly affect abandonment. These are bifurcation geometry (as expressed in α_1 and α_2), sinuosity and relative length. Sinuosity is defined here as channel length (L) divided by distance (D). Relative length is defined here as length of one bifurcated channel divided by the length of the other channel.

To test the significance of these parameters two graphs were constructed. Fig. 3.3-2 shows sinuosity plotted against deviation angle; the ratio L/D of the left channel plotted against α_1 et cetera. For reasons of simplicity the left deviating angles have been given a positive sign; this is also done in further analysis. In Fig. 3.3-3 relative length is plotted against deviation angle; L_1/L_2 is plotted against α_1 and L_2/L_1 is plotted against α_2. A square was used for channels that were abandoned in the following year. Both graphs consist of 124 plotted points.

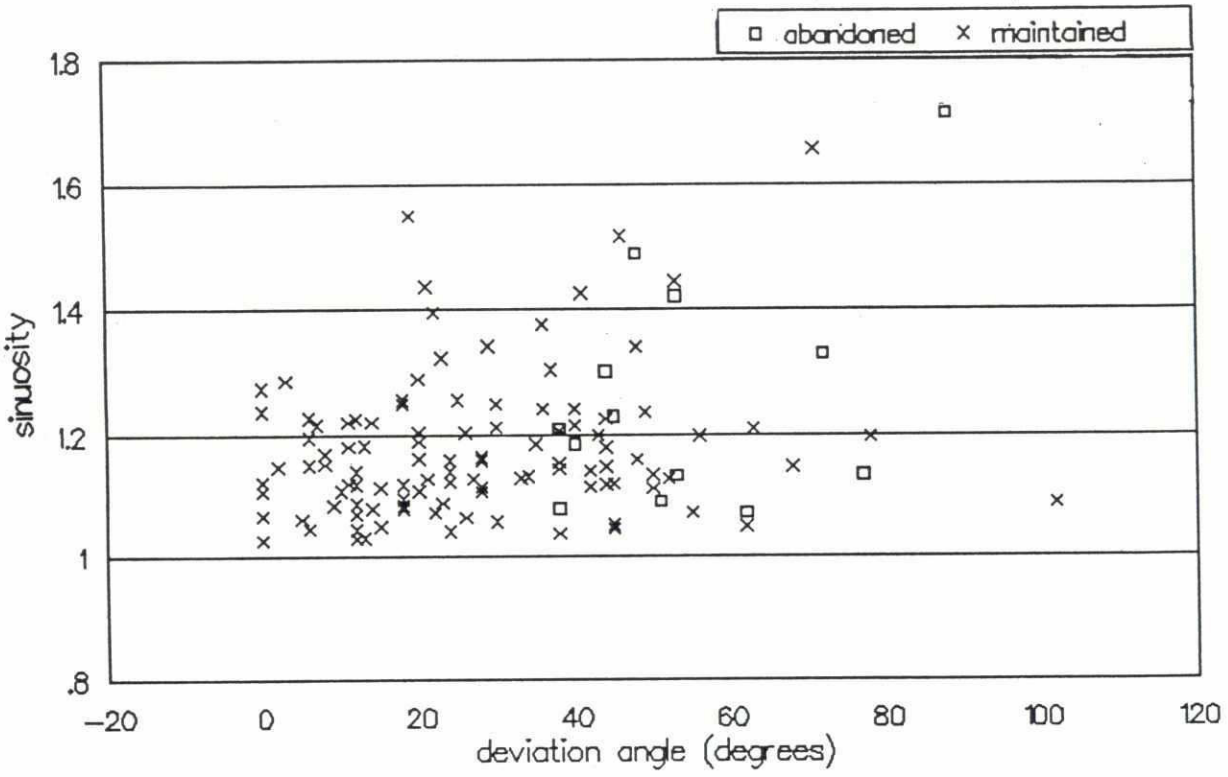


Fig. 3.3-2: Sinuosity versus deviation angle, labelled for abandonment

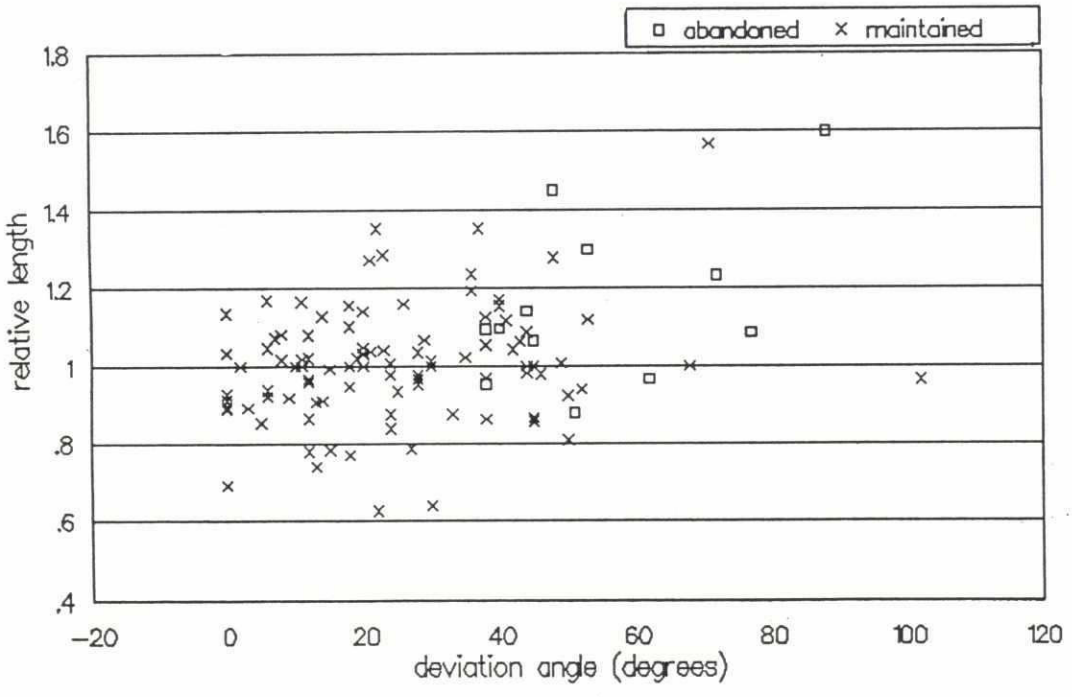


Fig. 3.3-3: Relative length versus deviation angle, labelled for abandonment

An inspection of the graphs leads to the following remarks:

- The sinuosity and relative length never exceed 1.7, this is low compared to meandering rivers;

- The angle, α, indicating channel deviation from upstream channel direction, seems to be a more important factor in channel abandonment than sinuosity or relative length;
- Abandonment seems only to take place when the angle, α, is larger than approximately 40°;
- The geometry of the bifurcation point (as expressed in α) greatly influences the sediment distribution, so the analysis supports the view that this distribution is an important factor in channel abandonment;
- The relative length corresponds to the cut-off ratio as used previously by Klaassen and van Zanten (1989) in their analysis of cut-off and abandonment phenomena. It seems that in Jamuna type of rivers where abandonment is virtually independent of the cut-off ratio, the sediment distribution as determined by the geometry is a much more important parameter than the cut-off ratio, and
- Changes in channel configuration greatly affect bifurcations. This complicated the analysis a great deal. Upstream changes may lead to a change in upstream channel direction or even abandonment. Downstream changes may disturb the parameters L and D. Both changes might obscure possible relations and limit the validity of the conclusions mentioned above.

To demonstrate the effect of channel angle on abandonment a bar-graph (Fig. 3.3-4) was constructed. For seven angle classes (0°-9°, 10°-19° etc.) a distinction was made between channels that were abandoned and channels that were maintained.

In Fig. 3.3-5 these frequencies are converted to percentages. A clear trend is visible now. With increasing angle, bifurcated channels have a higher probability of being abandoned.

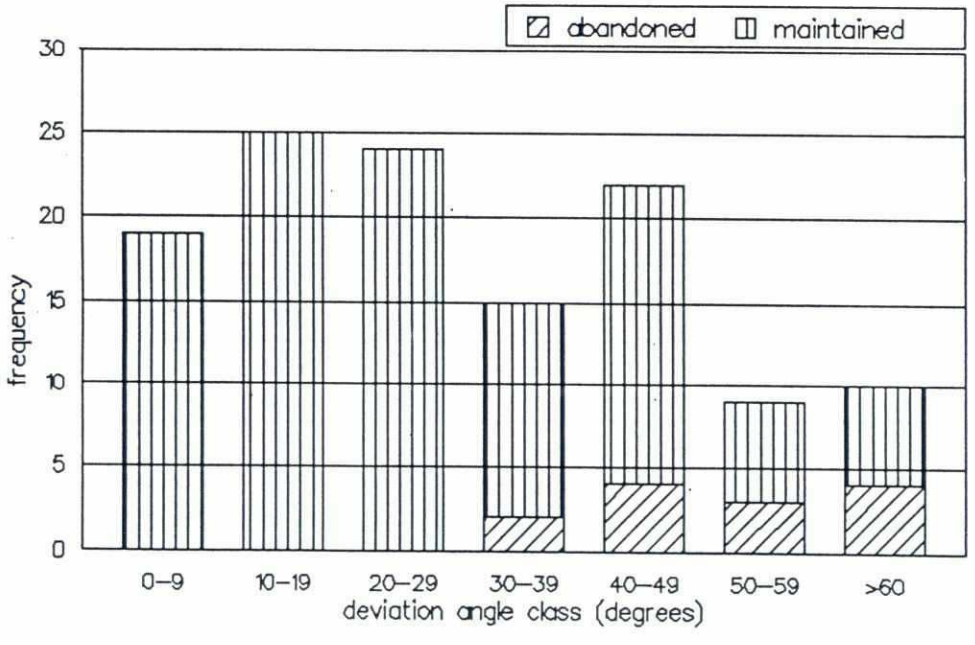


Fig. 3.3-4: Frequency of abandonment for different angle classes

R.P.O. LIBRARY

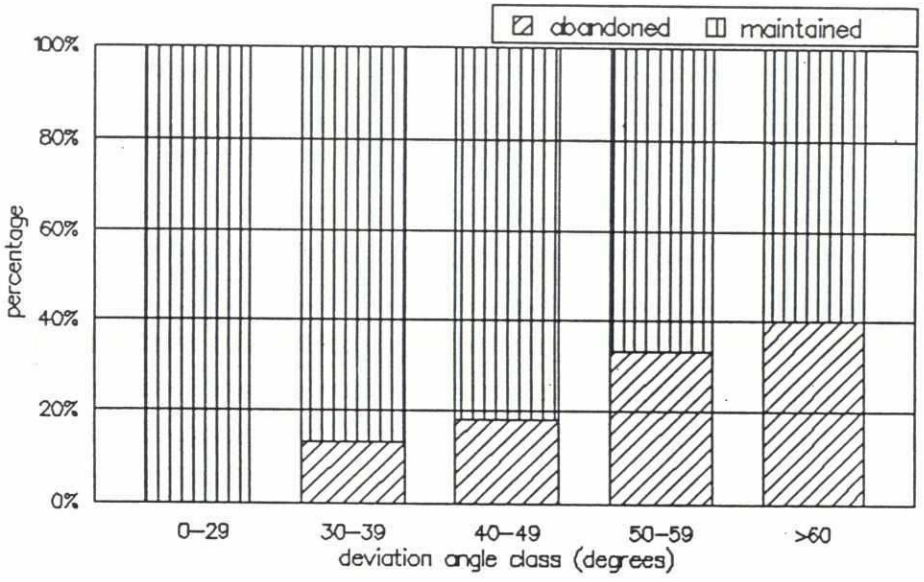


Fig. 3.3-5: Probability of abandonment for different angle classes

3.3.3 Influence of Bifurcation Asymmetry

A separate study element was directed at the influence of bifurcation asymmetry. A bifurcation was considered to be symmetric only when it met the following requirements:

- $| \, | \alpha_1 | - | \alpha_2 | \, | \leq 20°$; (the absolute value of the angle difference of the two bifurcated channels should be less than or equal to 20°), and
- $| W_1 - W_2 | / (W_1 + W_2) \leq 0.2$; (relative width difference should be less than or equal to 0.2).

The two quantities introduced above are referred to as degree of angle asymmetry and degree of width asymmetry.

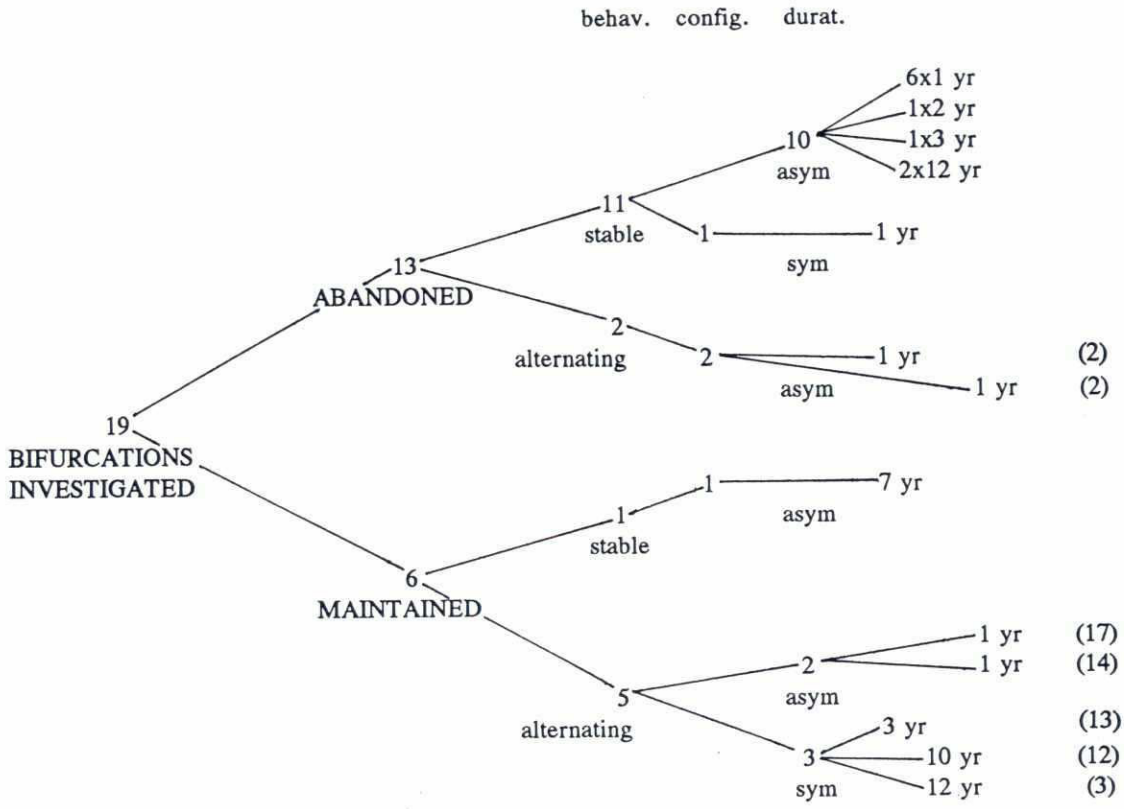
Masselink (1989) stated that asymmetric bifurcations were doomed to disappear within a year or two. From Fig. 3.3-6 it seems clear that asymmetry increases the probability on abandonment. But asymmetric bifurcations do not always disappear within two years; some of them exist up to twelve years and others, especially the ones that alternate between asymmetric and symmetric, remain to exist even over a longer period.

The relation between asymmetry and abandonment can also be seen from Fig. 3.3-7. The two asymmetry parameters, as defined above, were calculated for all the studied bifurcations. The abandoned bifurcations were indicated by a square symbol in the following figures.

From these graphs it can be observed that:

- symmetric bifurcations (using the critical values as given above) are rarely abandoned;
- increasing angle asymmetry seems to have a positive correlation with the probability on abandonment;

- increasing width asymmetry does not seem to increase the probability on abandonment, an opposite relation even seems visible, and
- abandonment seems more dependent upon angle difference than on width differences.



behav. : description of symmetric behaviour through time, the configuration could be stable through time or alternating between symmetric and asymmetric.
config.: configuration in last phase of existence.
durat. : duration of last phase; total time of existence, in case of alternating configuration,between brackets.

Fig. 3.3.6: Diagram of investigated bifurcations, abandonment and symmetric behaviour through time

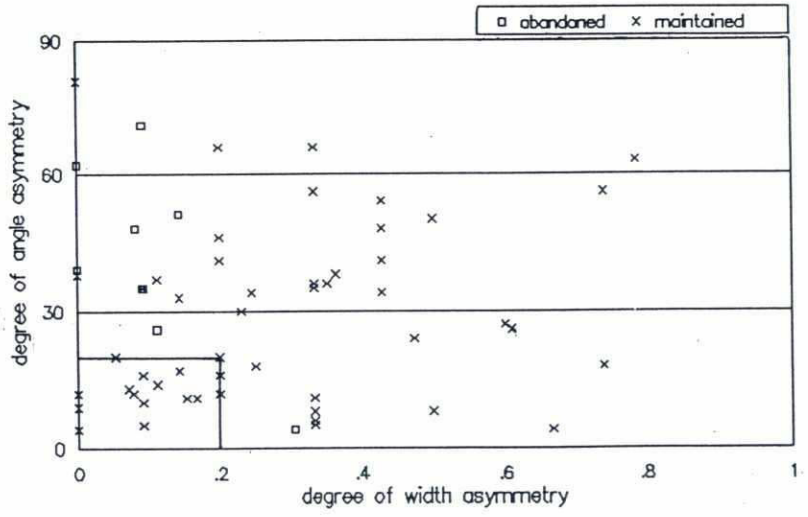


Fig. 3.3-7: Degree of angle asymmetry versus degree of width asymmetry, within the lower left box the symmetry requirements are met

In Fig. 3.3-8 a comparison is made between deviation angle and angle asymmetry. From this figure it is clear that deviation angle is a more reliable parameter for predicting abandonment than angle asymmetry. The deviation angle shows a clear lower boundary, from where abandonment is found. Such a limitation is not found for the angle asymmetry values.

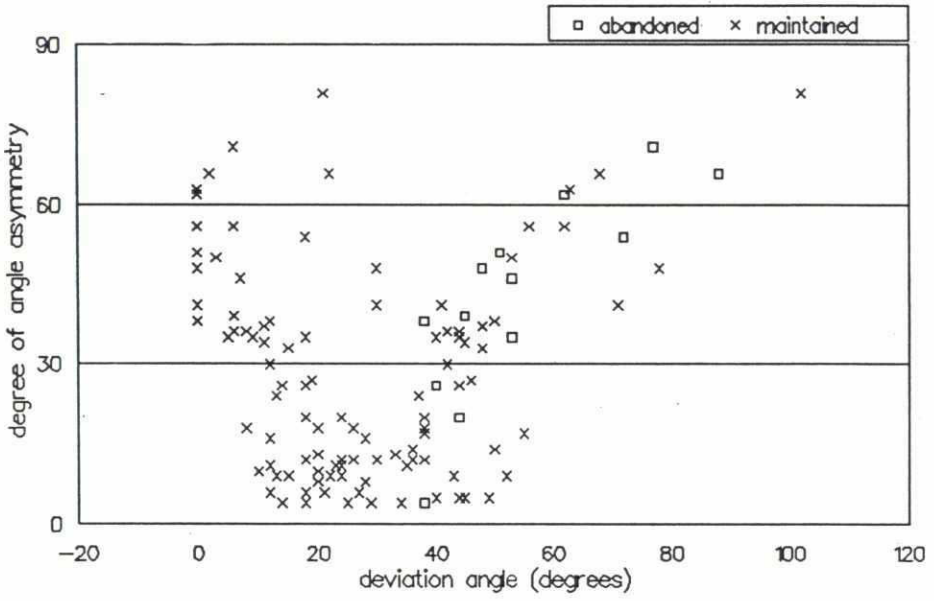


Fig. 3.3-8: Degree of angle asymmetry versus deviation angle, labelled for abandonment

The same is ilucidated by Fig. 3.3-9. In this figure the deviation angles of the two bifurcated channels are plotted, a label indicates which channel is abandoned. The part of the graph in which the angle symmetry requirement is met, is shaded.

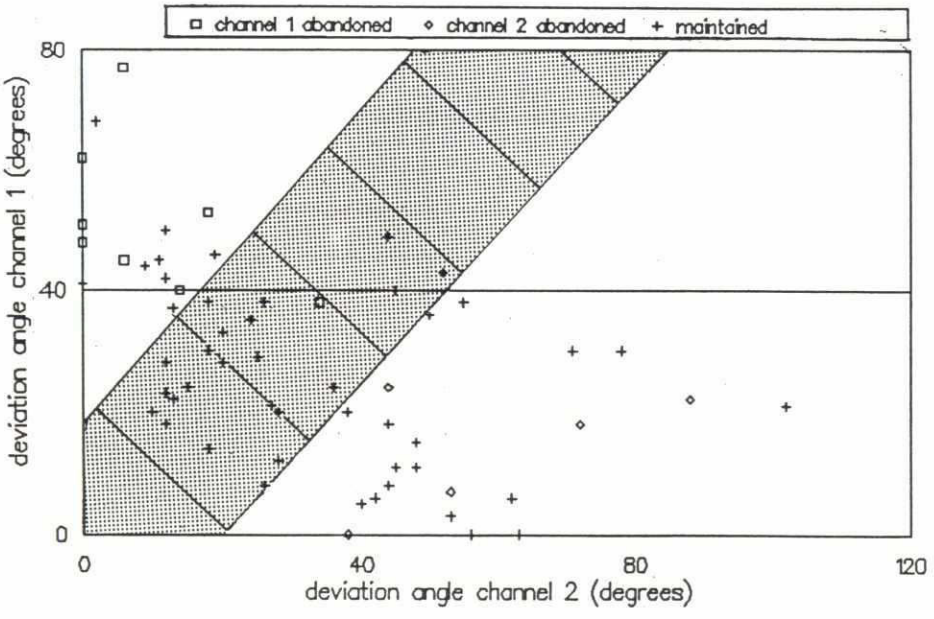


Fig. 3.3-9: Deviation angle, channel 1 versus channel 2, labelled for abandonment, shaded area meets angle symmetry requirement

3.3.4 Influence of Bifurcation Position

This subsection presents the results of a limited study on the importance of the bifurcation position in respect to abandonment.

For the exact position of the bifurcated channel three possibilities were distinguished: (i) the inner side of a bend, (ii) the outer side of a bend and (iii) no bend present within 2.5 km of the bifurcation. The latter situation includes cross-over and straight reaches.

First the maintained positions of the bifurcated channels were studied. As can be seen from Fig. 3.3-10, the maintained channels can be found on all the three positions, with each of them taking an approximately equal part. A different distribution can be found for the abandoned bifurcated channels (see Fig. 3.3-11). Most abandoned channels (almost 70 %) are situated in the inner side of the bend.

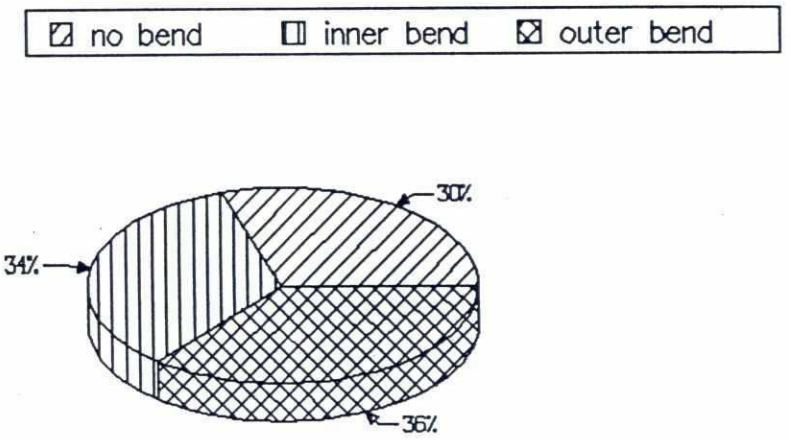


Fig. 3.3-10: Positions of the maintained bifurcated channels

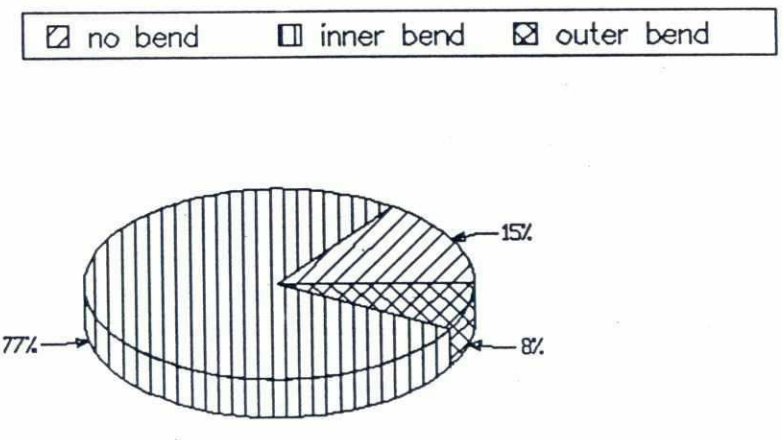


Fig. 3.3-11: Positions of the abandoned bifurcated channels

Fig. 3.3-12 and 3.3-13 show the shares of the different locations, for the individual angle classes. The shares are approximately equal for the maintained bifurcation angle classes. The abandoned bifurcations however show a peculiar spread of the location shares. The 30°-39° class consists completely of "no bend" channels. Two channels are found in this class, one situated in a cross-over and one situated in a straight reach. The only outer bend situated channel can be found in the highest angle class, notably with an angle greater than 60°.

It cannot be overemphasized that only a few (13) abandoned channels were studied, so it may be dangerous to base too many conclusions on the observations made above. However, to conclude that most abandoned channels were situated in the inner side of a bend seems to be on the safe side.

This is also what one would expect from the water-sediment distribution in a bend. As is stated by amongst others Leopold et al. (1964) stream flow can be divided into two components; a downstream component and a weaker, transverse component. This secondary flow is caused by the slow adaption of the water mass to the bend situation (inertia). This effect is especially strong in the upper layer of the water mass because of the higher velocity near the surface. To compensate for the transverse flow that is directed towards the outer-bank, an inner-bend directed return flow arises at the bottom of the stream. See Fig. 3.3-14 where the shaded area depicts the magnitude of the side-ways flow.

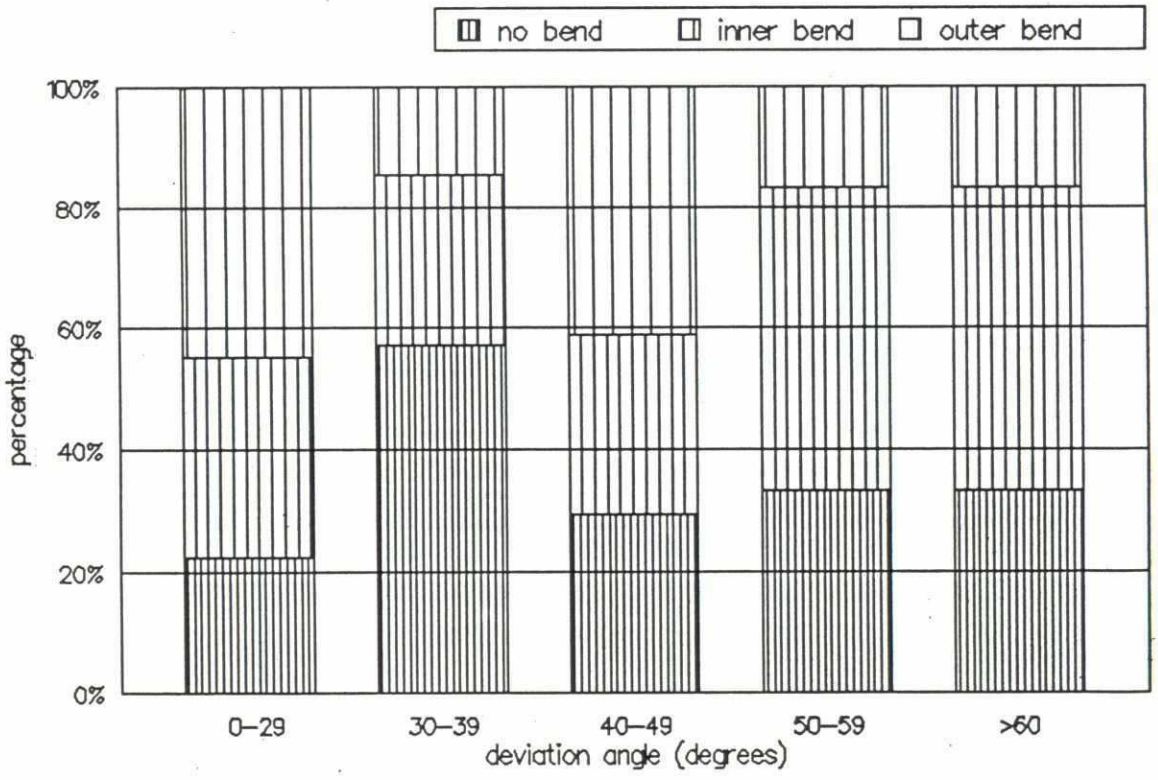


Fig. 3.3-12: Positions of the maintained bifurcated channels, differentiated for deviation angle class

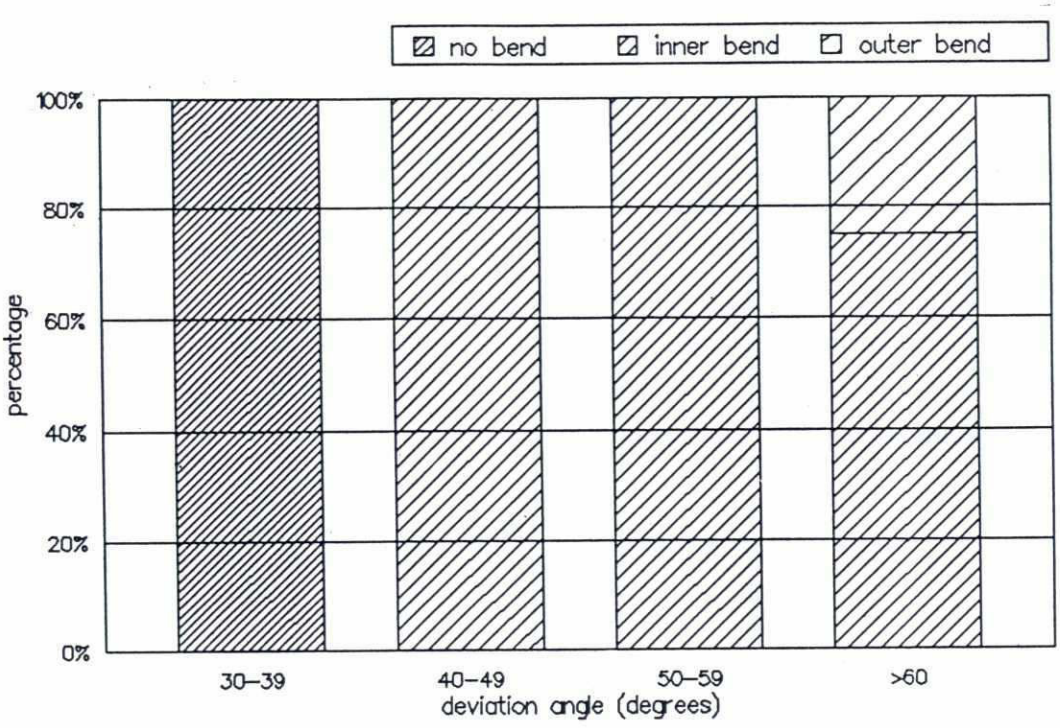


Fig. 3.3-13: Positions of the abandoned bifurcated channels, differentiated for deviation angle class

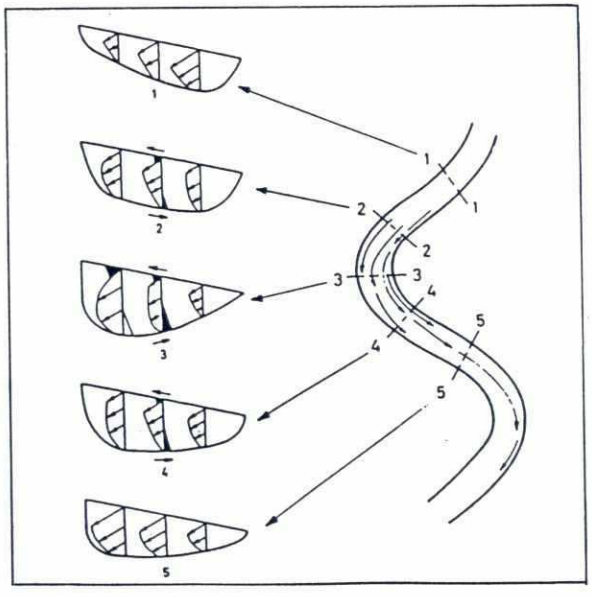


Fig. 3.3-14: Sketch showing pattern of flow in meanders

(Source: Leopold et al., 1964)

The bottom flow carries the bed load and most of the suspended load towards the inner bank. The abundance of sediment could probably explain the high probability on abandonment of channels which are situated in inner bends. Channels on the outer side of a bend have a larger probability on survival and apparently abandon only when they form a very large angle with the upstream channel. In that case one could speak of a short cut. Thus from the present data it seems that chute cut-offs only occur with very high angles, ($>60°$).

That abandonment of "no bend" channels is only found in the 30°-39° class, whilst in the maintained bifurcations graph they are found in all classes and could not be explained. It is probably due to the small sample size.

3.3.5 Migration of Bifurcations

A relation between bifurcation symmetry and migration was given by Masselink (1989). He found that a symmetric bifurcation migrated approximately 900 m/yr in the upstream direction. In this study a similar investigation was done.

For every year and for every bifurcation, the migration rate (in m/yr) was obtained from the difference images. Downstream migration was defined as positive. Then the symmetry criterion, as given in the Subsection 3.3.3, was applied to the bifurcations. Subsequently, a comparison was made with the migration rate of that year. The results are presented in a bar graph (see Fig. 3.3-15). With 19 bifurcations studied and an average life time of 3.25 years, 62 situations arise. It is to be noted that abandonment is only encountered in 13 situations.

From Fig. 3.3-15 it becomes clear that rapid negative (upstream) migration is only found in asymmetric bifurcations. The share of symmetric bifurcations increases with the transition from relatively slow upstream, to fast downstream migration.

The same trend is visible in Fig. 3.3-16. In this graph migration is plotted against angle asymmetry, labelled for relative width asymmetry. Definitions for these parameters are given in Subsection 3.3.3. The squares (width asymmetry 0.2 or less) with an angle asymmetry of 20° or less, mainly show a positive migration, displaying a big scatter as may be noted in the graph.

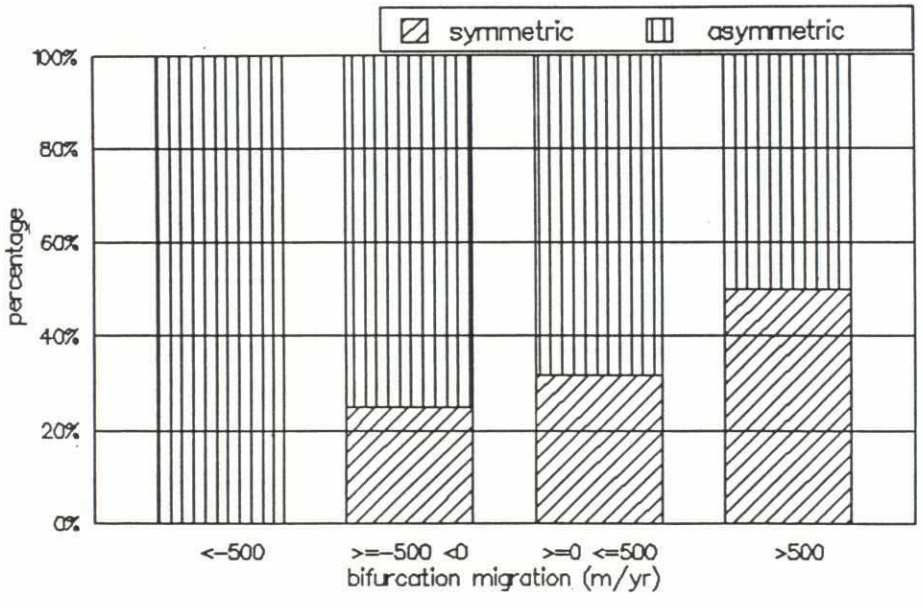


Fig. 3.3-15: Migration of symmetric and asymmetric bifurcations

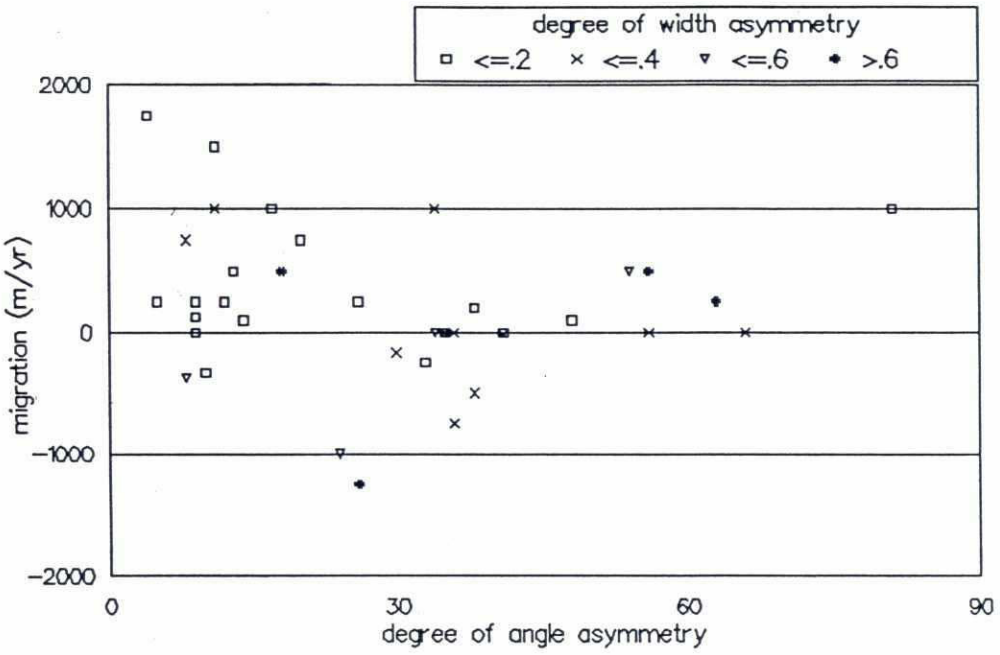


Fig. 3.3-16: Bifurcation migration versus angle asymmetry, labelled for width asymmetry

From Fig. 3.3-15 and 3.3-16 it may be concluded that symmetric bifurcations normally show downstream migration, but an unambiguous relation between symmetry and migration could not be found. An average speed of migration could not be obtained. These conclusions firmly oppose the statements made by Masselink (1989).

3.3.6 Conclusions of Bifurcation Analysis

From the study on bifurcations reported upon in the previous subsection the following conclusions can be drawn:

- It is clear that most of the bifurcations disappear in three years or less;
- Asymmetry seems to increase the probability of abandonment, but it is not a guarantee as was suggested by Masselink (1989). Some bifurcations that are alternately symmetric and asymmetric seem to be more stable;
- The bifurcation geometry seems to be a more important parameter in abandonment than sinuosity or relative length (cut-off ratio);
- Bifurcated channels that deviate more than approximately 40° from the upstream channel direction have a high probability of abandonment. This probability increases as deviation increases. A high deviation angle normally corresponds with asymmetry, and
- Abandoned bifurcated channels are most often situated in the inner side of a bend. This can possibly be explained from the sediment distribution. Sediment transport is directed towards inner bends.

3.4 WIDTH CHANGES OF BIFURCATED CHANNELS

In this section attention was given to the change in width of the studied bifurcated channels. Changes in channel width were studied in the same way as the abandonment of bifurcations. Abandonment was supposed to be an extreme case of channel narrowing. For the time being it was assumed that the influence of the width to depth ratio was small.

Since all images were taken from the same season, it was expected that the total discharge for a specific bifurcation was the same. An observed change in channel width should then be caused by a local change in discharge, presumably caused by an unfavourable deviation angle or sinuosity. So a limited study was done in which the change in width was related to certain planform parameters that were collected during this study.

From most of the bifurcated channels the width in one year was compared to the width in the following year. From this comparison the change was obtained and expressed as a percentage. Not all the bifurcations could be used, when for example for a bifurcation only data of one year were available, no comparison could be made. Also years in which an avulsion took place were not considered, since the bifurcated channels were supposed to be too much different compared to the ones in the year before.

First a frequency analysis was done for the distribution of the changes in width. See Fig. 3.4-1, the class width in this diagram is 30, the class centres are given underneath the bars. So -60 % means that a class stretches from -75 % until (but not including) -45 %. The population has an approximate normal distribution, with its centre around 0 % change, the arithmetic mean is 0.34 %, the standard deviation is large: 46 %. The distribution suggests a certain skewness to the right. Remarkable are the two occurrences in the 210 % class.

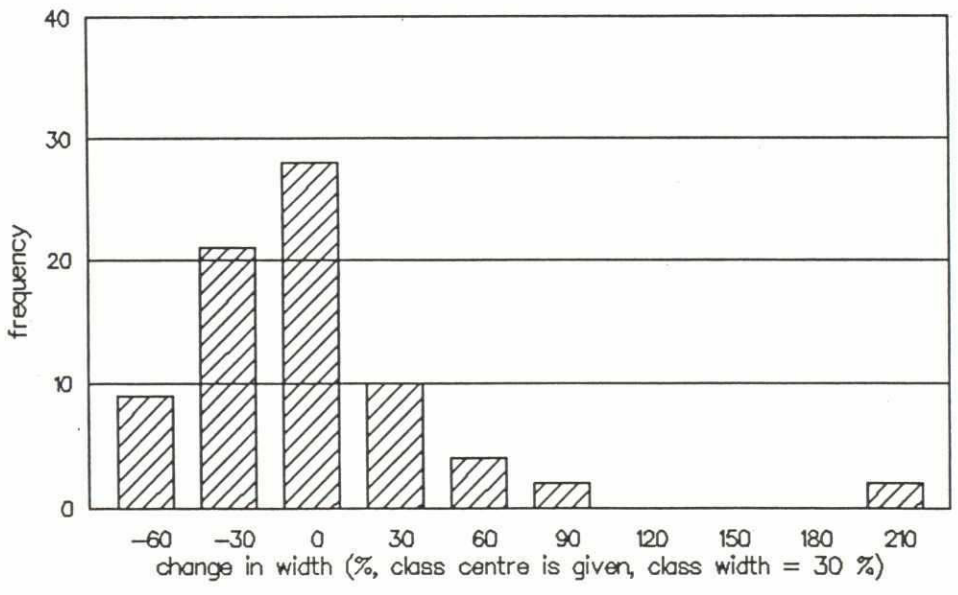


Fig. 3.4-1: Frequency distribution of the change in width data

Fig. 3.4-2 shows the relations between change in width and: first-year and second-year sinuosity, first- and second-year angle and two different asymmetry parameters. All images show approximately the same distribution, the change in width is distributed around zero and no relation is visible between any one of these parameters and the change in width. A possible explanation is perhaps that a changing parameter is compared to a stable parameter. It is possibly not the magnitude, but the change of a parameter that initiates a change in width. In the following graphs the change in width is compared to a changing parameter.

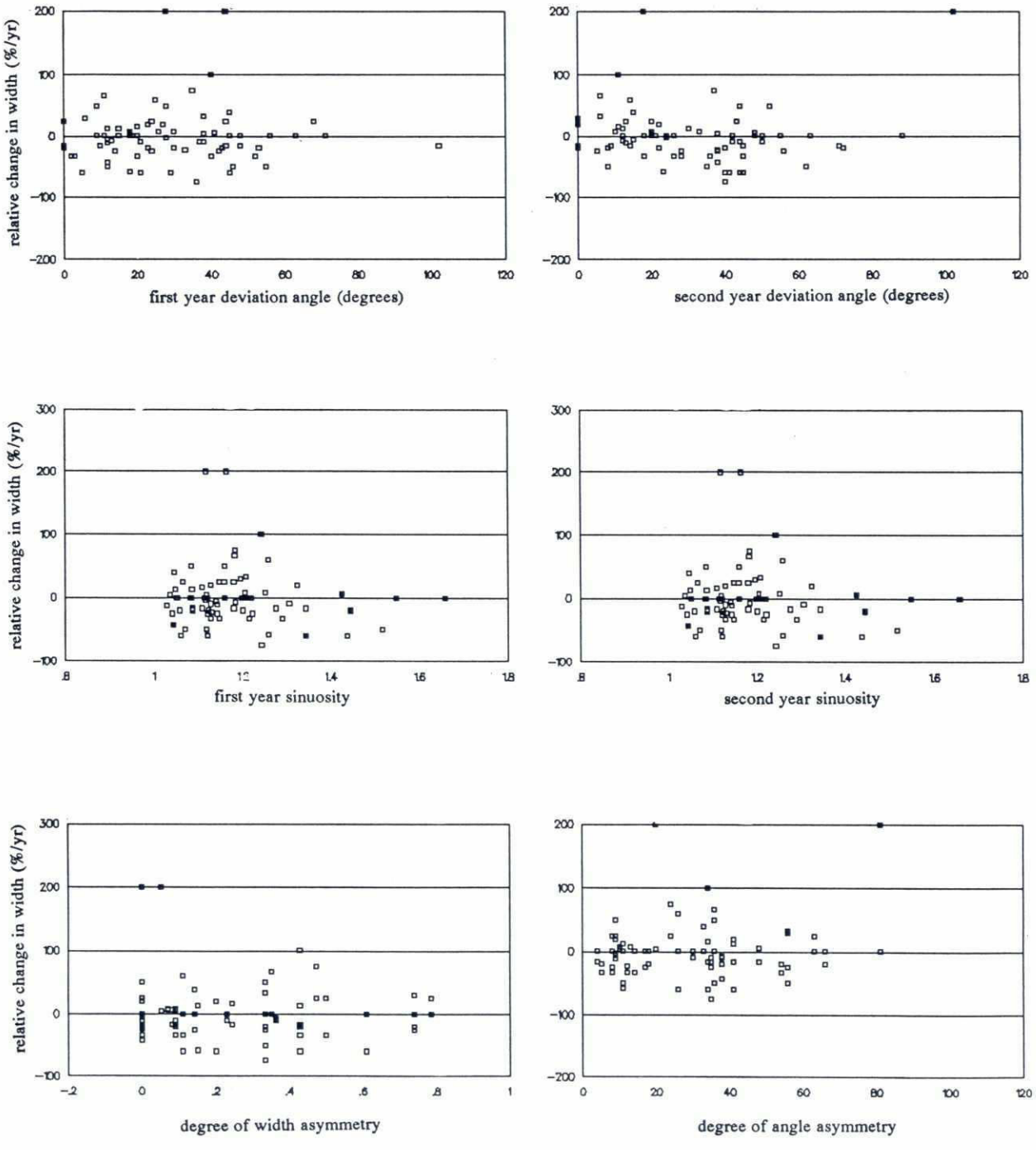


Fig. 3.4-2: Relative change in width versus various planform parameters

In Fig. 3.4-3 the change in width is compared to the change in angle (°/yr). An increase in angle, causing an unfavourable hydrodynamical situation was supposed to lead to a decrease in width. However, the figure does not show this relation. Fig. 3.4-4 compares the absolute change in width (m/yr) with change in angle. A slightly more convincing relation can be observed. Fig. 3.4-5 tests the relation between change in width in channel 1 and change in width in channel 2. If an increase in width in a channel does mean an increase in discharge then the other channel, which receives less water, should show a decrease in width. This is not evidenced in Fig. 3.4-5.

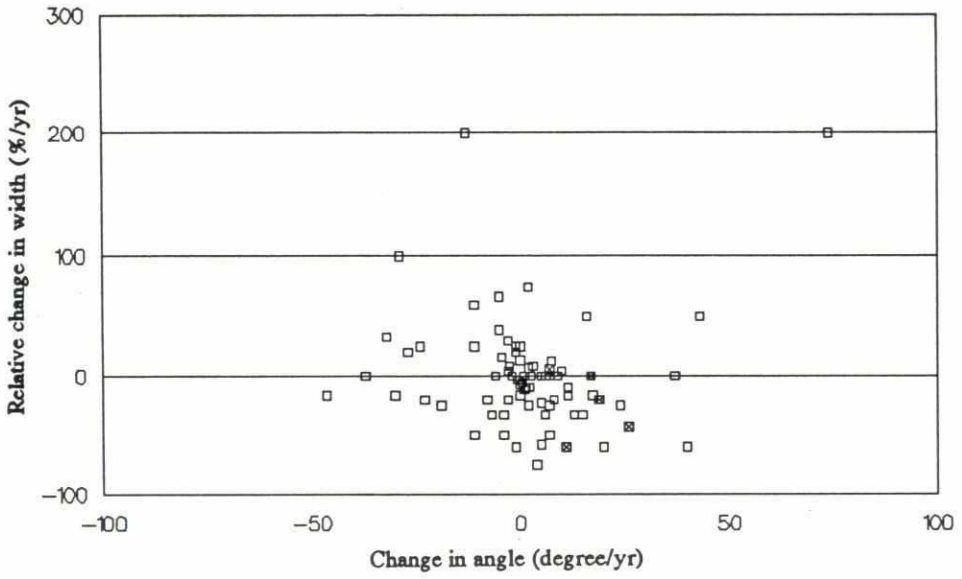


Fig. 3.4-3: Relative change in width versus change in angle

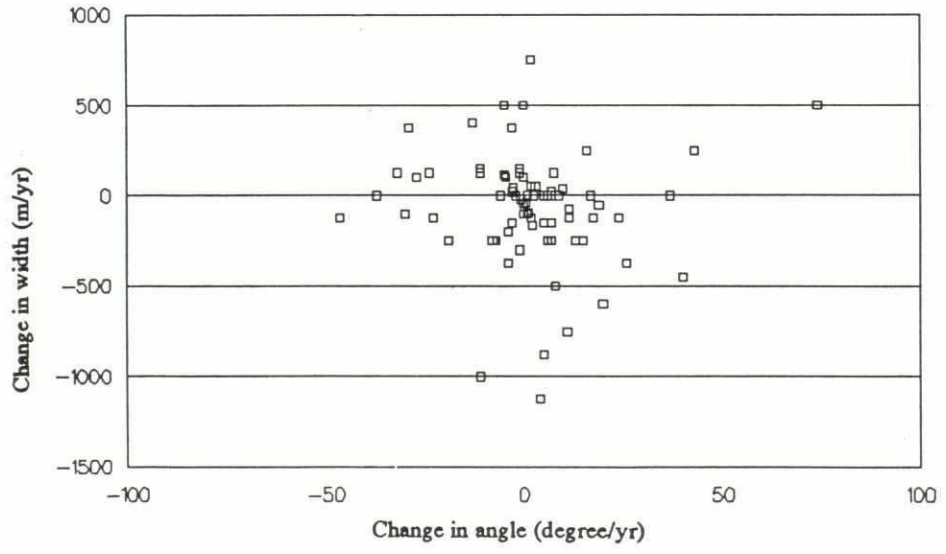


Fig. 3.4-4: Absolute change in width versus change in angle

As a conclusion one might say that change in width seems not to be strongly related with the magnitude of sinuosity, angle or symmetry parameter. Moreover, change in width does not seem significantly related to change in angle or width of the other channel either. If one assumes that change in width means change in discharge, the change in discharge is not convincingly related to any of the above mentioned parameters.

To explain the changes in width as observed in this study, one could think of an autonomous change in discharge, for example, caused by a different low flow discharge or a different acquisition date of the satellite images. Table 2.2-2 shows a list of the discharges at the image acquisition date. A different water distribution upstream of the bifurcation could also cause an autonomous change in discharge, this can be the case for second and lower order bifurcations.

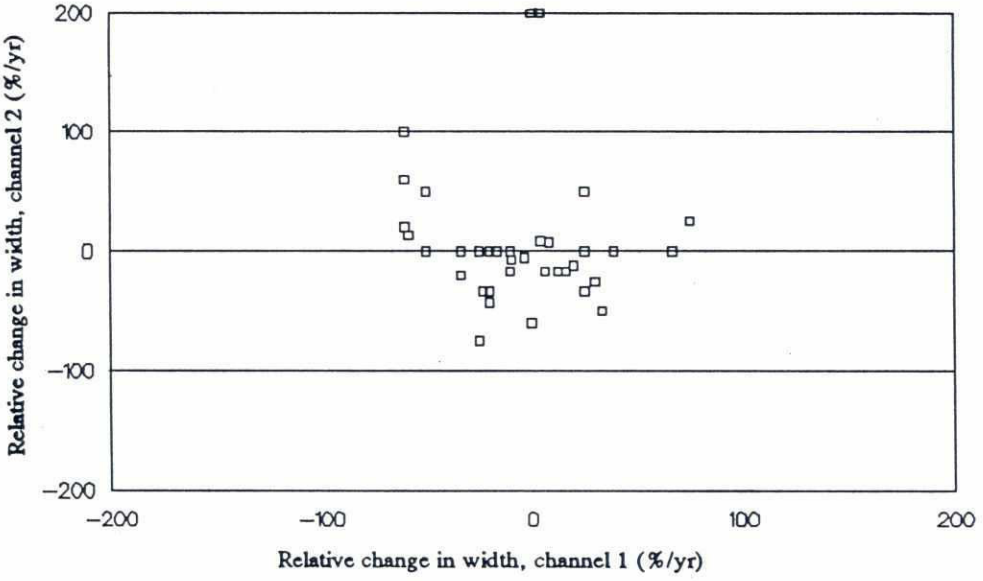


Fig. 3.4-5: Relative change in width, channel 1 versus channel 2

It is also possible that change in discharge expresses itself in other ways then change in width alone, for example also as change in depth or change in velocity. Change in width could then not unambiguously be related to a specific parameter.

That the decrease of discharge of a certain channel (the conveyance) expresses itself through shallowing rather than narrowing seems a likely possibility. Abandonment is supposed to be caused by a change in sediment distribution. So increased sedimentation, causing abandonment, is likely to cause shallowing.

3.5 MULTIPLE YEAR COMPOSITES

3.5.1 Introduction

Initially the processing of the data was limited to processing into single-year classified images and eventually into two-year composites or difference images. During this study the idea came up to develop more-year composites in which all single-year classified images are merged. It was hoped that such an image could help visualize and understand the long term dynamics of the Jamuna river.

For these more-year composites, all the images available were used. This series included fifteen images spread over a twenty year period (1973-1992). Two different kinds of composites were constructed. One indicates the number of water occurrences, the other visualises the successive river courses. For both composites simplified single-year classifications were used, including only two classes: water and land. The latter class includes sand, bare soil and vegetation. Note that the discharge differences of the images, as mentioned in the former chapter, also affect these composites. By the time this report was printed these composites were only available for the south image. The composites of the north image are still under preparation at the NLR.

3.5.2 Number of Water Occurrences

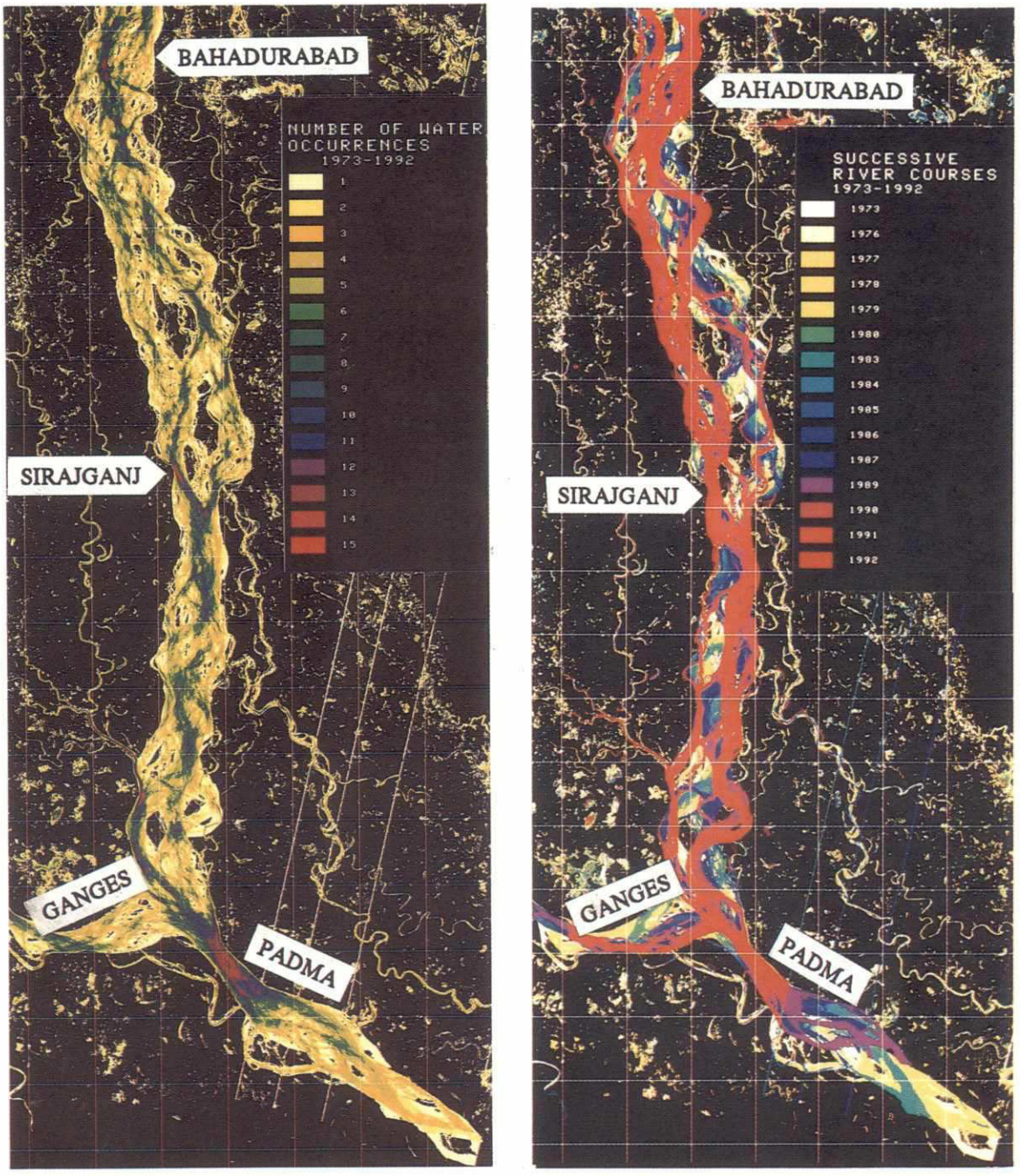
For the image indicating the number of water occurrences (see Fig. 3.5-1) simple addition was made, counting how many times a certain pixel was interpreted as water. If water occurred one time the pixel was given a whitish yellow colour. With an increasing number of water occurrences the colour gradually changes via yellow, green and blue into red.

This image gives a fair impression of the braiding zone, the preferred water ways (coloured in blue) and the stable river sites (coloured in red). Only a few of these stable river sites or nodal points exist. They seem to be located downstream from major confluences, which can be made up of two important Jamuna branches or of the Jamuna and a major tributary. Remarkable is the stabilizing effect of the Sirajganj embankment.

This composite also shows that very few chars are stable over a longer period. In former studies a reasonable long life (over thirty years) was expected for both the nodal points and the meta-stable islands (for example, FAP 1). The latter are defined as chars at or above dominant discharge. From the images presented here, it is clear that such long life-times are scarce.

3.5.3 Successive River Courses

The image indicating the successive river courses (see Fig. 3.5-1) was made by giving water occurrences of every year a unique colour.



(a) Number of water occurances

(b) Successive river courses

Fig. 3.5-1: Multi-year composites of low-flow satellite images of the deep channels of the Jamuna river (approximate scale 1:1,000,000)

Starting with whitish yellow for 1973 and, using the same colour series as in the other composite, ending with bright red for water in 1992, every new water occurrence overwrites the previous situation (whether water or land). The continuous red thus depicts the most recent river course. This image can be used to detect gradual shifts in the river planform. An example is the recent outflanking in the eastern branch just upstream of the Ganges confluence. Another remarkable feature can be seen north of Sirajganj. For a long time the Jamuna used to have two major branches there, but from 1987 onwards the eastern branch has been reduced in size continuously. A significant westward trend or a substantial widening of the Jamuna cannot be detected from this composite. Coleman (1969) indicated such trends for the 1830-1963 period. One might conclude that for the past twenty years the river was relatively stable in its present position, but the possibility of a longer term trend is still there.

Because these composites were only finished at the end of the research period they could not be incorporated fully in the analysis of the present study. But it is believed that the kind of images presented here, are a great help in visualizing the long term dynamics of an extremely active river like the Jamuna. Especially important locations, like stable river sites and preferred river courses are easy to detect.

3.6 TOWARDS A PREDICTIVE MODEL

The processes in the Jamuna river are so complex that they sometimes seem almost random. Therefore, it is important to reflect upon the predictability of these processes. The predictions are based on observations and on the availability of constituent elements for a predictive model. Both put limits to the predictability, as will be discussed hereafter. Based on this discussion the prospects of the development of a predictive model are indicated.

The observations do not provide complete information, and measurements are usually only estimates of the true state. In particular, the following problems can be mentioned:

- the resolution (pixel size) of the satellite images is on the order of 50 m;
- there are no data on the morphological changes during a flood; only the net end result can be seen on the satellite images taken in the dry season;
- cross-sections are not available for every channel;
- even when a cross-section is available for a certain channel, it is not necessarily representative because of the strong non-uniformity of the channels, and
- inundated banks cannot be distinguished from eroded banks on the satellite images; hence, higher stages produce spurious bank erosion on the images.

These sources of inaccuracy deteriorate the input of (the concepts of) the predictive model, and hence decrease the quality of the predictions.

The derivation of mathematical **predictive model** based on the underlying mechanisms involves many problems, due to the accumulation of residual effects in the integration over time and space, the possibility of chaotic behaviour, the interaction at larger scales with other

dynamic systems, and the necessity of including exceptional events that can be disregarded in predictions for shorter time spans.

The formal integration to larger scales results in a mathematical model consisting of a set of coupled partial differential equations. It reduces an infinite number of degrees of freedom to a number for which solving the equations is feasible. The procedure is not a direct integration from a small to a large scale, but a series of integration steps to ever higher levels in a cascade of scales. Due to the non-linearity of the system, each step produces closure terms for which additional relationships must be induced from observations. Examples of such relationships are eddy viscosity models in the integration over turbulent fluctuations, and velocity profiles in the integration over depth or width. The choice of additional relationships also determines whether the result of the integration is a bar-approach model or a channel-approach model. This stepwise integration procedure implies that information on processes on smaller scales is lost, and that descriptions on larger scales are added as premises for further deduction. The errors of the additional relationships are residual effects. They may cancel out on larger scales, but they may also accumulate and eventually become dominant, so that the model derived by formal integration cannot predict the actual phenomena. The main aim of the observations of phenomena on larger scales is therefore a careful determination of the additional relationships for closure.

The resulting mathematical model with only a few degrees of freedom can also have the property that small deviations accumulate and eventually lead to totally different predictions. Since the recognition of this chaotic behaviour of deterministic systems, the term 'chaos' has got a more restricted meaning in physics. It no longer refers to randomness in general, but to a special type of unpredictability, related to a sensitive dependence on initial conditions. Chaos in river morphology is still a hardly explored subject. There are indications of chaotic behaviour in models for the development of bed topography and meander bend migration (Mosselman, 1992), but whether these models really exhibit such behaviour is still to be investigated.

As the final mathematical predictive model has not been formulated yet, it is not possible to quantify the predictability in a formal way. From experience the Consultant estimates that the limit for bank erosion predictions is about 2 to 3 years. Prediction for a period of about five years ahead seems unrealistic in general, though some local phenomena are more persistent, for example major confluences, major bends and channels aligning active tectonic faults.

On larger scales, the dynamic system of a river interacts with the dynamic systems of (i) climate, (ii) geological activity, (iii) vegetation and (iv) human interference, which can also be regarded as an interaction with another dynamic system. These interactions are discussed below:

(i) Climate

Interactions with climate are not taken into account. Possible effects would be a change in the discharge hydrograph due to changes in precipitation distribution, and a change in boundary conditions at the confluence due to sea level rise.

(ii) Geological Activity

Bangladesh lies in one of the most active tectonic zones of the world (Coleman, 1969). It is generally recognized that major avulsions are controlled by tectonic migration of the Brahmaputra which is controlled by major faults or fractures in the earth's crust. However, there are indications that also the channel patterns within the present river course are influenced by tectonic activity. This could be one of the reasons that the river seems to have preferred courses.

(iii) Vegetation

Vegetation affects the bank erosion of smaller streams, but the larger the river, the less the influence will be. Roots are only present in the upper part, and bank materials can be sheared away by the flow up to depths of 10 m (Coleman, 1969). The insignificance of vegetation is supported by Masselink (1989), who did not find any correlation between bank erosion and the presence of vegetation.

(iv) Human interference

Human interference can produce significant changes of the river, but this does not generate an additional source of unpredictability. By building river training structures, the river system becomes less free and hence more predictable.

Predictions covering a long period are also made difficult by the possible occurrence of exceptional events. An earthquake could completely alter the present day trends and may result in a completely new orientation of the course of the river (as suggested by Coleman for the major shift of the Brahmaputra river from its former Old Brahmaputra course to the present Jamuna course).

Still however the above does not include that a predictive model cannot be developed. The characteristics of such a model would however be more complicated than the deterministic models presently in use. It seems that in this case a predictive model would consist of a combination of deterministic elements and probabilistic approach. Its constituent elements are starting to emerge. Some of these elements are typically like the graphs shown in the Section 3.2, 3.3 and 3.4 of this Annex. Hence the probability of occurrence of a certain phenomenon (like an abandonment to take place) is a function of some local parameters but can also be expressed as a certain probability distribution function the characteristics of which are linked to these local parameters.

The following conceptual model can be visualised: The present planform is determined, e.g. from satellite images. Then the probabilities of changes in the planform during the next flood are evaluated yielding possible planforms after one year with corresponding probabilities of occurrence. Then again these new planforms are evaluated and possible further developments during the next flood are indicated. This leads to a new set of possible planforms after 2 years, again with related probabilities of occurrence. This procedure can be repeated for a number of floods. The final result is a set of possible developments to the river system with their probability of occurrence. These can then be used e.g. for a study of how probable bank erosion at certain site over the coming years will be. In fact the above approach was used in evaluating the conditions in the test areas in Chapter 4.

The conceptual model proposed above is described as a combination of a deterministic and a probabilistic approach. It is clear from the above description that initially (in the first years) the deterministic part is the most influential in determining how the planform of the river will change. After some years however the probability of occurrence is gradually taking over. This implies that after some years (possibly some 5 years) the model will merely provide estimates of the state the river may be in, and becomes comparable to a statistical description of the river characteristics. In the first years however, the deterministic approach yields results that are steered from the existing planform characteristics and will provide useful results for planning preventive or remedial measures, e.g. in the case that a channel may become particularly aggressive over the coming years. Hence such a model will be very helpful in deciding on any bank protection works (FAP 21) and any remedial measures to mitigate the attack of the river (as studied under FAP 22).

It is against this background of limited predictability and the gradual emergence of a conceptual model that may predict the behaviour of the river over the coming years, that the following discussion on the conditions at the test areas in Chapter 4 has to be appreciated.

4 STUDY OF TEST AREAS

4.1 TEST AREAS

In the Technical Report No.1 (FAP 21/22, 1992) the following areas for test river training structures were pre-selected:

- Kamarjani
- Bahadurabad
- Chandanbaisa
- Nakalia

The pre-selection was based on various criteria, one of them being the certainty-of-attack. This criterion is evaluated here in more detail based on information (in particular satellite images) on the recent behaviour of the river system near the proposed test areas. This information became available over the last months as a result of the remote sensing study. In addition to this reassessment, the possibility of other sites is reconsidered on the basis of the new satellite images. The approach is outlined in Section 4.2. The actual analysis is described in Section 4.3 and the conclusions and recommendations are given in Section 4.4.

4.2 APPROACH

The evaluation of the certainty-of-attack criterion requires reliable predictions of future river geometry. These predictions are based on **observations** and on concepts for a **predictive model.**

Observations of the behaviour of the river is mainly inferred from satellite images and river cross-sections surveyed by the Morphology Division of the Bangladesh Water Development Board. These available observations are described in Chapter 2 of this ANNEX.

The **predictive model** aimed at is not available at this very moment, but some of its constituent elements are understood by now and computational rules are becoming available (see the Sections 3.2 and 3.3). These have been used instead in the present analysis. Ultimately the constituent elements of the model are based on fundamental laws describing water motion, sediment transport, bed erosion and sedimentation, and bank erosion and accretion. They are formulated for small volumes of water and sediment, and then integrated over time and space to larger scales. In their present form however they consist of fairly straight forward prediction graphs. Two types of approaches can be used: (i) bar approach and (ii) channel approach.

In the bar approach, the pattern changes are taken to be determined primarily by changes of a submerged bed topography. What typically can be predicted using the bar approach is the gradual movement downstream of a system of bars and channels as present near Kazipur. Hence also the location of the main attack and how it changes in time can be predicted with this approach.

In the channel approach, the patterns are schematized as a network of migrating bends, interconnected at bifurcations and confluences that are also migrating. Within this network, new channels can be created and existing channels can be abandoned. Typically the channel approach can be used for the prediction of bank erosion along curved channels, the probability of the occurrence of cut-offs, etc.

The reality will be a combination of bar and channel processes, so that neither of the approaches separately will be complete. However, constructing a model which includes both approaches will be very difficult.

In addition to the small-scale motion of water and sediment, two elements are to be kept in mind: the hypothesis of cyclicity and the hypothesis of preferred river courses, both suggested by Masselink (1989) and Klaassen and Masselink (1992). The cyclicity of the 50% conveyance position is presently being investigated within the present framework (see Chapter 2) and a period of about 20 to 25 years seems to be found. The preference for certain river courses to which the river regularly returns might exist because the sediment deposited in former abandoned channels is eroded more easily than the surrounding sediments, like Gilvear and Harrison (1991) have found for the river Tay in Scotland. It could also be related to active tectonic faults, which is currently being investigated in cooperation with the Municipal University of Amsterdam, the Netherlands.

4.3 ANALYSIS

4.3.1 General

In this section the conditions at the proposed test areas are assessed in more detail. The emphasis is on the recent developments and attempts are made to extrapolate this recent behaviour to predict the most probable behaviour of the river system at the proposed test areas over the years to come. In particular the probability of continued bank erosion is evaluated and estimates of this bank erosion are made for the near future. This is presented in one figure for each test area in which some possible developments are indicated together with the probability that a certain development may take place.

The probability of the future developments and of continued bank erosion at the test areas is presented here to underscore the uncertainties involved in the prediction of the future developments. By including predictions of the behaviour of the system during the flood of 1992, it will be possible after the flood to check on the accuracy of the predictions. It may be expected that the analysis of the satellite images as presently being carried out will result in improved possibilities for predicting the future behaviour of the river system. This will lead to better predictions and hence to guidelines when and where protective measures will be needed.

4.3.2 Kamarjani

Kamarjani and the Manos regulator are situated on the right bank of the Jamuna river at an approximate latitude of 25°22'. Cross-sections of this area are coded J-15. From 1973 to 1978, the river pattern here became more and more ragged, but the banks near Kamarjani and the Manos regulator were not under attack. The river had regained a simpler appearance in 1984 with a bifurcation at about 4 km downstream of the Manos regulator. Upstream of this bifurcation, widening and associated sedimentation produced an area of dissected chars. Further sedimentation caused these chars to coalesce and to integrate with the island downstream in 1986, thus shifting the bifurcation about 12 km upstream. Island growth by lateral accretion deflected the bifurcated channels outward. This induced severe bank erosion,

for which the right embankment had to be retired. This is the background of the massive bank erosion at Kamarjani and the Manos regulator after 1984. However, the corresponding migration rate has decreased now, and there seems to be a tendency that the eastern anabranch could become more important than the one near Kamarjani. Hence it is likely that the erosion may diminish in the years to come.

A cyclic repetition of channel patterns at Kamarjani could not be detected from the images. Rather, the impression of overall widening was dominant. It is interesting to note that in 1991 the island had been split in two by a node like crossing lying at the same location as the bifurcation of 1984, which supports the hypothesis that the river has preferred courses.

The processes prevailing from 1977 to 1984 can be understood best from the perspective of the bar approach, but for the behaviour from 1986 to now, and hence for predictions, the channel approach is more appropriate.

Based on the 1992 planform derived from the 1992 image and on the changes over the period 1989-1992 (see also Fig. 2.2-1 of the main report) an assessment was made of possible future developments at the Kamarjani test area. The results of that assessment are presented in Fig. 4.3-1.

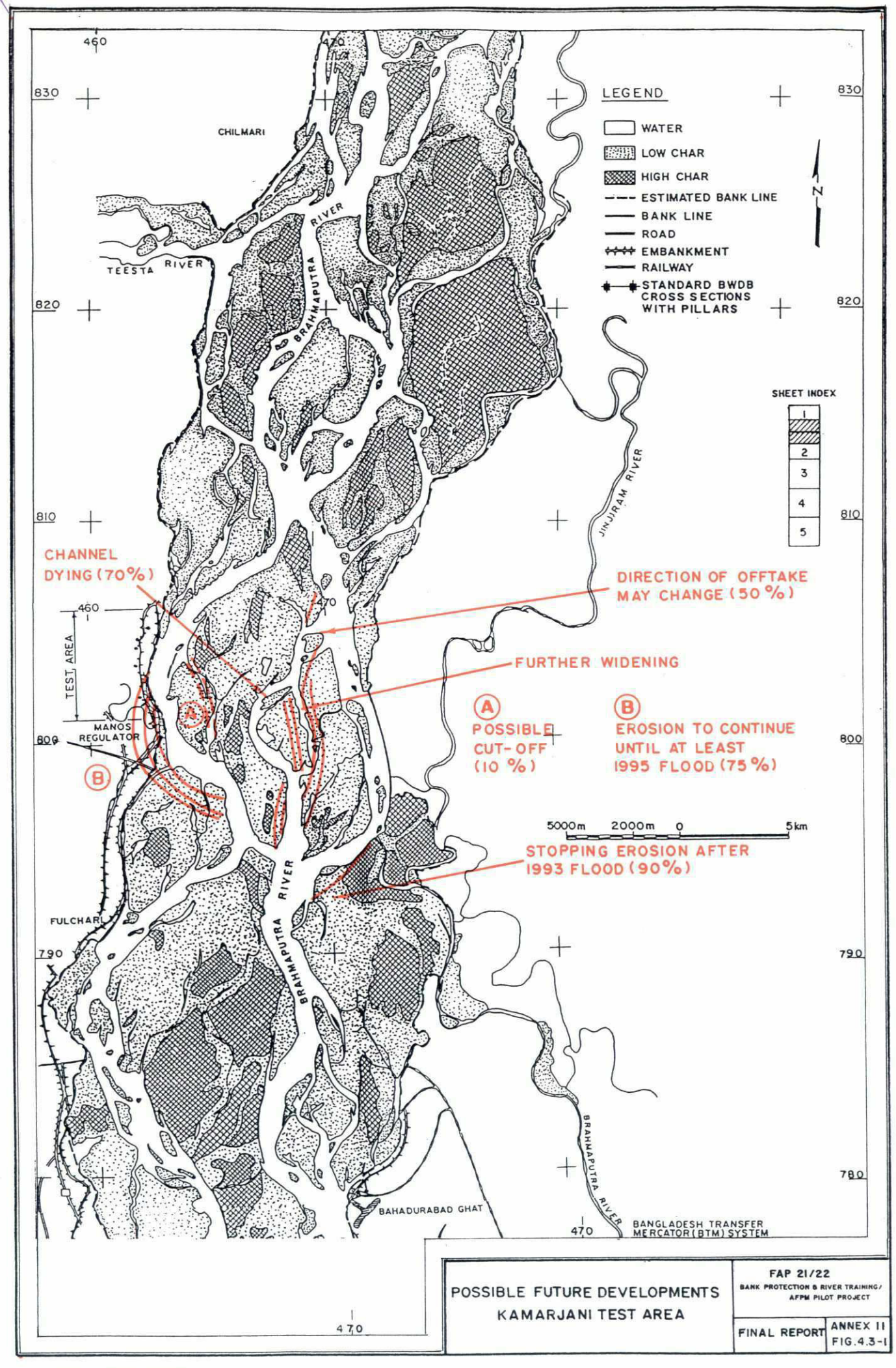
The following observations are made:

(i) In 1992 a mid char channel had developed that acts as a cut-off channel for the Eastern channel near Kamarjani. If this channel develops further the possibility exists that this channel is going to attract more water at the expense of the western channel. This may especially be the case if the minor channel west of the cut-off channel would be abandoned. Larger channels usually have smaller slopes, hence they tend to attract more water in a braided system.

(ii) The cut-off channel has only a good probability to remain in existence if the direction of the offtake changes slightly. It is expected (at a 90 % probability level) that the cut-off channel will continue to widen over the coming years. The curved pattern may induce the formation of a bend opposite to Kamarjani in due time.

(iii) Near Kamarjani two possible cut-offs can be identified. The probability that they will develop into a real cut-off is estimated to be very low because of the angle of the offtakes from the main stream direction.

Hence it is concluded that with a 75 % probability the bank erosion near Kamarjani will continue at least until 1995. The rate of bank erosion at the Kamarjani site for the period 1992-1995 is also indicated in Fig. 4.3-1. It is felt that this rate will hardly decelerate. As a consequence it may be expected that the Manos regulator will be eroded away before a test structure can be built. Developments after 1995 are increasingly difficult to predict, but it is estimated that the bank erosion will still continue, although probably at a slightly lesser rate.



POSSIBLE FUTURE DEVELOPMENTS
KAMARJANI TEST AREA

FAP 21/22
BANK PROTECTION & RIVER TRAINING/ AFPM PILOT PROJECT

FINAL REPORT | ANNEX 11 FIG.4.3-1

4.3.3 Bahadurabad

Bahadurabad lies on the left bank of the Jamuna river at latitude 25°09'. Cross-sections of this area are coded J-14. In 1973, there was only one main channel here. It had a strong meandering twist at about 10 to 15 km upstream of Bahadurabad ghat, outflanking into the left bank of the Jamuna. The river became more braided in the following years. Severe bank erosion had occurred upstream of Bahadurabad in 1976 as a combination of channel migration and widening associated with char formation. This bank erosion produced an embayment just upstream of Bahadurabad ghat. In 1984 a more orderly planform had appeared, mainly consisting of two anabranches on either side of an elongated island. These anabranches persisted from then to 1992. Since 1990, an important channel has been impinging on the bank south of Bahadurabad ghat, whereas the embayment which was formed between 1973 and 1976 silted up. The change-detection images of 1989-1991 and 1991-1992 show a continuation of this trend which can be expected to persist during the next two years. The bank downstream of Bahadurabad ghat seems therefore a most suitable area for bank protection test structures.

A cyclic repetition of channel patterns at Bahadurabad could not be detected from the images. Rather, the impression of widening prevailed. A return to a course which had been abandoned previously could not be recognized in the immediate vicinity of Bahadurabad. The channel approach offers the best base for predictions here.

Based on the 1992 planform derived from the 1992 image and changes over the period 1989-1992 (see also Fig. 2.2-2 of the main report) an assessment was made of possible future developments at the Bahadurabad test area. The results of the assessment are presented in Fig. 4.3-2.

The following observations are made:

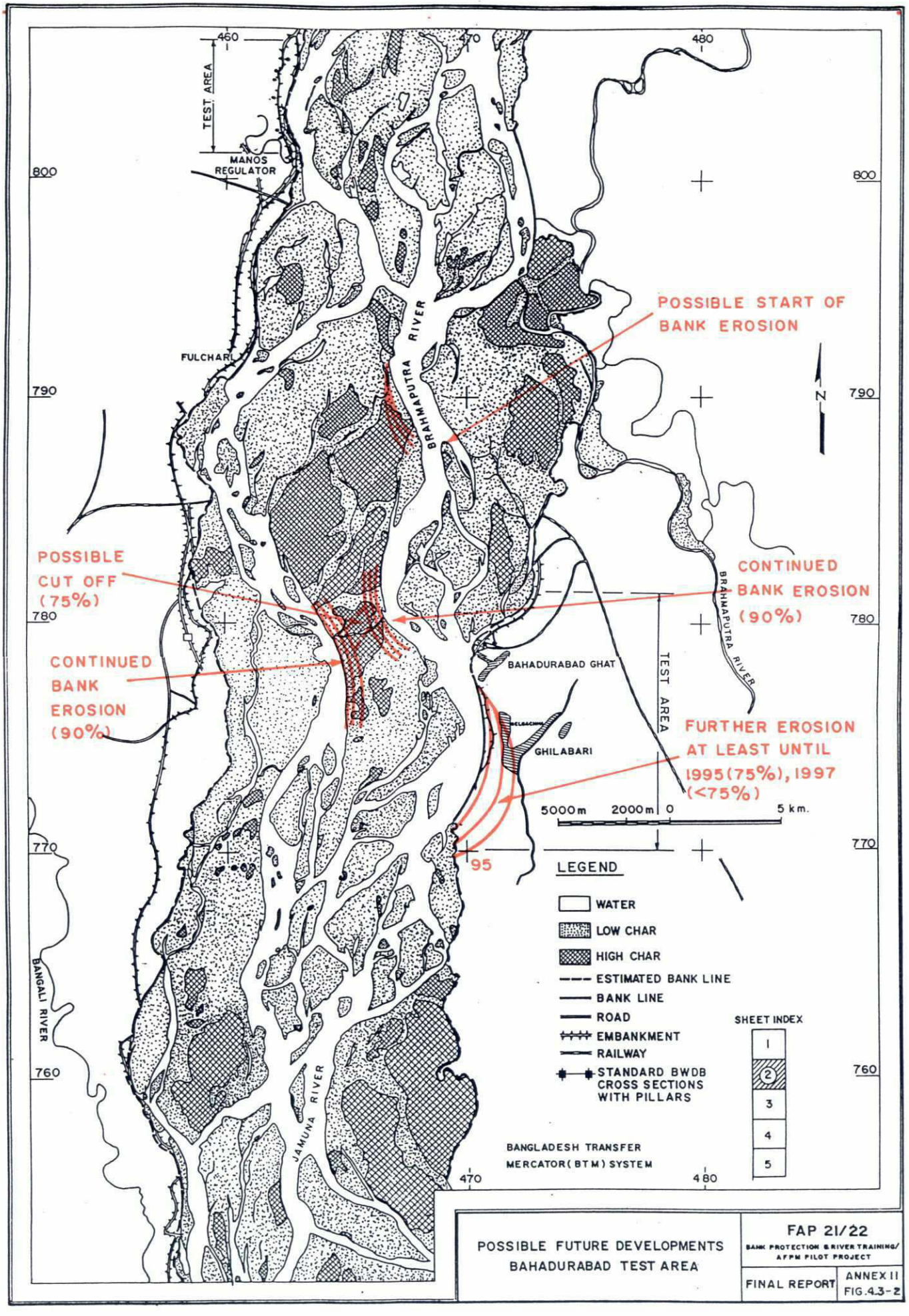
(i) Upstream of Bahadurabad two channels are present that have developed fair bends. One channel is located at in the eastern channel system and is in fact the main reason for the erosion downstream of Bahadurabad. The other channel is more connected to a system of mid char channels and bars.

(ii) It is expected that both channels will continue to erode, hence increasing the probability of a short-cut to develop in time, see Fig. 4.3-2. It is estimated that such a short-cut will have taken place in 1995 with a 75 % of probability.

(iii) In the past channels have existed at the possible future location of this short-cut and all of them carried water form the eastern reaches of the river to the western reaches.

(iv) If such a development would occur it would gradually reduce the rate of erosion south of Bahadurabad ghat.

The probability of continuing bank erosion at Bahadurabad is estimated at 75 % in 1995 and less than that for the years to come.


460
470
480
800
790
780
770
760
TEST AREA
MANOS REGULATOR
FULCHARI
BRAHMAPUTRA RIVER
POSSIBLE START OF BANK EROSION
N
POSSIBLE CUT OFF (75%)
CONTINUED BANK EROSION (90%)
CONTINUED BANK EROSION (90%)
BRAHMAPUTRA RIVER
BAHADURABAD GHAT
TEST AREA
GHILABARI
FURTHER EROSION AT LEAST UNTIL 1995(75%), 1997 (<75%)
5000m 2000m 0 5 km.
95
BANGALI RIVER
JAMUNA RIVER
LEGEND
WATER
LOW CHAR
HIGH CHAR
ESTIMATED BANK LINE
BANK LINE
ROAD
EMBANKMENT
RAILWAY
STANDARD BWDB CROSS SECTIONS WITH PILLARS
SHEET INDEX
1
2
3
4
5
BANGLADESH TRANSFER MERCATOR(BTM) SYSTEM
POSSIBLE FUTURE DEVELOPMENTS BAHADURABAD TEST AREA
FAP 21/22
BANK PROTECTION & RIVER TRAINING/ AFPM PILOT PROJECT
FINAL REPORT
ANNEX II FIG.4.3-2

4.3.4 Chandanbaisa

Chandanbaisa is situated on the right bank of the Jamuna river at latitude 24°48'. Its cross-section is coded J-11. Throughout the years, two anabranches can be identified here. In 1973, both anabranches lay far from Chandanbaisa, but in 1976 a bend had already migrated to the vicinity of this town. The two anabranches had considerably shifted westward in 1984. As a result, a relatively wide and braided anabranch aligned the right bank near Chandanbaisa from 1984 to 1991. Bars propagating through this anabranch exposed and protected the bank at Chandanbaisa alternately, thus offering favourable conditions for building test river training structures. In 1991, however, substantial sedimentation had occurred along the whole stretch of the bank. Char fragments grown together downstream of Chandanbaisa deflect the main flow thread eastward. Upstream of Chandanbaisa, a channel which dissects the medial char seems to gain importance. If this trend continues, then the main body of the flow will impinge on the bank upstream of Chandanbaisa, thus causing significant bank erosion. This trend cannot be counted upon too surely, though, so that the certainty-of-attack criterion is not satisfied very well here.

A cyclic repetition of channel patterns at Chandanbaisa could not be detected from the images. Again, the impression of widening and increased braiding prevailed. A comparison of the southern images from 1973 and 1989 offers an impressive illustration of this trend. A return to a preferred course could not be found in the immediate vicinity of Chandanbaisa.

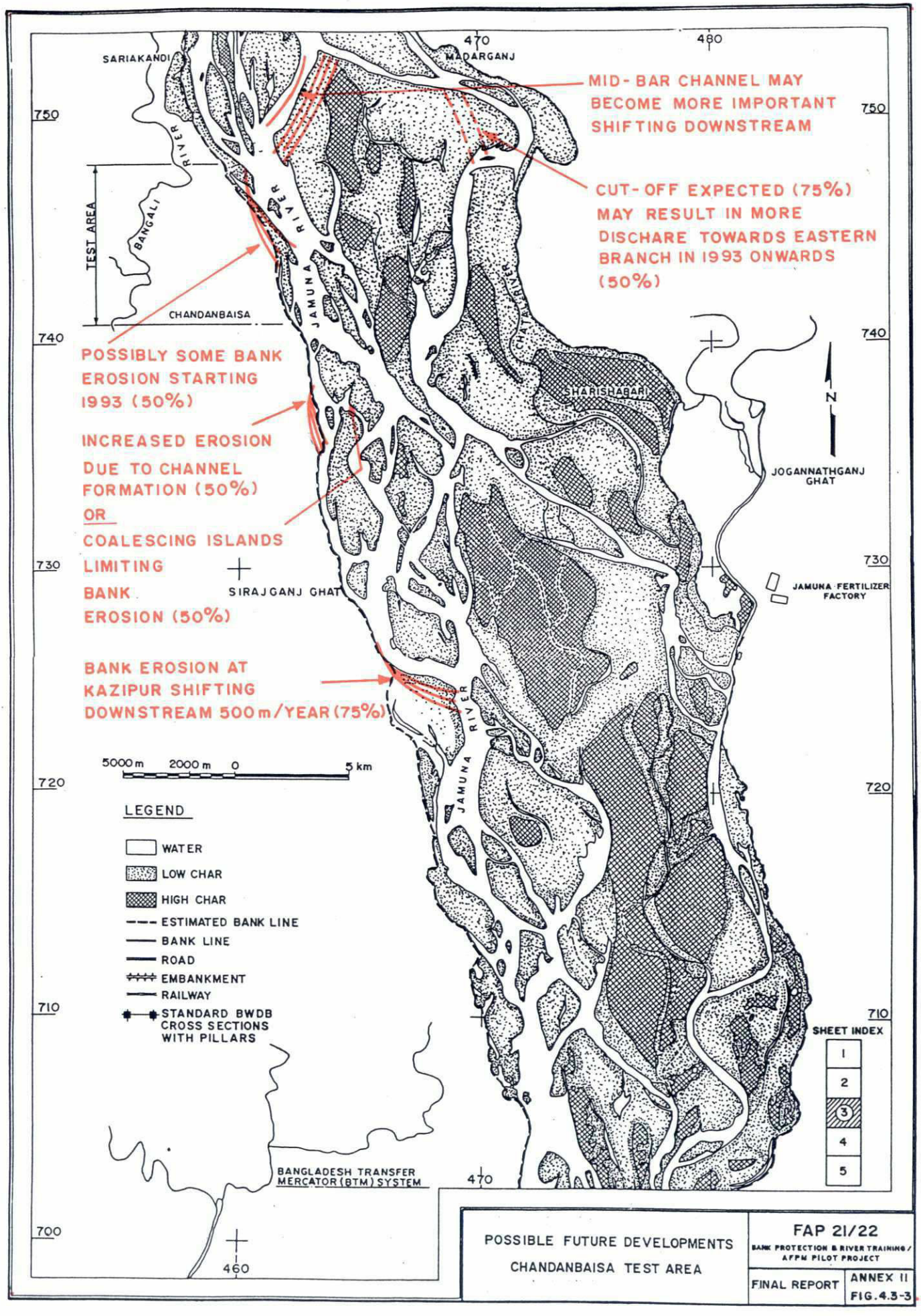
The sedimentation and char growth in this area can be understood best from the perspective of the bar approach, but the channel approach is the best base for a prediction of bank erosion upstream of Chandanbaisa. It should be noted that char erosion might even occur in a period in between the dates of two consecutive images which show char accretion. It is possible that scour occurs during the flood, after which substantial deposition takes place during the falling stage of the hydrograph.

Based on the 1992 planform derived from the 1992 image and changes over the period 1991-1992 (see also Fig. 2.2-3 of the main report) an assessment was made of possible future developments at the Chandanbaisa test area. The results of the assessment are presented in Fig. 4.3-3

The following observations are made:

(i) At present most of the discharge is passing along the western side of the river. The bend near Madarganj on the left side will probably be cut off in 1992 or 1993. The possibility exists (50 %) that this will induce the flow to shift gradually from the western bank to the eastern bank.

(ii) A mid-bar channel upstream of Chandanbaisa seems to gain importance. Because it is directed towards the western bank this channel may induce bank erosion in the test area.


SARIAKANDI
MADARGANJ
470
480
750
740
730
720
710
700
460
MID-BAR CHANNEL MAY BECOME MORE IMPORTANT SHIFTING DOWNSTREAM
CUT-OFF EXPECTED (75%) MAY RESULT IN MORE DISCHARE TOWARDS EASTERN BRANCH IN 1993 ONWARDS (50%)
POSSIBLY SOME BANK EROSION STARTING 1993 (50%)
INCREASED EROSION DUE TO CHANNEL FORMATION (50%) OR COALESCING ISLANDS LIMITING BANK EROSION (50%)
BANK EROSION AT KAZIPUR SHIFTING DOWNSTREAM 500 m/YEAR (75%)
TEST AREA
BANGALI RIVER
JAMUNA RIVER
CHATAL RIVER
CHANDANBAISA
SIRAJGANJ GHAT
SHARISHABARI
JOGANNATHGANJ GHAT
JAMUNA FERTILIZER FACTORY
N
5000 m 2000 m 0 5 km
LEGEND
WATER
LOW CHAR
HIGH CHAR
ESTIMATED BANK LINE
BANK LINE
ROAD
EMBANKMENT
RAILWAY
STANDARD BWDB CROSS SECTIONS WITH PILLARS
SHEET INDEX
1
2
3
4
5
BANGLADESH TRANSFER MERCATOR (BTM) SYSTEM
POSSIBLE FUTURE DEVELOPMENTS
CHANDANBAISA TEST AREA
FAP 21/22
BANK PROTECTION & RIVER TRAINING / AFPM PILOT PROJECT
FINAL REPORT
ANNEX II
FIG. 4.3-3

(iii) More downstream there will probably be no bank erosion owing to the coalescing islands formation mentioned before.

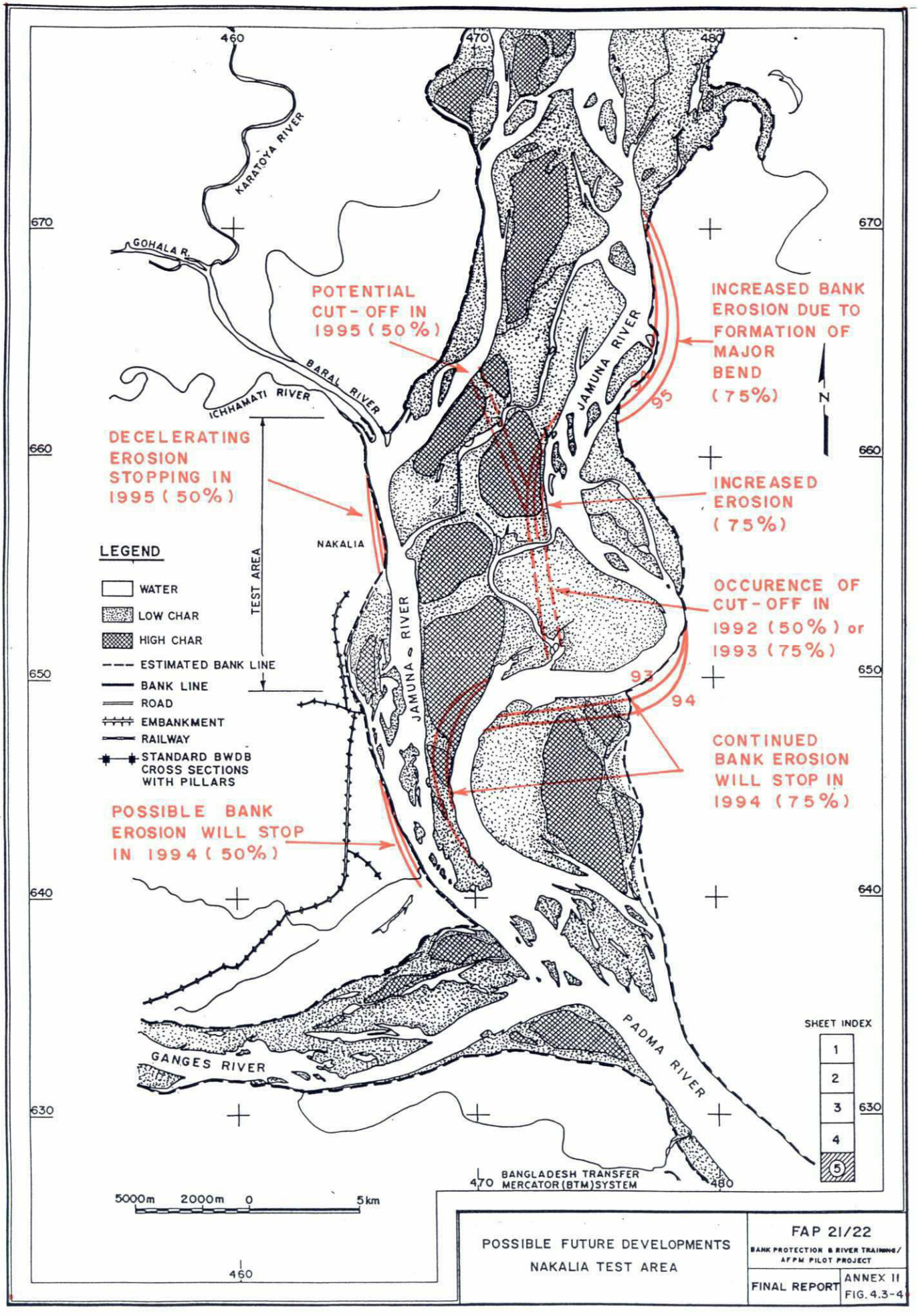
The possibility of bank erosion starting in 1993 is estimated to be about 50 %.

4.3.5 Nakalia

Nakalia lies on the right bank of the Jamuna river at latitude 24°01'. Cross-sections of this area are coded J-3. Downstream of Sirajganj, the Jamuna river is less braided and tends to assume a meandering planform. Despite the presence of chars and secondary channels, the main flow thread can easily be identified. In 1973, the river bifurcated near Nakalia around a char of less than 20 sq.km. This char grew later into a more stable, vegetated island, with two anabranches on either side of it. Further growth shifted the bifurcation point about 15 km upstream into the vicinity of Betil. From 1973 to 1984 the western anabranch was dominant. Severe bank erosion near Nakalia created an embayment in this period. In 1991 and 1992, however, the eastern anabranch became more important, and the embayment formed previously was filled with sediment. The 1989-1991 and 1991-1992 change-detection images show that the erosion is less than about 300 m per year. Meanwhile, the eastern channel between Chauhali and Aricha became much more active, and it is suggested to consider a test area along the left bank as an alternative. When doing so, one should anticipate the cut-off of the large bend which is likely to occur within two years. This alternative meets the preference expressed in the Terms of Reference for test sites on the left bank. Another option is that the test area is maintained on the right bank near Nakalia, with an additional guiding structure on the left bank to deflect the main flow thread to the west. This additional structure could be upstream of the present bifurcation in the area of Betil, or (better) further downstream, forcing channel creation through the island. For the latter option, the meandering planform of 1978 can serve as a guideline. It has a regular shape complying with the natural characteristics of the river.

A cyclic repetition of channel patterns at Nakalia could not be detected from the images. One might expect otherwise because the river is meandering here. It should be noted, however, that the wave length decreased. In 1978 and 1984 there were only five half-meanders between Sirajganj and the confluence with the Ganges, whereas there are six half-meanders in 1992. The decrease of wave length can be explained from a decrease of discharge, because in 1992 part of the discharge is conveyed by the western anabranch.

Again, significant widening occurred. The widening is such that the river between Sirajganj and the confluence with the Ganges might even loose the meandering appearance and become a fully braided river. A comparison of the southern images of 1973 and 1989 strongly suggests this possibility. A return to a course which had been abandoned previously could not be detected. The most appropriate base for predictions here is the channel approach.


460
470
480
670
660
650
640
630
KARATOYA RIVER
GOHALA R.
ICHHAMATI RIVER
BARAL RIVER
JAMUNA RIVER
POTENTIAL CUT-OFF IN 1995 (50%)
INCREASED BANK EROSION DUE TO FORMATION OF MAJOR BEND (75%)
95
N
DECELERATING EROSION STOPPING IN 1995 (50%)
INCREASED EROSION (75%)
NAKALIA
TEST AREA
OCCURENCE OF CUT-OFF IN 1992 (50%) or 1993 (75%)
93
94
CONTINUED BANK EROSION WILL STOP IN 1994 (75%)
POSSIBLE BANK EROSION WILL STOP IN 1994 (50%)
LEGEND
WATER
LOW CHAR
HIGH CHAR
ESTIMATED BANK LINE
BANK LINE
ROAD
EMBANKMENT
RAILWAY
STANDARD BWDB CROSS SECTIONS WITH PILLARS
SHEET INDEX
1
2
3
4
5
PADMA RIVER
GANGES RIVER
BANGLADESH TRANSFER MERCATOR (BTM) SYSTEM
5000m 2000m 0 5km
POSSIBLE FUTURE DEVELOPMENTS
NAKALIA TEST AREA
FAP 21/22
BANK PROTECTION & RIVER TRAINING / AFPM PILOT PROJECT
FINAL REPORT
ANNEX II
FIG. 4.3-4

Based on the 1992 planform derived from the 1992 image and changes over the period 1991-1992 (see also Fig. 2.2-4 of the main report) an assessment was made of possible future developments at the Nakalia test area. The results of the assessment are presented in Fig. 4.3-4.

The following observations are made:

(i) At present, a large bend exists opposite and slightly downstream that will experience a cut-off shortly. The probability that this cut-off will occur in 1992 is about 50 % and that it will have materialized in 1993 is 75 %.

(ii) Upstream of this bend there is another bend which is supposed to develop over the coming years.

(iii) This will trigger accelerated bank erosion just upstream of the cut-off discussed under (i). The effect of this bank erosion will be that the probability of a cut-off upstream will increase, see Fig. 4.3-4. This may lead to a reduction of the discharge in the western channel and hence a reduction of the bank erosion rate at Nakalia.

(iv) Another development may also influence the relative importance of the western channel. The eastern channel may gain importance due to the cut-off foreseen and the related movement of the bend in upstream direction. This may cause this channel to draw more water and this may result in a decrease of the bank erosion near Nakalia.

Based on the above observations, it is expected that the bank erosion at Nakalia will continue to reduce and may stop (with a 50 % probability) in 1994.

4.3.6 Other Possible Areas

It is clear form the previous subsection that the certainty-of-attack criterion is nowhere fully fulfilled at the four pre-selected test areas discussed above. Hence the Consultant has studied the recent developments in the river system to identify other areas which might have a larger probability of being attacked from 1994 onwards. The following are the observations of the other areas those have been reviewed:

(i) Right bank near Kazipur

At present there is an important migrating bend in this area. It is expected with a 75 % probability that this bend will continue to erode near Kazipur.

(ii) Left bank opposite to Kamarjani

The eastern anabranch is becoming more important here, conform Section 2.1, and attacks the left bank. However, present estimates are that this bank erosion will reduce or possibly even stop after the 1993 flood.

(iii) Left bank at Jamuna Bridge

Severe erosion occurs along the left bank at the proposed site of the Jamuna Bridge. Considering the river planform, this bank erosion can be expected to continue, unless a cut-off along the Western bank would develop.

(iv) Left bank between Chauhali and Aricha

This alternative has been discussed in Subsection 4.3.5. It seems worthwhile to keep this possible location in mind and to verify the developments at that location after the 1992 flood.

4.4 CONCLUSION AND RECOMMENDATIONS

At **Kamarjani** and the Manos regulator, the severe bank erosion after 1984 was related to the formation of a large island which deflected its anabranches outward. The corresponding migration rate may decrease in future, but substantial bank erosion will continue (at a 75 % probability level) until at least 1995.

The change-detection images of 1989-1991 and 1991-1992 show a continuation of bank erosion South of **Bahadurabad ghat** due to the impingement of a channel from upstream. In view of the present geometry of the area, this can be expected to continue during the next two years. The bank downstream of Bahadurabad ghat seems therefore a suitable area for bank protection test structures. Future developments may cause that the bank erosion rate to reduce after 1995.

Substantial sedimentation is occurring along the bank near **Chandanbaisa**. Chars in the downstream deflect the main flow thread to the east. It is plausible that the bank upstream of Chandanbaisa will erode in the near future, but the possibility for this does not satisfy the certainty-of-attack criterion very well.

Bank erosion at **Nakalia** appears to slow down. However, the eastern anabranch along the opposite bank is much more active, and it is suggested to consider a test area there as an alternative. When doing so, one should anticipate the cut-off of the large bend which is likely to occur within two years.

Neither cyclicity nor path preference could be seen in the channel patterns at the pre-selected sites. The overall widening is a much more striking phenomenon. This widening might have far reaching consequences for the reach between Sirajganj and the confluence with the Ganges, because the river might loose its meandering appearance and become fully braided here. A comparison of the southern images of 1973 and 1989 strongly suggests this possibility. An alternative explanation is that the river downstream of Sirajganj changes alternatively between more meandering and more braiding. More studies are needed to elucidate this aspect.

5 CONCLUSIONS

This chapter summarizes the most important conclusions of this report. The multiple-year composites seem to be valuable tools in visualizing the long term dynamics of the Jamuna river. Especially the number of water occurrences image has great engineering value. It shows the stable river sites, preferred river courses and stable chars. The latter are very rare. The existence of meta-stable islands, with a life-time of more than thirty years, as introduced by the FAP 1 study is not supported by the present survey. Both composites are believed to contain enough information to justify further analysis.

The relation between bank erosion and radius of curvature was thoroughly studied in the present report. The existing relations for the Jamuna, as found by Masselink (1989), were tried to be improved. This was done by introducing width in the relations, for example as a width to depth ratio. These results were not very promising, so a new method was applied.

The variation of the radius of curvature through the bend was introduced. A so called effective radius of curvature, in which part of the upstream curvature was included, was calculated by a computer program. Some bends that showed a similar planform over a number of years were selected. Of these bends the migration of the channel centre line was obtained at a number of coordinates. This migration was compared to the effective radius of curvature calculated for the same coordinates. Most of the individual bends showed a similar migration-effective radius relation. This relation is similar to the one found by Nanson and Hickin (1983). When the individual relations are plotted in one graph it becomes clear that the individual relations have limited general value.

For one bend a special investigation was done. A cyclic behaviour was discovered for the migration-effective radius of curvature relation through time. The coordinates in this bend showed, over a four-year period, alternately increasing and decreasing values for both migration and width. This specific study has limited value, since only one bend was investigated. However analysis has come out with some interesting trend and further research could be valuable.

Special attention in this report was given to bifurcations, these are locations in the river where water and sediment are divided. Most bifurcations disappeared, on the average after approximately three years. The study points out some important parameters in the abandonment process. Especially the deviation angle, the angle between upstream and bifurcated channel direction, seems important. When this angle gets larger than approximately 40°, a probability on abandonment arises that increases with increasing deviation angle. Asymmetry also appears to be important in the abandonment process. This holds especially for the degree of angle asymmetry.

A position on the inner side of a bend seems to increase the probability on abandonment of the bifurcated channel. This is supposedly caused by the sediment transport, which is directed

towards inner bends. Channels that are situated in straight reaches, cross-over reaches or on the outer side of a bend seem to be more stable. Bifurcated channels situated on the outer side of a bend apparently only abandon when they have a high deviation angle with the upstream channel.

The changes in width of the bifurcated channels were also investigated. The same planform parameters that influenced abandonment, were thought to affect changes in channel width. This could, however, hardly be proved with the present survey. The process of change in channel width seems more complex than the abandonment process.

Incorporation of depth parameter to this analysis could perhaps improve the results. A decrease of conveyance probably expresses itself through shallowing rather than narrowing. This would again support the view that sedimentation is the most important process in abandonment.

Bifurcations show both upstream and downstream migration. Upstream migration is almost only found with asymmetric bifurcations. Symmetric bifurcations normally show downstream migration.

REFERENCES

REFERENCES

AUTHOR/DATE	TITLE/PUBLISHER
Benson, M.A., (1965)	Spurious Correlation in Hydraulics and Hydrology, Journal of the Hydraulics Division, American Society of Civil Engineers, Vol. 91, HY 4
Coleman, J.M., (1969)	Brahmaputra River Channel Processes and Sedimentation, Sedimentary Geology Vol.3
Jonge, Z. de, (1988)	Image Processing: A Methodology Production of Statical and Dynamical Image Colour Composites of the Jamuna River in Bangladesh, State University Utrecht (Dept. of Physical Geography), The Netherlands/Delft Hydraulics
Klaassen, G.J. and Masselink, G., (1992)	Planform Changes of a Braided River with Fine Sand as Bed and Bank Material, Paper Presented During 5th International Symposium on River Sedimentation, Karlsruhe, Germany
Klaassen, G.J. and Zanten, B.H.J. van, (1989)	On Cut-off Ratios of Curved Channels, Paper Presented During XXIIIth IAHR Congress, Ottawa, Canada/Publication No. 444, Delft Hydraulics
Klaassen, G.J. and Vermeer, K., (1988)	Channel Characteristics of the Jamuna River, Bangladesh, Paper Presented During International Conference on River Regime, Wallingford, England
Leopold, L.B. et al., (1964)	Fluvial Processes in Geomorphology, Freeman, San Francisco
Masselink, G., (1989)	Morphological Processes in the Jamuna River, a Study Based on Landsat Images and Cross-Sectional Data, State University Utrecht (Dept. of Physical Geography), Netherlands/Delft Hydraulics

AUTHOR/DATE	TITLE/PUBLISHER
Nanson, G.C. and Hickin, E.J., (1983)	Channel Migration and Incision on the Beatton River, Journal of the Hydraulics Division, American Society of Civil Engineers, Vol. 109, No. 3
Noorbergen, H.H.S., (1989)	Multitemporal Analysis of a Braiding River, Technical Publication TP 89235 L, National Aerospace Laboratory (NLR), The Netherlands
Sir William Halcrow & Partners Ltd., (1991)	River Training Studies of the Brahmaputra River, Second Interim Report, Technical Annex 4, Morphological Studies.
Thijsse, J. Th., (1964)	Report on the Hydrology of East Pakistan, for the Planning Board of the Government of East Pakistan

APPENDICES

APPENDIX 1

LIST OF AVAILABLE MATERIAL

(NOT QUOTED IN THIS REPORT)

APPENDIX 1

LIST OF AVAILABLE MATERIAL

(NOT QUOTED IN THIS REPORT)

GEOLOGY

World Bank, (1985)	Geology and Ground Water Resources of Bangladesh, A Study for the World Bank South Asia Region, P.H. Jones Hydrogeology Inc., Baton Rouge, Louisiana
Khan, F.H., (1991)	Geology of Bangladesh, University Press, Dhaka
Ministry of Irrigation, Water Development and Flood Control, (1987),	Geology of Bangladesh, Master Plan Organization Technical Report No.4
Ministry of Energy and Mineral Resources, (1990)	Geological Map of Bangladesh, Geological Survey of Bangladesh, Dhaka
Morgan, J.P. and McIntire, W.G., (1959)	Quaternary Geology of the Bengal Basin, East Pakistan and India: Geological Society of America Bulletin, Vol. 70

TOPOGRAPHY

University of Dhaka, (1981),	Bangladesh in Maps
Burrard, Col. S.G., (1911/1914),	3 Maps Covering Complete Jamuna, Surveyed (1848/1875) with Corrections to (1911/1913), Based on Maps of Walker (1866), Scale 1:253,440
LaTouche, T.H.D., (1910)	The Journals of Major James Rennell (1764 to 1767), the Asiatic Society, Calcutta Incl. Map of Bengal and Bahar (Area Comparable to Bangladesh), Approx. Scale 1:1,300,000

Rennel, J., (1765) — A General Map of the River Brahmaputra, 5 Maps Covering the Brahmaputra River's Old Course from the Meghna Confluence to Deep in Assam (India), Approx. Scale 1:130,000, 1917 Reproduction, 1992 Quality Copy on Photographic Paper

Various Maps, (1914-1967) — 17 Maps, Mostly of the Sirajganj Area, Some do not Show the Jamuna River, Scales 1:50,000 to 1:250,000, All Xeroxes

Walker, J., (1866) — Indian Atlas Sheets 118 and 119, Covering North Part of the Jamuna River, Approx. Scale 1:250,000.

Wilcox, B.N.J., (1828) — Map of the Course of the Brahmaputra, Province of Assam (India), 91°-93° Longitude/ 26°-27° Latitude, Approx. Scale 1:250,000, 1992 Quality Copy on Photographic Paper

MORPHOLOGY/HYDROLOGY

Burger, J.W. et al., (1987) — Bank Erosion and Channel Processes in the Jamuna River, Bangladesh, Paper Presented During River Bank Erosion Symposium, Dhaka, Bangladesh

Chen, G. and Shen, H.W., (1983), — River Curvature-Width Ratio Effect on Shear Stress, River Meandering, Proceedings of ASCE Special Conference on Rivers

China-Bangladesh Joint Expert Team — Study Report on Flood Control and River Training Project on the Brahmaputra River in Bangladesh (1991), Vol.1: Analysis of Hydrology and River Morphology of the Brahmaputra River,

Howard, A.D. and Knutson, T.R., (1984) — Sufficient Conditions for River Meandering: A Simulation Approach, Water Resources Research, Vol. 20, No. 11

Klaassen, G.J. and Vermeer, K., (1988) — Channel Characteristics of the Jamuna River, Bangladesh, Paper Presented During International Conference on River Regime, Wallingford, England

Klaassen, G.J., (1992) — Experience from a Physical Model for a Bridge Across a Braided River with Fine Sand as Bed Material, Paper Presented During 5th International Symposium on River Sedimentation, Karlsruhe, Germany

Reineck, H.E. and Singh, I.B., (1980) — Depositional Sedimentary Environments, 2nd Edition, Springer -Verlag, Berlin

Sir William Halcrow and Partners Ltd. (1991) River Training Studies of the Brahmaputra River, First Interim Report, Technical Annex 2, Hydrology.

Ullah, H., (1987a) Computer Modelling of River Channel Changes in Alluvial Condition, First Interim Report: Analytical Study of Channel Changes of the Brahmaputra, Institute of Flood Control and Drainage Research, Bangladesh University of Engineering and Technology, Dhaka, Bangladesh

Ullah, H., (1987b) Changes of Bed Level and Cross-sectional Area of the Brahmaputra, Paper Presented During 31th Annual Convention of the Institution of Engineers, Khulna, Bangladesh

Williams, P.F. and Rust, B.R., (1969) The Sedimentology of a Braided River, Journal of Sediment, Petrol., Vol. 39, pp. 649-679.

REMOTE SENSING

Buiten, H.J. and Clevers, J.G.P.W. (red), (1990) Remote Sensing, Theorie en Toepassingen van Land Observatie, Pudoc, Wageningen, The Netherlands

RPT,NEDECO and BCL Jamuna Bridge Appraisal Study, Phase II, (1990), Annex 2, Remote Sensing Study,

FINMAP Monitoring the Jamuna River Using Satellite Images, (1991), Report of the Analysis of the Images,

Roque, N., (1983) Application of Remote Sensing Technology for Detecting Fluvial Changes of the Ganges and Brahmaputra-Jamuna River Courses in Bangladesh, University of New Mexico, Albuquerque, USA

Verhoef, W. and Noorbergen, H.H.S., (1988) Change Detection Methods Used in Jamuna River Project, Memorandum RR-88-022 L, National Aerospace Laboratory (NLR), The Netherlands

APPENDIX 2

ACCURACY OF SATELLITE IMAGE STUDY

APPENDIX 2

ACCURACY OF SATELLITE IMAGE STUDY

The following analysis has been carried out by a Z. de Jonge (1988), as part of his traineeship at Delft Hydraulics, which is thought to be relevant background information to the present study and is therefore incorporated here in an unedited version.

Accuracy Analysis of Satellite Image Correction and Interpretation

During correction and interpretation of satellite images errors are bound to occur. For example, while these errors cause horizontal deviations of boundaries between classes, it is necessary to know the mean values of these errors. In Table Ap.2-1 these errors are listed, additionally a 'significance value' is given. This significance value explains when a distance measured in a composite is significant, i.e. not an error but a truly apparent phenomenon, for example erosion. The possible places of occurrence of the errors are: (i) finding co-ordinates on a map, (ii) finding corresponding points in 1977 image, (iii) correcting the other images, (iv) classification, (v) measuring distances in a composite.

(i) Finding Co-ordinates on a Map

As a drawing line is about 0.2 mm wide, exact co-ordinates can never be obtained from a map. For this study two maps were used: 1:50,000 and 1:250,000. On the 1:50,000 map two ground control points were located; the exact co-ordinates can differ up to 10 m from the ones which were found. On the 1:250,000 map five ground control points were located; the exact co-ordinates can differ by 50 m (= 0.2 mm drawing line width) from the ones which were found. Thus an overall mean standard error of $(2 * 10 + 5 * 50)/ 7 \approx 40$ m is probable. A significance value of $2.5 * 40 = 100$ m gives here a probability of 97 %.

(ii) Finding Corresponding Points in the 1977 Image

While locating points in the 1977 image that correspond with the ground control points, errors are made owing to the age of the maps (1955/1957) and the size of the pixels in this image (80 x 80 m). The computer calculated a standard error of 50 m in N/S and E/W directions. So a standard error of $50 * \sqrt{2} \approx 70$ m is probable in NW/SE and NE/SW directions. The resulting mean standard error is $(50 + 70)/ 2 = 60$ m. In this case the significance value is $2.5 * 60 = 150$ m

W.A.R.P.O. LIBRARY DELFT

SATELLITE IMAGE ACCURACY ANALYSIS

Procedure/Problem	Error at	Average Standard Error (in m)		significance value (in m)
- Conversion of 1977-image to map co-ordinates	1:50,000			100
	1:250,000	40		150
	1977 image	60		
- Geometrical correction	other images	35		85
- Comparison at dynamical composites	1977 and other composite two	35		85
	other composites	40		125
- Comparison between composites and maps	1977/1:200.000 map	70		175
	other/1:200.000 map	80		200
- Location of a boundary on a 1977 composite	sand/water	15		40
	vegetation/water	30		75
	bare soil/water	30		75
- Location of a boundary on an other composite	sand/water vegetation/water	40		100
	bare soil/water	45		110
		45		110
- Distance between boundaries at statical composites*	water/sand - water/sand	20		50
	water/sand - water/veg.	35	1977	85
	water/veg. - water veg.	40		100
	water/sand - water/sand	40		100
	water/sand - water/veg.	50	other	125
	water/veg. - water/veg.	55		135
- Distances between boundaries at dynamic composites	water/sand - water/sand	45	1977-	110
	water/sand - water/veg.	45	other	110
	water/veg. - water sand	50		125
	water/veg. - water/veg.	55	other	135
	water/sand - water/sand	55	other	135
	water/veg. - water/veg.	60		150
	water/veg. - water/veg.	65		160

veg. = vegetation

* = in following cases vegetation and bare soil are equivalent

Table Ap.2-1: Image processing procedure with error values

(iii) Correcting the "Other" Images

After the correction of the other images the computed standard error in N/S and E/W direction was, on the average, 30 m. So in NW/SE and NE/SW direction the mean standard error is 40 m. The resulting mean standard error is (30 + 40)/2 = 35 m and therefore, the significance value is 2.5 * 35 $\approx$ 85 m. (Note: "other" images are all images except the one from 1977).

(iv) Classification (1977 image)

a) When considering the classification diagram, it is apparent that there are errors in the boundary regions between the classification clusters. 95 % possibility is there that in the composites only one pixel is wrongly classified at the boundaries between the classes. In most cases one pixel, representing bare soil, can be seen at the boundary sand/water. The exact boundary is in the centre of the pixel, taking into account a standard error (E/W, N/S) of 0.5 * 0.5 * 50 which is less than 15 m. In NW/SE and NE/SW direction the standard error is $< 15\sqrt{2} \approx 20$ m. Therefore, the significance value, in this special case is 40 m.

b) At the boundary vegetation/water either one vegetation pixel or one water pixel too many vegetation/water has been given. At the boundary bare soil/water the same also applies. Therefore, in these two cases a standard error of half a pixel size is for 95 % probable in both N/S and E/W direction; this error is 25 m. In NW/SE and NE/SW directions the standard error is 35 m. The resulting standard error is 30 m, thus giving a significance value of 2.5 * 30 = 75 m.

(v) Measuring Distances in a Composite

Measuring in a composite with scale 1:250,000 results in a standard error of 35 m (probability 97 %) which is due the accuracy of the measurement method.

If the preceding results are combined, the other accuracy values in Table Ap.2-1 can be explained.

The values thus calculated are used for different composite analysis as given in detail hereafter:

Comparison Between Maps and Statical Composites

When comparing a 1:200,000 map and a 1977 composite 1:250,000 the resulting error is $\sqrt{(40^2 + 60^2)} \approx 70$ m. The significance value is 175 m. When comparing a 1:200,000 map and an 'other' composite 1:250,000 the resulting error is $\sqrt{(40^2 + 60^2 + 35^2)} \approx 80$ m. The significance value is 200 m.

Comparing Statical Composites

When comparing a 1977 composite and the 'other' statical composite by means of a dynamical composite, the resulting error is the same as the classification error: 35 m; so the significance value is 85 m too. When comparing two 'other' statical composites by means

of a dynamical composite the resulting error is $\sqrt{(35^2 + 35^2)} \approx 50$ m. The significance value is 125 m. When comparing maps 1:200,000 and dynamical composites the resulting errors are $\sqrt{(40^2 + 60^2 + 35^2)} \approx 80$ m and $\sqrt{(40^2 + 60^2 + 50^2)} \approx 90$ m respectively. The significance values are 200 and 225 m respectively.

Boundary Displacements in Other Composites

By the effects of correction and classification (iii) and (iv) the resulting error in the 'other' statical composites are: a) at the land/water boundary a displacement of $\sqrt{(15^2 + 35^2)} \approx 40$ m with a significance value of 100 m; b) at the water/vegetation and the water/bare soil boundaries a displacement of $\sqrt{(30^2 + 35^2)} \approx 45$ m with a significance value of 110 m.

Distances Between Boundaries in the Statical Composites

Here the composites may be classified as (a) 1977 and (b) other.

(a) When measuring distances between boundaries in the 1977 composite (water/sand, water/vegetation and water/bare soil) three combinations are possible. First, a distance between two water/sand boundaries. There the resulting error is $\sqrt{(15^2 + 15^2)} \approx 20$ m; significance value 50 m. Second, a distance between a water/sand boundary and a water/vegetation or water/bare soil boundary: $\sqrt{(15^2 + 30^2)} \approx 35$ m. The significance value is 85 m. Third, a distance between two water/vegetation or and/or water/bare soil boundaries. The resulting error is $\sqrt{(30^2 + 30^2)} \approx 40$ m and the significance value is 100 m.

(b) When measuring the corresponding distances (see a) the following errors occur. First, $\sqrt{(20^2 + 35^2)} \approx 40$ m; significance value 100 m; Second, $\sqrt{(35^2 + 35^2)} \approx 50$ m; significance value 125 m; Third, $\sqrt{(40^2 + 35^2)} \approx 55$ m; significance value 135 m.

Distance Between Boundaries in the Dynamical Composites

In this discussion (c) stands for 1977/other and (d) for other/other.

(c) When measuring distances between the three already mentioned boundaries four combinations (= calculations) are possible: (i) the distance between two water/sand boundaries: $\sqrt{(15^2 + 40^2)} \approx 45$ m; significance value 115 m, (ii) the distance between a water/sand boundary of the 1977 part of the dynamical composite and a water/vegetation or water/bare soil boundary of the other part of the dynamical composite: $\sqrt{(15^2 + 45^2)} \approx 48$ m: significance value 115 m, (iii) the distance between a water/vegetation or water/bare soil boundary of the 1977 part of the dynamical composite and the water/sand boundary of the other part of the image: $\sqrt{(30^2 + 40^2)} \approx 50$ m; significance value 125 m and (iv) the distance between the water/vegetation and/or water/bare soil boundaries of the 1977 part and the other part of the dynamical composite: $\sqrt{(30^2 + 45^2)} \approx 55$ m; significance value 135 m.

d) When measuring distances between the three boundaries mentioned above in a dynamical composite composed of two other statical composites, then the following calculations should

be used: (i) when a distance between two sand/water boundaries is considered: $\sqrt{(40^2 + 40^2)} \approx 55$ m; significance value 135 m, (ii) when a distance between a water/sand boundary and a water/vegetation or water/bare soil boundary is considered: $\sqrt{(40^2 + 45^2)} \approx 60$ m; significance value 150 m and (iii) when a distance between water/vegetation and/or water/bare soil boundaries is considered: $\sqrt{(45^2 + 45^2)} \approx 65$ m; significance value 160 m. One standard error mentioned above (v) not to be neglected is the measurement error as a result of the measurement accuracy. After having done about 300 measurements a resulting standard error of 35 m was found, with an accuracy 2.5 m (97% probability level). Therefore, when in the second report distances are given, these should be taken into account. As the accuracy varies between 15 and 65 m as far as classification and correction errors are considered, the total accuracy varies between $\sqrt{(15^2 + 35^2)} \approx 40$ and $\sqrt{(65^2 + 35^2)} \approx 75$ m. Thus, the maximum significance value is $2.5 * 75 = 185$ m.

APPENDIX 3

DETERMINATION OF CHANNEL CENTRE CO-ORDINATES

APPENDIX 3

DETERMINATION OF CHANNEL CENTRE CO-ORDINATES

At the National Aerospace Laboratory (NLR) the following steps were taken, in order to derive the necessary input co-ordinates for the Meanplan calculations. This appendix is not a precise manual, but a simplified description of some relevant actions. Therefore some basic knowledge of the Reseda system is needed to understand the co-ordinates which may be described as followes:

(1) The relevant sub area of a single year classified image was loaded with MS (modify sub area). This was done to obtain an image with a decimation factor of 1, which means that no decimation took place.

(2) With the image control device the X and Y axis were changed in such a way that both in the horizontal and vertical direction 100 pixels covered a distance of 10 cm on the screen. The screen scale is then 1:50,000, 100 pixels represent 5,000 m.

(3) The smoothed channel centre line is described with the use of "rubber bands". These are line segments, plotted on the screen, if a starting and end co-ordinate are given. The derivation of the smoothed channel centre line is due to some subjective criteria. An overview of the encountered difficulties and the personal solutions that were applied can be found in the following appendix.

(4) The starting and end co-ordinates of the "rubber bands" were written on paper, a more sophisticated method is not available. These co-ordinates consist of a line and pixel number, these are the Y and X co-ordinate respectively. Finally these co-ordinates were inserted in a Supercalc spreadsheet.

APPENDIX 4

INCLUSION OF INFLUENCE OF UPSTREAM CURVATURE

APPENDIX 4

INCLUSION OF INFLUENCE OF UPSTREAM CURVATURE

In this appendix a short discussion is given on the use and importance of the adaptation length, λ, in the effective radius of curvature calculation. The adaptation length indicates how much of the upstream channel is taken into account.

To study the effect of this adaptation length, the Meanplan calculations were carried out for three different adaptation lengths, for all available reaches. The three different adaptation lengths were; 0 m, 5,000 m and 10,000 m (0 m thus only indicating local curvature). The calculated radii were used for constructing relative migration versus relative radius plots. Both the first and second year related migration were used. These graphs can be found in this appendix.

When studying these graphs the following observations come about:

- the 5,000 m and 10,000 m adaptation length give approximately the same results, 10,000 m seems to give slightly lower, highest values;
- the use of $\lambda = 0$ m results in more extreme graphs; very high or very low radii (as in Bend 2, reach 2, related to first year planform), or dense scatter clouds (same reach, related to second year planform);
- graphs that make use of the 5,000 m or 10,000 m adaptation length have a more moderate appearance; less extreme radii, dense cloud are stretched, and
- the individual $\lambda = 5{,}000$ m or 10,000 m graphs do show similar shapes.

Note however that when the migration is related to the first or second year curvature a substantial difference in graph appearance arises.

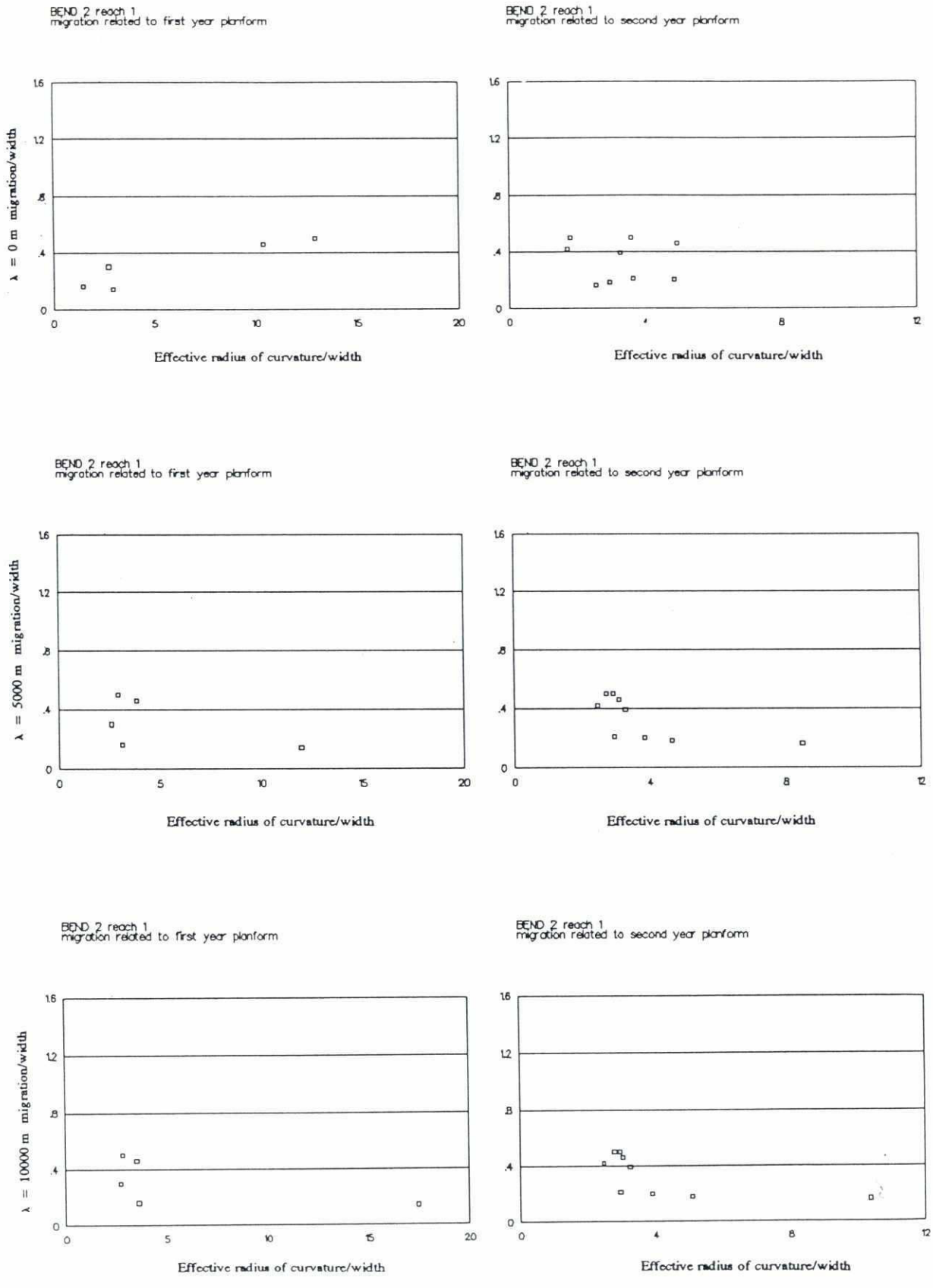


Fig. Ap.4-1: Improved bank erosion analysis migration-effective radius of curvature graphs

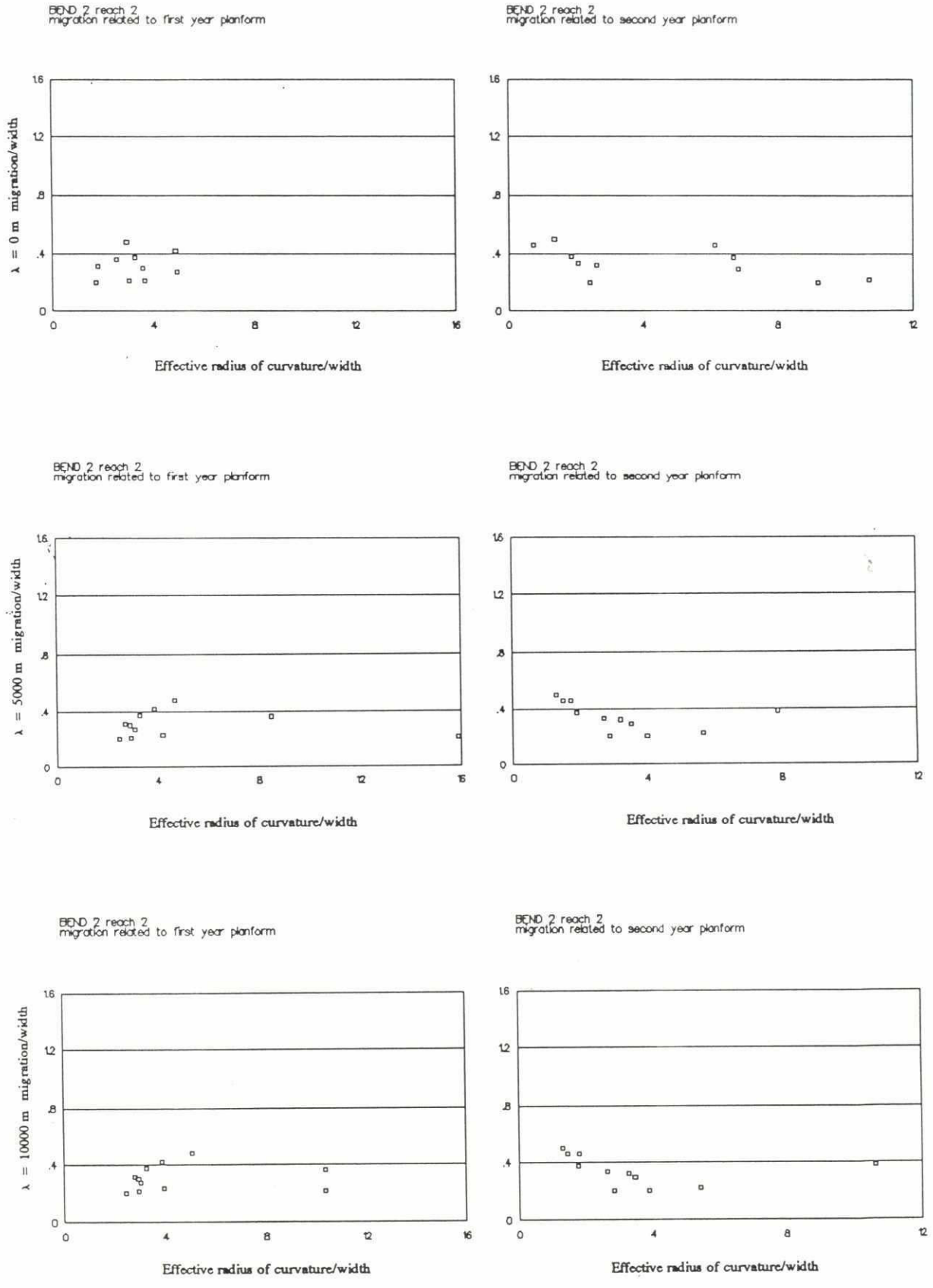


Fig. Ap.4-2: Improved bank erosion analysis migration-effective radius of curvature graphs

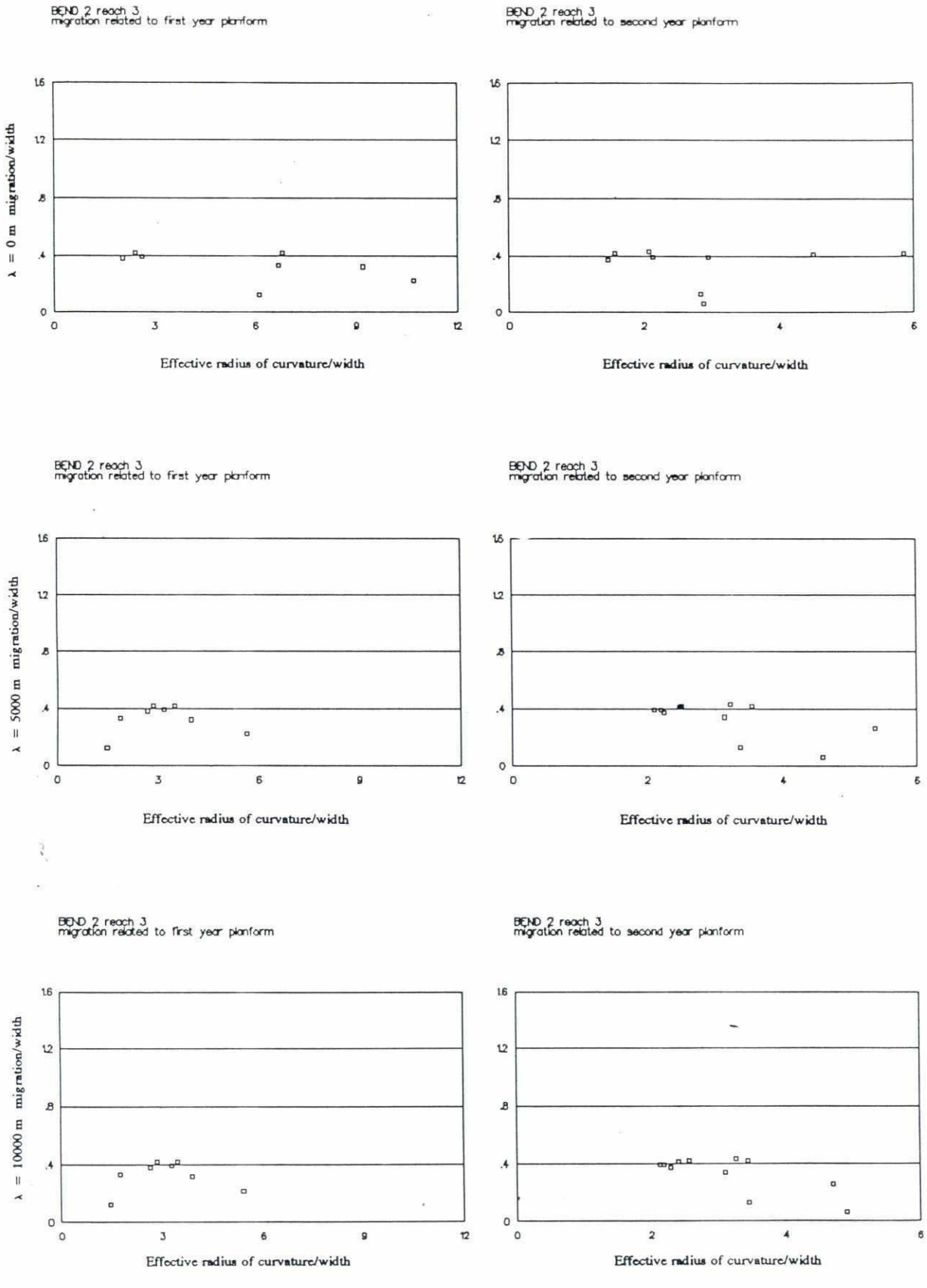


Fig. Ap.4-3: Improved bank erosion analysis migration-effective radius of curvature graphs

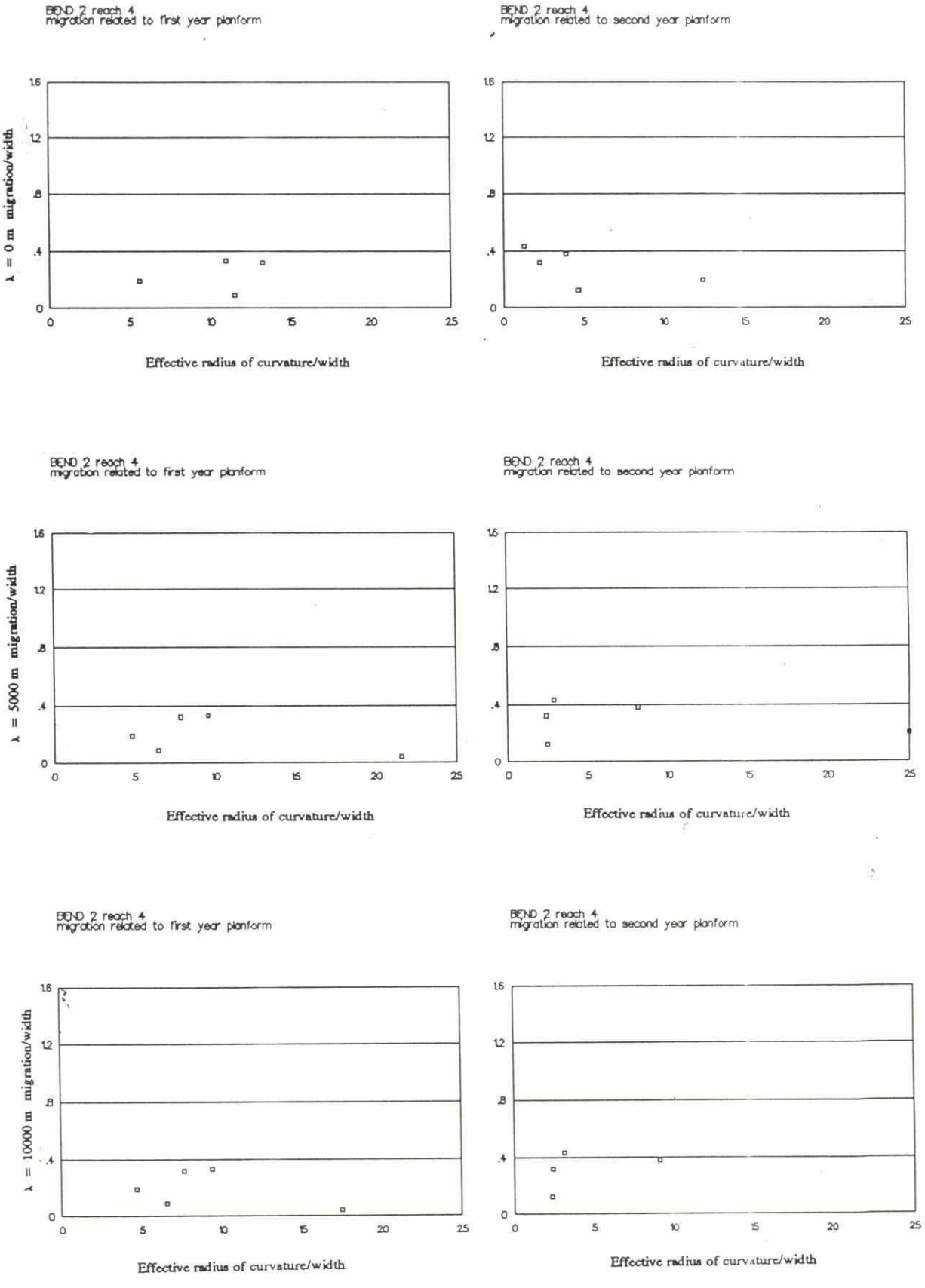


Fig. Ap.4-4: Improved bank erosion analysis migration-effective radius of curvature graphs

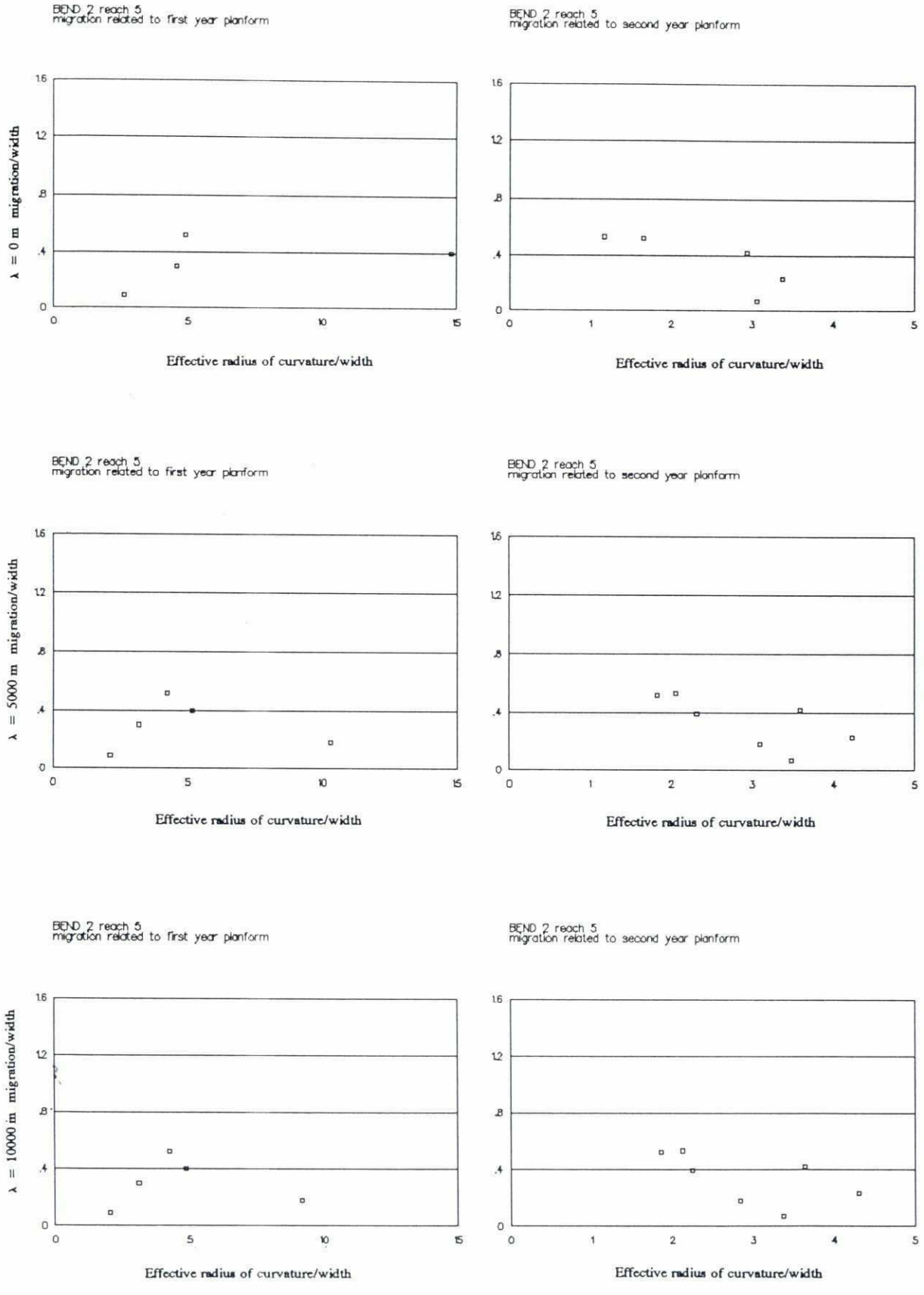


Fig. Ap.4-5: Improved bank erosion analysis migration-effective radius of curvature graphs

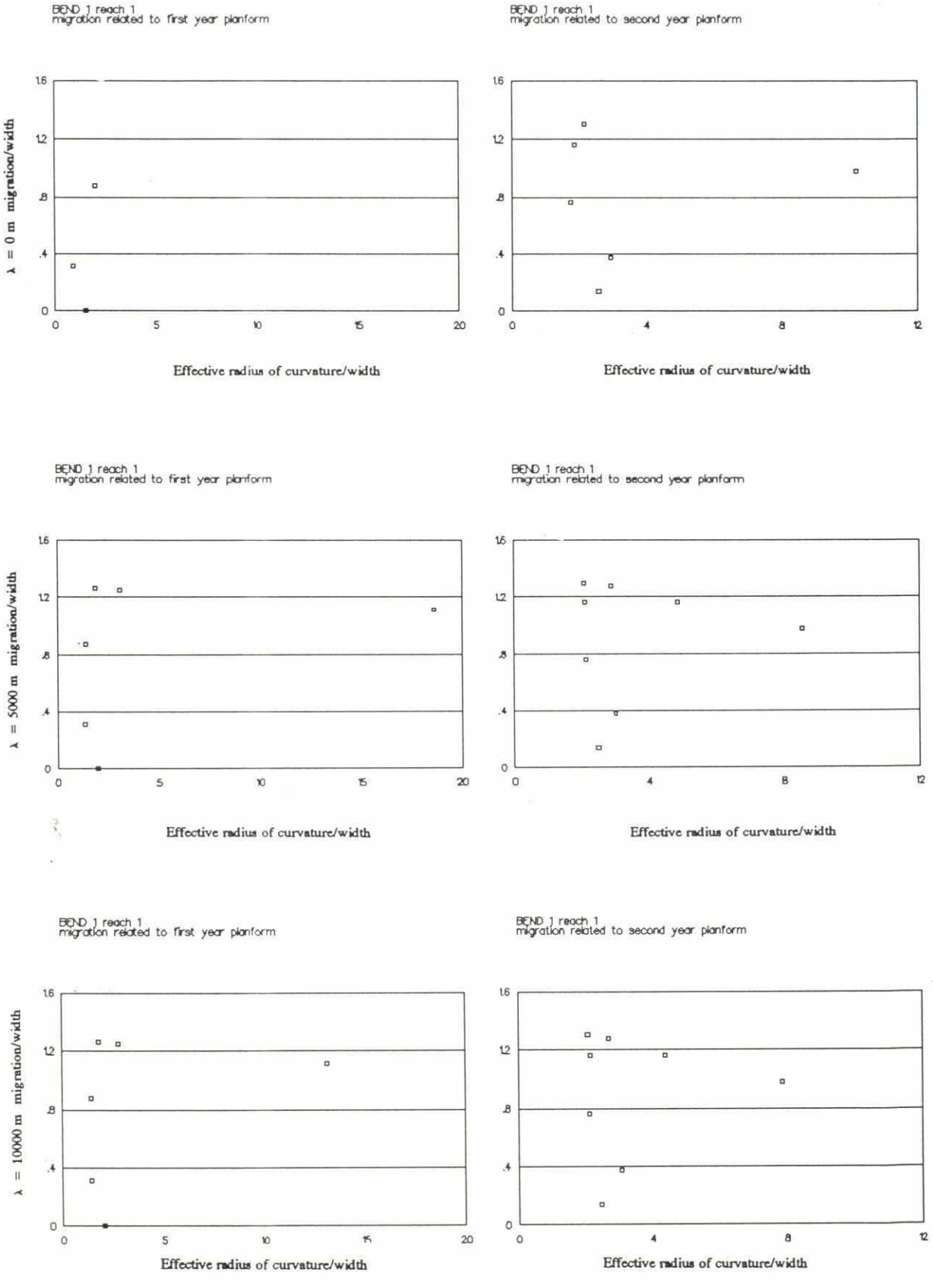


Fig. Ap.4-6: Improved bank erosion analysis migration-effective radius of curvature graphs

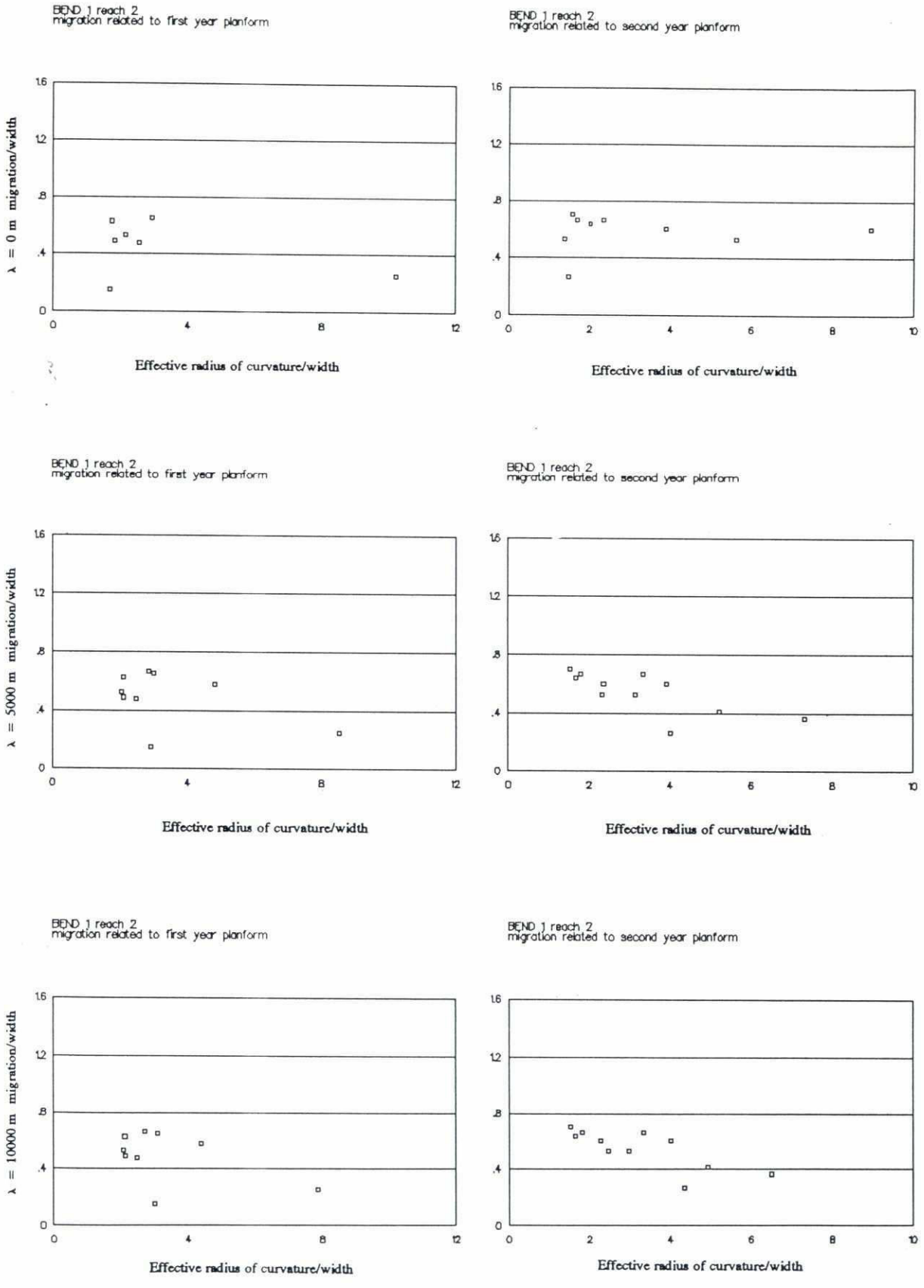


Fig. Ap.4-7: Improved bank erosion analysis migration-effective radius of curvature graphs

APPENDIX 5

COMPREHENSIVE DESCRIPTION OF BIFURCATIONS STUDIED

APPENDIX 5

COMPREHENSIVE DESCRIPTION OF BIFURCATIONS STUDIED

The following Table A5-1 represents the comprehensive description of bifurcations studied:

Bifurcation Code	Abandonment/ Maintained	Order	Location	Char Size	Life-Time (yr.)
BN 1	aban.	1	b	M	1
BN 2	aban.	2	b	M	1
BN 3	main.	2	c/b	S/L	17
BS 1	aban.	2	b	S	3
BS 2	aban.	2	b/s	S	2
BS 3	aban.	1	b	S	1
BS 4	aban.	2	b	S/M	1
BS 5	aban.	1	b/c	M/L	12
BS 6	main.	1/2	s/b	M/L	12
BS 7	main.	1	b	S	3
BS 8	aban.	1/2	b/s	L	12
BS 9	aban.	2/3	b	S	2
BS10	main.	2	c/s/b	L	13
BS11	aban.	2	b	L	1
BS12	aban.	2	b	S	1
BS13	aban.	3	c	S	1
BS14	aban.	2/3	b/s	M	2
BS15	main.	1	s/b	L	7
BS16	main.	2	s/b	L	5

Table Ap.5-1: Comprehensive description of bifurcations studied

The headings and notations used in the Table A11-2 are described hereunder:

Code:
B stands for bifurcation, N for North and S for South.

Abandonment/Maintained:
Abandonment indicates whether abandonment (aban.) of one of the bifurcated channels occurred or not. The latter case also includes disappearance of both channels because of an avulsion. Maintained (main.) in the remaining cases means that the bifurcation still existed in 1992, the last year that it could be studied.

Order:
Description of the importance of the channel reach upstream of the bifurcation. According to the terminology of Williams and Rust (1969), if the entire discharge is carried through one channel, this channel is defined to be of the first order. After a bifurcation in a first order channel, a second order channel arises. The dominant order has been given in this column.

Location:
For the situation at the bifurcation location three possibilities are distinguished:
b: the bifurcation is situated in a bend
c: the bifurcation is situated in a cross-over reach
s: the bifurcation is situated in a straight reach
The latter two situations should prevail for at least 2.5 km upstream of the bifurcation.

Char Size:
The size of the char that divides the two bifurcated size channels, is described in the following terms:
S (small) $<$ 10 km,
M (medium) $\geq$ 10 km and $<$ 20 km,
L (large) $\geq$ 20 km.

Life-Time:
The minimum life-time of a certain bifurcation is given here.

Due to the incomplete data series the actual life-time could not be reconstructed. For instance: a bifurcation was present in 1984, 1986 and 1987, but not in 1978 and 1989 (other years not available), its life-time is at least four years, but can be anything up to ten years.

207

BANK PROTECTION AND RIVER TRAINING (AFPM) PILOT PROJECT FAP 21/22

DRAFT FINAL REPORT PLANNING STUDY

ANNEX 12

SURVEYS

JANUARY 1993

ANNEX 12

SURVEYS

Table of Contents

		Page
1	**INTRODUCTION**	1
2	**BACKGROUND**	1
3	**CO-ORDINATE SYSTEMS**	1
4	**TOPOGRAPHIC AND HYDROGRAPHIC SURVEYS**	
4.1	Scope of Work	3
4.2	Technical Specifications, Standards	
4.2.1	Control Points	4
4.2.2	Horizontal Control	4
4.2.3	Vertical Control	4
4.2.4	Cross-section Survey	4
4.2.5	Drawings	4
4.3	Execution of Works by Subcontractors	
4.3.1	Schedule of Surveys/Subcontracts	5
4.3.2	Mobilization and Access to the Sites	6
4.3.3	Performance of Surveys and Methodology	7
4.3.4	Equipment	9
4.4	Additional Surveys Carried Out by the Consultant	
4.4.1	Scope of Surveys	10
4.4.2	Horizontal Control	10
4.4.3	Recording of Change of River Bankline and Bed Morphology	11

4.5	Results of Surveys	
4.5.1	Contour Maps and Cross-sections	13
4.5.2	Water Level Data	13
4.5.3	Lists of Control Points	15
4.5.4	Resumption of Control Levelling	18
4.5.5	Change of Bankline and Riverbed Profile	18
4.6	Hydrometric Measurements	
4.6.1	Kamarjani	19
4.6.2	Bahadurabad	19
5	**CONCLUDING REMARKS**	20

LIST OF FIGURES:

Fig.A.12-0 : Survey of Test Areas
Fig.A.12-1 : Kamarjani/Topographic and Hydrographic Survey of April/May 1992-Contour Map
Fig.A.12-2 : Kamarjani/Change of Bankline from May to October 1992 and Location of Cross-sections
Fig.A.12-3 : Kamarjani/Change of River Bank and Bed Profile from May to October 1992
Fig.A.12-4 : Kamarjani/Change of River Bank and Bed Profile from May to October 1992
Fig.A.12-5 : Kamarjani/Change of River Bank and Bed Profile from May to October 1992
Fig.A.12-6 : Kamarjani/Sample Surveys of Current Velocities
Fig.A.12-7 : Kamarjani/Basic Survey Data
Fig.A.12-8 : Bahadurabad/Topographic and Hydrographic Survey of April/May 1992-Contour Map
Fig.A.12-9 : Bahadurabad/Topographic and Hydrographic Survey of April/May 1992-Contour Map
Fig.A.12-10: Bahadurabad/Topographic and Hydrographic Survey of April/May 1992-Contour Map
Fig.A.12-11: Bahadurabad/Change of Bankline from May to October 1992, Northern Stretch
Fig.A.12-12: Bahadurabad/Change of Bankline from May to October 1992, Southern Stretch

Fig.A.12-13: Bahadurabad/Change of Bankline near Test Site from May to October 1992 and Location of Cross-sections
Fig.A.12-14: Bahadurabad/Change of River Bank and Bed Profile from May to October 1992
Fig.A.12-15: Bahadurabad/Change of River Bank and Bed Profile from May to October 1992
Fig.A.12-16: Bahadurabad/Sample Surveys of Current Velocities
Fig.A.12-17: Bahadurabad/Basic Survey Data
Fig.A.12-18: Bahadurabad/Basic Survey Data
Fig.A.12-19: Chandanbaisa/Topographic and Hydrographic Survey of April/May 1992-Contour Map
Fig.A.12-20: Chandanbaisa/Topographic and Hydrographic Survey of April/May 1992-Contour Map
Fig.A.12-21: Chandanbaisa/Basic Survey Data
Fig.A.12-22: Chandanbaisa/Basic Survey Data
Fig.A.12-23: Nakalia/Topographic and Hydrographic Survey of April/May 1992-Contour Map
Fig.A.12-24: Nakalia/Topographic and Hydrographic Survey of April/May 1992-Contour Map
Fig.A.12-25: Nakalia/Topographic and Hydrographic Survey of April/May 1992-Contour Map
Fig.A.12-26: Nakalia/Basic Survey Data
Fig.A.12-27: Nakalia/Basic Survey Data

LIST OF TABLES:

Table 3-1 : Comparison of different Transverse Mercator Projections 2
Table 4.3-1: Performance of topographic and hydrographic surveys 6
Table 4.5-1: Kamarjani-Water levels observed during echo soundings 13
Table 4.5-2: Bahadurabad-Water levels observed during echo soundings 14
Table 4.5-3: Chandanbaisa-Water levels observed during echo soundings 14
Table 4.5-4: Nakalia-Water levels observed during echo soundings 15
Table 4.5-5: Kamarjani-BTM co-ordinates and heights (PWD) of control points 16
Table 4.5-6: Bahadurabad-BTM co-ordinates and heights (PWD) of control points 16
Table 4.5-7: Chandanbaisa-BTM co-ordinates and heights (PWD) of control points 17
Table 4.5-8: Nakalia-BTM co-ordinates and heights (PWD) of control points 17
Table 4.5-9: Resumption of control levelling 18
Table 4.6-1: Summary of current measurements at Kamarjani 19
Table 4.6-2: Summary of Current Measurements at Bahadurabad 20

1 INTRODUCTION

This Annex deals with topographic and hydrographic surveys which were subcontracted to local surveying companies and carried out under the supervision of the Consultant, and additional surveys and hydrometric measurements carried out by the Consultant's own personnel and equipment. The latter surveys referred to control measurements and to record morphological changes caused by the flood of 1992.

2 BACKGROUND

Maps are a basic prerequisites for the planning of structures. Under the FAP 21/22 activities appropriate maps for the following tasks were required:

- final selection of test sites within the preselected areas;
- preparation of physical models;
- preparation of alternative preliminary designs of test structures, and
- observation of the extent of bank erosion.

Hydrometric measurements were aimed at providing additional hydrological data for physical modelling and the design of test structures.

A review of existing topographical maps and surveys executed in the past, in connection with other FAP activities, showed that they did not provide sufficient detailed and up-to-date information on the particular test areas of FAP 21. Consequently extensive topographic and hydrographic surveys had to be performed. They were scheduled to be finished before the monsoon period of 1992 as a basis for the above mentioned tasks, and were supplemented by surveying the morphological changes caused by the flood of 1992.

3 CO-ORDINATE SYSTEMS

Various co-ordinate systems resulting from the different projections are in use in Bangladesh and are applied by the various institutions for their mapping. These different systems are causing imminent problems when comparisons have to be made or survey works to be carried out.

The situation can be summarized as follows:

- official maps of Bangladesh prepared under the responsibility of SOB are based on a "Lambert Conformal Conic Projection". Since it has a number of disadvantages, it is intended to utilize another system in the future. However, no final decision has been taken so far;
- the Universal Transverse Mercator (UTM) projection is commonly used throughout the world, but also for some mapping in Bangladesh;

- many information from other sources are based on geographical co-ordinates of latitude and longitude only, which are normally not useful for plane surveying and large scale mapping;
- standard handhold GPS-receivers are normally based on geographical co-ordinates too, or alternatively on UTM co-ordinates which require conversion, when using a small GPS-receiver for position fixing in the field and another type of co-ordinates is required.
- SPOT image maps bear geographical co-ordinates and in addition a plane cartesian co-ordinate system which is also a Transverse Mercator Projection but is using other parameters than UTM (e.g. ellipsoid, scale factor, central meridian);
- Finnmap recommends a system called BTM (Bangladesh Transverse Mercator) which is also based on a Transverse Mercator Projection similar to the SPOT TM system but with some alteration. Landsat images used by FAP 19 for digital mapping are also related to the BTM system.

A comparison of different Transverse Mercator Projections used in Bangladesh is given in the following table:

Parameters	Universal Transverse Mercator Projection (UTM)	Bangladesh Transverse Mercator Projection (BTM)	SPOT Transverse Mercator Projection (SPOT TM)
Projection	Transv.Mercator	Transv.Mercator	Transv.Mercator
Ellipsoid	WGS 1984	Everest 1830	Everest spheroid
Scale Factor	0.9996	0.9996	0.9998
Central Meridian	87°/93°	90° E	90° E
Latitude of Origin	0°(equator)	0°(equator)	0°(equator)
False Easting	500000 m	500000 m	500000 m
False Northing	0 m	- 2000000 m	0 m
UTM Zone	45/46	-	-

Table 3-1: Comparison of different Transverse Mercator Projections

The previous explanations clearly show the necessity to introduce a uniform projection/co-ordinate system for use by FAP activities as suggested by FAP 19 (c.f. Technical Notes Series No.1 of FAP 19 of 24 May, 1992).

Following the proposal of FAP 19, the FAP 21/22 project has decided to set up their maps and plans utilizing the tentative BTM system because most of the recent information at FAP 21/22 (e.g. Landsat images) are based on that system.

FAP 21/22 acknowledges the valuable assistance given by FAP 19 in converting co-ordinates to/from different projections.

4 TOPOGRAPHIC AND HYDROGRAPHIC SURVEYS

4.1 SCOPE OF WORK

Based on the results given in the "Technical Report No.1 - Preselection of Test Areas" - of March 1, 1992 four areas along the Jamuna had been selected for the implementation of test structures:

- Kamarjani (north of Manos Regulator);
- downstream of Bahadurabad ghat;
- Chandanbaisa, and
- Nakalia.

The locations of the surveyed areas are shown on Fig.A.12-0.

W.A.R.P.O. LIBRARY.

The scope of works had to fulfil the following conditions:

- sufficient coverage in order to give enough flexibility and information for an optimum site selection;
- scale of mapping, arrangement and density of survey adequate for physical modelling, and
- construction of survey pillars including horizontal and vertical control survey for reestablishing/identifying particular survey areas at a later date.

The following basic parameters had been fixed for that:

- cross-section survey at approx. 200 m intervals;
- length of cross-sections approx. 3 km (1.5 km on the landside and 1.5 km on the waterside);
- extension of surveys along the Jamuna: Kamarjani 5 km, Bahadurabad 12 km, Chandanbaisa 10 km and Nakalia 12 km;
- layout plans in the scale of 1:5,000 with contour line equidistances of 0.25 m, and
- cross-sections in the scale of 1:2,000/100.

4.2 TECHNICAL SPECIFICATIONS, STANDARDS

Bangladeshi regulations and standards of accuracy for surveying works had to be applied in general. For the present survey the following specific terms had been stipulated and formed part of the contract with the surveying companies:

4.2.1 Control Points

(1) Placement of 70 (seventy) reinforced concrete pillars in sheltered and safe locations at four test ares, the points to be used as on-shore control points, and for later follow-up surveys;
(2) location of pillars being identified by the Consultant;
(3) the T-shaped pillars having dimension of 15 cm x 15 cm x 90 cm marked with respective numbers, brass rod anchored at the top of the pillars.

4.2.2 Horizontal Control

(1) Connection of survey to BTM system by second order closed traverse survey;
(2) accuracy typical for engineering surveys, i.e. for unadjusted horizontal distances: 1 in 10,000 and for unadjusted horizontal angles: $10\sqrt{N}$ sec;
(3) reference control points and co-ordinates for connection being provided by the Consultant.

4.2.3 Vertical Control

(1) Connection of heights to PWD datum, carried out as double levelling or closed back on the starting point;
(2) accepted misclosure for a line not to exceed $\pm\ 12\sqrt{K}$ mm - where K is the length of the circuit in kilometers;
(3) reference BM points and values being provided by the Consultant.

4.2.4 Cross-section Survey

(1) Cross-sections extending on landside part being surveyed by terrestrial method, and on waterside part by hydrographical means;
(2) waterside profiles in line with those measured onshore; the connection of both being made properly in view of elevation and location;
(3) bathymetric survey being performed from a boat, and water depths being measured by echo-sounder;
(4) position fix being done by intersection and resection, or other appropriate means;
(5) temporary gauges placed at distances of about 2 km, and water levels recorded for proper connection to PWD datum; the gauges connected to PWD datum by levelling, and
(6) spot heights on land taken at 50 m distances on the average.

4.2.5 Drawings

(1) Preparation of topographical maps, scale 1:5,000 in accordance with the professional standards;

(2) preparation of cross-section drawings, horizontal scale 1:2,000, vertical scale 1:100.

4.3 EXECUTION OF WORKS BY SUBCONTRACTORS

4.3.1 Schedule of Surveys/Subcontracts

Some constraints were imposed on the schedule of the surveys due to the dependence on other activities and conditions:
On the one hand the field works had to be finalized before the monsoon rains and therefore- due to the quite extensive volume of works - to be started as early as possible. On the other hand, the subcontracts could not be awarded and the surveys not be started before the test areas were identified by the Consultant and agreed upon by FPCO. But all preparations were made to permit the immediate beginning of the field works after approval of the test areas by FPCO. Fortunately the field works could be concluded without being too much hampered by bad weather conditions at the end of May 1992. Due to the fact that a further area near Nakalia had to be investigated upon request of FPCO, the Consultant decided to split the works into two packages and to employ two different surveying companies. Six bids were submitted by local surveying companies. After evaluation of these offers contracts were awarded to:

(a) Hydroland Survey Ltd. Kalabagan, Dhaka-1205;
(b) The Surveyors & The Realtors, Dhaka-1000.

After signing the contract on 02.04.1992, Hydroland actually started the field work on 11.04.1992 at three sites, at Kamarjani, Bahadurabad and Chandanbaisa. The Surveyors & The Realtors signed the contract with the Consultant on 08.04.1992 and started on 12.04.1992 at Nakalia. Both survey subcontractors completed the field works by the end of May, 1992 in accordance with the contractual time schedule.

The Table 4.3-1 describes the course of activities and the periods of execution for each test area.

Test Area	Type and Volume of Works	Work Period	
		From	To
Kamarjani (North of Manos Regulator)	**Survey:**		
	- Erection of pillars (10 Nos.)	11.04.92	21.04.92
	- Height connection of Kamarjani BM to Manos regulator BM	03.05.92	08.05.92
	- Height connection of pillars	13.04.92	21.04.92
	- Erection of temporary gauges	13.04.92	21.04.92
	- Traverse survey	02.05.92	06.05.92
	- Cross-section survey, water	13.04.92	21.04.92
	- Cross-section survey, land	15.04.92	09.05.92
	Drawings:		
	- Layout plans (date of completion)	-	11.07.92
	- Cross-sections (date of completion)	-	07.07.92
Bahadurabad	**Survey:**		
	- Erection of pillars (20 Nos.)	15.04.92	30.04.92
	- Height connection of BM	21.04.92	30.04.92
	- Height connection of pillars	21.04.92	07.05.92
	- Erection of temporary gauges	21.04.92	30.04.92
	- Traverse survey	14.05.92	20.05.92
	- Cross-section survey, water	21.04.92	21.05.92
	- Cross-section survey, land	21.04.92	21.05.92
	Drawings:		
	- Layout plans (date of completion)	-	17.07.92
	- Cross-sections (date of completion)	-	11.07.92
Chandanbaisa	**Survey:**		
	- Erection of pillars (20 Nos.)	12.04.92	21.04.92
	- Height connection of BM	13.04.92	21.04.92
	- Height connection of pillars	13.04.92	30.04.92
	- Erection of temporary gauges	13.04.92	30.04.92
	- Traverse survey	08.05.92	14.05.92
	- Cross-section survey, water	13.04.92	30.04.92
	- Cross-section survey, land	13.04.92	14.05.92
	Drawings:		
	- Layout plans (date of completion)	-	11.07.92
	- Cross-sections (date of completion)	-	11.07.92
Nakalia	**Survey:**		
	- Erection of pillars (20 Nos.)	12.04.92	16.04.92
	- Height connection of BM	18.04.92	29.04.92
	- Height connection of pillars	23.04.92	09.05.92
	- Erection of temporary gauges		
	- Traverse survey	16.04.92	14.05.92
	- Cross-section survey, water	09.05.92	17.05.92
	- Cross-section survey, land	10.05.92	12.05.92
	Drawings:		
	- Layout plans (date of completion)	-	13.07.92
	- Cross-sections (date of completion)	-	13.07.92

Table 4.3-1: Performance of topographic and hydrographic surveys

4.3.2 Mobilization and Access to the Sites

All 4 test areas were inspected by the Consultant and the survey contractors prior to the actual field works in order to fix the limits of the survey areas in the field, to mark the locations for the pillars and to discuss the work programme. The contractors proved to be familiar with the site condition which could be realized from their logistic approach.

Especially at Bahadurabad and Chandanbaisa the accessibility from the landside is rather difficult, but to a certain extent also at Kamarjani test area. Furthermore, the landside movement is handicapped by a poorly developed transport infrastructure and the lack of accommodation.

Hydroland Survey Ltd. therefore mobilized and operated from the waterside. Two hired passenger ships of about 25 m length served for mobilization and travelling from Dhaka to the sites, for accommodation, as drafting office and for storage of equipment at the various places. A number of smaller country boats was used in addition for transportation of the survey crews in the field, and - equipped with an echo sounder and navigational instruments - for the bathymetric surveys.

The Nakalia test area showed a much better accessibility from the landside and far better conditions in view of mobility, supply, accommodation etc. than the other test areas. The Surveyors & The Realtors mobilized from the landside but travelled in the field by hired country boats which were also used for the echo soundings. A rented house of corrugated iron at Nagarbari ghat served the survey crews as accommodation and office.

4.3.3 Performance of Surveys and Methodology

(1) General approach

At the beginning of the field works the Consultant and the contractors identified the limits of the survey areas and fixed the locations of the control stations. Furthermore, the Consultant provided initial bench-mark data and co-ordinate figures for the connection of the surveys to the generic system. During the whole period of the field works the Consultant made extensive field visits in order to guide the works, to discuss and solve problems which arose during the surveys, and to check the works at random, using own equipment. The professional and supporting personnel of both survey companies was in general adequately staffed to permit a simultaneous working in all required disciplines, like bathymetry, topography, traversing, levelling etc.

Hydroland Survey Ltd. was working in general in two test areas simultaneously. They started at Chandanbaisa and Kamarjani first and concentrated their staff and activities on Bahadurabad after finishing the first two places.

The Surveyors & The Realtors worked with a lower number of employees, since they had to survey one test area only.

The following survey works have been carried out in total:

-	construction of survey fix points (pillars)	-	70 numbers
-	traversing/horizontal control survey	-	67 km
-	connecting/control levelling	-	97 km

- topographic cross-section survey - 336 km
- hydrographic cross-section survey - 290 km

(2) Control stations

The fixed points/control stations consist of T-shaped reinforced concrete pillars of the dimensions of 15 x 15 x 90 cm, placed in sheltered locations as far as possible. Numbering of pillars at the test areas has been given in the following order:

(a)	Kamarjani	:	FAP 21.01 to FAP 21.10
(b)	Bahadurabad	:	FAP 21.11 to FAP 21.30
(c)	Chandanbaisa	:	FAP 21.31 to FAP 21.50
(d)	Nakalia	:	FAP 21.51 to FAP 21.70

The location of the control points as well as the traverse data (angles and distances) are shown on Fig.A.12-7 (Kamarjani); Fig.A.12-17 and Fig.A.12-18 (Bahadurabad); Fig.A.12-21 and Fig.A.12-22 (Chandanbaisa), and Fig.A.12-26 and Fig.A.12-27 (Nakalia).

(3) Traversing

The newly established pillars at all test areas were traversed with EDM and theodolite to obtain a local traverse network. Co-ordinates of these pillars have been provided in BTM grid system. (For more details see also Subsection 4.4.2).

(4) Levelling

Control levelling has been made by double levelling at Kamarjani, Bahadurabad and Chandanbaisa. At Nakalia the levelling connected several stations along the line for checking, and has finally been closed on two stations. The heights of newly established pillars and cross-section surveys were determined with reference to the bench-marks (BM) located at each test site.

(5) Cross-section survey

The cross-sections on the landside areas have been surveyed using conventional techniques (chaining and levelling), whereas the bathymetric cross-sections have been recorded by means of echo-sounders installed on small country boats. The survey boat was tracked along prefixed parallel lines at about 200 m intervals. The lines were arranged perpendicularly to transit lines, which were arranged almost parallelly to the river banks.

For the conning of the boats when running soundings, markers (poles with flags) were fixed on the shore or on chars. The boat was then run down each track, the steersman lining himself in with the successive pairs of shore stations.

The position of the survey boat was fixed in intervals by the resection method (Hydroland) using sextants on the boat and by the intersection method (The Surveyors & The Realtors) using theodolites on land. To link both position fixes with the depth records, marks were printed on the graph paper of the echo sounder, simultaneously with the position fixes.

On-shore levelling was done from the water line of the high bank and over the high bank as well as along the desired distances. Levelling was furthermore applied over the chars, falling in line with the cross section.

(6) Reduction of depths and heights

Soundings (depths) taken along the bathymetric cross-sections (including levelling over chars) as well as the spot levels (heights) taken along the on-shore cross-sections were reduced to PWD datum level.

(7) Water level gauges

For proper connection of the soundings to PWD datum, temporary gauges were placed at about 2 km apart at each test area and water levels were recorded at half hour intervals during the soundings. These gauges were levelled and connected with the BM located within the test areas.

(8) Topographic survey

For the survey of salient topographical features of importance such as mosques, buildings, embankments, roads etc. in addition plane table surveying as well as chain surveying was applied in some areas.

4.3.4 Equipment

The equipment used for the surveys complied fully with the requirements for such tasks. Part of the available electronic equipment formed the electronic distance measuring equipment and the echo-sounders. A problem for the operation of electronic equipment in the field, especially in remote areas, is the power supply for charging of batteries. Therefore, Hydroland Survey Ltd. operated a generator for this purpose.

The following equipment was used for surveys in total:

(1) Instruments	Numbers
- EDM tacheometer (Pentax)	1
- EDM, fitted with theodolite	1
- sextant	6
- theodolite Pentax FG-18	1
- theodolite (Russian type)	1
- graphic echo sounder	3
- level instrument	6
- auto level	3
- plane table equipment	5
- scientific calculator	6
- station pointer	2
- diagonal scale	2

-	measuring chain	2
-	measuring tape	2
-	echo test disc	2

(2) vessels

-	survey and accommodation launch	2
-	mechanised craft	6

The more sophisticated equipment of the Consultant was employed for checking and supporting the contractors' work as well as for own additional surveys.

4.4 ADDITIONAL SURVEYS CARRIED OUT BY THE CONSULTANT

4.4.1 Scope of Surveys

Besides the continuous supervision of the field works of the subcontractors the additional surveys of the Consultant had inter alia the following objectives:

- provision of co-ordinates of control points for the connection to the given co-ordinate system;
- recording of the river bankline at the test sites after the 1992 flood, and
- recording of the riverbed morphology at the test sites after the 1992 flood.

4.4.2 Horizontal Control

As co-ordinate system for its mapping FAP 21/22 has adopted the tentative Bangladesh Transverse Mercator (BTM) projection which was introduced by FAP 18 and is also in use by FAP 19, too (see also Chapter 3). The intention of that decision was to connect all topographical and hydrographic surveys to the recently established FM GPS control points, and by this to use existing BTM co-ordinates for the calculation of the horizontal control surveys. Unfortunately co-ordinates of FM GPS pillars could not be obtained, contrary to all expectations. In order to solve the problem the Consultant used his own portable GPS receiver for the establishment of a basic co-ordinate network, however without differential correction and therefore with a reduced accuracy.

The co-ordinates of the used hand-held GPS receiver are generally given in geographical co-ordinates of latitude and longitude or alternatively in UTM of northing and easting. Since the surveys required a grid co-ordinate system, the UTM mode was used. There are several position fixing modes differing from each other in terms of time required and accuracy delivered, the most accurate (and the slowest) being the 3 D mode where more than 4 satellites are tracked at the same time. For position fixing in the 3 D mode the accuracy is given in the manufacturer's manual with about 15 m and 40 m for the "Selective Availability" (operation mode of the satellite operator) switched "off" or "on", respectively. Generally the "Selective Availability" is switched on.

(1) Applied method for the retrieval of BTM co-ordinates for control points

In order to improve the accuracy of the data all positions were collected in 3 D mode only, and each pillar's position was determined by collection of multiple positions at each point and by calculating the average. As far as possible, points were collected only when a favourable satellite geometry was available. In addition, the control points were interconnected by 2nd order traversing from which co-ordinates in a arbitrary system had been calculated first. This survey ensured the internal accuracy of the horizontal control framework.

In order to check the reliability of the UTM co-ordinates of the GPS survey the relative positions of the points to each other were then compared in both systems. The most reasonable two points with a sufficiently large distance from each other were selected and the tentative UTM co-ordinates corrected in such a way to keep the given authorized length, calculated from the local co-ordinates of the traverse survey. All local co-ordinates of the remaining points were than transformed into the UTM-system on the basis of these two points. Since BTM co-ordinates could not be obtained from the GPS receiver, another transformation from UTM to BTM became necessary. As both projections are based on different ellipsoids a special programme was required - and available with FAP 19 - to do the conversions.

(2) Remarks and recommendations

Because of the limited accuracy of the GPS survey a residual error in the co-ordinates of some ten meters may still be expected. That is to say that a displacement could appear when BTM co-ordinates originated in other and more precise sources (e.g. from Finnmap GPS points) would be combined with those from the above described surveys. However the internal (relative) accuracy of the control points of FAP 21 is not affected by a possible displacement. As already explained before, the internal accuracy is based on traverses, and thus differences should not appear when surveys will be based on co-ordinates of FAP 21 only. Nevertheless an adjustment is recommended for future surveys, when BTM co-ordinates from the precise GPS survey of FAP 18 are available.

4.4.3 Recording of Change of River Bankline and Bed Morphology

In order to provide information on the extent of erosion and the change of the river bed morphology occurred during the flood season of 1992, the Consultant performed additional echo soundings at the two selected test sites at Kamarjani and Bahadurabad in the month of October 1992. Longitudinal and transverse river profiles were recorded by means of an echo sounder installed on the Consultant's speed boat. The soundings were reduced to PWD datum by gauge readings. For position fixing of the moving boat the Consultant's microwave system was used.

(1) Equipment

The equipment used by the Consultant for the additional surveys (including hydrometric measurements) consists of the following items:

- working boat (inflatable rubber boat with rigid GRP hull) and 50 HP outboard motor;
- microwave range-range position fixing system (Trisponder);
- electronic current probe with sensors for current speed, depth (pressure), direction (fluxgate compass) and data terminal;
- portable winch;
- water sampler;
- digital echo sounder;
- electronic tacheometer (EDM)
- levelling equipment, and
- hand-hold GPS receiver.

To carry the boat to the sites a boat trailer had been built by a Bangladeshi workshop according to a design prepared by the Consultant, and fixing devices have been constructed to carry the instruments on the boat (e.g. winch, echo sounder, transducer, master station of Trisponder etc.).

A very important tool for position fixing in connection with all investigations was the Trisponder navigation system, since it permits a precise and continuous survey of the boat's position on the river. A detailed description is given in the subsequent para.

(2) Position fixing by microwave system

For position fixing the RACAL DECCA Trisponder microwave system was used. The system is able to fix positions up to 80 km, when "line-of-sight" conditions prevail. The system provides the user with the capability to achieve accuracies of position fix of a moving vessel typically on the order of 3 meters with updates of 1 second.

To determine the position of the moving speed boat the "range-range" technique is used: distances are measured from the master unit on the boat to two remote shore station placed on known points. These were established beforehand on suitable places under consideration of the following conditions: free line-of-sight, good coverage of the area to be surveyed, well-conditioned triangles for accuracy. This required remote stations partly on chars and partly on the riverbanks. To get the relation to the basic survey of April/May the points were connected to existing control pillars from the former survey by means of traversing and trilateration, using the EDM equipment. When running echo sounding profiles, position fixes with simultaneous marks on the echo sounder were taken approximately every 30 second and registered by a printer.

Also the bankline after the flood period was surveyed by the Trisponder system. The boat was sailed along the bankline as close as possible at a distance of about 5 metres, and the position was fixed at all relevant changes of the bankline. Finally, co-ordinates were calculated from the registered range-data and plotted on the basic maps in the scale 1:5,000.

4.5 RESULTS OF SURVEYS

After evaluation of all field records, calculations, plotting, etc. the following data and documents have been prepared:

4.5.1 Contour Maps and Cross-sections

The following survey maps and cross-section drawings are available in A1-size:

	Kamarjani	Bahadurabad	Chandanbaisa	Nakalia
contour and sounding maps 1:5000	3	6	5	7
cross-sections 1:2000/100	26	61	52	66

The drawings formed the basis for different tasks of the Project (in particular for physical modelling), and were partly reduced, generalised or modified according to the different requirements. Generalized and reduced editions of the topographical maps in the scale of 1:20,000 of all investigated areas are attached to this ANNEX at the end. See Figures A.12-1 (Kamarjani); A.12-8 to A.12-9 (Bahadurabad); A.12-19 and A.12-20 (Chandanbaisa), and A.12-23 to A.12-25 (Nakalia). The original A1 full-size drawings are kept in the Consultant's office.

4.5.2 Water Level Data

The water levels, recorded at each test area for the time when echo soundings have been made, are compiled in the following Tables 4.5-1 to 4.5-4. The figures are located to PWD datum.

Date	Reduced Level (m - PWD)				
	Time				
	6:00 h	9:00 h	12:00 h	15:00 h	18:00 h
15.04.92	-	-	16.49	16.49	16.49
16.04.92	16.50	16.50	16.50	16.50	16.50
17.04.92	16.50	16.50	16.50	16.50	16.50
18.04.92	16.54	16.55	16.57	16.50	16.57
19.04.92	16.75	16.76	16.77	16.80	16.86
20.04.92	17.13	17.14	17.16	17.19	17.24

Note: The figures indicate the water levels in the areas, where echo sounding have been carried out at the same time.

Table 4.5-1: Kamarjani-Water levels observed during echo soundings

Date	Reduced Level (m - PWD)				
	Time				
	6:00 h	9:00 h	12:00 h	15:00 h	18:00 h
25.04.92	-	15.94	15.93	15.91	15.89
26.04.92	15.83	15.83	15.81	15.80	15.79
27.04.92	15.71	15.70	15.69	15.69	15.68
07.05.92	15.15	15.14	15.14	15.13	15.13
08.05.92	15.14	15.14	15.14	15.14	15.14
09.05.92	15.13	15.13	15.13	15.13	15.14
15.05.92	15.16	15.17	15.18	15.19	15.19
16.05.92	15.20	15.19	15.18	15.17	15.16
17.05.92	15.17	15.17	15.18	15.20	15.21
18.05.92	15.00	15.00	14.99	14.98	14.98

Note: The figures indicate the water levels in the areas, where echo sounding have been carried out at the same time.

Table 4.5-2: Bahadurabad-Water levels observed during echo soundings

Date	Reduced Level (m - PWD)				
	Time				
	6:00 h	9:00 h	12:00 h	15:00 h	18:00 h
19.04.92	11.54	11.54	11.56	11.58	11.60
20.04.92	11.76	11.79	11.85	11.91	11.94
21.04.92	12.38	12.41	12.45	12.49	12.52
22.04.92	12.68	12.74	12.18	12.81	12.84
23.04.92	13.00	13.00	13.01	13.01	13.02
24.04.92	13.14	13.13	13.11	13.10	13.08
25.04.92	13.02	13.00	12.99	12.92	12.96
27.04.92	12.57	12.55	12.54	12.52	12.51

Note: The figures indicate the water levels in the areas, where echo sounding have been carried out at the same time.

Table 4.5-3: Chandanbaisa-Water levels observed during echo soundings

Date	Reduced Level (m - PWD)			Between cross-sections
	Time			
	9:00 h	12:00 h	15:00 h	No. - No.
09.05.92	5.08	5.09	5.09	33 - 36
10.05.92	5.54	5.54	5.53	0 - 5
12.05.92	5.54	5.55	5.54	6 - 12
13.05.92	5.28	5.28	5.28	37 - 65
14.05.92	5.57	5.57	5.57	13 - 18
15.05.92	5.56	5.57	5.57	19 - 24
16.05.92	5.44	5.44	5.43	25 - 32
Note: The figures indicate the water levels in the areas, where echo sounding have been carried out at the same time.				

Table 4.5-4: Nakalia-Water levels observed during echo soundings

4.5.3 Lists of Control Points

In the following tables, BTM co-ordinates and elevations related to PWD datum, of all control points of the four test areas are shown. The tables show furthermore the BM points and height figures to which the levellings had been connected. The elevation figure is related to the top of the point.

To permit discovering or re-establishing of the control points in the field for follow-up surveys, traverse data are compiled in Figures A.12-7 (Kamarjani), A.12-17 and A.12-18 (Bahadurabad), A.12-21 and A.12-22 (Chandanbaisa), and A.12-26 and A.12-27 (Nakalia).

No. of Control Point	Co-ordinates (BTM)		Elevation m (PWD)
	Easting (m)	Northing (m)	
FAP 21.01	462,674.65	805,806.03	23.619
FAP 21.02	462,291.22	805,502.93	21.604
FAP 21.03	462,521.84	805,178.59	21.966
FAP 21.04	461,935.77	804,621.22	20.663
FAP 21.05	462,144.11	803,710.17	23.279
FAP 21.06	462,007.93	803,055.47	24.129
FAP 21.07	462,253.07	802,776.41	24.185
FAP 21.08	462,514.26	802,097.95	24.166
FAP 21.09	462,653.40	801,496.16	24.628
FAP 21.10	462,784.85	801,354.44	23.802
FMBM 7603	-	-	20.590
FMBM 7604	-	-	22.620
BMTS-416 at Manos Regulator	-	-	24.720

Table 4.5-5: Kamarjani-BTM co-ordinates and heights (PWD) of control points

No. of Control Point	Co-ordinates (BTM)		Elevation m (PWD)
	Easting (m)	Northing (m)	
FAP 21.11	470,606.09	780,117.04	20.055
FAP 21.12	470,286.58	779,429.53	20.853
FAP 21.13	470,222.82	778,514.20	19.056
FAP 21.15	470,624.51	776,053.66	18.898
FAP 21.16	470,830.15	775,448.04	18.266
FAP 21.17	470,534.65	774,261.16	18.760
FAP 21.18	469,359.43	771,929.79	18.549
FAP 21.19	469,090.25	770,741.10	19.557
FAP 21.20	469,436.73	768,672.92	18.439
FAP 21.21	469,780.20	768,424.28	20.368
FAP 21.22	469,584.85	770,588.74	19.294
FAP 21.23	470,308.70	771,294.10	19.511
FAP 21.24	471,457.13	774,064.67	20.101
FAP 21.25	471,319.71	775,238.02	19.228
FAP 21.26	471,333.41	776,393.75	21.047
FAP 21.27	471,234.40	777,494.02	19.923
FAP 21.28	471,025.65	778,115.34	20.139
FAP 21.29	470,634.32	779,024.61	20.763
FAP 21.30	470,724.31	779,929.74	21.909
FMGPS 764	-	-	20.310
FMBM 5244	-	-	19.850
FMBM 5215	-	-	19.060

Table 4.5-6: Bahadurabad-BTM co-ordinates and heights (PWD) of control points

No. of Control Point	Co-ordinates (BTM)		Elevation m (PWD)
	Easting (m)	Northing (m)	
FAP 21.31	460,193.68	746,857.19	18.349
FAP 21.32	460,168.94	746,305.29	16.537
FAP 21.33	460,416.83	745,868.36	19.738
FAP 21.34	460,781.75	745,733.16	17.761
FAP 21.35	460,620.19	745,180.26	15.877
FAP 21.36	460,869.21	744,796.98	17.164
FAP 21.37	460,965.54	744,205.47	18.860
FAP 21.38	461,061.80	743,771.99	16.823
FAP 21.39	460,897.33	743,354.30	15.866
FAP 21.40	461,102.24	742,972.20	16.367
FAP 21.41	461,450.01	742,652.28	16.340
FAP 21.42	461,613.48	741,863.78	18.902
FAP 21.43	462,147.49	741,035.82	18.818
FAP 21.44	462,449.49	740,537.00	16.097
FAP 21.45	462,238.12	739,917.55	16.225
FAP 21.46	462,647.28	739,519.64	17.341
FAP 21.47	462,600.29	738,999.64	15.222
FAP 21.48	462,670.64	738,791.34	15.819
FAP 21.49	462,448.55	738,416.28	15.995
FAP 21.50	462,860.42	737,803.92	16.524
FMGPS 750	-	-	16.380
FMBM 7214	-	-	16.260

Table 4.5-7: Chandanbaisa-BTM co-ordinates and heights (PWD) of control points

No. of Control Point	Co-ordinates (BTM)		Elevation m (PWD)
	Easting (m)	Northing (m)	
FAP 21.51	464,621.62	661,467.58	12.223
FAP 21.52	464,941.65	660,367.91	10.671
FAP 21.53	465,146.10	659,157.96	11.543
FAP 21.54	465,522.12	658,048.56	10.666
FAP 21.55	465,731.88	656,933.17	10.195
FAP 21.56	465,796.24	655,742.85	11.395
FAP 21.57	465,085.51	654,649.54	9.605
FAP 21.58	464,685.34	653,601.50	10.821
FAP 21.59	464,131.06	652,366.34	10.208
FAP 21.60	463,758.53	650,849.22	10.171
FAP 21.61	464,117.56	649,474.44	9.495
FAP 21.62	463,588.96	649,325.43	13.079
FAP 21.63	463,577.42	650,685.44	13.356
FAP 21.64	463,387.55	652,336.48	13.321
FAP 21.65	463,534.02	653,700.45	13.775
FAP 21.66	464,396.76	655,028.78	13.310
FAP 21.67	464,837.68	655,991.03	13.265
FAP 21.68	464,925.79	657,569.29	13.521
FAP 21.69	464,805.28	659,027.76	13.614
FAP 21.70	464,279.52	661,306.01	13.526
FMBM 6525	-	-	11.600
Kaitola Pump Station	-	-	12:210

Table 4.5-8: Nakalia-BTM co-ordinates and heights (PWD) of control points

4.5.4 Resumption of Control Levelling

The closing errors of the levelling loopes of the control levelling for each test area are compiled in the following table.

Test Area	Starting Point	End Point	Distance (double running)	Permitted error	Surveyed error
Kamarjani	FMBM 7603	BM FAP 21/10	16x2 = 32 km	68 mm	20 mm
Bahadurabad	FM GPS 764	BM FAP 21/11	28.5x2 = 57 km	91 mm	13 mm
Chandanbaisa	FM GPS 750	BM FAP 21/50	16x2 = 32 mm	68 mm	15 mm
Nakalia	FM BM 6525 via Koitola Pump Station	BM FAP 21/66	29 km (single running)	65 mm	17 mm

Table 4.5-9: Resumption of control levelling

4.5.5 Change of Bankline and Riverbed Profile

The re-survey of the banklines and cross sections in Kamarjani and Bahadurabad is being compared with the situation surveyed in April/May'92 in Fig. A.12-2 to A.12-5 for Kamarjani and in Fig. A.12-11 to A.12-15 for Bahadurabad. The drawings show that considerable erosion has been taken place. The maximum loss of land was about 300 m at Kamarjani and 200 m at Bahadurabad. This is in the range of the prediction, given in the morphological study, and thus stating the forecast.

Measuring the courses of the riverbanks and the cross sections, echo soundings were made continuously during travelling. Very deep scour holes close to the embankment were observed at the end of October (e.g. > 20 m in front of the high and primary school north of Manos regulator). Longitudinal soundings showed dunes upto 2.5 m high at both places with strong currents and strong surface turbulences.

4.6 HYDROMETRIC MEASUREMENTS

According to the description in Task 8 of the Scope of Works of the Consulting Agreement the hydrometric surveys have to be understood as complementary works, to be carried out if and when required. Thus, they were performed at random without following a fixed schedule.

The purpose of the measurements was to provide data on flow velocities and directions at selected points of the test areas. Therefore fix point current measurements by means of an electronic probe have been carried out in Kamarjani and Bahadurabad and supplemented by float tracking.

4.6.1 Kamarjani

The fix point current measurements were carried out at three locations close to the eroding embankment:

(a) about 800 m;
(b) about 1800 m, and
(c) about 2900 m north of Manos regulator.

Floats were tracked along the test area over a width of about 500 m from the river bank, and the position along their course was fixed by means of the Trisponder system. The float vanes were placed at 1.5 m below the water surface. The floats were followed by the speed boat, and position fixes were taken when passing the floats. Together with the fixes the time was recorded and the velocities were calculated. The plot of the measured float tracks is shown on Fig.A.12-6.

The results of the sample surveys of current velocities at Kamarjani are given in Table 4.6-1.

Location	Date	Water Level m PWD	Velocity m/s	Remark
(a)	21.07.92	21.32	3.2	Fix point
(b)	21.07.92	21.32	3.1	Fix point
(c)	21.07.92	21.32	2.9	Fix point
(d)	28.10.92	18.10	1.7	Float track

Table 4.6-1: Summary of current measurements at Kamarjani

According to figures recorded by the Water Board at the gauge near the Manos regulator, the water level during the fix point measurements represented the highest recorded level in 1992.

4.6.2 Bahadurabad

The fix point measurements were made at one location close to the eroding embankment near Belgachha village, and float tracks were measured in front of Belgacha village and in front of Bahadurabad railway ghat. Again the float vanes were arranged at 1.5 m below the surface of the water. The measurements were done in the same way as described for Kamarjani. The plot of the float ways is shown on Fig.A.12-16.

Current measurements in the Bahadurabad reach have also been undertaken by FAP 24 (River Survey) in September 1992. The measurements included velocity verticals in a river cross-section situated at about 1.5 km south of the railway ghat. Two verticals from these measurement (those near the bankline) can be considered as representative for the test site.

The results of the current measurements supplemented by the two measurements of FAP 24 are compiled Table 4.6-2.

Location	Date	Water Level m PWD	Velocity m/s	Remark
A	16.09.92	17.80	1.2-1.4	Source: FAP 24
B	19.09.92	17.80	1.6-1.8	Source: FAP 24
C	22.07.92	19.10	2.8	Fix point
Railway ghat	31.10.92	16.20	1.5	Float track
Belgacha	01.11.92	16.80	1.2	Float track

Note:
The location of point A (velocity vertical of FAP 24) is about 900 away from the bankline, the location of point B about 150 m. C represents a fixed point current measurement of FAP 21/22, taken in front of Belgacha in the main flow channel near the eroding bankline.

Table 4.6-2: Summary of current measurements at Bahadurabad

5 CONCLUDING REMARKS

Although the surveys had to be carried out under a very tight time schedule for four areas simultaneously, the field works were organized in such a way that they could be finalized before the start of the monsoon rains.

Every effort was also made to prepare the necessary survey maps and cross section drawings as quickly as possible, as to permit the construction of the physical models without delay.

The performance of the works and the results of the survey campaign can hence be considered as quite satisfactory.

The survey results formed the basis for the different tasks of the study and have been processed further according to the requirements. The drawings attached to this Annex represent a selection of the surveys and show their most important results.

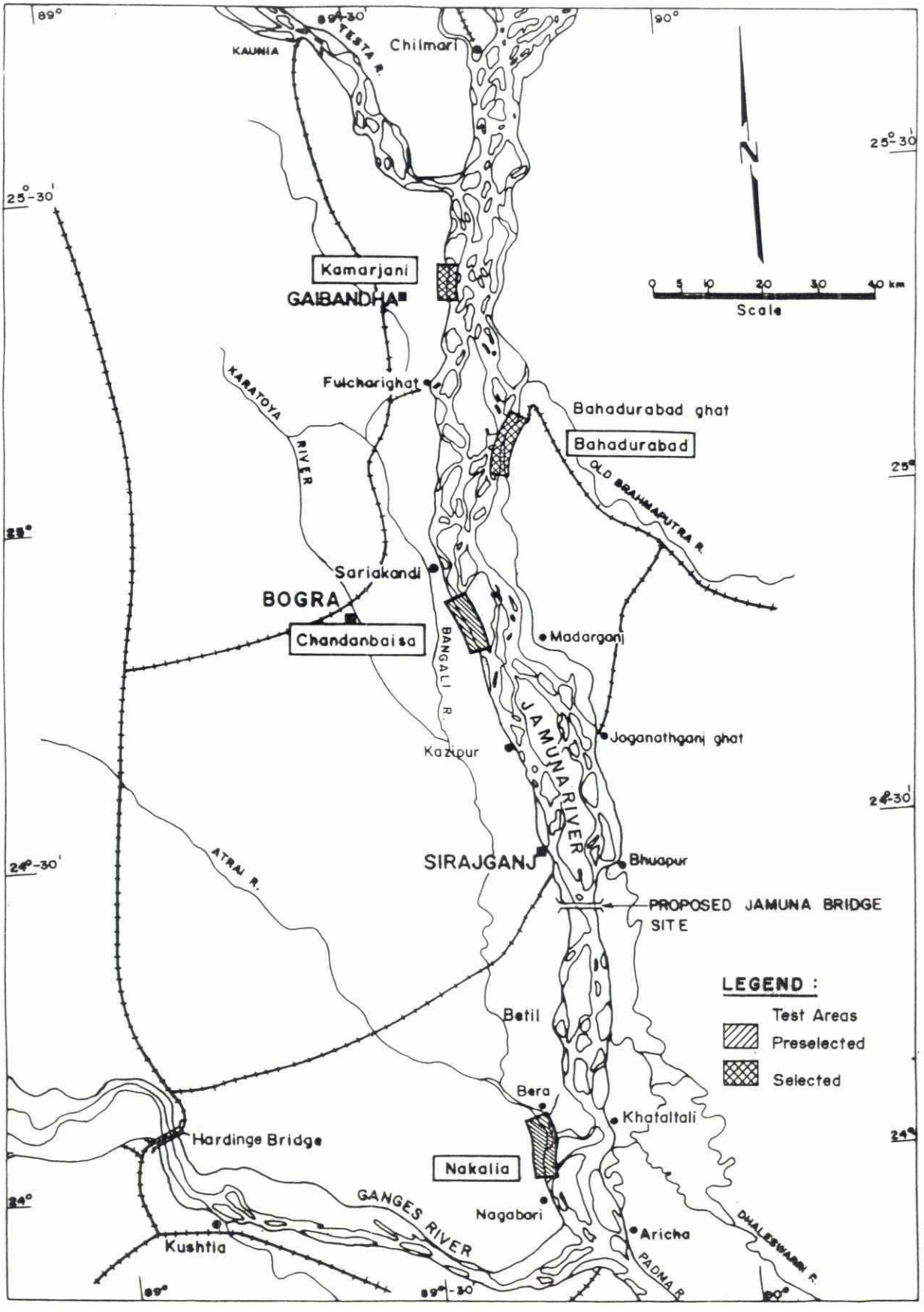
The full-scale drawings (size A 1) of all surveys are not attached to this Annex. They will remain with the Consultant as basis for tasks and follow-up works of the future project phases (e.g. detailed topographical and cadastral surveys for the Test and Implementation Phase).

Co-ordinate figures in this Annex are given in tentative BTM terms. It is recommended (see Subsection 4.4.2) to connect the pillars of the test sites to FM GPS control stations of FAP 18 in connection with future surveys, when co-ordinates of these points are available, and to adjust the tentative BTM figures, if required.

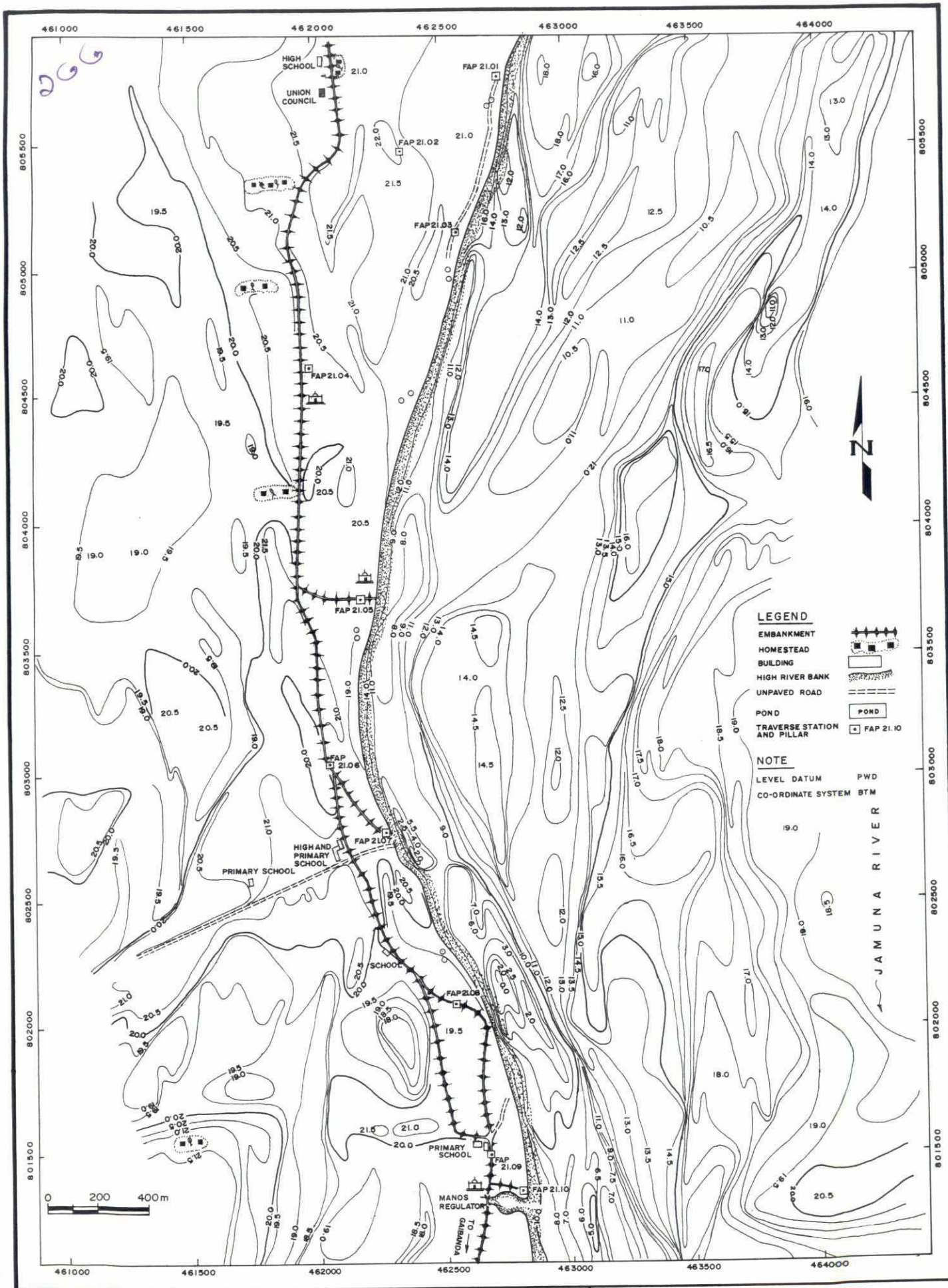
All elevations are related to PWD datum which is 0.46 m above SOB datum.

Co-ordinate figures in this Annex are given in tentative BTM terms. It is recommended (see Subsection 4.4.2) to connect the pillars of the test sites to FM GPS control stations of FAP 18 in connection with future surveys, when co-ordinates of these points are available, and to adjust the tentative BTM figures, if required.

All elevations are related to PWD datum which is 0.46 m above SOB datum.



SURVEY OF TEST AREAS	**FAP - 21/22** BANK PROTECTION AND RIVER TRAINING / (AFPM) PILOT PROJECT
	FINAL REPORT | FIG. A.12 - 0



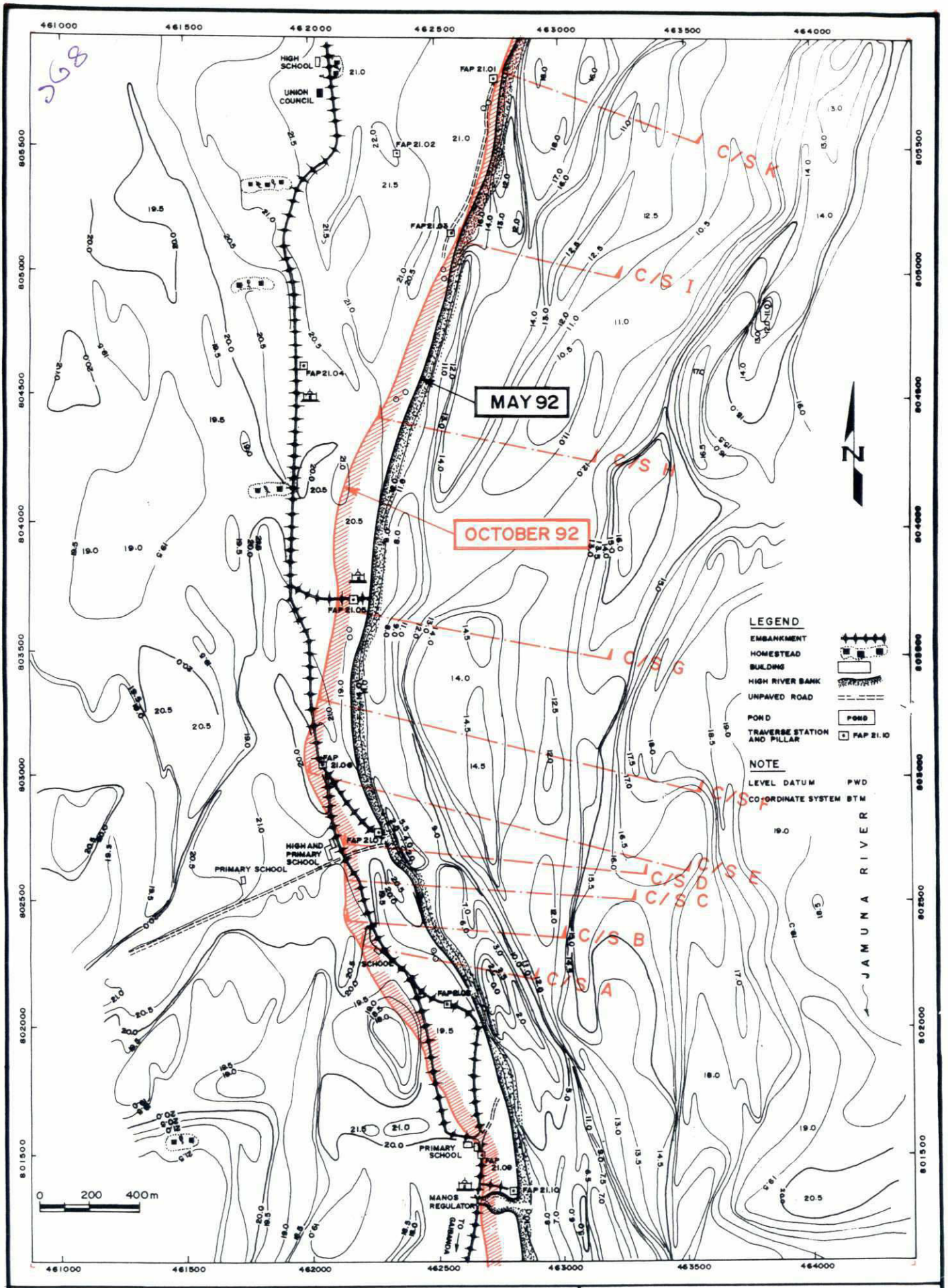
KAMARJANI
TOPOGRAPHIC AND HYDROGRAPIC SURVEY OF APRIL/MAY 1992
CONTOUR MAP

FAP – 21/22

BANK PROTECTION AND RIVER TRAINING/ (AFPM) PILOT PROJECT

FINAL REPORT

FIG. A.12–1



KAMARJANI

CHANGE OF BANKLINE
FROM MAY TO OCTOBER 1992
AND LOCATION OF CROSS SECTIONS

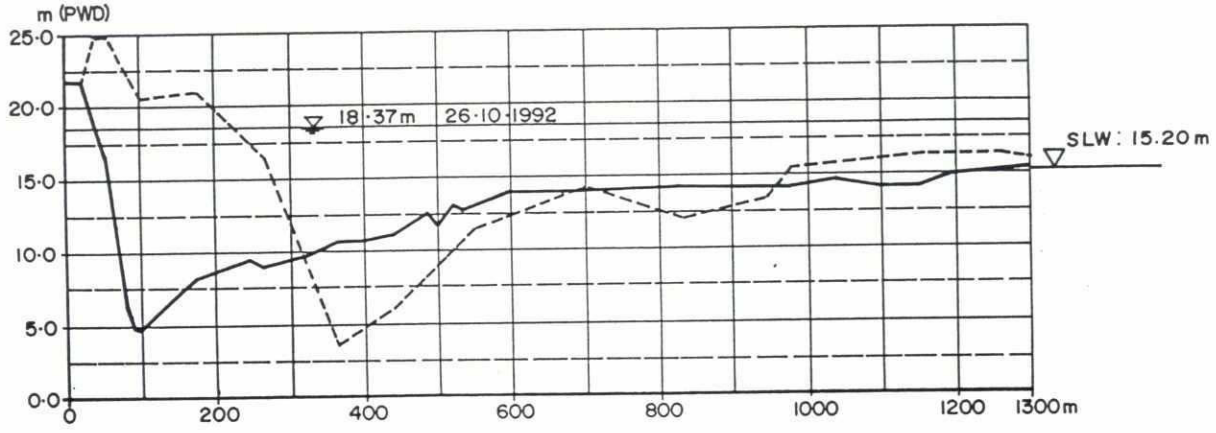
FAP – 21/22

BANK PROTECTION AND RIVER TRAINING/
(AFPM) PILOT PROJECT

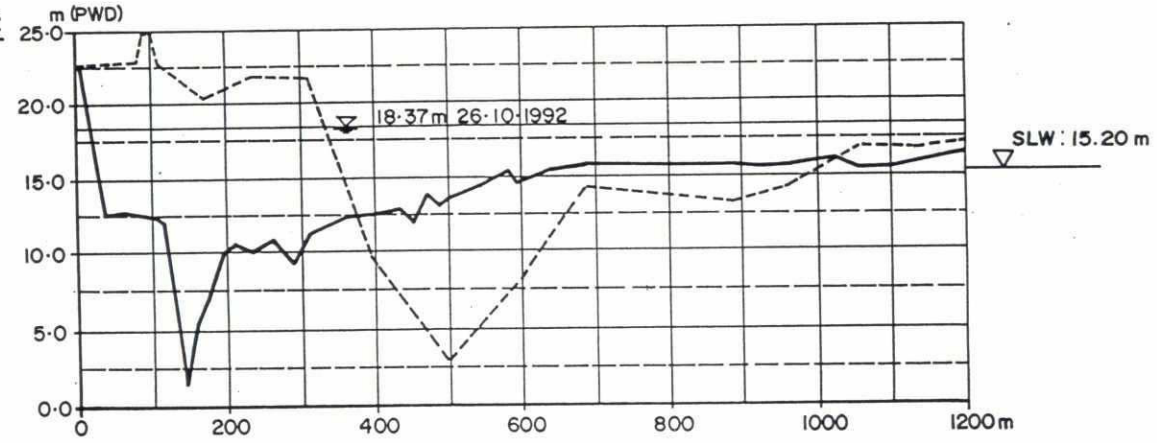
FINAL REPORT | FIG. A. 12–2

FIG. A. 12-2

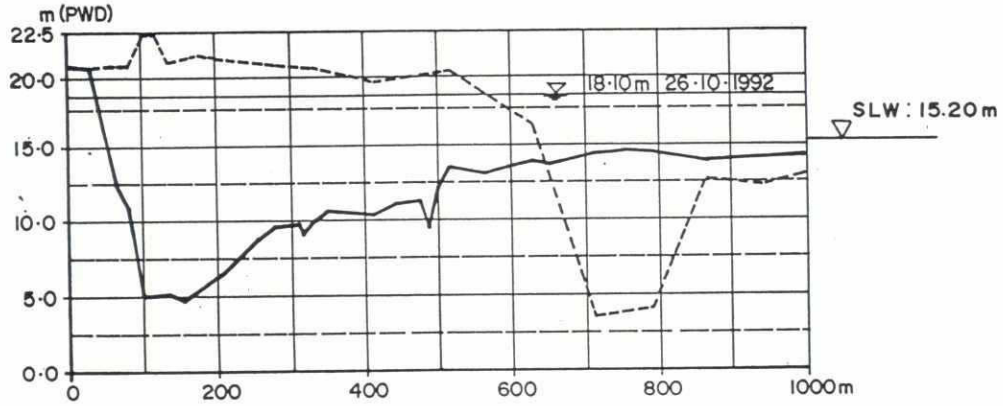
C/S D



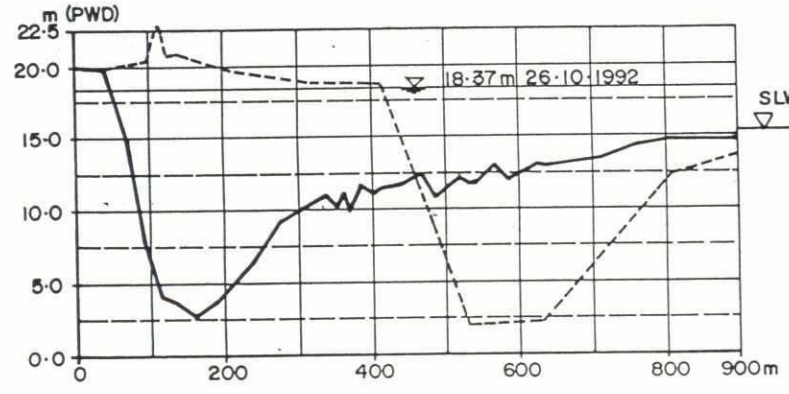
C/S C



C/S B



C/S A



LEGEND

------- MAY 1992

——— OCTOBER 1992

NOTE

LOCATION SEE FIG. A.12–2

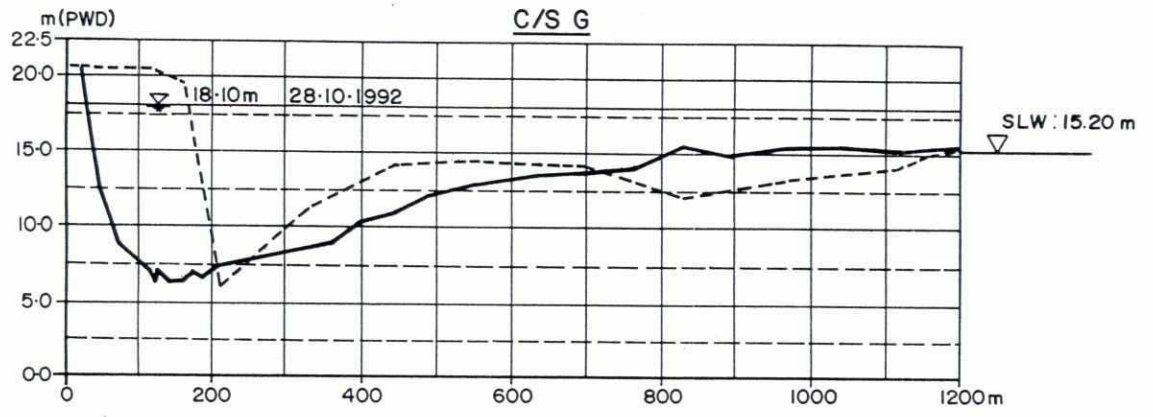
KAMARJANI

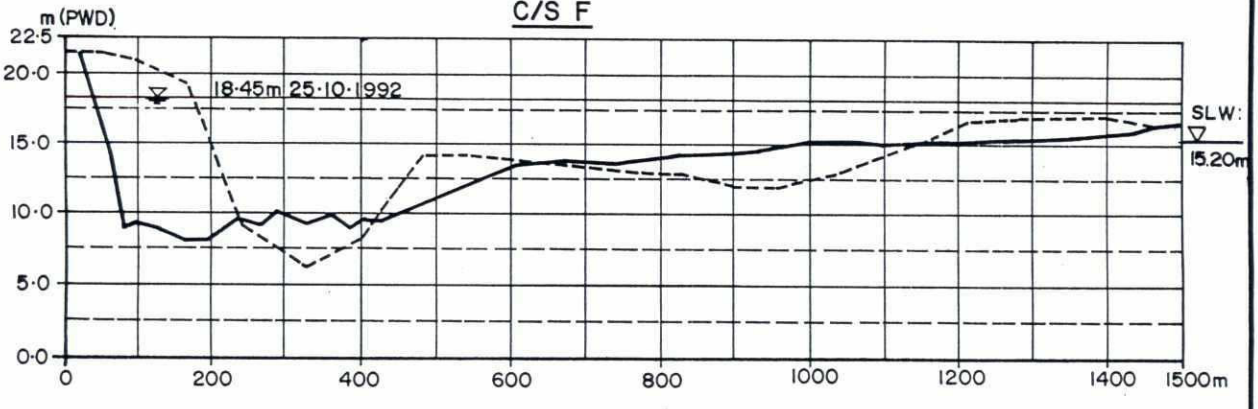
CHANGE OF RIVER BANK AND BED PROFILE
FROM MAY TO OCTOBER 1992

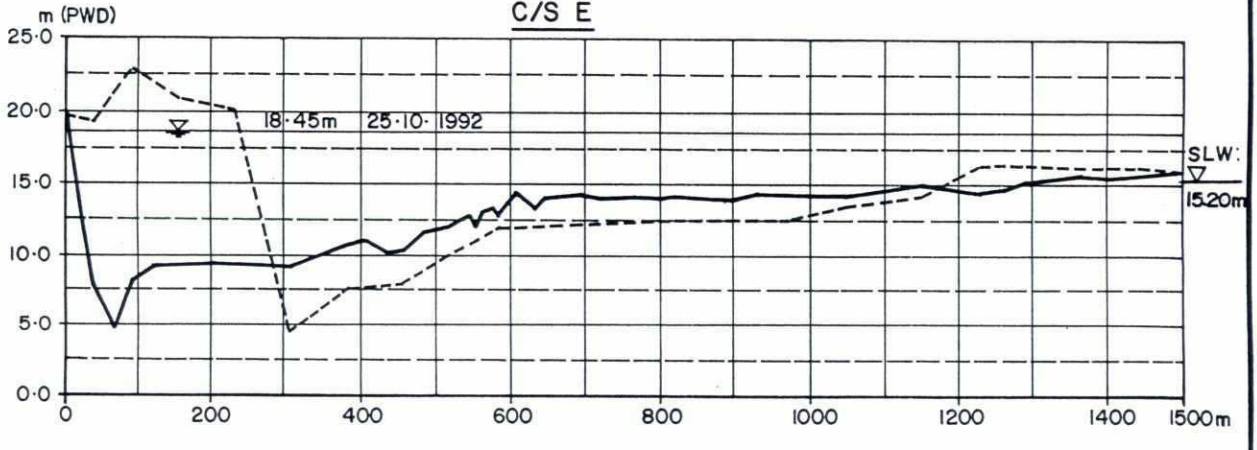
FAP — 21/22

BANK PROTECTION AND RIVER TRAINING/
(AFPM) PILOT PROJECT

FINAL REPORT | FIG. A. 12–3







LEGEND

------- MAY 1992

——— OCTOBER 1992

NOTE

LOCATION SEE FIG. A. 12 – 2

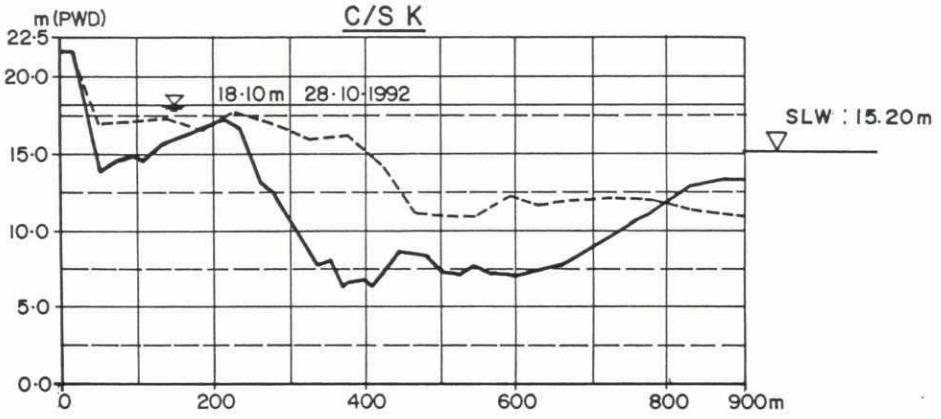
KAMARJANI

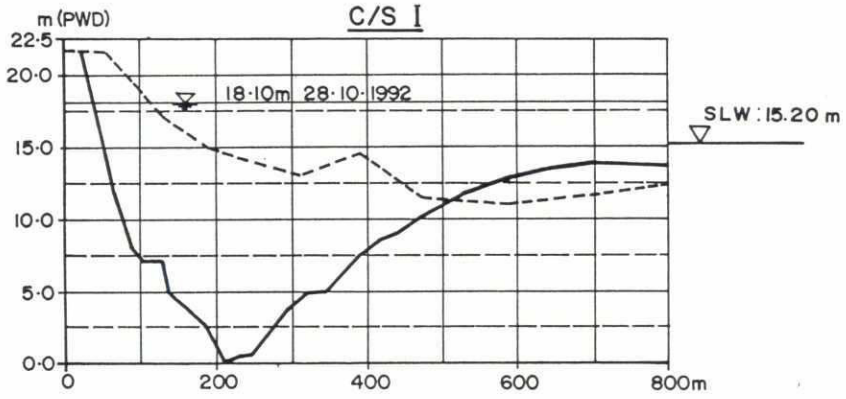
CHANGE OF RIVER BANK AND BED PROFILE
FROM MAY TO OCTOBER 1992

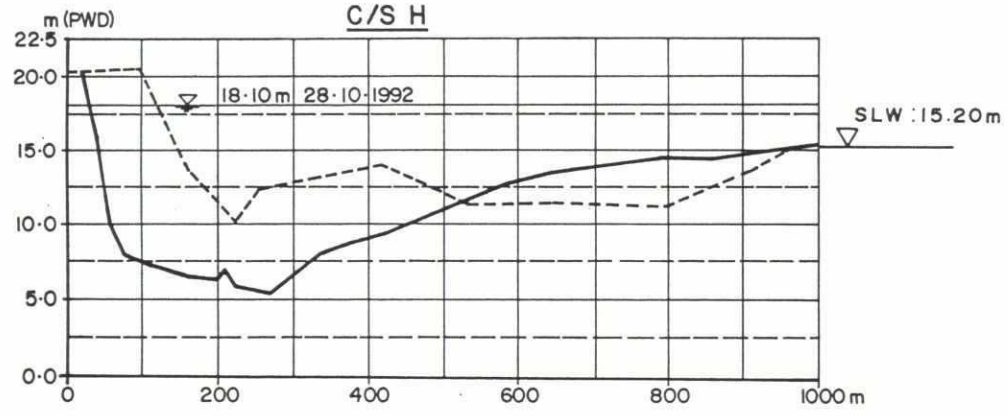
FAP – 21/22

BANK PROTECTION AND RIVER TRAINING/
(AFPM) PILOT PROJECT

FINAL REPORT | FIG. A. 12–4







LEGEND

------- MAY 1992

——— OCTOBER 1992

NOTE

LOCATION SEE FIG. A.12—2

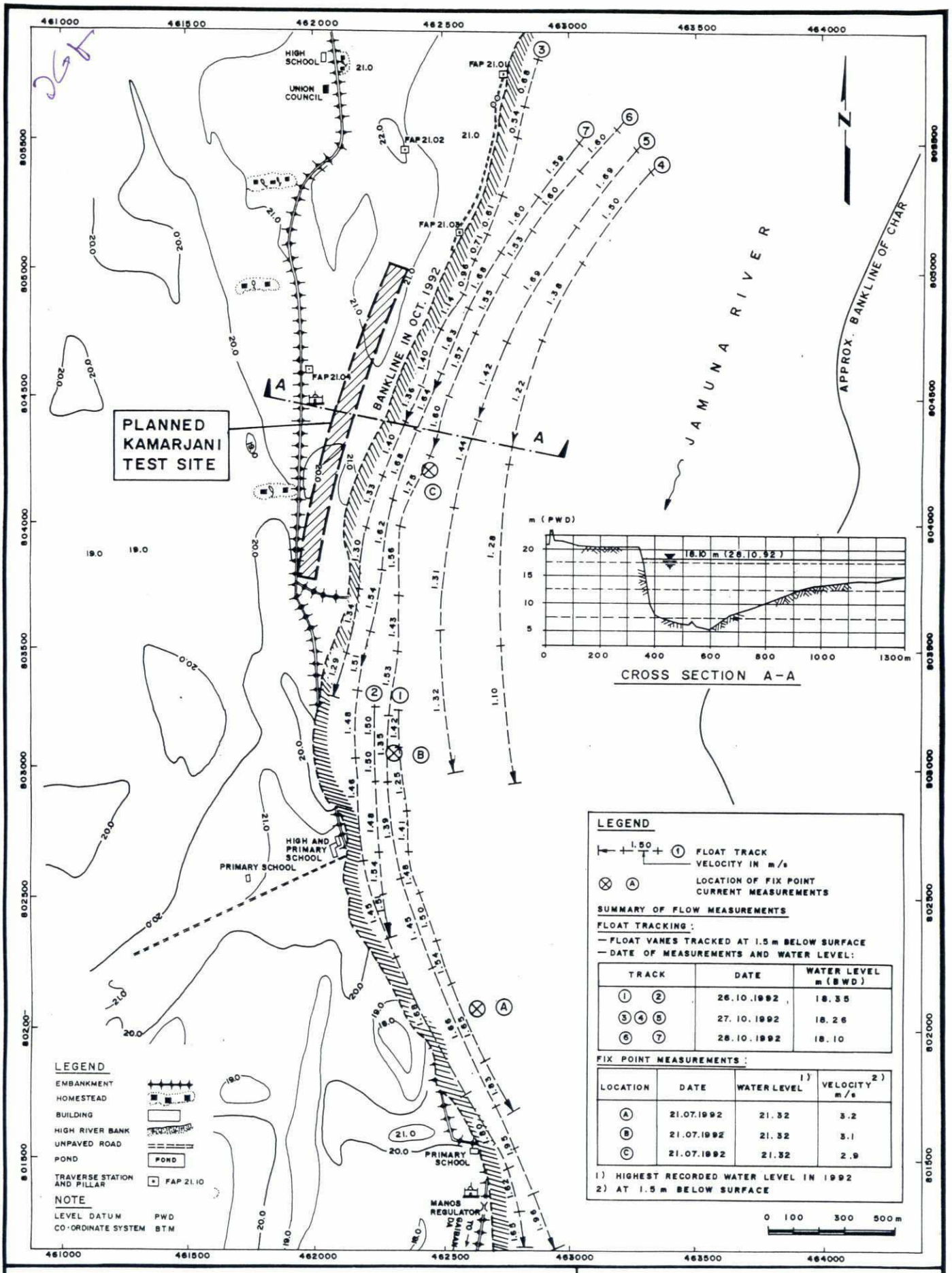
KAMARJANI

CHANGE OF RIVER BANK AND BED PROFILE
FROM MAY TO OCTOBER 1992

FAP — 21/22

BANK PROTECTION AND RIVER TRAINING/
(AFPM) PILOT PROJECT

FINAL REPORT | FIG. A.12—5



TRACK	DATE	WATER LEVEL m (PWD)
① ②	26.10.1992	18.35
③ ④ ⑤	27.10.1992	18.26
⑥ ⑦	28.10.1992	18.10

LOCATION	DATE	WATER LEVEL 1)	VELOCITY 2) m/s
Ⓐ	21.07.1992	21.32	3.2
Ⓑ	21.07.1992	21.32	3.1
Ⓒ	21.07.1992	21.32	2.9

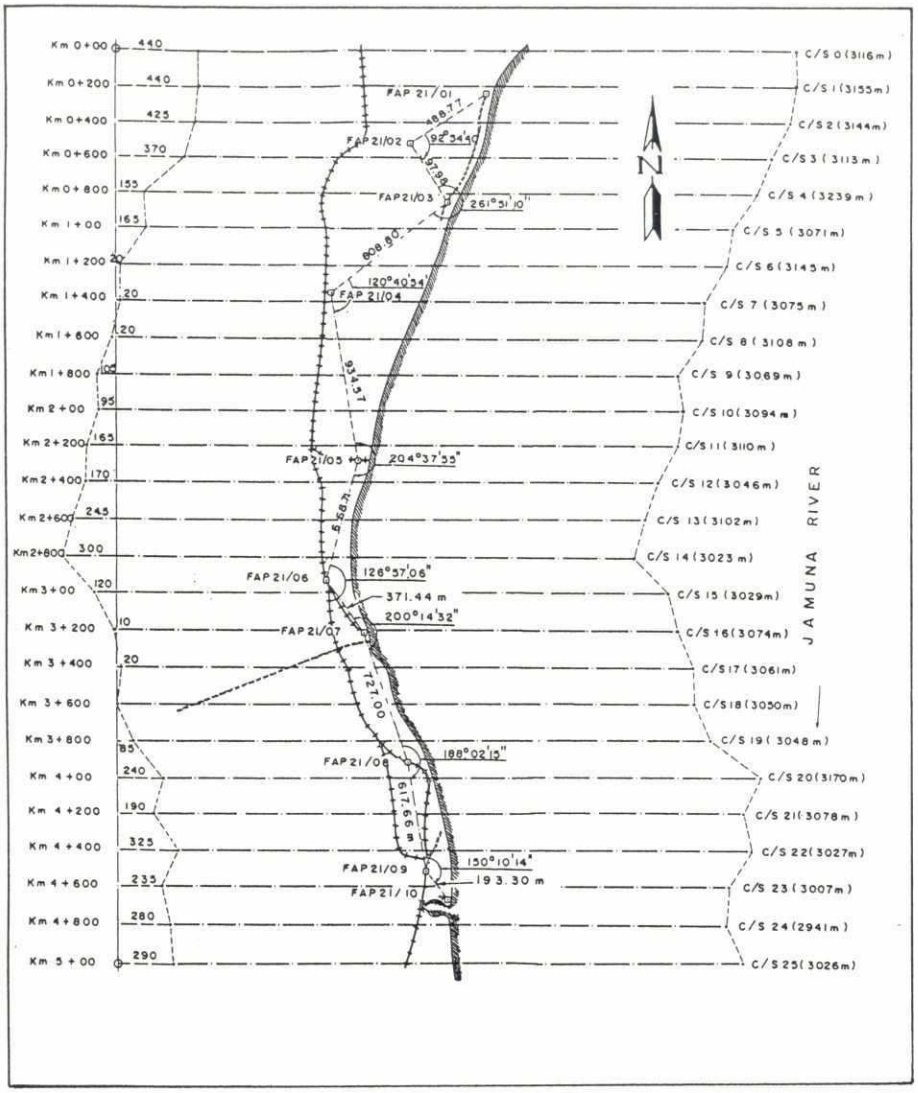
KAMARJANI

SAMPLE SURVEYS OF CURRENT VELOCITIES

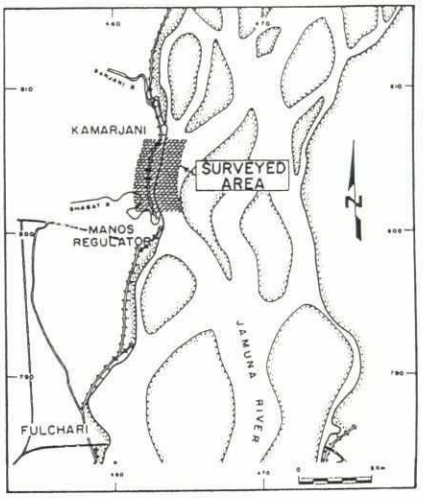
FAP – 21/22

BANK PROTECTION AND RIVER TRAINING / (AFPM) PILOT PROJECT

FINAL REPORT | FIG. A.12–6



LOCATION OF CROSS SECTIONS AND CONTROL POINTS



LOCATION OF SURVEY AREA

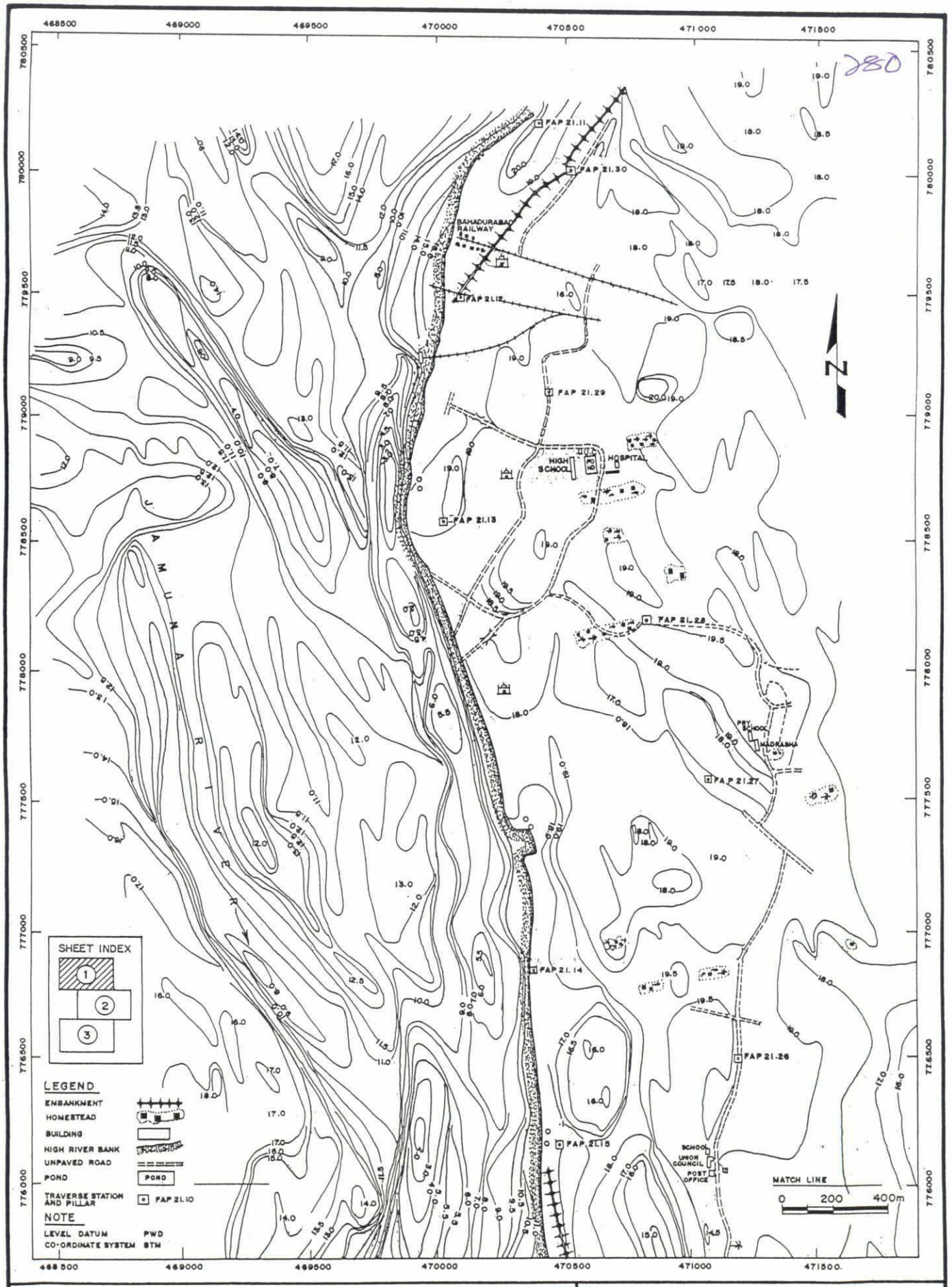
No. of Control Point	Co-ordinates (BTM)		Elevation m (PWD)
	Easting (m)	Northing (m)	
FAP 21.01	462,674.65	805,806.03	23.619
FAP 21.02	462,291.22	805,502.93	21.604
FAP 21.03	462,521.84	805,178.59	21.966
FAP 21.04	461,935.77	804,621.22	20.663
FAP 21.05	462,144.11	803,710.17	23.279
FAP 21.06	462,007.93	803,055.47	24.129
FAP 21.07	462,253.07	802,776.41	24.185
FAP 21.08	462,514.26	802,097.95	24.166
FAP 21.09	462,653.40	801,496.16	24.628
FAP 21.10	462,784.85	801,354.44	23.802
FMBM 7603	-	-	20.590
FMBM 7604	-	-	22.620
BMTS-416 at Manos Regulator	-	-	24.720

BTM CO-ORDINATES AND HEIGHTS (PWD)
OF CONTROL POINTS

KAMARJANI
BASIC SURVEY DATA
(SURVEYED APRIL / MAY 1992)

FAP – 21/22
BANK PROTECTION AND RIVER TRAINING/
(AFPM) PILOT PROJECT

FINAL REPORT | FIG. A.12 – 7

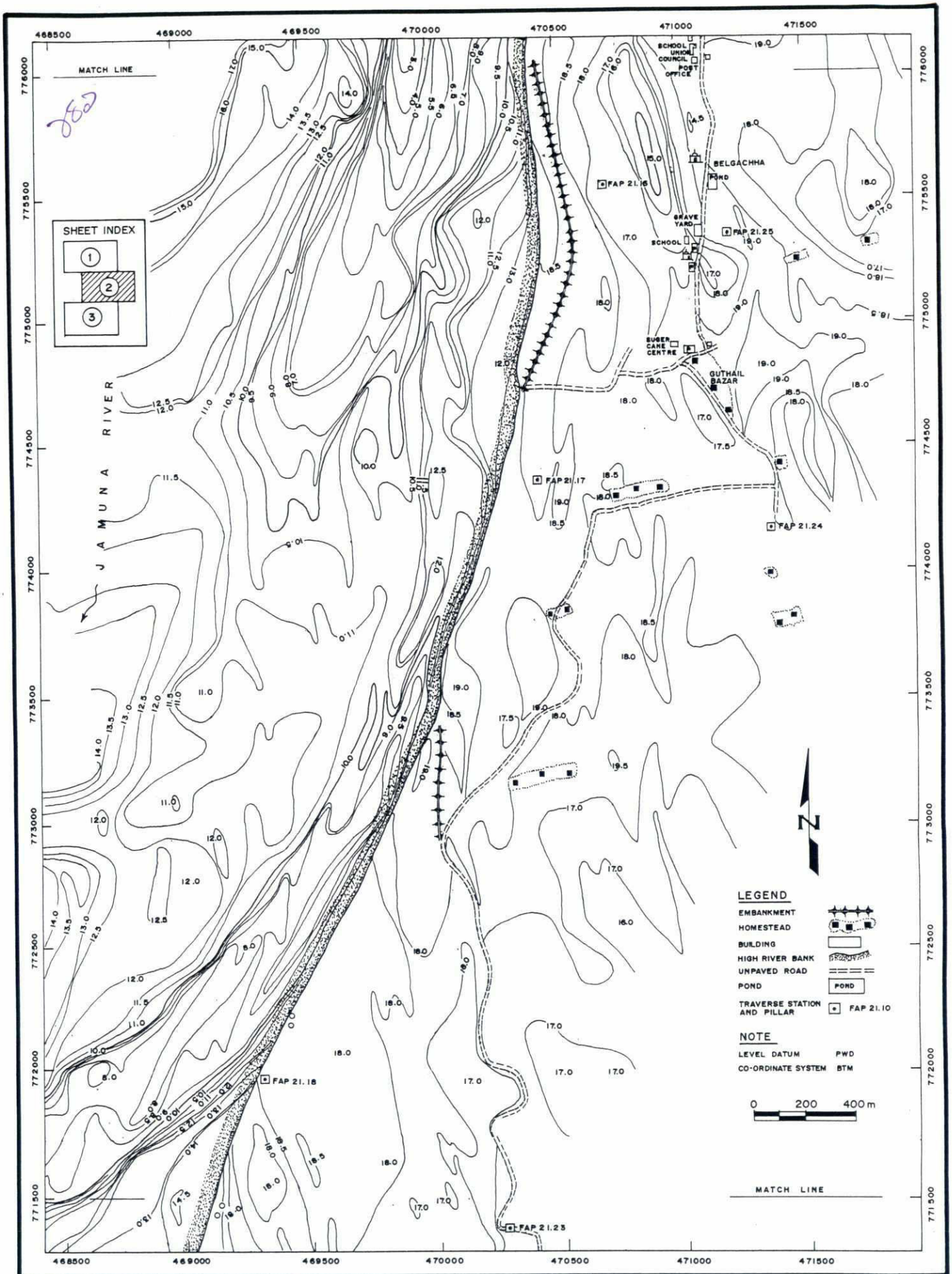


BAHADURABAD
TOPOGRAPHIC AND HYDROGRAPIC SURVEY OF APRIL / MAY 1992
CONTOUR MAP

FAP - 21/22

BANK PROTECTION AND RIVER TRAINING/ (AFPM) PILOT PROJECT

FINAL REPORT | FIG. A.12 - 8



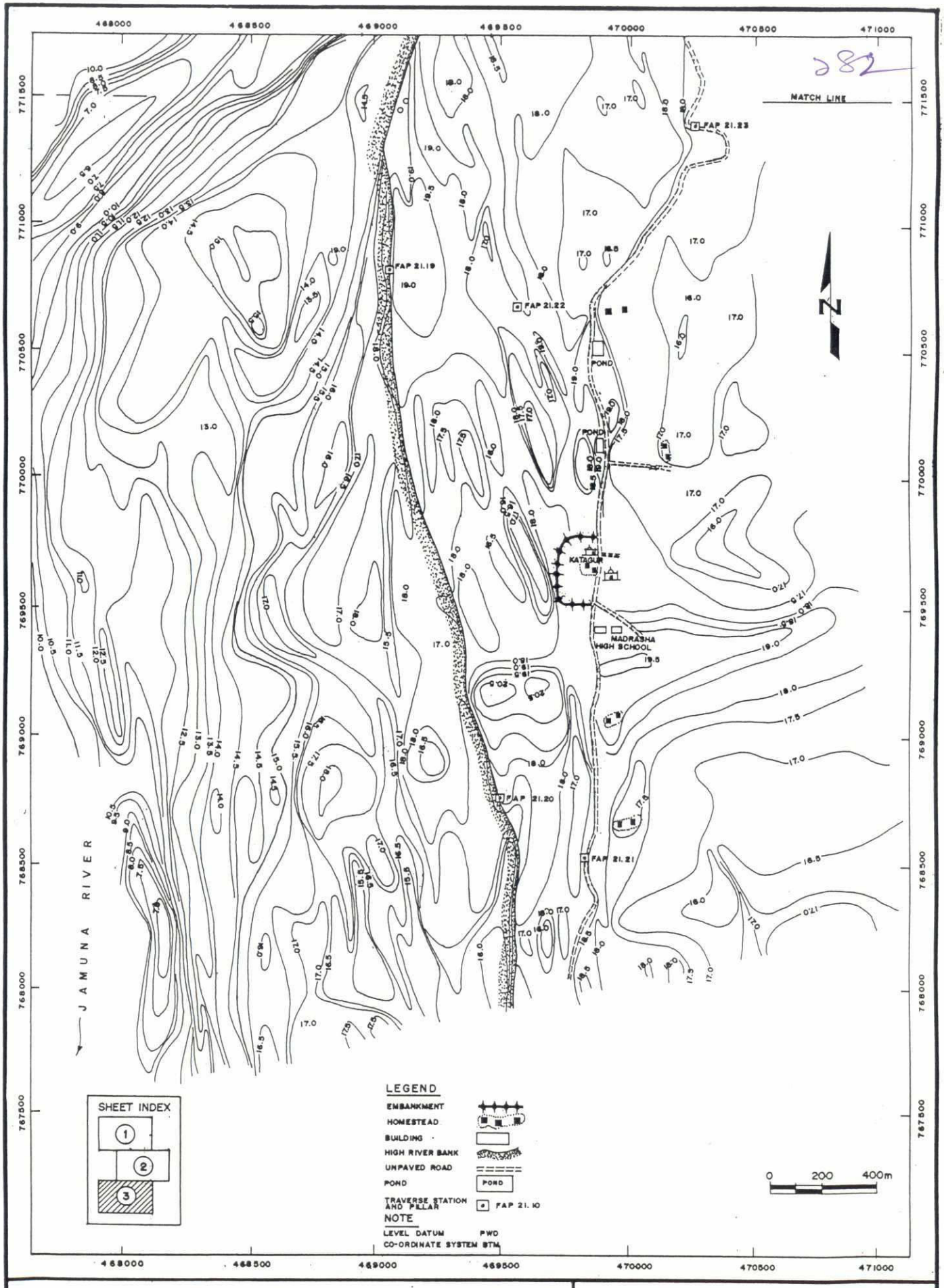
BAHADURABAD

TOPOGRAPHIC AND HYDROGRAPIC SURVEY OF APRIL / MAY 1992 CONTOUR MAP

FAP - 21/22

BANK PROTECTION AND RIVER TRAINING/ (AFPM) PILOT PROJECT

FINAL REPORT | FIG. A.12 - 9

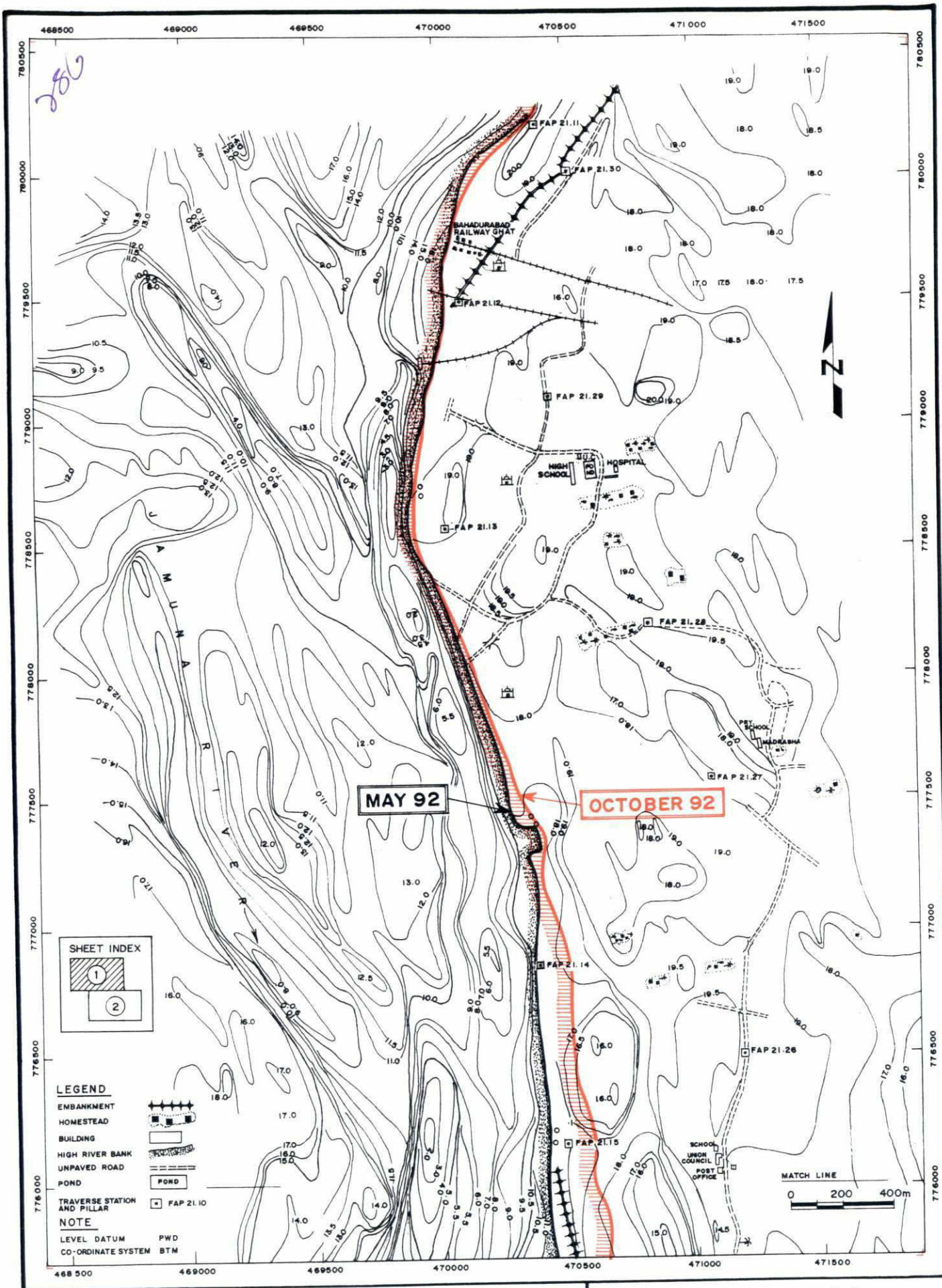


BAHADURABAD
TOPOGRAPHIC AND HYDROGRAPIC SURVEY OF APRIL / MAY 1992
CONTOUR MAP

FAP - 21/22

BANK PROTECTION AND RIVER TRAINING / (AFPM) PILOT PROJECT

FINAL REPORT | FIG. A.12-10



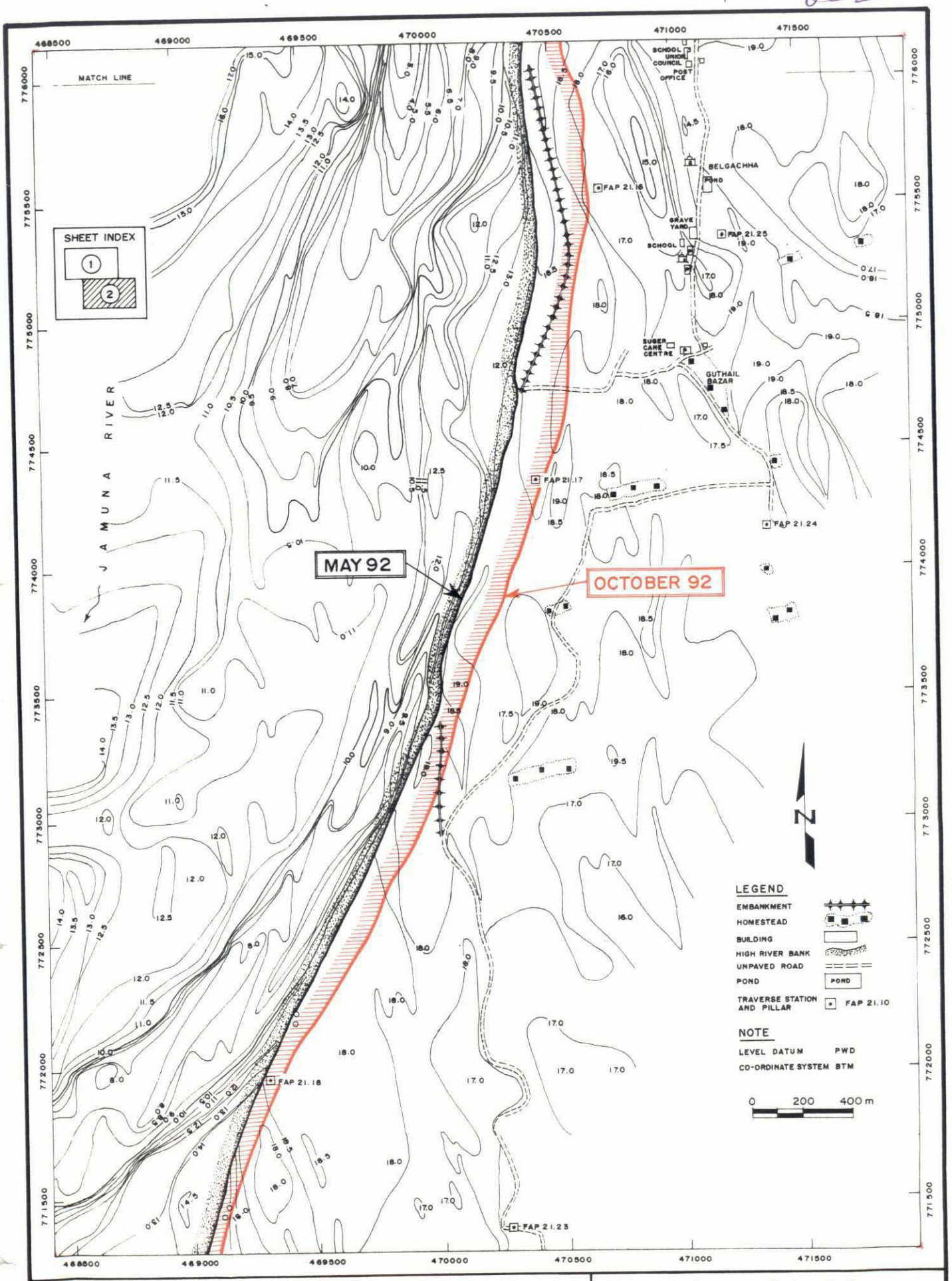
BAHADURABAD
CHANGE OF BANKLINE FROM MAY TO OCTOBER 1992 NORTHERN STRETCH

FAP - 21/22

BANK PROTECTION AND RIVER TRAINING/ (AFPM) PILOT PROJECT

FINAL REPORT

FIG. A.12-11



BAHADURABAD

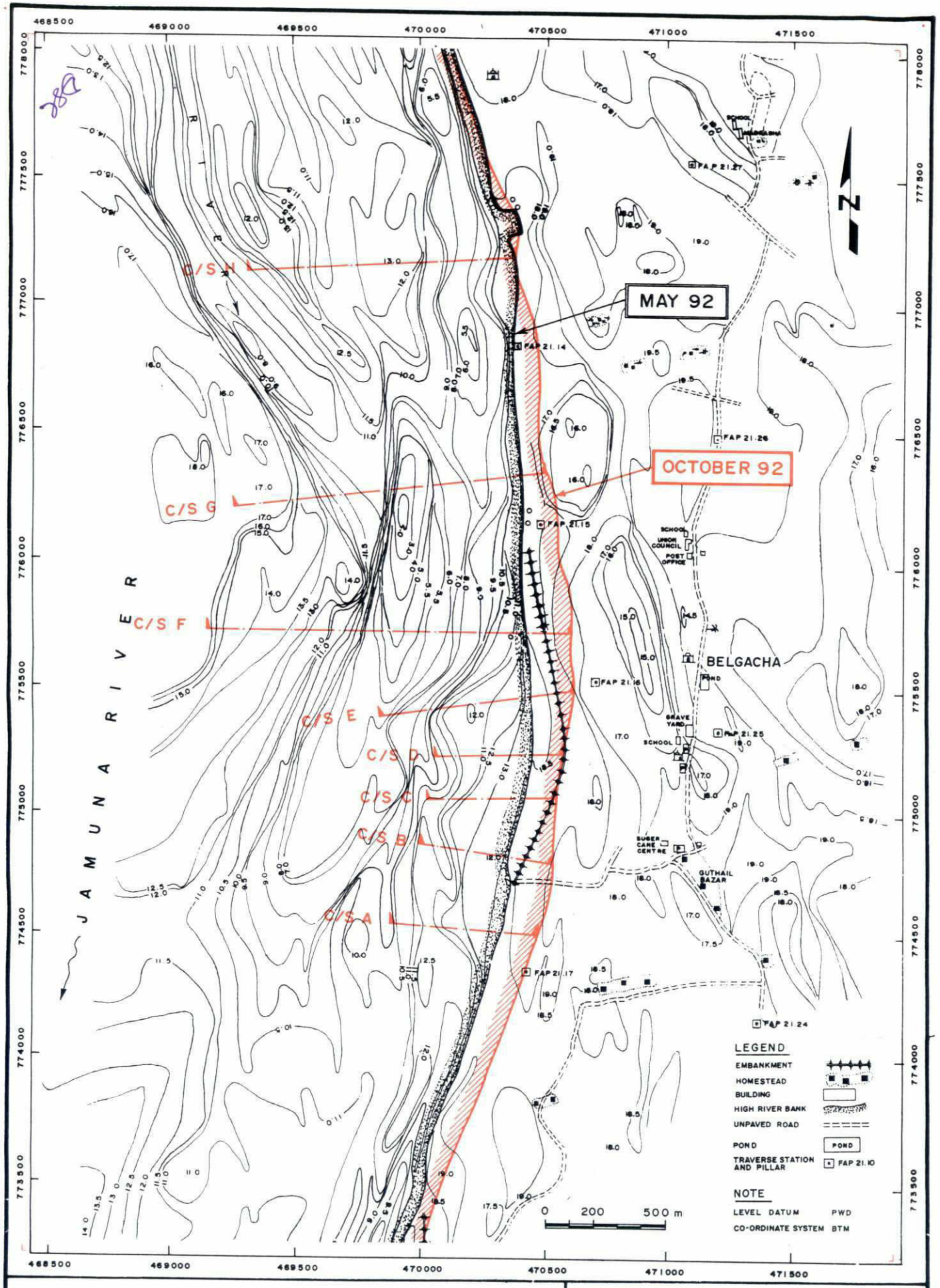
CHANGE OF BANKLINE FROM MAY TO OCTOBER 1992 SOUTHERN STRETCH

FAP - 21/22

BANK PROTECTION AND RIVER TRAINING/ (AFPM) PILOT PROJECT

FINAL REPORT | FIG. A.12-12

FIG. A 12-12



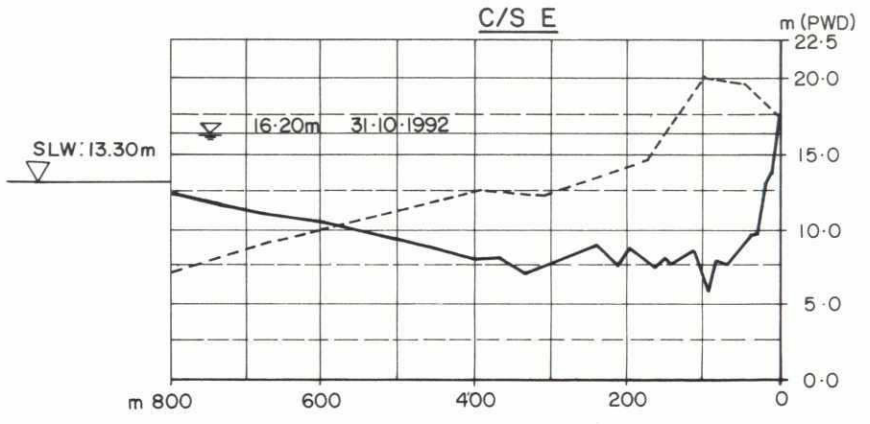
BAHADURABAD

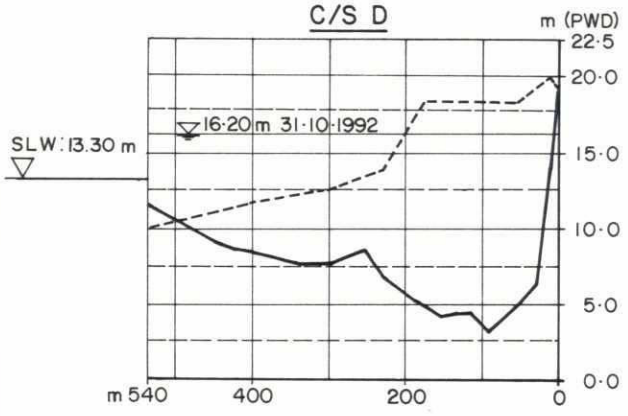
CHANGE OF BANKLINE NEAR TEST SITE
FROM MAY TO OCTOBER 1992
AND LOCATION OF CROSS SECTIONS

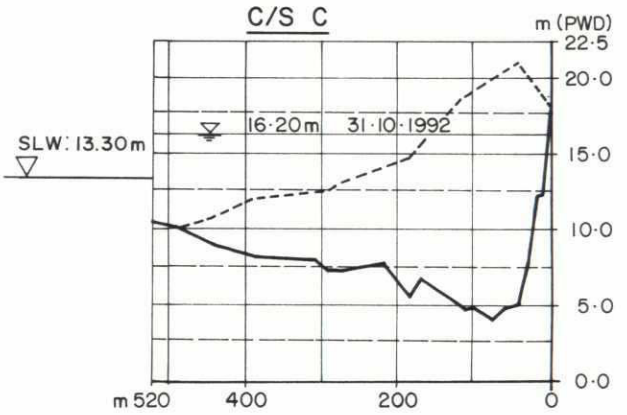
FAP - 21/22

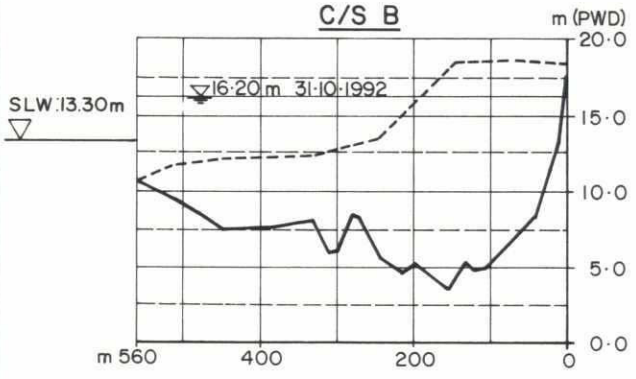
BANK PROTECTION AND RIVER TRAINING/
(AFPM) PILOT PROJECT

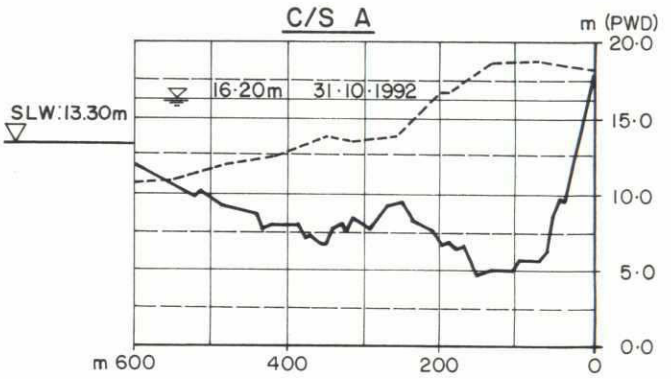
FINAL REPORT | FIG. A.12-13











LEGEND

------- MAY 1992

——— OCTOBER 1992

NOTE

LOCATION SEE FIG. A.12-13

BAHADURABAD

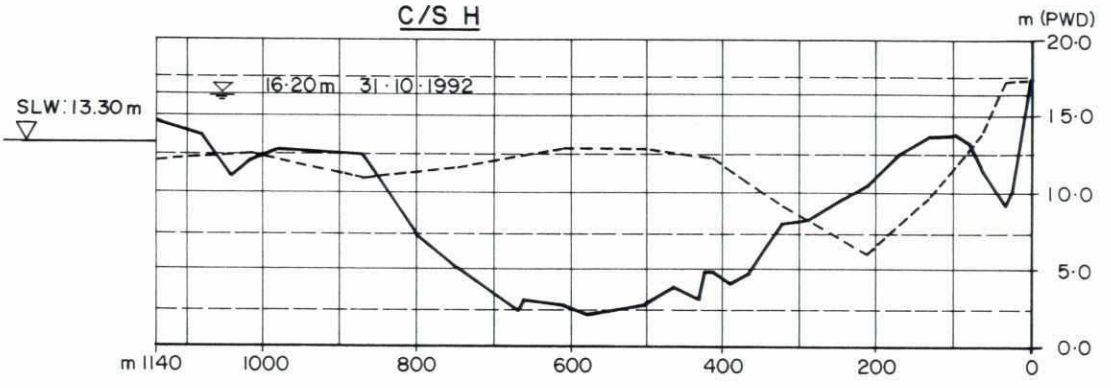
CHANGE OF RIVER BANK AND BED PROFILE FROM MAY TO OCTOBER 1992

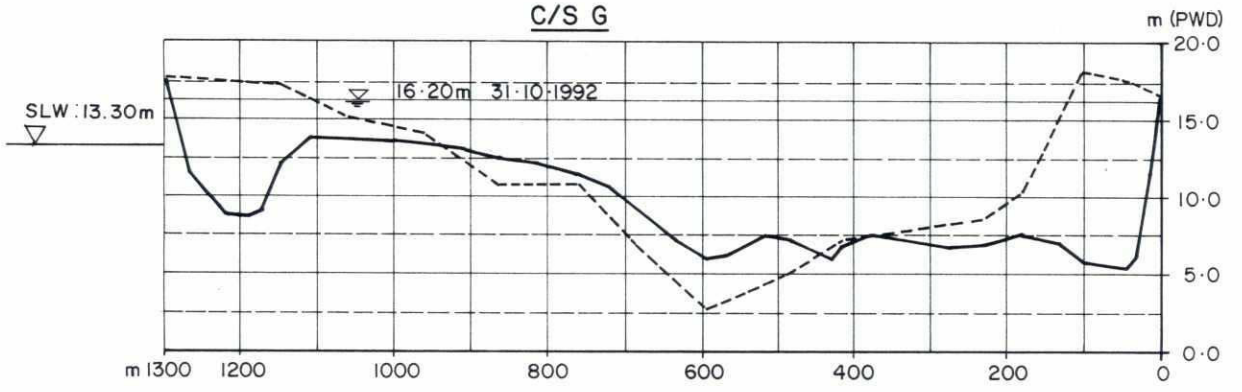
FAP — 21/22

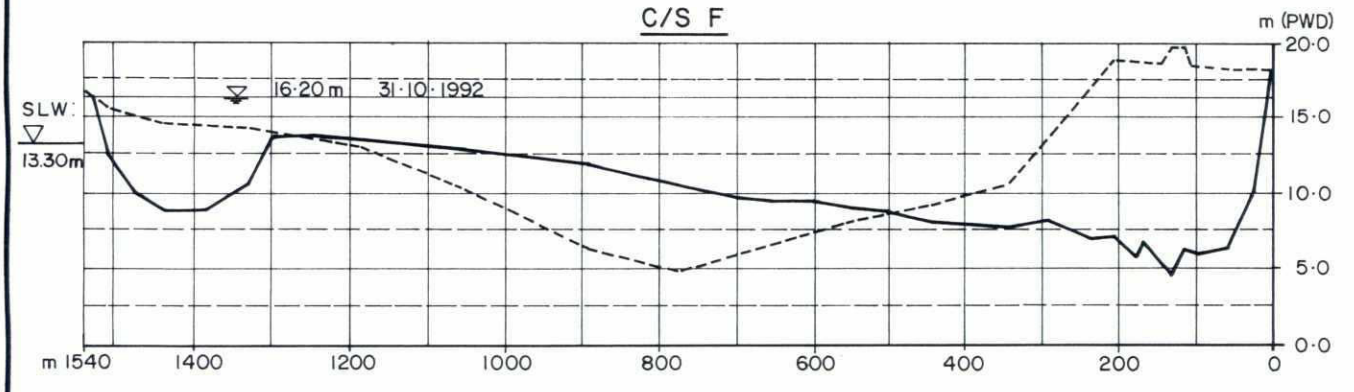
BANK PROTECTION AND RIVER TRAINING/ (AFPM) PILOT PROJECT

FINAL REPORT

FIG. A.12-14







LEGEND

------- MAY 1992

——— OCTOBER 1992

NOTE

LOCATION SEE FIG. A.12-13

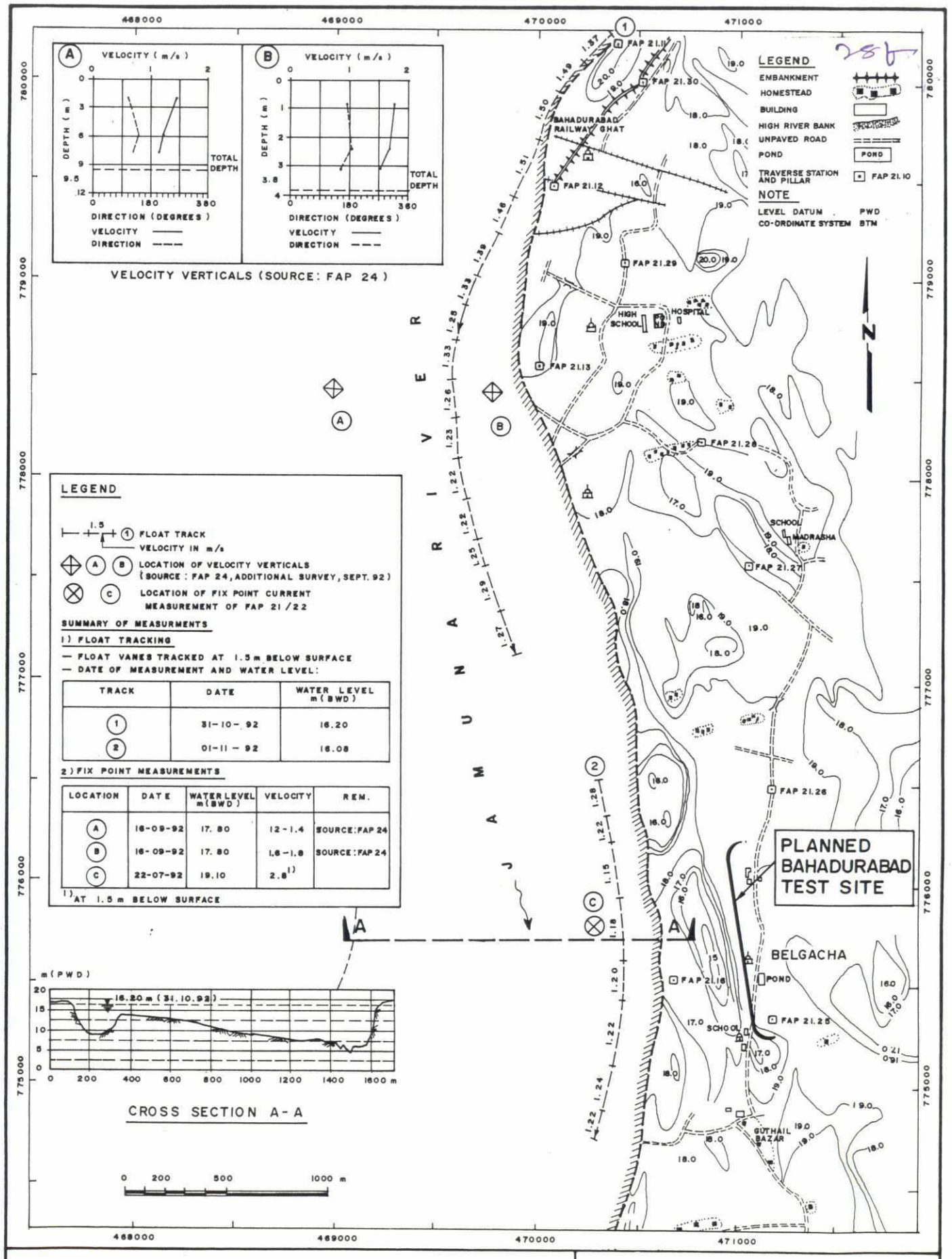
BAHADURABAD

CHANGE OF RIVER BANK AND BED PROFILE
FROM MAY TO OCTOBER 1992

FAP — 21/22

BANK PROTECTION AND RIVER TRAINING/
(AFPM) PILOT PROJECT

FINAL REPORT | FIG. A.12-15

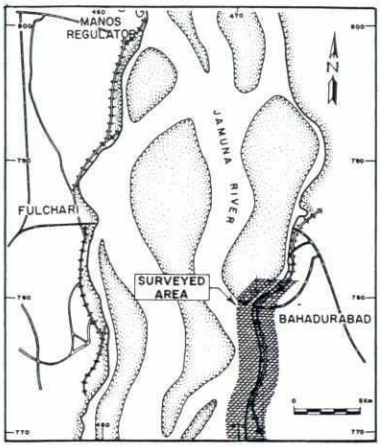


BAHADURABAD
SAMPLE SURVEYS OF CURRENT VELOCITIES

FAP – 21/22

BANK PROTECTION AND RIVER TRAINING / (AFPM) PILOT PROJECT

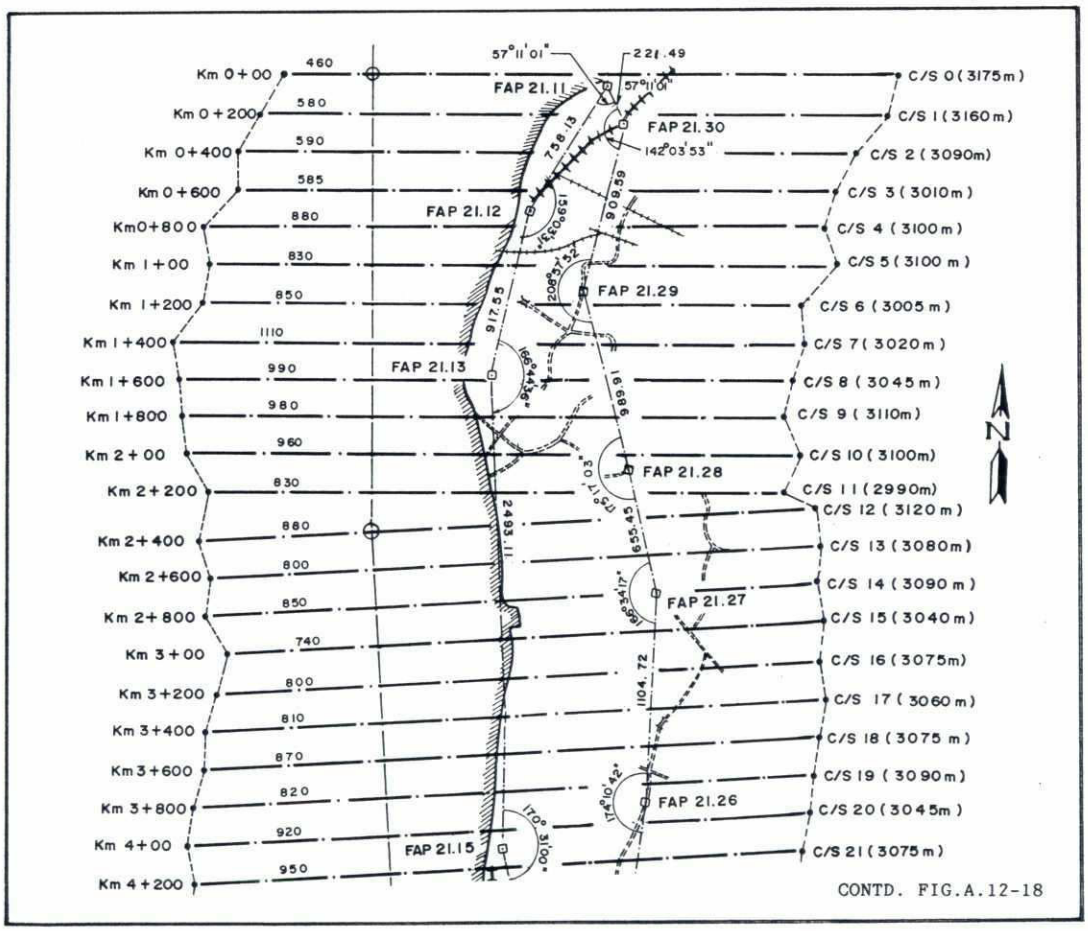
FINAL REPORT | FIG. A.12-16



LOCATION OF SURVEY AREA

No. of Control Point	Co-ordinates (BTM)		Elevation m (PWD)
	Easting (m)	Northing (m)	
FAP 21.11	470,606.09	780,117.04	20.055
FAP 21.12	470,286.58	779,429.53	20.853
FAP 21.13	470,222.82	778,514.20	19.056
FAP 21.15	470,624.51	776,053.66	18.898
FAP 21.16	470,830.15	775,448.04	18.266
FAP 21.17	470,534.65	774,261.16	18.760
FAP 21.18	469,359.43	771,929.79	18.549
FAP 21.19	469,090.25	770,741.10	19.557
FAP 21.20	469,436.73	768,672.92	18.439
FAP 21.21	469,780.20	768,424.28	20.368
FAP 21.22	469,584.85	770,588.74	19.294
FAP 21.23	470,308.70	771,294.10	19.511
FAP 21.24	471,457.13	774,064.67	20.101
FAP 21.25	471,319.71	775,238.02	19.228
FAP 21.26	471,333.41	776,393.75	21.047
FAP 21.27	471,234.40	777,494.02	19.923
FAP 21.28	471,025.65	778,115.34	20.139
FAP 21.29	470,634.32	779,024.61	20.763
FAP 21.30	470,724.31	779,929.74	21.909
FMGPS 764	-	-	20.310
FMBM 5244	-	-	19.850
FMBM 5215	-	-	19.060

BTM CO-ORDINATES AND HEIGHTS (PWD)
OF CONTROL POINTS



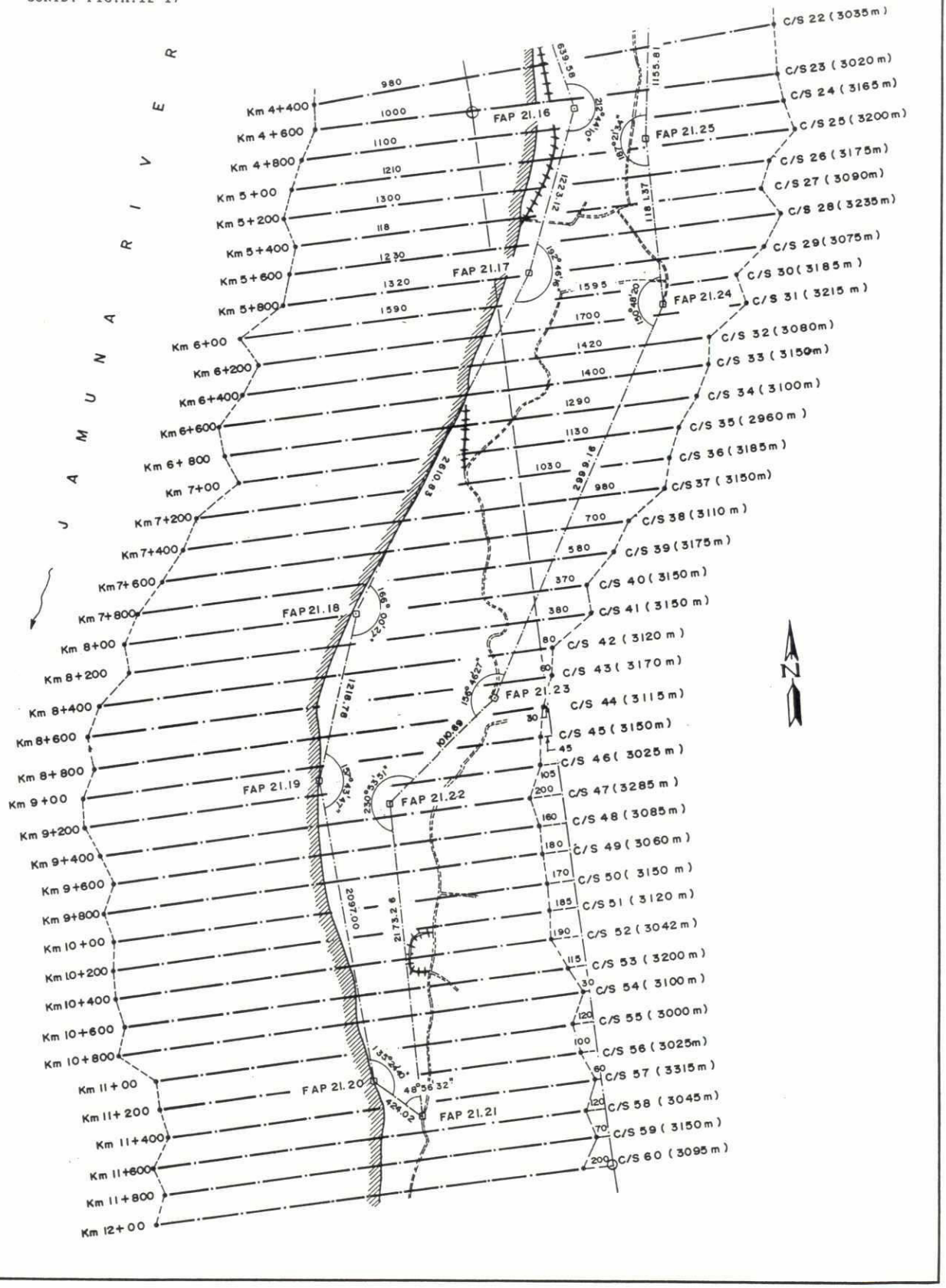
LOCATION OF CROSS SECTIONS AND CONTROL POINTS

BAHADURABAD
BASIC SURVEY DATA
(SURVEYED APRIL / MAY 1992)

FAP – 21/22
BANK PROTECTION AND RIVER TRAINING / (AFPM) PILOT PROJECT

FINAL REPORT | FIG. A. 12 - 17

CONTD. FIG.A.12-17

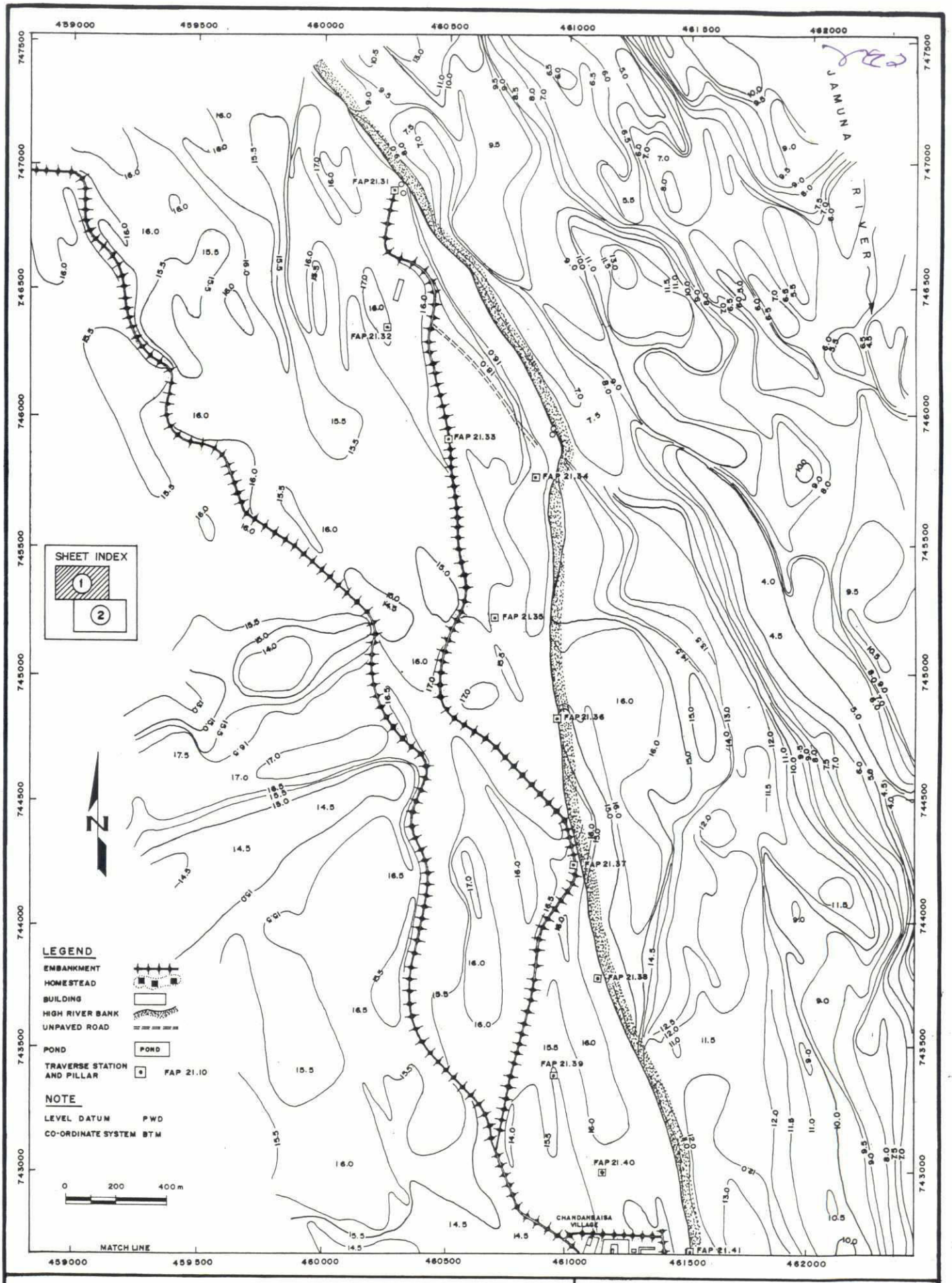


LOCATION OF CROSS SECTIONS AND CONTROL POINTS

BAHADURABAD
BASIC SURVEY DATA
(SURVEYED APRIL / MAY 1992)

FAP – 21/22
BANK PROTECTION AND RIVER TRAINING / (AFPM) PILOT PROJECT

FINAL REPORT | FIG. A. 12-18

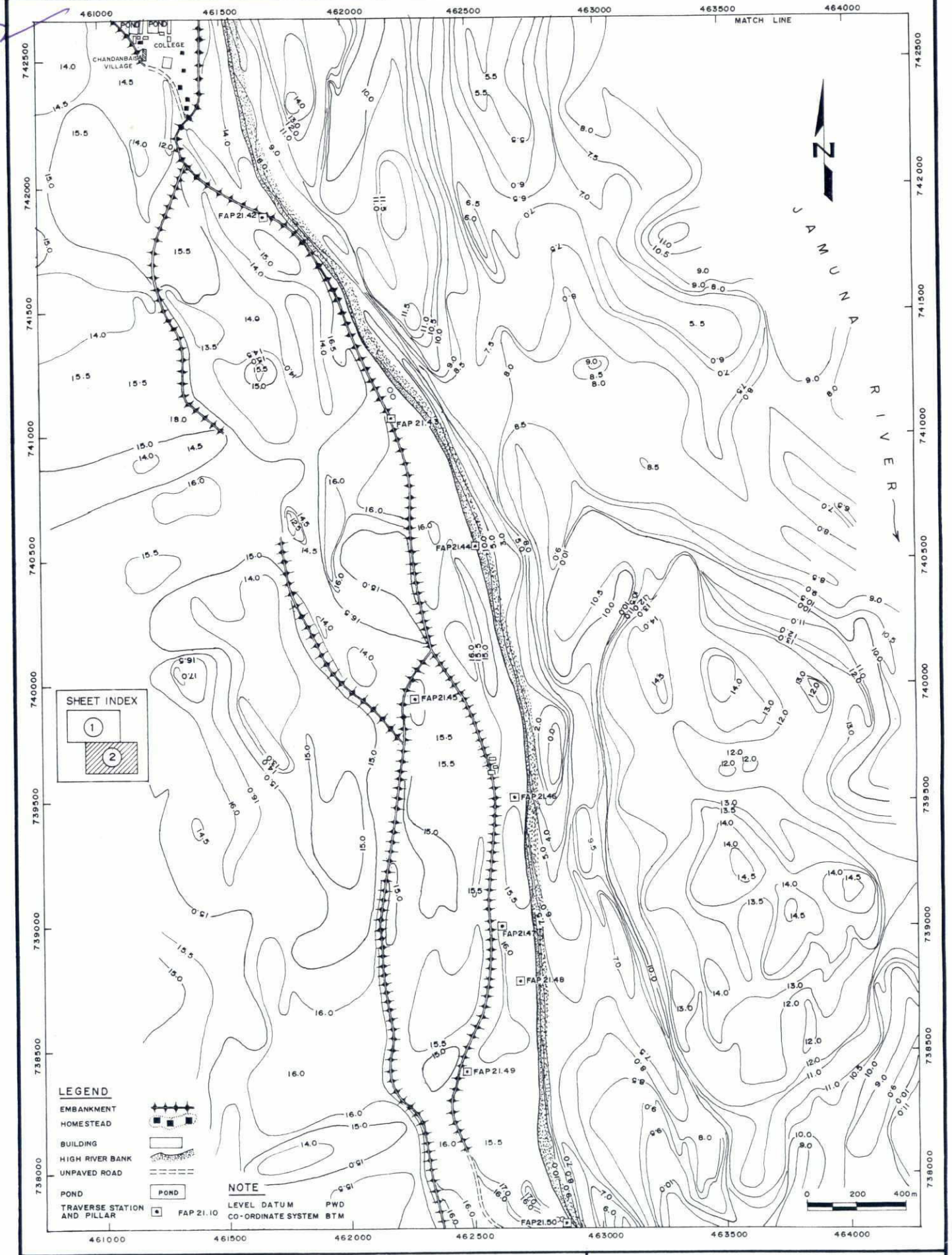


CHANDANBAISA
TOPOGRAPHIC AND HYDROGRAPIC SURVEY OF APRIL / MAY 1992
CONTOUR MAP

FAP – 21/22

BANK PROTECTION AND RIVER TRAINING/ (AFPM) PILOT PROJECT

FINAL REPORT | FIG. A. 12–19

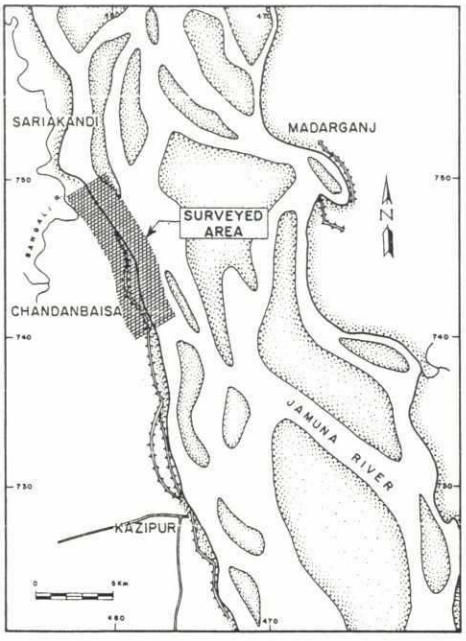


CHANDANBAISA
TOPOGRAPHIC AND HYDROGRAPIC SURVEY OF APRIL / MAY 1992
CONTOUR MAP

FAP - 21/22

BANK PROTECTION AND RIVER TRAINING/ (AFPM) PILOT PROJECT

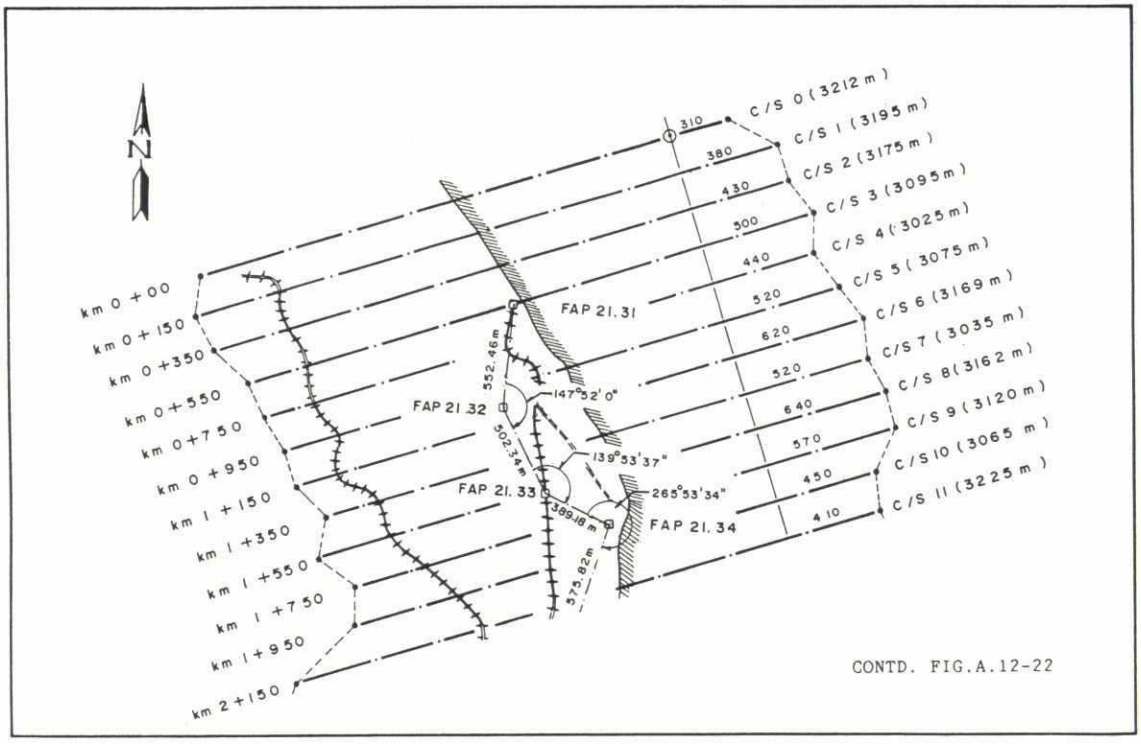
FINAL REPORT | FIG. A.12—20



LOCATION OF SURVEY AREA

No. of Control Point	Co-ordinates (BTM)		Elevation m (PWD)
	Easting (m)	Northing (m)	
FAP 21.31	460,193.68	746,857.19	18.349
FAP 21.32	460,168.94	746,305.29	16.537
FAP 21.33	460,416.83	745,868.36	19.738
FAP 21.34	460,781.75	745,733.16	17.761
FAP 21.35	460,620.19	745,180.26	15.877
FAP 21.36	460,869.21	744,796.98	17.164
FAP 21.37	460,965.54	744,205.47	18.860
FAP 21.38	461,061.80	743,771.99	16.823
FAP 21.39	460,897.33	743,354.30	15.866
FAP 21.40	461,102.24	742,972.20	16.367
FAP 21.41	461,450.01	742,652.28	16.340
FAP 21.42	461,613.48	741,863.78	18.902
FAP 21.43	462,147.49	741,035.82	18.818
FAP 21.44	462,449.49	740,537.00	16.097
FAP 21.45	462,238.12	739,917.55	16.225
FAP 21.46	462,647.28	739,519.64	17.341
FAP 21.47	462,600.29	738,999.64	15.222
FAP 21.48	462,670.64	738,791.34	15.819
FAP 21.49	462,448.55	738,416.28	15.995
FAP 21.50	462,860.42	737,803.92	16.524
FMGPS 750	-	-	16.380
FMBM 7214	-	-	16.260

BTM CO-ORDINATES AND HEIGHTS (PWD)
OF CONTROL POINTS



CONTD. FIG.A.12-22

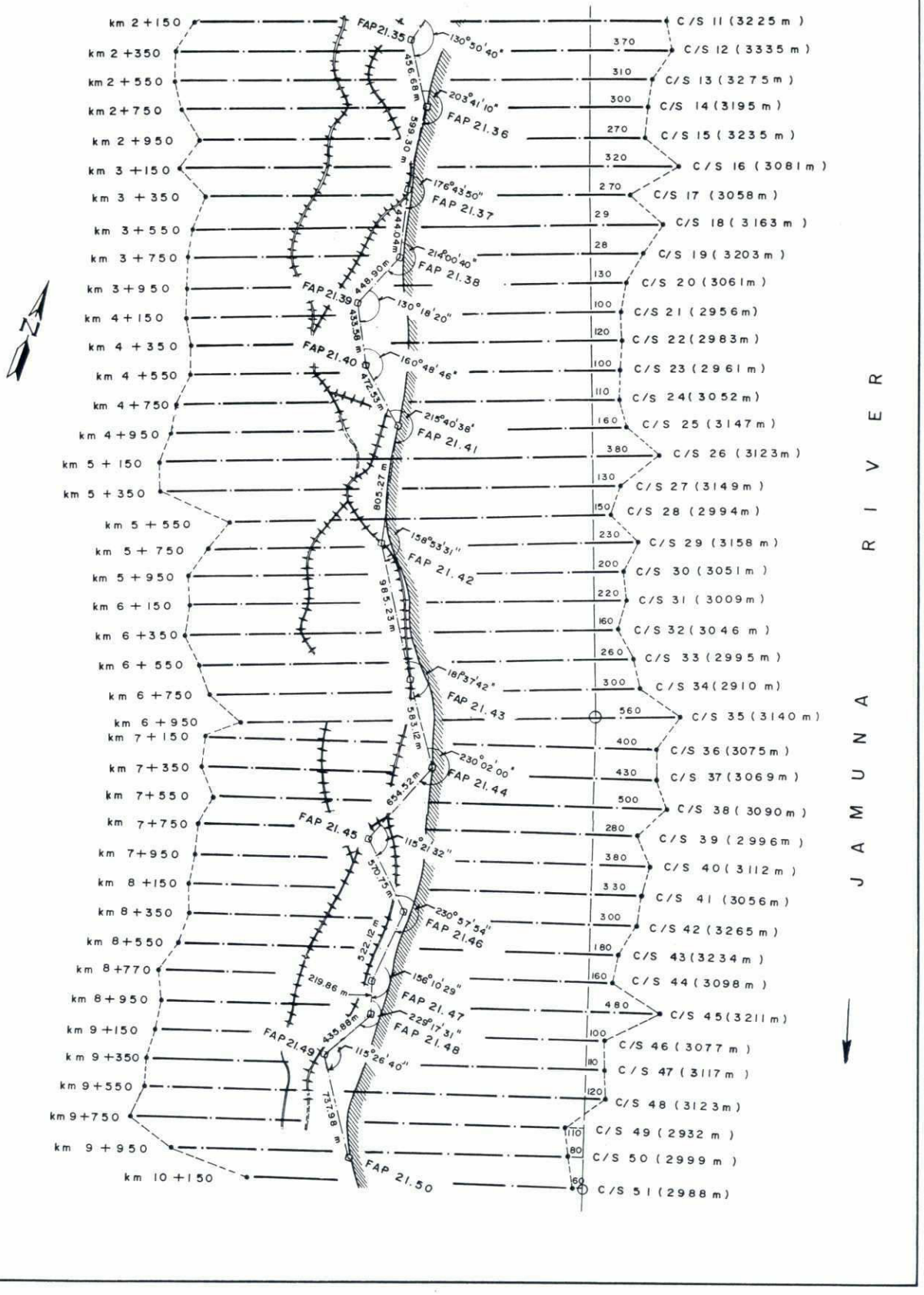
LOCATION OF CROSS SECTIONS AND CONTROL POINTS

CHANDANBAISA
BASIC SURVEY DATA
(SURVEYED APRIL / MAY 1992)

FAP – 21/22
BANK PROTECTION AND RIVER TRAINING/
(AFPM) PILOT PROJECT

FINAL REPORT | FIG. A.12 - 21

CONTD. FIG.A.12-21



LOCATION OF CROSS SECTIONS AND CONTROL POINTS

CHANDANBAISA

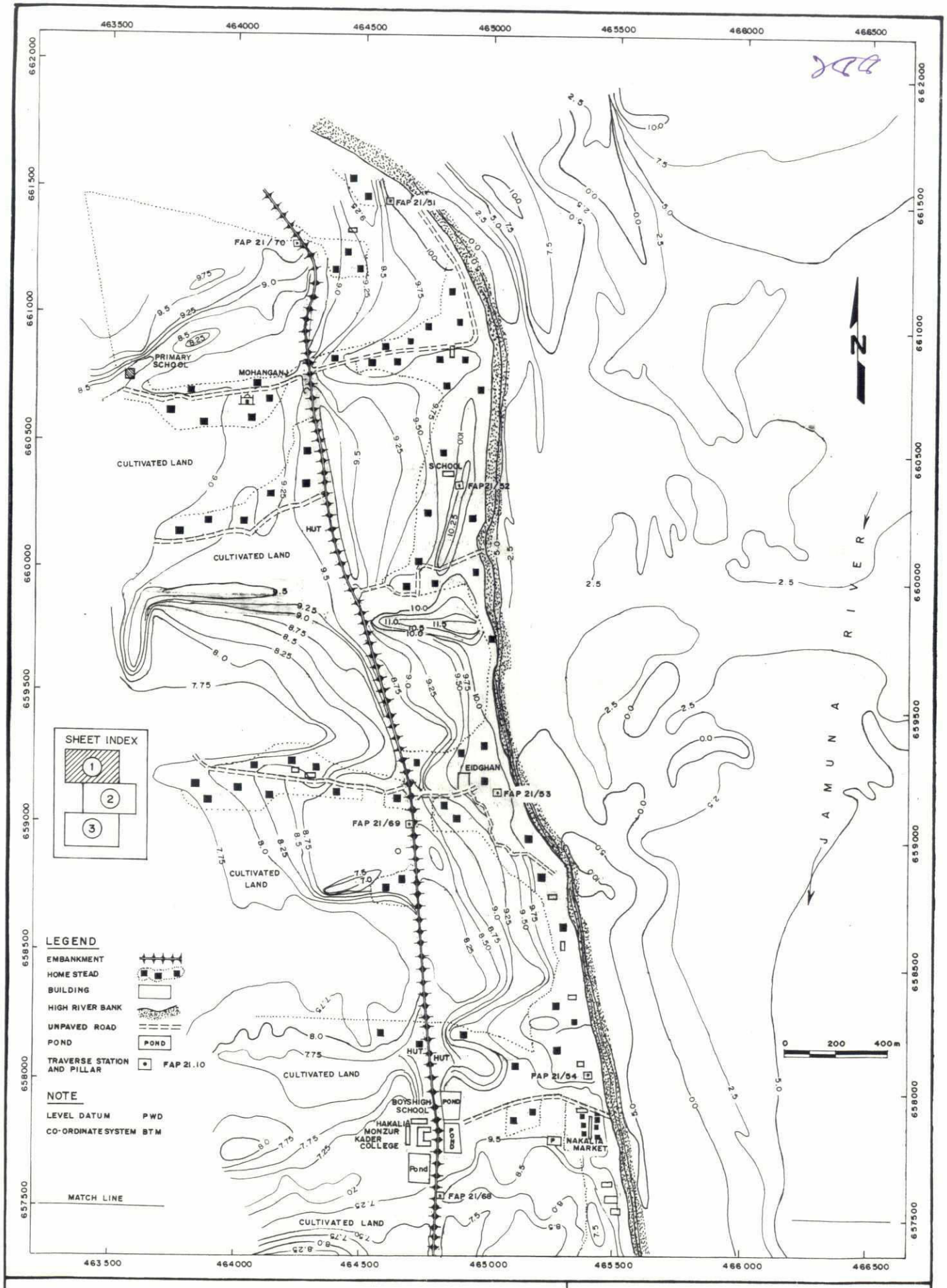
BASIC SURVEY DATA

(SURVEYED APRIL / MAY 1992)

FAP – 21/22

BANK PROTECTION AND RIVER TRAINING / (AFPM) PILOT PROJECT

FINAL REPORT | FIG. A.12-22

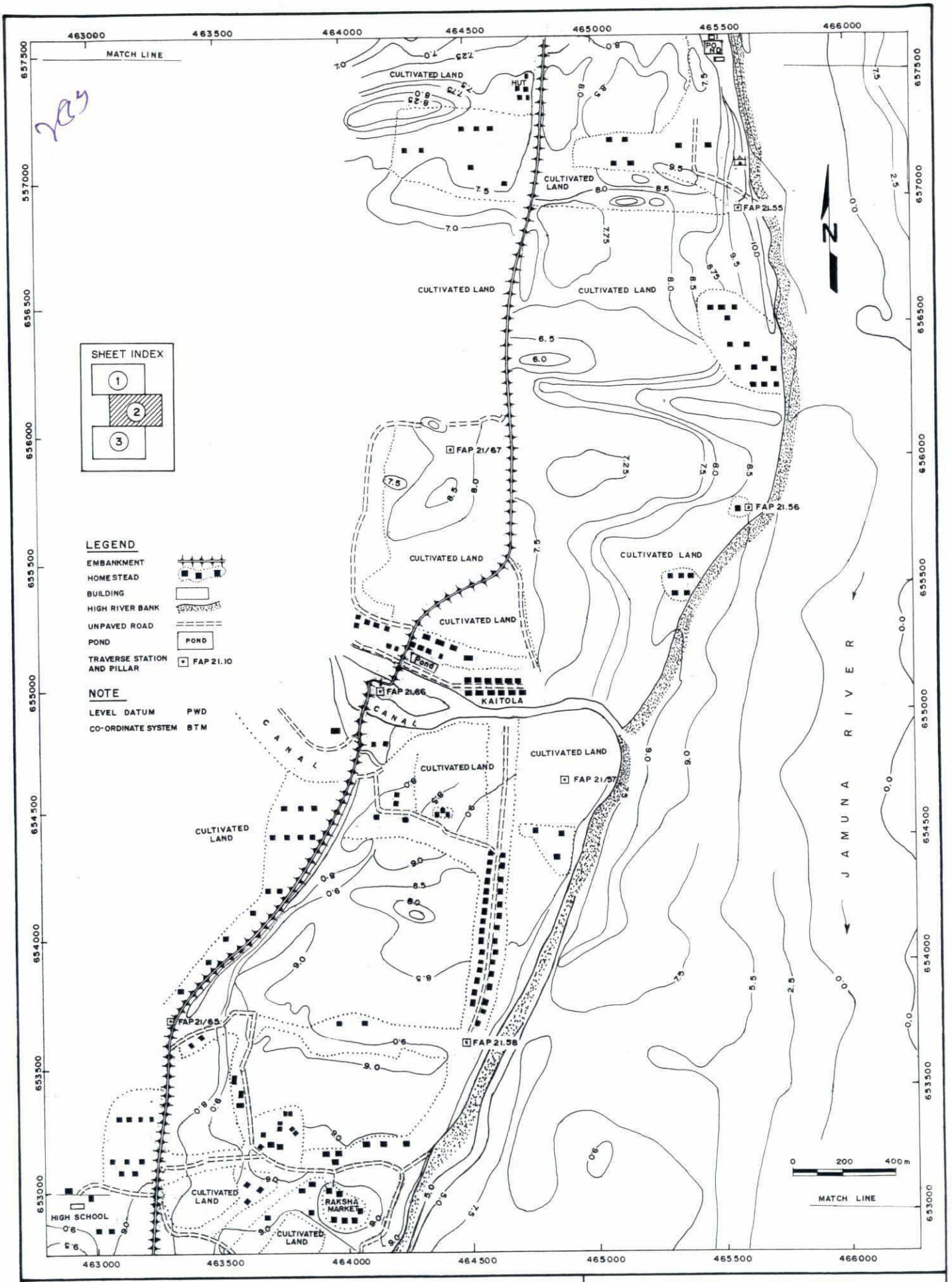


NAKALIA
TOPOGRAPHIC AND HYDROGRAPIC SURVEY OF APRIL / MAY 1992
CONTOUR MAP

FAP - 21/22

BANK PROTECTION AND RIVER TRAINING/ (AFPM) PILOT PROJECT

FINAL REPORT | FIG. A.12-23



NAKALIA

TOPOGRAPHIC AND HYDROGRAPIC SURVEY OF APRIL / MAY 1992

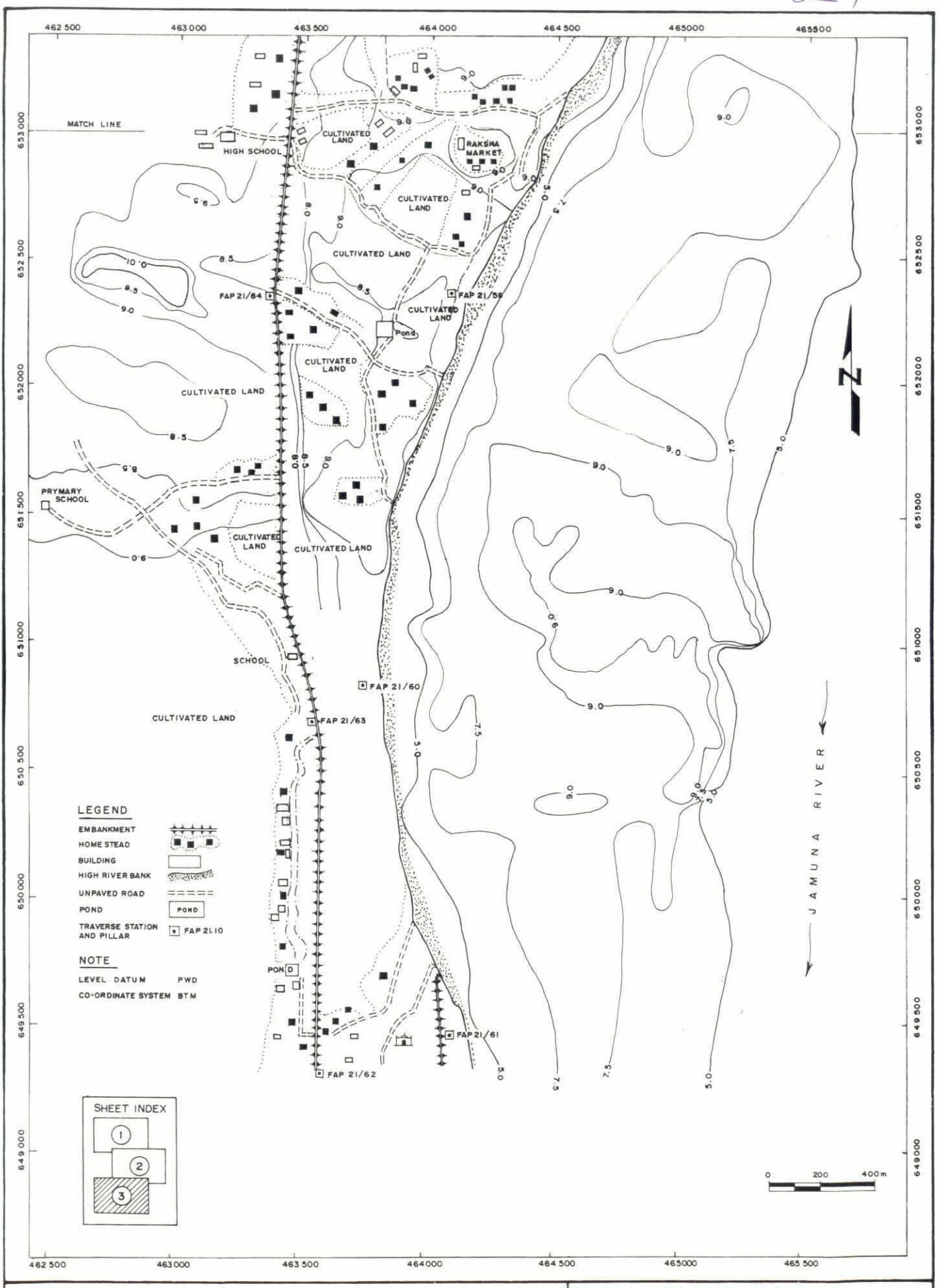
CONTOUR MAP

FAP - 21/22

BANK PROTECTION AND RIVER TRAINING/ (AFPM) PILOT PROJECT

FINAL REPORT

FIG. A.12—24



NAKALIA

TOPOGRAPHIC AND HYDROGRAPIC SURVEY OF APRIL / MAY 1992

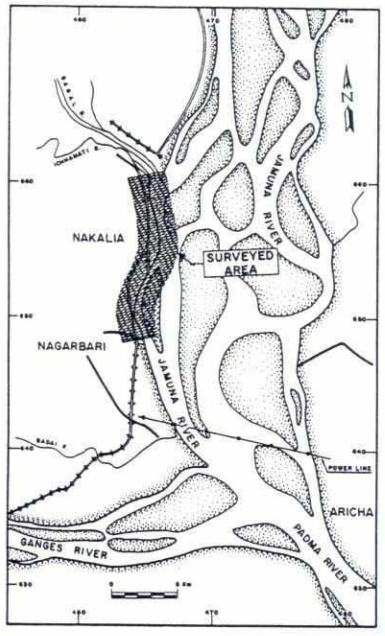
CONTOUR MAP

FAP – 21/22

BANK PROTECTION AND RIVER TRAINING / (AFPM) PILOT PROJECT

FINAL REPORT

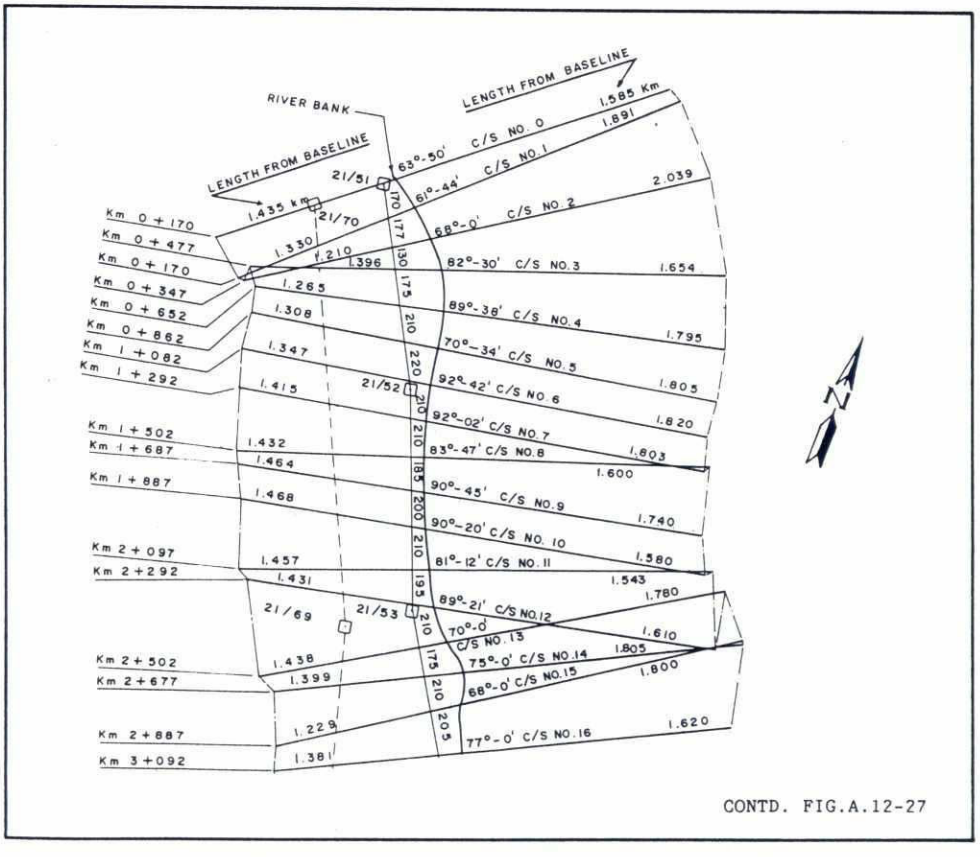
FIG. A.12–25



LOCATION OF SURVEY AREA

No. of Control Point	Co-ordinates (BTM)		Elevation m (PWD)
	Easting (m)	Northing (m)	
FAP 21.51	464,621.62	661,467.58	12.223
FAP 21.52	464,941.65	660,367.91	10.671
FAP 21.53	465,146.10	659,157.96	11.543
FAP 21.54	465,522.12	658,048.56	10.666
FAP 21.55	465,731.88	656,933.17	10.195
FAP 21.56	465,796.24	655,742.85	11.395
FAP 21.57	465,085.51	654,649.54	9.605
FAP 21.58	464,685.34	653,601.50	10.821
FAP 21.59	464,131.06	652,366.34	10.208
FAP 21.60	463,758.53	650,849.22	10.171
FAP 21.61	464,117.56	649,474.44	9.495
FAP 21.62	463,588.96	649,325.43	13.079
FAP 21.63	463,577.42	650,685.44	13.356
FAP 21.64	463,387.55	652,336.48	13.321
FAP 21.65	463,534.02	653,700.45	13.775
FAP 21.66	464,396.76	655,028.78	13.310
FAP 21.67	464,837.68	655,991.03	13.265
FAP 21.68	464,925.79	657,569.29	13.521
FAP 21.69	464,805.28	659,027.76	13.614
FAP 21.70	464,279.52	661,306.01	13.526
FMBM 6525 Kaitola pump station	-	-	11.600
	-	-	12.210

BTM CO-ORDINATES AND HEIGHTS (PWD) OF CONTROL POINTS



CONTD. FIG.A.12-27

LOCATION OF CROSS SECTIONS AND CONTROL POINTS

NAKALIA

BASIC SURVEY DATA

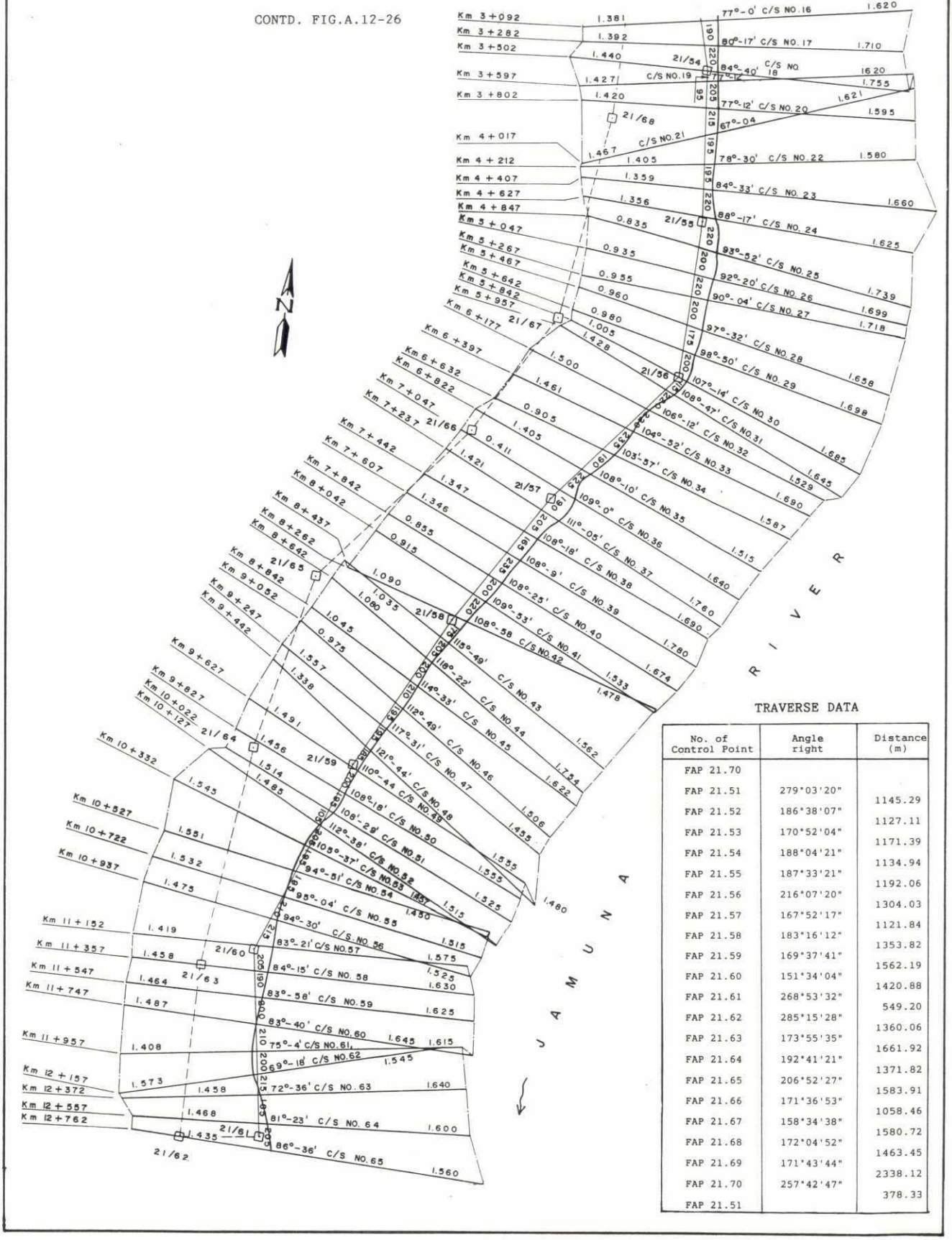
(SURVEYED APRIL / MAY 1992)

FAP – 21/22

BANK PROTECTION AND RIVER TRAINING / (AFPM) PILOT PROJECT

FINAL REPORT | FIG. A. 12 - 26

CONTD. FIG.A.12-26



TRAVERSE DATA

No. of Control Point	Angle right	Distance (m)
FAP 21.70		
FAP 21.51	279°03'20"	1145.29
FAP 21.52	186°38'07"	1127.11
FAP 21.53	170°52'04"	1171.39
FAP 21.54	188°04'21"	1134.94
FAP 21.55	187°33'21"	1192.06
FAP 21.56	216°07'20"	1304.03
FAP 21.57	167°52'17"	1121.84
FAP 21.58	183°16'12"	1353.82
FAP 21.59	169°37'41"	1562.19
FAP 21.60	151°34'04"	1420.88
FAP 21.61	268°53'32"	549.20
FAP 21.62	285°15'28"	1360.06
FAP 21.63	173°55'35"	1661.92
FAP 21.64	192°41'21"	1371.82
FAP 21.65	206°52'27"	1583.91
FAP 21.66	171°36'53"	1058.46
FAP 21.67	158°34'38"	1580.72
FAP 21.68	172°04'52"	1463.45
FAP 21.69	171°43'44"	2338.12
FAP 21.70	257°42'47"	378.33
FAP 21.51		

LOCATION OF CROSS SECIONS AND CONTROL POINTS

NAKALIA
BASIC SURVEY DATA
(SURVEYED APRIL / MAY 1992)

FAP – 21/22
BANK PROTECTION AND RIVER TRAINING/ (AFPM) PILOT PROJECT

FINAL REPORT | FIG. A.12 - 27

BANK PROTECTION AND RIVER TRAINING
(AFPM) PILOT PROJECT
FAP 21/22

DRAFT FINAL REPORT
PLANNING STUDY

ANNEX 13

SUBSOIL INVESTIGATIONS

JANUARY 1993

ANNEX 13

SUBSOIL INVESTIGATIONS

Table of Contents

		Page
1	INTRODUCTION	1
2	FIELD TESTS	1
3	LABORATORY TESTS	4
4	EVALUATION	6

LIST OF FIGURES

A.13-0	:	Test areas
A.13-1 to 7	:	Location maps of soil exploratory works
A.13-8	:	Types of soils laboratory tests executed
A.13-9	:	Sketch of cones used in Cone Penetration Tests
A.13-10	:	Piezometer installed
A.13-11 to 26	:	Soil test results
A.13-27 to 36	:	Cone Penetration tests
A.13-37 to 81	:	Grain size distributions
A.13-82 to 88	:	Consolidation tests
A.13-89 to 93	:	Unconfined Compression tests
A.13-94 to 98	:	Triaxial tests

LIST OF TABLES

Table 2-1	:	Co-ordinates and ground levels of locations of field investigations	4

1 INTRODUCTION

This Annex contains the results of geotechnical investigations performed in the field and the laboratory as well as their evaluation. Exploratory borings, penetration and permeability tests were executed in the selected test areas to obtain information on soil strata, their density and permeability. On selected representative samples extracted from the borings standard soil mechanics tests were performed in the laboratory in order to obtain data on soil properties such as grain size distribution, unit weight, consistency, density, compressibility and shear strength required for the preliminary design works.

2 FIELD TESTS

(a) Equipment

The tender documents for the exploratory works left it to the bidders as to which method they will apply for sinking the boreholes, either light percussion or wash boring. All bidders preferred the latter one since this method is more common in Bangladesh.

However, as no continuous accurate sampling can be expected by the water or mud circulating method, and representative soil samples could only be obtained from the SPT split spoon sampler.

The contractor engaged two drilling machines for the field work:

1. Koken heavy duty drilling machine RK-2 (weight about 3.0 tons)
2. Tone boring rig THS/IC (weight about 1.5 tons)

Both machines were used simultaneously at different locations for sinking of holes and execution of Standard Penetration Tests. In addition the hydraulic gear of the Koken drilling machine was suitable for the performance of the Cone Penetration Tests. The main equipment was supplemented by two engine operated high pressure mud pumps.

(b) Mobilization and Access to the Sites

All 4 test areas were inspected by the Consultant and his subcontractor in advance of the actual field works, in order to study the access conditions from the land and river side and to mark the test locations.

Generally, the accessibility from land side was found to be rather difficult, because of the low level of the existing infrastructure and in addition it often required to pass through cultivated lands.

The distance between test locations and the next accessible road (normally unpaved surface) in each test area ranged between:

Kamarjani	:	200-300 m
Bahadurabad ghat	:	200-2000 m with few cross bars
Chandanbaisa	:	2-14 km including crossing of the Bengali river
Nakalia	:	300-600 m

Under these conditions it was agreed upon with the subcontractor to mobilize and approach each test location with the whole equipment from the river side. A 12 m long steel boat was used for transporting and shifting the equipment from one test location to the other. Sloped ramps were prepared at the river banks to load and unload the drilling equipment to and from the boat, respectively.

During soil exploratory field work, the water levels showed generally a rising tendency. Except in Kamarjani area, where the level fluctuated up and down in the range of 0.2 m, the level rose up to about one meter in the course of the investigations. It resulted in bank heights above river water level at different landing places as follows:

Kamarjani	:	2.0 - 3.0 m
Bahadurabad ghat	:	2.5 - 4.0 m
Chandanbaisa	:	1.0 - 1.8 m
Nakalia	:	1.0 - 5.0 m

(c) Drilling of Boreholes for SPT

As already mentioned under para (a) the wash boring method was adopted to sink the boreholes. The soil at the bottom of the hole was loosened by a 95 mm dia bit and carried to the surface by water recirculating under high pressure. To avoid collapsing of the hole, a 125 mm diameter casing was driven, generally 8 to 10 m deep. Below this depth drilling mud was used for hole stabilization. For determination of the character and consistency of the soil strata, Standard Penetration Tests were carried out at 1.5 m intervals and disturbed soil samples collected from the split spoon sampler.

Undisturbed soil samples from cohesive layers could be obtained by means of open tube samplers of 75 mm diameter, but hardly below water level. Better results would have been obtained with a thin walled sampler or a piston sampler which, however, were not available in Bangladesh. The dimensions of the split barrel sampler which was used for soil sampling and Standard Penetration Test procedure correspond to the specifications of ASTM D 1586.

Fig. A.13-11 through A.13-26 present the respective data, comprising depth below ground level, 'N'-value (No. of blows) and soil sampling for Standard Penetration Tests as well as main laboratory test results.

(d) Penetrometer Tests

Ten Penetrometer Tests were performed in the test areas by using mechanical cone penetrometers. Two types of penetrometer cones were used:

Type 1 : mantle cone and
Type 2 : friction jacket cone.

Both have been manufactured in Bangladesh according to the sizes laid down in ASTM D 3441. Fig. A.13-9 shows dimensions of the cone penetrometers used. While Type 1 could be used for measuring the cone resistance only, Type 2 was suitable for measuring cone resistance as well as local skin friction. The procedure of measuring the forces on the cone and friction sleeve was repeated at regular intervals of depths, normally at 20 cm. At some test locations the test had to be discontinued due to jamming of the cone mechanism, caused by soil particles which penetrated between sliding surfaces. The reason for this effect was most probably the presence of very fine grained soils in the test area. However, after extracting and cleaning the cone penetrometer the test could be resumed.

Fig. A.13-27 through A.13-36 present illustrative diagrammes of measured cone resistance and skin friction at different test locations.

(e) Permeability Test

For determination of the in-situ permeability of the subsoil, one piezometer has been installed at each test area. Fig. A.13-10 shows the details of piezometers installed. The depth of the piezometers ranges between 6 and 8 m below ground surface. For installation of piezometers the boreholes were drilled by wash boring method. The annular space between strainer and hole was filled with coarse sand beyond the upper level of the strainer and bentonite balls and cement bentonite grout was used as sealing material above that level.

The in-situ permeability test was conducted as a "Constant Head Test" in accordance with the recommendations laid down in BS 5930: 1981. To perform the test, the piezometer was filled with clean water up to the top of piezometer stand pipe which was approx. 1.0 m above the ground level. This water level was kept by adding additional water until a steady rate of flow could be observed. Prior to the test, the static ground water level was checked in the piezometer.

Location No.	BTM- Co-ordinates		Ground level (m PWD)	Water level (m PWD)
	Eastings	Northings		
GA 1	462462	802286	19.3	17.26 (30.4.92)
GA 2	462132	803572	20.5	17.33 (2.5.92)
GA 3	462340	804520	20.8	-
GA 4	462490	805007	20.4	17.46 (4.5.92)
GA 5	462656	805693	20.9	17.58 (5.5.92)
BA 1	470120	778660	18.9	15.68 (14.5.92)
BA 2	470520	777340	18.9	15.05 (17.5.92)
BA 3	470580	776030	18.1	15.12 (10.5.92)
BA 4	470460	774490	18.4	15.06 (12.5.92)
BA 5	470100	773230	18.5	-
BA 6	469480	772160	18.9	-
BA 7	469170	771400	19.0	-
CH 1	460210	746872	15.0	-
CH 2	462136	741141	13.0	11.56 (19.4.92)
CH 3	462830	737822	15.5	12.46 (21.4.92)
CH 4	460835	745917	15.3	13.11 (24.4.92)
NK 1	465020	660890	7.9	-
NK 2	465140	659340	8.5	-
NK 3	465500	658440	10.0	-
NK 4	465440	658510	10.5	-
NK 5	465650	657650	10.2	-
NK 6	465830	656720	10.5	-
NK 7	465880	656280	9.8	-

GA - Kamarjani BA - Bahadurabad
CH - Chandanbaisa NK - Nakalia

Table 2-1: Co-ordinates and ground levels of locations of field investigations

3 LABORATORY TESTS

(a) Grain Size Distribution

The determination of the distribution of particle sizes in soils found at the test areas were performed by sieving and, where necessary, by a sedimentation process on disturbed and undisturbed samples in accordance with ASTM D 422. The results obtained from these tests were the basis for identification and classification of the different types of soil as per ASTM D 2487 as shown in Fig. A.13-37 through 81.

(b) Specific Gravity

The specific gravity being the ratio of the weight in air of a given volume of a material at a recorded temperature to the weight in air of an equal volume of distilled water at a recorded temperature was determined by means of pycnometer test as per ASTM D 854. The results are listed in Fig. A.13-11 through 26.

(c) Unit Weight

The dry unit weight being the weight of soil solids per unit of total volume of soil and the submerged unit weight being the weight of the solids in air minus the weight of water displaced by the solids per unit of volume of soil were determined in accordance with common international standards (see Fig. A.13-11 to 26).

(d) Moisture Content

Since the amount of water in soils can influence their behaviour considerably, the moisture content of soils is a soil mechanics characteristic which is most frequently determined especially on fine soils. It is the amount of water within the pore space between the soil grains which is removable by oven drying at 105-110° C expressed as a percentage of the mass of dry soil. Tests were executed as per ASTM D 2216 and results are compiled in Fig. A.13-11 through 26.

(e) Plasticity

The plasticity index (PI) of fine-grained cohesive soils is a most useful way of identifying and classifying such soils. It is defined as the numerical difference between the liquid limit (LL) and the plastic limit (PL) of the soil.

$$PI = LL\text{-}PL$$

Liquid limit and plastic limit are known as the Atterberg limits and are to be determined in accordance with ASTM D 423 and D 424. Liquid limit (LL) is the water content at which soil passes from the plastic to the liquid state and the plastic limit is defined to be the water content at which a soil passes from the plastic state to the solid state and becomes too dry to be in a plastic condition. Results of relevant tests are listed in Fig. A.13-11 to 26.

(f) Compressibility

The compressibility of the soil is the measure of the amount by which the soil will compress when loaded and allowed to consolidate. The consolidation depends mainly on the permeability of the soil, especially of fine soils such as clay or silt.

Soil parameters needed for the estimation of the rate of settlement and of the time within which settlement will be complete are determined by the standard oedometer consolidation test as per ASTM D 2435. The results of the oedometer tests are illustrated as log-pressure/voids ratio curves (e/log p curve) out of which compressibility coefficients needed for the estimation of settlements of buildings and structures can be determined.

Relevant tests were performed on selected undisturbed cohesive samples and the curves are shown in Fig. A.13-82 to 88. Compressibility coefficients are listed in Fig. A.13-11 to 26.

(g) Shear Strength

Shear strength is the maximum shear resistance which a soil can offer under defined conditions of effective pressure and drainage. Under drained conditions that means the soil being consolidated under the prevailing normal load the shear strength consists of two components, notably being the angle of shear resistance which is due to friction between the particles and the cohesion.

$$\tau = c + \sigma \tan \varphi$$

with τ = shear stress
c = cohesion
φ = angle of shear resistance (angle of internal friction)

Angle of shear resistance and cohesion are the shear parameters. In case they were determined under drained conditions they are called effective shear parameters. If the soil is under undrained condition which means unconsolidated the prevailing shear resistance of the soil is called undrained shear strength. It is measured immediately after the application of stress and before drainage of water can take place.

$$\tau = c_u$$

with c_u = undrained shear strength

Shear parameters can be determined from undisturbed samples by several different tests. In this case the effective shear parameters being necessary for the calculation of the final stability were determined by testing of selected undisturbed cohesive soil samples in a triaxial testing apparatus under drained conditions. Relevant shear diagrammes are shown in Fig. A.13-94 to 98 and the values are listed in Fig. A.13-11 to 26.

The c_u-values needed for the calculation of the initial stability were determined by the unconfined compression test. Details of relevant tests are illustrated on Fig. A.13-89 to 93 and their results are compiled in Fig. A.13-11 to 26.

4 EVALUATION

(a) Kamarjani

At Kamarjani the subsoil consists mainly of poorly graded micaceous silty fine to medium sand (group SM) with a silt content between 8 and 28 %, with a mean value of 16 %, covered in some areas by slightly clayey sandy silt with a thickness of about 5 m (group CL

to ML).

The groundwater table was measured at the time of investigation in the range of 1.8 to 4.0m below surface. According to the visual classification and the classification of soils for engineering purposes as per ASTM D 2487 the cover layer of cohesive soil is of low plasticity and of medium to stiff consistency only. The effective shear parameters were determined in the following ranges:

φ = 25° to 29°
c = 13.8 to 20.7 kN/m^2

with mean values as follows:

φ = 27.7°
c = 14 kN/m^2

The coefficient of uniformity of the silty sand is between 3 and 8. Its relative density down to depths between 8 and 15 m is loose, with increasing tendency below this levels, but only below approx. 20 m depth it is medium dense to dense.

The coefficient of permeability is about 3×10^{-5} m/s and the effective angle of internal friction is assumed to be

φ = 27.5°

with a negligible amount of cohesion.

(b) Bahadurabad

Also in the selected test area of Bahadurabad the subsoil consists mainly of poorly graded silty sand with traces of mica and a content of silt between 9 and 21 % (mean value 13 %). Cohesive layers of clayey sandy silt to sandy silt (group CL to ML) were found as cover layers with thickness up to 5.5 m, but also as about 2 m thick layers down to a depth of 11.5m below surface.

The groundwater table at the time of field investigations was between 2.5 and 3.3 m below surface. The plasticity of the clayey sandy silt and sandy silt was as per visual classification only low and according to the results of standard penetration tests its consistency medium to stiff.

Effective shear parameters of cohesive layers:

φ = 29° to 35°
c = 0 to 11.7 kN/m^2

with the following mean values:

$\varphi = 33°$
$c = 0 \ kN/m^2$

According to the standard penetration tests and the cone penetration tests the relative density of the silty sand with a coefficient of uniformity between 2 and 9 was only loose down to approximately 5.0 m; below this level it was medium dense and at depths between 16 and 24 m medium dense to dense. The coefficient of permeability was estimated to be about $3*10^{-5}$ m/s and the effective angle of internal friction:

$\varphi = 27.5°$

without cohesion.

(c) Chandanbaisa

Cohesive layers of slightly clayey sandy silt and sandy silt (group CL to ML) were observed on the top down to about 4.5 m. But also in this test area the soil consists mainly of micaceous silty sand (group SM) with a content of silt in the range of 4 to 37 % and a mean value of 17 %. The groundwater table at the time of execution of borings was determined to 3.0 to 3.6 m below surface.

The CL- and ML-group soil was of low plasticity and as per standard penetration tests and cone penetration tests of medium consistency only. Its effective shear parameters were measured to

$\varphi = 26°$ to $28°$
$c = 20.7$ to $26.2 \ kN/m^2$

The mean values are:

$\varphi = 28.5°$
$c = 17 \ kN/m^2$

For the main layer of silty sand the following soil mechanics properties are applicable:

Coefficient of uniformity	:	2 to 8
Coefficient of permeability	:	$4.5*10^{-5}$ m/s

Relative density as per SPT and CPT:

Down to 5 - 8 m	:	loose
below 16 - 20 m	:	medium dense to dense

Effective angle of internal friction	:	$\varphi = 27.5°$
Effective cohesion	:	$c = 0$ kN/m^2

(d) Nakalia

At Nakalia cohesive soil layers were determined on the top, but also in depths between 3.5 and 10.5 m and from 13.5 to 15 m. According to the visual classification and the plasticity chart as per ASTM D 2487 this soil is to be classified clayey sandy silt to sandy silt (group CL to ML). Its plasticity index was determined in the range of 12 to 22 and the consistency according to the results of SPT is only soft to medium. The following effective shear parameters were obtained from the laboratory tests:

$\varphi = 22°$ to $30°$
$c = 11.7$ to 13.8 kN/m^2

with a mean value $\varphi = 30°$ and no cohesion.

The applicable soil mechanics properties of the main layer of silty sand with traces of mica are the following:

silt content	:	6 to 24 %, mean value 15 %
coefficient of uniformity	:	2 to 7
coefficient of permeability	:	$3*10^{-5}$ m/s
effective angle of internal friction	:	$\varphi = 27.5°$
effective cohesion	:	$c = 0$ kN/m^2

The results obtained from SPT and CPT show that the relative density of the silty sand layers down to 5 to 18 m is only loose. The beginning of a medium to dense density is not uniform in the investigated test area and was ascertained between 13 to 21 m depth.

The groundwater table at the time of investigation was found between 2.0 and 4.0 m below surface.

(e) Summary

The results of field investigations and laboratory tests show very similar conditions of soil in the investigated test areas. The top layer consists mostly of slightly clayey to clayey, sandy silt of low plasticity. The amount of clay is in the range of 3 and 33 %, and the moisture content between 26 and 39 %. According to the visual classification and the laboratory tests it is to be classified as CL to ML as per soil classification chart of ASTM D 2487.

The effective shear parameters determined in the soil mechanics laboratory of BUET for the individual test areas range as follows:

$\varphi = 22°$ to $35°$
$c = 0$ to 26.2 kN/m^2

In order to have theoretical values of the angle of internal friction and the cohesion as a basic for the statical calculations for design works, the mean values of all tests were determined and are as follows:

$\varphi = 31°$
$c = 3.3\ kN/m^2$

Below this cohesive top layer the subsoil consists mainly of micaceous silty sand the density of which is increasing with depth from loose to medium dense to dense at a depth of 16 to 24 m below surface. The silt content ranges between 4 and 37 % and the coefficient of uniformity between 2 and 9. The coefficient of permeability is about 3 to $4x10^{-5}$ m/s and the effective angle of internal friction is assumed to be $\varphi = 27.5°$ without cohesion.

In order to compare the results of the subsoil investigations the reports of other projects have been studied. According to the geotechnical investigations undertaken by FAP 1 along the right bank of the Jamuna, the vertical stratification for design works had been assumed as follows:

Down to a depth of about 10 m clays and silts of low plasticity and non-plastic silts (group CL and ML), followed by non-plastic silty fine sand (group SM) down to about 20 m below surface. Between a depth of about 20 to 30 m the soil was described as non-plastic slightly silty medium fine sand and medium fine sand (group SP-SM and SP). The sands are extremely uniform, generally with a coefficient of uniformity of between 2 and 3 and they are all described as being slightly micaceous. The permeability is explained to be "consistent with SM/SP and SP soil". The bulk density of all layers recommended for use in the stability analysis is 19.5 kN/m^3 and the effective angle of internal friction $\varphi = 28°$ for the layers down to 10 m depth, $\varphi = 32°$ for layers between 10 and 20 m and $\varphi = 33°$ for the third layer between 20 and 30m depth, all without effective cohesion.

According to the investigations undertaken for the Jamuna Bridge Project, three different layers along the river bank had been recognized. Down to 4 m below ground level mainly silt only, followed by fine silty sand and starting from about 30 m the soil consists of fine to medium slightly silty sand. The layers along the right bank are described to appear coarser than those along the east bank and the coefficient of uniformity is in the range of 2 to 2.5 on the west bank and of 2 to 3.9 on the east bank. The coefficient of permeability was established as approximately $4 * 10^{-5}$ m/s on the west and about $2 * 10^{-5}$ m/s an the east bank. The angle of internal friction is given between 36° and 41° and the cohesion is described as practically absent.

In ANNEX 7 to the Draft Final Feasibility Report of FAP 3.1 of October 1992 the alluvial soils are described as "poorly graded silty fine sand to sandy silt" with an indication "that in general coarsening of grain sizes appears with depth from silty material (ML to CL) to silty sand (SM) and poorly graded or single sized fine sand (SP)". The soils are generally

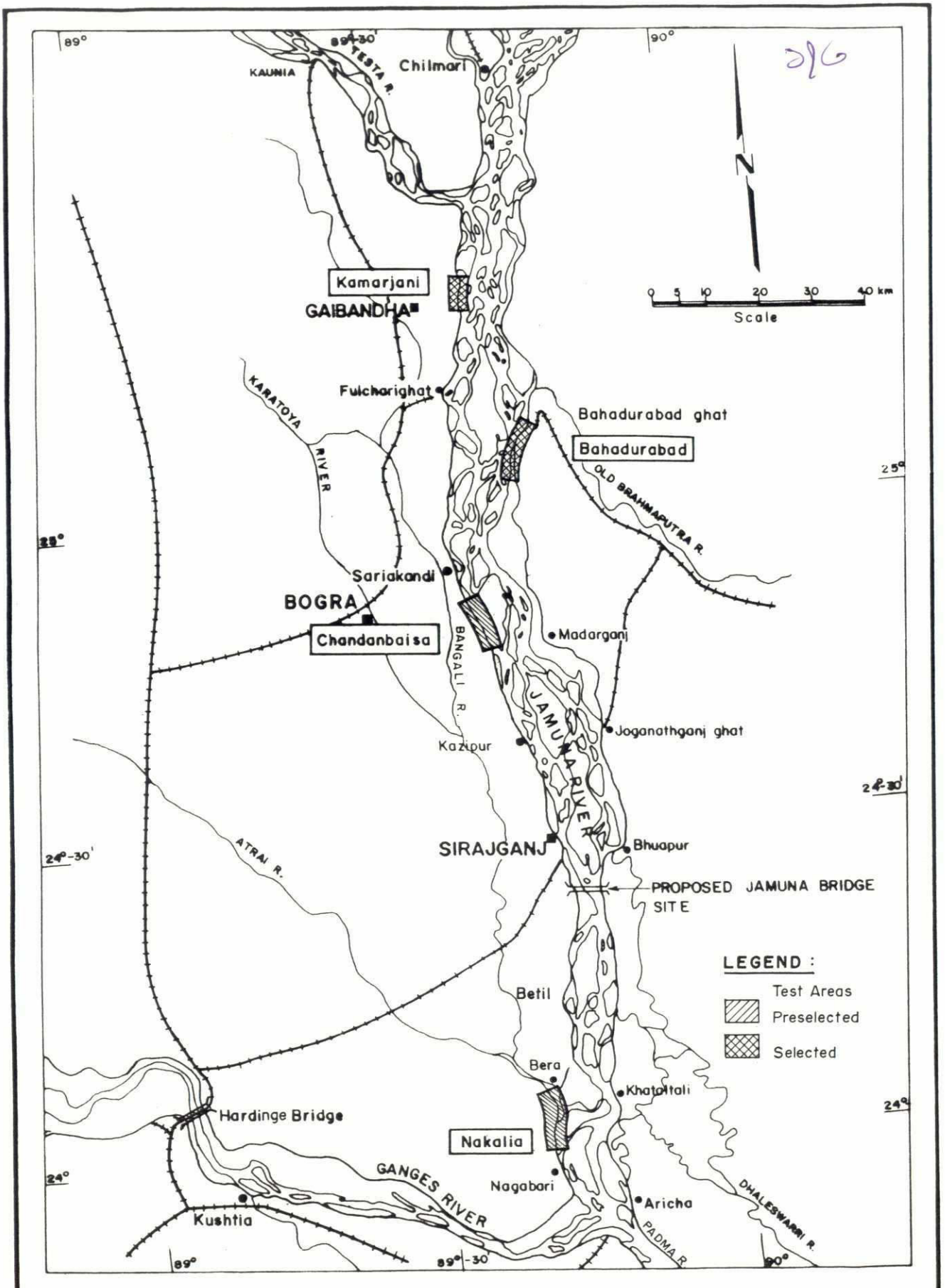
in loose state to about 5-10 m depths. Below this level the density and the grain sizes increase with depth. The shear strength of the fine sandy , silty soil is determined to be on an average of 27.5° with a cohesion of 15 kN/m^2. The permeability determined in boreholes by constant head tests is on an average of 10^{-6} to 10^{-7} m/s, but increases for sandy soil (SM-SP) to 10^{-5} m/s.

This description shows that the FAP 21/22 subsoil investigations are in line with results of other projects. Along the Jamuna the following tendencies could be observed:

(i) close to the surface slightly cohesive soil stratum was encountered the depth of which is on an average of about 5 m;

(ii) below that slightly cohesive stratum loosely to medium densely packed micaceous silty fine sand is found until a depth of about 20 m, and

(iii) finally, medium dense to dense silty fine sand is found at depths larger than about 20 m.

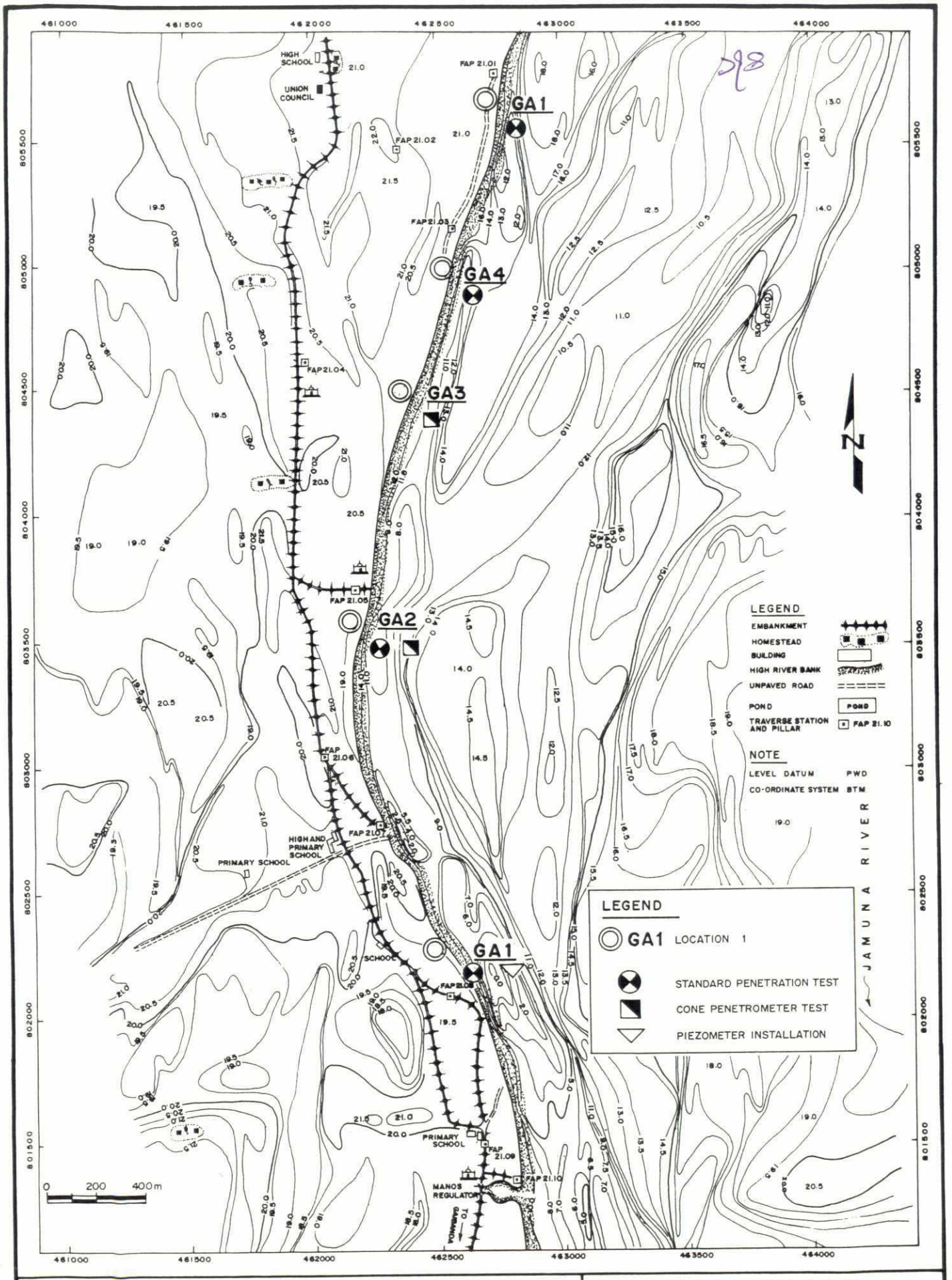


TEST AREAS

FAP - 21/22

BANK PROTECTION AND RIVER TRAINING / (AFPM) PILOT PROJECT

FINAL REPORT | FIG. A.13-0



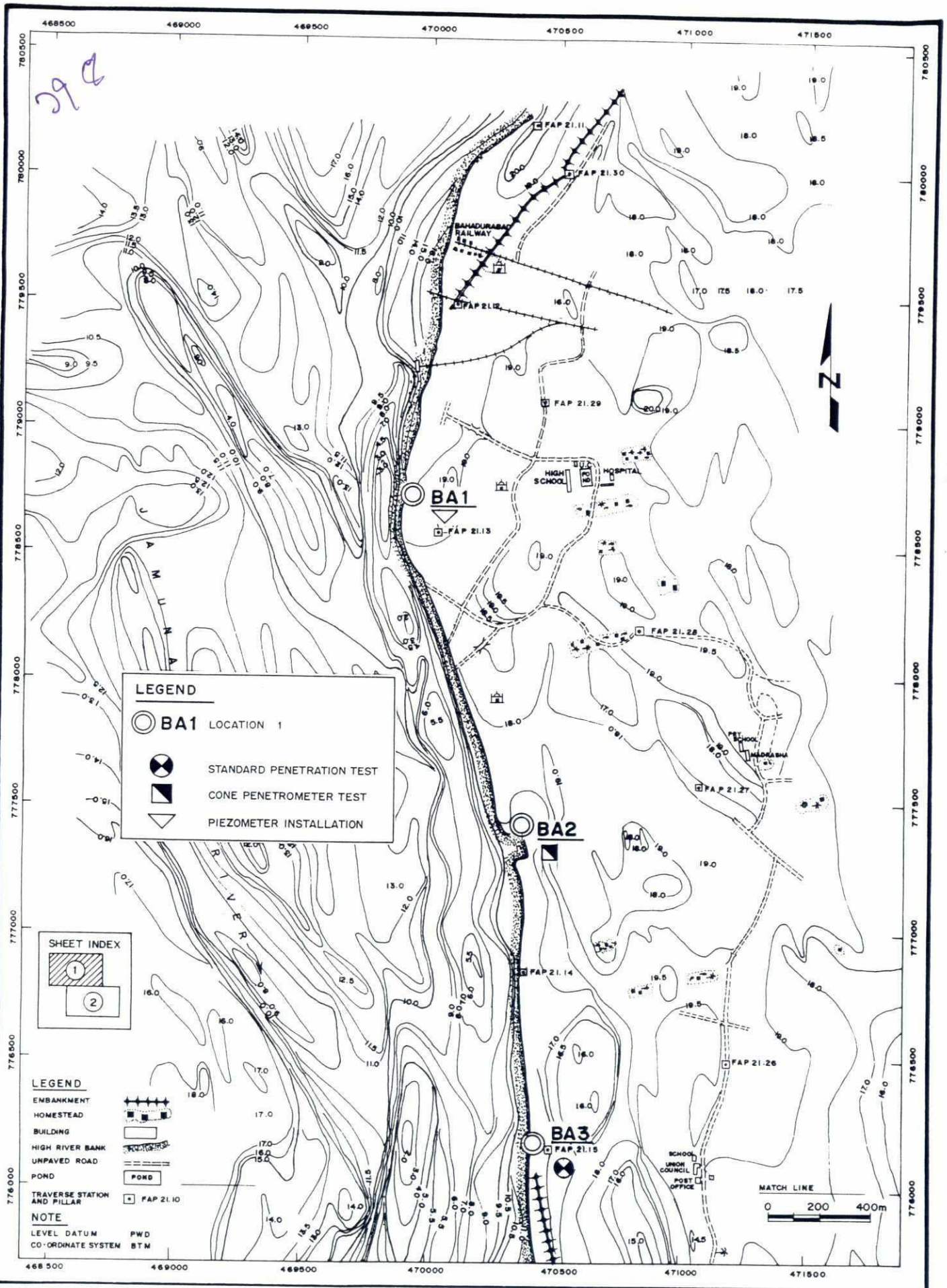
KAMARJANI
LOCATION MAP OF SOIL EXPLORATORY WORKS

(BASED ON SURVEY OF APRIL / MAY 1992)

FAP – 21/22

BANK PROTECTION AND RIVER TRAINING / (AFPM) PILOT PROJECT

FINAL REPORT | **FIG. A. 13 – 1**



BAHADURABAD
LOCATION MAP OF SOIL EXPLORATORY WORKS

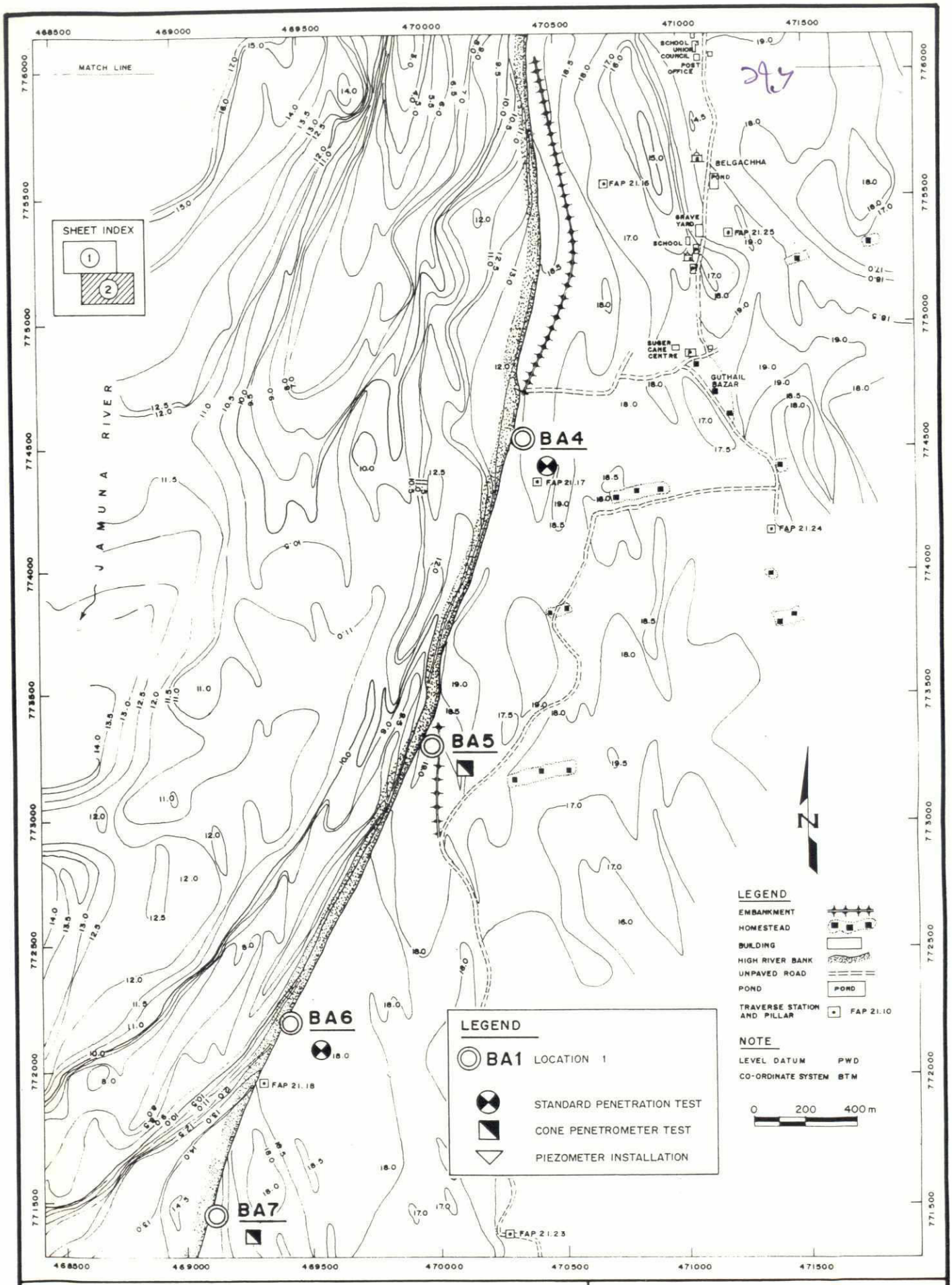
(BASED ON SURVEY OF APRIL / MAY 1992)

FAP - 21/22

BANK PROTECTION AND RIVER TRAINING/ (AFPM) PILOT PROJECT

FINAL REPORT

FIG. A.13-2

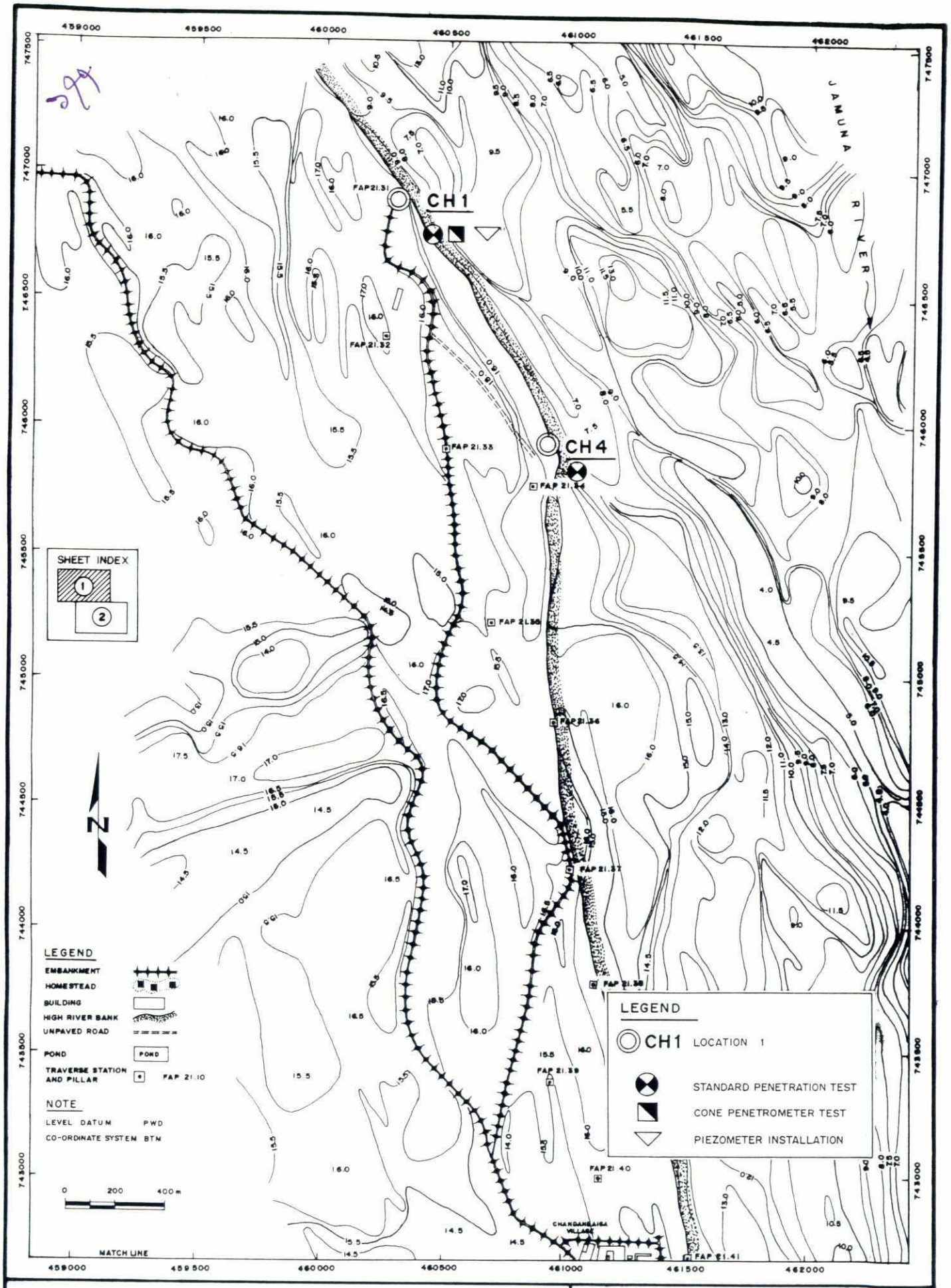


BAHADURABAD
LOCATION MAP OF SOIL EXPLORATORY WORKS
(BASED ON SURVEY OF APRIL/MAY 1992)

FAP - 21/22

BANK PROTECTION AND RIVER TRAINING/ (AFPM) PILOT PROJECT

FINAL REPORT | FIG. A.13-3



CHANDANBAISA

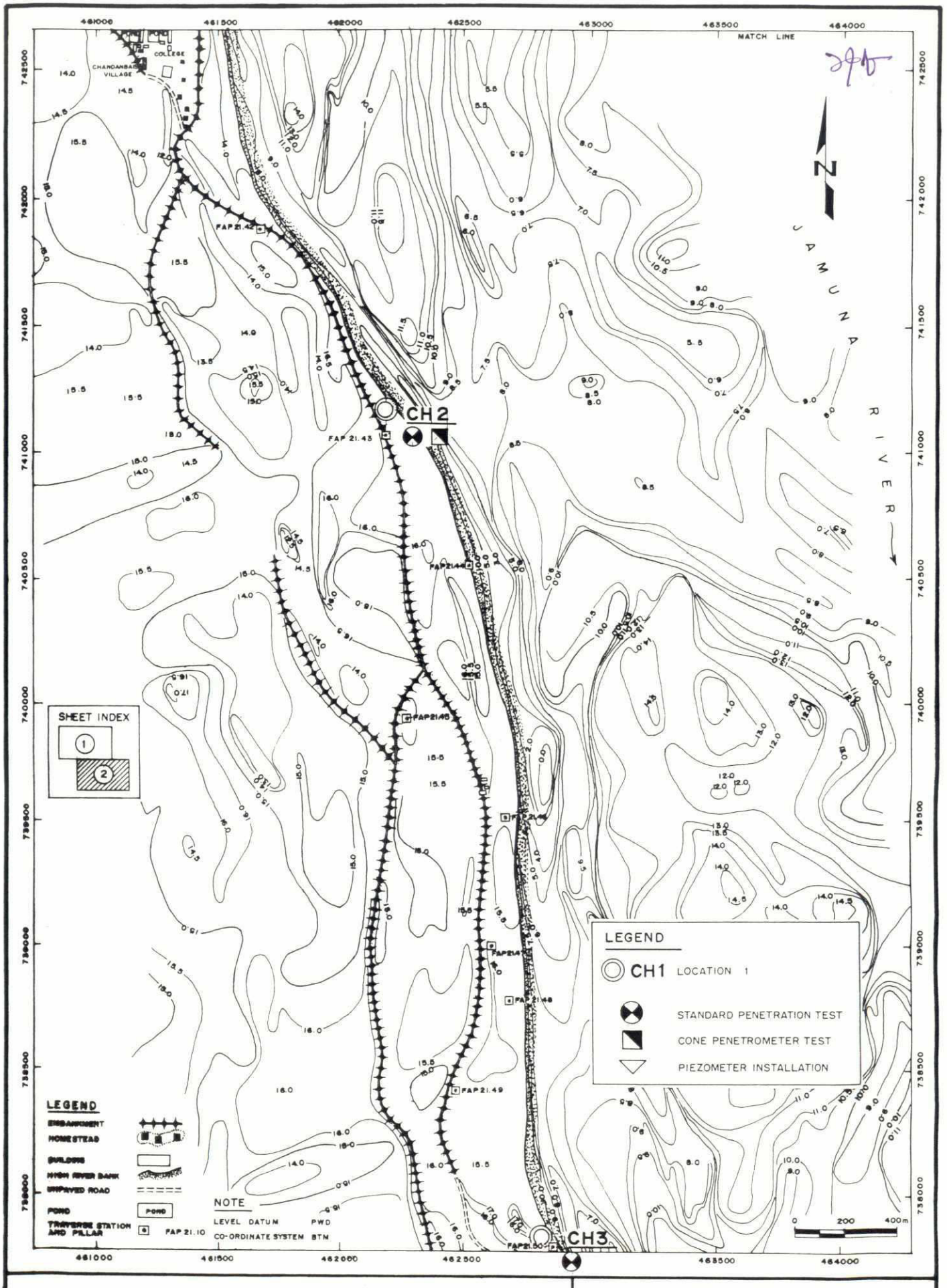
LOCATION MAP OF SOIL EXPLORATORY WORKS

(BASED ON SURVEY OF APRIL / MAY 1992)

FAP – 21/22

BANK PROTECTION AND RIVER TRAINING / (AFPM) PILOT PROJECT

FINAL REPORT | FIG. A.13-4



CHANDANBAISA

LOCATION MAP OF SOIL EXPLORATORY WORKS

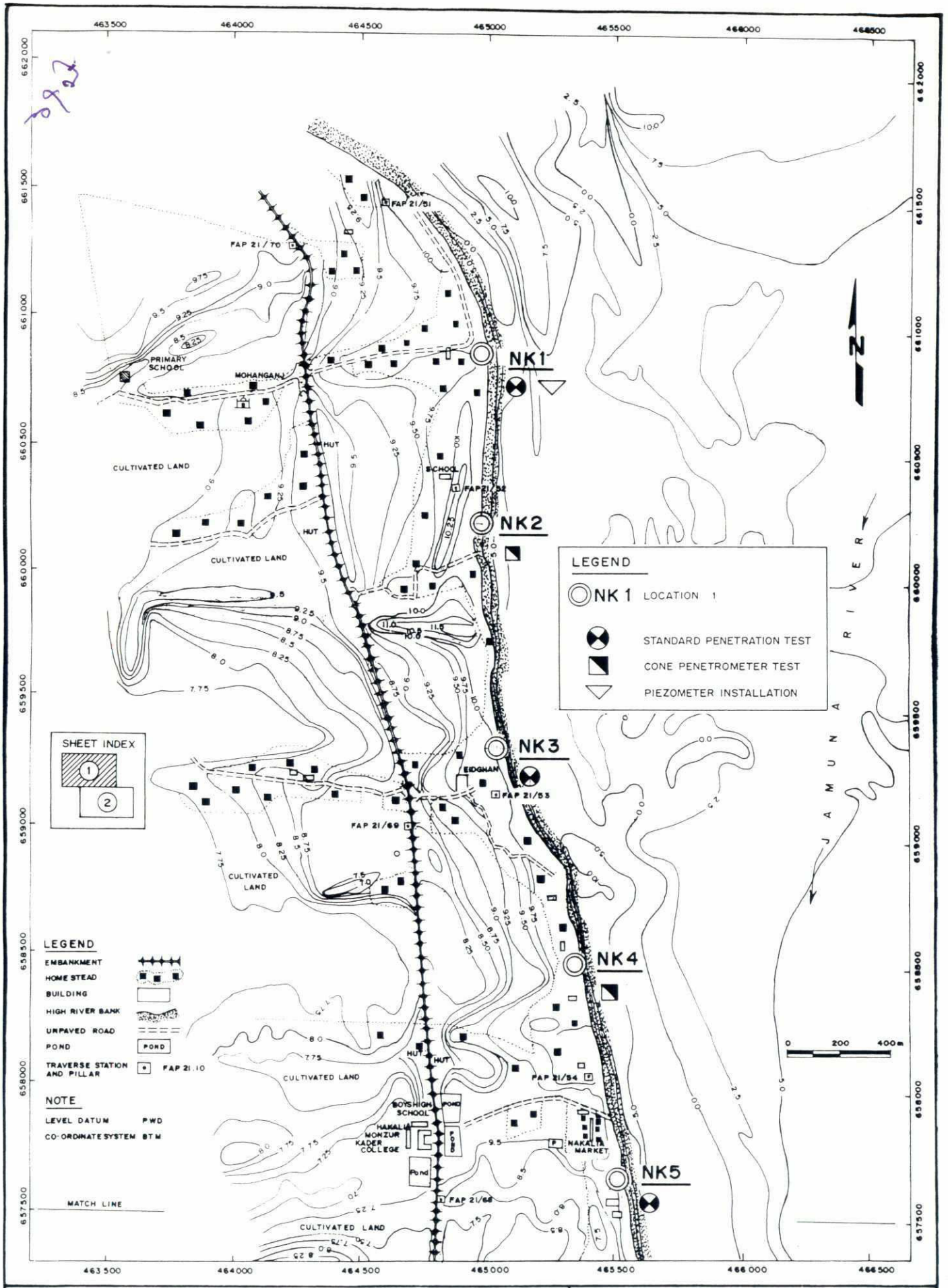
(BASED ON SURVEY OF APRIL / MAY 1992)

FAP - 21/22

BANK PROTECTION AND RIVER TRAINING/ (AFPM) PILOT PROJECT

FINAL REPORT

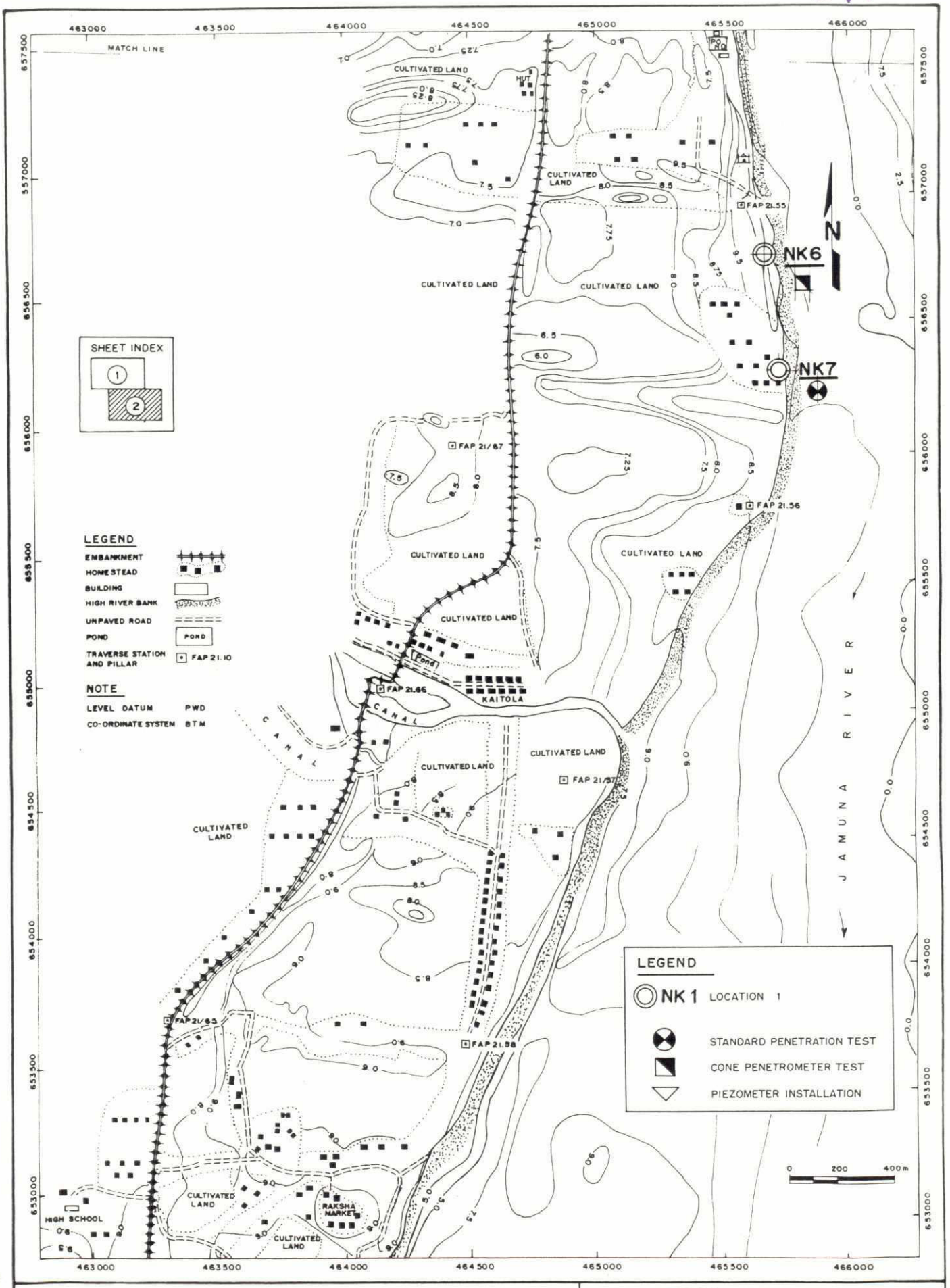
FIG. A.13-5



NAKALIA
LOCATION MAP OF SOIL EXPLORATORY WORKS
(BASED ON SURVEY OF APRIL / MAY 1992)

FAP - 21/22
BANK PROTECTION AND RIVER TRAINING/ (AFPM) PILOT PROJECT

FINAL REPORT | FIG. A.13-6



NAKALIA
LOCATION MAP OF SOIL EXPLORATORY WORKS
(BASED ON SURVEY OF APRIL/MAY 1992)

FAP - 21/22
BANK PROTECTION AND RIVER TRAINING/ (AFPM) PILOT PROJECT

FINAL REPORT | FIG. A.13-7

LABORATORY TESTS PERFORMED (Nos.)

LOCATION	BH	S	MC	G	AL	UW	TA	UC	C
KAMARJANI (GA)	1	4	1	1*		1	1*		1*
	2	5	1			1	1*		
	4	5							
	5	7	2			2	1*	1	
BAHADURABAD (BA)	1	8	3	1+1*	2	3	2*	1	1
	3	5			1				
	4	5							
	6	9							
CHANDANBAISA (CH)	1	13		1					
	2	13							
	3	13		1					
	4	9	3		1	2	2*	1	
NAKALIA (NK)	1	9	1	1	2	1		1	1
	3	7	2		2	2	1*	1	2
	5	6	1		1	1	1*		1
	7	7			1				1
TOTAL TESTS EXECUTED		125	14	6	10	13	9	5	7
TESTS ASKED FOR		101	14	7	15	13	11	6	9

LEGEND

BH = BORE HOLE

S = GRAIN SIZE DISTRIBUTION

MC = MOISTURE CONTENT

G = SPECIFIC GRAVITY

AL = ATTERBERG LIMITS

UW = UNIT WEIGHT

TA = TRIAXIAL COMPRESSION TEST (Consolidated drained)

UC = UNCONFINED COMPRESSION TEST

C = CONSOLIDATION TEST

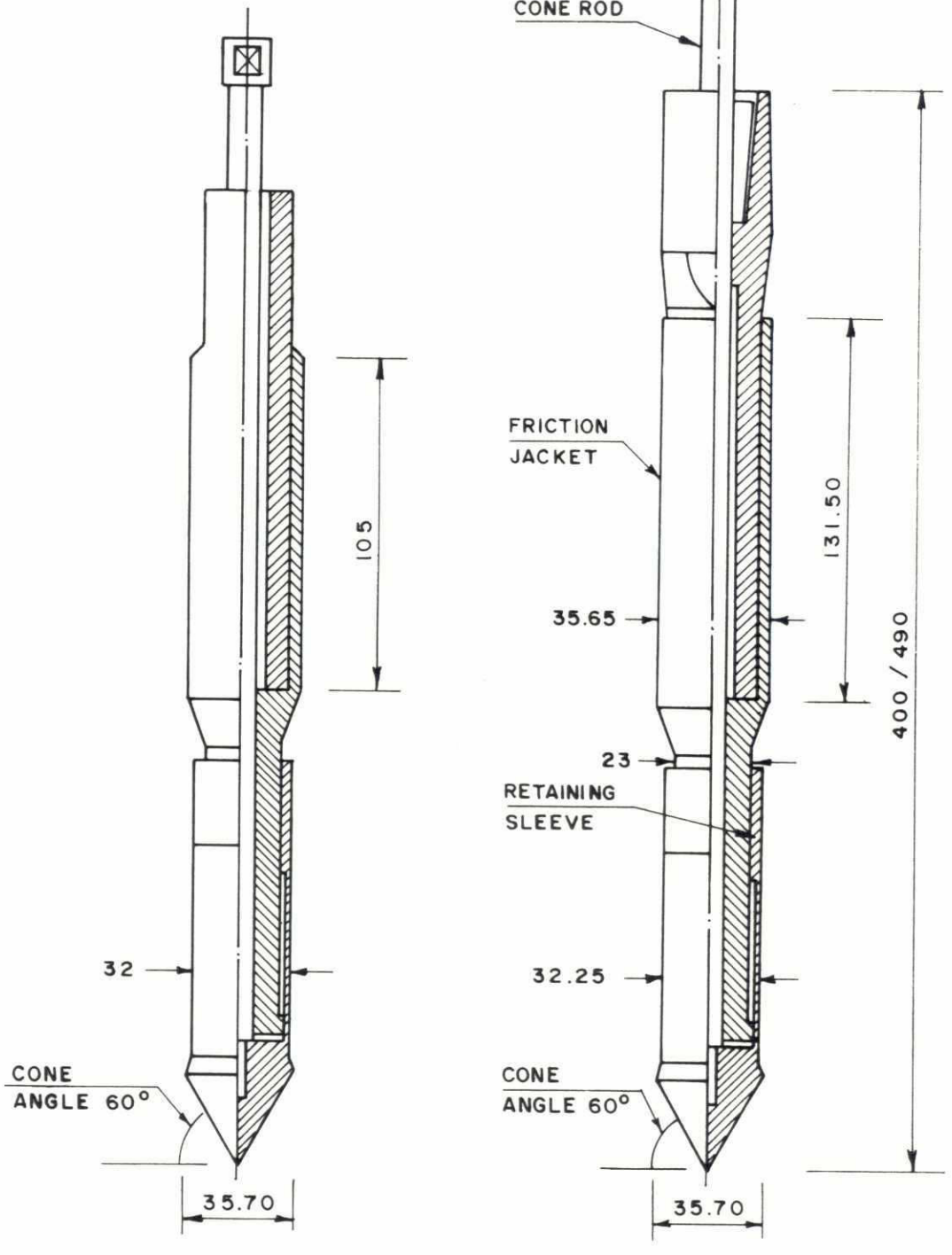
NOTE : Tests nos having asterik mark were executed at Soil Mechanics Laboratory, BUET.

TYPE OF SOILS LABORATORY TESTS EXECUTED

FAP – 21/22

BANK PROTECTION AND RIVER TRAINING/ (AFPM) PILOT PROJECT

FINAL REPORT | FIG. A.13-8



MANTLE CONE

FRICTION JACKET CONE

ALL DIMENSIONS ARE IN MILLIMETER

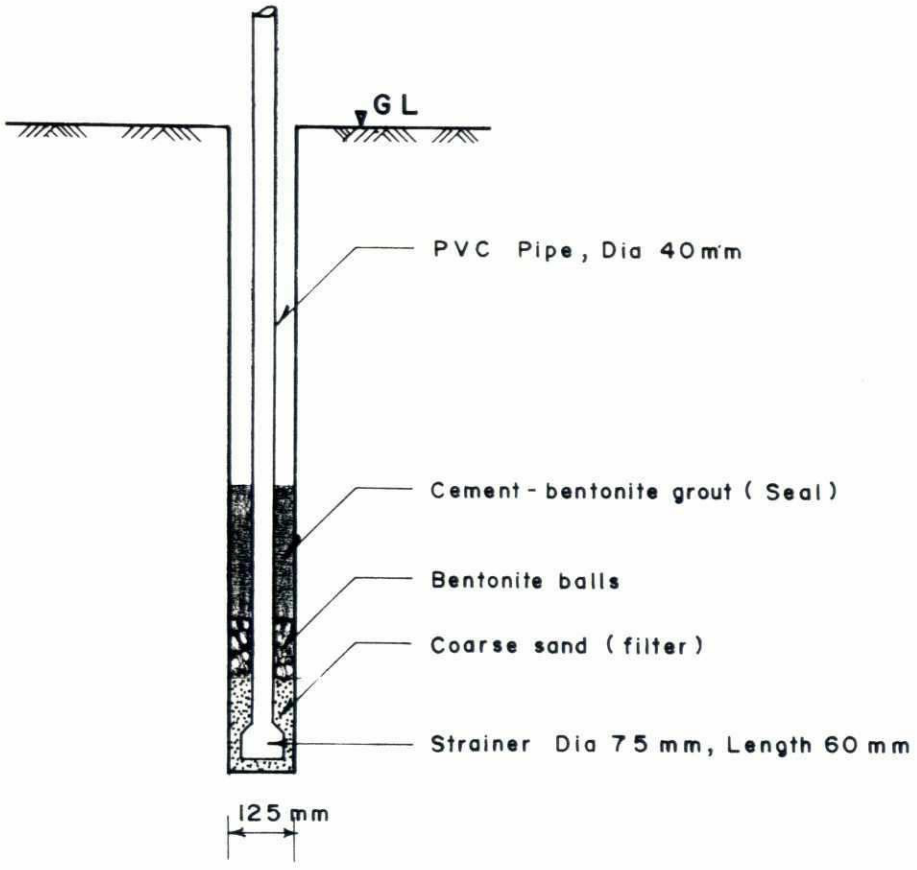
WORKS EXECUTED BY FOUNDATION CONSULTANTS LTD.

SKETCHES OF CONES USED IN CONE PENETROMETER TEST

FAP-21/22

BANK PROTECTION AND RIVER TRAINING/ (AFPM) PILOT PROJECT

FINAL REPORT | FIG. A.13-9



SCHEMATIC DIAGRAM OF PIEZOMETER INSTALLED FOR IN-SITU PERMEABILITY BY CONSTANT HEAD METHOD

Particulars of piezometer installed	GA — 1	BA — 1	NK — 1
Date of installation	29 - 4 - 92	8 - 5 - 92	24 - 5 - 92
Date of test	1 - 5 - 92	11 - 5 - 92	28 - 5 - 92
Boring depth below G.L	6.07 m	7.50 m	7.77 m
Length of PVC pipe	7.00 m	8.34 m	8.71 m
GWT from G.L on test date	2.90 m	3.60 m	3.00 m
Length of PVC above G.L	0.95 m	0.88 m	1.05 m
Length of filter materiel (as measured)	0.18 m	0.17 m	0.21 m
Soil at filter level	Fine sand with little silt	Fine to med sand, little silt	Fine sand, little silt
Time for steady flow of 3 litres	4m 33secs	2m 42 secs	2m 25 secs

PIEZOMETER INSTALLED

FAP - 21/22

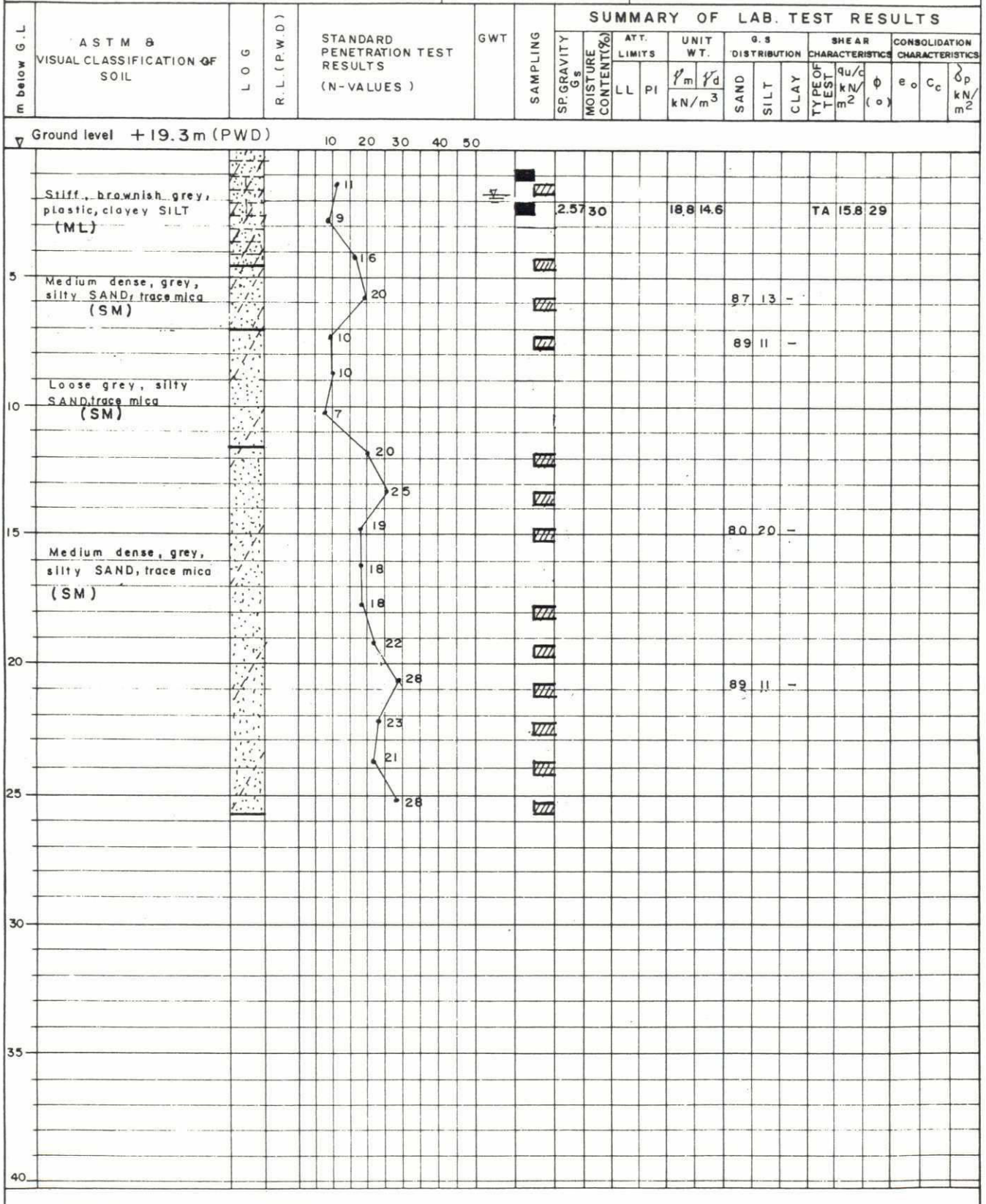
BANK PROTECTION AND RIVER TRAINING/ (AFPM) PILOT PROJECT

FINAL REPORT | FIG. A.13-10

LOCATION : KAMARJANI

BORE HOLE NO. GA-1

METHOD OF BORING : WASH
DIA OF BORING : 100 mm.
DATE OF EXECUTION : 30-4 to 1-5-92



LEGEND

- Sand
- CLay
- Silt
- Undisturbed Sample from Test Pit
- Disturbed Sample from Bore hole
- Undisturbed Sample from Bore hole

T.A Triaxial shear test
U. C. Unconfined Compression test

WORKS EXECUTED BY FOUNDATION CONSULTANTS LTD.

SOIL TEST RESULTS

FAP-21/22

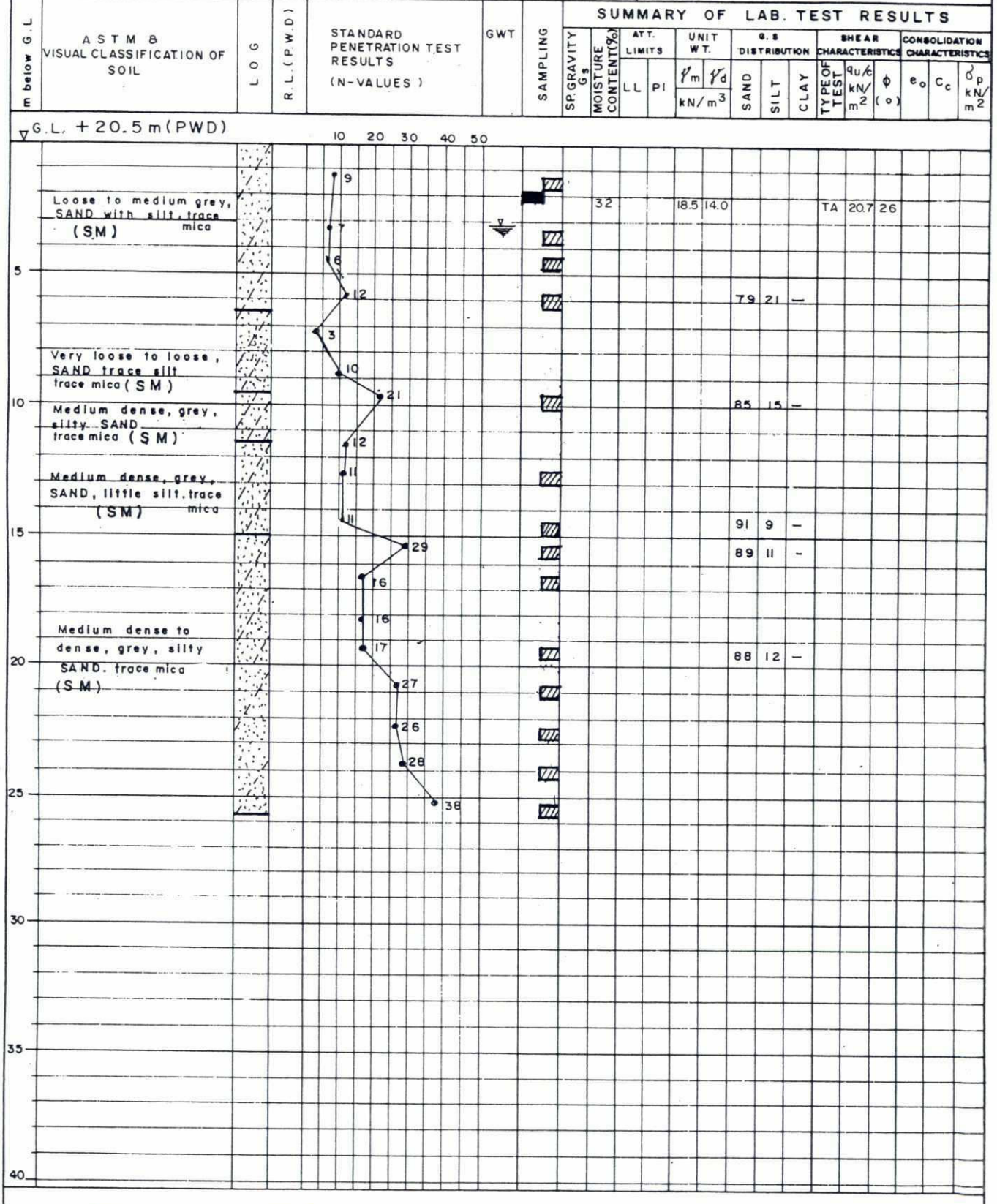
BANK PROTECTION AND RIVER TRAINING/ (AFPM) PILOT PROJECT

FINAL REPORT | FIG. A.13-11

LOCATION : KAMARJANI

BORE HOLE NO. GA-2

METHOD OF BORING : WASH
DIA OF BORING : 100mm
DATE OF EXECUTION : 2-5 to 3-5-92



LEGEND

- Sand
- CLay
- Silt
- Undisturbed Sample from Test Pit
- Disturbed Sample from Bore hole
- Undisturbed Sample from Bore hole

T.A Triaxial shear test
U. C. Unconfined Compression test

WORKS EXECUTED BY FOUNDATION CONSULTANTS LTD.

SOIL TEST RESULTS

FAP-21/22

BANK PROTECTION AND RIVER TRAINING/ (AFPM) PILOT PROJECT

FINAL REPORT

FIG. A. 13-12

LOCATION : KAMARJANI	BORE HOLE NO. GA – 4	METHOD OF BORING : WASH DIA OF BORING : 100 mm. DATE OF EXECUTION : 4-5 to 5-5-92	

SUMMARY OF LAB. TEST RESULTS

m below G.L	ASTM & VISUAL CLASSIFICATION OF SOIL	LOG	R.L.(P.W.D)	STANDARD PENETRATION TEST RESULTS (N-VALUES)	GWT	SAMPLING	SP. GRAVITY G_s	MOISTURE CONTENT (%)	ATT. LIMITS LL	ATT. LIMITS PI	UNIT WT. γ_m kN/m³	UNIT WT. γ_d kN/m³	G.S DISTRIBUTION SAND	G.S DISTRIBUTION SILT	G.S DISTRIBUTION CLAY	SHEAR CHARACTERISTICS TYPE OF TEST	SHEAR CHARACTERISTICS q_u/c kN/m²	SHEAR CHARACTERISTICS ϕ (°)	CONSOLIDATION CHARACTERISTICS e_o	CONSOLIDATION CHARACTERISTICS C_c	CONSOLIDATION CHARACTERISTICS σ_p kN/m²
	GL. + 20.4 m (PWD)			10 20 30 40 50																	
	Loose, brownish grey, SAND with silt, trace mica (SM)			6									72	28	–						
				11																	
5				10																	
	Loose to medium dense, brownish grey, silty SAND, trace mica (SM)			16									85	15	–						
				12									78	22	–						
				29																	
10	Medium dense, brownish grey, SAND with silt trace mica (SM)			13																	
				16																	
				20									86	14	–						
15	Medium dense, brownish grey, silty SAND, trace mica (SM)			18																	
				19																	
				20																	
20	Dense, brownish grey, SAND little silt, trace mica (SM)			35									92	8	–						
25																					
30																					
35																					
40																					

LEGEND

- Sand
- CLay
- Silt

- Undisturbed Sample from Test Pit
- Disturbed Sample from Bore hole
- Undisturbed Sample from Bore hole

T.A Triaxial shear test

U. C. Unconfined Compression test

WORKS EXECUTED BY FOUNDATION CONSULTANTS LTD.

SOIL TEST RESULTS

FAP-21/22

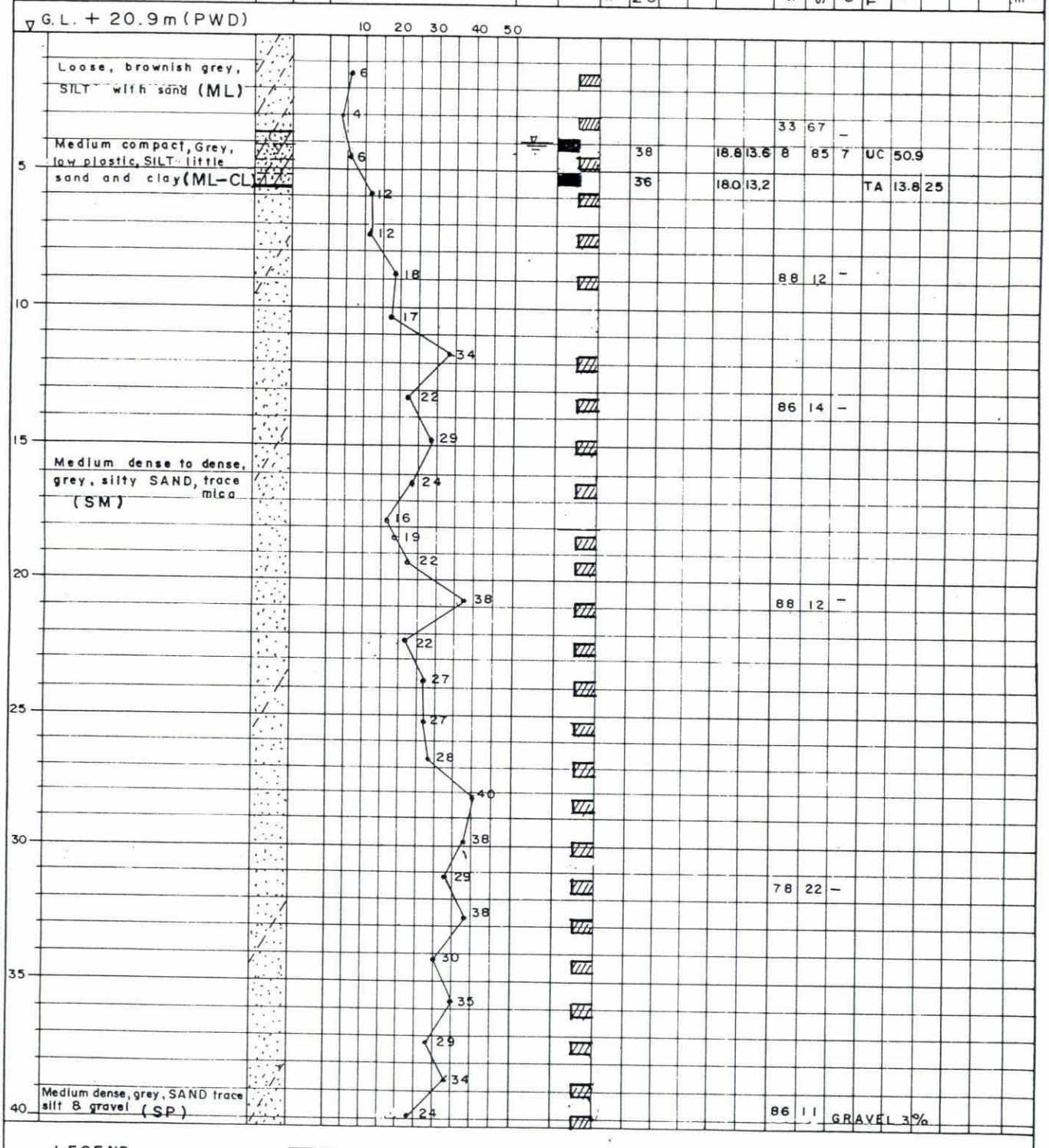
BANK PROTECTION AND RIVER TRAINING/ (AFPM) PILOT PROJECT

FINAL REPORT | FIG. A. 13-13

LOCATION : KAMARJANI

BORE HOLE NO. GA – 5

METHOD OF BORING : WASH
DIA OF BORING : 100mm
DATE OF EXECUTION : 3–5 to 5–5–92



m below G.L	ASTM & VISUAL CLASSIFICATION OF SOIL	LOG	R.L. (PWD)	STANDARD PENETRATION TEST RESULTS (N-VALUES)	GWT	SAMPLING	SUMMARY OF LAB. TEST RESULTS														
							SP. GRAVITY Gs	MOISTURE CONTENT (%)	ATT. LIMITS LL	ATT. LIMITS PI	UNIT WT. γm kN/m³	UNIT WT. γd kN/m³	G.S DISTRIBUTION SAND	G.S DISTRIBUTION SILT	G.S DISTRIBUTION CLAY	SHEAR CHARACTERISTICS TYPE OF TEST	SHEAR CHARACTERISTICS qu/c kN/m²	SHEAR CHARACTERISTICS φ (°)	CONSOLIDATION CHARACTERISTICS p_o	CONSOLIDATION CHARACTERISTICS C_c	CONSOLIDATION CHARACTERISTICS σ_p kN/m²
5	Loose, brownish grey, SILT with sand (ML)												33	67	–						
	Medium compact, Grey, low plastic, SILT little sand and clay (ML–CL)							38			18.8	13.6	8	85	7	UC	50.9				
								36			18.0	13.2				TA	13.8	25			
10													88	12	–						
15	Medium dense to dense, grey, silty SAND, trace mica (SM)												86	14	–						
20													88	12	–						
25																					
30													78	22	–						
35																					
40	Medium dense, grey, SAND trace silt & gravel (SP)												86	11	GRAVEL 3%						

LEGEND

Sand
CLay
Silt

Undisturbed Sample from Test Pit
Disturbed Sample from Bore hole
Undisturbed Sample from Bore hole

T.A Triaxial shear test.
U. C. Unconfined Compression test

WORKS EXECUTED BY FOUNDATION CONSULTANTS LTD.

SOIL TEST RESULTS

FAP-21/22

BANK PROTECTION AND RIVER TRAINING/ (AFPM) PILOT PROJECT

FINAL REPORT

FIG. A. 13–14

LOCATION : BAHADURABAD

BORE HOLE NO. BA — 1

METHOD OF BORING : WASH
DIA OF BORING : 100mm
DATE OF EXECUTION : 8 — 5 to 9-5-92

SUMMARY OF LAB. TEST RESULTS

E below G.L	ASTM 8 VISUAL CLASSIFICATION OF SOIL	L.O.G	R.L (PWD)	STANDARD PENETRATION TEST RESULTS (N-VALUES)	GWT	SAMPLING	SP. GRAVITY Gs	MOISTURE CONTENT (%)	ATT. LIMITS LL	ATT. LIMITS PI	UNIT WT. γ_m kN/m³	UNIT WT. γ_d kN/m³	G.S DISTRIBUTION SAND	G.S DISTRIBUTION SILT	G.S DISTRIBUTION CLAY	SHEAR CHARACTERISTICS TYPE OF TEST	SHEAR CHARACTERISTICS qu/c kN/m²	SHEAR CHARACTERISTICS ϕ (°)	CONSOLIDATION CHARACTERISTICS e_o	CONSOLIDATION CHARACTERISTICS C_c	CONSOLIDATION CHARACTERISTICS σ_p kN/m²
	GL. + 18.9 m (PWD)			10 20 30 40 50																	
	Low plastic, Brownish grey, sandy SILT (ML)			2				31			17.6	13.4				TA	0	35			
				6									11	89	—						
	Grey medium plastic, SILT with clay little sand (CL)						2.55	39	43	22	18.1	13.0	10	56	34	TA	11.7	29	0.87	0.19	
				11				26	46	27	19.5	15.5	16	77	7	UC	207				
5	Brownish grey, low plastic, sandy SILT little clay (ML – CL)			12																	
				14									79	21	—						
	Medium dense, brownish grey SAND with silt, trace mica (SM)			13																	
10	Low plastic Grey, SILT with sand trace clay (ML)			4									22	77	1						
				13																	
				15			2.67														
15				18																	
				16																	
				17																	
				17																	
20				18									88	12	—						
	Medium dense grey, silty SAND, trace mica (SM)			19																	
				21																	
				29																	
25				40									80	20	—						
				33																	
				30																	
	Dense to very dense, grey, silty SAND, trace mica (SM)			30																	
30				37																	
				59									81	19	—						
				72																	
35				35																	
				42																	
				54																	
40				69																	

LEGEND

- Sand
- CLay
- Silt

- Undisturbed Sample from Test Pit
- Disturbed Sample from Bore hole
- Undisturbed Sample from Bore hole

T.A Triaxial shear test
U. C. Unconfined Compression test

WORKS EXECUTED BY FOUNDATION CONSULTANTS LTD.

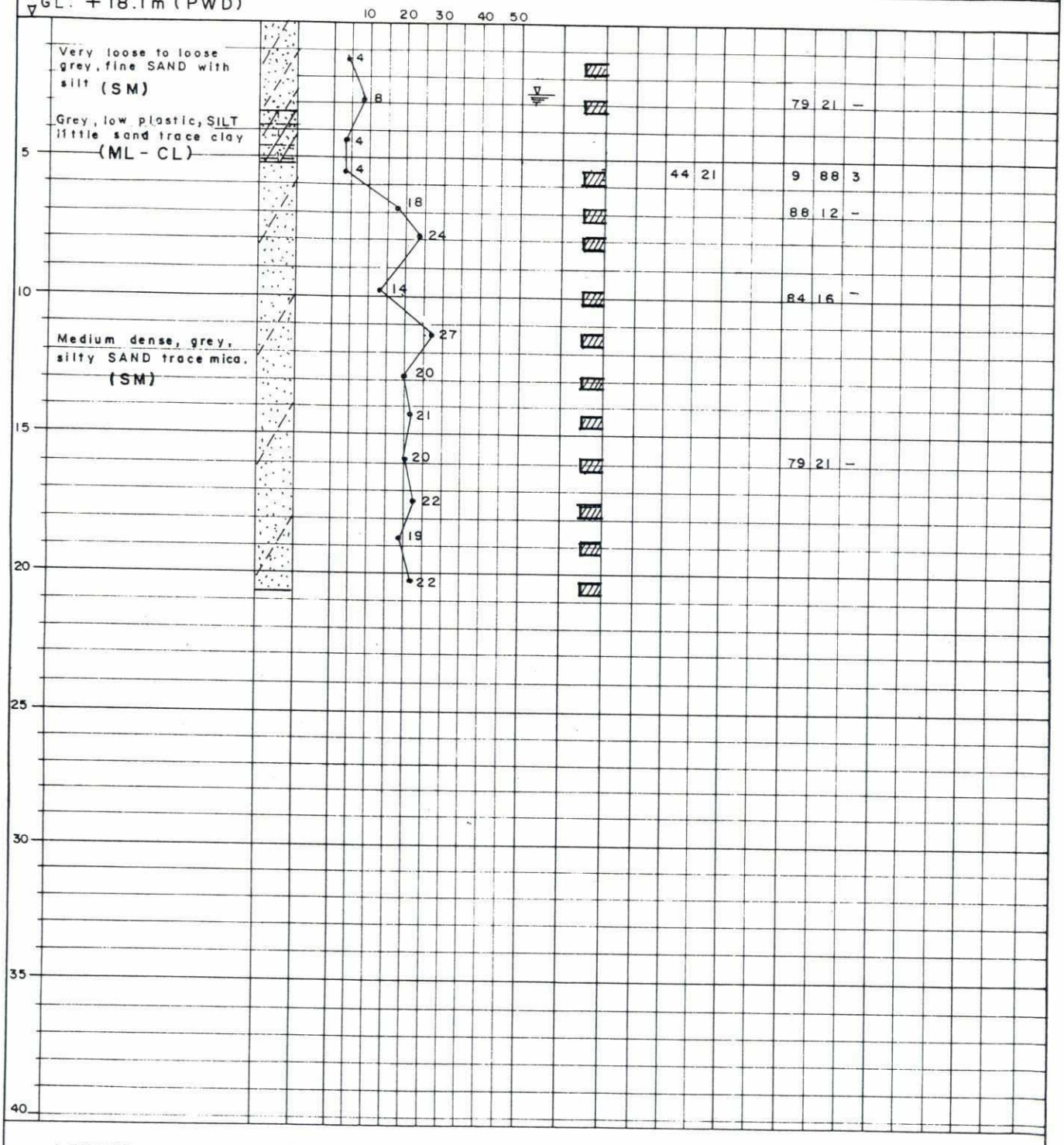
SOIL TEST RESULTS

FAP - 21 / 22

BANK PROTECTION AND RIVER TRAINING / (AFPM) PILOT PROJECT

FINAL REPORT | FIG. A. 13-15

LOCATION : BAHADURABAD	BORE HOLE NO. BA-3	METHOD OF BORING : WASH DIA OF BORING : 100 mm DATE OF EXECUTION : 8-5 to 9-5-92



LEGEND

- Sand
- CLay
- Silt
- Undisturbed Sample from Test Pit
- Disturbed Sample from Bore hole
- Undisturbed Sample from Bore hole
- T.A Triaxial shear test
- U.C. Unconfined Compression test

WORKS EXECUTED BY FOUNDATION CONSULTANTS LTD.

SOIL TEST RESULTS

FAP-21/22

BANK PROTECTION AND RIVER TRAINING/ (AFPM) PILOT PROJECT

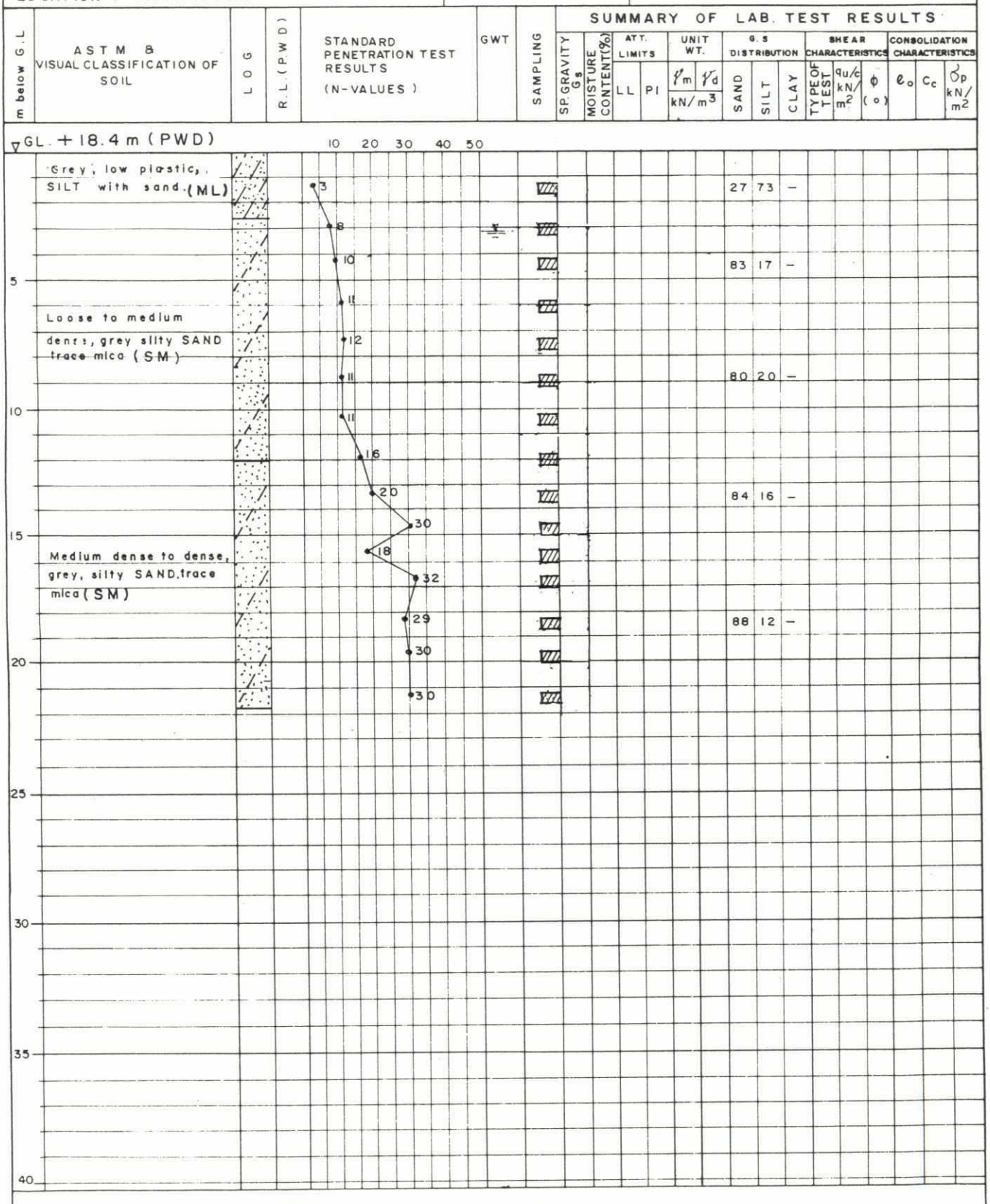
FINAL REPORT | FIG. A.13-16

7220

LOCATION : BAHADURABAD

BORE HOLE NO. BA — 4

METHOD OF BORING : WASH
DIA OF BORING : 100 mm.
DATE OF EXECUTION : 10-5 to 11-5-92



LEGEND

Sand
Clay
Silt

Undisturbed Sample from Test Pit
Disturbed Sample from Bore hole
Undisturbed Sample from Bore hole

T.A Triaxial shear test
U.C. Unconfined Compression test

WORKS EXECUTED BY FOUNDATION CONSULTANTS LTD.

SOIL TEST RESULTS

FAP-21/22

BANK PROTECTION AND RIVER TRAINING/ (AFPM) PILOT PROJECT

FINAL REPORT | FIG. A.13-17

LOCATION : BAHADURABAD

BORE HOLE NO. BA-6

METHOD OF BORING : WASH
DIA OF BORING : 100 mm
DATE OF EXECUTION : 12-5 to 13-5-92

m below G.L	ASTM & VISUAL CLASSIFICATION OF SOIL	LOG	R.L (P.W.D)	STANDARD PENETRATION TEST RESULTS (N-VALUES)	GWT	SAMPLING	SUMMARY OF LAB. TEST RESULTS																
							SP. GRAVITY G_s	MOISTURE CONTENT (%)	ATT. LIMITS LL	ATT. LIMITS PI	UNIT WT. γ_m kN/m³	UNIT WT. γ_d kN/m³	G.S DISTRIBUTION SAND	G.S DISTRIBUTION SILT	G.S DISTRIBUTION CLAY	SHEAR CHARACTERISTICS TYPE OF TEST	SHEAR CHARACTERISTICS q_u/c kN/m²	SHEAR CHARACTERISTICS ϕ (°)	CONSOLIDATION CHARACTERISTICS e_o	CONSOLIDATION CHARACTERISTICS C_c	CONSOLIDATION CHARACTERISTICS σ_p kN/m²
	GL. +18.9 m (PWD)			10 20 30 40 50																			
	Loose, grey, sandy SILT trace clay, mica (ML)			5									42	51	7								
				5																			
5				22									82	18	–								
				19									91	9									
				16									84	16	–								
				15																			
10	Medium dense, grey, silty SAND (SM) trace mica			21									82	18	–								
				20																			
				18									91	9	–								
15				17																			
				20																			
				22									86	14	–								
20				23									88	12	–								
				22																			
25																							
30																							
35																							
40																							

LEGEND

- Sand
- CLay
- Silt

- Undisturbed Sample from Test Pit
- Disturbed Sample from Bore hole
- Undisturbed Sample from Bore hole

T.A Triaxial shear test
U. C. Unconfined Compression test

WORKS EXECUTED BY FOUNDATION CONSULTANTS LTD.

SOIL TEST RESULTS

FAP-21/22

BANK PROTECTION AND RIVER TRAINING/ (AFPM) PILOT PROJECT

FINAL REPORT

FIG. A.13-18

LOCATION : CHANDANBAISA

BORE HOLE NO. CH-1

METHOD OF BORING : WASH
DIA OF BORING : 100 mm.
DATE OF EXECUTION : 12-4 to 14-4-92

m below G.L	ASTM & VISUAL CLASSIFICATION OF SOIL	LOG	R.L.(P.W.D)	STANDARD PENETRATION TEST RESULTS (N-VALUES)	GWT	SAMPLING	SUMMARY OF LAB. TEST RESULTS: SP. GRAVITY Gs	MOISTURE CONTENT(%)	ATT. LIMITS: LL	PI	UNIT WT. kN/m³: γm	γd	G.S DISTRIBUTION: SAND	SILT	CLAY	SHEAR CHARACTERISTICS: TYPE OF TEST	qu/c kN/m²	φ (°)	CONSOLIDATION CHARACTERISTICS: eo	Cc	σp kN/m²
	GL. + 15.0 m (PWD)			10 20 30 40 50																	
	Loose to medium dense, grey, SAND with silt trace mica (SM)			12									78	22	–						
				9	▽								77	23	–						
5	Very loose, grey, SAND with silt trace mica (SM)			3									65	35	–						
				12																	
				14									84	16	–						
				15																	
10				20																	
	Medium dense to very dense, grey, silty fine SAND trace mica (SM)			18																	
				24									81	19	–						
15				29																	
				22									84	16	–						
				20																	
20													90	10	–						
	Very dense grey SAND trace mica (SM)			82																	
				24																	
				31									76	24	–						
25				34									85	15	–						
	Dense, grey, silty SAND trace mica (SM)			27																	
				33																	
				36																	
30				33									92	8	–						
				49																	
	Very dense, grey SAND, little silt, trace mica (SM)			48									94	6	–						
35				60																	
				80									80	20	–						
				>50																	
40				>50									90	10	–						

LEGEND

- Sand
- CLay
- Silt

- Undisturbed Sample from Test Pit
- Disturbed Sample from Bore hole
- Undisturbed Sample from Bore hole

T.A Triaxial shear test
U. C. Unconfined Compression test

WORKS EXECUTED BY FOUNDATION CONSULTANTS LTD.

SOIL TEST RESULTS

FAP - 21 / 22

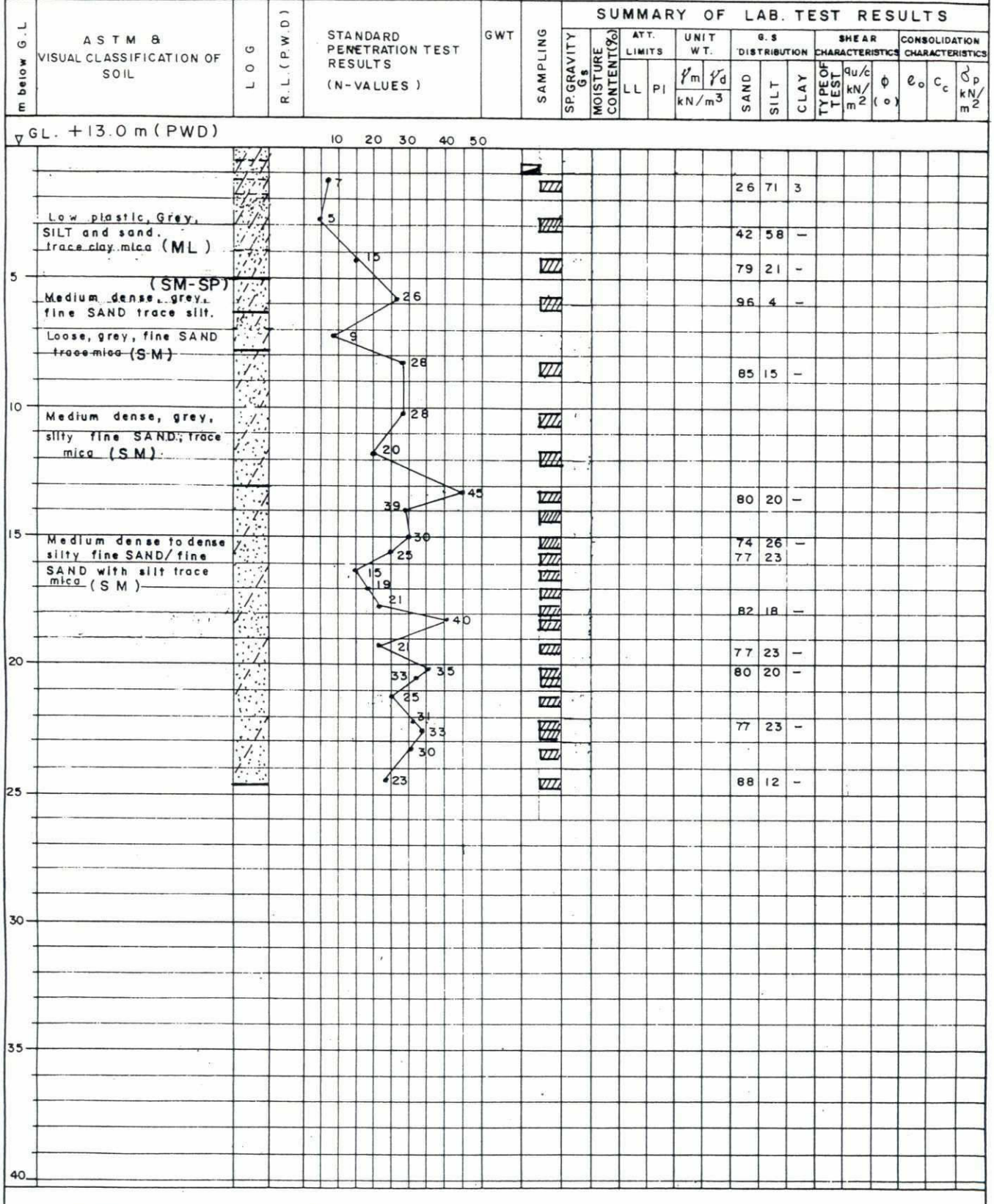
BANK PROTECTION AND RIVER TRAINING/ (AFPM) PILOT PROJECT

FINAL REPORT | FIG. A. 13 - 19

LOCATION : CHANDANBAISA

BORE HOLE NO. CH – 2

METHOD OF BORING : WASH
DIA OF BORING : 100 mm.
DATE OF EXECUTION : 14-4 to 15-4-92



LEGEND

- Sand
- CLay
- Silt
- Undisturbed Sample from Test Pit
- Disturbed Sample from Bore hole
- Undisturbed Sample from Bore hole

T.A Triaxial shear test.
U. C. Unconfined Compression test

WORKS EXECUTED BY FOUNDATION CONSULTANTS LTD.

SOIL TEST RESULTS

FAP-21/22

BANK PROTECTION AND RIVER TRAINING/ (AFPM) PILOT PROJECT

FINAL REPORT | FIG. A. 13–20

LOCATION : CHANDANBAISA.

BORE HOLE NO. CH - 3

METHOD OF BORING : WASH
DIA OF BORING : 100mm.
DATE OF EXECUTION : 22-4 to 23-4-92

SUMMARY OF LAB. TEST RESULTS

m below G.L	ASTM & VISUAL CLASSIFICATION OF SOIL	LOG	R.L (P.W.D)	STANDARD PENETRATION TEST RESULTS (N-VALUES)	GWT	SAMPLING	SP. GRAVITY Gs	MOISTURE CONTENT (%)	ATT. LIMITS LL	ATT. LIMITS PI	UNIT WT. γ_m kN/m³	UNIT WT. γ_d kN/m³	G.S DISTRIBUTION SAND	G.S DISTRIBUTION SILT	G.S DISTRIBUTION CLAY	SHEAR CHARACTERISTICS TYPE OF TEST	SHEAR CHARACTERISTICS qu/c kN/m²	SHEAR CHARACTERISTICS φ (°)	CONSOLIDATION CHARACTERISTICS e_o	CONSOLIDATION CHARACTERISTICS C_c	CONSOLIDATION CHARACTERISTICS γ_p kN/m²
	GL. + 15.5 m (PWD)			10 20 30 40 50																	
	Loose, brownish grey, fine SAND with silt, trace mica (SM)			7, 6									63	37	–						
	Grey, low plastic, sandy SILT little clay (ML-CL)			26			2.67						14	80	6						
5				25									80	20	–						
				12, 15, 21									83	17	–						
													86	14	–						
10	Medium dense, grey, silty fine to medium SAND trace mica (SM)			18, 21									88	12	–						
				43									88	12	–						
15				16, 28, 29									86	14	–						
	Very dense, grey SAND, little silt trace mica (SM)			57									92	8	–						
20	Medium dense, grey to dark grey, silty fine to medium SAND trace mica (SM)			18, 29									85	15	–						
				28, 26									84	16							
25													82	18	–						
30																					
35																					
40																					

LEGEND

- Sand
- CLay
- Silt

- Undisturbed Sample from Test Pit
- Disturbed Sample from Bore hole
- Undisturbed Sample from Bore hole

T.A Triaxial shear test
U. C. Unconfined Compression test

WORKS EXECUTED BY FOUNDATION CONSULTANTS LTD.

SOIL TEST RESULTS

FAP - 21 / 22

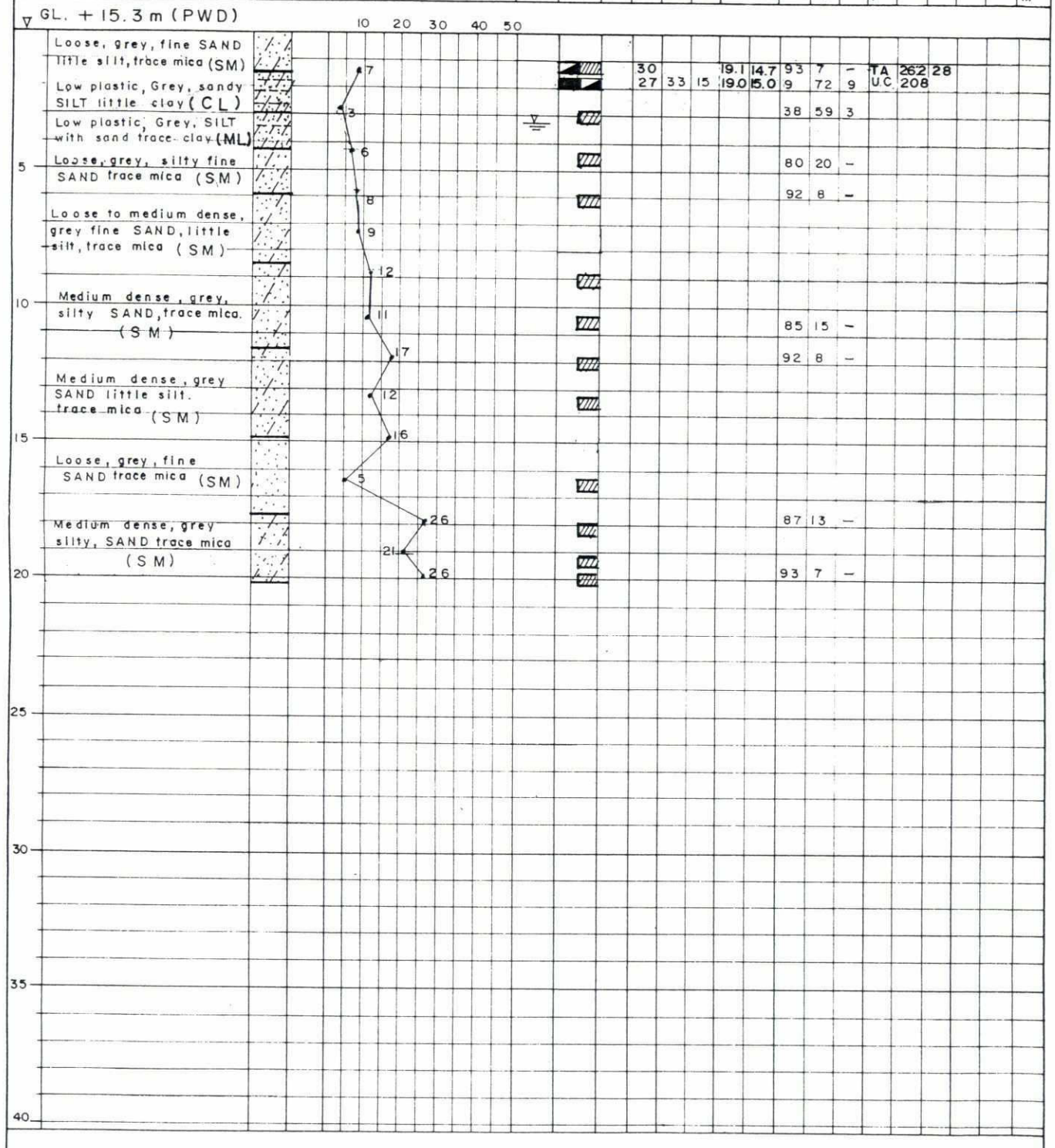
BANK PROTECTION AND RIVER TRAINING/ (AFPM) PILOT PROJECT

FINAL REPORT | FIG. A.13 - 21

LOCATION : CHANDANBAISA

BORE HOLE NO. CH – 4

METHOD OF BORING : WASH
DIA OF BORING : 100 mm
DATE OF EXECUTION : 23-4 to 24-4-92



LEGEND

- Sand
- CLay
- Silt
- Undisturbed Sample from Test Pit
- Disturbed Sample from Bore hole
- Undisturbed Sample from Bore hole
- T.A Triaxial shear test
- U. C. Unconfined Compression test

WORKS EXECUTED BY FOUNDATION CONSULTANTS LTD.

SOIL TEST RESULTS

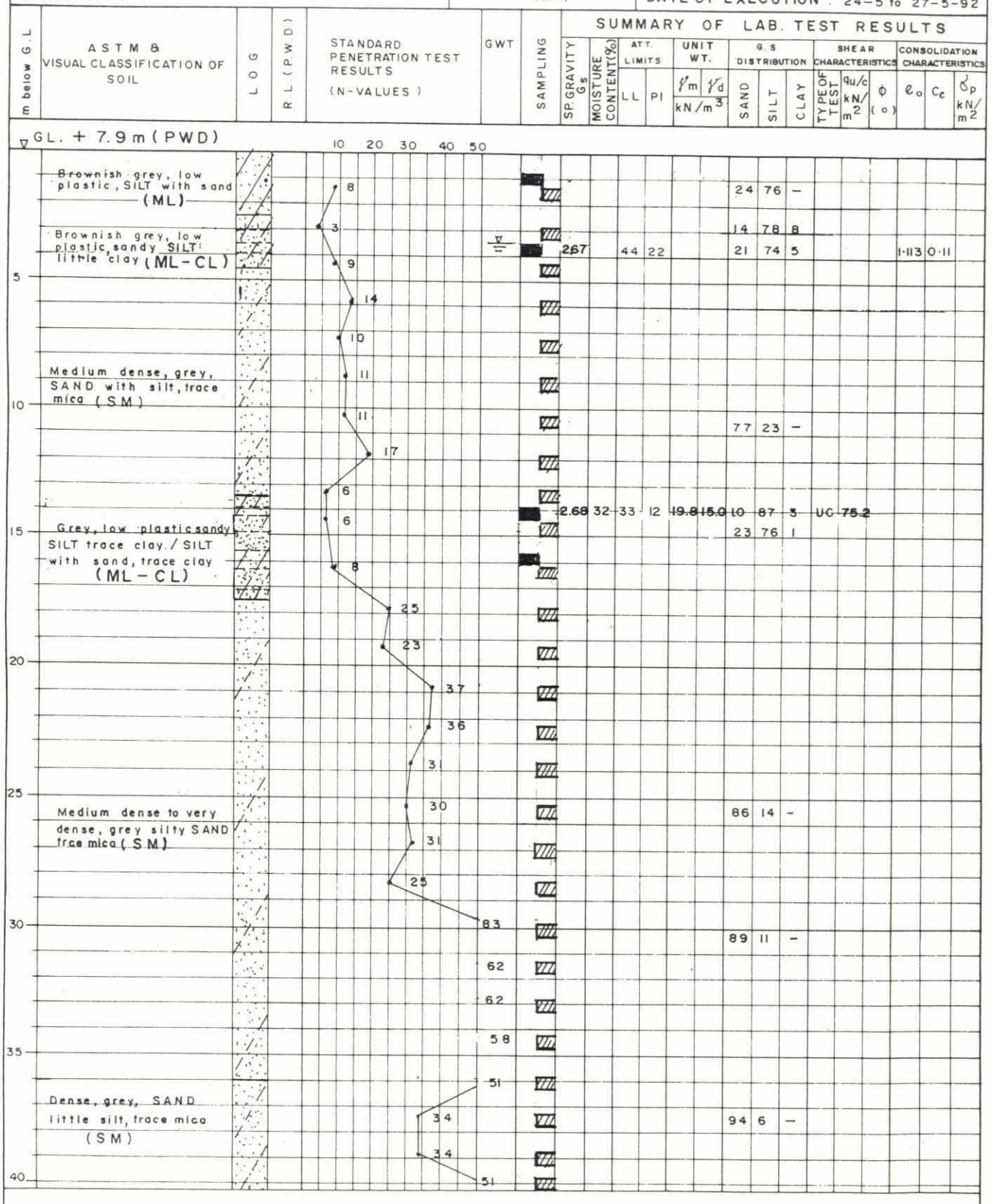
FAP-21/22

BANK PROTECTION AND RIVER TRAINING/ (AFPM) PILOT PROJECT

FINAL REPORT

FIG. A. 13-22

LOCATION : NAKALIA	BORE HOLE NO. NK-1	METHOD OF BORING : WASH DIA OF BORING : 100mm DATE OF EXECUTION : 24-5 to 27-5-92



LEGEND

- Sand
- Clay
- Silt

- Undisturbed Sample from Test Pit
- Disturbed Sample from Bore hole
- Undisturbed Sample from Bore hole

T.A Triaxial shear test

U.C. Unconfined Compression test

WORKS EXECUTED BY FOUNDATION CONSULTANTS LTD.

SOIL TEST RESULTS

FAP-21/22

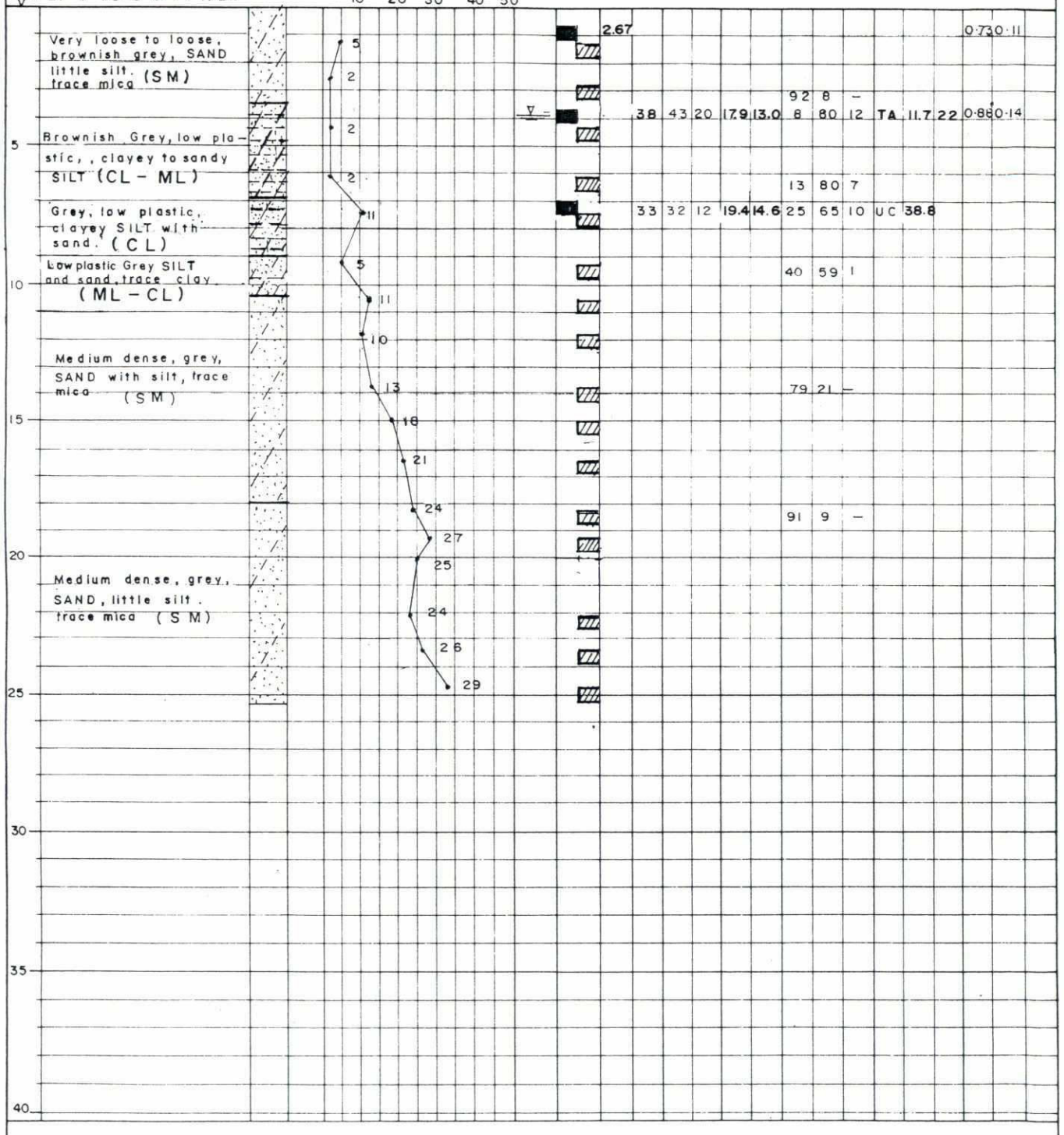
BANK PROTECTION AND RIVER TRAINING/ (AFPM) PILOT PROJECT

FINAL REPORT | FIG. A.13-23

LOCATION : NAKALIA.

BORE HOLE NO. NK-3

METHOD OF BORING : WASH
DIA OF BORING : 100 mm
DATE OF EXECUTION : 24-5 to 25-5-92



LEGEND

- Sand
- CLay
- Silt
- Undisturbed Sample from Test Pit
- Disturbed Sample from Bore hole
- Undisturbed Sample from Bore hole

T.A Triaxial shear test
U. C. Unconfined Compression test

WORKS EXECUTED BY FOUNDATION CONSULTANTS LTD.

SOIL TEST RESULTS

FAP - 21 / 22

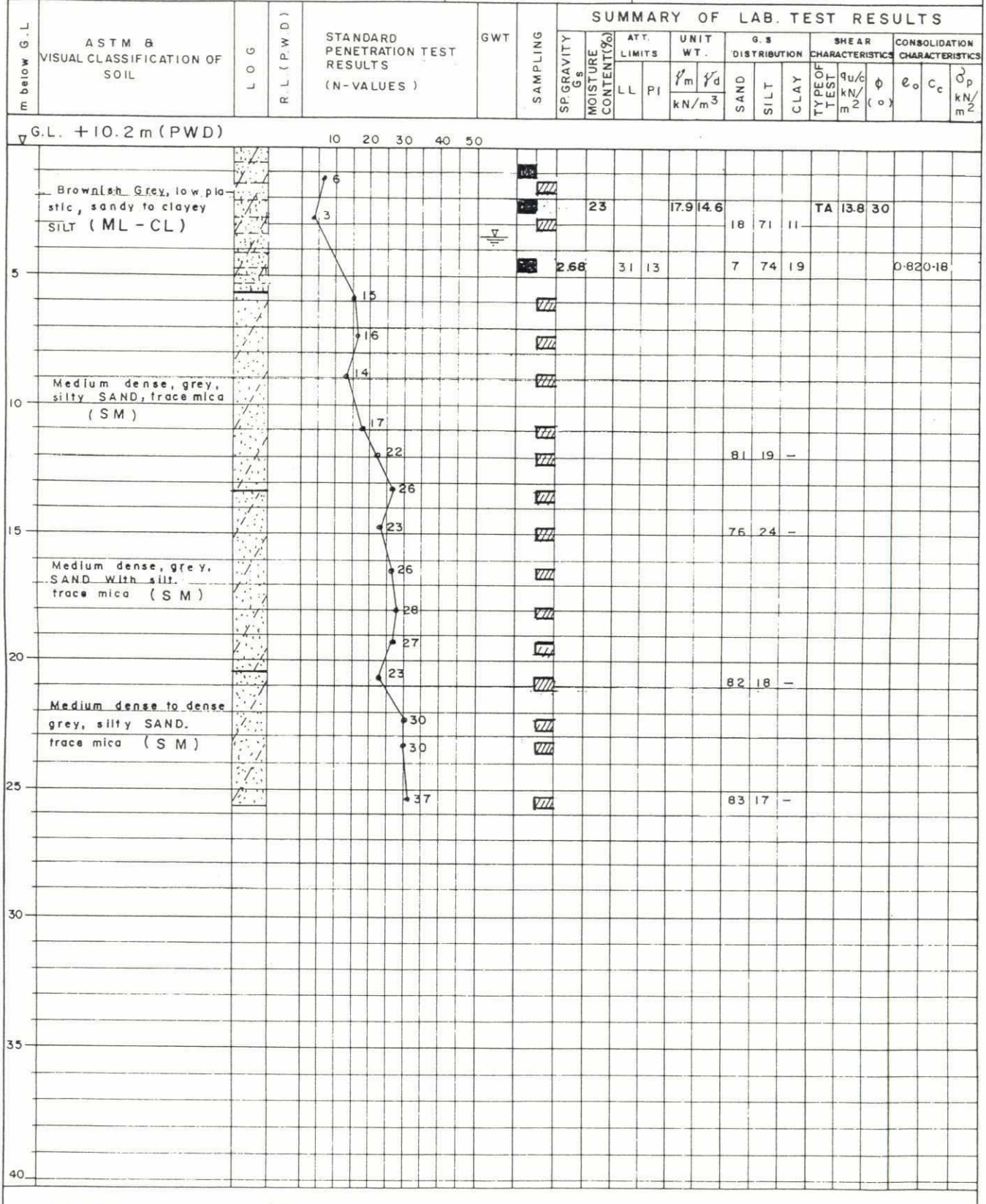
BANK PROTECTION AND RIVER TRAINING/ (A F P M) PILOT PROJECT

FINAL REPORT | FIG. A. 13 - 24

LOCATION : NAKALIA

BORE HOLE NO. NK-5

METHOD OF BORING : WASH
DIA OF BORING : 100mm
DATE OF EXECUTION : 27-5 to 28-5-92



SUMMARY OF LAB. TEST RESULTS

m below G.L	ASTM & VISUAL CLASSIFICATION OF SOIL	LOG	R.L (P.W.D)	STANDARD PENETRATION TEST RESULTS (N-VALUES)	GWT	SAMPLING	SP. GRAVITY Gs	MOISTURE CONTENT(%)	ATT. LIMITS LL	ATT. LIMITS PI	UNIT WT. γ_m kN/m³	UNIT WT. γ_d kN/m³	G.S DISTRIBUTION SAND	G.S DISTRIBUTION SILT	G.S DISTRIBUTION CLAY	SHEAR CHARACTERISTICS TYPE OF TEST	SHEAR CHARACTERISTICS q_u/c kN/m²	SHEAR CHARACTERISTICS ϕ (°)	CONSOLIDATION CHARACTERISTICS e_o	CONSOLIDATION CHARACTERISTICS C_c	CONSOLIDATION CHARACTERISTICS σ_p kN/m²
	Brownish Grey, low plastic, sandy to clayey SILT (ML-CL)			6, 3				23			17.9	14.6	18	71	11	TA	13.8	30			
5				15, 16, 14			2.68		31	13			7	74	19				0·820	0·18	
10	Medium dense, grey, silty SAND, trace mica (SM)			17, 22, 26									81	19	–						
15				23, 26, 28									76	24	–						
20	Medium dense, grey, SAND with silt, trace mica (SM)			27, 23									82	18	–						
25	Medium dense to dense grey, silty SAND, trace mica (SM)			30, 30, 37									83	17	–						
30																					
35																					
40																					

LEGEND

- Sand
- CLay
- Silt

- Undisturbed Sample from Test Pit
- Disturbed Sample from Bore hole
- Undisturbed Sample from Bore hole

T.A Triaxial shear test
U.C. Unconfined Compression test

WORKS EXECUTED BY FOUNDATION CONSULTANTS LTD.

SOIL TEST RESULTS

FAP-21/22

BANK PROTECTION AND RIVER TRAINING/ (AFPM) PILOT PROJECT

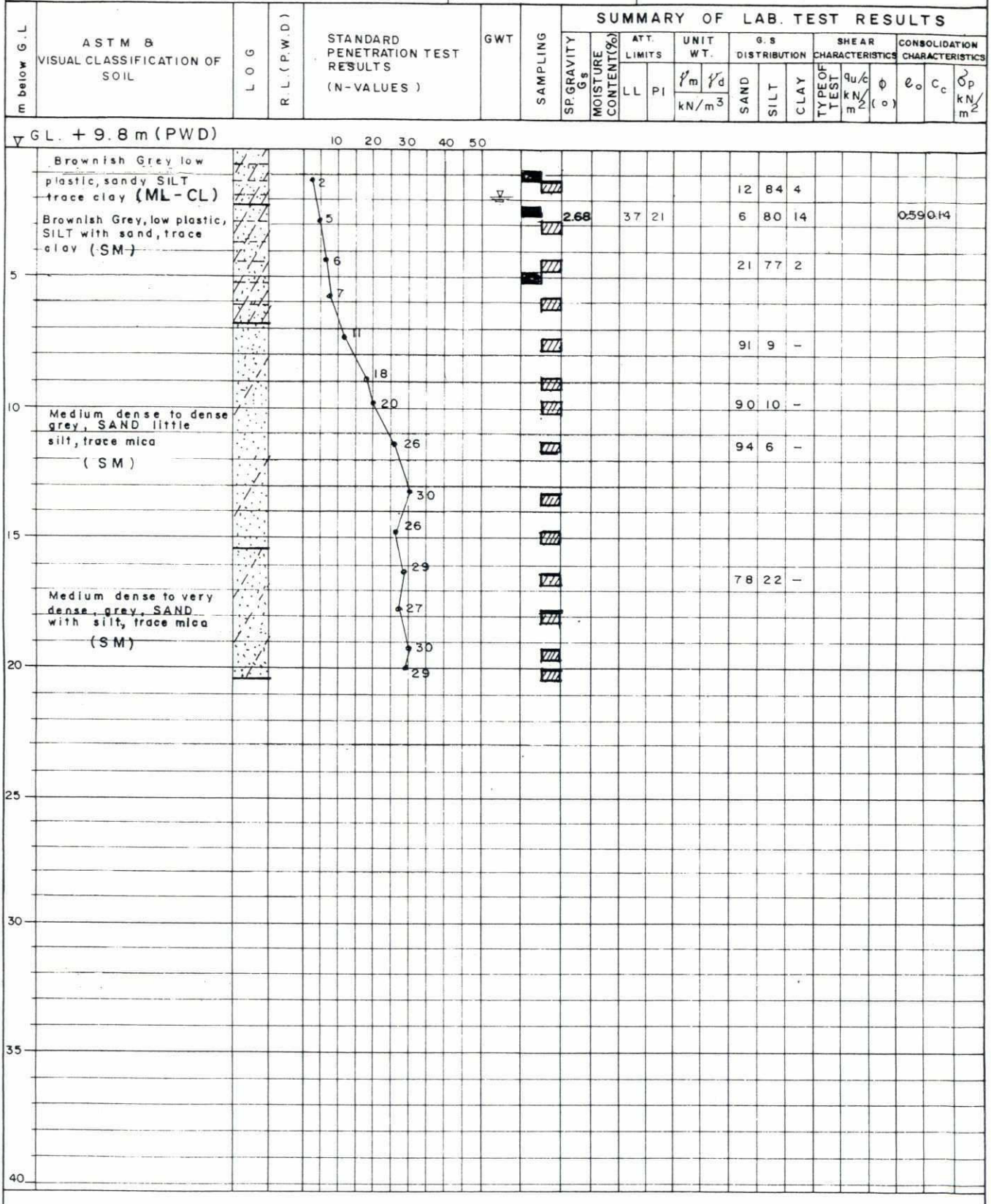
FINAL REPORT

FIG. A. 13÷25

LOCATION : NAKALIA.

BORE HOLE NO. NK-7

METHOD OF BORING : WASH
DIA OF BORING : 100 mm
DATE OF EXECUTION : 29-5 to 30-5-92



LEGEND

- Sand
- Clay
- Silt

- Undisturbed Sample from Test Pit
- Disturbed Sample from Bore hole
- Undisturbed Sample from Bore hole

T.A Triaxial shear test
U.C. Unconfined Compression test

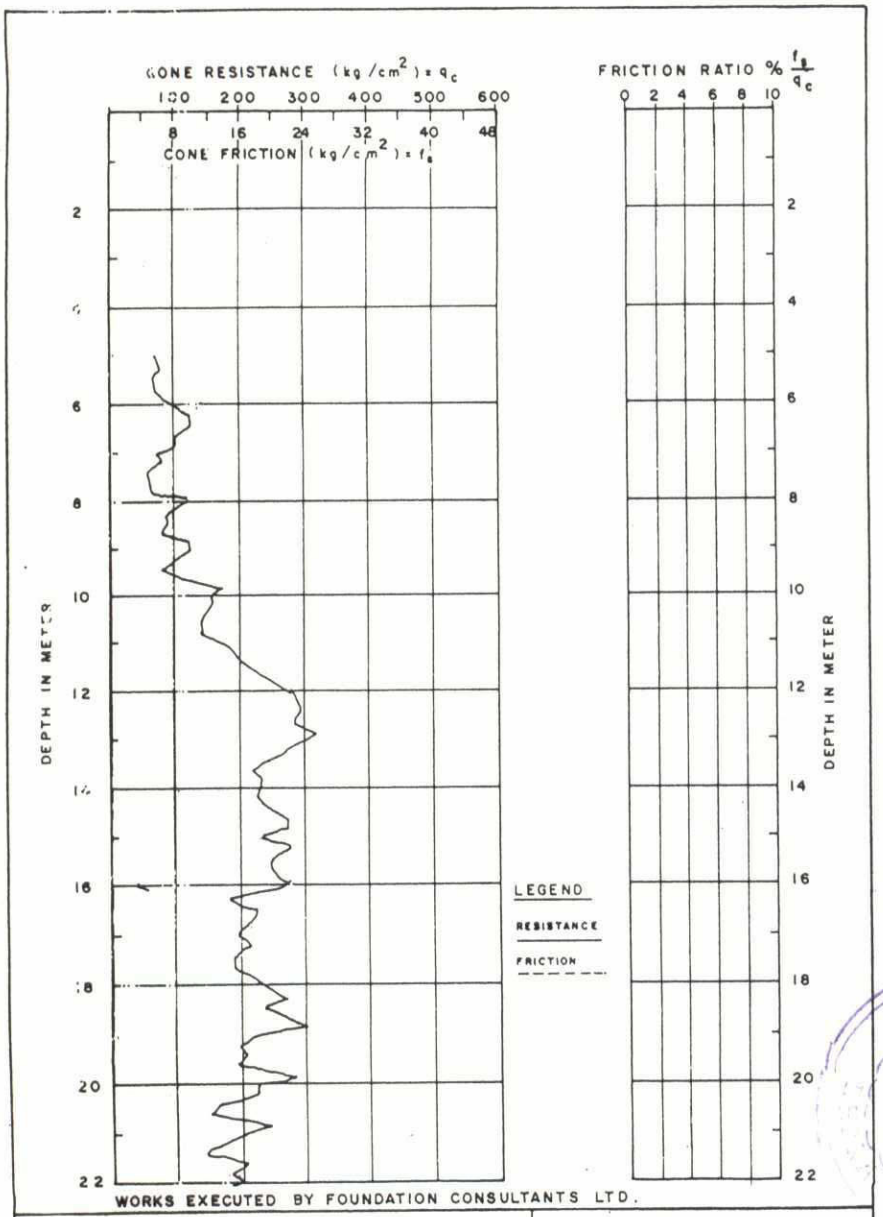
WORKS EXECUTED BY FOUNDATION CONSULTANTS LTD.

SOIL TEST RESULTS

FAP-21/22

BANK PROTECTION AND RIVER TRAINING/ (AFPM) PILOT PROJECT

FINAL REPORT | FIG. A. 13-26



CONE PENETRATION TEST

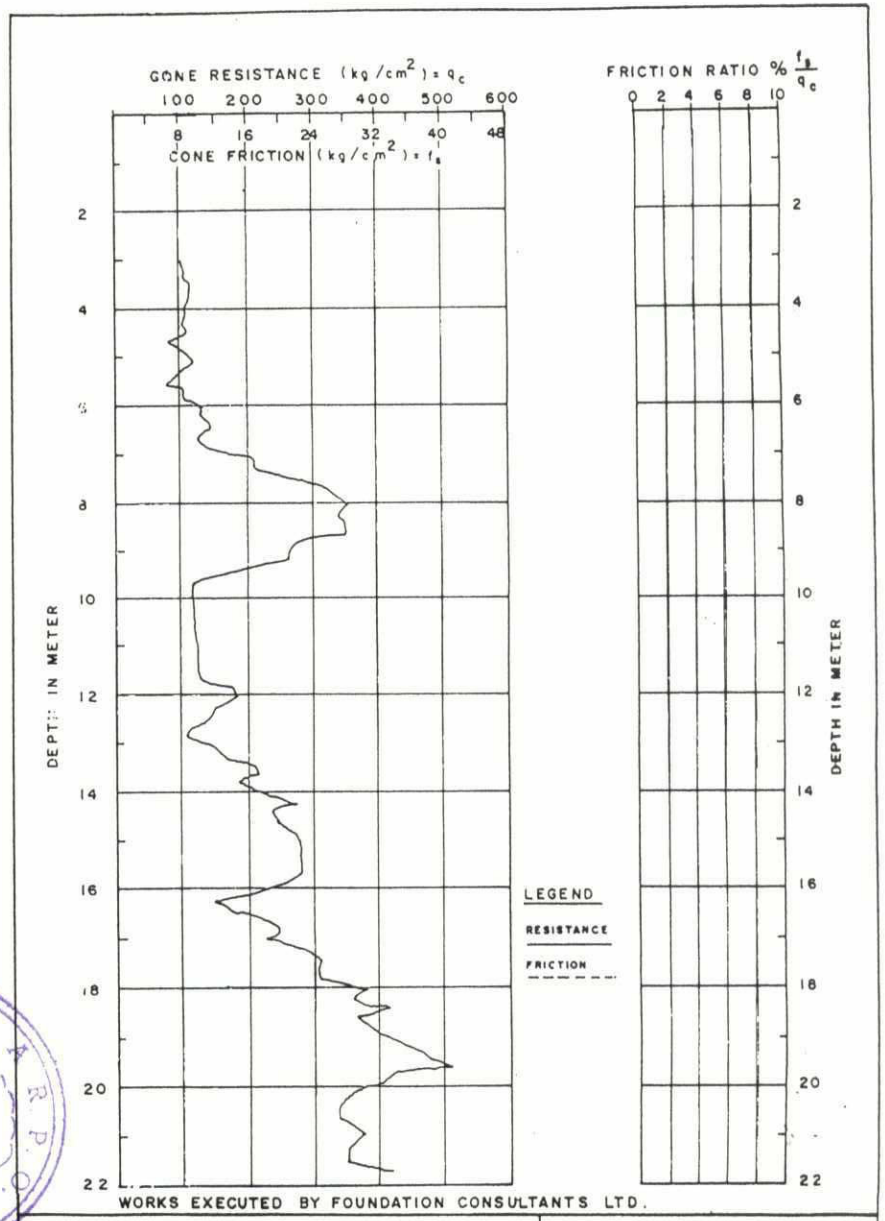
LOCATION: KAMARJANI-2

FAP-21/22

BANK PROTECTION AND RIVER TRAINING/ (AFPM) PILOT PROJECT

FINAL REPORT | FIG. A.13-27

W.A.P.R.O. LIBRARY.



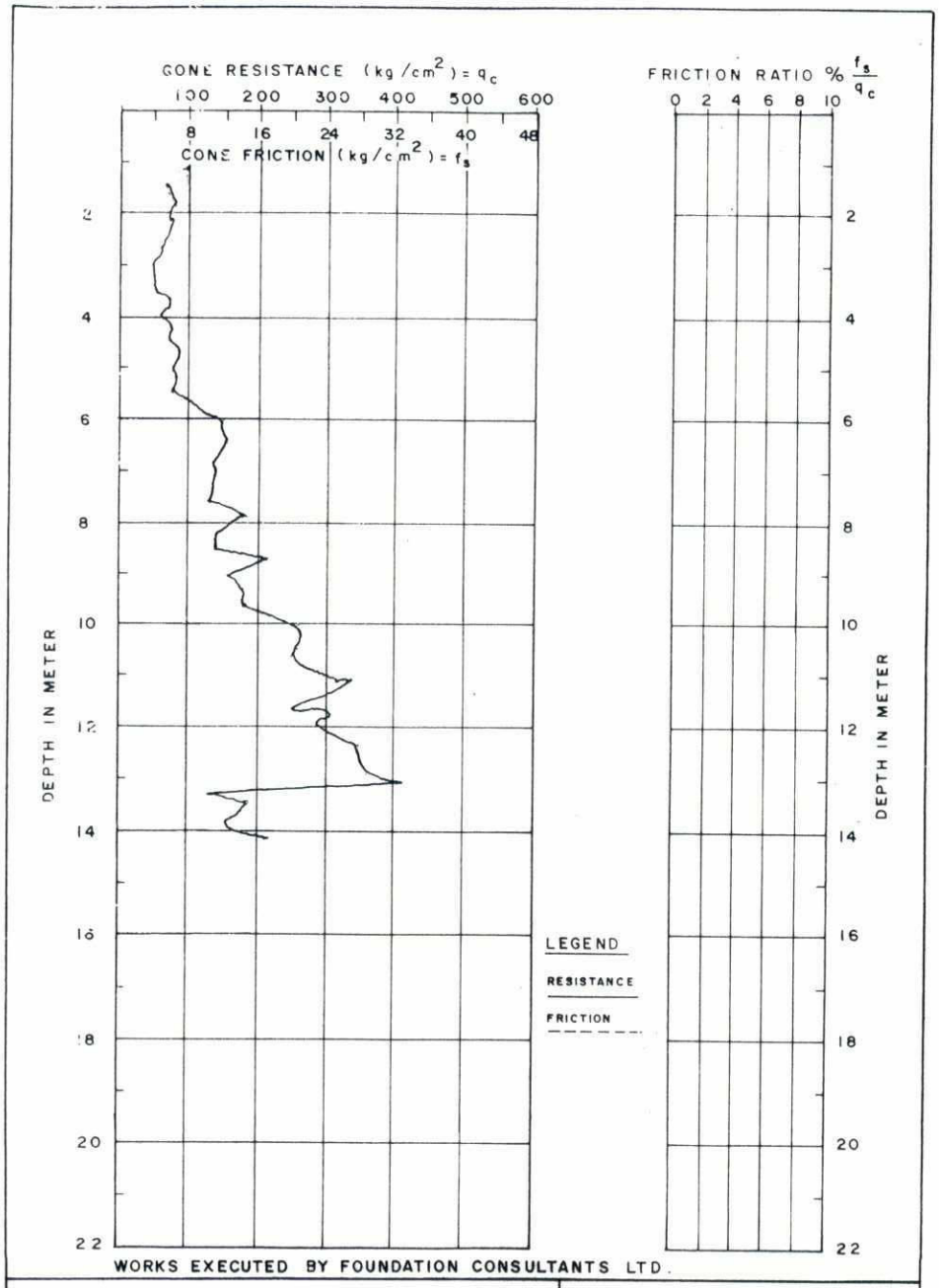
CONE PENETRATION TEST

LOCATION: KAMARJANI-3

FAP-21/22

BANK PROTECTION AND RIVER TRAINING/ (AFPM) PILOT PROJECT

FINAL REPORT | FIG. A.13-28



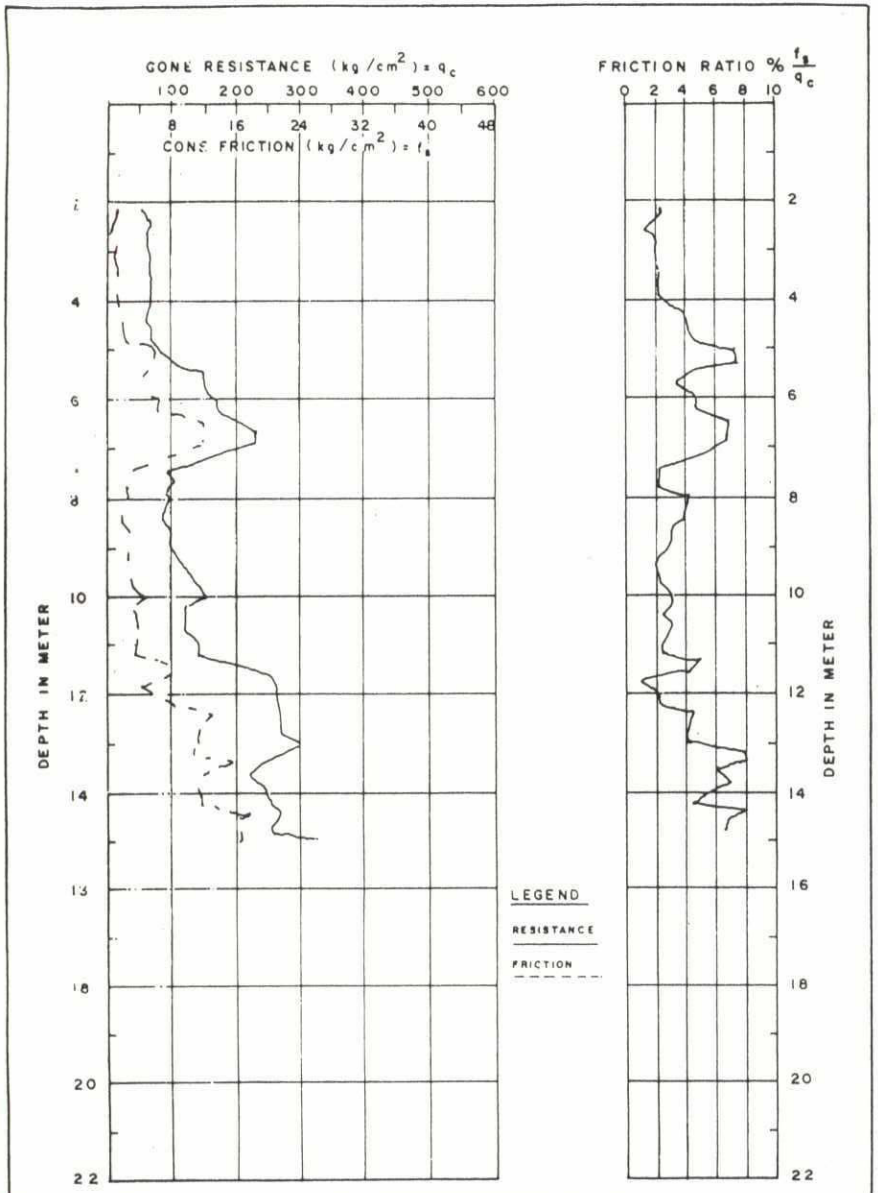
CONE PENETRATION TEST

LOCATION: BAHADURABAD - 2

FAP - 21/22

BANK PROTECTION AND RIVER TRAINING/ (AFPM) PILOT PROJECT

FINAL REPORT | FIG. A.13 - 29



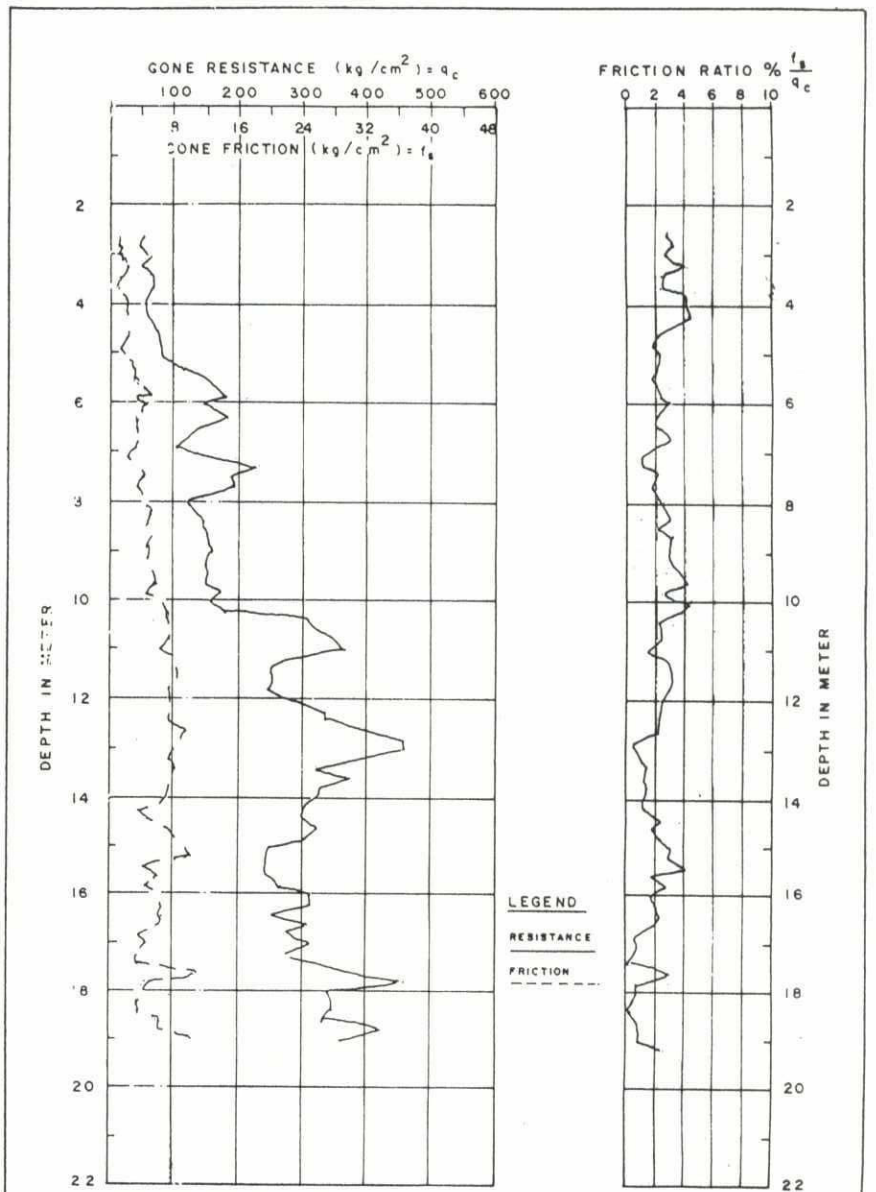
CONE PENETRATION TEST

LOCATION: BAHADURABAD - 5

FAP-21/22

BANK PROTECTION AND RIVER TRAINING/ (AFPM) PILOT PROJECT

FINAL REPORT | FIG. A.13-30



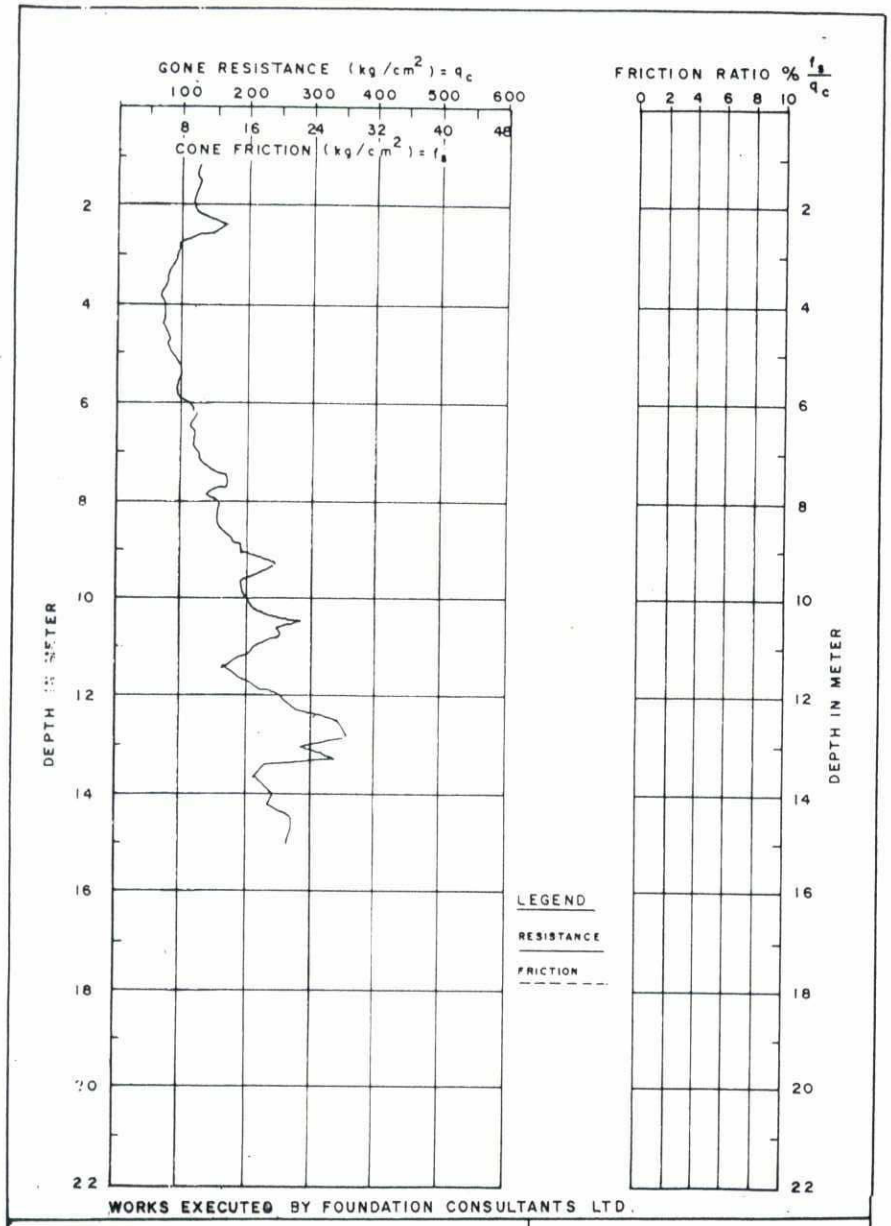
CONE PENETRATION TEST

LOCATION: BAHADURABAD - 7

FAP-21/22

BANK PROTECTION AND RIVER TRAINING/ (AFPM) PILOT PROJECT

FINAL REPORT | FIG. A.13-31



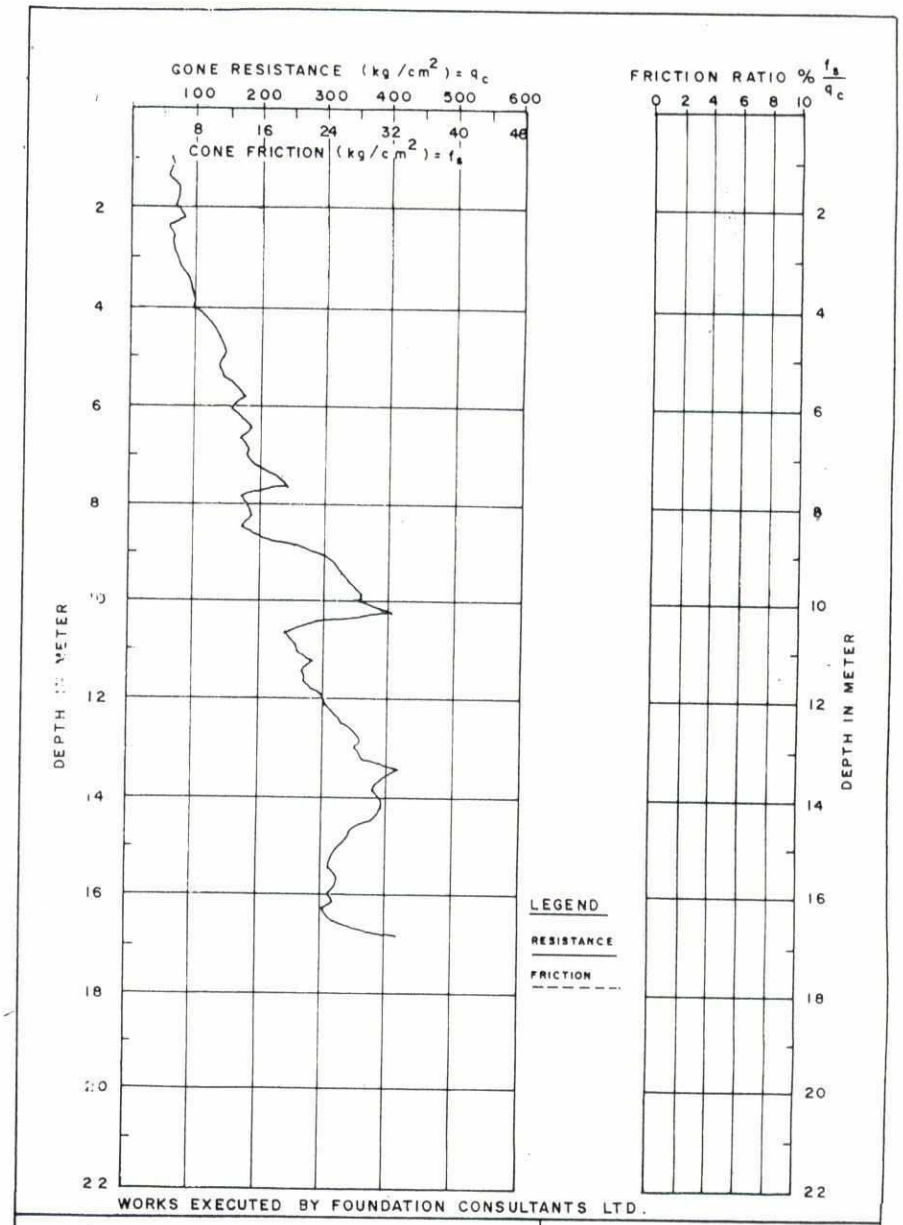
CONE PENETRATION TEST

LOCATION: CHANDANBAISA – 1

FAP – 21/22

BANK PROTECTION AND RIVER TRAINING / (AFPM) PILOT PROJECT

FINAL REPORT | FIG. A.13–32



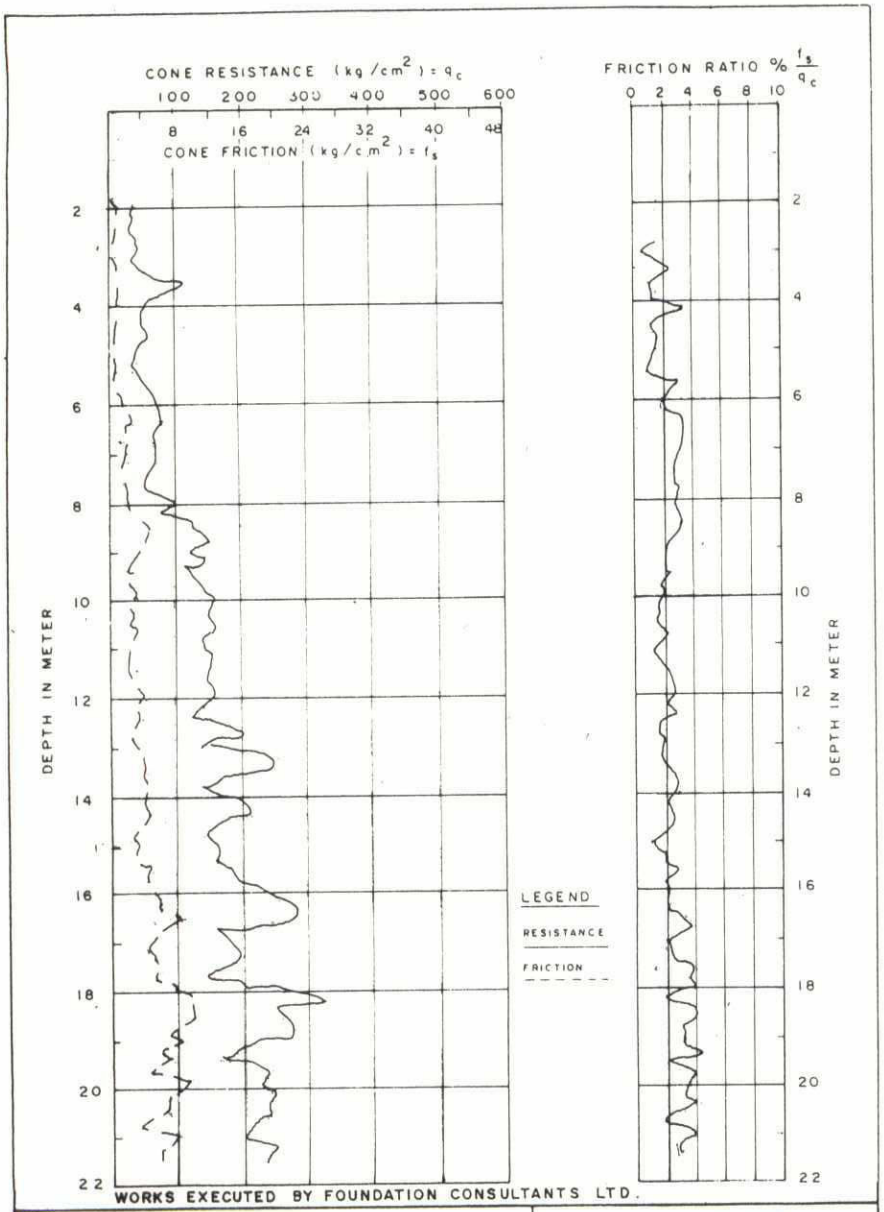
CONE PENETRATION TEST

LOCATION: CHANDANBAISA–2

FAP – 21/22

BANK PROTECTION AND RIVER TRAINING / (AFPM) PILOT PROJECT

FINAL REPORT | FIG. A.13–33



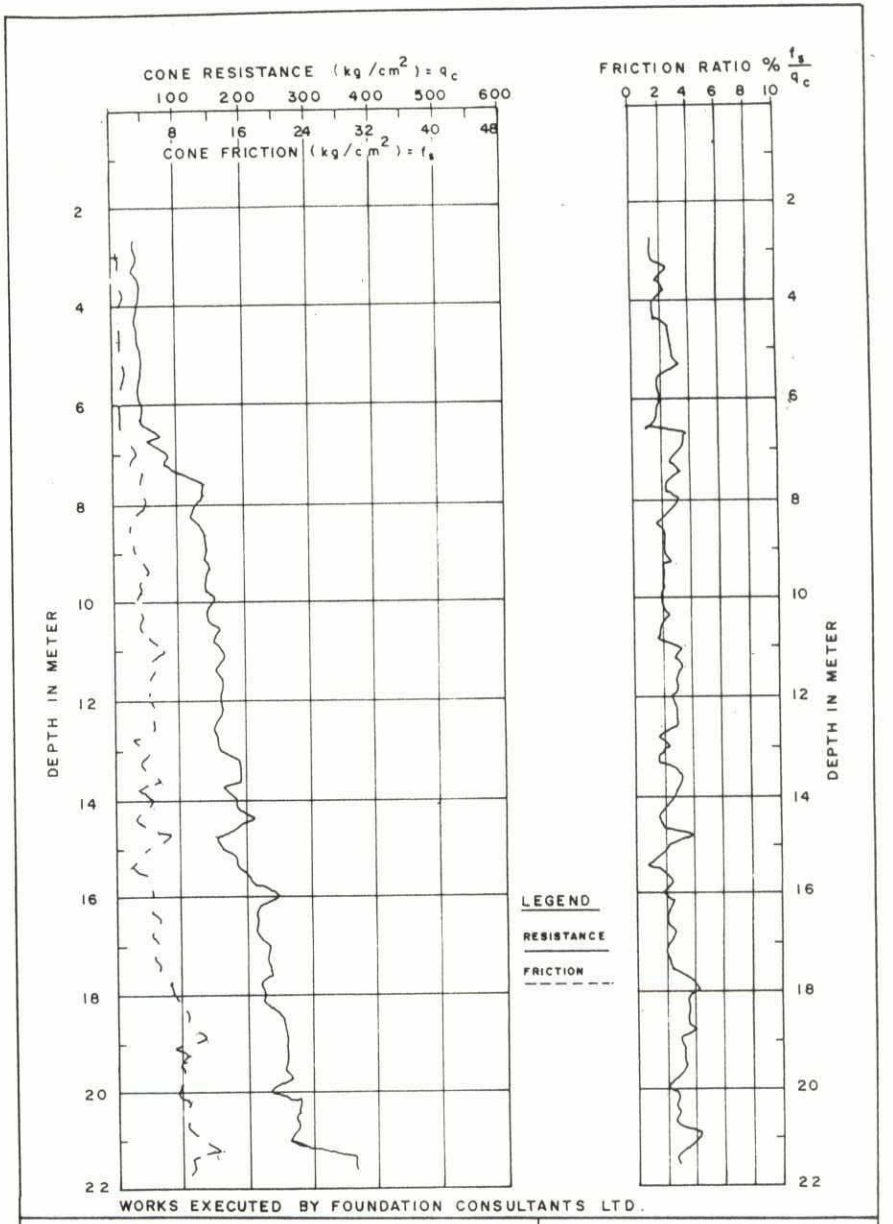
CONE PENETRATION TEST

LOCATION: NAKALIA – 2

FAP – 21/22

BANK PROTECTION AND RIVER TRAINING/ (AFPM) PILOT PROJECT

FINAL REPORT | **FIG. A.13–34**



CONE PENETRATION TEST

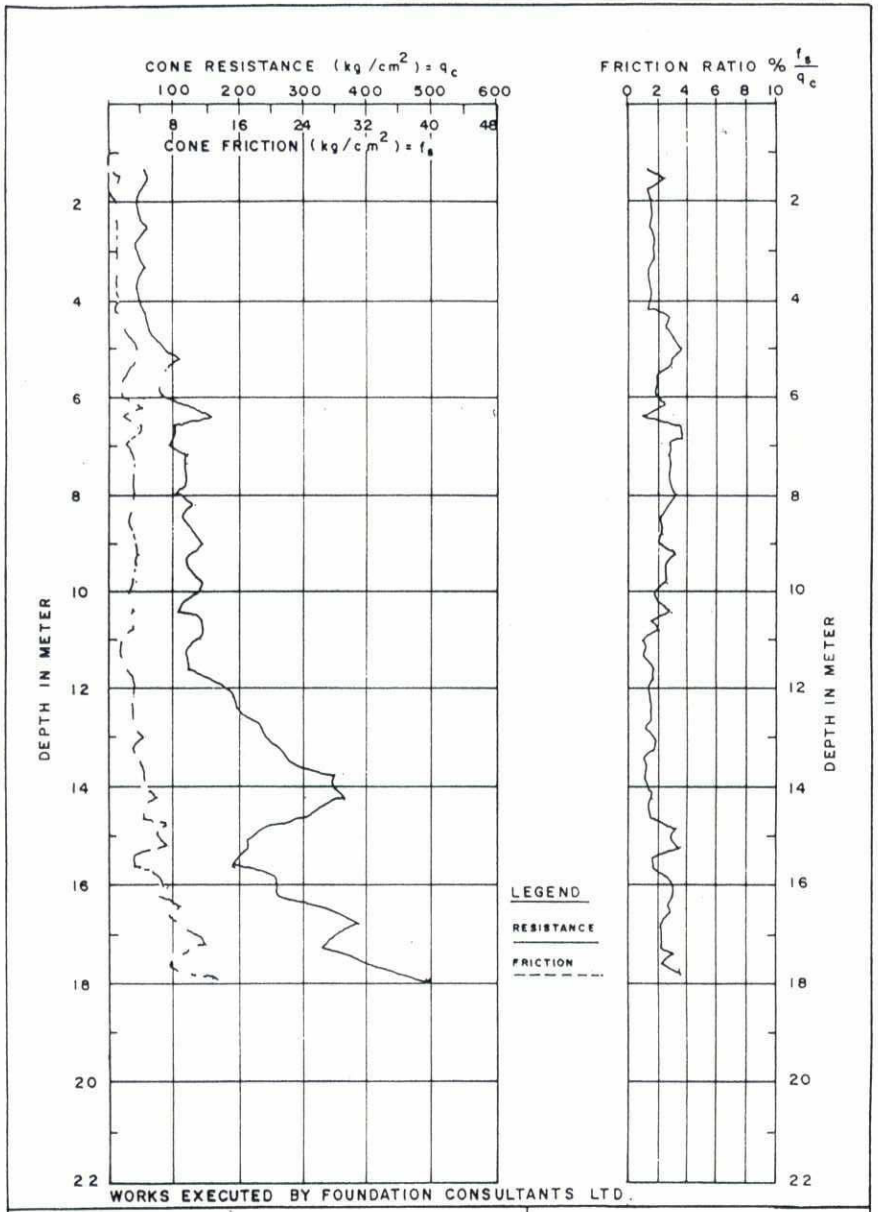
LOCATION: NAKALIA – 4

FAP – 21/22

BANK PROTECTION AND RIVER TRAINING/ (AFPM) PILOT PROJECT

FINAL REPORT | **FIG. A.13–35**

208



CONE PENETRATION TEST

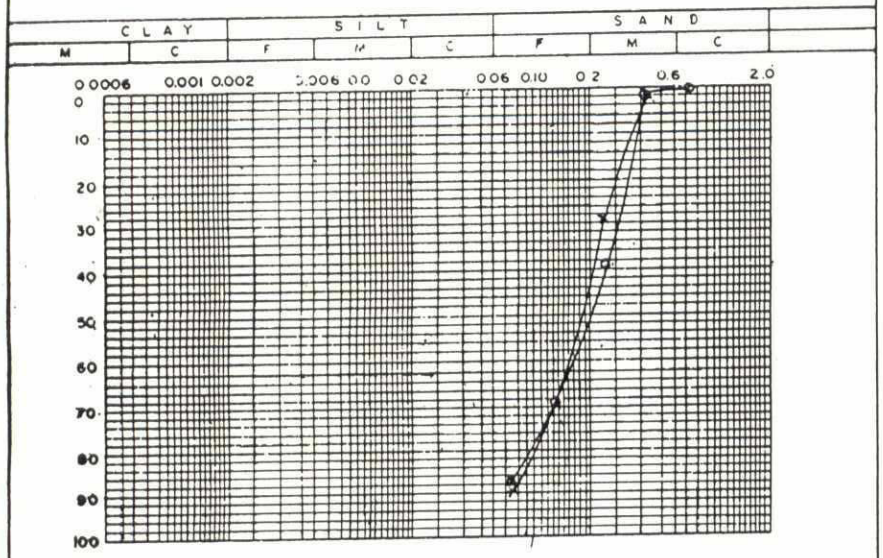
LOCATION: NAKALIA – 6

FAP – 21/22

BANK PROTECTION AND RIVER TRAINING/ (AFPM) PILOT PROJECT

FINAL REPORT | FIG. A. 13 – 36

SOIL INVESTIGATION | LOCATION : KAMARJANI



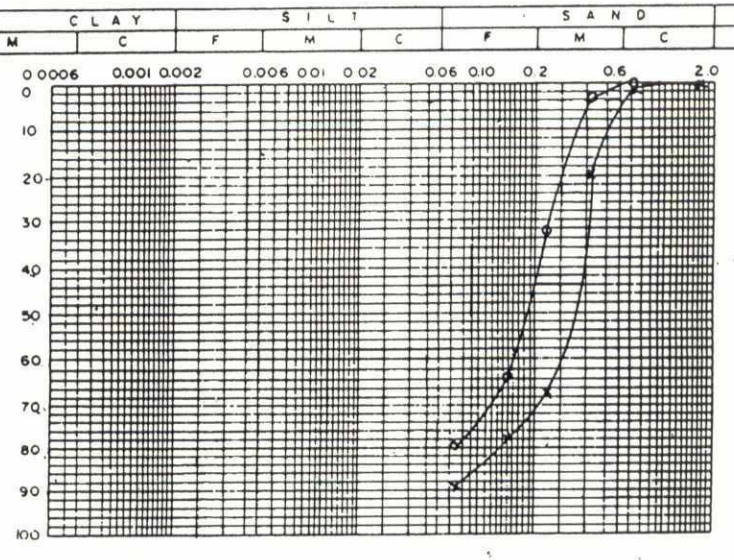
SYMBOL	BORE HOLE NO.	SAMPLE NO.	DEPTH (m)	CLASSIFICATION	CLAY %	SILT %	SAND %	REMARKS D_{60}
0 0 0	GA – 1	D – 4	5.85–6.3m	SM	—	13	87	.26mm
X X X	GA – 1	D – 5	7.35–7.8m	SM	—	11	89	.22mm

WORKS EXECUTED BY FOUNDATION CONSULTANTS LTD.

GRAIN SIZE DISTRIBUTION

FAP-21/22
BANK PROTECTION AND RIVER TRAINING/ (AFPM) PILOT PROJECT
FINAL REPORT | FIG. A.13-37

SOIL INVESTIGATION | LOCATION : KAMARJANI



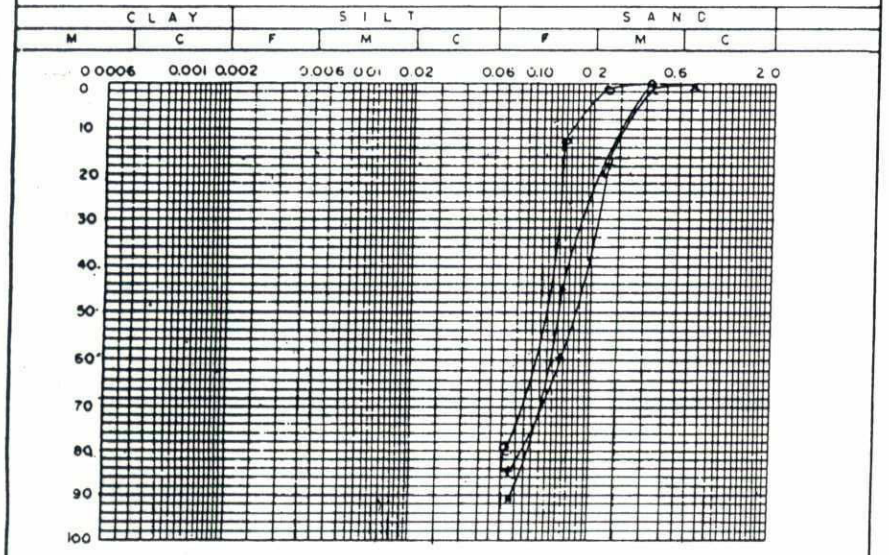
SYMBOL	BORE HOLE NO.	SAMPLE NO.	DEPTH (m)	CLASSIFICATION	CLAY %	SILT %	SAND %	REMARKS D_{60}
0 0 0	GA – 1	D – 10	14.85–15.3m	SM	—	20	80	.25mm
X X X	GA – 1	D – 14	20.85–21.3m	SM	—	11	89	.4mm

WORKS EXECUTED BY FOUNDATION CONSULTANTS LTD.

GRAIN SIZE DISTRIBUTION

FAP-21/22
BANK PROTECTION AND RIVER TRAINING/ (AFPM) PILOT PROJECT
FINAL REPORT | FIG. A.13-38

SOIL INVESTIGATION | LOCATION : KAMARJANI



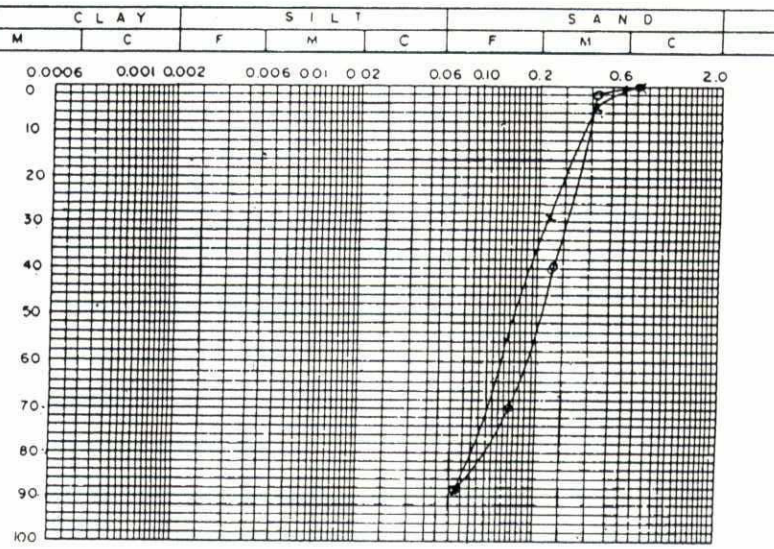
SYMBOL	BORE HOLE NO.	SAMPLE NO.	DEPTH (m)	CLASSIFICATION	CLAY %	SILT %	SAND %	RENARKS D_{60}
0 0 0	GA – 2	D – 4	5.95 – 6.39m	SM	—	21	79	.13mm
X X X	GA – 2	D – 7	9.66 – 10.11m	SM	—	15	85	.2mm
– · – · –	GA – 2	D – 10	14.75 – 15.2m	SM	—	9	91	.16mm

WORKS EXECUTED BY FOUNDATION CONSULTANTS LTD.

GRAIN SIZE DISTRIBUTION

FAP - 21/22
BANK PROTECTION AND RIVER TRAINING/ (AFPM) PILOT PROJECT
FINAL REPORT | FIG. A.13-39

SOIL INVESTIGATION | LOCATION : KAMARJANI



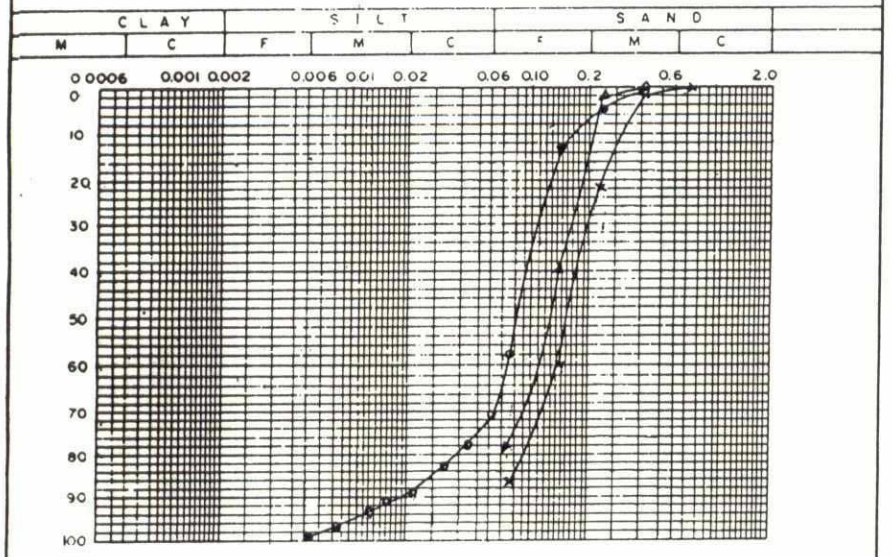
SYMBOL	BORE HOLE NO.	SAMPLE NO.	DEPTH (m)	CLASSIFICATION	CLAY %	SILT %	SAND %	RENARKS D_{60}
0 0 0	GA – 2	D – 11	15.35 – 15.8m	SM	—	11	89	.27mm
X X X	GA – 2	D – 14	19.3 – 19.75m	SM	—	12	88	.185mm

WORKS EXECUTED BY FOUNDATION CONSULTANTS LTD.

GRAIN SIZE DISTRIBUTION

FAP - 21/22
BANK PROTECTION AND RIVER TRAINING/ (AFPM) PILOT PROJECT
FINAL REPORT | FIG. A.13-40

SOIL INVESTIGATION	LOCATION : KAMARJANI

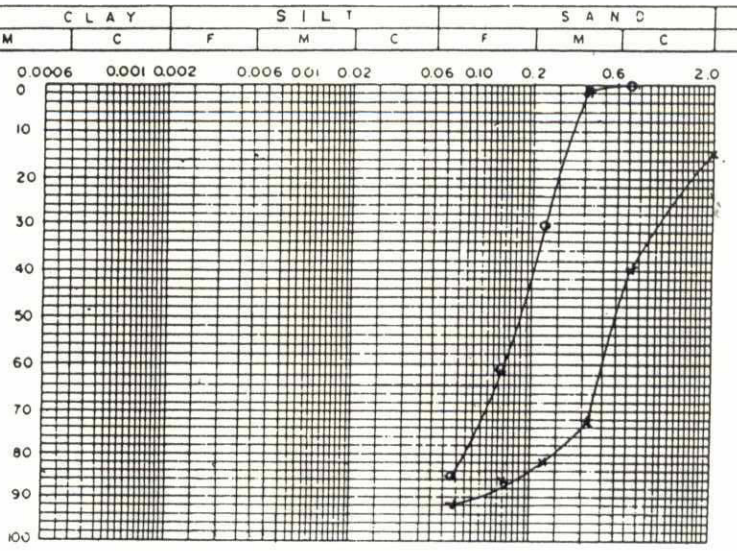


SYMBOL	BORE HOLE NO.	SAMPLE NO.	DEPTH (m)	CLASSIFICATION	CLAY %	SILT %	SAND %	REMARKS D_{60}
0 0 0	GA – 4	D – 1	1.35 – 1.8 m	SM	—	28	72	.092mm
X X X	GA – 4	D – 5	7.85 – 8.3m	SM	—	15	85	.17mm
Δ Δ Δ	GA – 4	D – 6	9.35 – 9.8m	SM	—	22	78	.15mm

WORKS EXECUTED BY FOUNDATION CONSULTANTS LTD.

GRAIN SIZE DISTRIBUTION	FAP – 21/22 BANK PROTECTION AND RIVER TRAINING/ (AFPM) PILOT PROJECT	
	FINAL REPORT	FIG. A.13 – 41

SOIL INVESTIGATION	LOCATION : KAMARJANI

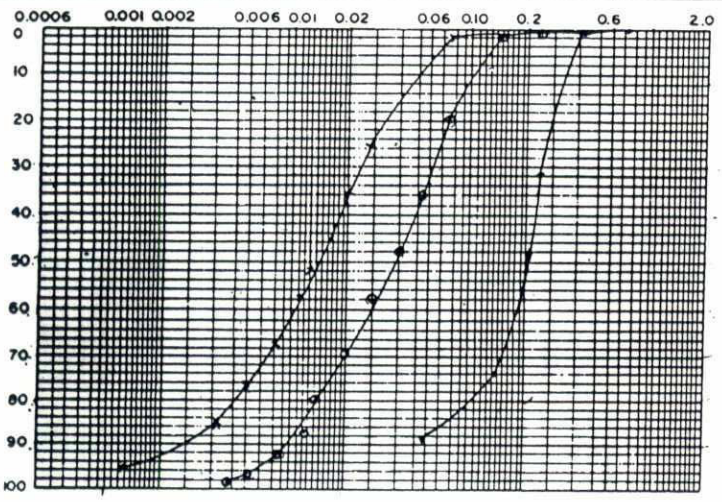


SYMBOL	BORE HOLE NO.	SAMPLE NO.	DEPTH (m)	CLASSIFICATION	CLAY %	SILT %	SAND %	REMARKS D_{60}
0 0 0	GA – 4	D – 9	14.15 – 14.6m	SM	—	14	86	.2 mm
X X X	GA – 4	D – 13	19.85 – 20.3m	SM	—	8	92	.72mm

WORKS EXECUTED BY FOUNDATION CONSULTANTS LTD.

GRAIN SIZE DISTRIBUTION	FAP – 21/22 BANK PROTECTION AND RIVER TRAINING/ (AFPM) PILOT PROJECT	
	FINAL REPORT	FIG. A.13 – 42

SOIL INVESTIGATION	LOCATION : KAMARJANI

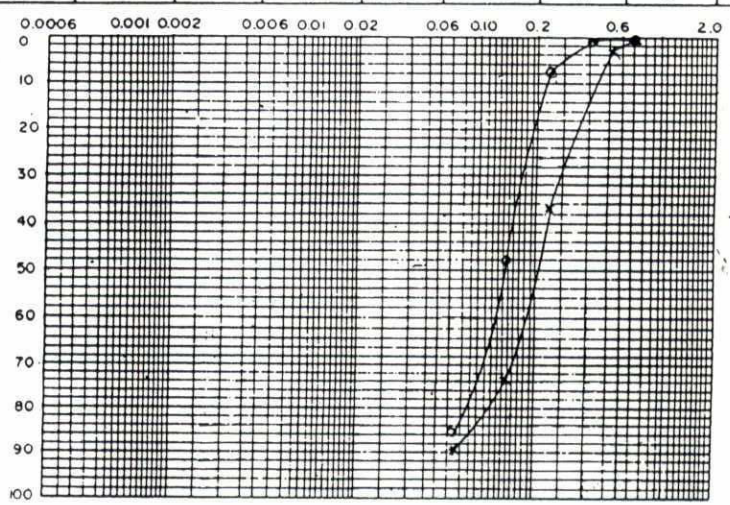


SYMBOL	BORE HOLE NO.	SAMPLE NO.	DEPTH (m)	CLASSIFICATION	CLAY %	SILT %	SAND %	REMARKS D_{60}
o o o	GA – 5	D – 2	3.2 – 3.65m	ML	—	67	33	.048mm
x x x	GA – 5	UD – 2	3.8 – 4.25m	ML — CL	7	85	8	.018mm
· · ·	GA – 5	D – 6	8.8 – 9.25m	SM	—	12	88	.23mm

WORKS EXECUTED BY FOUNDATION CONSULTANTS LTD.

GRAIN SIZE DISTRIBUTION	FAP - 21/22 BANK PROTECTION AND RIVER TRAINING/ (AFPM) PILOT PROJECT
	FINAL REPORT | FIG. A.13 – 43

SOIL INVESTIGATION	LOCATION : KAMARJANI

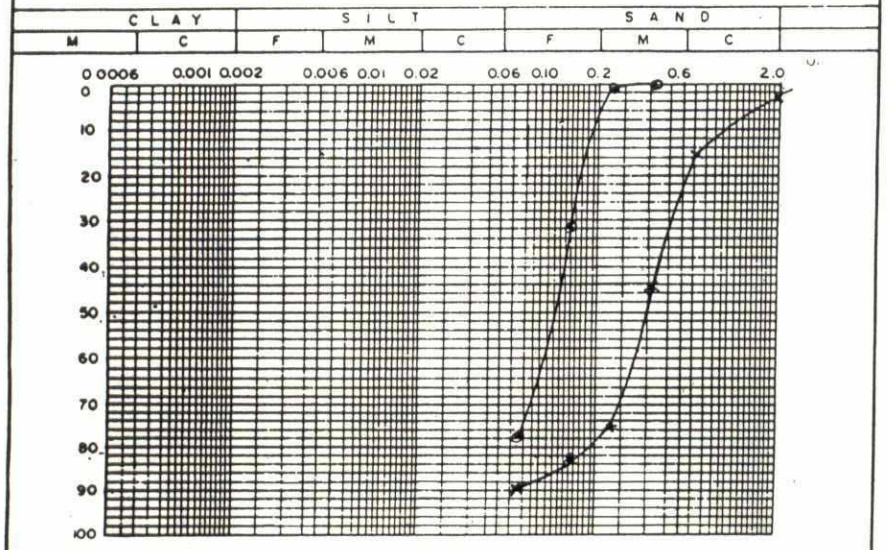


SYMBOL	BORE HOLE NO.	SAMPLE NO.	DEPTH (m)	CLASSIFICATION	CLAY %	SILT %	SAND %	REMARKS D_{60}
o o o	GA – 5	D – 9	13.35 – 13.8m	SM	—	14	86	.016mm
x x x	GA – 5	D – 15	20.85 – 21.3m	SM	—	12	88	.25mm

WORKS EXECUTED BY FOUNDATION CONSULTANTS LTD.

GRAIN SIZE DISTRIBUTION	FAP - 21/22 BANK PROTECTION AND RIVER TRAINING/ (AFPM) PILOT PROJECT
	FINAL REPORT | FIG. A.13 – 44

SOIL INVESTIGATION | LOCATION : KAMARJANI



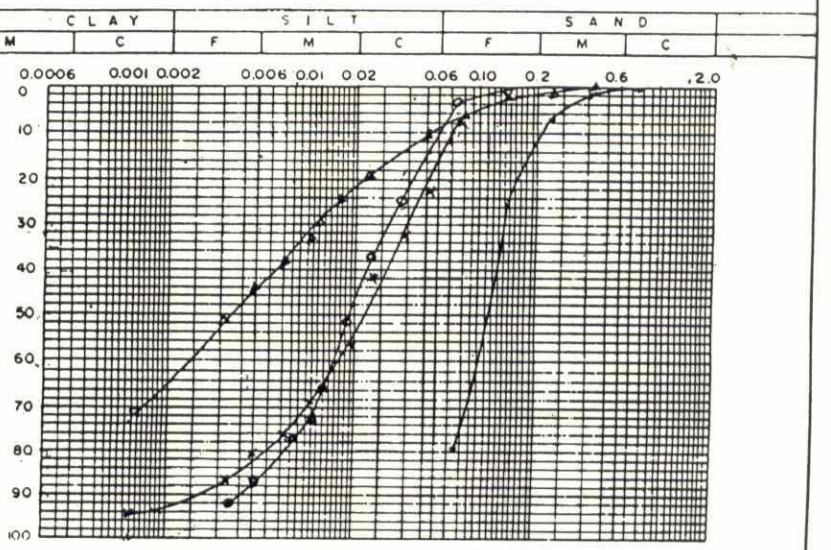
SYMBOL	BORE HOLE NO.	SAMPLE NO.	DEPTH (m)	CLASSIFICATION	CLAY %	SILT %	SAND %	RENARKS D_{60}
0 0 0	GA – 5	D – 22	31.35 – 31.8m	SM	—	22	78	.14mm
X X X	GA – 5	D – 28	39.8 – 40.25m	SM	—	11	89	.45mm

WORKS EXECUTED BY FOUNDATION CONSULTANTS LTD.

GRAIN SIZE DISTRIBUTION

FAP - 21/22
BANK PROTECTION AND RIVER TRAINING/ (AFPM) PILOT PROJECT
FINAL REPORT | FIG. A.13 – 45

SOIL INVESTIGATION | LOCATION : BAHADURABAD



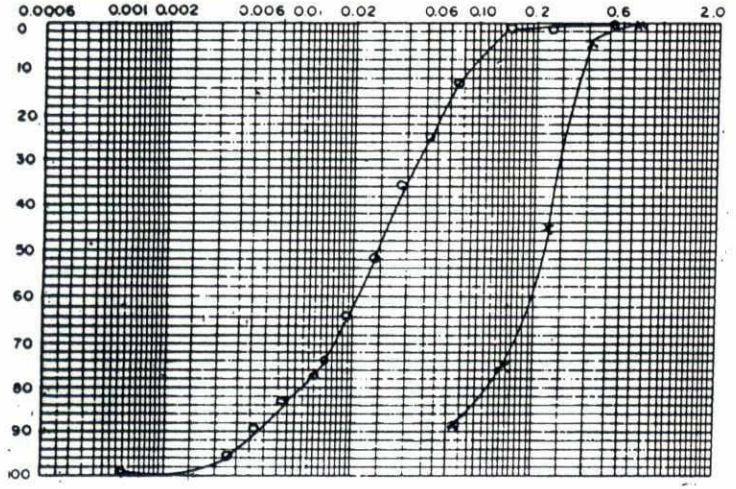
SYMBOL	BORE HOLE NO.	SAMPLE NO.	DEPTH (m)	CLASSIFICATION	CLAY %	SILT %	SAND %	RENARKS D_{60}
0 0 0	BA – 1	D – 1	1.5 – 1.95m	ML	—	89	11	.024mm
X X X	BA – 1	UD – 3	3.5 – 3.95m	ML — CL	7	77	16	.032mm
·—·—·	BA – 1	D – 4	5.85 – 6.3m	SM	—	21	79	.13mm
Δ Δ Δ	BA – 1	UD – 2	2.15 – 2.6m	CL	34	56	10	.0077mm

WORKS EXECUTED BY FOUNDATION CONSULTANTS LTD.

GRAIN SIZE DISTRIBUTION

FAP - 21/22
BANK PROTECTION AND RIVER TRAINING/ (AFPM) PILOT PROJECT
FINAL REPORT | FIG. A.13 – 46

SOIL INVESTIGATION	LOCATION : BAHADURABAD

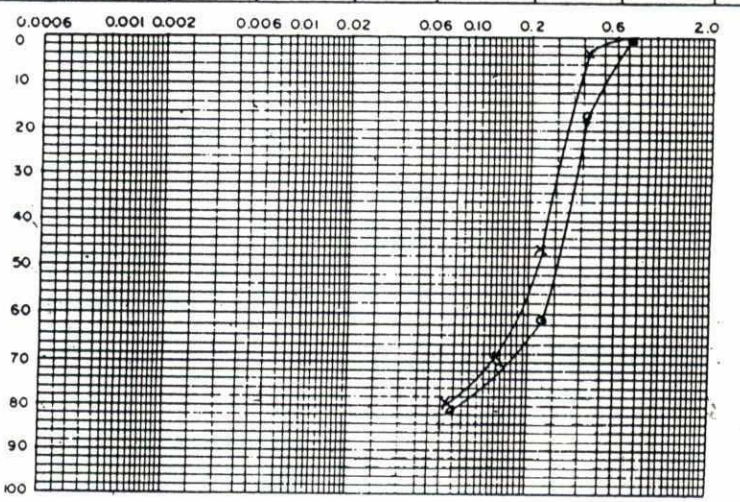


SYMBOL	BORE HOLE NO.	SAMPLE NO.	DEPTH (m)	CLASSIFICATION	CLAY %	SILT %	SAND %	REMARKS D_{60}
o o o	BA – 1	D – 8	10.85 – 11.3m	ML	1	77	22	.036mm
X X X	BA – 1	D – 16	19.85 – 20.3m	SM	—	12	88	.27mm

WORKS EXECUTED BY FOUNDATION CONSULTANTS LTD.

GRAIN SIZE DISTRIBUTION	FAP – 21/22 BANK PROTECTION AND RIVER TRAINING/ (AFPM) PILOT PROJECT
	FINAL REPORT | FIG. A. 13 – 47

SOIL INVESTIGATION	LOCATION : BAHADURABAD

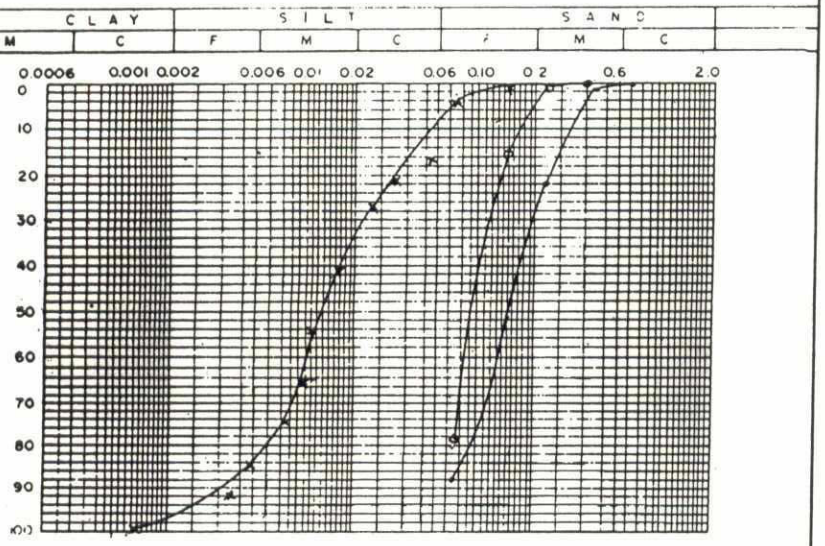


SYMBOL	BORE HOLE NO.	SAMPLE NO.	DEPTH (m)	CLASSIFICATION	CLAY %	SILT %	SAND %	REMARKS D_{60}
o o o	BA – 1	D – 18	23.85 – 24.3m	SM	—	20	80	.35mm
X X X	BA – 1	D – 25	32.5 – 32.95m	SM	—	19	81	.26mm

WORKS EXECUTED BY FOUNDATION CONSULTANTS LTD.

GRAIN SIZE DISTRIBUTION	FAP – 21/22 BANK PROTECTION AND RIVER TRAINING/ (AFPM) PILOT PROJECT
	FINAL REPORT | FIG. A. 13 – 48

SOIL INVESTIGATION | LOCATION : BAHADURABAD



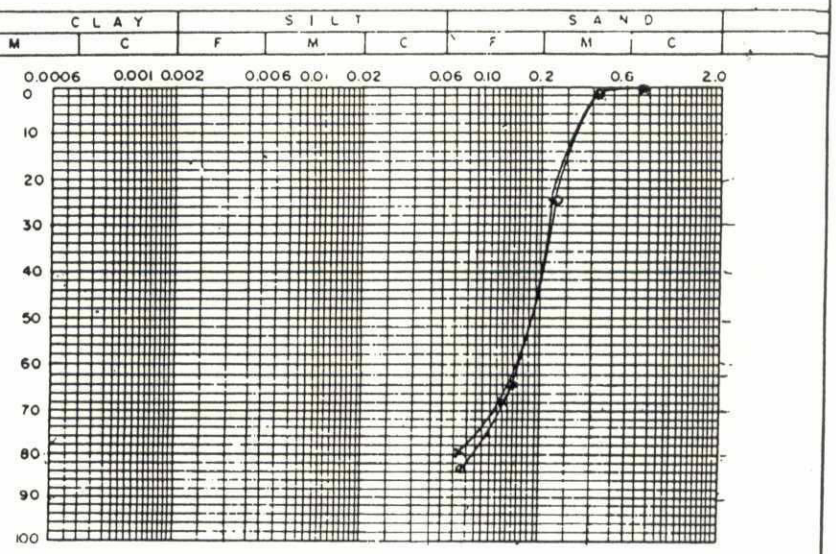
SYMBOL	BORE HOLE NO.	SAMPLE NO.	DEPTH (m)	CLASSIFICATION	CLAY %	SILT %	SAND %	REMARKS D_{60}
0 0 0	BA – 3	D – 2	2.85–3.3 m	SM	—	21	79	.1 mm
X X X	BA – 3	D – 4	5.35–5.85m	ML — CL	3	88	9	.017mm
—·—·—	BA – 3	D – 5	6.85–7.3m	SM	—	12	88	.19 mm

WORKS EXECUTED BY FOUNDATION CONSULTANTS LTD.

GRAIN SIZE DISTRIBUTION

FAP - 21/22
BANK PROTECTION AND RIVER TRAINING/ (AFPM) PILOT PROJECT
FINAL REPORT | FIG. A.13–49

SOIL INVESTIGATION | LOCATION : BAHADURABAD



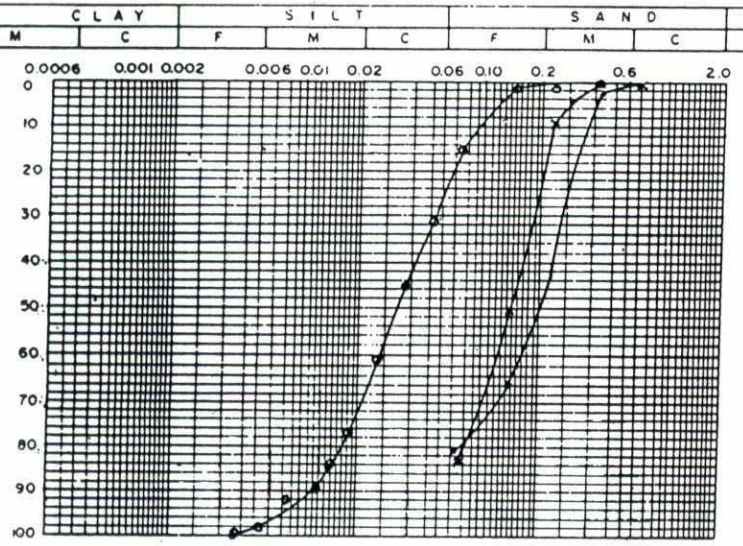
SYMBOL	BORE HOLE NO.	SAMPLE NO.	DEPTH (m)	CLASSIFICATION	CLAY %	SILT %	SAND %	REMARKS D_{60}
0 0 0	BA – 3	D – 7	9.85–10.3 m	SM	—	16	84	.2 mm
X X X	BA – 3	D – 11	15.85–16.3 m	SM	—	21	79	1.21mm

WORKS EXECUTED BY FOUNDATION CONSULTANTS LTD.

GRAIN SIZE DISTRIBUTION

FAP - 21/22
BANK PROTECTION AND RIVER TRAINING/ (AFPM) PILOT PROJECT
FINAL REPORT | FIG. A.13–50

SOIL INVESTIGATION | LOCATION : BAHADURABAD



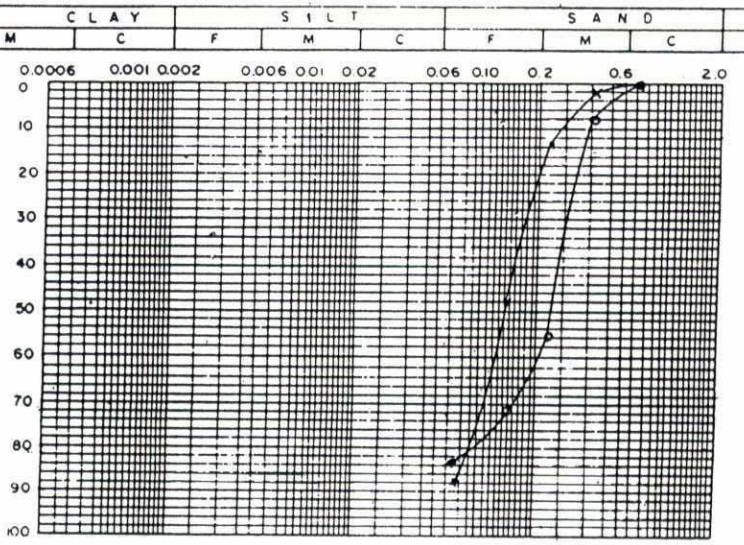
SYMBOL	BORE HOLE NO.	SAMPLE NO.	DEPTH (m)	CLASSIFICATION	CLAY %	SILT %	SAND %	REMARKS D_{60}
o o o	BA — 4	D — 1	1.35 — 1.8 m	ML	—	73	27	.04 mm
x x x	BA — 4	D — 3	4.35 — 4.8 m	SM	—	17	83	.17 mm
·—·—·	BA — 4	D — 6	8.85 — 9.3 m	SM	—	20	80	.25 mm

WORKS EXECUTED BY FOUNDATION CONSULTANTS LTD.

GRAIN SIZE DISTRIBUTION

FAP - 21/22
BANK PROTECTION AND RIVER TRAINING/ (AFPM) PILOT PROJECT
FINAL REPORT | FIG. A.13-51

SOIL INVESTIGATION | LOCATION : BAHADURABAD



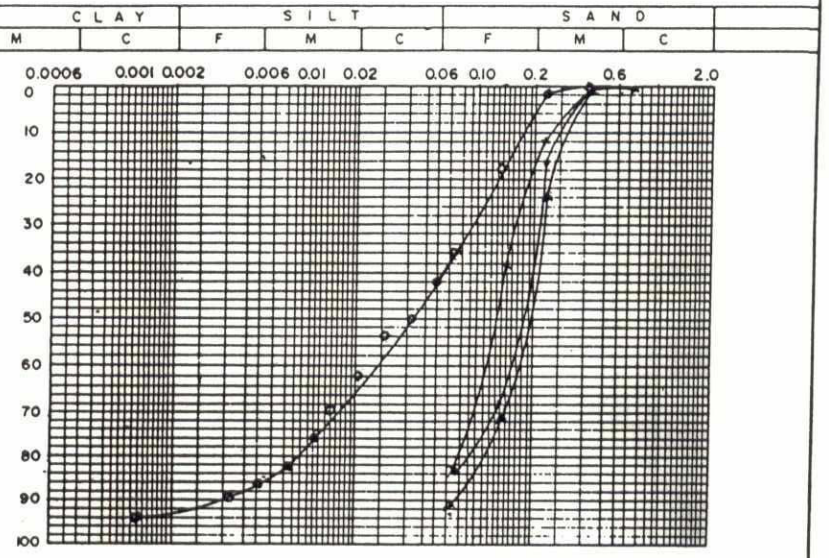
SYMBOL	BORE HOLE NO.	SAMPLE NO.	DEPTH (m)	CLASSIFICATION	CLAY %	SILT %	SAND %	REMARKS D_{60}
o o o	BA — 4	D — 9	13.33 — 13.78m	SM	—	16	84	.15mm
x x x	BA — 4	D — 13	18.35 — 18.8m	SM	—	12	88	.29mm

WORKS EXECUTED BY FOUNDATION CONSULTANTS LTD.

GRAIN SIZE DISTRIBUTION

FAP - 21/22
BANK PROTECTION AND RIVER TRAINING/ (AFPM) PILOT PROJECT
FINAL REPORT | FIG. A.13-52

SOIL INVESTIGATION | LOCATION : BAHADURABAD



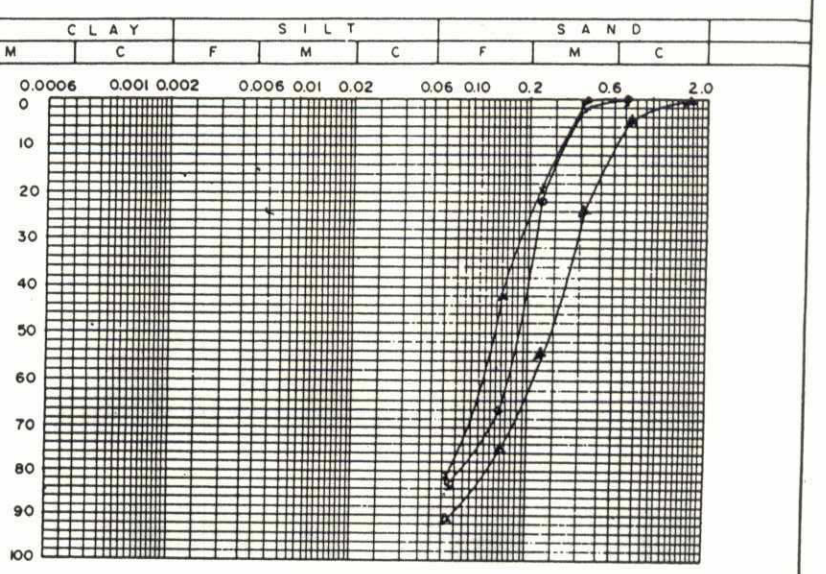
SYMBOL	BORE HOLE NO.	SAMPLE NO.	DEPTH (m)	CLASSIFICATION	CLAY %	SILT %	SAND %	REMARKS D_{60}
o o o	BA — 6	D — 1	1.42 – 1.87m	ML	7	51	42	.062mm
x x x	BA — 6	D — 3	4.35 – 4.8m	SM	—	18	82	.10mm
Δ Δ Δ	BA — 6	D — 4	6 — 6.45m	SM	—	9	91	.22mm
·—·—·	BA — 6	UD — 2	1.5 – 1.95m	SM	—	17	83	.2mm

WORKS EXECUTED BY FOUNDATION CONSULTANTS LTD.

GRAIN SIZE DISTRIBUTION

FAP - 21/22
BANK PROTECTION AND RIVER TRAINING/ (AFPM) PILOT PROJECT
FINAL REPORT | FIG. A.13–53

SOIL INVESTIGATION | LOCATION : BAHADURABAD



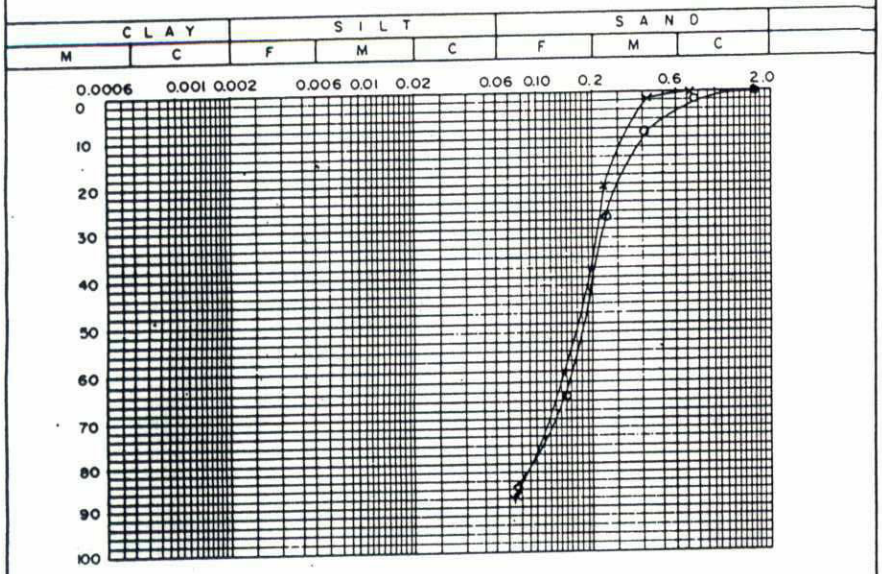
SYMBOL	BORE HOLE NO.	SAMPLE NO.	DEPTH (m)	CLASSIFICATION	CLAY %	SILT %	SAND %	REMARKS D_{60}
o o o	BA — 6	D — 5	7.4 – 7.85m	SM	—	16	84	.2mm
x x x	BA — 6	D — 7	10.4 – 10.85m	SM	—	18	82	.15mm
Δ Δ Δ	BA — 6	D — 9	13.4 – 13.85m	SM	—	9	91	.33mm

WORKS EXECUTED BY FOUNDATION CONSULTANTS LTD.

GRAIN SIZE DISTRIBUTION

FAP - 21/22
BANK PROTECTION AND RIVER TRAINING/ (AFPM) PILOT PROJECT
FINAL REPORT | FIG. A.13–54

SOIL INVESTIGATION | LOCATION : BAHADURABAD



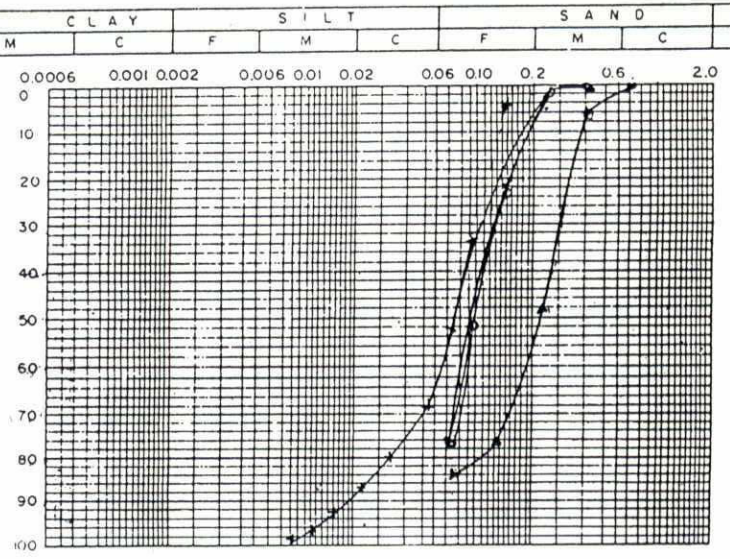
SYMBOL	BORE HOLE NO.	SAMPLE NO.	DEPTH (m)	CLASSIFICATION	CLAY %	SILT %	SAND %	REMARKS D_{60}
o o o	BA — 6	D — 11	18.4 — 18.85m	SM	—	14	86	.2mm
x x x	BA — 6	D — 13	19.4 — 19.85m	SM	—	12	88	.19mm

WORKS EXECUTED BY FOUNDATION CONSULTANTS LTD.

GRAIN SIZE DISTRIBUTION

FAP - 21/22
BANK PROTECTION AND RIVER TRAINING/ (AFPM) PILOT PROJECT
FINAL REPORT | FIG. A.13-55

SOIL INVESTIGATION | LOCATION : CHANDANBAISA



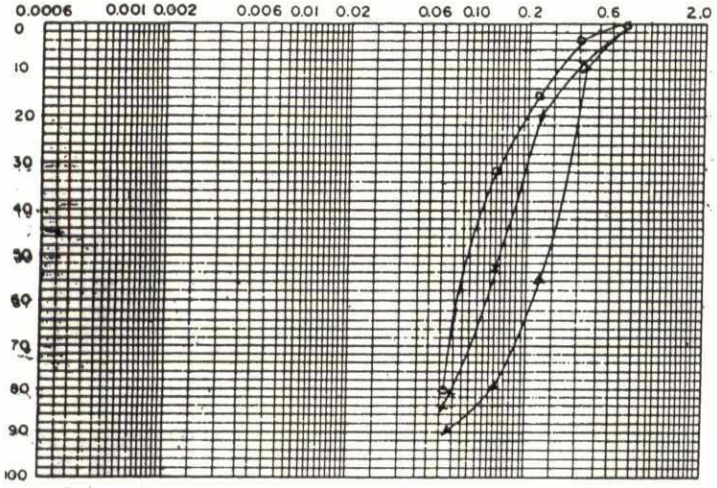
SYMBOL	BORE HOLE NO.	SAMPLE NO.	DEPTH (m)	CLASSIFICATION	CLAY %	SILT %	SAND %	REMARKS D_{60}
o o o	CH — 1	D — 1	1.68 — 2.13m	SM	—	22	78	.12mm
x x x	CH — 1	D — 3	4.5 — 4.95m	SM	—	35	65	.088mm
Δ Δ Δ	CH — 1	D — 5	7.5 — 7.95m	SM	—	16	84	.28mm
— · — ·	CH — 1	D — 2	3 — 3.45m	SM	—	23	77	.12mm

WORKS EXECUTED BY FOUNDATION CONSULTANTS LTD.

GRAIN SIZE DISTRIBUTION

FAP - 21/22
BANK PROTECTION AND RIVER TRAINING/ (AFPM) PILOT PROJECT
FINAL REPORT | FIG. A.13-56

SOIL INVESTIGATION | LOCATION : CHANDANBAISA



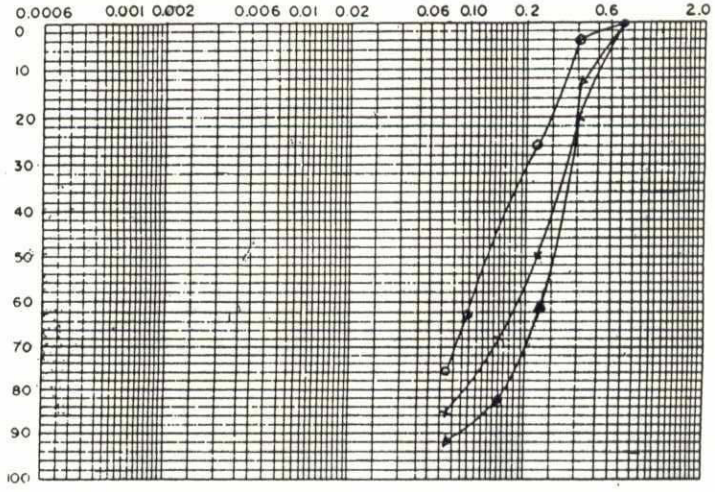
SYMBOL	BORE HOLE NO.	SAMPLE NO.	DEPTH (m)	CLASSIFICATION	CLAY %	SILT %	SAND %	REMARKS D_{60}
o o o	CH — 1	D — 9	14.15 — 14.6m	SM	—	19	81	.12mm
x x x	CH — 1	D — 11	16.05 — 16.5m	SM	—	16	84	.18mm
Δ Δ Δ	CH — 1	D — 13	19.35 — 19.8m	SM	—	10	90	.31mm

WORKS EXECUTED BY FOUNDATION CONSULTANTS LTD.

GRAIN SIZE DISTRIBUTION

FAP - 21/22
BANK PROTECTION AND RIVER TRAINING/ (AFPM) PILOT PROJECT
FINAL REPORT | FIG. A.13-57

SOIL INVESTIGATION | LOCATION : CHANDANBAISA



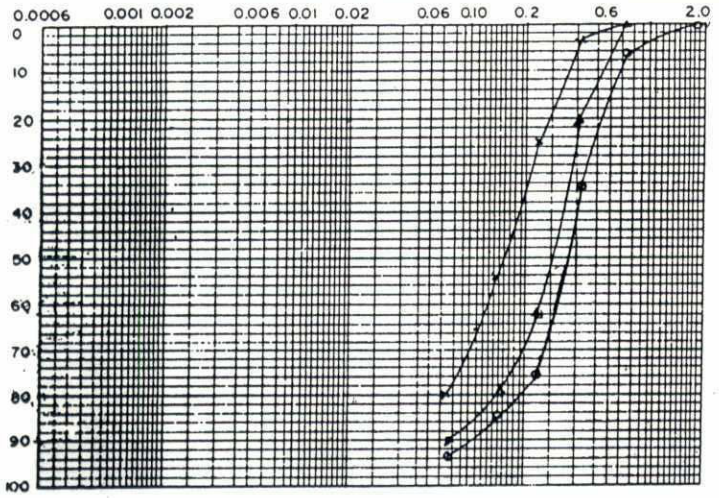
SYMBOL	BORE HOLE NO.	SAMPLE NO.	DEPTH (m)	CLASSIFICATION	CLAY %	SILT %	SAND %	REMARKS D_{60}
o o o	CH — 1	D — 16	24 — 24.45m	SM	—	24	76	.16mm
x x x	CH — 1	D — 17	25.5 — 25-95m	SM	—	15	85	.3mm
Δ Δ Δ	CH — 1	D — 21	31.35 — 31.8m	SM	—	8	92	.35mm

WORKS EXECUTED BY FOUNDATION CONSULTANTS LTD.

GRAIN SIZE DISTRIBUTION

FAP - 21/22
BANK PROTECTION AND RIVER TRAINING/ (AFPM) PILOT PROJECT
FINAL REPORT | FIG. A.13-58

SOIL INVESTIGATION	LOCATION : CHANDANBAISA

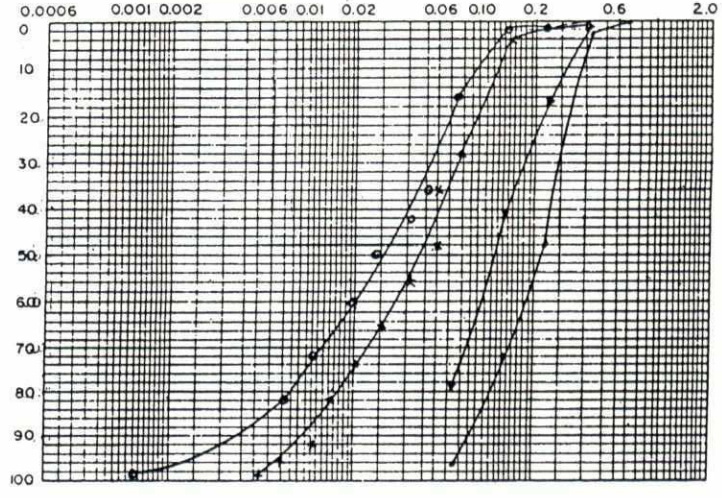


SYMBOL	BORE HOLE NO.	SAMPLE NO.	DEPTH (m)	CLASSIFICATION	CLAY %	SILT %	SAND %	REMARKS D_{60}
o o o	CH — 1	D — 23	34.8 — 35.25m	SM	—	6	94	.4mm
x x x	CH — 1	D — 25	37.35 — 37.8m	SM	—	20	80	.18mm
Δ Δ Δ	CH — 1	D — 27	40.5 — 40.95m	SM	—	10	90	.34mm

WORKS EXECUTED BY FOUNDATION CONSULTANTS LTD.

GRAIN SIZE DISTRIBUTION	FAP - 21/22 BANK PROTECTION AND RIVER TRAINING/ (AFPM) PILOT PROJECT	
	FINAL REPORT	FIG. A.13-59

SOIL INVESTIGATION	LOCATION : CHANDANBAISA

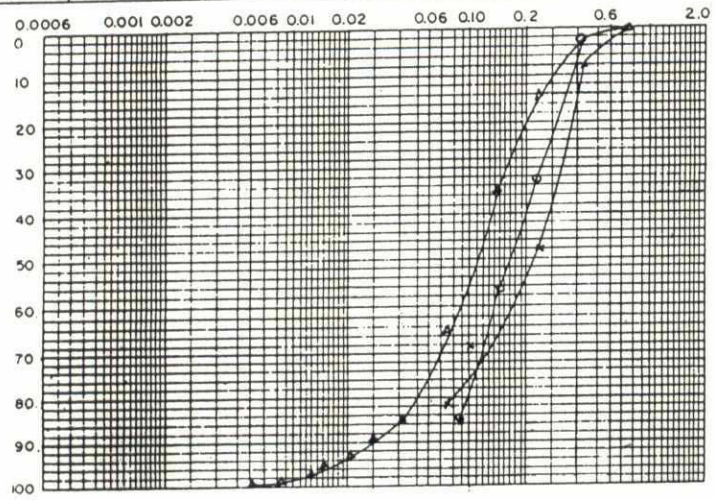


SYMBOL	BORE HOLE NO.	SAMPLE NO.	DEPTH (m)	CLASSIFICATION	CLAY %	SILT %	SAND %	REMARKS D_{60}
o o o	CH II — 2	D — 1	1.35 — 1.8m	ML	3	71	26	.04mm
x x x	CH — 2	D — 2	2.85 — 3.3m	ML	—	58	42	.06mm
Δ Δ Δ	CH — 2	D — 3	4.35 — 4.8m	SM	—	21	79	.15mm
·—·—·	CH — 2	D — 4	5.85 — 6.3m	SM — SP	—	4	96	.27mm

WORKS EXECUTED BY FOUNDATION CONSULTANTS LTD.

GRAIN SIZE DISTRIBUTION	FAP - 21/22 BANK PROTECTION AND RIVER TRAINING/ (AFPM) PILOT PROJECT	
	FINAL REPORT	FIG. A.13-60

SOIL INVESTIGATION | LOCATION : CHANDANBAISA



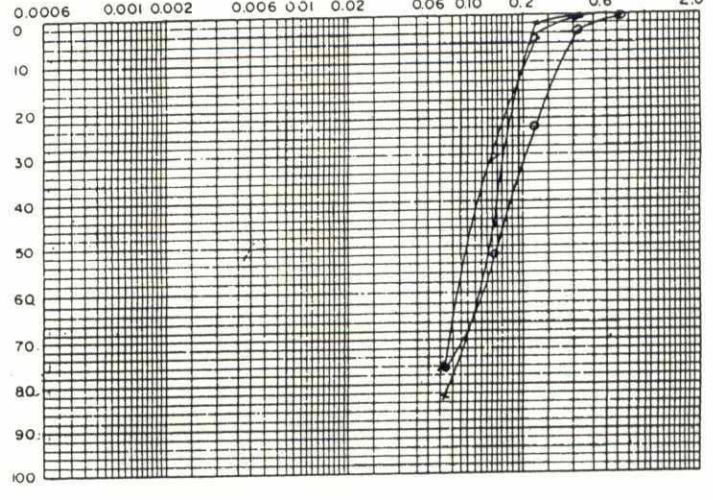
SYMBOL	BORE HOLE NO.	SAMPLE NO.	DEPTH (m)	CLASSIFICATION	CLAY %	SILT %	SAND %	REMARKS D_{60}
o o o	CH — 2	D — 6	8.55 – 9 m	SM	—	15	85	.2 mm
x x x	CH — 2	D — 9	13.35 – 13.8m	SM		20	80	.28mm
Δ Δ Δ	CH — 2	D — 11	14.85 – 15.3m	SM		26	74	.14mm

WORKS EXECUTED BY FOUNDATION CONSULTANTS LTD.

GRAIN SIZE DISTRIBUTION

FAP - 21/22
BANK PROTECTION AND RIVER TRAINING/ (AFPM) PILOT PROJECT
FINAL REPORT | FIG. A.13-61

SOIL INVESTIGATION | LOCATION : CHANDANBAISA



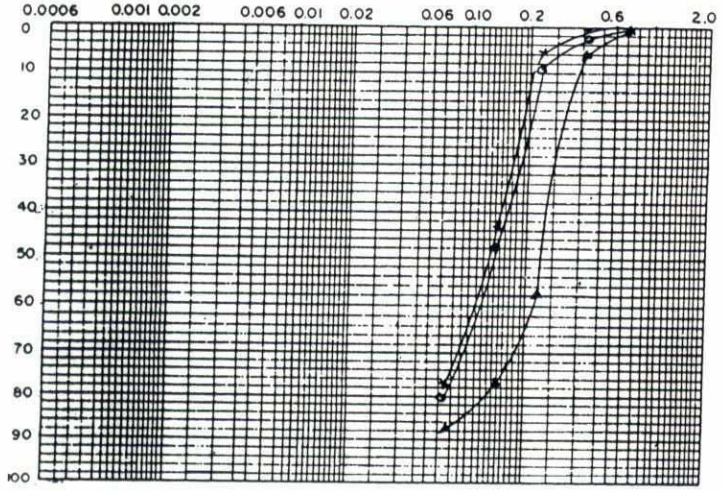
SYMBOL	BORE HOLE NO.	SAMPLE NO.	DEPTH (m)	CLASSIFICATION	CLAY %	SILT %	SAND %	REMARKS D_{60}
o o o	CH — 2	D — 12	15.6 – 16.06m	SM	—	23	77	.18mm
x x x	CH — 2	D — 15	17.85 – 18.3m	SM	—	18	82	.15mm
Δ Δ Δ	CH — 2	D — 17	19.35 – 19.8m	SM	—	23	77	.12mm

WORKS EXECUTED BY FOUNDATION CONSULTANTS LTD.

GRAIN SIZE DISTRIBUTION

FAP - 21/22
BANK PROTECTION AND RIVER TRAINING/ (AFPM) PILOT PROJECT
FINAL REPORT | FIG. A.13-62

SOIL INVESTIGATION	LOCATION : CHANDANBAISA

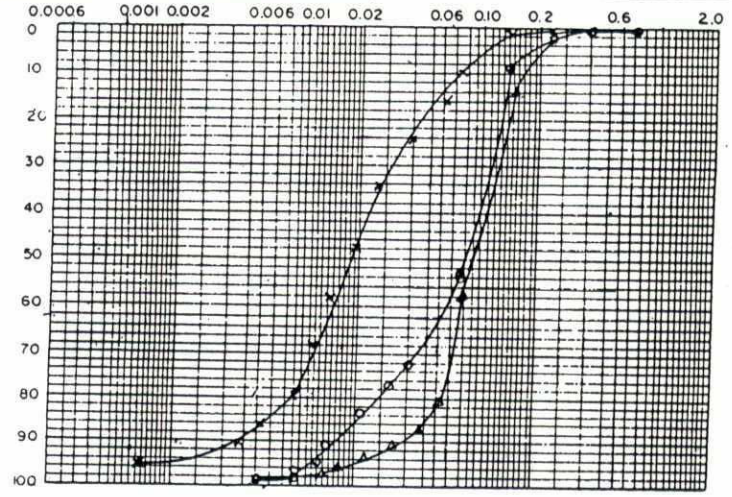


SYMBOL	BORE HOLE NO.	SAMPLE NO.	DEPTH (m)	CLASSIFICATION	CLAY %	SILT %	SAND %	REMARKS D_{60}
o o o	CH — 2	D — 18	20.10 – 20.55m	SM	—	20	80	.16mm
x x x	CH — 2	D — 21	23.05 – 22.5m	SM	—	23	77	.15mm
Δ Δ Δ	CH — 2	D — 24	24.3 – 24.75m	SM	—	12	88	.28mm

WORKS EXECUTED BY FOUNDATION CONSULTANTS LTD.

GRAIN SIZE DISTRIBUTION	FAP - 21/22 BANK PROTECTION AND RIVER TRAINING/ (AFPM) PILOT PROJECT
	FINAL REPORT | FIG. A.13-63

SOIL INVESTIGATION	LOCATION : CHANDANBAISA

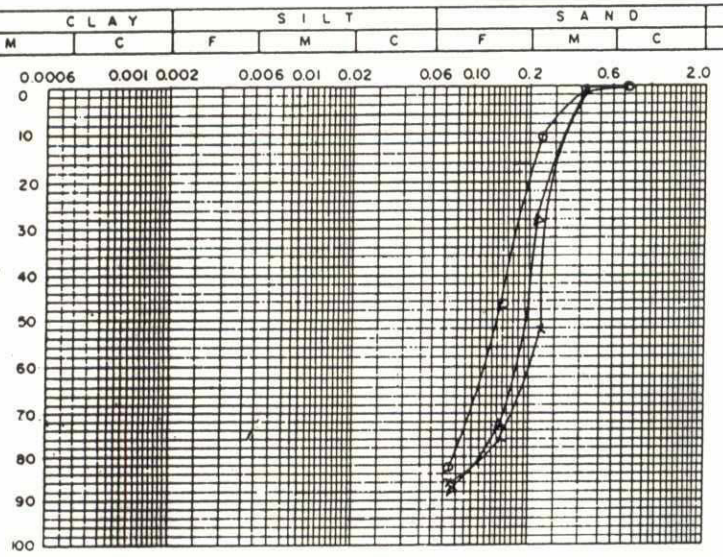


SYMBOL	BORE HOLE NO.	SAMPLE NO.	DEPTH (m)	CLASSIFICATION	CLAY %	SILT %	SAND %	REMARKS D_{60}
o o o	CH — 3	D — 1	1.35 – 1.85 m	SM	—	37	63	.1mm
x x x	CH — 3	D — 2	2.85 – 3.3m	ML — CL	6	80	14	.023mm
Δ Δ Δ	CH — 3	D — 3	4.35 – 4.8m	SM	—	20	80	.11mm

WORKS EXECUTED BY FOUNDATION CONSULTANTS LTD.

GRAIN SIZE DISTRIBUTION	FAP - 21/22 BANK PROTECTION AND RIVER TRAINING/ (AFPM) PILOT PROJECT
	FINAL REPORT | FIG. A.13-64

SOIL INVESTIGATION | LOCATION : CHANDANBAISA



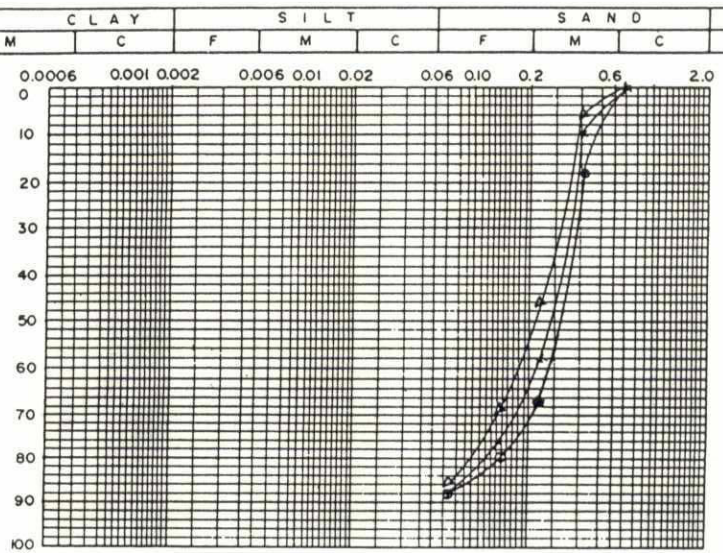
SYMBOL	BORE HOLE NO.	SAMPLE NO.	DEPTH (m)	CLASSIFICATION	CLAY %	SILT %	SAND %	REMARKS D_{60}
o o o	CH — 3	D — 4	5.85 – 6.3m	SM	—	17	83	.16mm
x x x	CH — 3	D — 5	7.35 – 7.8m	SM	—	14	86	.25mm
Δ Δ Δ	CH — 3	D — 7	8.85 – 9.3m	SM	—	12	88	.21mm

WORKS EXECUTED BY FOUNDATION CONSULTANTS LTD.

GRAIN SIZE DISTRIBUTION

FAP - 21/22
BANK PROTECTION AND RIVER TRAINING/ (AFPM) PILOT PROJECT
FINAL REPORT | FIG. A.13 - 65

SOIL INVESTIGATION | LOCATION : CHANDANBAISA



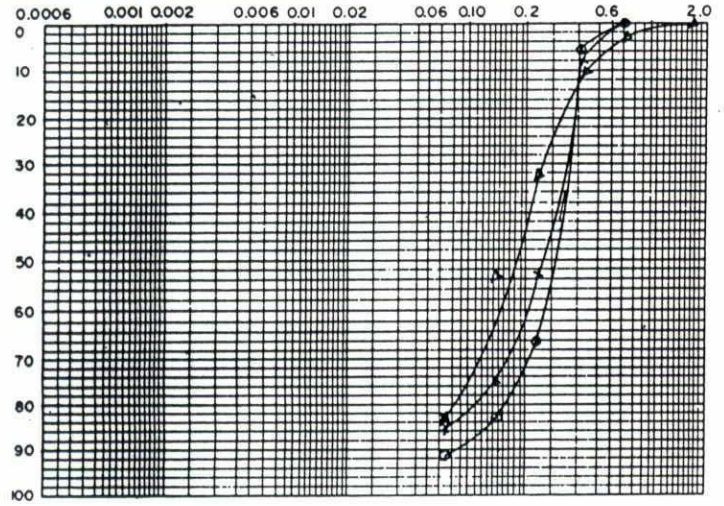
SYMBOL	BORE HOLE NO.	SAMPLE NO.	DEPTH (m)	CLASSIFICATION	CLAY %	SILT %	SAND %	REMARKS D_{60}
o o o	CH — 3	D — 8	10.35 – 10.8m	SM	—	12	88	.37mm
x x x	CH — 3	D — 10	13.35 – 13.8m	SM	—	12	88	.32mm
Δ Δ Δ	CH — 3	D — 12	16.35 – 16.8m	SM	—	14	86	.29mm

WORKS EXECUTED BY FOUNDATION CONSULTANTS LTD.

GRAIN SIZE DISTRIBUTION

FAP - 21/22
BANK PROTECTION AND RIVER TRAINING/ (AFPM) PILOT PROJECT
FINAL REPORT | FIG. A.13 - 66

SOIL INVESTIGATION	LOCATION : CHANDANBAISA

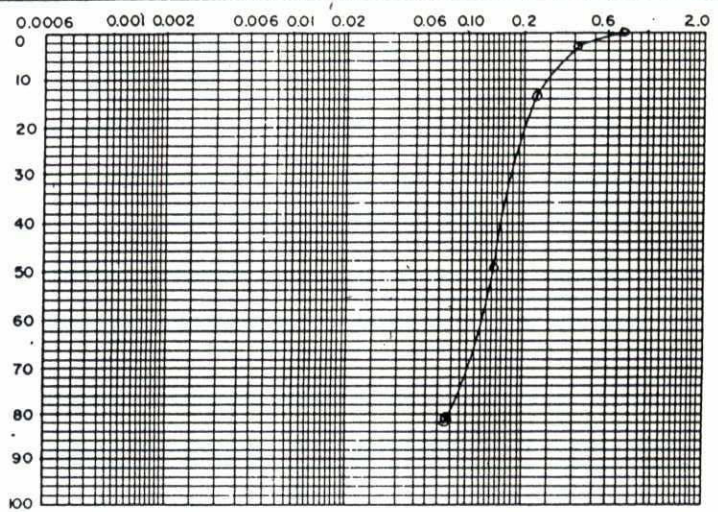


SYMBOL	BORE HOLE NO.	SAMPLE NO.	DEPTH (m)	CLASSIFICATION	CLAY %	SILT %	SAND %	REMARKS D_{60}
o o o	CH — 3	D — 14	19.35-19.8m	SM	—	8	92	.33mm
x x x	CH — 3	D — 16	22.35-22.8m	SM	—	15	85	.32mm
Δ Δ Δ	CH — 3	D — 17	23.85-24.3m	SM	—	16	84	.22mm

WORKS EXECUTED BY FOUNDATION CONSULTANTS LTD.

GRAIN SIZE DISTRIBUTION	FAP-21/22 BANK PROTECTION AND RIVER TRAINING/ (AFPM) PILOT PROJECT
	FINAL REPORT | FIG. A.13-67

SOIL INVESTIGATION	LOCATION : CHANDANBAISA

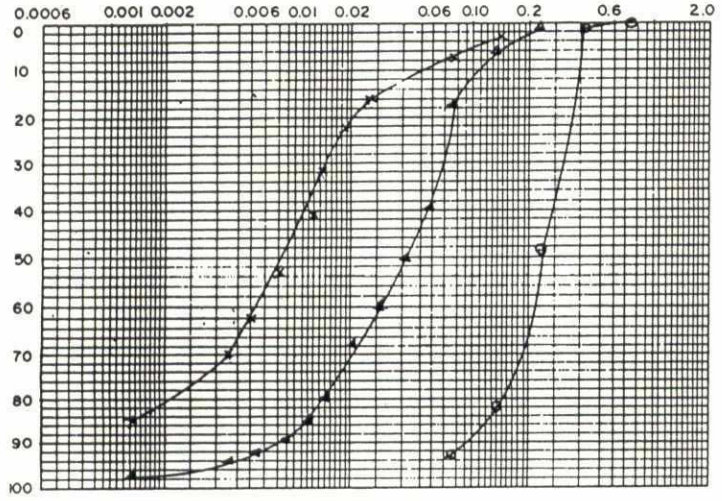


SYMBOL	BORE HOLE NO.	SAMPLE NO.	DEPTH (m)	CLASSIFICATION	CLAY %	SILT %	SAND %	REMARKS D_{60}
o o o	CH — 3	D — 18	24.85-25-3m	SM	—	18	82	.15mm

WORKS EXECUTED BY FOUNDATION CONSULTANTS LTD.

GRAIN SIZE DISTRIBUTION	FAP-21/22 BANK PROTECTION AND RIVER TRAINING/ (AFPM) PILOT PROJECT
	FINAL REPORT | FIG. A.13-68

SOIL INVESTIGATION | LOCATION : CHANDANBAISA



SYMBOL	BORE HOLE NO.	SAMPLE NO.	DEPTH (m)	CLASSIFICATION	CLAY %	SILT %	SAND %	REMARKS D_{60}
o o o	CH — 4	D I(A)	1.34 - 1.5m	SM	—	7	93	.29mm
x x x	CH — 4	D I(B)	1.5 — 1.79m	CL	19	72	9	.011mm
Δ Δ Δ	CH — 4	D — 2	2.85 - 3.3m	ML — CL	3	59	38	.055mm

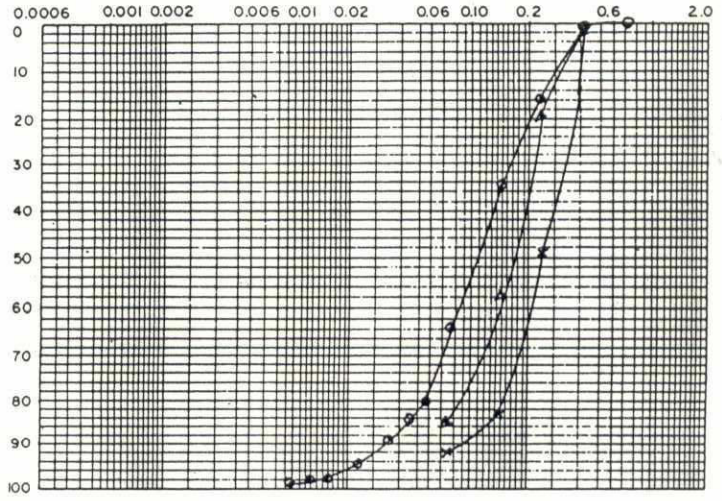
WORKS EXECUTED BY FOUNDATION CONSULTANTS LTD.

GRAIN SIZE DISTRIBUTION

FAP - 21/22
BANK PROTECTION AND RIVER TRAINING/ (AFPM) PILOT PROJECT
FINAL REPORT | FIG. A.13-69

W.A.P.D.A. LIBRARY.

SOIL INVESTIGATION | LOCATION : CHANDANBAISA



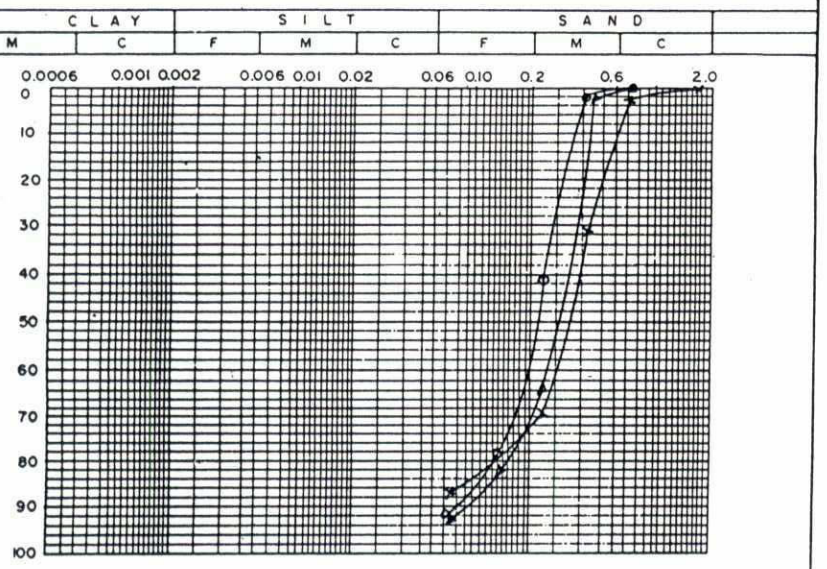
SYMBOL	BORE HOLE NO.	SAMPLE NO.	DEPTH (m)	CLASSIFICATION	CLAY %	SILT %	SAND %	REMARKS D_{60}
o o o	CH — 4	D — 3	4.43 - 4.88m	SM	—	20	80	.13mm
x x x	CH — 4	D — 4	5.92 - 6.37m	SM	—	8	92	.28mm
Δ Δ Δ	CH — 4	D — 7	10.35 - 10.8m	SM	—	15	85	.19mm

WORKS EXECUTED BY FOUNDATION CONSULTANTS LTD.

GRAIN SIZE DISTRIBUTION

FAP - 21/22
BANK PROTECTION AND RIVER TRAINING/ (AFPM) PILOT PROJECT
FINAL REPORT | FIG. A.13-70

SOIL INVESTIGATION | LOCATION : CHANDANBAISA



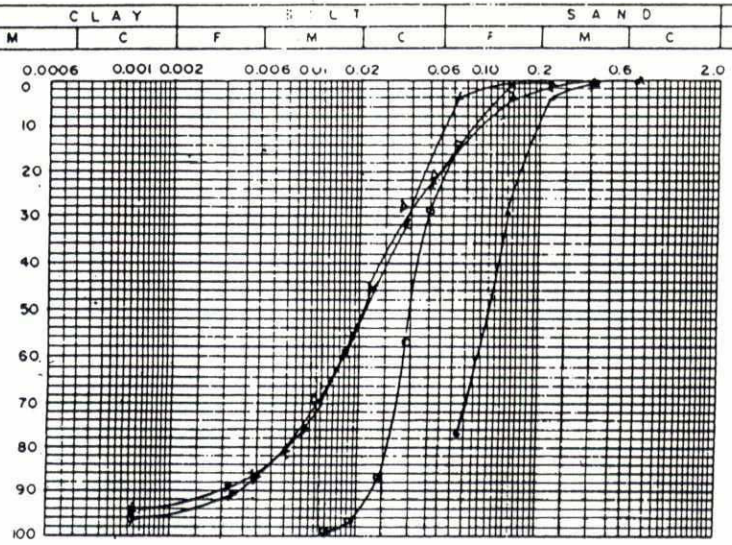
SYMBOL	BORE HOLE NO.	SAMPLE NO.	DEPTH (m)	CLASSIFICATION	CLAY %	SILT %	SAND %	REMARKS D_{60}
o o o	CH — 4	D — 8	11.83 – 12.3m	SM	—	8	92	.25mm
x x x	CH — 4	D — 12	18 — 18.45m	SM	—	13	87	.4mm
Δ Δ Δ	CH — 4	D — 14	19.85 – 20.3m	SM	—	7	93	.35mm

WORKS EXECUTED BY FOUNDATION CONSULTANTS LTD.

GRAIN SIZE DISTRIBUTION

FAP - 21/22
BANK PROTECTION AND RIVER TRAINING/ (AFPM) PILOT PROJECT
FINAL REPORT | FIG. A.13-71

SOIL INVESTIGATION | LOCATION : NAKALIA



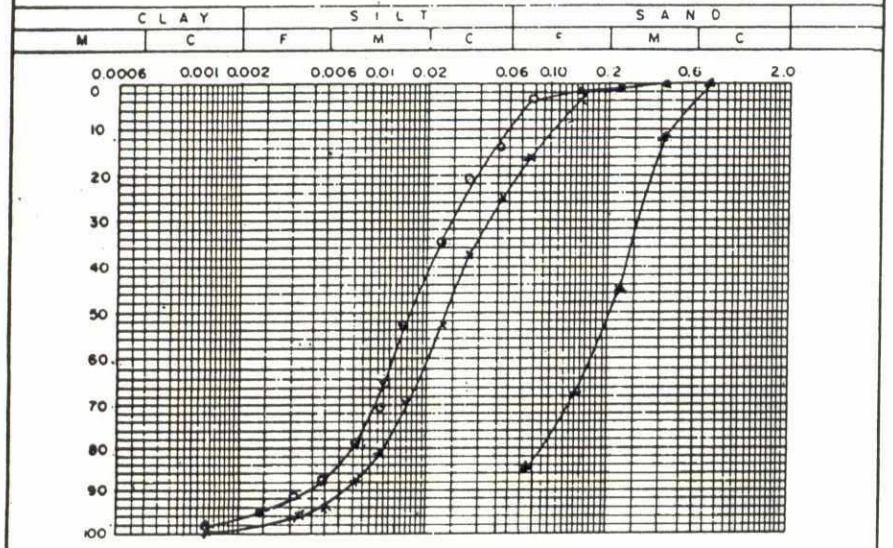
SYMBOL	BORE HOLE NO.	SAMPLE NO.	DEPTH (m)	CLASSIFICATION	CLAY %	SILT %	SAND %	REMARKS D_{60}
o o o	NK — 1	D — 1	1.35 – 1.8 m	ML	—	76	24	.045mm
x x x	NK — 1	D — 2	2.85 – 3.3m	ML — CL	8	78	14	.031mm
Δ Δ Δ	NK — 1	UD — 2	3.5 – 3.85m	ML — CL	5	74	21	.028mm
.—.—.	NK — 1	D — 7	10.35 – 10.8m	SM	—	23	77	.125mm

WORKS EXECUTED BY FOUNDATION CONSULTANTS LTD.

GRAIN SIZE DISTRIBUTION

FAP - 21/22
BANK PROTECTION AND RIVER TRAINING/ (AFPM) PILOT PROJECT
FINAL REPORT | FIG. A.13-72

SOIL INVESTIGATION	LOCATION : NAKALIA

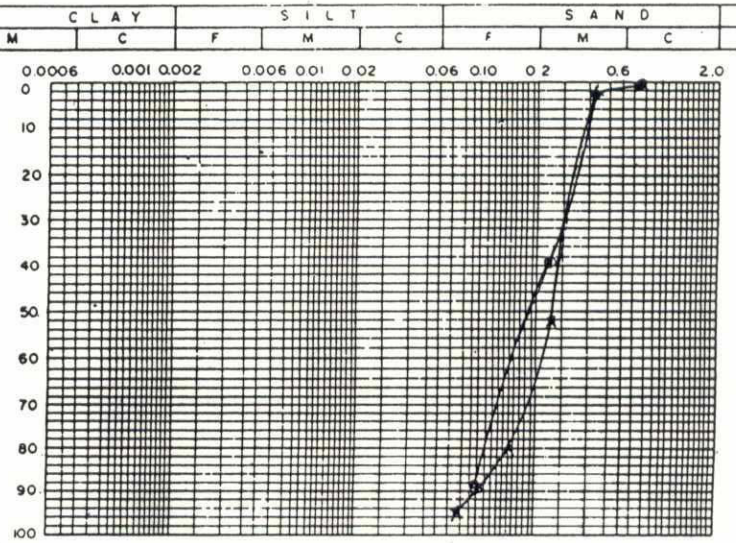


SYMBOL	BORE HOLE NO.	SAMPLE NO.	DEPTH (m)	CLASSIFICATION	CLAY %	SILT %	SAND %	REMARKS D_{60}
o o o	NK — 1	UD—3	14.04 – 14.49m	CL	3	87	10	.021mm
x x x	NK — 1	D — 10	14.85 – 15.3m	ML — CL	1	76	23	.034mm
Δ Δ Δ	NK — 1	D —17	25.35 – 25.8m	SM	—	14	86	.28mm

WORKS EXECUTED BY FOUNDATION CONSULTANTS LTD.

GRAIN SIZE DISTRIBUTION	FAP - 21/22 BANK PROTECTION AND RIVER TRAINING/ (AFPM) PILOT PROJECT	
	FINAL REPORT	FIG. A.13 – 73

SOIL INVESTIGATION	LOCATION : NAKALIA

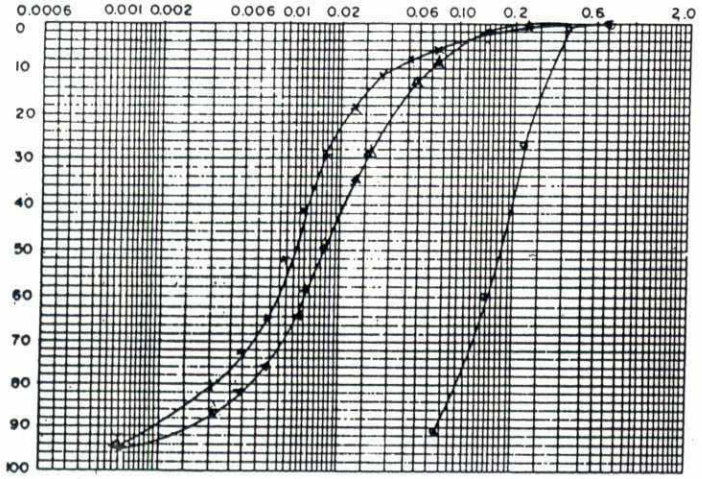


SYMBOL	BORE HOLE NO.	SAMPLE NO.	DEPTH (m)	CLASSIFICATION	CLAY %	SILT %	SAND %	REMARKS D_{60}
o o o	NK — 1	D — 20	29.85 – 30.3m	SM	—	11	89	.25mm
x x x	NK — 1	D — 25	37.35 – 37.8m	SM	—	6	94	.28mm

WORKS EXECUTED BY FOUNDATION CONSULTANTS LTD.

GRAIN SIZE DISTRIBUTION	FAP - 21/22 BANK PROTECTION AND RIVER TRAINING/ (AFPM) PILOT PROJECT	
	FINAL REPORT	FIG. A.13 – 74

SOIL INVESTIGATION | LOCATION : NAKALIA



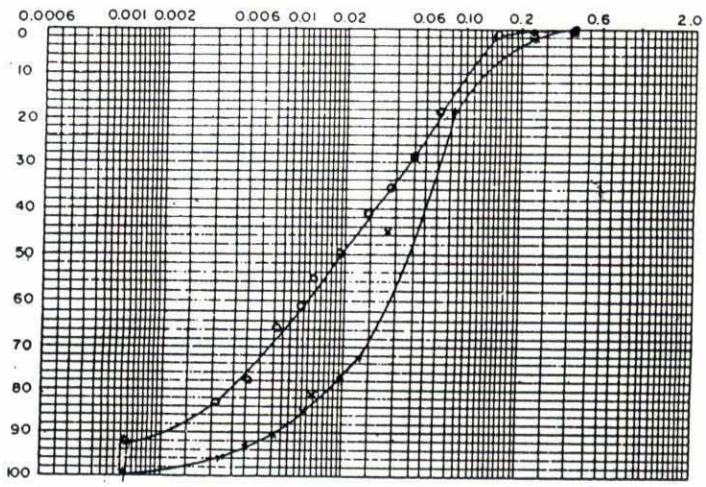
SYMBOL	BORE HOLE NO.	SAMPLE NO.	DEPTH (m)	CLASSIFICATION	CLAY %	SILT %	SAND %	REMARKS D_{60}
o o o	NK — 3	D — 2	2.85 – 3.3m	SM	—	8	92	.02mm
x x x	NK — 3	UD — 2	3.75 – 4.2m	CL	12	80	8	.014mm
Δ Δ Δ	NK — 3	D — 4	6.35 – 6.8m	ML — CL	7	80	13	.021mm

WORKS EXECUTED BY FOUNDATION CONSULTANTS LTD.

GRAIN SIZE DISTRIBUTION

FAP - 21/22
BANK PROTECTION AND RIVER TRAINING/ (AFPM) PILOT PROJECT
FINAL REPORT | FIG. A.13-75

SOIL INVESTIGATION | LOCATION : NAKALIA



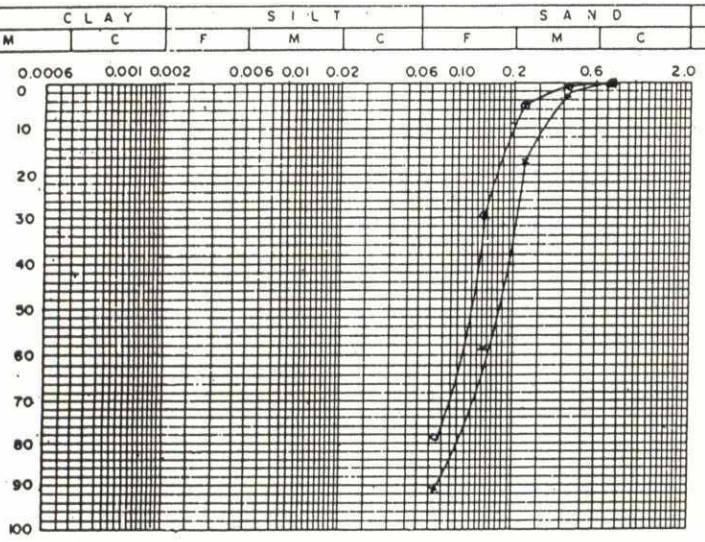
SYMBOL	BORE HOLE NO.	SAMPLE NO.	DEPTH (m)	CLASSIFICATION	CLAY %	SILT %	SAND %	REMARKS D_{60}
o o o	NK — 3	UD — 3	7.0 – 7.45m	CL	10	65	25	.031mm
x x x	NK — 3	D — 6	9.35 – 9.8m	ML — CL	1	59	40	.061mm

WORKS EXECUTED BY FOUNDATION CONSULTANTS LTD.

GRAIN SIZE DISTRIBUTION

FAP - 21/22
BANK PROTECTION AND RIVER TRAINING/ (AFPM) PILOT PROJECT
FINAL REPORT | FIG. A.13-76

SOIL INVESTIGATION	LOCATION : NAKALIA

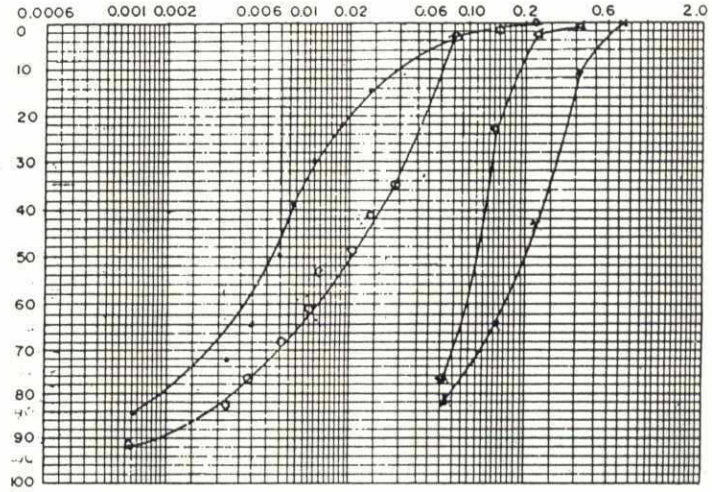


SYMBOL	BORE HOLE NO.	SAMPLE NO.	DEPTH (m)	CLASSIFICATION	CLAY %	SILT %	SAND %	REMARKS D_{60}
o o o	NK — 3	D — 9	13.85–14.3m	SM	—	21	79	.13mm
x x x	NK — 3	D — 12	18.35–18.8m	SM	—	9	91	.18mm

WORKS EXECUTED BY FOUNDATION CONSULTANTS LTD.

GRAIN SIZE DISTRIBUTION	FAP-21/22 BANK PROTECTION AND RIVER TRAINING/ (AFPM) PILOT PROJECT
	FINAL REPORT | FIG. A.13-77

SOIL INVESTIGATION	LOCATION : NAKALIA

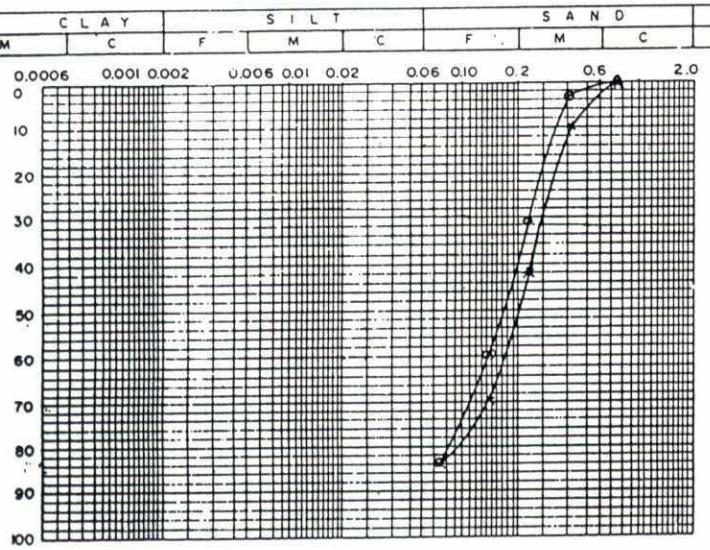


SYMBOL	BORE HOLE NO.	SAMPLE NO.	DEPTH (m)	CLASSIFICATION	CLAY %	SILT %	SAND %	REMARKS D_{60}
o o o	NK — 5	D — 2	2.85–3.3m	ML — CL	11	71	18	.032mm
x x x	NK — 5	D — 7	11.85–12.3m	SM	—	19	81	.26mm
Δ Δ Δ	NK — 5	D — 9	14.05–15.3m	SM	—	24	76	.12mm
·—·—·	NK — 5	UD — 3	4.35–4.8m	CL	19	74	7	.095mm

WORKS EXECUTED BY FOUNDATION CONSULTANTS LTD.

GRAIN SIZE DISTRIBUTION	FAP-21/22 BANK PROTECTION AND RIVER TRAINING/ (AFPM) PILOT PROJECT
	FINAL REPORT | FIG. A.13-78

SOIL INVESTIGATION | LOCATION : NAKALIA



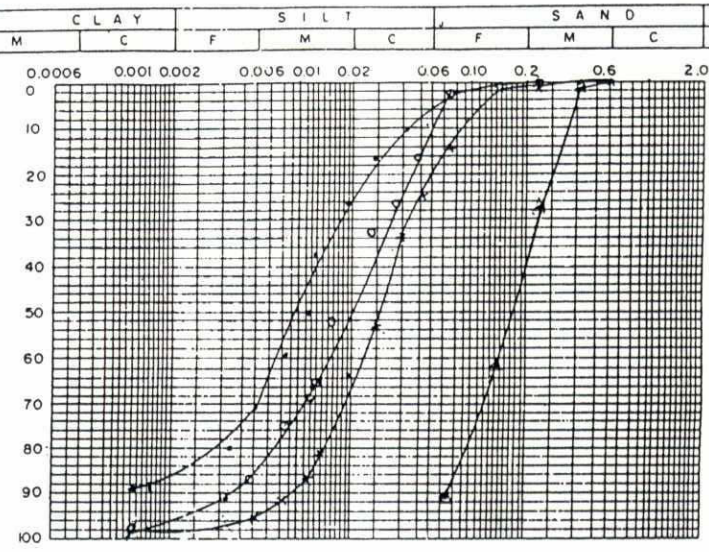
SYMBOL	BORE HOLE NO.	SAMPLE NO.	DEPTH (m)	CLASSIFICATION	CLAY %	SILT %	SAND %	REMARKS D_{60}
o o o	NK — 5	D — 13	20.85–21.5m	SM	—	18	82	.2mm
x x x	NK — 5	D — 16	25.35–25.8m	SM	—	17	83	.25mm

WORKS EXECUTED BY FOUNDATION CONSULTANTS LTD.

GRAIN SIZE DISTRIBUTION

FAP-21/22
BANK PROTECTION AND RIVER TRAINING/ (AFPM) PILOT PROJECT
FINAL REPORT | FIG. A.13-79

SOIL INVESTIGATION | LOCATION : NAKALIA



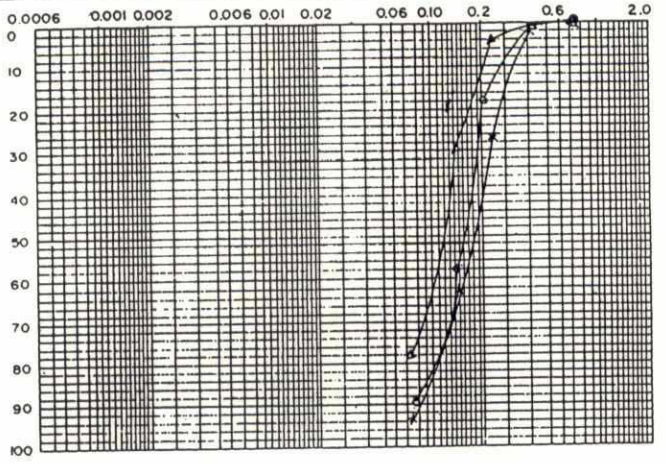
SYMBOL	BORE HOLE NO.	SAMPLE NO.	DEPTH (m)	CLASSIFICATION	CLAY %	SILT %	SAND %	REMARKS D_{60}
o o o	NK — 7	D — 1	1.35–1.8m	ML	4	84	12	.028mm
x x x	NK — 7	D — 3	4.35–4.8m	ML	2	77	21	.038mm
Δ Δ Δ	NK — 7	D — 5	7.35–7.8m	SM	—	9	91	.2mm
·—·—·	NK — 7	UD — 2	2.4–2.85m	CL	14	80	6	.012mm

WORKS EXECUTED BY FOUNDATION CONSULTANTS LTD.

GRAIN SIZE DISTRIBUTION

FAP-21/22
BANK PROTECTION AND RIVER TRAINING/ (AFPM) PILOT PROJECT
FINAL REPORT | FIG. A.13-80

SOIL INVESTIGATION	LOCATION : NAKALIA



SYMBOL	BORE HOLE NO.	SAMPLE NO.	DEPTH (m)	CLASSIFICATION	CLAY %	SILT %	SAND %	REMARKS D_{60}
o o o	NK — 7	D — 7	8.75 – 9.2 m	SM	—	10	90	.17 mm
x x x	NK — 7	D — 8	11.25 – 11.7 m	SM	—	6	94	.2 mm
Δ Δ Δ	NK — 7	D — 11	15.75 – 16.20 m	SM	—	22	78	.13 mm

WORKS EXECUTED BY FOUNDATION CONSULTANTS LTD.

GRAIN SIZE DISTRIBUTION	FAP - 21/22 BANK PROTECTION AND RIVER TRAINING/ (AFPM) PILOT PROJECT	
	FINAL REPORT	FIG. A.13 - 81

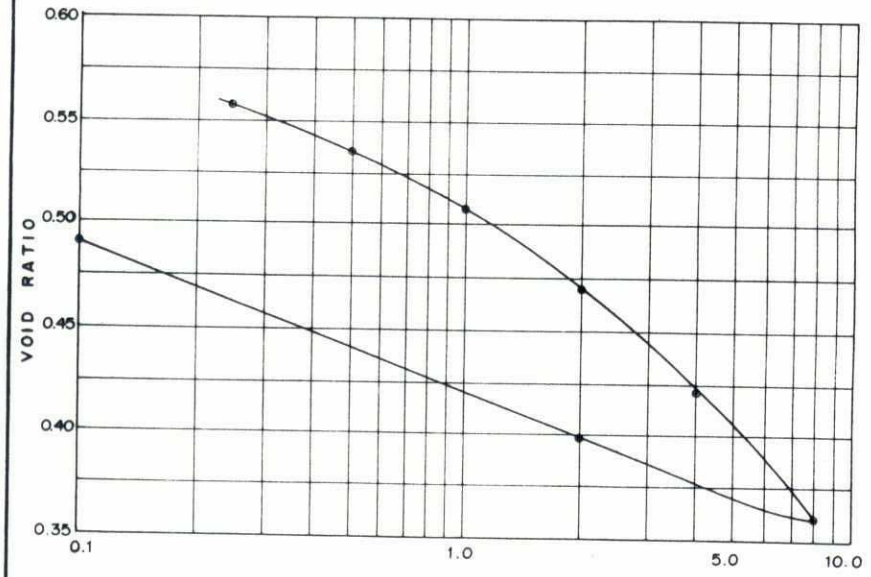
22T

BH. NO: GA 1 SAMPLE NO : U.D – 2 DEPTH : 1.80 – 2.25 m

DESCRIPTION OF SAMPLE : Stiff grey clayey silt.

INITIAL WATER CONTENT : 29.7 % FINAL WATER CONTENT :

SP. GR. OF SOIL : 2.57



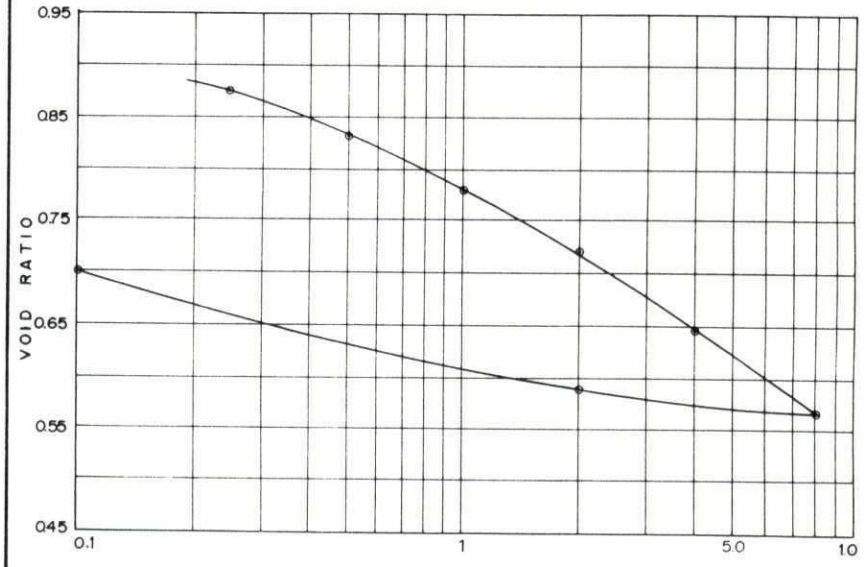
CONSOLIDATION TEST	FAP – 21/22 BANK PROTECTION AND RIVER TRAINING / (A F P M) PILOT PROJECT	
	FINAL REPORT	FIG. A.13 – 82

BH. NO: BA 1 SAMPLE NO : U.D – 2 DEPTH : 2.15 – 2.60 m

DESCRIPTION OF SAMPLE : Silt with clay.

INITIAL WATER CONTENT : 39.1% FINAL WATER CONTENT :

SP. GR. OF SOIL : 2.55



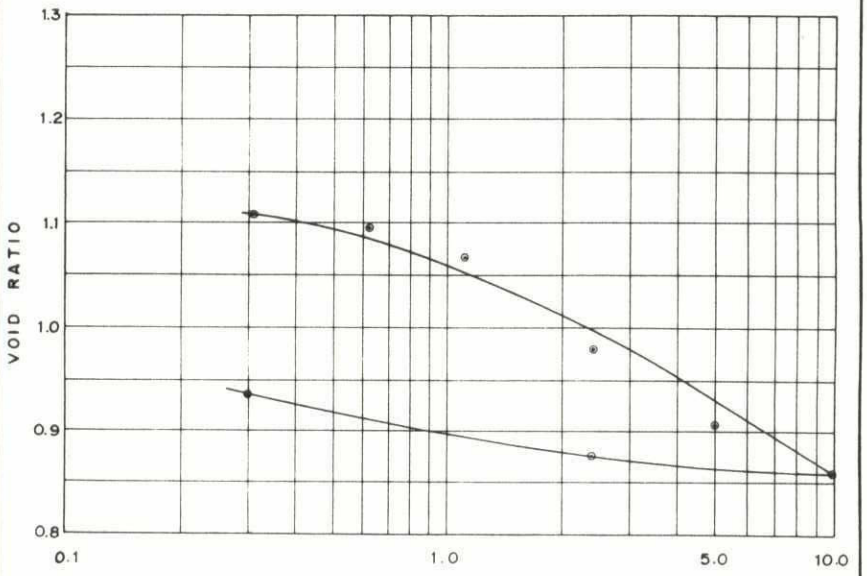
CONSOLIDATION TEST	FAP – 21/22 BANK PROTECTION AND RIVER TRAINING / (A F P M) PILOT PROJECT	
	FINAL REPORT	FIG. A.13 – 83

BH. NO: NK-1 SAMPLE NO: UD-2 DEPTH: 3.5 - 3.95 m

DESCRIPTION OF SAMPLE: Sandy silt, trace clay

INITIAL WATER CONTENT: FINAL WATER CONTENT: 26 %

SP. GR. OF SOIL: 2.67



CONSOLIDATION TEST

FAP - 21/22

BANK PROTECTION AND RIVER TRAINING / (A F P M) PILOT PROJECT

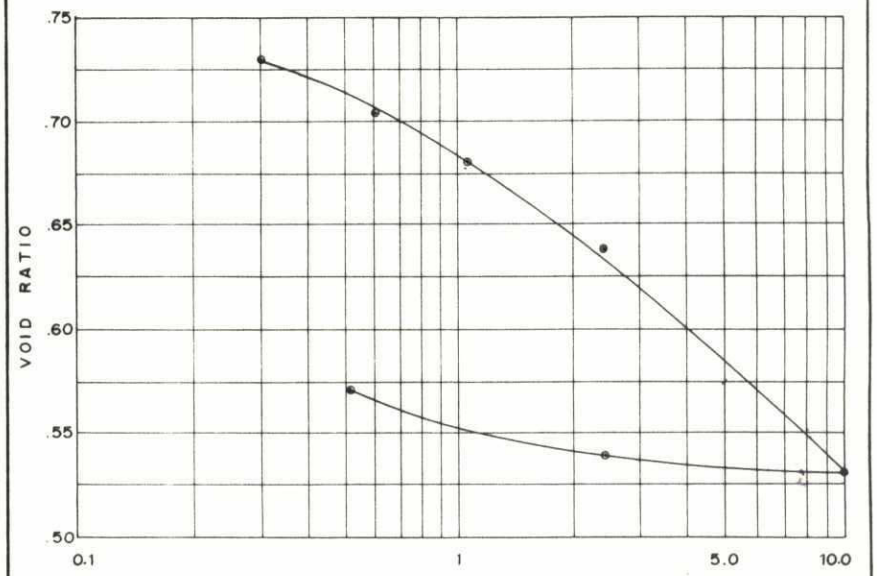
FINAL REPORT | FIG. A.13-84

BH. NO: NK-3 SAMPLE NO: UD-1 DEPTH: 0.7 - 1.15 m

DESCRIPTION OF SAMPLE: Silty sand

INITIAL WATER CONTENT: FINAL WATER CONTENT: 31 %

SP. GR. OF SOIL: 2.67



CONSOLIDATION TEST

FAP - 21/22

BANK PROTECTION AND RIVER TRAINING / (A F P M) PILOT PROJECT

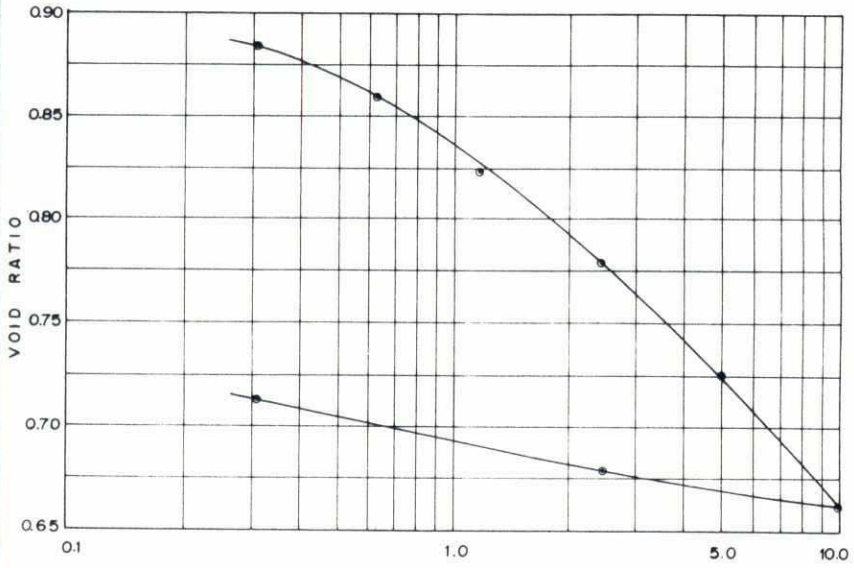
FINAL REPORT | FIG. A.13-85

BH. NO: NK-3 SAMPLE NO: UD-2 DEPTH: 3.75-4.2 m

DESCRIPTION OF SAMPLE: Clayey silt, little sand.

INITIAL WATER CONTENT: FINAL WATER CONTENT: 29%

SP. GR. OF SOIL: 2.67 %



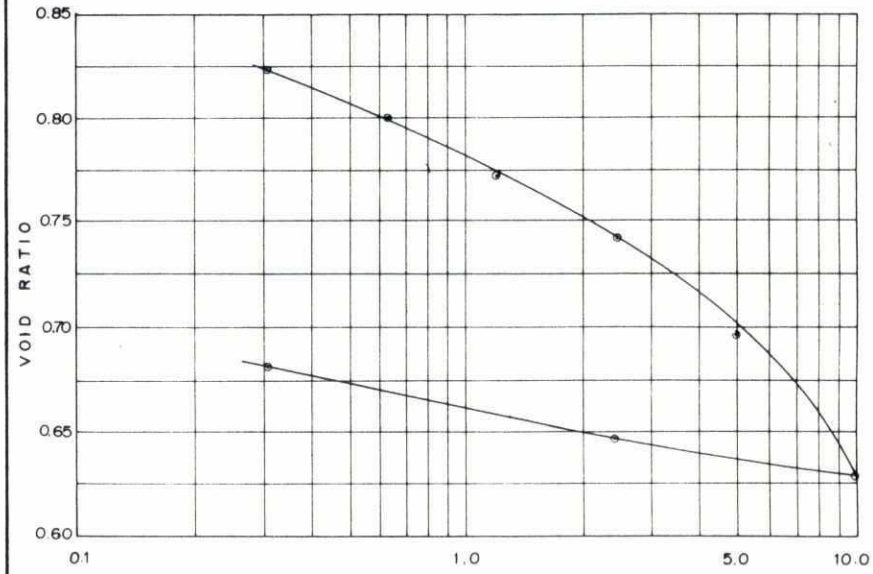
CONSOLIDATION TEST	FAP - 21/22 BANK PROTECTION AND RIVER TRAINING / (AFPM) PILOT PROJECT	
	FINAL REPORT	FIG. A.13-86

BH. NO: NK-5 SAMPLE NO: UD-3 DEPTH: 4.35-4.8 m

DESCRIPTION OF SAMPLE: Clayey silt, little sand.

INITIAL WATER CONTENT: FINAL WATER CONTENT: 30%

SP. GR. OF SOIL: 2.68



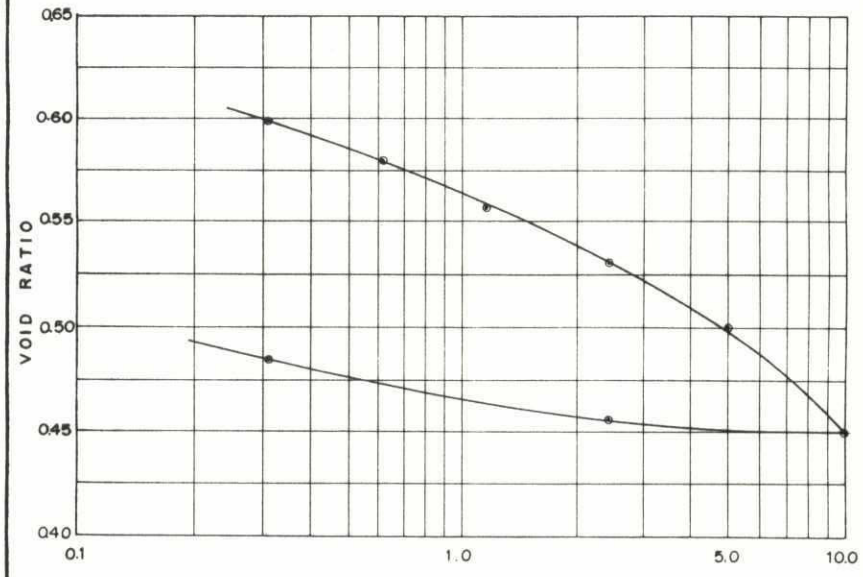
CONSOLIDATION TEST	FAP - 21/22 BANK PROTECTION AND RIVER TRAINING / (AFPM) PILOT PROJECT	
	FINAL REPORT	FIG. A.13-87

BH. NO: NK-7 SAMPLE NO: UD-2 DEPTH: 2.4 - 2.85 m

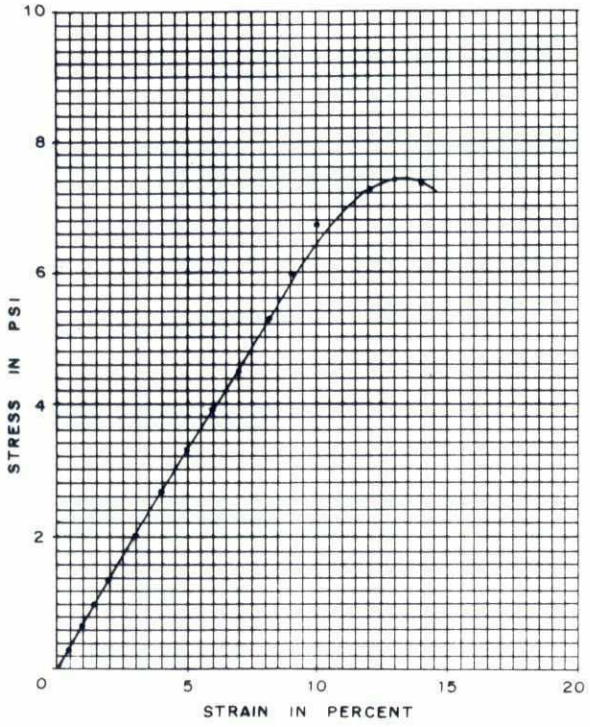
DESCRIPTION OF SAMPLE: Silt with sand, trace clay.

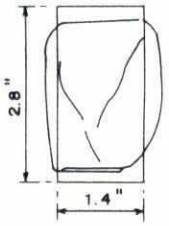
INITIAL WATER CONTENT: FINAL WATER CONTENT: 29%

SP. GR. OF SOIL: 2.68



CONSOLIDATION TEST	FAP - 21/22 BANK PROTECTION AND RIVER TRAINING / (AFPM) PILOT PROJECT	
	FINAL REPORT	FIG. A.13-88





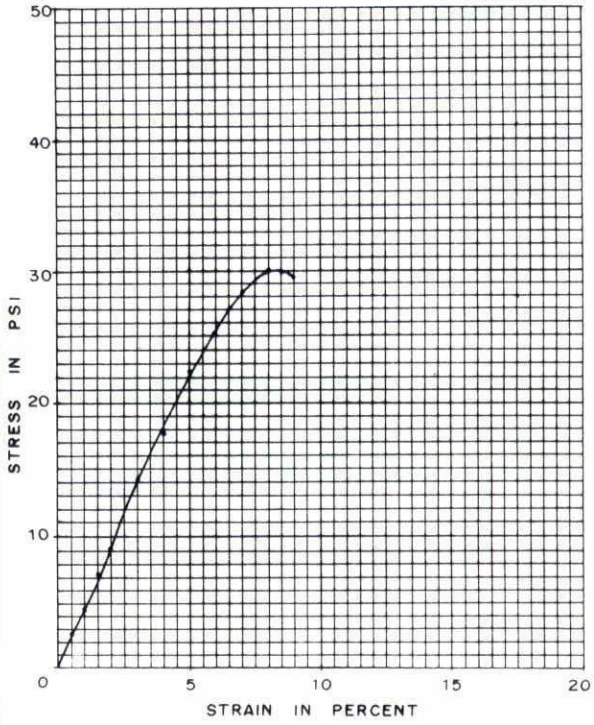
FAILURE SKETCH

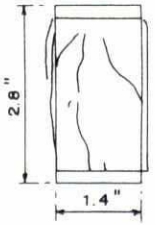
BORING NO.	SAMPLE NO.	DEPTH IN M	UNCONFINED COMP. STRENGTH PSI	PERCENT STRAIN AT FAILURE	UNIT WT. SAT. KN/m^3	UNIT WT. DRY KN/m^3	MOISTURE CONTENT
GA-5	UD-2	3.8-4.2	7.41	13	18.8	13.6	38.35%

UNCONFINED COMPRESSION TEST

FAP – 21/22
BANK PROTECTION AND RIVER TRAINING/ (AFPM) PILOT PROJECT

FINAL REPORT | FIG. A.13-89





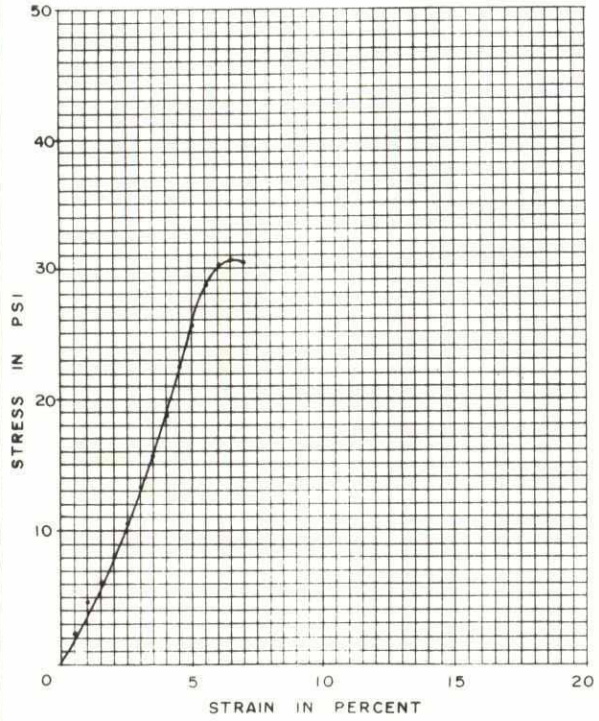
FAILURE SKETCH

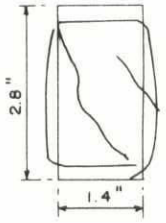
BORING NO.	SAMPLE NO.	DEPTH IN M	UNCONFINED COMP. STRENGTH PSI	PERCENT STRAIN AT FAILURE	UNIT WT. SAT. KN/m^3	UNIT WT. DRY KN/m^3	MOISTURE CONTENT
BA-1	UD-3	3.5-3.9	30.12	8	19.5	15.5	25.6%

UNCONFINED COMPRESSION TEST

FAP – 21/22
BANK PROTECTION AND RIVER TRAINING/ (AFPM) PILOT PROJECT

FINAL REPORT | FIG. A.13-90





FAILURE SKETCH

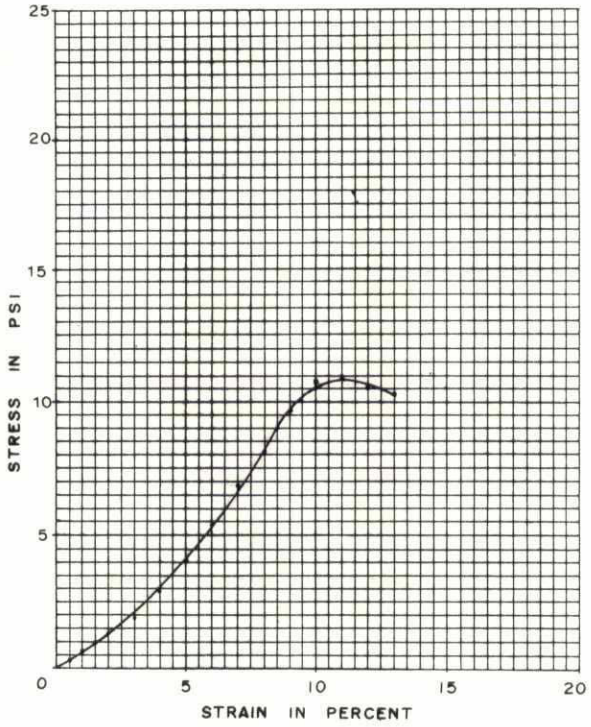
BORING NO.	SAMPLE NO.	DEPTH	UNCONFINED COMP. STRENGTH PSI	PERCENT STRAIN AT FAILURE	UNIT WT. SAT. KN/m^3	UNIT WT. DRY KN/m^3	MOISTURE CONTENT
CH-4	UD-1	1-1.5	30.25	6	19.0	15.0	26.7%

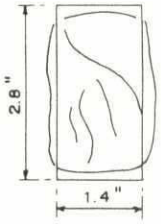
UNCONFINED COMPRESSION TEST

FAP – 21/22

BANK PROTECTION AND RIVER TRAINING/ (AFPM) PILOT PROJECT

FINAL REPORT | FIG. A.13-91





FAILURE SKETCH

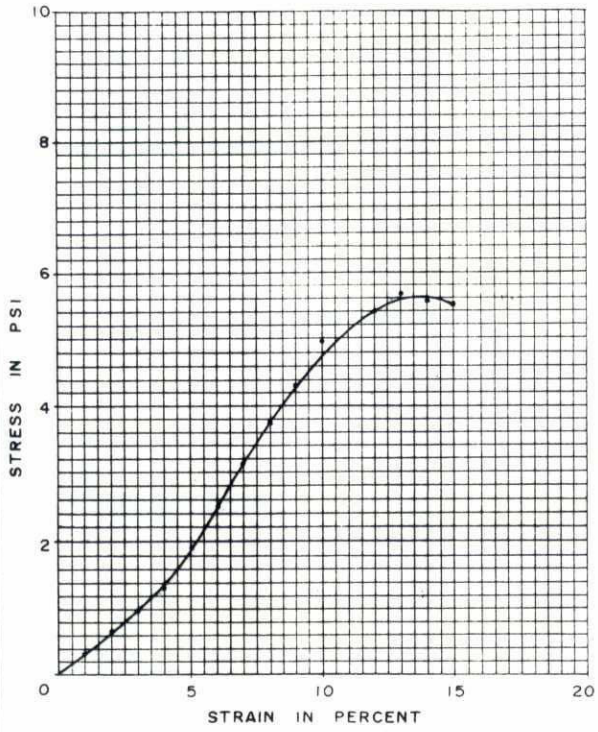
BORING NO.	SAMPLE NO.	DEPTH IN M	UNCONFINED COMP. STRENGTH PSI	PERCENT STRAIN AT FAILURE	UNIT WT. SAT. KN/m^3	UNIT WT. DRY KN/m^3	MOISTURE CONTENT
NK-1	UD-3	14-14.5	10.9	11	19.80	15.0	32.43%

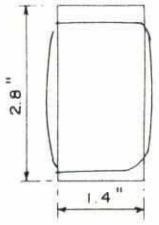
UNCONFINED COMPRESSION TEST

FAP – 21/22

BANK PROTECTION AND RIVER TRAINING/ (AFPM) PILOT PROJECT

FINAL REPORT | FIG. A.13-92





FAILURE SKETCH

BORING NO.	SAMPLE NO.	DEPTH IN M	UNCONFINED COMP. STRENGTH PSI	PERCENT STRAIN AT FAILURE	UNIT WT. SAT. KN/m³	UNIT WT. DRY KN/m³	MOISTURE CONTENT
NK-3	UD-3	7-7.4	5.63	13	19.4	14.6	32.53%

UNCONFINED COMPRESSION TEST

FAP - 21/22

BANK PROTECTION AND RIVER TRAINING / (AFPM) PILOT PROJECT

FINAL REPORT | FIG. A.13-93

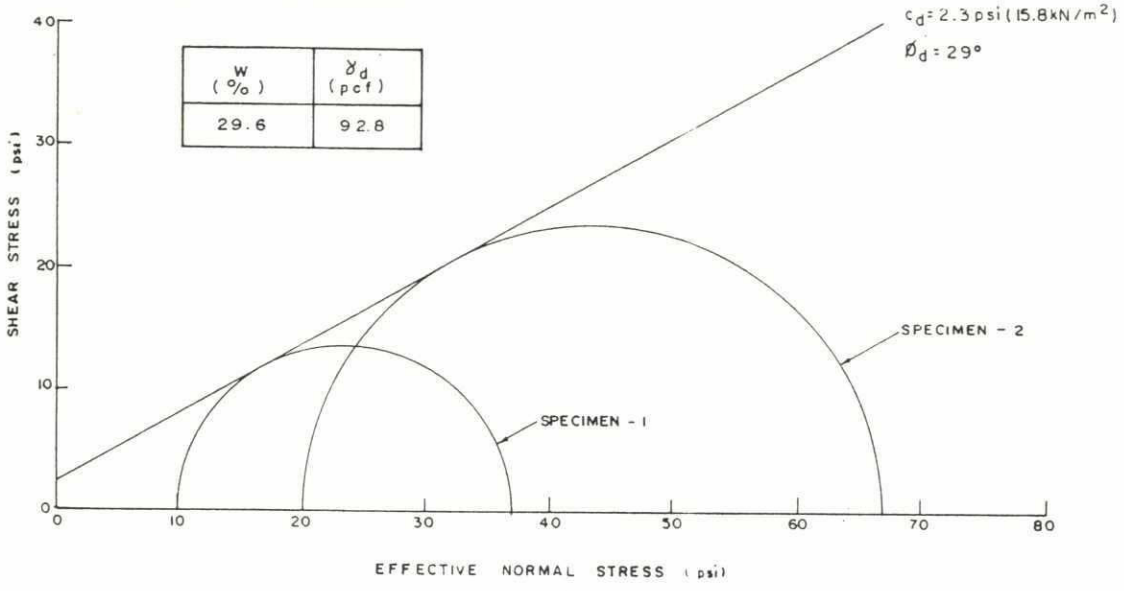
CONSOLIDATED DRAINED TRIAXIAL COMPRESSION TEST

BORE HOLE NO. GA—1

SAMPLE NO. UD-2

DEPTH: 1.80 — 2.25m

W (%)	γ_d (pcf)
29.6	92.8



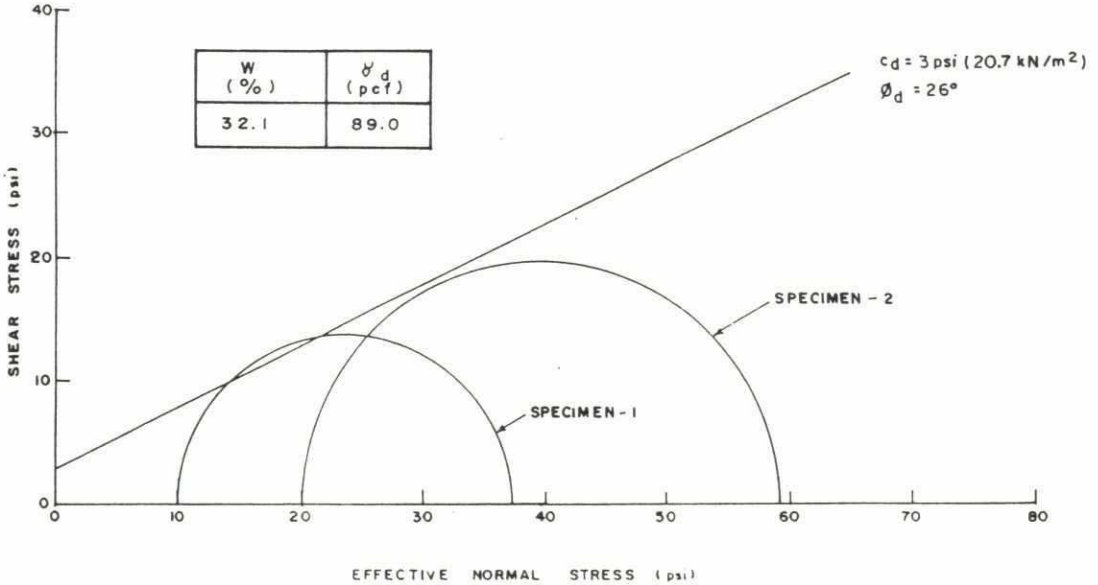
CONSOLIDATED DRAINED TRIAXIAL COMPRESSION TEST

BORE HOLE NO. GA-2

SAMPLE NO. UD-1

DEPTH: 1.85 - 2.30 m

W (%)	γ_d (pcf)
32.1	89.0



TRIAXIAL TESTS

FAP - 21/22

BANK PROTECTION AND RIVER TRAINING / (AFPM) PILOT PROJECT

FINAL REPORT | FIG. A.13-94

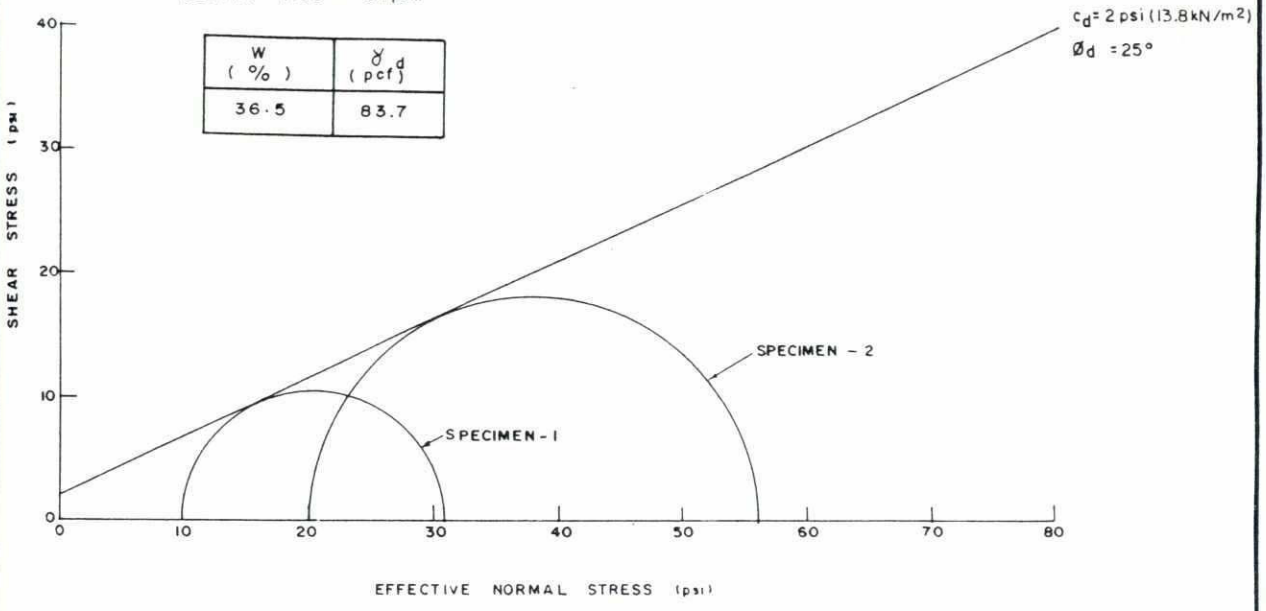
CONSOLIDATED DRAINED TRIAXIAL COMPRESSION TEST

BORE HOLE NO. GA – 5

SAMPLE NO. UD – 3

DEPTH: 4.95 — 5.40m

W (%)	γ_d (pcf)
36.5	83.7



TRIAXIAL TESTS

FAP – 21/22

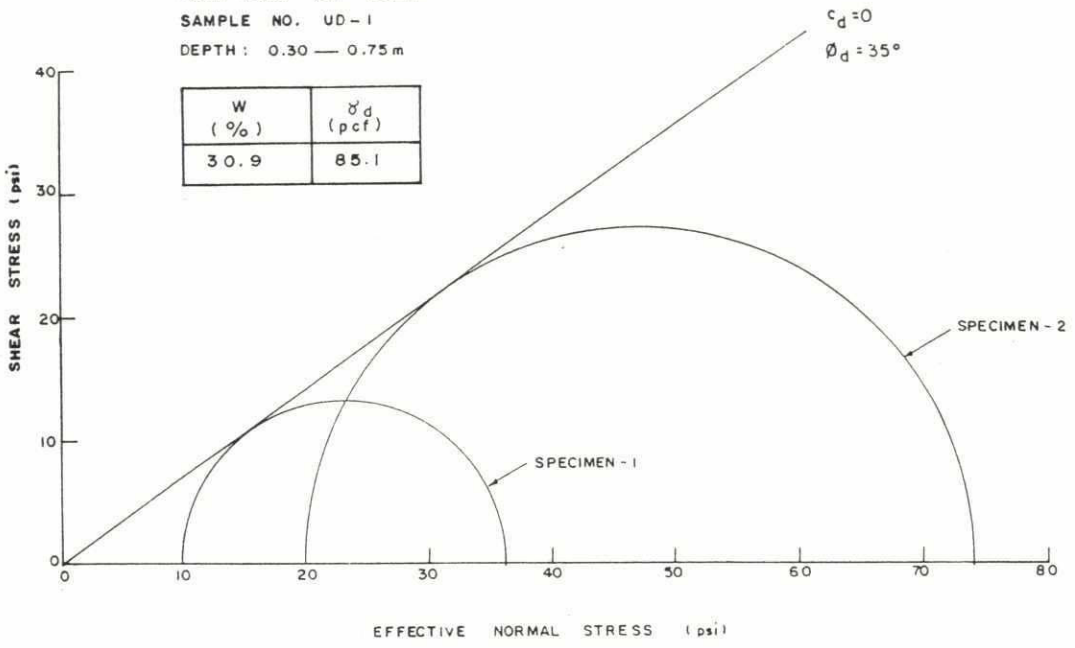
BANK PROTECTION AND RIVER TRAINING / (AFPM) PILOT PROJECT

FINAL REPORT | FIG. A.13-95

CONSOLIDATED DRAINED TRIAXIAL COMPRESSION TEST

BORE HOLE NO. BA–1
SAMPLE NO. UD – 1
DEPTH : 0.30 — 0.75 m

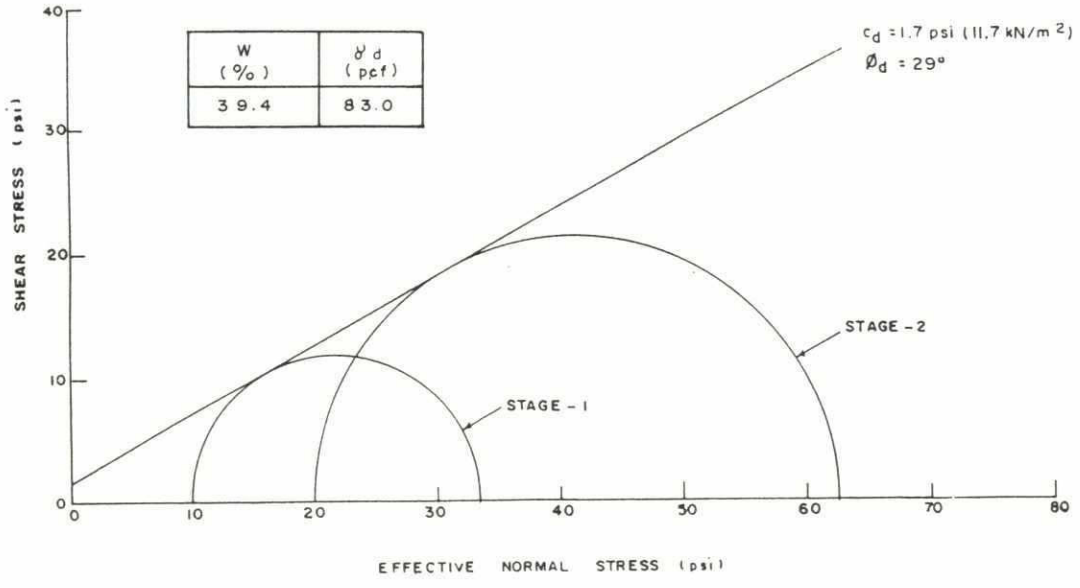
W (%)	γ_d (pcf)
30.9	85.1



CONSOLIDATED DRAINED TRIAXIAL COMPRESSION TEST

BORE HOLE NO. BA–1
SAMPLE NO. UD –2
DEPTH : 2.15 — 2.60 m

W (%)	γ_d (pcf)
39.4	83.0



TRIAXIAL TESTS

FAP – 21/22

BANK PROTECTION AND RIVER TRAINING / (AFPM) PILOT PROJECT

FINAL REPORT

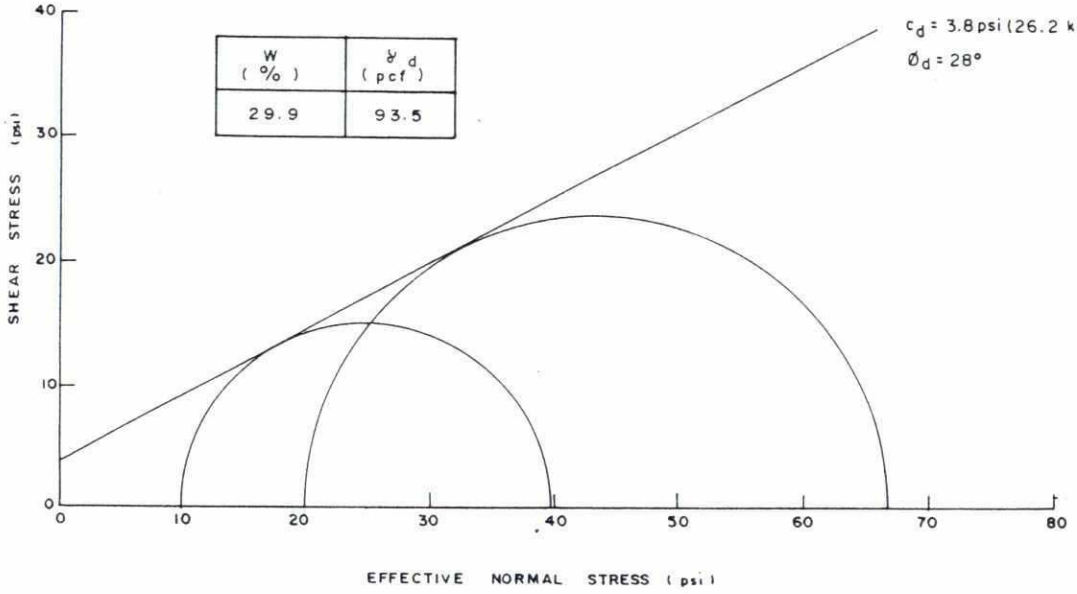
FIG. A.13 – 96

CONSOLIDATED DRAINED TRIAXIAL COMPRESSION TEST

BORE HOLE NO. CH-4
SAMPLE NO. UD-18
DEPTH : 1.0 — 1.5m

W (%)	γ_d (pcf)
29.9	93.5

c_d = 3.8psi (26.2 kN/m²)
ϕ_d = 28°

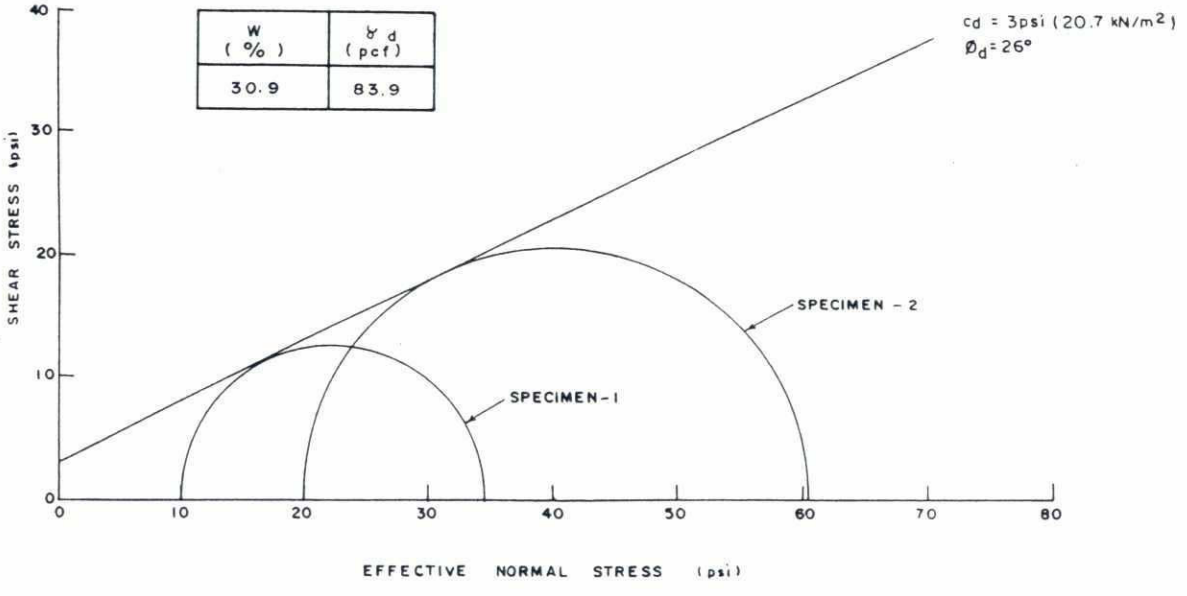


CONSOLIDATED DRAINED TRIAXIAL COMPRESSION TEST

BORE HOLE NO. CH-4
SAMPLE NO. UD-1
DEPTH : 1.56 — 2.00m

W (%)	γ_d (pcf)
30.9	83.9

cd = 3psi (20.7 kN/m²)
ϕ_d = 26°



TRIAXIAL TESTS

FAP - 21/22

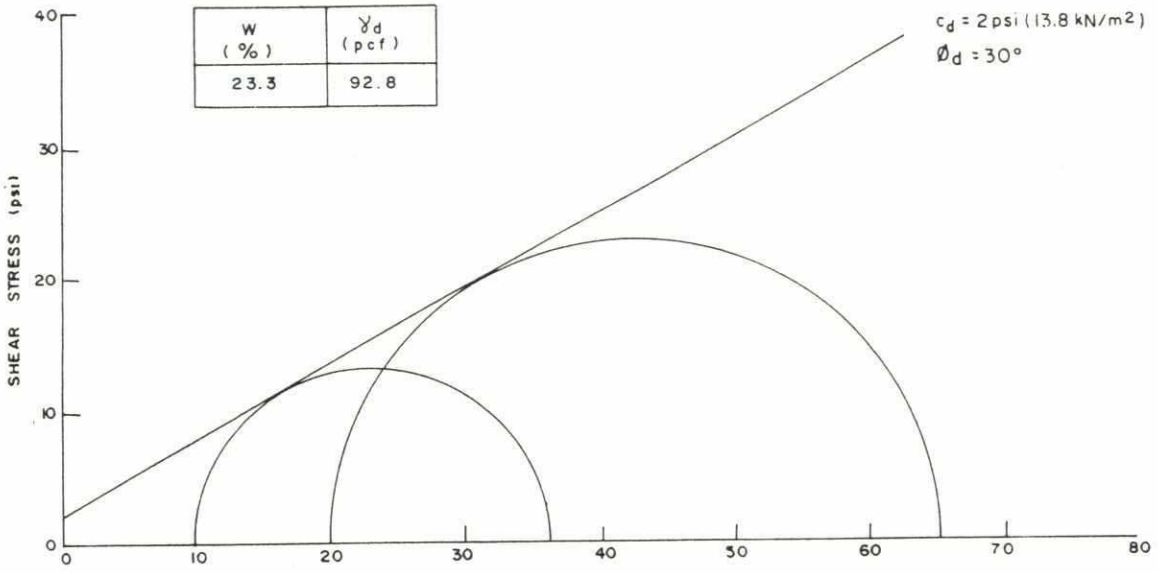
BANK PROTECTION AND RIVER TRAINING / (AFPM) PILOT PROJECT

FINAL REPORT | FIG. A.13-97

CONSOLIDATED DRAINED TRIAXIAL COMPRESSION TEST

BORE HOLE NO. NK — 5
SAMPLE NO. UD2
DEPTH: 2.00 — 2.45m

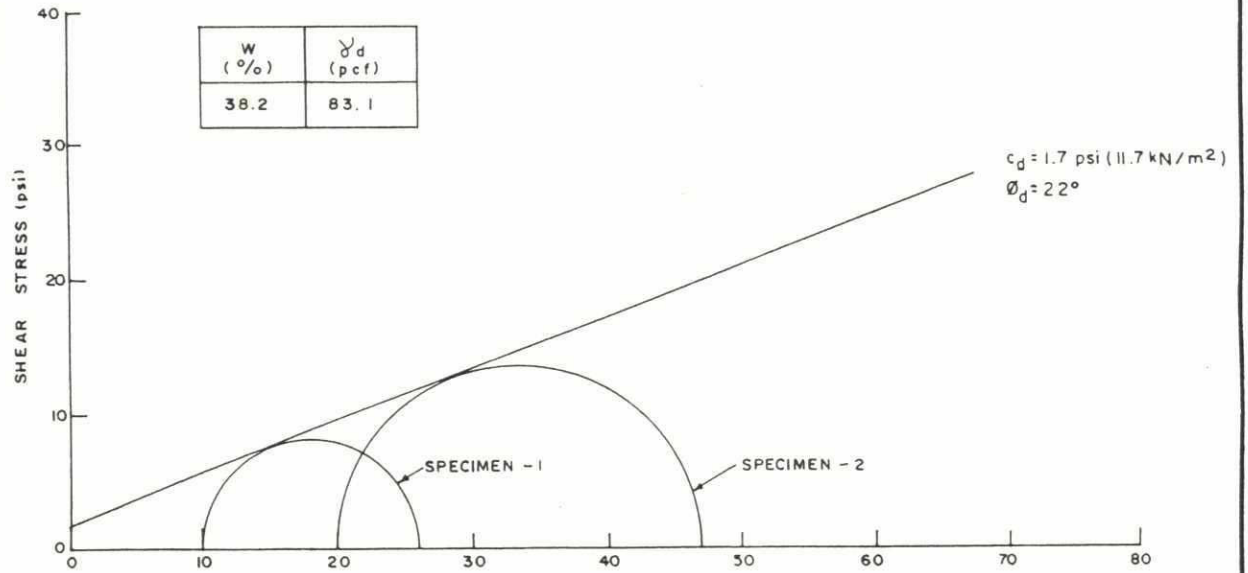
W (%)	γ_d (pcf)
23.3	92.8



CONSOLIDATED DRAINED TRIAXIAL COMPRESSION TEST

BORE HOLE NO. NK—3
SAMPLE NO. UD-2
DEPTH: 3.75 — 4.20m

W (%)	γ_d (pcf)
38.2	83.1



NOTE: TESTS WERE CARRIED OUT ON REMOULDED SPECIMENS.

TRIAXIAL TESTS

FAP — 21/22

BANK PROTECTION AND RIVER TRAINING / (AFPM) PILOT PROJECT

FINAL REPORT | FIG. A.13-98

২৪৩

BANK PROTECTION AND RIVER TRAINING (AFPM) PILOT PROJECT FAP 21/22

DRAFT FINAL REPORT

ANNEX 14

PHYSICAL MODEL TESTS



JANUARY 1993

ANNEX 14

PHYSICAL MODEL TESTS

Table of Contents

		Page
1	**INTRODUCTION**	1
2	**RIVER RESEARCH INSTITUTE FACILITIES**	2
3	**KAMARJANI MODEL**	
3.1	Introduction	3
3.2	The Bathymetry of the Model Area	3
3.3	Scaling	
3.3.1	Introduction	5
3.3.2	Similitude of Local Scour	6
3.3.3	Similitude of the Flow Field	7
3.3.4	Scales	7
3.3.5	Estimation of the Time Scale of Scour Development	8
3.4	Boundary Conditions	10
3.5	Model Construction	11
3.6	Measurement Devices	12
3.7	Test Programme	13
3.8	Presentation of the Results	15
3.9	Analysis	
3.9.1	Introduction	18
3.9.2	Flow Velocities Along the Bank	19
3.9.3	Flow Velocities Near the Groynes	21
3.9.4	Scour Depth Near the Groynes	22
3.10	Conclusions	25

		Page
4	**BAHADURABAD MODEL**	
4.1	Introduction	28
4.2	The Bathymetry of the Model Area	29
4.3	Scaling	
4.3.1	Introduction	30
4.3.2	Similitude of Local Scour	31
4.3.3	Similitude of the Flow Field	31
4.3.4	Scales	31
4.3.5	Estimation of the Time Scale of Scour Development	34
4.4	Boundary Conditions	34
4.5	Model Construction	35
4.6	Measurement Devices	36
4.7	Test Programme	37
4.8	Presentation of the Results	38
4.9	Analysis	40
4.10	Conclusions	46

LIST OF FIGURES

Fig. 3.10-1:	Layout of a falling apron around a permeable groyne	26
Fig. 4.9-1:	Sketch of flow pattern in test T2	45
Fig. 4.9-2:	Sketch of flow pattern in test T3	45
Fig. A.14-1:	Location of open air model area RRI, Faridpur	47
Fig. A.14-2:	Plan of model area of RRI	48
Fig. A.14-3:	Kamarjani site survey	49
Fig. A.14-4:	Kamarjani site cross-section	50
Fig. A.14-5:	Kamarjani model longitudinal section of thalweg	51
Fig. A.14-6:	Kamarjani model typical cross-section	52
Fig. A.14-7:	Kamarjani model layout plan	53
Fig. A.14-8:	Kamarjani model longitudinal section	54
Fig. A.14-9:	Bahadurabad and Kamarjani model sieve analysis of bed sand	55
Fig. A.14-10:	Kamarjani model, 3 tested groynes	56
Fig. A.14-11:	Kamarjani model test T2	57

Page

Fig. A.14-12:	Kamarjani model test T2	58
Fig. A.14-13:	Kamarjani model test T2, flow line and velocity profile	59
Fig. A.14-14:	Kamarjani model test T2, longitudinal and cross-section	60
Fig. A.14-15:	Kamarjani model test T2, deepest point of scour hole	61
Fig. A.14-16:	Kamarjani model test T3, plan of permeable groyne	62
Fig. A.14-17:	Kamarjani model test T3, permeable groyne	63
Fig. A.14-18:	Kamarjani model test T3, flow line and velocity profile	64
Fig. A.14-19:	Kamarjani model test T3, groyne no.1 longitudinal and cross-section	65
Fig. A.14-20:	Kamarjani model test T3, deepest point of scour hole	66
Fig. A.14-21:	Kamarjani model test T5	67
Fig. A.14-22:	Kamarjani model test T5	68
Fig. A.14-23:	Kamarjani model test T5, flow line and velocity profile	69
Fig. A.14-24:	Kamarjani model test T5, profile of deepest scour hole groyne no.1	70
Fig. A.14-25:	Kamarjani model test T5, deepest point of scour hole	71
Fig. A.14-26:	Kamarjani model test T7, plan of permeable groyne	72
Fig. A.14-27:	Kamarjani model test T7	73
Fig. A.14-28:	Kamarjani model test T7, flow line and velocity profile	74
Fig. A.14-29:	Kamarjani model test T7, profile of deepest scour hole groyne no.1	75
Fig. A.14-30:	Kamarjani model test T7, deepest point of scour hole	76
Fig. A.14-31:	Kamarjani model test T10	77
Fig. A.14-32:	Kamarjani model test T10	78
Fig. A.14-33:	Kamarjani model test T10, flow line and velocity profile	79
Fig. A.14-34:	Kamarjani model test T10, longitudinal and cross-section groyne no.1	80
Fig. A.14-35:	Kamarjani model test T10, longitudinal and cross-section groyne no.2	81
Fig. A.14-36:	Kamarjani model test T10, longitudinal and cross-section groyne no.3	82
Fig. A.14-37:	Kamarjani model test T10, deepest point of scour hole	83
Fig. A.14-38:	Kamarjani model scour depth as a function of blockage and slope	84
Fig. A.14-39:	Location of Bahadurabad and expected bank erosion	85
Fig. A.14-40:	Bahadurabad site survey	86
Fig. A.14-41:	Bahadurabad cross-section	87
Fig. A.14-42:	Bahadurabad model different approach channels	88
Fig. A.14-43:	Bahadurabad model cross-sections type A	89
Fig. A.14-44:	Bahadurabad model cross-sections type B	90
Fig. A.14-45:	Bahadurabad model cross-sections type C	91
Fig. A.14-46:	Layout of Bahadurabad model	92
Fig. A.14-47:	Bahadurabad scale model	93
Fig. A.14-48:	Bahadurabad model layout of three upstream termination	94
Fig. A.14-49:	Bahadurabad model revetment slope 1:3, 1:4 and vertical sheet pile	95
Fig. A.14-50:	Bahadurabad model test T2 layout plan	96

Page

Fig. A.14-51:	Bahadurabad model test T2, flow line and velocity profile	97
Fig. A.14-52:	Bahadurabad model test T2, velocity along the revetment	98
Fig. A.14-53:	Bahadurabad model test T2, long sections of scour hole	99
Fig. A.14-54:	Bahadurabad model test T2, velocity along the revetment	100
Fig. A.14-55:	Bahadurabad model test T2, cross-section of scour holes	101
Fig. A.14-56:	Bahadurabad model test T2, layout plan	102
Fig. A.14-57:	Bahadurabad model test T3, flow line and velocity profile	103
Fig. A.14-58:	Bahadurabad model test T3, velocity along the revetment	104
Fig. A.14-59:	Bahadurabad model test T3, long sections of scour hole	105
Fig. A.14-60:	Bahadurabad model test T3, measurement of bed erosion	106
Fig. A.14-61:	Bahadurabad model test T3, cross-section of scour holes	107
Fig. A.14-62:	Bahadurabad model test T5, layout plan	108
Fig. A.14-63:	Bahadurabad model test T5, flow line and velocity profile	109
Fig. A.14-64:	Bahadurabad model test T5, velocity along the revetment	110
Fig. A.14-65:	Bahadurabad model test T5, long sections of scour hole	111
Fig. A.14-66:	Bahadurabad model test T5, measurement of bed erosion	112
Fig. A.14-67:	Bahadurabad model test T5, cross-section of scour holes	113
Fig. A.14-68:	Bahadurabad model test T7, layout plan	114
Fig. A.14-69:	Bahadurabad model test T7, flow line	115
Fig. A.14-70:	Bahadurabad model test T7, velocity along the revetment	116
Fig. A.14-71:	Bahadurabad model test T7, long sections of scour hole	117
Fig. A.14-72:	Bahadurabad model test T7, measurement of bed erosion	118
Fig. A.14-73:	Bahadurabad model test T7, cross-section of scour holes	119
Fig. A.14-74:	Bahadurabad model test T7, layout plan	120
Fig. A.14-75:	Bahadurabad model test T10, flow line and velocity profile	121
Fig. A.14-76:	Bahadurabad model test T10, long sections of scour holes	122
Fig. A.14-77:	Bahadurabad model test T10, bed erosion	123
Fig. A.14-78:	Bahadurabad model test T10, cross-sections of scour holes	124
Fig. A.14-79:	Bahadurabad model local scour depth as a function of revetment slope	125
Fig. A.14-80:	Bahadurabad model local scour depth as a function of revetment slope and channel alignment	126

Page

LIST OF TABLES

Table 3.3-1:	Main scale factors	8
Table 3.4-1:	Hydrologic data for boundary conditions	10
Table 3.7-1:	Characteristics of the groynes in the different tests	14
Table 3.8-1:	Measured water level gradient for the discharge according to the Froude condition	17
Table 3.8-2:	Measured water level gradient for the increased discharge	17
Table 3.9-1:	Maximum flow velocity along the bank between the groynes	20
Table 3.9-2:	Maximum flow velocities around a groyne at a radius of 30 m to 125 m from the groyne head	21
Table 3.9-3:	Distances from the groyne where the maximum flow velocity has been measured in the local grid	22
Table 3.9-4:	The maximum flow velocity with a radius less than 19 m from the groyne head	22
Table 3.9-5:	Equilibrium maximum local scour depths near groynes	23
Table 3.10-1:	The maximum flow velocity upstream of the first groyne	27
Table 3.10-2:	Maximum local scour depths for permeable groynes with a blockage of 20 % to 30 % near the head of the groyne	28
Table 4.3-1:	Main scale factors	32
Table 4.3-2:	Main data for tests T1 and T2 in cross-section 6, upstream of the revetment	33
Table 4.3-3:	Main data for tests T3 and T4 in cross-section 6, upstream of the revetment	33
Table 4.3-4:	Main data for tests T5, T6 and T7 in a cross-section upstream of the revetment	33
Table 4.3-5:	Main data for tests T8, T9 and T10 in a cross-section upstream of the revetment	34
Table 4.4-1:	Hydrologic data for boundary conditions	35
Table 4.7-1:	Test programme for a revetment	37
Table 4.8-1:	Measured water level gradient in the movable bed portion	39
Table 4.9-1:	Maximum flow velocities and maximum scour depths	41
Table 4.9-2:	Maximum flow velocity near the revetment, bed protection and falling apron	42
Table 4.9-3:	Angle of the approach channel with the revetment	44

Page

LIST OF PHOTOS

Photo - 1:	Test T2	upstream groyne, deepest point of scour hole	127
Photo - 2:	Test T9	upstream groyne	127
Photo - 3:	Test T4	upstream groyne with bed protection	128
Photo - 4:	Test T6	upstream groyne head with bed protection	128
Photo - 5:	Test T5	upstream groyne without bed protection, deepest point of scour hole	128
Photo - 6:	Test T9	upstream termination with radius 50 m	129
Photo - 7:	Test T4	upstream termination with radius 450 m	129
Photo - 8:	Test T2	upstream termination with radius 50 m	129
Photo - 9:	Test T3	upstream termination with radius 450 m	130
Photo - 10:	Test T6	upstream termination of a vertical wall, radius 450 m	130
Photo - 11:	Test T10	upstream termination with a row of piles	130

1 INTRODUCTION

Deep scour holes may be formed around bank protection test structures along the Jamuna river, in the river bed of non-cohesive fine sand. For the design of these test structures the maximum depths of the expected scouring and the maximum flow velocities around the structures are design parameters, which were investigated in a physical model. For the location to build the test structures two most promising test areas were selected, one on the right bank between Kamarjani and the Manos regulator and the other one on the left bank south of Bahadurabad. The proposed test structure near Kamarjani is a series of groynes which were tested in the Kamarjani model. The proposed test structure near Bahadurabad is a revetment which has a length of approximately 1 km and this revetment was investigated in the Bahadurabad model.

The physical model investigations were conducted in two physical models at the River Research Institute (RRI) in Faridpur. These model investigations contributed to the determination of the hydraulic and morphological design conditions regarding flow velocities and scour depths for the test structures. These contributions consisted of:

- an optimization of the alignment of the test structures, shape of the head of the groynes, upstream termination of the revetment regarding flow velocities and scour depths, and
- the measurement of the flow velocities which determine the distribution of the hydraulic load on the top layer of the test structures.

The draft Terms of Reference for these model investigations were submitted to the RRI on May 12, 1992. The RRI sent the first technical and financial proposal on June 26, 1992. In order to optimise this proposal with the various constraints (time schedule among other things) a series of meetings between the RRI and the Consultant took place on June (29 and 30) and July (6, 11, 25 and 26), 1992. The contract documents for the model investigations of Kamarjani test area and Bahadurabad test area were signed on July 26, 1992.

The Consultant had requested the reservation of space in the first permanent hall for physical models in RRI. But it appeared that this hall could not be in operation before the end of 1992 due to some delay in the completion of the hydraulic circuit. Notwithstanding the less accuracy of the results of a test, the solution of open air models had to be chosen as an alternative. These open air models were covered partially by temporary sheds.

In the proposal of the Project three model investigations were planned. To complete the model investigations within the planning phase of this Project, it was necessary to construct and to operate these models parallely. The water circulation (pumps and supply canals) for the open air models and the available instruments were only sufficient to operate one model at a time. Furthermore, the price of a model investigation in RRI has increased so much between 1991 (date of the Project proposal) and 1992 that, added to the other reasons, it has

appeared more reasonable to reduce the test programme from three to two open air model investigations.

This report gives a summary of the modelling activities and investigations. The facilities of RRI for physical model investigations are described in short (see Chapter 2). Next the results with a series of groynes in the Kamarjani model are described in detail in Chapter 3 and the results of a revetment in the Bahadurabad model has been given in Chapter 4. The presentation of the results of each model investigation is followed by the main conclusions.

2 RIVER RESEARCH INSTITUTE FACILITIES

The River Research Institute in Faridpur has a soil mechanics department and a hydraulics department. The hydraulics department has the following facilities for scale model investigations: two test halls (each one with a length of 100 m and a width of 30 m) and an out door model area of 130 m wide and 260 m long, see Fig. A.14-1. The test halls were not available for physical model investigations during the study phase of FAP 21/22, because these halls including the hydraulic circuit were under construction at that time.

The out-door model area is a platform composed of nine compartments, three of them are 125 m by 40 m and six of them are 60 m by 38 m (see the map in Fig. A.14-2). All these compartments are supplied with water by a network of canals. After passing the models, the model discharge returns to different collect canals which are connected with the sump for the pumps. These pumps return the model discharge to the supply canals.

The compartments used for the present studies were number 1 and number 3 (each being 125 m x 40 m in size). The maximum capacity of the pumps and the supply canals is 0.6 m^3/s. The effective head between the supply and collect canals is about 1.3 m only and this limits the discharge effective available in the model.

All the nine compartments are filled up with sand whose mean grain size diameter is about 0.18 mm. Only one type of sand is available for model investigation.

A model has an inflow and an outflow section with fixed bed and between these inflow and outflow sections the model has a movable bed. In order to protect the models from rain and wind (the model investigation took place during the monsoon season) a temporary shed was built covering the whole movable bed portion.

3 KAMARJANI MODEL

3.1 INTRODUCTION

Along the right bank of the Jamuna river, the test area between Kamarjani and the Manos regulator (at the mouth of the Ghagat river) is situated at an approximate latitude of 25°20' to 25°23', see the map in Fig. A.14-3 which is based on the Landsat images of March 1992.

As part of the morphological study an assessment was made about possible future developments of the bank line at the Kamarjani test area based on the 1992 planform and on the observed changes in the channel pattern over the period 1973-1992, (see Fig. A.14-3) with the predicted future bank lines. As far as the right bank is concerned, the morphological study has concluded that with a tentative 75 % probability the bank erosion near Kamarjani will continue atleast until 1995. The rate of bank erosion at the Kamarjani site for the period 1992-1995 is also indicated in Fig. A.14-3. It is felt that there is very little chance of deceleration of this rate. As a consequence it may be expected that the Manos regulator will be eroded away before a test structure can be built there. Developments after 1995 are increasingly difficult to predict, but it is estimated that the bank erosion will still continue, although probably at a slightly lesser rate.

The groynes to be studied in the physical model are expected to be implemented after the monsoon season of 1993. Accordingly the tests have been carried out with the consistent banklines after the monsoon 1993. The results of these tests can probably be also used to predict the local scour holes and the maximum flow velocities for the following years, 1994 and 1995, because the reduced curvature of the predicted bank line in those years will have a very small influence on the scour depths and the flow velocities.

The approximate layout of the groynes including the connection to an extension of existing embankments is indicated in Fig. A.14-3. Information on different aspects of the physical model as for example, the bed geometry, the boundary conditions, the main data of the model and the model construction is given in details in sections 3.2 to 3.6. The test programme and the measurements during a test are described in Section 3.7. The results and their analysis are summarized in sections 3.8 and 3.9. Finally the conclusions of this model investigation are given in Section 3.10.

3.2 THE BATHYMETRY OF THE MODEL AREA

The bank of the Jamuna river between Kamarjani and the Manos regulator has been surveyed over a stretch of about five kilometers in March 1992 . The distance between the cross-sections in this survey is about 200 m. These cross-section surveys cover a total width of about 3 km, with about 1.5 km on the landside and 1.5 km on the riverside. For the land area, heights have been measured at an interval of 50 m and for the river area the bathymetric survey has been performed from a boat and the depth was recorded continuously.

The results of the survey are presented in a layout plan at a scale 1:5,000 and in cross-sections at a distorted scale: 1:2,000 horizontal and 1:100 vertical. In a reduction of this general layout plan contour lines corresponding to 7 m and 14 m +PWD have been drawn, see Fig.A.14-3. For a comparison, the 1 in 2 years flood level is 21.60 m +PWD. Some representative cross-sections such as number 8, 12, 14 and 20 are shown in Fig. A.14-4. The location of these cross-sections is indicated in Fig. A.14-3.

The thalweg of the outflanking channel and the secondary channel is presented in a longitudinal section, as per the information of the surveyed cross-sections see Fig. A.14-5. From this graph it can be seen that the outflanking channel is subject to severe scouring near cross-sections 12 and 19 where the scour holes reach a level of 3.35 m and 0.00 m +PWD respectively, corresponding to a depth of 18.25 m and 21.60 m under the 1 in 2 years flood level. These scour holes can not be explained by the typical bed profiles in the bend of an outflanking channel, which is mentioned as bend scour. Probably these scour holes can be considered as confluence scour holes, because the locations of the scour holes seem to correspond to the confluence of secondary channels, as shown in Fig. A.14-3. Upstream of cross-section 10 a small channel can be identified along the right bank. The main channel flow is directly hitting the bank and at that location it forms a confluence with the secondary channel. Near the cross-section 11 the outflanking channel divides into two secondary channels which are separated by a low char. The main channel flows along the bank. These two channels join up near cross-section 19.

The maximum depth of a confluence scour hole can be estimated as a function of the depths of the tributaries and of their approach angle by:

$$\frac{h_s}{h} = 1.292 + 0.037\,\theta \qquad (3.2\text{-}1)$$

in which

θ	=	the angle between the centre lines of the channels	(degrees)
h_s	=	the maximum scour depth at the confluence	(m)
h	=	the mean of the depth of the channels upstream of the confluence	(m)

The application of this formula for the two scour holes results in a scour depth of respectively 18.5 m and 23 m under the 1 in 2 years flood water level, whereas the observation shows 18.3 m and 22 m. This confirms the explanation of confluence scour as one of the most explicative phenomenon.

However, these peculiarities are not assumed to be permanent and probably will not occur after the monsoon of 1993 and 1994. These confluences of relatively small channels may be changed completely after one major annual flood. Anyhow, they explain the scour near the bank but do not explain completely the erosion of the bank itself.

The construction of the groynes is planned to be completed after the 1993 monsoon. At that time the location of the bankline, as well as the river bed geometry itself will probably be changed. During a period of a few months just before the start of the construction of the physical models the bankline had already shifted by about 200 m, reaching close to the Manos regulator. Therefore it would have been pointless to represent all the details of the surveyed bathymetry of March 1992 with a high degree of accuracy in the physical model.

The choice has been made to carry out the scale investigation with the expected banklines assessed by the morphological studies and to keep only the main features of the cross-sections which are assessed to remain unchanged during the next two or three years. The main feature of Kamarjani model area is the bend beginning near cross-section number 10 and ending near the Manos regulator (cross-section number 23). The proposed groynes will be located in this bend (near cross-sections 14, 15 and 16). The beginning of this bend corresponds also to the point where the main channel joins the bank because of the gradual disappearance of a shallow area near the right bank. This shallow area is the continuation of a low char situated more upstream. These features were maintained after the schematization of the survey data.

The cross-section of the outflanking channel is the average of the measured cross-sections. The depths of the shallow area and of the main channel upstream of the bend are the averages of the depths observed during the survey of the cross-sections 1 and 9. The corresponding levels are about 15 m and 11 m +PWD respectively.

The cross-section represented in the model for the bend is an average of the observed cross-sections 12 and 23. The beginning of a shallow area at about 400 m of the right bank has been represented in the model, so that the general concentration of the flow on the right bank is correctly simulated (cross-sections 4 to 7 of the model, see Fig. A.14-7). In the beginning of the bend the cross-sections have been moulded by interpolation between the defined cross-sections (cross-section 1.1 to 3 of the model, as shown in layout plan Fig. A.14-7).

3.3 SCALING

3.3.1 Introduction

In the physical models for Kamarjani and Bahadurabad the flow field and the local scour around bank protection structures should be reproduced at scale. The principles of similitude of local scour holes in the physical models are summarized in Subsection 3.3.2. Next the scale condition for the reproduction of the flow field around structures is described in Subsection 3.3.3. From these conditions the scales of the main parameters of the non-distorted models are determined (Subsection 3.3.4). Finally an estimation of the time scale of the scour hole development is given in Subsection 3.3.5.

3.3.2 Similitude of Local Scour

In a physical model the same scour hole depths can be reproduced as in the prototype if certain scale laws and scale conditions are fulfilled. In a physical model not only the water depth, the model discharge etc. should be scaled according to the basic scale laws and scale conditions, but also the bed material in case of a local scour model or a movable bed model.

An important dimensionless shear stress parameter for sediment transport and bed erosion is the Shields parameter ϕ:

$$\phi = \frac{h\ I}{\frac{\rho_s - \rho}{\rho} * D_{50}} \qquad (3.3\text{-}1)$$

in which

h	=	water depth	(m)
I	=	hydraulic gradient	(-)
ρ_s	=	density of the bed material	(kg/m^3)
ρ	=	density of water	(kg/m^3)
D_{50}	=	mean sand diameter	(m)

For an undistorted model in which sand is the bed material, the sediment transport can be reproduced in the model at scale if the D_{50} is reproduced at the length scale. The sediment transport of the Jamuna river is fine sand. If this sand is scaled at the length scale the diameter of model sand will become equal to diameter of silt or clay. However, the properties and the transportation characteristics of silt and clay particles are completely different from the properties and the transportation characteristics of sand. Therefore the sand of the Jamuna river can not be scaled in the model to reproduce the sediment transport intensity in the model.

A solution for this problem could be to select a material with a low density for the movable bed in the model, for example by using a light weight material, such as bakelite, coal dust or polystyrene etc. However, these materials are sensitive for pollution by algae, therefore not suitable for an open air model with a water temperature of about 30°C. In principle a model with light weight material should have its own water circulation circuit so that it does not loose materials or spoil the other models. Such a facility is not available in the River Research Institute (RRI). Furthermore all these materials are much more expensive than sand. For these reasons the use of light weight materials had to be discarded.

Tilting of the model, which would increase the hydraulic gradient in the model and would allow the selection of fine sand can not be adopted here. The angle of tilting would be big and as a consequence serious deviations of all other hydraulic parameters had to be accepted. Only a small tilting of the model as an additional measure has been adopted here.

For these reasons it has been chosen, not to follow the scale condition for the representation of the sediment transport intensity in the model. However, it is possible to reproduce the phenomenon of local scour holes in the vicinity of an obstacle. This problem has been the subject of many investigations and a general conclusion is that once the conditions of general sediment motion have been established in a stream, there will be no further increase in scour depth with an increase of the flow velocity, because the increase in sediment transport capacity of the flow is the difference between the equilibrium sediment transport from upstream of the scour hole and the maximum sediment transport capacity in the scour hole, which is almost constant and depends on the geometry of the structure and cross-section.

In the Jamuna river the critical mean flow velocity for the initiation of sediment transport is between 0.2 and 0.4 m/s in shallow water. It is much less than the mean flow velocity during the floods and therefore the maximum scour depths can be reached within one season only.

In the model, according to the scale and the depth of the channel to be reproduced the critical mean velocity is between 0.1 and 0.3 m/s and these flow velocities are slightly less than this critical flow velocity in the prototype. A scale condition is that in the model the mean flow velocity should be greater than this critical value, atleast twice. In these condition the scour hole characteristics will not be influenced by the size of the bed material but, like on the prototype, will be influenced only by the flow pattern and the geometry of the structure and cross-section.

3.3.3 Similitude of the Flow Field

Froude condition:
In a physical model the water level gradient around structures can be modelled if the Froude condition is fulfilled. A scale effect in this water level gradient around a structure also causes a deviation in the flow pattern around the structure. The flow separation near the upstream termination and the size of the eddy will slightly change if the Froude condition is not fulfilled. In the physical model with a revetment these possible deviations are of secondary importance for the overall flow field because the flow field is mainly determined by the model boundaries and the model hydraulic roughness.

3.3.4 Scales

The geometric length scale for the undistorted model has been chosen carefully at 75 in order to find an optimization between the limitations of the test facility (such as size of the compartments available in the outdoor model area, available discharge), hydraulic conditions (one of the main objective was to observe the same bed forms ripples everywhere in the model in order to get a constant roughness) and big enough practical conditions (size of groynes, depth, etc.) to permit precise measurements.

The general layout and the boundaries of the model are presented in Fig. A.14-7. The length of the modelled area is about 2,400 m which is sufficient to simulate the effects of a series of groynes in the model. The inflow upstream of the first groyne has a length of about 1,300 m. The width of the modelled area is about 440 m in the section with the groynes.

The main scale factors for a reproduction of the flow field are determined by this length scale and the Froude condition, see Table 3.3-1. The main scale factors for a reproduction of the local scour holes in the model are determined by this length scale and the condition that the mean flow velocity is about twice the critical flow velocity for the sediment, see Table 3.3-1. The model values in this table are based on cross-section 9.

			Froude Similitude		Scour Similitude	
Parameter	Unit	Prototype	Scale Factor	Model	Scale Factor	Model
Length	m	2400	75	32	75	32
Width	m	450	75	6	75	6
Mean water depth	m	12.8	75	0.171	75	0.171
Cross-sectional area	m^2	5780	5625	1.03	5625	1.03
flow velocity	m/s	2.03	8.66	0.23	5.075	0.4
Discharge	m^3/s	11700	48714	0.24	28.547	0.412
Water level	m +PWD	21.6	-	-	-	-
Sediment diameter	mm	0.2	1.2	0.18	1.2	0.18

Table 3.3-1: Main scale factors

For each test, in order to measure the flow velocities after development of the scour holes, the model has been operated first with a high discharge to reproduce the local scour holes. This first part of the test lasted 16 hours during which the bed level was regularly measured (once or twice per hour). Flow velocities and flow lines were also measured in order to compare the velocity field corresponding to the Froude condition (low discharge). At the end of this part of the test the model was emptied for additional observations (shape of the scour holes, bed forms, contourlines, etc.). In a second stage, the model was operated with a low discharge corresponding to the Froude condition. In this part of the test the general velocity field as well as the flow lines were measured again. More detailed measurements of the velocity field were made near the groynes. For both the discharges water levels were measured in order to assess the hydraulic roughness of the model bed. In the first six tests the low discharges flowed in the bed moulded by the high discharge. As a result the roughness of the model bed was increased because of the high ripples, with a height of about 3 cm. For the last tests (T6 to T10) the bed was superficially smoothed between the two discharges, so that the ripples for the low discharge beings less, with a height of about 1 cm, the scale effect of the too high model bed roughness was reduced.

3.3.5 Estimation of the Time Scale of Scour Development

An estimation of the time scale for the development of the local scour holes is made on the assumption of bed load transport. In the physical model the sediment transport is in the

transition between bed load transport and suspended sediment transport. In the prototype, where the suspended sediment transport is dominant the development of the local scour holes will be much faster than this estimation based on bed load transport.

The bed load sediment transport formula of Meyer-Peter and Muller reads:

$$G = 8 \frac{\rho}{\rho_a} \frac{s}{s-1} B [g D (s - 1)]^{\frac{3}{2}} [\alpha \frac{h I}{(s - 1) D} - \phi]^{\frac{3}{2}} \qquad (3.3\text{-}2)$$

in which

ρ	=	specific weight of water
ρ_a	=	apparent specific weight of the sand
s	=	density of the sand
B	=	width of the river
D	=	mean diameter of the sand
h	=	water depth
I	=	hydraulic gradient
ϕ	=	Shields parameter
α	=	coefficient, function of the bed forms

$$\alpha = (\frac{k_s}{k_r})^{\frac{3}{2}} \qquad (3.3\text{-}3)$$

in which

k_s	=	Strickler coefficient with the dunes or ripples
k_r	=	Strickler coefficient of the flat bed

The scale of factor of the parameter x is defined as n_x = x in prototype divided by x in the model. In an undistorted model ($n_B = n_h = \lambda$) in which the sand is almost the same as in the prototype $n_s = n_D = 1$:

$$n_G = \lambda \frac{\left[\alpha_m \frac{\lambda h_p I_m}{(s - 1) D_p} - \phi_m \right]^{\frac{3}{2}}}{\left[\alpha_p \frac{h_p I_p}{(s - 1) D_p} - \phi_p \right]^{\frac{3}{2}}} \qquad (3.3\text{-}4)$$

in which

n_G	=	scale factor of the bed load transport	(-)

A calculation with the values of the different parameters for the Jamuna river shows that

$$\alpha \frac{h I}{(s - 1) D} \gg \phi_p$$

For large transport rates the shear velocity is much more than the critical velocity.

On the Jamuna $k_r \simeq 26 / (D_{90})^{1/6} \simeq 100$ and $k_s \simeq 40$ (corresponding to a Chézy coefficient of 60). k_r model = K_r proto, so $\alpha_m/\alpha = (K_s \text{ model}/k_s \text{ proto})^{3/2}$. In the models k_s has been estimated to be equal to 31 assuming that Strickler coefficient for model and prototype is the same.

The formula is simplified to:

$$n_G = \lambda \left[\lambda \left(\frac{k_{sm}}{k_{sp}} \right)^{3/2} * \frac{I_m}{I_p} - \frac{0.033}{\alpha \dfrac{h_p I_p}{(s-1) D_p}} \right]^{3/2} \qquad (3.3\text{-}5)$$

It has been found for the high discharge, in the movable part of the model that $I_m \equiv 0.00082$ ($I_p \simeq 7.5*10^{-5}$). A numerical application with $h_p = 12$ m gives sediment transport of value, $G = 1.9*10^{-4}$ m^2/s.

The time scale of scour development is the ratio of the volume scale by bed transport rate scale:

$$t_s = \frac{V_s}{G_s} = \frac{\lambda^3}{1.9 * 10^{-4}} \simeq 0.012 \qquad (3.3\text{-}6)$$

As a results 1 hour model is equal to 80 hours i.e. 3 days and 8 hours in prototype and 16 hours model is about 53 days in prototype.

The development of the scour hole has been measured during 16 hours in the model. This time scale has been derived assuming bed load transport. In the Jamuna river suspended sediment transport is dominant over the bed load transport (see ANNEX 2) and therefore the real time scale will probably be smaller than estimated.

3.4 BOUNDARY CONDITIONS

Three types of boundary conditions are needed in the physical models: (i) an upstream boundary condition at the inflow of the model, (ii) a downstream boundary condition at the outflow of the model, and (iii) a lateral boundary condition because in the model, the whole width of an outflanking channel is not modelled.

The upstream boundary condition is the discharge and the discharge distribution along the upstream boundary of the model. The characteristic discharges in a complete cross-section of the Jamuna river near Kamarjani are determined in the hydrologic study, as is given in the following table (also see ANNEX 5).

Return Period	Discharge (m^3/s)	Water Level (m +PWD)
2 years	70,200	21.60
10 years	91,000	22.25
100 years	117,000	22.89

Table 3.4-1: Hydrologic data for boundary conditions

In the Jamuna river the critical depth averaged flow velocity for the initiation of sediment transport is between 0.2 and 0.4 m/s. In the channels of the Jamuna river the depth averaged flow velocities are often more than twice as much. For example, the mean flow velocity in a channel cross-section is about 2 m/s for the 1 in 2 years flood, that means that the conditions for a full development of the scour holes near obstacles probably reacheds quickly. This supports the selection of the 1 in 2 years flood for the tests in the physical model.

The model does not represent the total width of the outflanking channel, but only a part of about 440 m from the right bank. In the part of the channel with this width only a portion of the total discharge of 70,200 m^3/s flows. This portion of discharge is estimated at 11,700 m^3/s if a cross-sectional area of about 5,800 m^2 a water level gradient of $7.5*10^{-5}$ and a value of the bed roughness coefficient $C \approx 60\ m^{0.5}/s$ are assumed.

The lateral boundary condition is the location of the left boundary of the model. This boundary is not the left bank of the outflanking channel, but it is a flow line of the prototype in order to represent a portion where the discharge is constant. The width of the model is sufficient to prevent any influence by the groynes on this flow line. This boundary flow line was simulated by a 2-dimensional mathematical model. The results of that study were not available in time for the construction of the model and this flow line boundary has been estimated first and compared with the results of the mathematical model afterwards. The estimation was found to be very close to the simulation result.

The downstream boundary condition is the water level to be adjusted in the model by tailgates. The water level corresponding to the 1 in 2 year flood represented on the model is 21.6 m +PWD, see Table 3.4-1.

3.5 MODEL CONSTRUCTION

The hydraulic circuit of the outdoor model area is a gravitational type. The available head difference between the supply canal and the collect canal is about 1.3 m. And this means that the elevation of the model has to be fixed carefully, which has to take into account on one hand the head losses, such as (i) losses in the pipes between the supply canal and the weir, (ii) losses through all the devices for tranquilization of the flow and (iii) losses by the tailgates. On the other hand the model elevation should permit the drainage of the lowest points in the movable bed of the physical model. The selected relative elevation of the different devices is indicated in a longitudinal section of the model, see Fig. A.14-8.

The main characteristics of the sand for the movable bed in the physical model are D_{90} = 0.27 mm, D_{50} = 0.18 mm and about 5 % of silt. The sieve curves of some of the samples of the sand are presented in Fig. A.14-9.

In the movable sand bed of the physical model the flow creates ripples which make the bed too rough compared to the roughness which is determined according to the scale laws and the bed roughness in the field. The movable bed portion of the model has been strictly limited to the location of the test structures for which scours are studied, because of this scale effect by these ripples. This minimization of the length of the movable portion also limits the increase of the slope of the water surface which is induced by these ripples.

After a test is completed the fixed bed part of the model is drained by lowering the tailgates. The movable bed portion of the model is isolated by impermeable walls from the surrounding model area and an additional drainage to a small reservoir was made to control the water level in this movable bed portion of the model. By this means it was possible to keep a constant water level after a test and so as to materialize the contour lines with threads to characterize a local scour hole.

3.6 MEASUREMENT DEVICES

Introduction

In a model test the following type of measurements are made: (a) the discharge, (b) the water levels at different places in the model, (c) the scour depths, and (d) the flow velocities. The detail of the devices are described and the accuracy of these measurements is estimated hereafter.

Discharge

The discharge is determined from the measured water level upstream of 2 rectangular weirs. The characteristics for the left bank weir are, width = 1.80 m, height = 0.665 m and for the right bank weir width = 1.82 m, height = 0.720 m.

The discharge as a function of water level upstream of the weir is given by the formula :

$$Q = \left[0.403 + 0.053 * \frac{h_w}{p} \right] \sqrt{2\,g} * b \left[\left(h_w + \frac{u_w^2}{2\,g} \right)^{1.5} - \left(\frac{u_w^2}{2\,g} \right)^{1.5} \right] \qquad (3.6\text{-}1)$$

in which

b	=	width of the weir	(m)
g	=	acceleration by gravity	(m/s^2)
h_w	=	vertical distance between the crest of the weir and the upstream water level	(m)
p	=	height of the crest of the weir above the bottom	(m)
Q	=	discharge passing the weir	(m^3/s)
u_w	=	the average flow velocity in the cross-section in which h_w has been measured	(m/s)

Because of changes in power supply to the pumps during a test, the water level upstream of the weir was not constant. The accuracy of the discharge measurement is estimated to be about 5 %.

Water level

The water levels were measured in point gauges connected to the model by drainage pipes buried under the movable bed. The purpose was to measure a smooth level along a flow line in the middle of the channel. As the pipes were too often blocked they have been directly connected with the bank above the bed. The accuracy of the measured levels is about ± 0.075 m (1 mm in the model).

Scour depth

For the measurements of the scour holes threads are tightened between the banks, and the distance between the thread and the top of the sand bed is measured with a scale. During the test the sand bed is not visible because of the water turbidity and the sediment transport. During lowering of the scale a sudden increase in the resistance mark the top of the sand bed. It was not possible to keep the reference line constant because of sag of thread. Obviously this simple method is not very accurate. From an analysis of these measurements the accuracy is estimated at ± 0.3 m (4 mm in the model) for absolute levels and this accuracy is sufficient for this model investigation.

Flow velocity

The magnitude of the flow velocities have been measured with an OTT Current meter. This current meter is not precise enough to measure flow velocities less than 0.08 m/s in the model which corresponds to 0.7 m/s in the prototype. The accuracy of the flow velocity measurements is about 5 % and these measurements were less accurate than expected. With this type of instruments an accuracy within a range of 1 to 2 % is possible.

3.7 TEST PROGRAMME

A test programme of 10 tests with a series of three groynes have been carried out in this physical model investigation. These groynes were located at the predicted bankline after the monsoon of 1993 (III'94). Around each groyne in the movable bed the scour depths and the flow velocities had to be measured. The main characteristics of this test programme is presented in Table 3.7-1. Test T1 is not a complete test and was used to have an experience in the model operation. A section of some typical groynes in Test T2, T3 and T10 is presented in Fig. A.14-10.

W A R. P. O. LIBRARY. DHAKA

Test No.	Length		Spacing	Permeability of groynes			Length Impermeable	Falling Apron
	chn (m)	lnd (m)	(m)	1 (%)	2 (%)	3 (%)	(m)	(m)
T2	20	80	300	0	0	0	100	yes
T3	40	80	300	30	30	0	0 0 100	yes
T4	40	80	300	50	50	50	0	yes
T5	40	80	300	0	0	0	120	no
T6	40	80	450	50	50	-	0	yes
T7	80	80	450	50	50	-	24	yes
T8	40	80	300	30/50	30/50	30/50	24	no
T9	41	80	300	20/30/ 40/50	20/30/ 40/50	20/30/ 40/50	60	no
T10	61	80	300	20/30/ 40/50	20/30/ 40/50	20/30/ 40/50	80	no

chn = length of the groyne into the channel.
lnd = length of the groyne on the attached char in front of the embankment,
Permeability = percentage blocked by the piles of a cross-section through the axis of the groyne.

Table 3.7-1: Characteristics of the groynes in the different tests

The length of the groyne as given in Table 3.7-1 is measured from the predicted bankline after the flood in 1993. Some additional information about each test is given hereafter:

Test T2: Three impermeable groynes had been built with different slopes of the head and the sides: (i) 1:4 for the upstream Groyne 1, (ii) 1:3.5 for the middle Groyne 2, and (iii) 1:3 for the downstream Groyne 3. For each groyne the axis was perpendicular to the bank line.

Test T3: Groynes 1 and 2 were permeable groynes (upstream) and Groyne 3 is an impermeable groyne which was identical to Groyne 3 in Test T2. The groyne axis was perpendicular to the bank. A permeable groyne was made of 2 parallel pile rows. Around the groynes a falling apron with a final equilibrium slope of 1:2 represented in the model as a fixed mortar layer was made under the initial bed level.

Test T5: The test had been carried out with 3 impermeable groynes made of a vertical plate (sheet piling). In the test no falling apron limited the local scour holes, which developed freely.

Test T8: The axis of the groynes made an angle of 15° with a line perpendicular to the bank line. The groynes were pointing in upstream direction. The permeability of the groyne was 50 % which increased over a length of 20 m near the head of the groyne to 70 %. The first 24 m of the groyne near the embankment were impermeable. The permeable part did not had a prefixed falling apron which limits the development of the local scour holes.

Test T9: The axis of the groynes made an angle of 15° with a line perpendicular to the bank line. The groynes were pointing in upstream direction. The impermeable part connected to the embankment had a length of 60 m and the permeable part was also 60 m. The permeability of the groynes was progressively increased from 50 % to 80 % towards the head.

Test T10: The difference with Test T9 is that the length of the impermeable part had been increased by 20 m to 80 m (its limit corresponded to the 1993 bankline). The length of the permeable part was 60 m and as a consequence the whole groyne was 20 m longer.

3.8 PRESENTATION OF THE RESULTS

The complete and intermediary results are available at the Project office and in the River Research Institute (Faridpur). The most interesting results are presented for some selected tests (T2, T3, T5, T7 and T10) in graphical form in, Fig. A.14-11 to A.14-37. The complete results which are presented in graphs and tables, provide a series of informations concerning the tests which is summarised hereafter.

Scouring

Different aspects of the scouring have been presented in graphs: (i) the maximum local scour depth as a function of time, and (ii) several cross-sections of the local scour at different moment during the test. The general bed erosion has been measured as a function of time, but has not been presented in any graph.

Maximum local scour depth

A graph showing the deepest point of the local scour hole near each groyne as function of time permits to check if an equilibrium has been reached at the end of the test see Fig. A.14-15, A.14-20, A.14-25 and A.14-30. If not, the evolution of the maximum depths was extrapolated in order to estimate the equilibrium maximum scour depth. In most cases this extrapolation added a few metres to the maximum measured scour depth after 16 hours. In some tests the deepest point of the local scour hole shifted in downstream direction. In such a test the deepest point was not measured in the same location during the test. After completion of a test some photographs were taken of the scour hole, see photos 1 to 5.

Local scour depths

For each groyne the bed levels in two longitudinal-sections and two cross-sections passing through the head of the groyne and through the deepest point of the local scour hole are

made at different times during a test. The initial and the final bed level at the end of the test are included in these graphs, see for example Fig. A.14-14, A.14-19, A.14-24, A.14-29, A.14-34, A.14-35 and A.14-36. In these sections the prefixed falling apron, if any has been built in the model, has been drawn so that the junction between the bed and the assumed final position of the falling apron appears clearly.

From these graphs longitudinal and lateral slopes of the scour holes can be estimated.

Scouring of the movable bed

General bed erosion can have some influence on the local scour depths. To check the general bed erosion in the movable part of the model, the bed levels were measured in three points which were in the middle of the channel that means at about 240 m from the right bank and not located near the groynes, are presented as a function of the time. These points were influenced by the presence of the groynes. The variation of their levels was the result of the sediment transport in the model which was responsible for the erosion of the bed. The supply of sand upstream of the model partially limits, but cannot completely prevent general bed erosion. A too big supply of sand has a negative effect to create too much sedimentation in the upstream cross-sections of the model without more benefits downstream. In the first tests this general bed erosion might have had a small influence on the measured local scour depths, but in the final tests general bed erosion was small and its influence on the local scour depths was negligible.

Flow lines

A few flow lines have been sketched in the plan of the model for the Froude discharge, see Fig. A.14-13, A.14-18, A.14-23, A.14-28 and A.14-33. Flow lines have been especially studied near the right bank so as to appreciate the diversion of the flow by the groynes. The comparison between the flow lines with the two different discharges in the same test shows that the flow pattern for the study of scouring is fairly the same, as it should be, to the flow lines measured with the discharge corresponding to Froude condition.

Flow velocity field

The general flow field is characterised by the flow velocities which were measured in 6 standard cross-sections. In these standard cross-sections 4, 7, 10, 11, 14 and 18 the flow velocity was measured at half the water depth at an interval of about 40 m, see Fig. A.14-13, A.14-18, A.14-23, A.14-28 and A.14-33.

Flow velocity near the groynes

For each test the flow velocities were measured in a local grid around the head of the groyne to determine the velocity gradient in a cross-section near a groyne.

Water level measurements and estimation of the water level gradient

In each test the water level had been measured using four point gauges installed along the model for the discharge according to the Froude condition and for increased discharge. These

water levels have been used to define the position of the downstream tailgate and to estimate the water level gradient.

The water level gradient in the movable bed portion of the model followed from the water level difference measured between point gauge 1, 2, 3 and 4, see Tables 3.8-1 and 3.8-2 for the tests T2 to T10.

Test No.	T2	T3	T4	T5	T6	T7	T8	T9	T10
	(10^{-5})								
Slope between point gauge 1 and 2	18	19	23	18	25	43	34	59	48
Slope between point gauge 2 and 3	11	10	11	15	5	20	23	25	17
Slope between point gauge 3 and 4	-	-	-	-	-	131	13	75	29

Table 3.8-1: Measured water level gradient for the discharge according to the Froude condition

Test No.	T2	T3	T4	T5	T6	T7	T8	T9	T10
	(10^{-5})								
Slope between point gauge 1 and 2	54	52	63	61	70	76	104	110	115
Slope between point gauge 2 and 3	79	68	83	106	95	96	75	76	67
Slope between point gauge 3 and 4	-	-	-	-	-	189	229	208	104

Table 3.8-2: Measured water level gradient for the increased discharge

The large variations in the measured water level gradient can be explained due to the following:

- The accuracy of the water level reading with a point gauge is about 0.5 to 1 mm. The accuracy of the water level gradient is determined by a substraction of two water levels which differed slightly.
- The water levels should be measured along one flow line in the model. Some point gauges were connected with the bank and others measured the water level in the middle of the model, so a transverse gradient in the water level was mixed up with longitudinal gradient.
- The model discharge fluctuated considerably especially during the first 6 tests and these fluctuations created small waves with a period of 20 to 30 minutes in the model.
- The variable bed roughness and the general bed erosion in the movable bed portion, as well as artificial sediment supply to reduce this general bed erosion had a disturbing influence on the water level gradient.

All these effects together resulted in rather big variations in determining the water level gradient.

A first approximation of the roughness of the fixed bed part of the model Chézy coefficients, $C = 36\ m^{0.5}/s$ were calculated with the original parameters (cross-sectional area $\simeq 1.01\ m^2$, a hydraulic radius $\simeq 0.135$ m, and an average slope $32*10^{-5}$ for the discharge according to the Froude condition and $79*10^{-5}$ for the increased discharge) for the discharge according to the Froude condition and $C = 40\ m^{0.5}/s$ for the increased discharge. The average value $C = 38\ m^{0.5}/s$ can be considered as an inaccurate approximation of the hydraulic roughness of the fixed bed portion. Because this value when substituted in the White-Colebrook formula gives a hydraulic roughness $k_s = 0.01$ m and this value is too high for a smooth cemented surface.

For the movable bed, if the last tests are considered for which the bed erosion was rather limited, the mean wetted area was $1.45\ m^2$ and the hydraulic radius was 0.205 m. With these values $C = 25\ m^{0.5}/s$ was calculated for the discharge according to the Froude condition and $C = 22\ m^{0.5}/s$ for the increased discharge, which gives an average value $C = 24\ m^{0.5}/s$ for the movable bed portion, but probably this value is not very accurate. Compared with $C = 60\ m^{0.5}/s$ in the prototype the model bed is much too rough. Therefore the length of the movable bed part was designed as small as possible.

3.9 ANALYSIS

3.9.1 Introduction

The analysis of the results of the tests has been done giving emphasis on the following aspects:

- the maximum flow velocities near the bank between the groynes (Subsection 3.9.2);
- the maximum flow velocities in the vicinity of the structure, especially near the head of the groyne (Subsection 3.9.3), and
- the maximum depths in the local scour holes near the groynes (Subsection 3.9.4).

These are the most important aspects for the design of the groynes. The analysis of the side slopes of the local scour holes is not included in the presented analysis.

Analysis of the flow velocities

The flow velocities which were measured in the standard cross-sections in both stages of a test with different model discharges, are compared with each other. The scale factors are such for the different discharges that the flow velocities measured in the model correspond to the same flow velocity in the prototype. Without a scale effect due to the increase of the model discharge and the too high hydraulic roughness, the mean flow velocities as well as the distribution of the flow velocities should be the same. Variations in the mean flow velocity can only result from slight variations in the area of a cross-section in the movable

bed or more often from uncertainties in the measurement of the discharge due to great variation of supply canal water level. The differences between the mean flow velocities are on the average 0.1 m/s with extreme values of 0.4 m/s.

For comparing the flow velocity distributions in the same cross-section between the two discharges, it is recommended to make the mean flow velocity of these distributions the same for both discharges. For a given test and a selected cross-section the difference between the observed mean flow velocity and the average flow velocity were calculated for all the tests in the same cross-section. The average of these differences for all the cross-sections of one test determined the correction of the flow velocity distribution. These comparisons showed that the model discharge was not constant during a test, because the supply channel of the water circuit does not have an overflow weir.

3.9.2 Flow Velocities Along the Bank

The flow velocities near the bank and between the groynes were compared with the flow velocities near the bank without groynes. In the calibration Test T1 the general flow velocity field was measured without groynes. For the other tests the measurements of flow velocities further upstream of the first groyne can also be used.

In cross-sections 4 and 7 upstream of the groynes the average flow velocity near the bank was about 2.3 m/s and the average flow velocity of the whole cross-section was 2.6 to 2.7 m/s with a return period of about 2 years. These flow velocities are higher than the critical flow velocity required for the initiation of bank erosion and a continuous bank erosion can be expected.

The groynes are planned to be built after the monsoon of 1993. It is assumed that during the construction and planning the bank line will retreat by about 20 m.

From tests T6 to T10, the flow velocity above the flood plain in front of the embankment has been measured to have an impression of the future rate of bank erosion. For all the tests performed the presence or absence of ripples on the bank between the groynes were examined. Ripples appeared at the beginning of sediment motion and the corresponding depth averaged flow velocity was about 0.18 m/s. For the first part of the test with an increased discharge, this will correspond to 0.9 m/s in prototype conditions. This phenomena was used to estimate if the mean flow velocity was higher than about 0.9 m/s above the flood plain.

For Test T2, big eddies developed downstream of the groynes. These eddies were responsible for important flow velocities near the bank and ripples have appeared everywhere along the bank and on the flood plain.

In Test T3, the permeable groynes (opening 70 %) prevented the development of eddies between the groynes. It was observed however that between groynes 1 and 2 ripples cover

the flooded bank indicating still strong flow velocities near the bank. Between second permeable groyne and the third impermeable groyne the bed had remained flat, due to the impermeability of the third groyne.

By reducing the permeability of the groyne down to 50 % in Test T4, the length of disturbed bed along the bank had been reduced to half of the total distance between the groynes (see Photo 3).

In Test T5 a strong eddy had developed between the groynes and the whole area of the flooded bank was covered by ripples in a similar pattern as in Test T2, see Photo 5. For the tests (T6 to T10) the velocities near the bank are given in Table 3.9-1.

Test No.	Maximum Flow Velocity Between Groynes 1 and 2 (m/s)	Maximum Flow Velocity Between Groynes 2 and 3 (m/s)	Spacing/ Effective Groyne Length	Spacing/ Total Groyne Length
T6	0.8	0.7	7.5	3.7
T7	0.7	0.6	4.5	2.8
T8	1.0	0.8	5.0	2.5
T9	0.6	0.5	4.9	2.5
T10	0.3	0.2	3.7	2.1

Table 3.9-1: Maximum flow velocity along the bank between the groynes

Between tests T6 and T7 the length of the permeable groynes had been increased and the result was a reduction of the flow velocity along the bank with 0.1 m/s. In Test T7 the first 24 m of the groyne near the bank were impermeable to avoid erosion of the bank near the groyne and also to reduce the flow velocities along the bank between the groynes.

With Test T8, the groyne axis mades an angle of 75° with upstream bank instead of 90° in the previous tests, and the opening of the last 19 m near the head had been increased to 70%. The increase in the opening had a direct effect on the flow velocity which had been increased along the bank with 0.3 m/s for downstream Groyne 1 and with 0.15 m/s for downstream Groyne 2.

For Test T9, the length of the groyne corresponding to the width of the flood plain at 19 m +PWD was impermeable and in the channel a short section of 60 m was permeable. The permeability of that section increased progressively from 50% to 80% towards the head of the groyne. The flow velocities near the bank between the groynes were low and no ripples were observed near the bank. Nevertheless as for the previous test was concerned the flood plain had been eroded especially in the middle between the groynes where the bank had retreated 25 m to 30 m. In the vicinity of the groynes the bank had retreated by about 20 m, see Photo 2.

For this reason the impermeable part of the groyne had been lengthened by 20 m in Test T10. It is the only test in which the critical flow velocity corresponding to the beginning of motion of sand (about 0.3 m/s for the prototype) had not been exceeded along the bank between the groynes.

Regarding the reduction of the flow velocity along the bank between the groynes tests T9 and T10 have shown the best results and the value of the ratio between the spacing of the groynes and the effective length, defined as the length from the head of the groyne to the stabilized bank line is recommended to be between 3.7 and 4. The ratio between this spacing of the groynes and the total length of the groynes (from the embankment to the groyne head) is recommended between 2 and 2.5.

3.9.3 Flow Velocities Near the Groynes

The flow velocities have been measured in a local grid around the groynes between 75 m upstream and 112 m downstream of the groyne and between 38 m and 75 m towards the left bank. The maximum flow velocities measured in this area are presented in Table 3.9-2. These flow velocities can be compared with the mean flow velocities in the corresponding cross-sections of 2.2 and 2.3 m/s.

Test No.	T2	T3	T4	T5	T6	T7	T8	T9	T10
	(m/s)	(m/s)	(m/s)	(m/s)	(m/s)	(m/s)	(m/s)	(m/s)	(m/s)
Groyne 1	3.1 -	3.0 (2.8)	2.6 (2.3)	2.8 (2.7)	2.6 (2.9)	2.5 -	2.7 (2.8)	2.5 (2.6)	2.8 -
Groyne 2	2.7 -	2.9 (2.7)	2.7 (2.4)	2.6 (2.5)	2.5 (2.8)	2.6 -	2.7 (2.8)	2.5 (2.6)	2.7 -
Groyne 3	3.9 -	3.2 (3.0)	2.9 (2.6)	2.5 (2.4)			2.6 (2.7)	2.6 (2.7)	2.7 -

The corrected flow velocities are mentioned first followed by the measured value between brackets.

Table 3.9-2: Maximum flow velocities around a groyne at a radius of 30 m to 125 m from the groyne head

The maximum flow velocity of 3.9 m/s has been observed near the head of third impermeable groyne in Test T2. Around a permeable groyne the maximum flow velocity is 2.9 m/s at a distance 70 to 80 m from the groyne, see Table 3.9-3. However, at a shorter distance of 20 m from the permeable groyne lowest flow velocities of 2.3 to 2.6 m/s were measured, see Table 3.9-4.

Test No.	T2	T3	T4	T5	T6	T7	T8	T9	T10
	(m)	(m)	(m)	(m)	(m)	(m)	(m)	(m)	(m)
Groyne 1	125	99	94	94	75	68	27	68	77
Groyne 2	104	124	38	27	77	42	42	38	96
Groyne 3	114	51	70	114			38	94	77

Table 3.9-3: Distances from the groyne where the maximum flow velocity has been measured in the local grid

Test No.	T2	T3	T4	T5	T6	T7	T8	T9	T10
	(m/s)	(m/s)	(m/s)	(m/s)	(m/s)	(m/s)	(m/s)	(m/s)	(m/s)
Groyne 1	1.9	2.4	2.3	2.0	2.3	2.3	2.6	2.3	2.3
Groyne 2	1.6	2.7	2.4	1.9	2.3	2.3	2.4	2.4	2.4
Groyne 3	2.4	2.6	2.2	2.0			2.3	2.3	2.5

The corrected flow velocities are mentioned only.

Table 3.9-4: The maximum flow velocity with a radius less than 19 m from the groyne head

3.9.4 Scour Depth near the Groynes

Different types of scour are measured near the groynes:

- local scour depth due to strong vortices;
- constriction scour near the impermeable groyne head;
- local scour around the piles of the permeable groyne, and
- so-called bed form scour.

The measurements in the tests are emphasised on the local scour hole, because this local scour hole is the most important amongst the different types of scour. The extrapolated maximum scour depth in the local scour holes is summarized in Table 3.9-5. It can be mentioned that the initial bed level around the groynes was at 6.4 m +PWD in all tests and the local scour depth was measured from this initial bed level.

Test No.	Groyne No.	Deepest Point	Local Scour Depth	Falling Apron	Permeability of the Groyne
		(m +PWD)	(m)		(%)
T2	1 2 3	- 24 - 10 - 15	30.4 16.4 21.4	Yes	0 0 0
T3	1 2 3	- 4 - 4 - 16	10.4 10.4 22.4	Yes	70 70 0
T4	1 2 3	- 12 - 5 - 12	18.4 11.4 18.9	Yes	50 50 0
T5	1 2 3	- 25 - 29 - 23	31.4 35.4 29.4	Yes	0 0 0
T6	1 2 3	- 14 - 12 *	20.4 18.4 *	Yes	50 50 50
T7	1 2 3	- 15 - 13 *	21.4 19.4 *	Yes	50 50 50
T8	1 2 3	- 3 - 3 - 3	9.4 9.4 9.4	No	50-70 50-70 50-70
T9	1 2 3	- 1 0 2	5.4 6.4 4.4	No	Progressive Permeability
T10	1 2 3	0 - 1 0	6.4 7.4 6.4	No	Progressive Permeability

* Third groyne is situated in the cemented portion of the model.

Table 3.9-5: Equilibrium maximum local scour depths near groynes

The passage of ripples (height of about 2 cm to 3 cm on the model, equivalent to 2 m prototype) can create fluctuations (however smaller) in the evolution of the scour holes. Added to the relative uncertainty of the scour measurements, an overall accuracy of 1 m is estimated for these scour depths.

The deepest scour holes appeared with the completely impermeable groynes in tests T2, T3 and T5. In those tests the equilibrium maximum scour depth is more than 20 m.

The results of tests T3 and T4 show clearly that an increase of the permeability of the groyne results in a reduction of the maximum scour depth. The equilibrium maximum scour depth as a function of the permeability of the head of the groyne is shown in Fig. A.14-38. This reduction of the scour depth is almost a linear function of the permeability.

A wider spacing of the groynes results in an increase of the maximum scour depth. Without a falling apron around the row of piles the maximum local scour depth near the head of the groyne is reduced by 2 m to 3 m.

In some tests the upstream groyne protected the second groyne for a full flow attack and therefore the maximum scour depth near the second groyne can be something less than the maximum scour depth near the first groyne.

The reduction of the slope of the head of an impermeable groyne results in a modest reduction of the maximum scour depth, see graph in Fig. A.14-38 in which the results of tests T2, T3 and T5 are used.

A description of the test results in various tests is given hereafter:

(1) In tests T4 and T6 the groynes were the same (except the third groyne which has been replaced by a permeable groyne like the others), but only the spacing between the groynes was increased from 300 m in T4 to 450 m in T6. The influence of this modification can be measured on the second groyne which is less protected, 450 m downstream of the upstream groyne and in which scour depth has increased by 60 % (18.4 m instead of 11.4 m). Its scour depth was 450 m, nearly same as the first groyne. This shows that with a spacing of 450 m the local scour holes of the groynes were independent and the downstream groyne was no more protected by the upstream one.

(2) Between tests T6 and T7 the distance of 450 m had been kept but the length of the groyne had been increased by 40 m. The depth of scour hole near the first groyne in Test T7 was about the same as the depth of scour hole in Test T6.

(3) For the upstream groyne in Test T8 the maximum scour depth is even less than in Test T4 in which all the impermeable part opening was 70 %. This can be explained by:
- in T4 the groynes had a prefixed falling apron which was not built in Test T8;
- a slight modification of the angle between the groyne and the bank, and
- the permeability near the head of the groyne is dicisive for the depth of the maximum scour depth.

The falling apron as shown on Fig. 3.10-1 was represented in its expected final position with a 1:2 slope under the initial bed level. The local scour near the groyne head is increased by the presence of the fixed falling apron. This increase can be considered as a partial compensation for the increased blockage by the falling apron.

In Test T4 scouring between the piles was prevented with the prefixed falling apron. As a consequence scouring developed exclusively near the head of the groyne. In Test T8 the scouring occured over the whole length of the groyne with scour depths between 1.5 m and 2 m. Therefore the increase of flow section was well distributed laterally and the observed scour depth beyond the groyne head was less.

In Test T9, the first 60 m of the groyne from the embankment were impermeable and the following 60 m of the groyne was made permeable. The permeability was very progressive with four different steps from 50 to 80 % near the head of the groyne. The maximum scour depths were slightly less than the maximum scour depths in Test T8. This test shows that an impermeable groyne does not generate big local scour holes provided a permeable extension is added to the head of the groyne.

Test T10 has been studied to observe the influence of an increase of the length of the impermeable part of the groyne, the length and opening of the permeable part remaining the same. The head of the impermeable part coincided with the location of the bankline at the time of construction. A slight increase of the maximum scour depth with 1 m to 2 m had occurred near the piles of the groynes (maximum being located between 15 m and 35 m from the groyne head towards the right bank).

Some erosion of the flood plain was observed near the head of the impermeable part of the groyne. This erosion diminished almost completely at 20 m downstream of the groyne centre line. The efficiency of a series of groynes increases starting from the upstream to downstream.

3.10 CONCLUSIONS

The detail analysis of the results and the subsequent discussions of the physical model test are the basis for the conclusions given here.

In all the tests a moderate attack on the bank is simulated and a return period of 2 to 5 years is expected for the simulated water levels and the discharges. These conditions are expected to be observed during the monitoring period after completion of the construction of the test structures.

An optimized lay-out of the groynes is a combination of an impermeable part on the flood plain and a permeable part in the channel. This impermeable part of the groyne protects the bank by reducing the flow velocities along the bank. The permeable part has to have a progressively increasing permeability towards the head of the groyne and this part prevents the strong vortices and eddies which are observed near impermeable groynes and which induce deep local scour holes downstream of the groyne head.

Length

The length of the impermeable part of the groyne depends on the spacing of the groynes and on the place where the bank line should be stabilized to guarantee sufficient safety width of the flood plain in front of the embankment. The impermeable part had a length of 60 m to 80 m in the model tests. For Kamarjani test structure the impermeable part should be extended by about 20 m beyond this stabilized bank line and the permeable part of the groyne should have a length of about 60 m.

Spacing

The value of the ratio between the spacing of the groynes and the effective length of the groynes is recommended between 3.7 and 4. The value of the ratio between this spacing and the total length of the groynes (from the embankment to the groyne head) is recommended between 2 and 2.5.

Single or double row of piles

A single row of piles has almost the same effectiveness regarding the flow field and the scour depths as a double row of piles. However, a double row of piles may be required for the stability of the structure.

Bed protection

The initial bed around the piles of the permeable part of the groyne erodes atleast 5 to 6 m and this bed erosion requires longer and stronger piles than in case this local scour is prevented by a bed protection. This bed protection can be a falling apron. The length and the width of this falling apron is determined by the local scour holes. In the model tests a final slope of a falling apron was assumed at 1:2. The layout of a thin falling apron is sketched in Fig. 3.10-1.

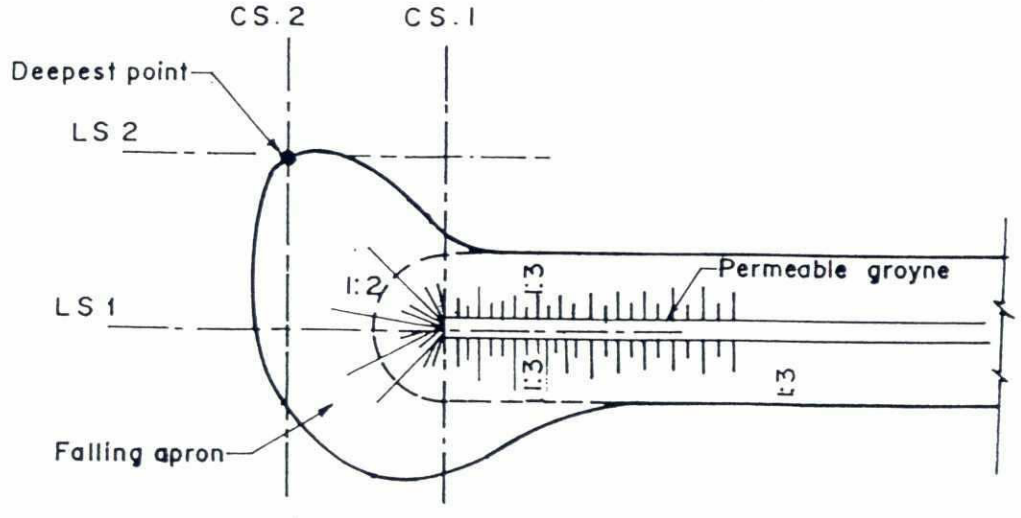


Fig. 3.10-1: Lay-out of a falling apron around a permeable groyne

Maximum flow velocity along the bank

With the optimized layout of the groynes and the recommended spacing of the groynes, the flow velocities along the bank between the groynes are reduced between 0.3 m/s to 0.5 m/s. These depth averaged flow velocities are just below the critical flow velocity for bank erosion and therefore a stabilized bank without erosion is expected.

Maximum flow velocity for the bed protection or falling apron

Upstream of the first groyne of a series of groynes the maximum flow velocities were determined for the design of the bed protection or falling apron, see Table 3.10-1.

Type of Groyne	0 to 20 m Infront of the Head of Groyne	0 to 20 m from Head of Groyne Towards the Bank	20 m to 60 m from Head of Groyne Towards the Bank
	(m/s)	(m/s)	(m/s)
Impermeable groyne	2.3	1.0	0.8
Permeable groyne	2.3	2.3	2.1

Table 3.10-1: The maximum flow velocity upstream of the first groyne

The upstream flow velocities in this table were measured at 19 m and 86 m upstream of the first groyne. If a permeable groyne is considered the upstream flow velocities are much higher than the flow velocities upstream of an impermeable groyne. These flow velocities increase if the permeability of the groyne increases. The maximum flow velocities for a groyne with a gradually increasing permeability towards the head (tests T9 and T10) are presented in Table 3.10-1.

Scour depths

For an impermeable groyne with a slope 1:3 of the head, the maximum local scour depths was 23 m below the initial bed level. For steeper slopes this depth increased up to 35 m for a vertical wall. For more gentle slopes of the head of the groyne a slight reduction in the maximum scour depth can be expected. In addition near the head of the groyne a few metres constriction scour should be expected.

Permeable groynes

The design scour depth near a permeable groyne is located downstream of the head of the groyne. Around each pile of a permeable groyne also a small local scour hole develops with a maximum scour depth of 2 to 3 times the pile diameter. This scour depth is less if the water depth around the pile is less than about 7 times the pile diameter. Usually the water depth is more than 7 times the pile diameter. This small scour hole around each pile can be superimposed on the local scour hole near the head of the groyne.

The local scour hole near the head of the groyne is a function of the permeability near the head. This permeability is expressed in percentage blocked by the piles of a cross-section through the axis of the groyne. A tentative linear relationship has been drawn in a graph with the results of the model tests, see Fig. A.14-38. The maximum scour depth is also dependant on the spacing between the groynes: the a spacing of more than recommended values as given in ratio between spacing and length of groyne results in a deeper scour hole. In some

tests a fixed falling apron was built in and this apron prevented scouring between the piles by which the effective blockage of the cross-section through the axis of the groyne was reduced. In some other tests no fixed falling apron was built and a relatively less deep local scour hole was measured. If the effective blockage is based on the area including the scouring in the axis of the groyne, all test results confirm the tentative relationship for the tests with a falling apron.

Return Period	Local Scour Depths with Falling Apron	Local Scour Depths without Falling Apron
(years)	(m)	(m)
2	8 - 11	4 - 8

Table 3.10-2: Maximum local scour depths for permeable groynes with a blockage of 20 % to 30 % near the head of the groyne and with and without a falling apron

An increase in the water depth level results in a small increase of the scour depth. On one side the scour depths without a falling apron are smaller than the scour depths with a falling apron, but on the other side the length and the strength of the piles can be reduced if a falling apron is applied. Therefore the design scour depths for both situations are given.

4 BAHADURABAD MODEL

4.1 INTRODUCTION

Along the left bank of the Jamuna river the test area south of Bahadurabad is situated at an approximate latitude of 25°09', see the map in Fig. A.14-39 which is based on the Landsat images of March 1992.

As part of the morphological study an assessment was made of possible future developments of the bank line at the Bahadurabad test area based on the 1992 planform and on the observed changes in the channel pattern over the period 1973-1992, see Fig. A.14-39 with the predicted future bank lines for the period 1992-1995. As far as the left bank is concerned, the morphological study has concluded that the bank erosion near Bahadurabad will continue atleast until 1995. Upstream of Bahadurabad a short-cut can develop between the main channels with a 75 % probability in 1995. As a consequence of such a short-cut the rate of bank erosion south of Bahadurabad will reduce gradually after 1995.

The revetment is planned to be implemented after the flood season of 1994. Accordingly the tests in a physical model have been carried out with the consistent banklines after the monsoon of 1994 and 1995. The results of these tests can probably also be used to predict the local scour holes and the maximum flow velocities for the following years, up to 1996, because the embayment upstream of the revetment will probably stabilize after 1995 and the flow pattern around the revetment will be covered by one of the extreme flow patterns studied in this model.

The approximate layout of the revetment are indicated in Fig. A.14-40. Information on different aspects of the physical model as the bed geometry, the boundary conditions, the main data of the model and the model construction is given in detail in sections 4.2 to 4.6. The test programme and the measurements during a test are described in sections 4.7 and 4.8. The results and the analysis of these results are summarized in Section 4.9. Finally the conclusions of this model investigation are given in Section 4.10.

4.2 THE BATHYMETRY OF THE MODEL AREA

The bank of the Jamuna river in the test area south of Bahadurabad has been surveyed over a stretch of about ten kilometers in March 1992. In this survey the distance between the cross-sections was about 200 m. These cross-sections surveys covered a total width of about 3 km, with about 1.5 km on the landside and 1.5 km on the waterside. For the land area, survey have been carried out at an interval of 50 m. For the water area the bathymetric survey has been performed from a boat and the depth was recorded continuously. The results of the survey are presented in a layout plan at a scale 1:5,000 and in cross-sections at a distorted scale: 1:2,000 horizontal and 1:100 vertical. In a reduction of this general layout plan contour lines corresponding to 7 m, 10 m and 14 m +PWD have been drawn, see Fig. A.14-40. For comparison, the 1 in 2 years flood level is 19.78 m +PWD. The bathymetry shows a complicated geometry with three deep channels with scour holes. The most upstream scour hole (cross-section 7) and the deepest one with a maximum scour depth up to -3.7 m +PWD are close to the left bank. These scour holes are probably formed by a combination of a confluence of two secondary channels and by the development of a typical bend profile. A second scour hole in cross-section 20 is the result of a confluence of a secondary channel along the char and the channel along the left bank. This scour hole with a maximum scour depth up to 1.83 m +PWD is less deep than the upstream scour hole. Downstream of this second scour hole a bend scour profile starts to develop again along the left bank. This bathymetry has been measured during the low discharge season and therefore it is possible that some secondary channels were formed by so-called retarded scour. During flood conditions these secondary channels can shift rather quickly and the normal bend profile is expected to be the dominant element in the bed bathymetry. Therefore the measured profiles were averaged to determine an average bend profile with extreme alignments of these secondary approach channels to the revetment, which has been moulded in the physical model.

Some representative cross-sections 12, 18, 24, 30, 36 and 42 are shown in Fig. A.14-41. The location of these cross-sections is indicated in Fig. A.14-40.

The construction of the revetment is planned to be completed after the 1994 flood. At that time the location of the bankline, as well as the river bed geometry itself will be changed. During a period of a few months just before the start of the construction of the physical models the bankline had already shifted by about 100 m (more or less) as predicted by the morphological study. Therefore the predicted future bank lines have been built in the physical model and the average bend profile with an extreme alignment of the approach channels has been shifted to that predicted bank line.

These extreme alignments were selected for the expected maximum scour depths near the revetments. Three different alignments A, B and C with small differences in the cross-section of the approach channel were tested, see Fig. A.14-42. The cross-section of the approach channels was determined from the surveyed cross-sections in the prototype, see Fig. A.14-43 for alignment type A, Fig. A.14-44 for alignment type B and Fig. A.14-45 for alignment type C.

Alignment type A represented an outflanking channel with some embayment upstream of the revetment. The thalweg of that channel has a level of 8.0 m +PWD near the revetment. The flow was expected to be diverted by the revetment and considerable scour depths were expected.

In alignment type B the thalweg of the approach channel was shifted to the middle of the channel and the extrapolation of this thalweg crossed the revetment just at the upstream termination.

In alignment type C the thalweg made a maximum angle with the revetment and the thalweg was directed to a middle section of the revetment. A shallow area developed between the approach channel and the bank.

4.3 SCALING

4.3.1 Introduction

In the physical models for Kamarjani and Bahadurabad the flow field and the local scour around bank protection structures had to be reproduced at scale. The principles of similitude of local scour holes in the physical models are summarized in Section 4.3.2. Next the scale condition for the reproduction of the flow field around structures is described in Section 4.3.3. From these conditions the scales of the main parameters of the non-distorted models were determined (Section 4.3.4).

4.3.2 Similitude of Local Scour

In a physical model the correct scour hole depths can be simulated as in the prototype if certain scale laws and scale conditions were fulfilled. In a physical model not only the water depth, the model discharge etc. should be scaled according the basic scale laws and scale conditions, but also the bed material in case of a local scour model or a movable bed model.

In the model, according to the scale and the depth of the channel to be reproduced the critical mean velocity was between 0.1 and 0.3 m/s and these flow velocities were slightly less than the critical flow velocity in the prototype. A scale condition is that in the model the mean flow velocity should be greater than this critical value, atleast twice. If this condition is fulfilled, then the scour hole characteristics are not influenced by the size of the bed material but, like on the prototype, only by the flow pattern and the geometry of the structure and cross-section.

4.3.3 Similitude of the Flow Field

In a physical model the water level gradient around structures can be modelled if the Froude condition is fulfilled. A scale effect in this water level gradient around a structure also causes a deviation in the flow pattern around the structure. The flow separation near the upstream termination and the size of the eddy will slightly change if the Froude condition is not fulfilled. In the physical model with a revetment these possible deviations are of secondary importance for the overall flow field because the flow field is mainly determined by the model boundaries and the model hydraulic roughness.

4.3.4 Scales

The geometric length scale for the undistorted model has been chosen carefully at 60 in order to find an optimization between all the limitations of the test facility (size of the compartments available in the outdoor model area, discharge available), hydraulic conditions and large enough practical conditions (size of groynes, depth, etc.) to permit precise measurements.

The general layout and the boundaries of the model are presented in Fig. A.14-46. The length of the modelled area is about 1,750 m which is sufficient to simulate the scouring near the upstream half of the revetment in the model. The total length of the revetment is about 1,000 m. The inflow upstream of the upstream termination has a length of about 1,250 m. The width of the modelled area is about 510 m in the section with the revetment.

The main scale factors for a reproduction of the flow field are determined by this length scale and the Froude condition, see Table 4.3-1. The main scale factors for a reproduction of the local scour holes in the model are determined by this length scale and the condition that the

mean flow velocity is about twice the critical flow velocity for the sediment. Main scale factors are also given in Table 4.3-1. The model values in that table are based on cross-section 9.

Parameter	Unit	Prototype	Froude Similitude		Scour Similitude	
			Scale Factor	Model	Scale Factor	Model
Length	m	1750	60	29	60	29.2
Width	m	550	60	9.17	60	9.17
Mean water depth	m	9.41	60	0.157	60	0.157
Cross-sectional area	m^2	5,180	3600	1.44	3600	1.44
flow velocity	m/s	1.66	7.75	0.21	4.15	0.4
Discharge	m^3/s	8,618	27900	0.300	14900	0.575
Water Level	m +PWD	19.78	-	-	-	-
Sediment diameter	mm	0.2	1.2	0.18	1.2	0.18

Table 4.3-1: Main scale factors

For each test, in order to measure the flow velocities after development of the scour holes, the model has been operated first with a high discharge to reproduce the local scour holes. This first part of the test lasted 16 hours during which the bed level was regularly measured (once or twice per hour). Flow velocities and flow lines were also measured in order to be compared with the flow velocity field corresponding to the Froude condition (low discharge). At the end of this part of the test the model was emptied for additional observations (shape of the scour holes, bed forms, contourlines, etc.). In a second stage the model was operated with the low discharge corresponding to the Froude condition. In this part of the test the general velocity field was measured again as well as the flow lines. More detailed measurements of the velocity field were made near the revetment. For both of the discharges water levels were measured in order to assess the roughness of the model bed. In the first six tests the low discharges flowed on the bed moulded by the high discharge. As a result the roughness of the model bed was increased because of the high ripples (about 3 cm). For the last tests the bed was superficially smoothed between the two discharges, so that the height of the ripples for the low discharge was reduced to about 1 cm and the scale effect in the model roughness was reduced.

In the main scale factors a small differentiation can be made for tests with different alignments of the approach channel. For the alignments A, B and C these data are given in Table 4.3-2, 4.3-3, 4.3-4 and 4.3-5. The changes are due to the geometric changes in the tests with different channel alignments.

Main data for all the tests upstream of the revetment are presented in Table 4.3-2 through 4.3-5.

			Froude Similitude		Scour Similitude	
Parameter	Unit	Prototype	Scale Factor	Model	Scale Factor	Model
Length	m	1700	60	28.3	60	28.3
Width	m	550	60	9.2	60	9.2
Mean depth	m	9.41	60	0.157	60	0.157
Cross-sectional area	m^2	5180	3600	1.44	3600	1.44
Mean velocity	m/s	1.66	7.75	0.21	4.15	0.40
Discharge	m^3/s	8618	27885	0.309	14960	0.576
Water Level	m +PWD	19.78	-	-	-	-

Table 4.3-2: Main data for tests T1 and T2 in cross-section 6, upstream of the revetment

			Froude Similitude		Scour Similitude	
Parameter	Unit	Prototype	Scale Factor	Model	Scale Factor	Model
Length	m	1700	60	28.3	60	28.3
Width	m	483	60	8.05	60	8.05
Mean depth	m	9.72	60	0.162	60	0.162
Cross-sectional area	m^2	4695	3600	1.30	3600	1.30
Mean velocity	m/s	1.66	7.75	0.21	4.15	0.40
Discharge	m^3/s	7790	27885	0.280	14960	0.521
Water Level	m +PWD	19.78	-	-	-	-

Table 4.3-3: Main data for tests T3 and T4 in cross-section 6, upstream of the revetment

			Froude Similitude		Scour Similitude	
Parameter	Unit	Prototype	Scale Factor	Model	Scale Factor	Model
Length	m	1700	60	28.3	60	28.3
Width	m	500	60	8.33	60	8.33
Mean depth	m	9.01	60	0.150	60	0.150
Cross-sectional area	m^2	4506	3600	1.25	3600	1.25
Mean velocity	m/s	1.66	7.75	0.21	4.15	0.40
Discharge	m^3/s	7480	27885	0.268	14960	0.500
Water Level	m+PWD	19.78	-	-	-	-

Table 4.3-4: Main data for tests T5, T6 and T7 upstream of the revetment

			Froude Similitude		Scour Similitude	
Parameter	Unit	Prototype	Scale Factor	Model	Scale Factor	Model
Length	m	1700	60	28.3	60	28.3
Width	m	610	60	10.2	60	10.2
Mean depth	m	7.55	60	0.126	60	0.126
Cross-sectional area	m^2	4605	3600	1.28	3600	1.28
Mean velocity	m/s	1.66	7.75	0.21	4.15	0.40
Discharge	m^3/s	7645	27885	0.274	14960	0.511
Water Level	m+PWD	19.78	-	-	-	-

Table 4.3-5: Main data for tests T8, T9 and T10 upstream of the revetment

4.3.5 Estimation of the Time Scale of Scour Development

The estimation of the time scale of the scour development follows the same approach as described for the Kamarjani model. In this approach the following values are assumed:

- the hydraulic roughness of the movable bed of the model, C = 37 $m^{0.5}/s$;
- the water level gradient i = 0.00135, and
- average water depth h = 9 m.

With these values $n_G = 8.5*10^{-4}$ and $n_s = 183$ are calculated. This means that 1 hour in the model corresponds to about 8 days in the prototype. During a test the scour measurements took 16 hours which corresponds to about 4 months in the prototype. This time scale is derived assuming bed load transport. But in the Jamuna river suspended sediment transport is dominant above the bed loead transport, and therefore the real time scale will probably be shorter than estimated.

4.4 BOUNDARY CONDITIONS

Three types of boundary conditions are needed in this type of physical models: an upstream boundary condition at the inflow of the model, a downstream boundary condition at the outflow of the model and a lateral boundary condition because in the model the whole width of an outflanking channel is not modelled.

The upstream boundary condition is the discharge and the discharge distribution along the upstream boundary of the model. The characteristic discharges in a complete cross-section of the Jamuna near Bahadurabad are determined in the hydrologic study. Hydrologic data is given in Table 4.4-1 (see also ANNEX 5).

Return Period	Discharge (m^3/s)	Water Level (m + PWD)
2 years	64,300	19.78
10 years	83,200	20.20
100 years	106,900	20.72

Table 4.4-1: Hydrologic data for boundary conditions

In the Jamuna river the critical depth averaged flow velocity for the initiation of sediment transport is between 0.2 m/s and 0.4 m/s. In the channels of the Jamuna river the depth averaged flow velocities are often more than twice as much. For example, the mean flow velocity in a channel cross-section is about 2 m/s for the 1 in 2 years flood. That means that the conditions for a full development of the scour holes near obstacles are probably reached quickly. This supports the selection of the 1 in 2 years flood for the tests in the physical model.

The model does not represent the total width of the outflanking channel, but only a part of about 550 m from the left bank. In a channel with this width only a portion of the total discharge of 64,300 m^3/s flows. This portion is estimated at 7500 m^3/s to at 8620 m^3/s, see Table 4.3-2 to 4.3-5.

The lateral boundary condition is the location of the right boundary of the model. This boundary is not the right bank of the outflanking channel, but it is a flow line of the prototype in order to represent a portion where the discharge is constant. The width of the model is sufficient to prevent any influence of this flow line on the flow field near the revetment. This boundary flow line was determined by a 2-dimensional mathematical model simulation. The results of that study were not available in time for the construction of the model and therefore this flow line boundary has been estimated first and compared with the results of the mathematical model afterwards.

The downstream boundary condition is the water level to be adjusted in the model by tailgates. The water level corresponding to the 1 in 2 year flood represented on the model is 19.78 m +PWD, see Table 4.4-1.

4.5 MODEL CONSTRUCTION

The hydraulic circuit of the outdoor model area is a gravitational type. The available head difference between the supply canal and the collect canal is about 1.3 m and this means that the elevation of the model has to be fixed carefully, which has to take into account the head losses, such as (i) losses in the pipes between the supply canal and the weir, (ii) losses through all the devices for tranquilization of the flow and (iii) losses by the tailgates. The

model elevation should also permit the drainage of the lowest points in the movable bed of the physical model. The selected relative elevation of the different devices is indicated in a longitudinal section of the model, see Fig. A.14-47.

The main characteristics of the sand for the movable bed in the physical model are D_{90} = 0.27 mm, D_{50} = 0.18 mm and about 5 % of silt; these values are the same as the characteristic values of the sand in the Kamarjani model.

In the movable sand bed of the physical model the flow creates ripples which make bed too rough compared with the roughness which is determined according to the scale laws and the bed roughness in the field. The movable bed portion of the model has been strictly limited to the location of the test structures, because of this scale effect by these ripples. This minimization of the length of the movable portion also limits the increase of the slope of the water surface which is induced by these ripples.

After a test is completed the fixed bed part of the model is drained by lowering the tailgates. The movable bed portion of the model was isolated by impermeable walls from the surrounding model area and an additional drainage to a small reservoir was made to control the water level in this movable bed portion of the model. By these means it was possible to keep a constant water level after a test and to materialize the isolines with threads to characterize a local scour hole.

4.6 MEASUREMENT DEVICES

Introduction

In a model test the following type of measurements are made: the discharge, the water levels at different places in the model, the scour depths and the flow velocities. The devices which were used in Bahadurabad model are the same as the devices used in the Kamarjani model and these devices has already been described in Section 3.6. However, some details are different in discharge measurement in Bahadurabad model.

Discharge

The discharge is determined from the measured water level upstream of 1 rectangular weir with a width = 1.80 m and the height = 0.665 m. The discharge as function of the water level upstream of the weir is given by the formula (4.6-1) :

$$Q = (0.403 + 0.053 * \frac{h_w}{p}) \sqrt{2g} * b [(h_w + \frac{u_w^2}{2g})^{1.5} - (\frac{u_w^2}{2g})^{1.5}] \qquad (4.6\text{-}1)$$

in which

b	=	width of the weir	(m)
g	=	acceleration by gravity	(m/s^2)
h_w	=	vertical distance between the crest of the weir and the upstream water level	(m)

p	=	height of the crest of the weir above the bottom	(m)
Q	=	discharge passing the weir	(m^3/s)
u_w	=	the average flow velocity in the cross-section in which h_w has been measured	(m/s)

Because of changes in the pumps power during a test, the level upstream the weir was not constant. The accuracy of the discharge measurement is estimated about 5 %.

4.7 TEST PROGRAMME

A test programme of 10 tests with a revetment have been carried out in this physical model investigation. Around the upstream part of the revetment in the movable bed the scour depths and the flow velocities were measured. The main characteristics of this test programme is presented in Table 4.7-1. Test T1 is not a complete test and was used to get experience in the model operation. A plan of the different lay-outs of the upstream termination is presented in Fig. A.14-48. A typical cross-section of the revetment is given in Fig. A.14-49.

Test No.	Channel Alignment	Slope of Revetment	Radius of Upstream Termination (m)
T1	A	1 : 3	50
T2	A	1 : 3	50
T3	A	1 : 3	450
T4	A	1 : 4	450
T5	B	1 : 4	450
T6	B	vertical	450
T7	B	1 : 4	no
T8	C	1 : 3	450
T9	C	1 : 3	50
T10	C	1 : 3	50 + pile row

A, B and C are different alignments of the approach channel as indicated in Fig. A.14-42.

Table 4.7-1: Test programme for a revetment

4.8 PRESENTATION OF RESULTS

The complete and intermediary results are available at the Project office and in the River Research Institute (Faridpur). The most interesting results are presented for some selected tests (T2, T3, T5, T7 and T10) in graphs, Fig. A.14-50 to A.14-78. The complete results which are presented in graphs and tables, give the following information:

General flow velocity field

In the standard cross-sections 2, 5, 9, 12 and 15 the flow velocities have been measured at an interval of about 50 m and at half the water depth, see for eaxample Fig. A.14-51. These measurements have been made for the Froude discharge and the increased discharge. The scale factors are such for the different discharges that the flow velocities measured in the model correspond to the same flow velocity in the prototype. So the mean velocities as well as the distribution of the velocities should be the same, if there was no scale effect due to the increase of the discharge.

Differences in the mean flow velocity of the Froude discharge and the increased discharge can result from: (i) slight variations of the area in the movable bed, (ii) from variations in the model discharge due to considerable variations of the water level in the supply canal, and (iii) inaccuracy of the flow velocity measurement. In some tests differences between these mean velocities have reached 0.4 m/s (20 % of the average flow velocity). More commonly they are about 0.2 m/s (10 % of the average flow velocity). In order to be able to compare the velocity distribution between the two discharges, it is necessary to take into account these possible differences in the mean flow velocity.

Flow velocity along the revetment

The flow velocities are measured at different distances from the revetment crest: (i) at 30 m from the crest and 4.20 m below the water surface, (ii) at 45 m from the crest and 6 m below the water surface, (iii) at 60 m at half the initial water depth, (iv) at 90 m at half the initial water depth, and (v) at 120 m at half the initial water depth. These flow velocities are measured in all the cross-sections of the revetment, see Fig. A.14-52, A.14-58, A.14-64 and A.14-70. The location of these measuring point are indicated in these graphs.

In these graphs the acceleration of the flow is along the revetment and contribute to the determination of the design flow velocity near the top layer of the revetment.

Flow lines

A few flow lines have been sketched in the plan of the model for low and high discharges, see for example Fig. A.14-51, A.14-57, A.14-63, A.14-69 and A.14-75. Flow lines have been especially studied near the left bank with the revetment so that the flow forms eddies in front of the revetment. The comparison between the flow lines with the two different discharges showed that the flow pattern for the study of scouring was fairly the same, as it should be, to the flow lines measured with the discharge corresponding to Froude condition.

Water level measurements and estimation of the water level gradient

In each test the water level has been measured with four point gauges along the model for the discharge according to the Froude condition and for the increased discharge, see for example Fig. A.14-57 and A.14-46. The measurements of the most upstream point gauge seem to be unreliable, probably because the connecting pipe was blocked. These water levels have been used to define the position of the downstream tailgate and to estimate the water level gradient.

The water level gradient in the movable bed portion of the model followed from the water level difference between point gauge 2 and 4, see Table 4.8-1 with the water level gradient for tests T2 to T10.

Test No.	Water Level Gradient Between Point Gauges 2 and 4	
-	Froude Discharge	Increased Discharge
-	(10^{-4})	(10^{-4})
T2	3.3	12.3
T3	5.1	13.6
T4	4.6	11.8
T5	3.1	11.7
T6	4.3	12.5
T7	5.4	20.0
T8	2.9	11.2
T9	2.4	13.8
T10	-	-
Mean	3.9	13.5

Table 4.8-1: Measured water level gradient in the movable bed portion

The average Chézy coefficient for the movable bed is estimated at 27 $m^{0.5}/s$, if the cross-sectional area = 1.44 m^2 and a hydraulic radius = 0.157 m are assumed. This value of the Chézy coefficient is probably too low.

For the fixed bed portion with a cemented top layer it is assumed that the roughness is the same as for the cemented portion of the Kamarjani model, that means a value of the Chézy coefficient around 38 $m^{0.5}/s$. However, these values are also not accurate.

Scouring

Different aspects of the scouring have been presented in graphs: (i) the maximum local scour depth as a function of time and (ii) cross-sections of the local scour hole and the general bed erosion as a function of time.

Maximum scour depth

A graph with the deepest point levels of the local scour hole in front of the revetment together with the deepest point levels in other cross-sections perpendicular to the revetment as function of time has been used to analyses if an equilibrium has been reached at the end of the test, see for example Fig. A.14-60, A.14-66, A.14-72 and A.14-77. If not, the evolution of the maximum depths was extrapolated in order to estimate the equilibrium maximum scour depth. In most cases this extrapolation added a few metres to the maximum measured scour depth after 16 hours.

Local scour depths

In different cross-sections along the revetment the deepest points were determined, each 4 model hours and are presented in a graph with the elevation of the thalweg of the local scour hole at different times as a function of the distance from the upstream termination of the revetment. The initial and the final bed level at the end of the test are included in these graphs, see for example Fig. A.14-53, A.14-59, A.14-65, A.14-71 and A.14-76.

Cross-sections of the scour hole

The bed levels measured in the cross-sections perpendicular to the revetment are drawn in a graph for the cross-section through the deepest point of the scour hole and for the first upstream and downstream cross-section, see for example Fig. A.14-55, A.14-61, A.14-67, A.14-73 and A.14-78.

In these cross-sections the fixed top layer of the revetment and the prefixed falling apron, if any, built in the model has been drawn so that the junction between the bed and the assumed final position of the falling apron appears clearly. From these graph longitudinal and lateral slopes of the scour holes can be estimated.

Scouring of the movable bed

General bed erosion can have some influence on the local scour depths. To check the general bed erosion in the movable part of the model the bed levels measured in three points which were in the middle of the channel at 210 m from the revetment are presented as a function of the time. The variation of the bed levels is the result of the sediment transport in the model. The supply of sand upstream of the model partially limits it but cannot completely prevent general bed erosion. A too big supply of sand has for effect to create too much sedimentation in the upstream cross-sections of the model without downstream benefits. In the first tests this general bed erosion might have had a small influence on the measured local scour depths, but in the final tests general bed erosion was small and its influence on the local scour depths was negligible.

4.9 ANALYSIS

The following aspects have been analyzed with respect to flow field and local scouring of the river bed:

- shape of the upstream termination,
- slope of the revetment, and
- alignment of the approach channel.

The influence of the slope of the revetment, the shape of the termination and the alignment of the approach channel at the maximum flow velocities and the maximum scour depths are used for the determination of the design criteria. As part of the analysis also an estimation of the width of the bed protection or falling apron is given based on the measured scour depths.

Some representative results which were used in the analysis are given in Fig. A.14-50 to A.14-77. The main results regarding the maximum flow velocity and the maximum scour depth for tests T2 to T10 are summarized in Table 4.9-1.

Test No.	Approach Channel	Slope of Revetment	Initial Bed Level	Maximum Scour Depth		Maximum Flow Velocity at		
						30 m	45 m	60 m
			(m +PWD)	(m +PWD)	(m)	(m/s)	(m/s)	(m/s)
T2	A	1:3	10	-10.0	20	2.1	2.6	3.0
T3	A	1:3	9	-2	11	2.3	2.5	2.7
T4	A	1:4	9	1	8	2.5	2.6	2.7
T5	B	1:4	9.5	2.5	7	1.9	2.1	2.4
T6	B	vertical	9.5	-6	15.5	2.0	-	2.3
T7	B	1:4	9.0	2	7	2.0	2.1	2.4
T8	C	1:3	9.5	5	4.5	2.0	2.0	2.1
T9	C	1:3	9.0	-5.5	14.5	1.5	2.2	2.2
T10	C	1:3	9.0	-4	13	1.4	1.7	1.9

Table 4.9-1: Maximum flow velocities and maximum scour depths

For the top layer of a revetment made with a slope 1 : 3 or a vertical wall and the bed protection or the falling apron as continuation of the top layer, different maximum flow velocities are presented in Table 4.9-2.

Element of the Structure	Location of Measurement	Maximum Flow Velocity (m/s)
Top layer of revetment 1 : 3 (1)	30 m	2.5
Bed protection and falling apron (2)	45 m	2.7
Bed protection and falling apron (3)	60 m	2.7

Table 4.9-2: Maximum flow velocity near the revetment, bed protection and falling apron

The numbers (1), (2) and (3) refer to locations where the flow velocity was measured in the physical model, see cross-section in Fig. A.14-49. These locations were more or less at half the water depth. The flow velocities in Table 4.9-2 are depth averaged flow velocities. Near the water surface some higher flow velocities can be expected.

Shape of upstream termination

The first ideas on a revetment as a test structure with different types of top layers was a slightly curved revetment with both upstream and downstream termination with a small radius of 50 m at the crest of the revetment, see Fig. A.14-48 and Photo 6. The results of Test T2 with such a revetment showed that if the approach channel had eroded a small embayment upstream of the revetment the flow can not follow the sharp radius of the revetment and the flow separated with an eddy in front of the most upstream test top layers. This separation results in variable hydraulic load on the different top layers and a comparison of the behaviour and the small damages become difficult. Therefore it is important to prevent a separation of the flow near the upstream termination of a test revetment. Two solutions were tested: an increase of the radius of the termination to about 450 m and a termination with a radius of 50 m combined with a pile row as a flow guiding screen, see Fig. A.14-48 and photos 7 and 11. The length of this row was about 250 m. With both solutions it was possible to prevent such a separation point and to create a more uniform hydraulic load along the revetment.

Characteristic flow lines and flow velocities measured in Test T3 with the radius of the termination about 450 m are shown in Fig. A.14-57. The flow lines followed along the left bank at the upstream termination of the revetment without flow separation. Along the revetment the flow velocities decreased slightly from 2.25 m/s upstream to 1.75 m/s downstream with a return period about 2 years, see Fig. A.14-57. This decrease can be explained by the development of a boundary layer along the revetment.

From the analysis of Test T10 it is expected that the same effect could have been reached with a much shorter row of piles with a length of 50 m only. The vortex as measured in Test T2 had been reduced and confined on the revetment (the revetment foot is now out of the vortex) but the reduction of the scour depth was not significant. This solution must not

probably be disregarded but additional tests should be done to increase the efficiency of such a screen regarding the flow field and the local scour depths and to minimize its length.

The length of the eddy in Test T2 depended on the curvature of the flow lines up to the reattachment point at the revetment. The relatively too high bed roughness created by the ripples in the movable bed reduced the radius of curvature of the flow lines. This reduction was considered as a scale effect. The correct length of the eddy in Test T2 was computed with the 2-dimensional mathematical model. The design flow velocities and the design scour depths are not influenced by this scale effect.

The measured maximum scour depths along the revetment were concentrated near the head of the revetment. The maximum scour depth can be reduced by 8 to 10 m if the radius of the upstream termination is increased from 50 m to about 450 m. The pile row reduces the maximum scour depth slightly with 1 to 2 m (Test T10 compared with Test T9), see Photo 11.

In the prototype it is expected that the scour hole was expected to have a much elongated shape along the revetment and these maximum scour depths will also be found more downstream along the revetment. Therefore the width and the strength of the bed protection or falling apron should not be reduced going in downstream direction. This has been confirmed with Test T7 with a continuous revetment in which test the same maximum scour depths were measured as near the upstream termination in Test T5.

A cross-section of the scour hole perpendicular to the revetment is presented in Fig. A.14-59 and A.14-73.

Slope of the revetment

The influence of the slope of the revetment can be estimated by comparing the results of Test T3 with a slope 1:3, with Test T4 with a slope 1:4 and other parameters are the same for both tests, see photos 7 and 9. An other comparison is made between Test T5 with a slope 1:4 and Test T6 with a vertical protection (like sheet piling), see Photo 10.

The main results of this comparison are summarized regarding the maximum flow velocities and the maximum scour depths.

Flow velocities: A revetment with a slope 1:4 (i.e. in Test T4) protrudes more into the channel than a revetment with a slope 1:3 (Test T3), if the crest line is kept in the same position. Therefore the cross-sectional area near the upstream termination is smaller with the slope 1:4 than with the slope 1:3. As the discharge is constant the flow velocities are a bit increased with the slope 1:4 than in the tests with the slope 1:3. Then the measured flow velocities near the head are 0.1 m/s to 0.5 m/s, the value is higher with 1:4 slope than with 1:3 slope. More downstream the flow velocities above a 1:4 slope are lower than above a 1:3 slope.

Maximum scour depths: The general tendency regarding maximum scour depth is that the value reduces if the slope becomes more gentle. A tentative relationship between the maximum scour depth and the slope of the revetment is sketched in Fig. A.14-79 and A.14-80. Following are the observations:

- a slope of 1:3 reduces the maximum scour depth near a vertical wall with 6 m to 7 m, and
- a slope of 1:4 reduces the maximum scour depth near a slope of 1:3 with 3 m to 4 m.

This relationship is valid for the maximum depth of the local scour hole. For other points of the local scour hole upstream or downstream of this maximum the influence of the slope is less pronounced.

Approach channel

Three different approach channel alignments A, B and C have been tested in the physical model and the main results of these tests are summarized regarding the maximum flow velocities and the maximum scour depths.

Flow velocities: The most unfavourable channel alignment is alignment A, with the thalweg close to the outflanking upstream bank. Other alignments result in 0.2 m/s to 0.5 m/s lower than maximum flow velocity. This means that the alignments B and C are comparable, with alignment C slightly less favourable than alignment B.

These results can be explained by the changes of two important parameters from one test to another: (i) the angle between the upstream flow direction and the direction of the revetment and (ii) the so-called angle of incidence of the flow and the protrusion of the revetment. This angle is defined in the Fig. 4.9-1 and 4.9-2.

Type Approach Channel	Angle of Incidence with the Revetment
-	(degrees)
A	162
B	147
C	149

Table 4.9-3: Angle of the approach channel with the revetment

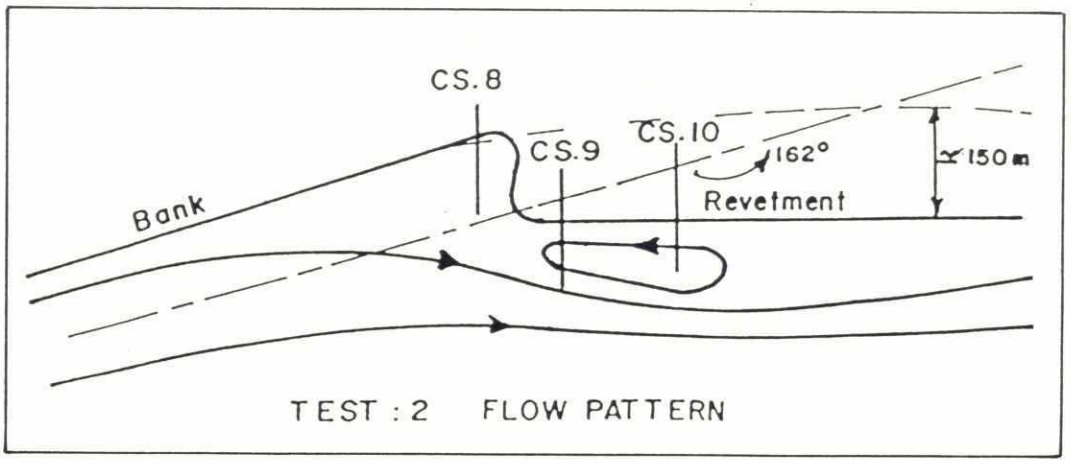


Fig. 4.9-1: Sketch of flow pattern in test T2

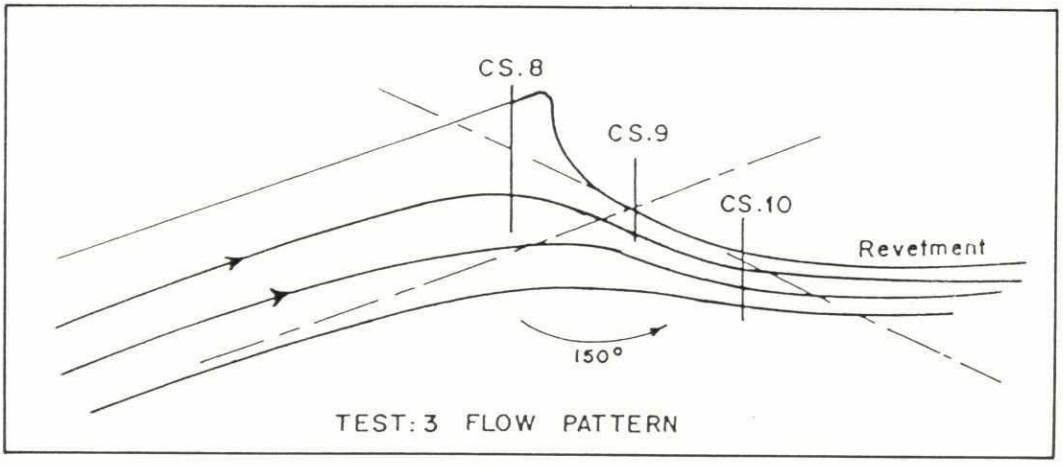


Fig. 4.9-2: Sketch of flow pattern in test T3

Maximum scour depths:

The maximum scour depth has been observed in cross-section 10 for Test T2 and in cross-section 13 A for Test T9, which crosses the center of the eddy. With Test T3 the upstream part of the revetment (about the first 250 m) has been pivoted, which has no effect to increase the angle of incidence of the flow or to remove the separation point, the flow line being in this test parallel to the bank, see Fig. 4.9-1.

In the tests with the approach channel alignment B the layout of the revetment is fairly the same as the layout of the revetment in the test with approach channel alignment A. On the other hand the incidence of the main flow has been reduced in alignment B compared with alignment A and above all the deepest channel has been shifted towards the right bank so that the head of the revetment is no more directly exposed to the main flow. So this is equivalent to a reduction of the protrusion of the revetment.

The maximum scour depth in alignment A is most unfavourable. The scour depth 1.5 m to 2 m more than in alignment B and 5.5 m more than in alignment C, see the tentative relationships sketched in Fig. A.14-80.

4.10 CONCLUSIONS

A prediction of future flow patterns in the channels of the Jamuna river and future bank lines is part of the morphologic study. For the design of a revetment south of Bahadurabad three extreme alignments of the approach channel to the revetment have been tested. The most unfavourable alignment regarding flow velocities and local scour depths close to the revetment is embankment upstream of the revetment.

A short termination with a radius of 50 m can create a flow separation near the upstream termination and this results in a widely varying flow attack on the different test sections of the revetment. This can be prevented with the following measures:

- increasing the radius of the upstream termination to 450 m, or
- to place a pile row near the upstream termination.

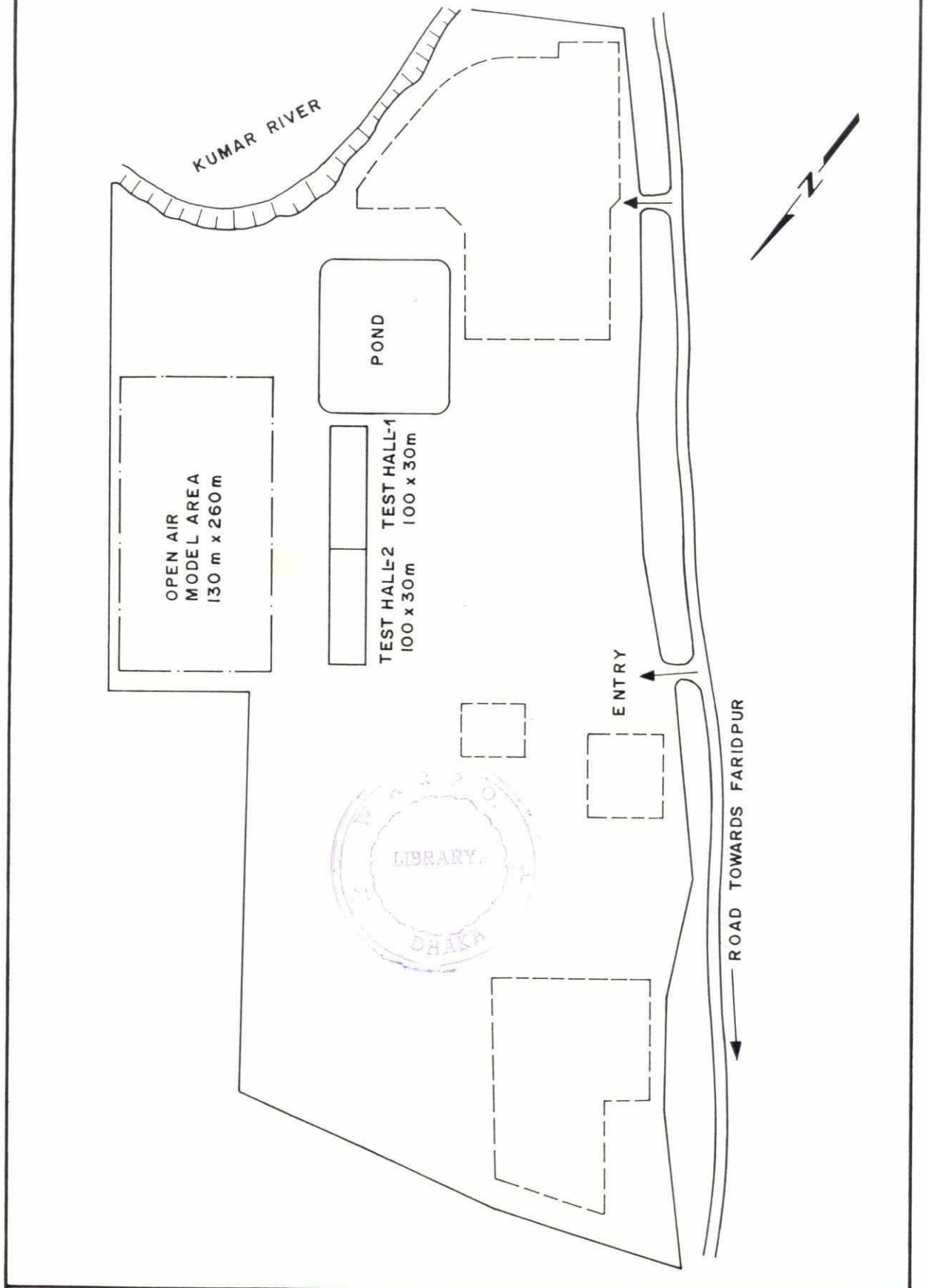
With these two solutions the maximum flow velocity at half the water depth is 2.5 m/s for the top layer, 3 m/s for the falling apron and the maximum scour depth for revetment is:

- with slope 1:3 between 11 m to 13 m, and
- with slope 1:4 between 7 m to 9 m.

These maximum flow velocities and maximum scour depths are expected to be observed with a return period of about 2 years. A general tendency is that the maximum local scour depth near a steep slope of the revetment is deeper than the maximum local scour depth near a gentle slope. This advantage of a gentle slope has to be balanced with the disadvantage of more material for the top layer of the revetment, for example from 1:3 to 1:4 the width of the top layer is increased by about 10 m.

Along the revetment going in downstream direction no reduction of the values should be applied, because these maximum values can be observed at every location along the revetment depending on the approach channel.

The shape of the scour hole determines the width of the falling apron assuming that the falling apron should reach up to the maximum scour depth. A width of 20 to 30 m of the falling apron is sufficient for the considered revetment under a flow attack with a return period of about 2 years.

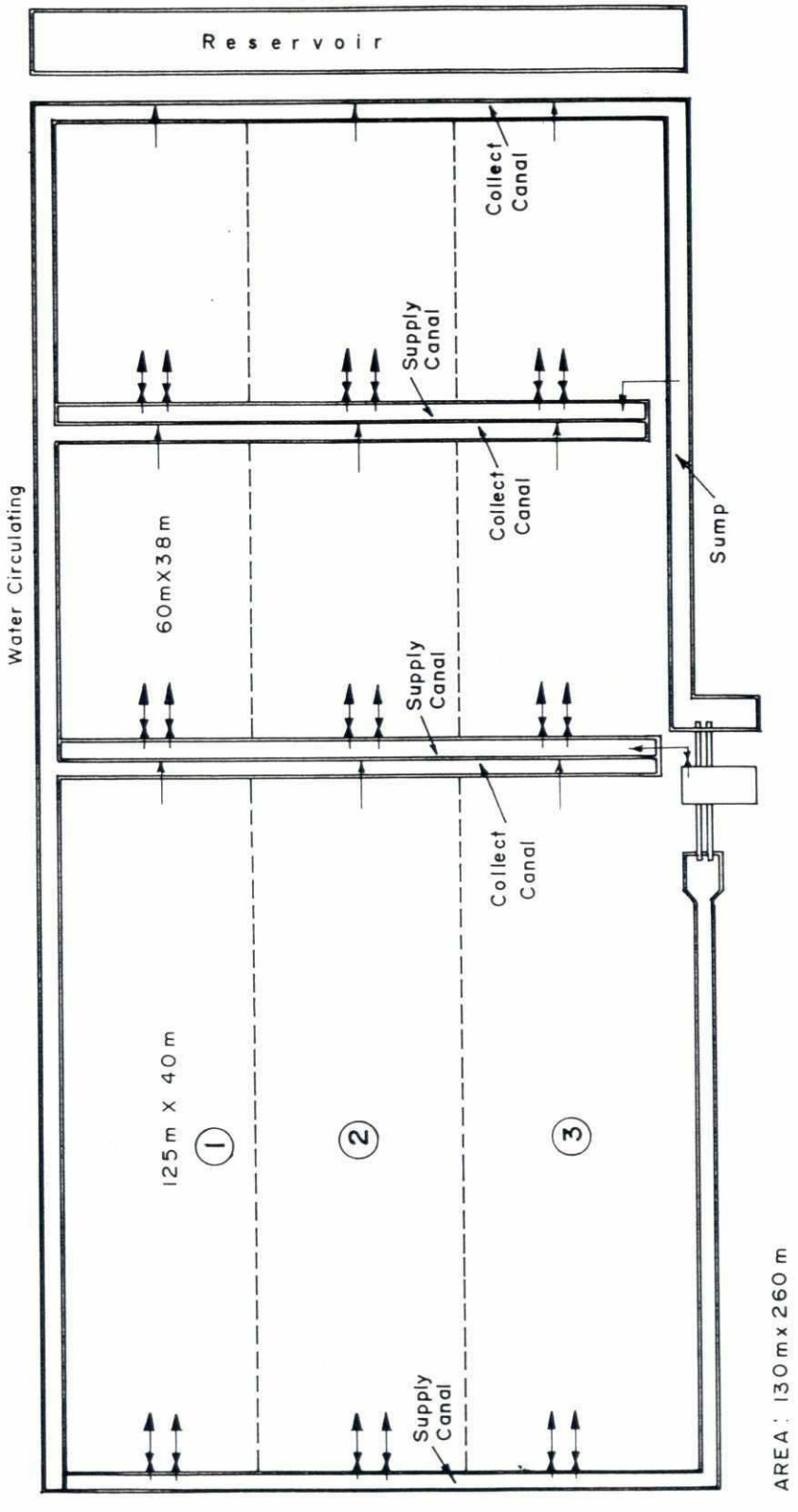


LIBRARY
DHAKA

LOCATION OF OPEN AIR MODEL AREA
R R I, FARIDPUR

FAP – 21/22
BANK PROTECTION AND RIVER TRAINING / (AFPM) PILOT PROJECT

FINAL REPORT | FIG. A.14–1

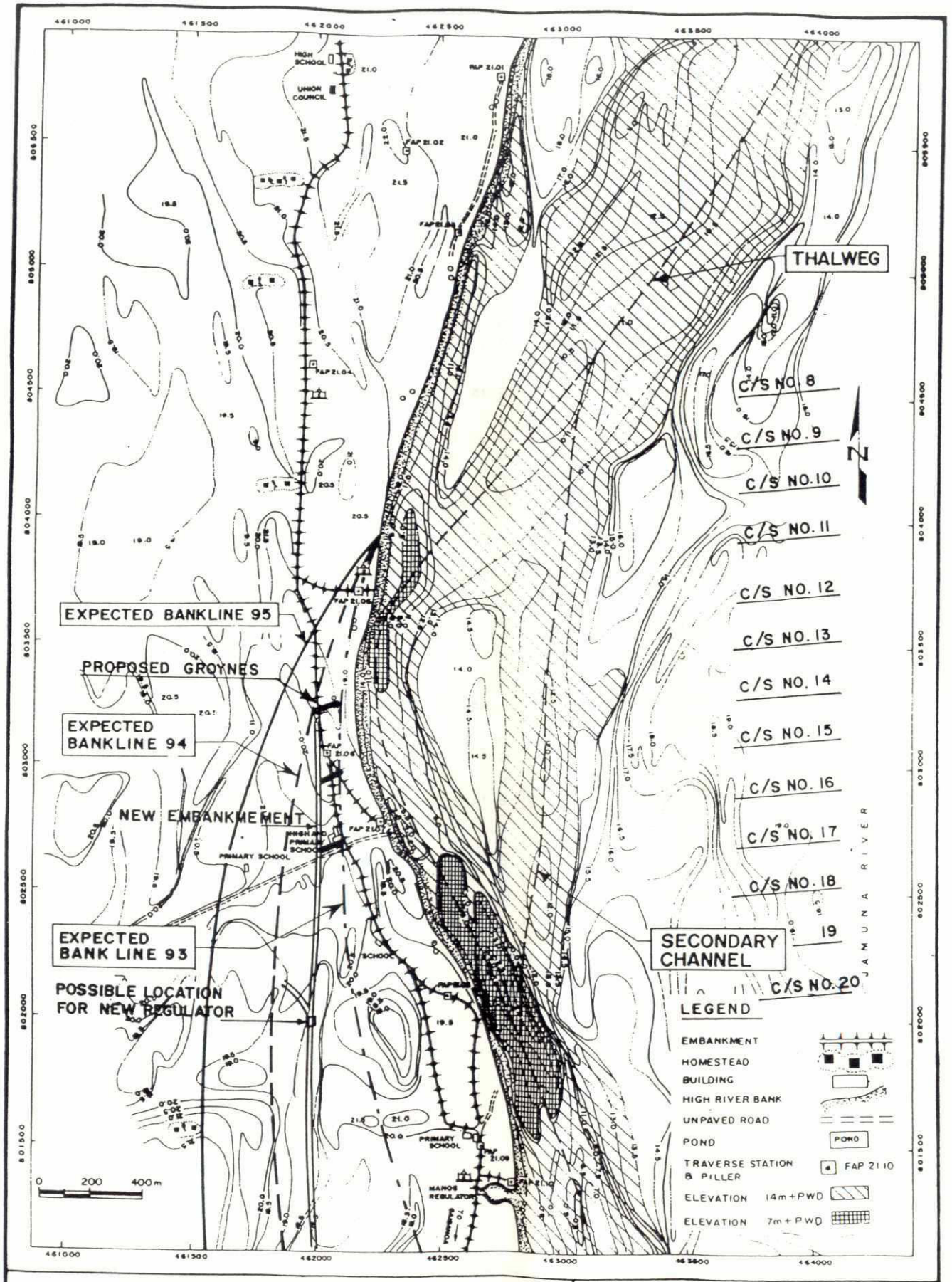


PLAN OF MODEL AREA OF RRI

FAP – 21/22

BANK PROTECTION AND RIVER TRAINING / (AFPM) PILOT PROJECT

FINAL REPORT | FIG. A.14 – 2

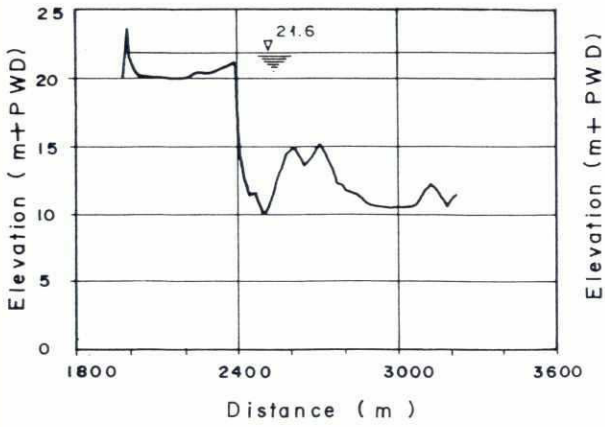


KAMARJANI SITE SURVEY

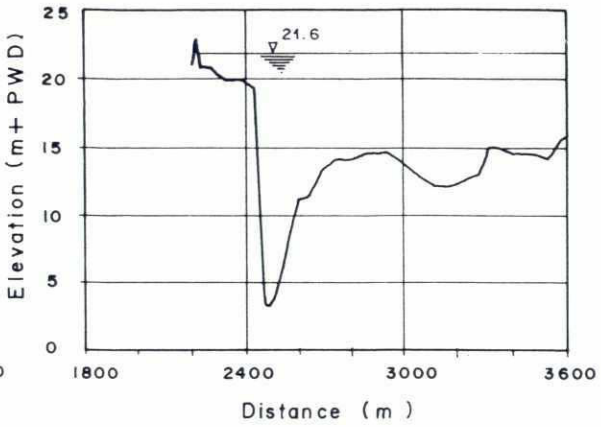
FAP - 21/22

BANK PROTECTION AND RIVER TRAINING / (AFPM) PILOT PROJECT

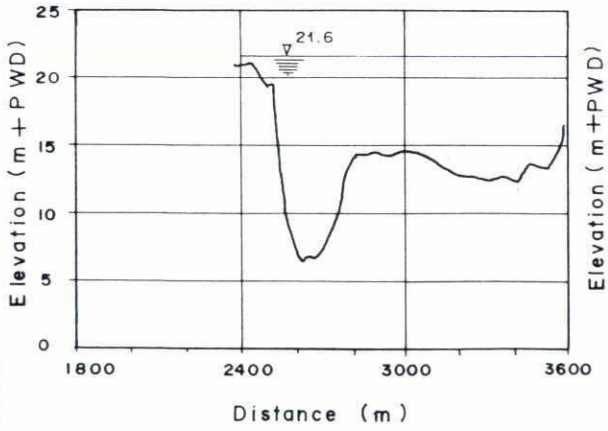
FINAL REPORT | FIG. A.14-3



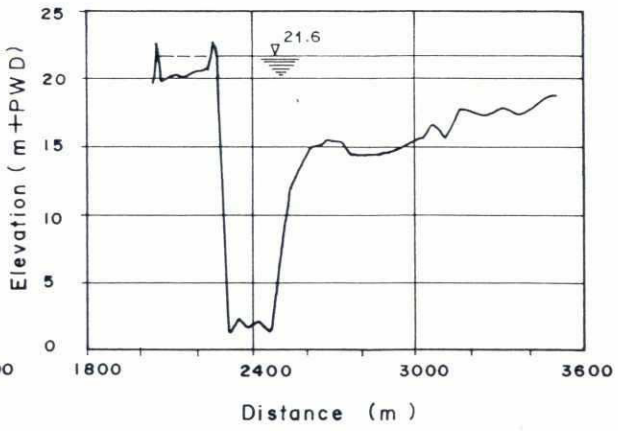
CROSS-SECTION NO. 8



CROSS-SECTION NO. 12



CROSS-SECTION NO. 14



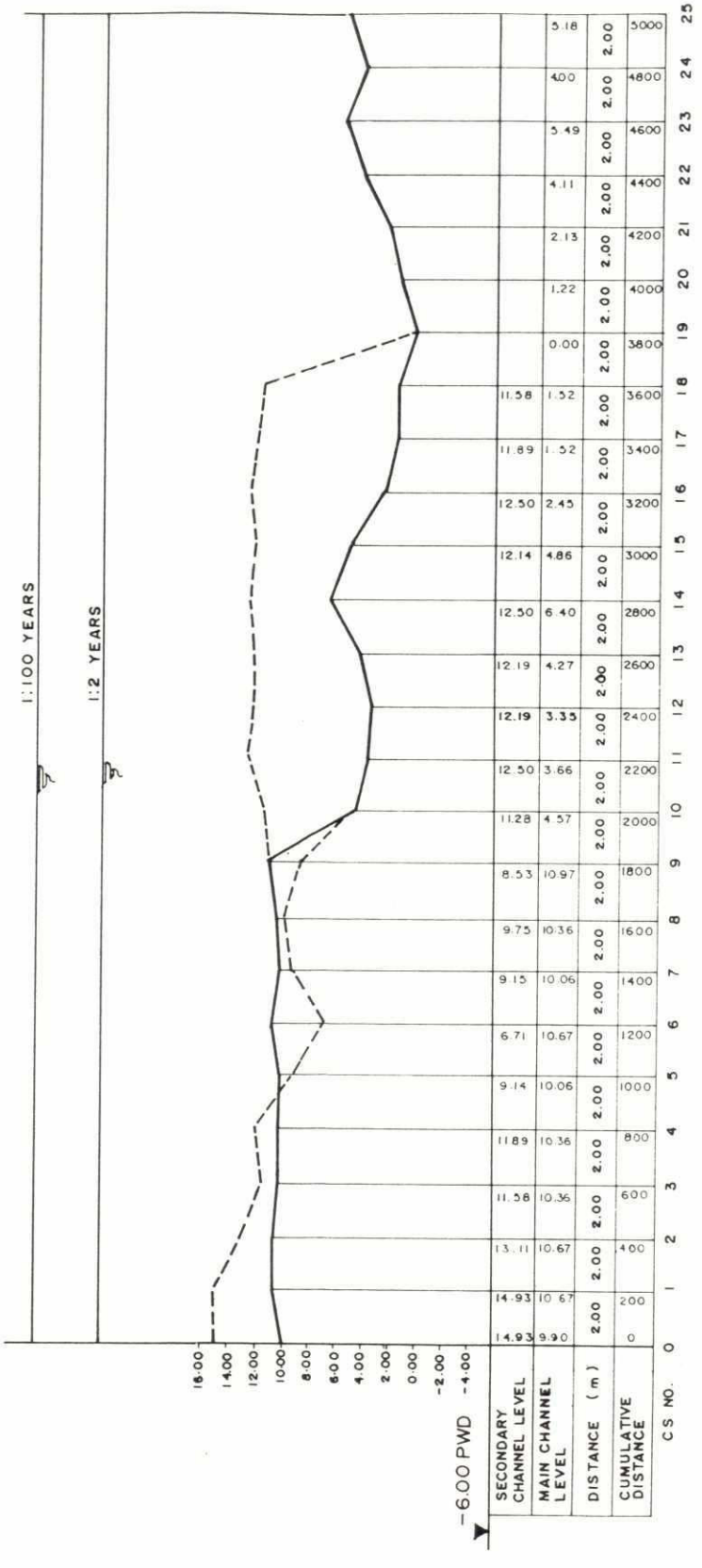
CROSS-SECTION NO. 20

KAMARJANI SITE CROSS-SECTION

FAP – 21/22

BANK PROTECTION AND RIVER TRAINING / (AFPM) PILOT PROJECT

FINAL REPORT | FIG. A.14 - 4



KAMARJANI MODEL

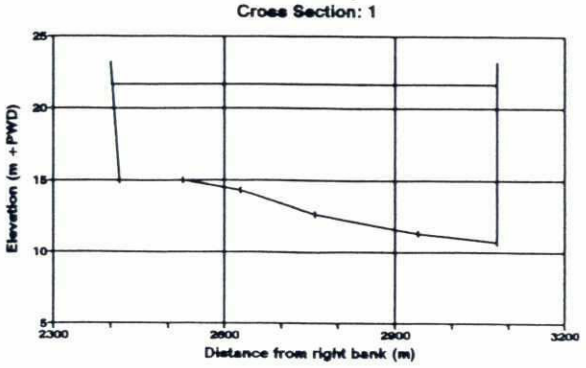
LONGITUDINAL SECTION OF THALWEG

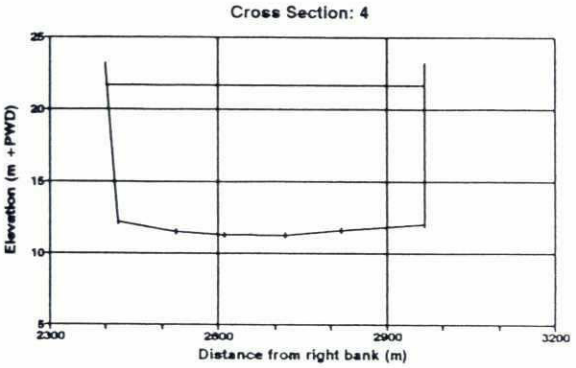
SURVEY OF MARCH 1992

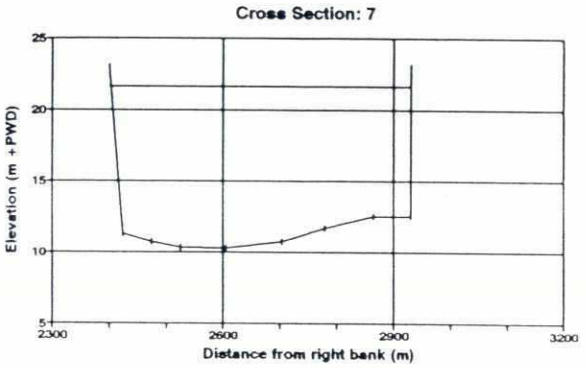
FAP – 21/22

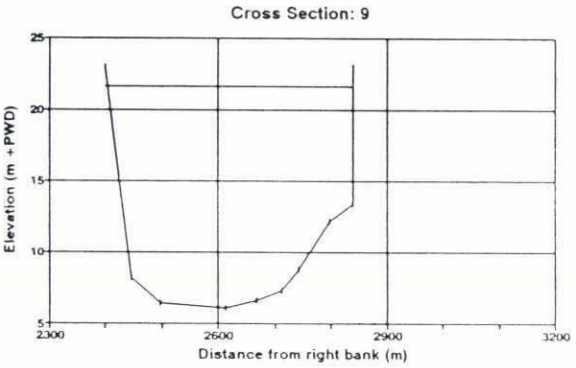
BANK PROTECTION AND RIVER TRAINING / (AFPM) PILOT PROJECT

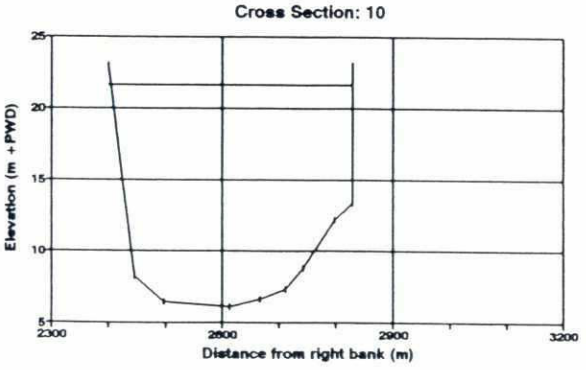
FINAL REPORT | FIG. A. 14 – 5

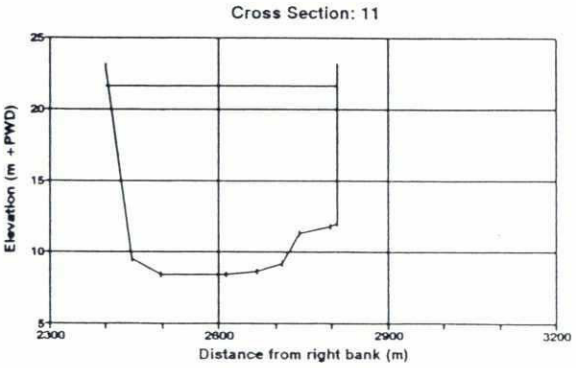




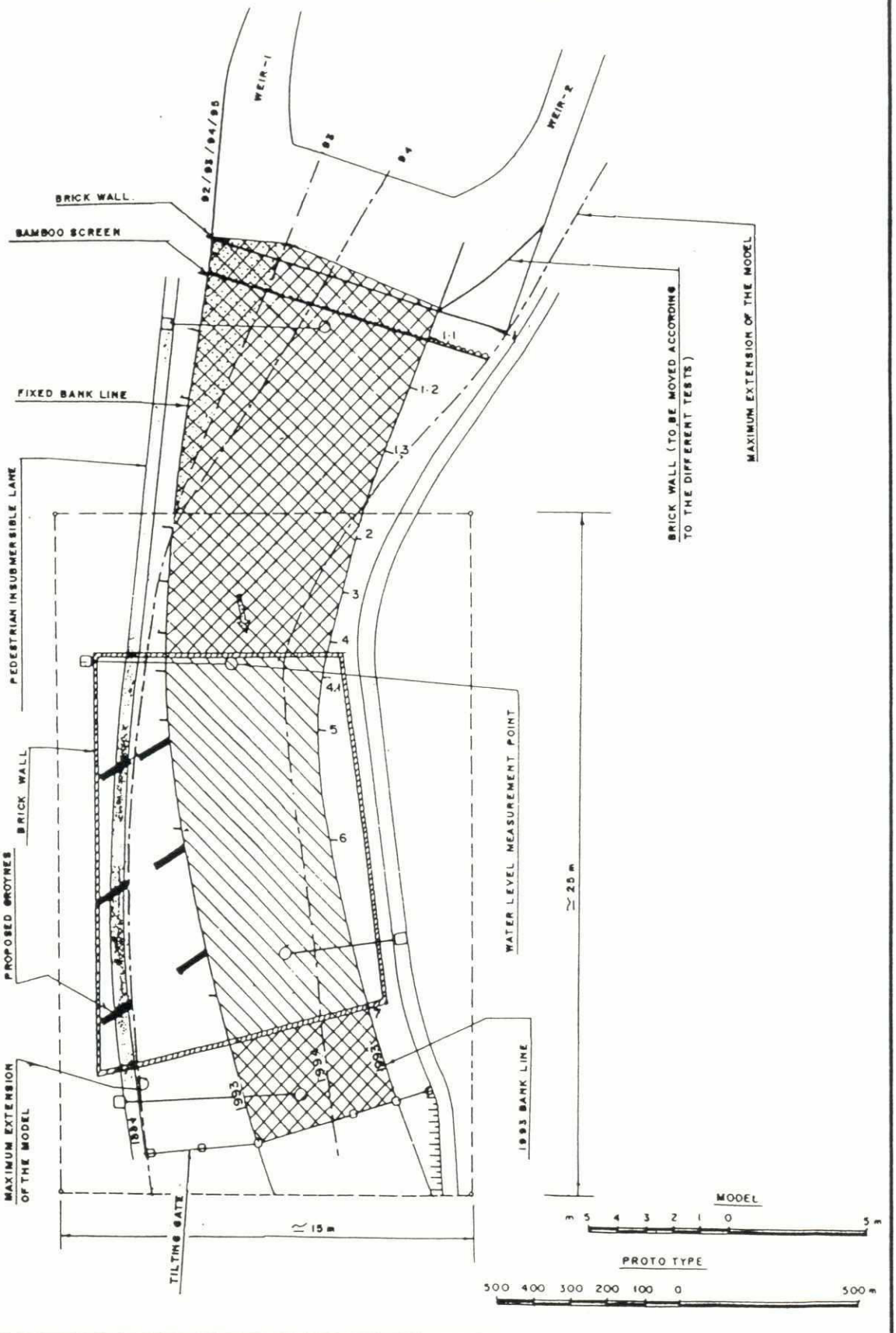








KAMARJANI MODEL TYPICAL CROSS SECTION	FAP – 21/22 BANK PROTECTION AND RIVER TRAINING / (AFPM) PILOT PROJECT	
	FINAL REPORT	FIG. A.14–6



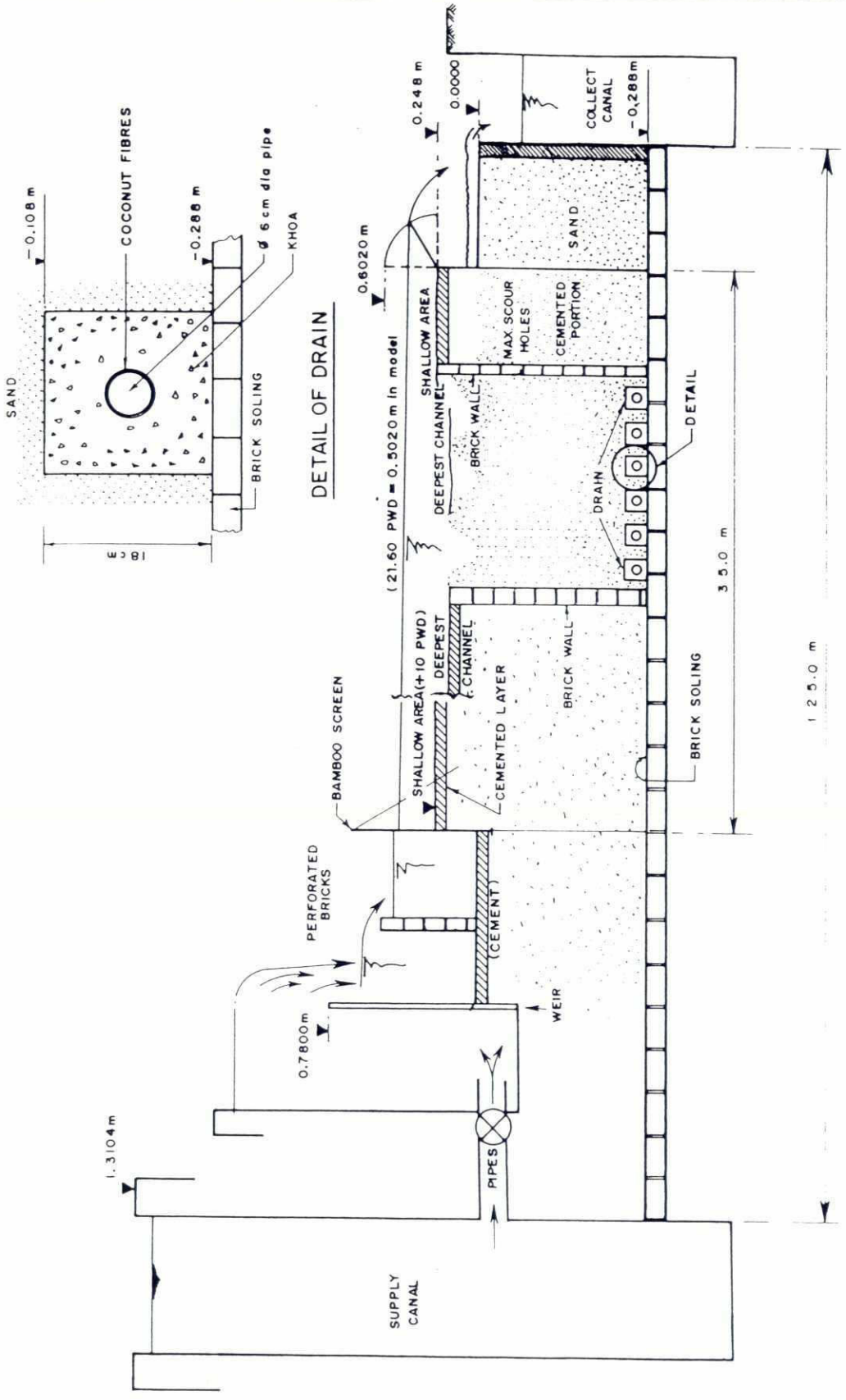
KAMARJANI MODEL LAYOUT PLAN

FAP – 21/22

BANK PROTECTION AND RIVER TRAINING / (AFPM) PILOT PROJECT

FINAL REPORT | FIG. A.14 – 7

GDA

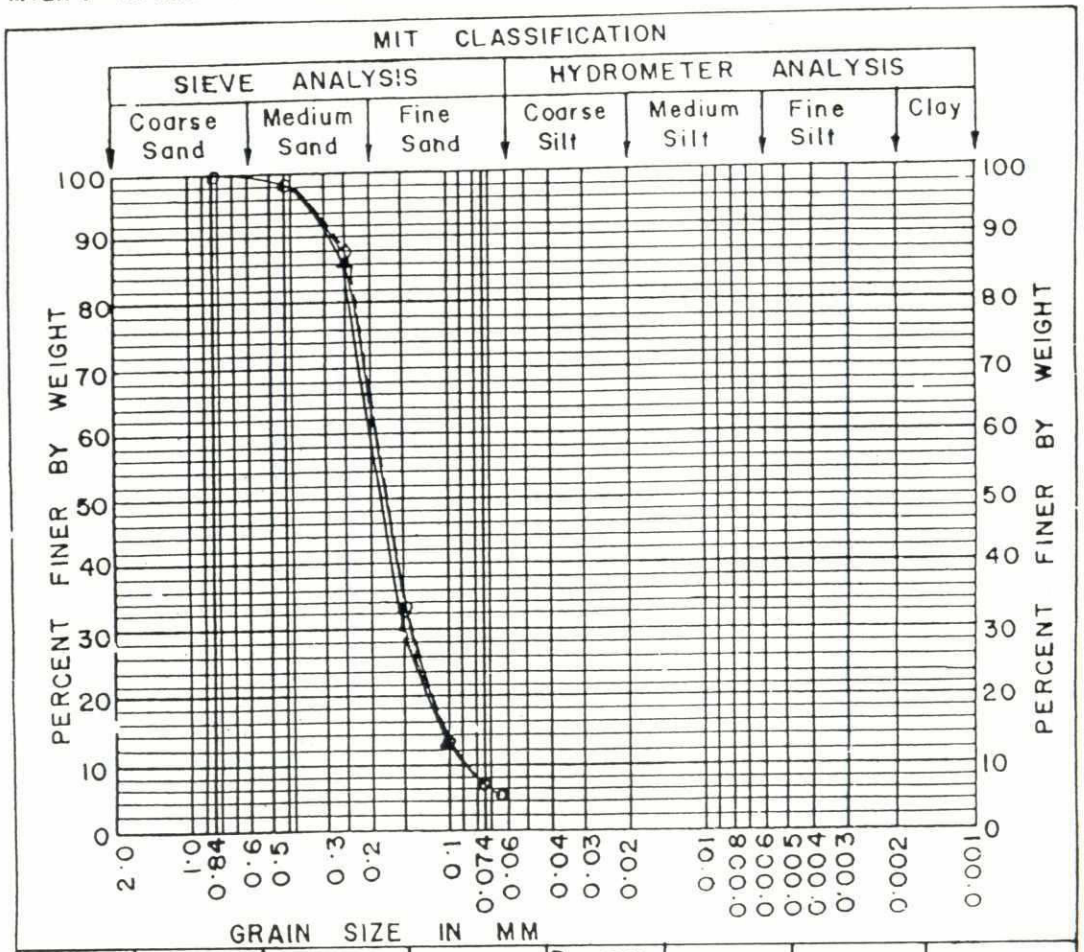


KAMARJANI MODEL LONGITUDINAL SECTION	FAP – 21/22 BANK PROTECTION AND RIVER TRAINING / (AFPM) PILOT PROJECT	
	FINAL REPORT	FIG. A.14 – 8

902

GRADATION CURVES OF BED MATERIALS

RIVER :— KAMARJANI MODEL STATION :— R. R. I.

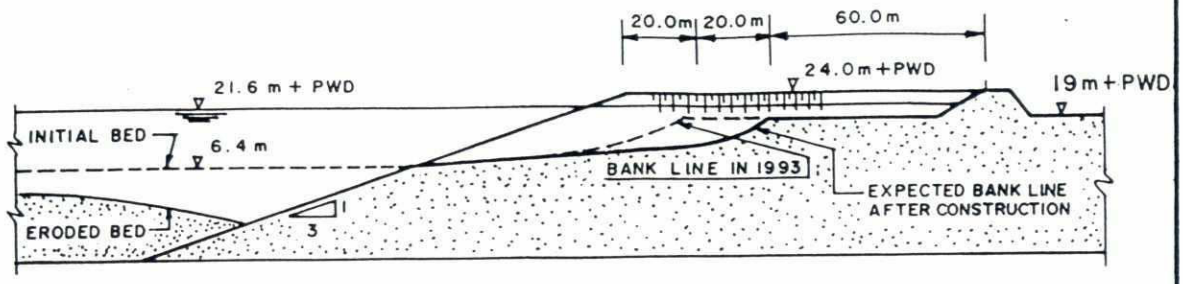


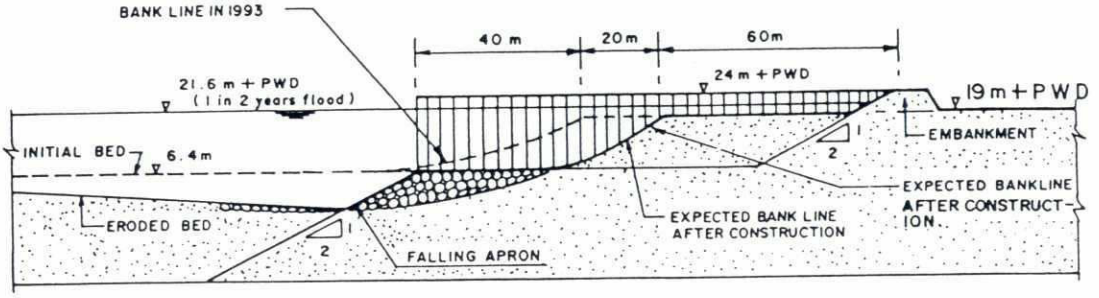
DATE	LEGEND	SAMPLE NO	DEPTH, FT.	D_{50} mm	SILT	MICA	LOCATION
24·8·92	o o o	1	—	0·176	5 %	<0·5%	Up stream
"	Δ Δ Δ	2	—	0·180	6 %	"	Middle
"	------	3	—	0·176	6 %	"	Down stream

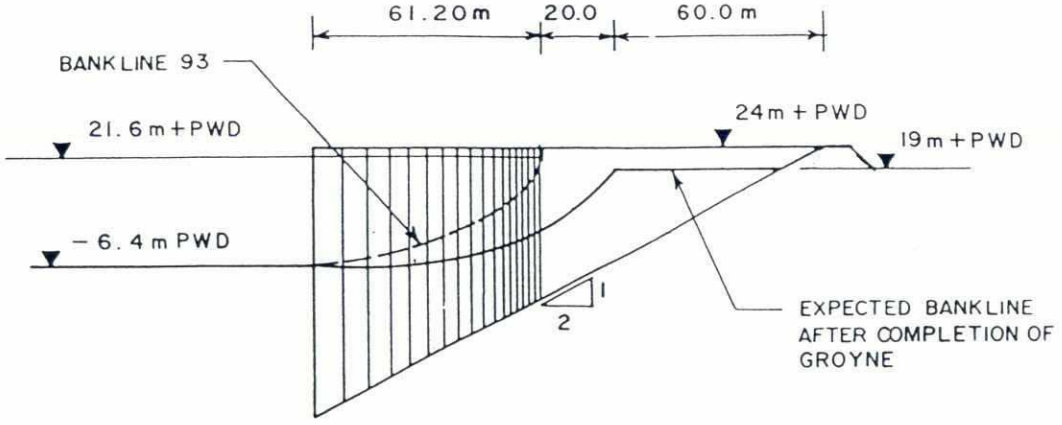
BAHADURABAD & KAMARJANI MODEL
SIEVE ANALYSIS OF BED SAND

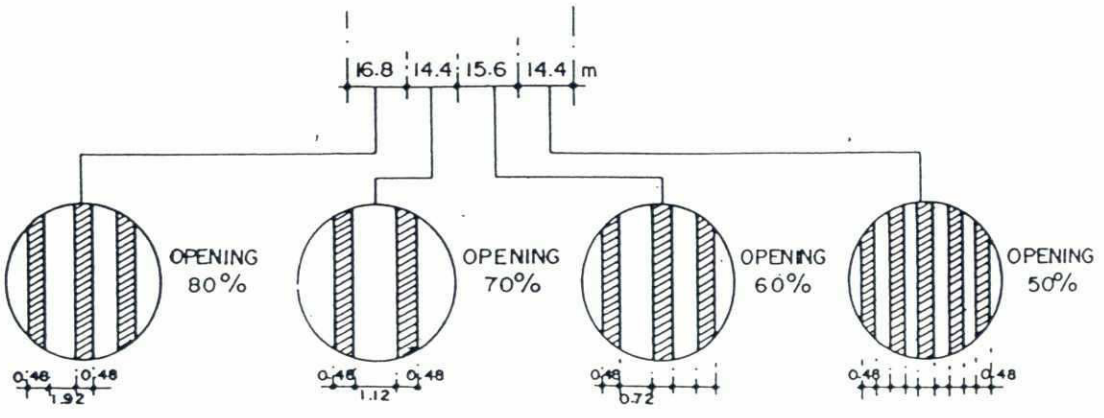
FAP – 21/22
BANK PROTECTION AND RIVER TRAINING / (AFPM) PILOT PROJECT

FINAL REPORT | FIG. A.14 – 9







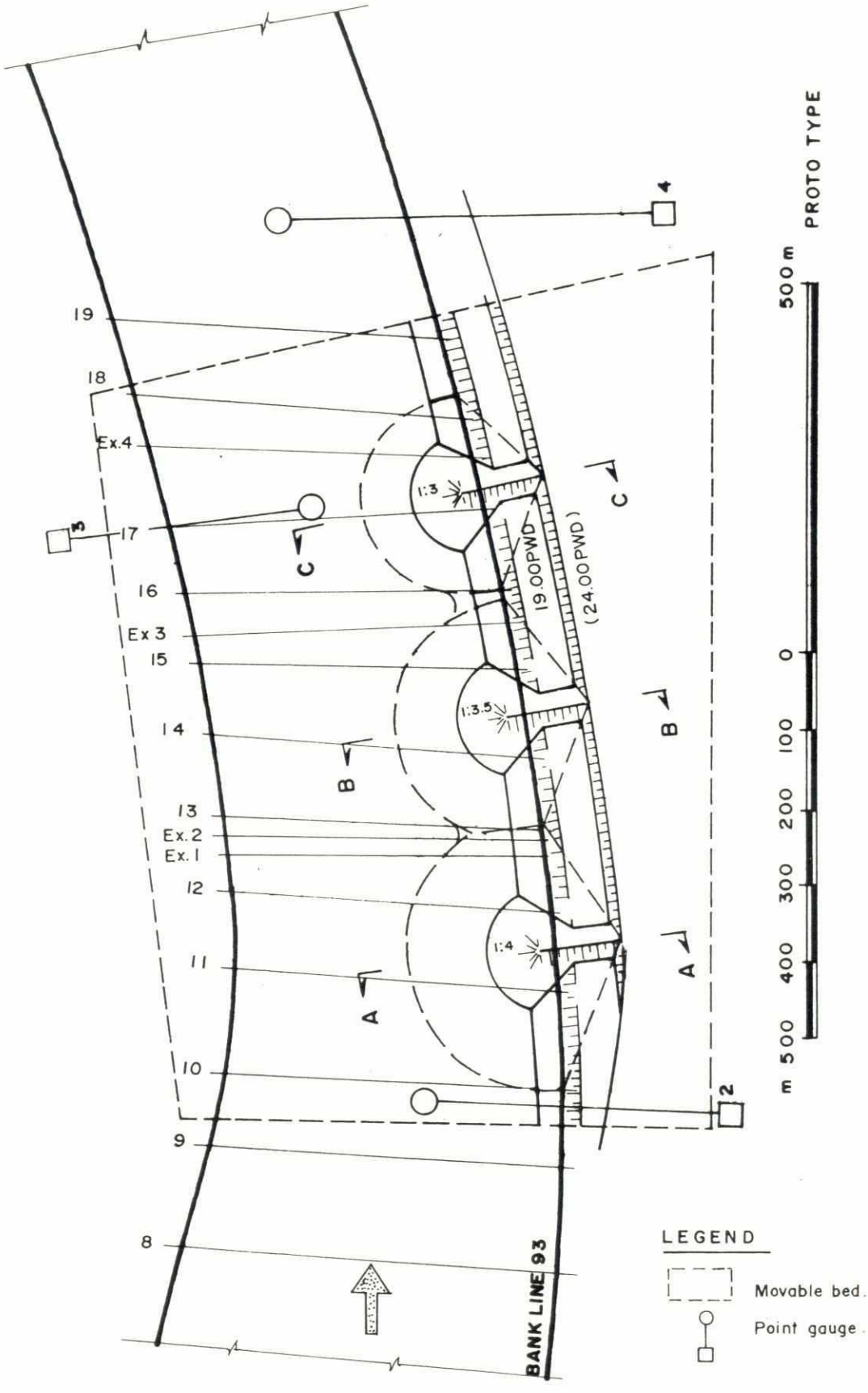


KAMARJANI MODEL
3 TESTED GROYNES

FAP – 21/22

BANK PROTECTION AND RIVER TRAINING / (AFPM) PILOT PROJECT

FINAL REPORT | FIG. A.14-10



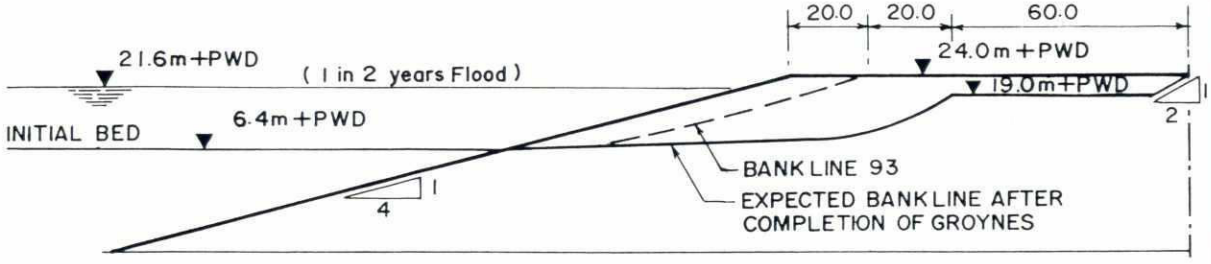
KAMARJANI MODEL

TEST T 2

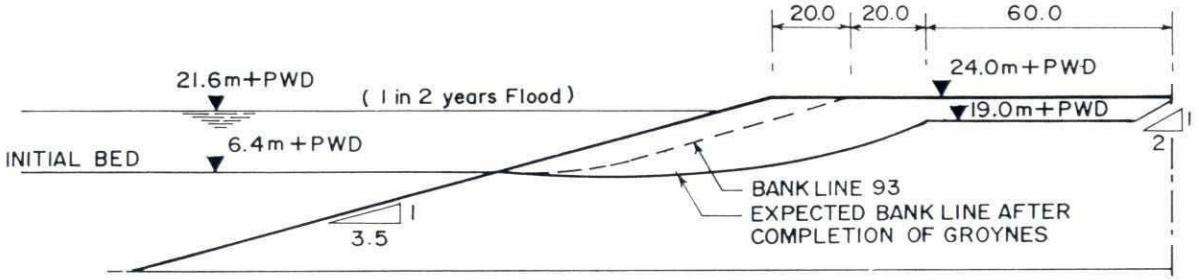
FAP - 21/22

BANK PROTECTION AND RIVER TRAINING / (AFPM) PILOT PROJECT

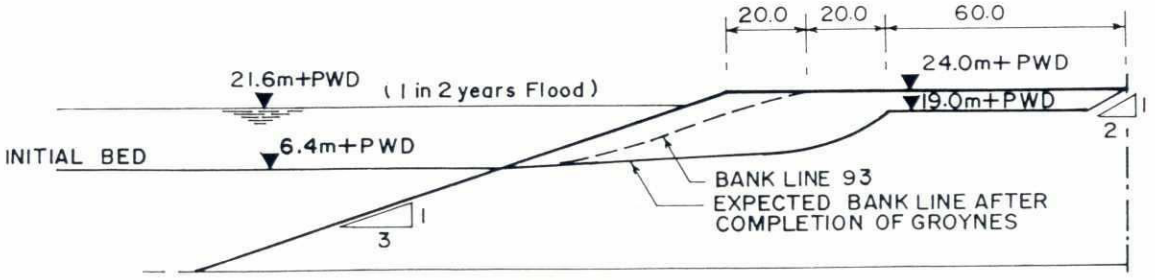
FINAL REPORT | FIG. A.14-11



1 ST GROYNE
SECTION A-A



2 ND GROYNE
SECTION B-B



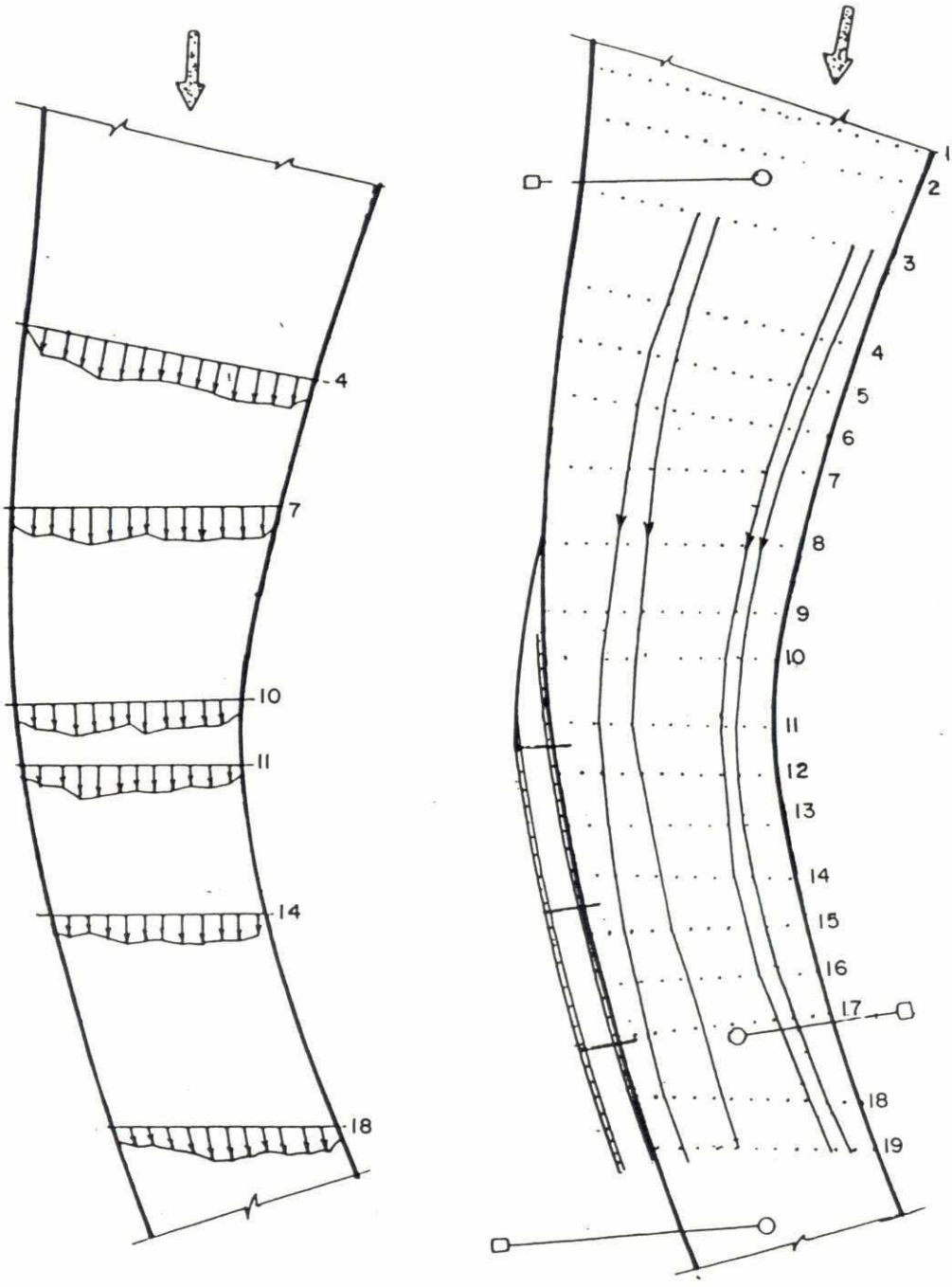
3 RD GROYNE
SECTION C-C



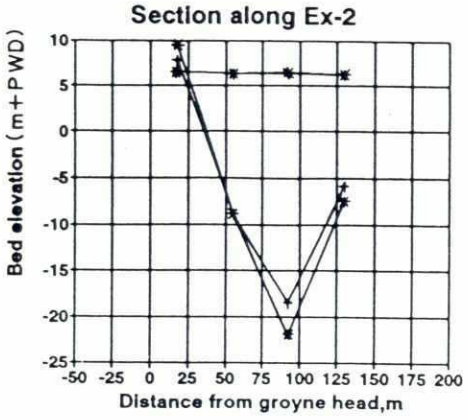
KAMARJANI MODEL
TEST T 2

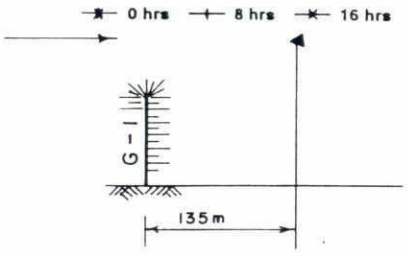
FAP – 21/22
BANK PROTECTION AND RIVER TRAINING/
(AFPM) PILOT PROJECT

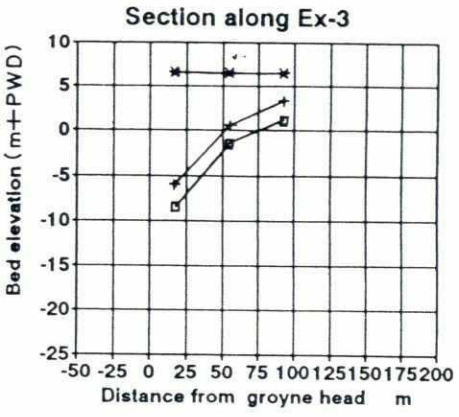
FINAL REPORT | FIG. A.14-12

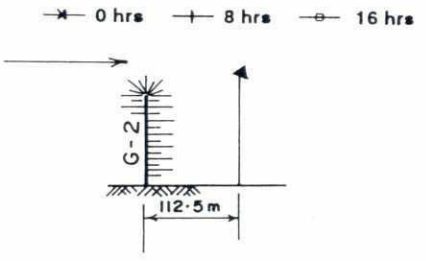


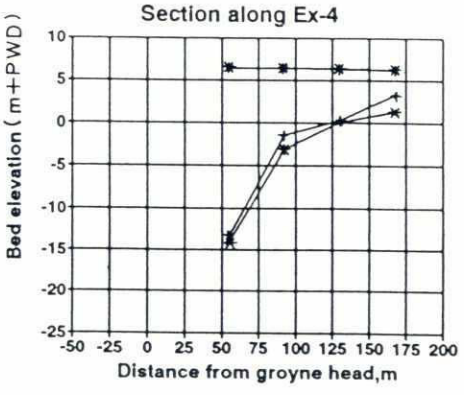
KAMARJANI MODEL TEST T 2 FLOW LINE & VELOCITY PROFILE	FAP – 21/22 BANK PROTECTION AND RIVER TRAINING / (AFPM) PILOT PROJECT	
	FINAL REPORT	FIG. A.14-13

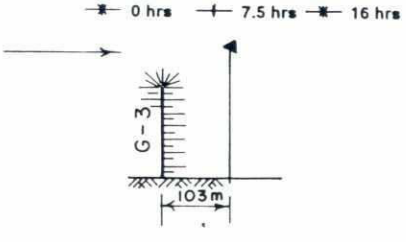










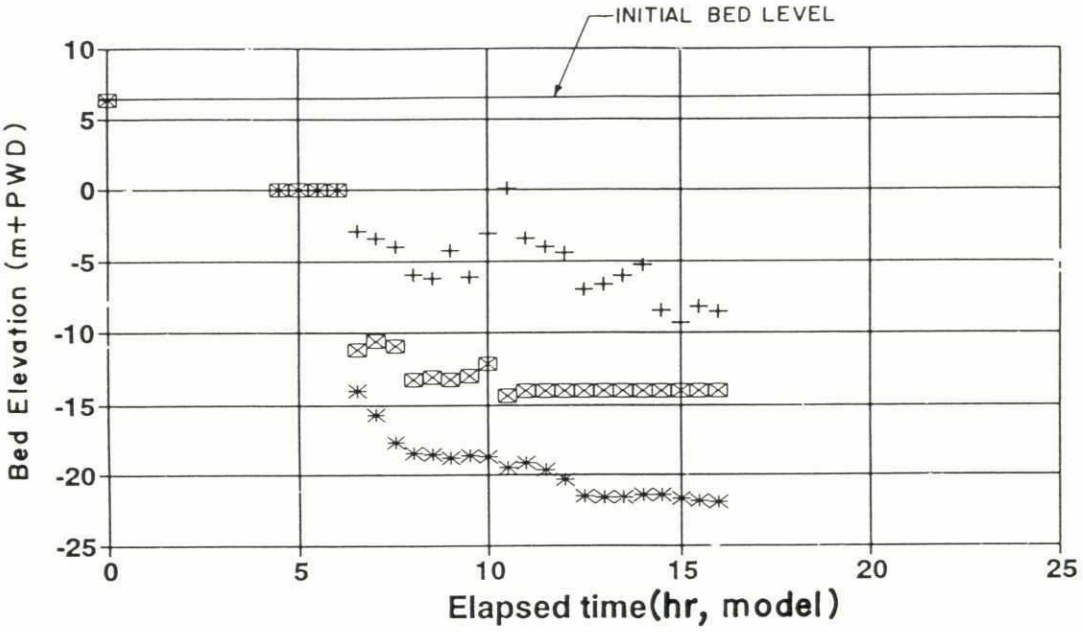


LEGEND

1. LOCATION OF DEEPEST POINT ... ... ◀

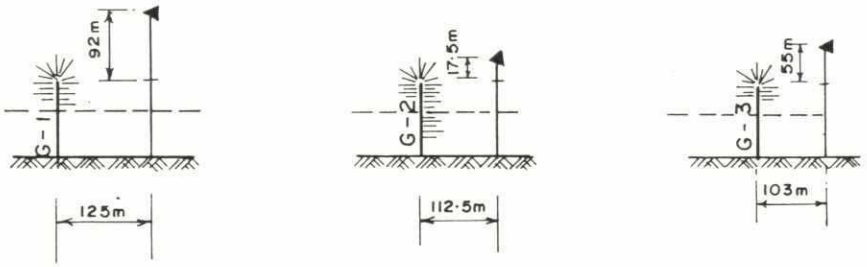
GROYNE NUMBER 1 ... ... G-1

KAMARJANI MODEL TEST T 2 LONGITUDINAL AND CROSS SECTION	**FAP – 21/22** BANK PROTECTION AND RIVER TRAINING / (AFPM) PILOT PROJECT
	FINAL REPORT | FIG. A.14-14



All groynes are impermeable with 20 m projection from '93 B/L

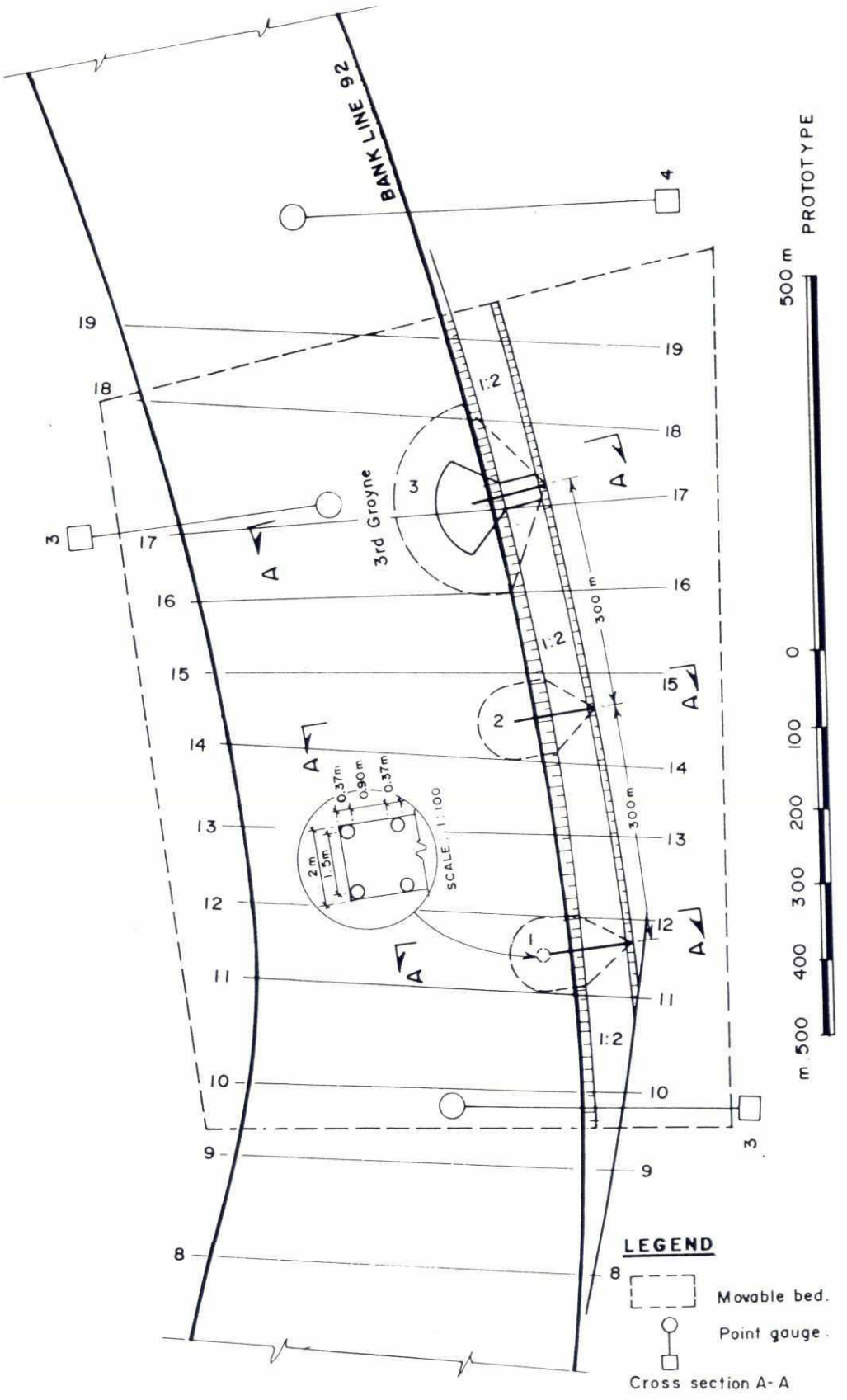
✳ Groyne-1 + Groyne-2 ⊠ Groyne-3



LEGEND

1. LOCATION OF DEEPEST POINT ---- ◀

KAMARJANI MODEL TEST T 2 DEEPEST POINT OF SCOUR HOLE	FAP – 21/22 BANK PROTECTION AND RIVER TRAINING / (AFPM) PILOT PROJECT	
	FINAL REPORT	FIG. A. 14–15



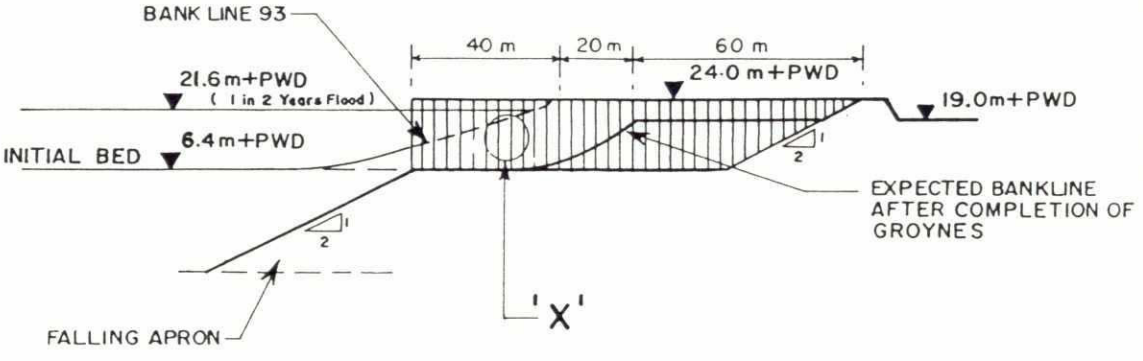
KAMARJANI MODEL
PLAN OF PERMEABLE GROYNE
TEST T 3

FAP – 21/22

BANK PROTECTION AND RIVER TRAINING / (AFPM) PILOT PROJECT

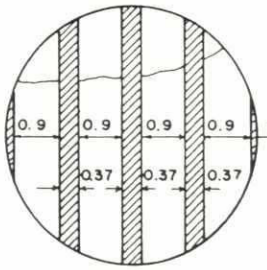
FINAL REPORT

FIG. A.14-16



SECTION A-A / B-B

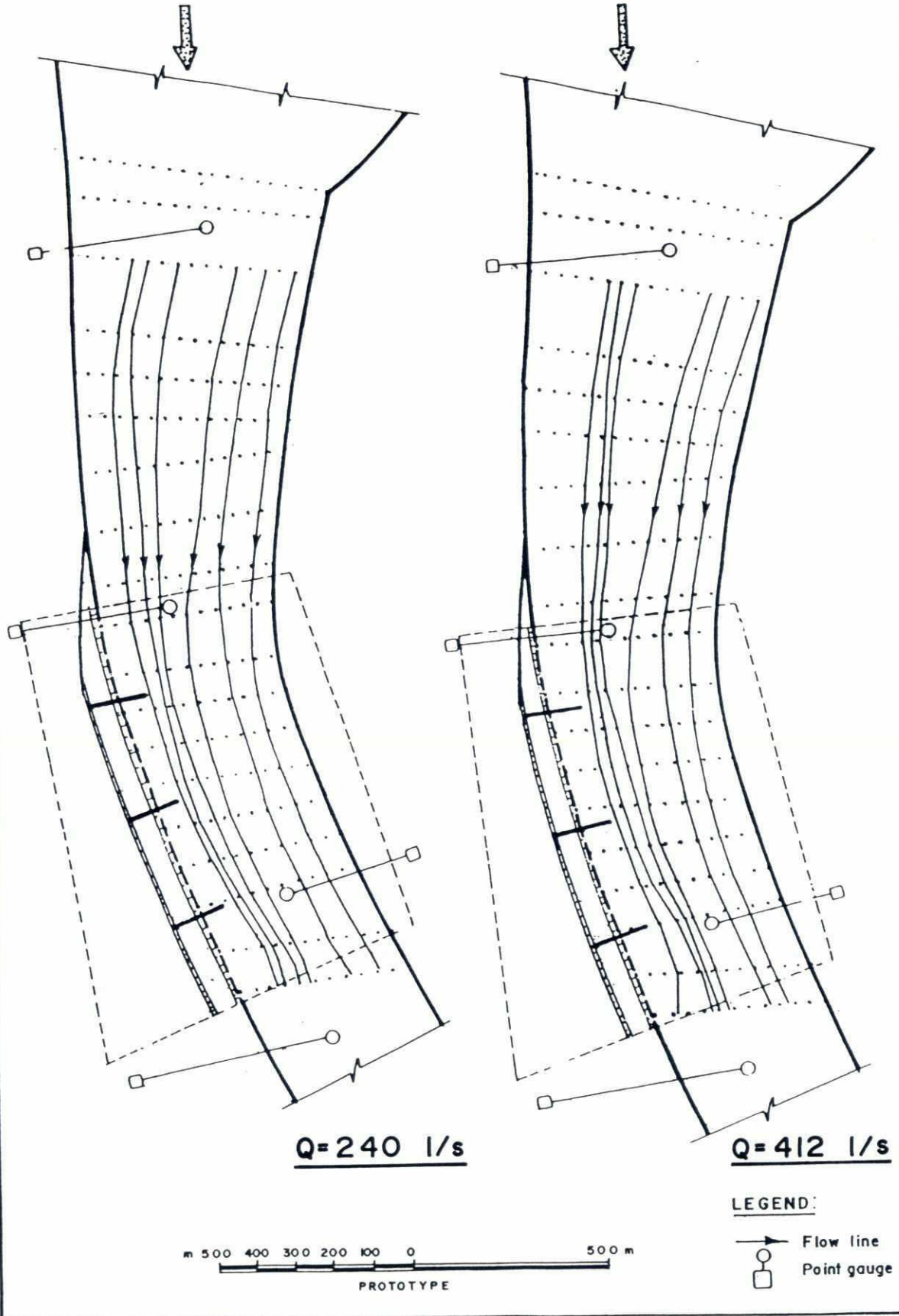




OPENING 70%

DETAIL OF 'X'

KAMARJANI MODEL PERMEABLE GROYNE TEST T 3	FAP – 21/22 BANK PROTECTION AND RIVER TRAINING / (AFPM) PILOT PROJECT	
	FINAL REPORT	FIG. A.14-17

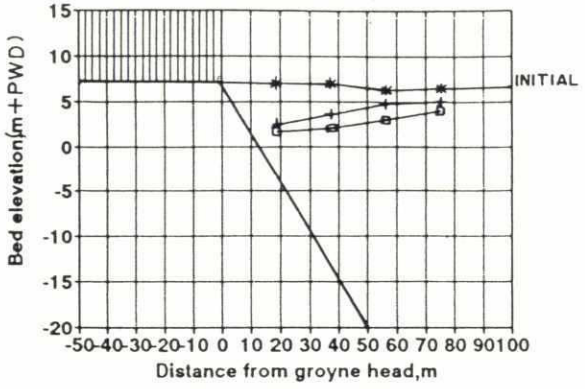


KAMARJANI MODEL
TEST T 3
FLOW LINE

FAP – 21/22
BANK PROTECTION AND RIVER TRAINING / (AFPM) PILOT PROJECT

FINAL REPORT | FIG. A.14-18

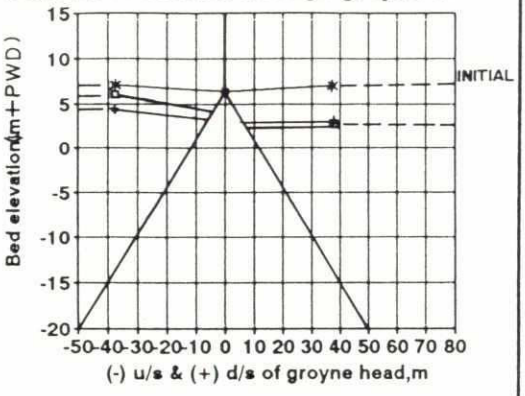
Section along the groyne-1



0 hrs 8 hrs 16 hrs



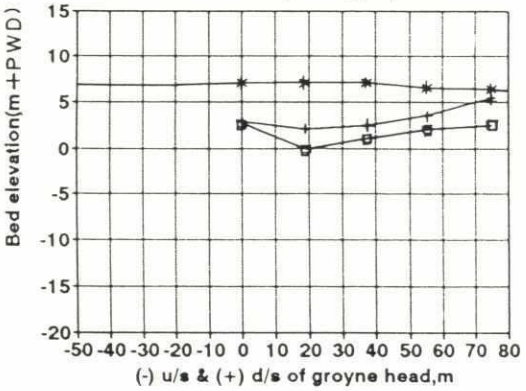
Transverse section through groyne head



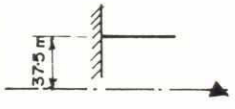
0 hrs 8 hrs 16 hrs



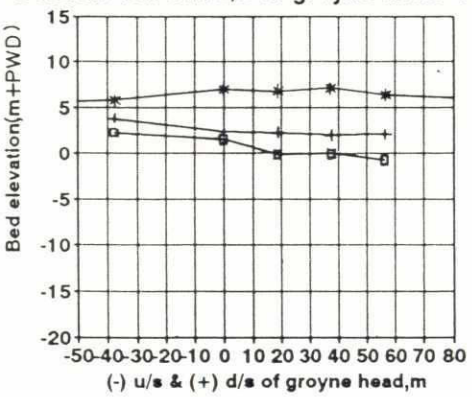
Section 37.5 m d/s of groyne-1



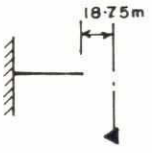
0 hrs 8 hrs 16 hrs



Section 18.75 m d/s of groyne head -1



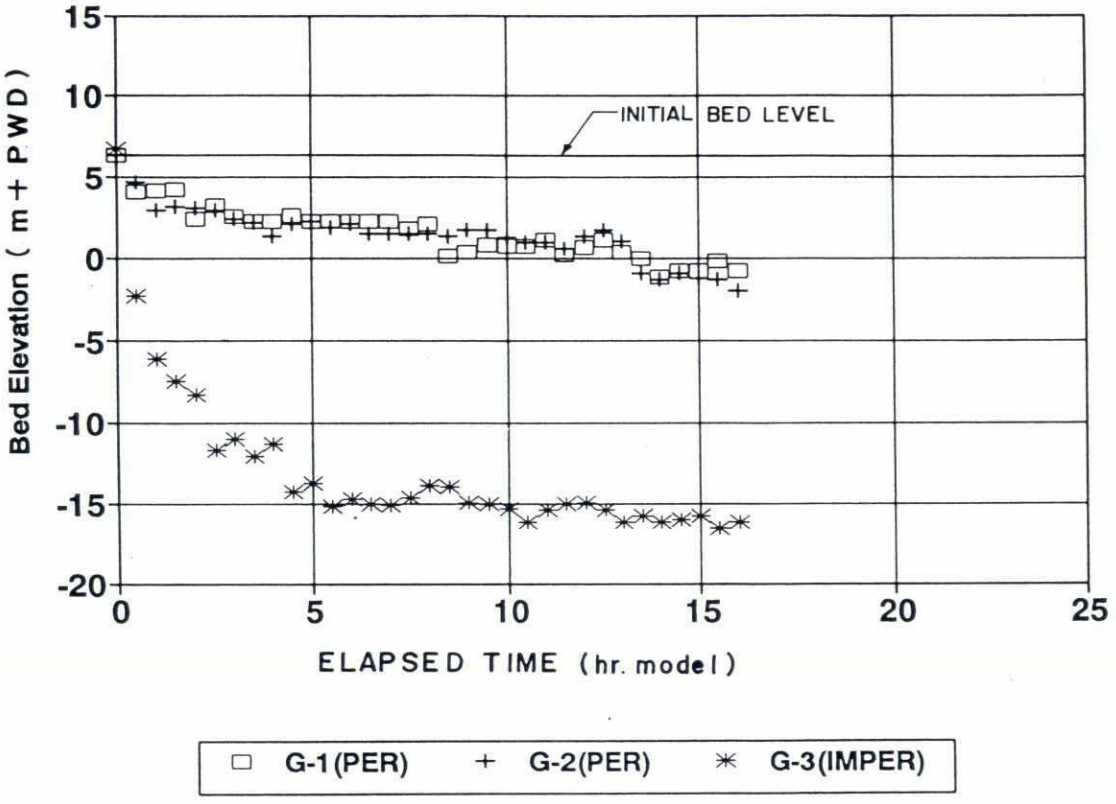
0 hrs 8 hrs 16 hrs



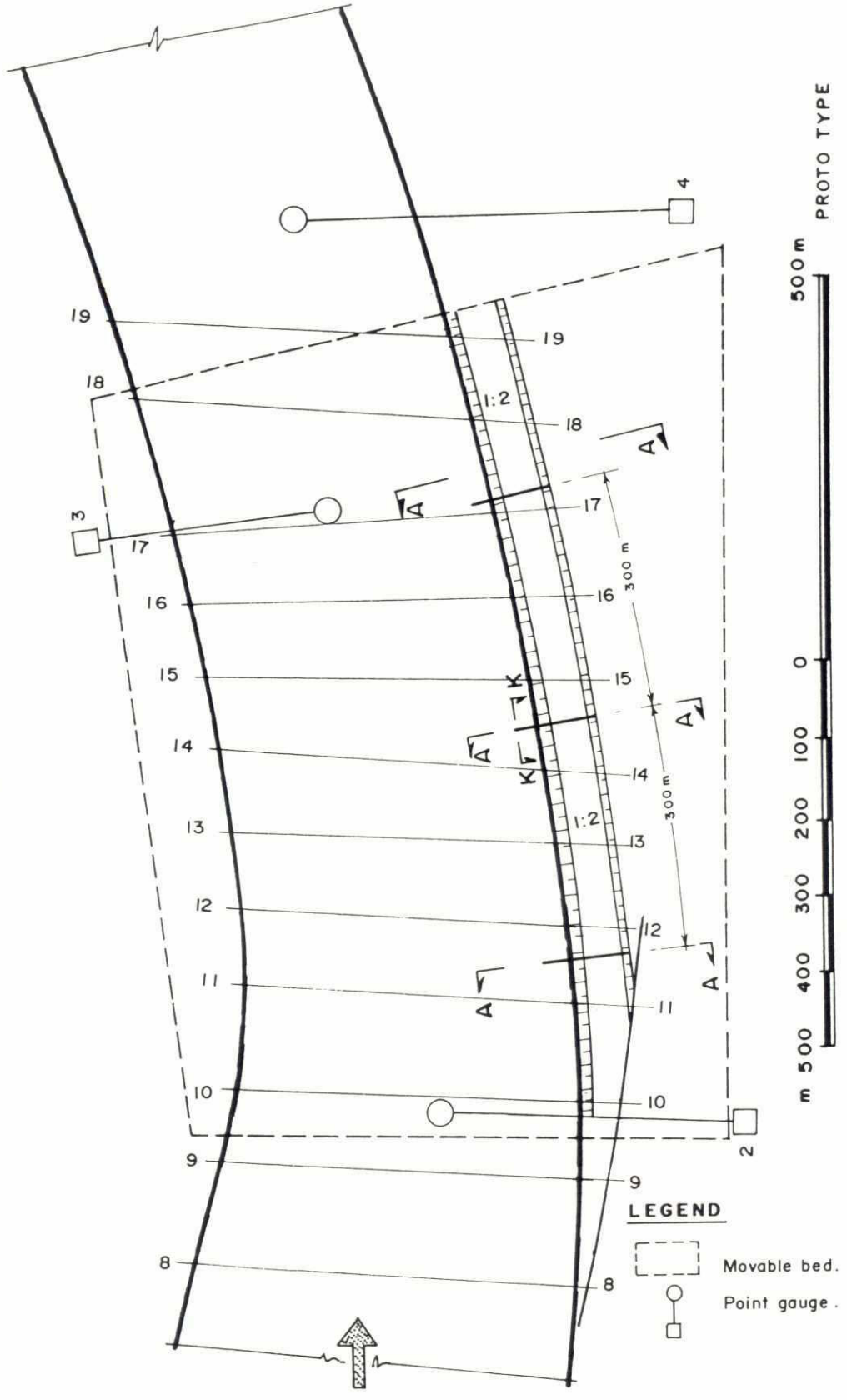
LEGEND

1. LOCATION OF DEEPEST POINT ... ... ◀

KAMARJANI MODEL TEST T 3 GROYNE NO. 1 LONGITUDINAL AND CROSS SECTION	**FAP – 21/22** BANK PROTECTION AND RIVER TRAINING / (AFPM) PILOT PROJECT FINAL REPORT | FIG. A.14-19



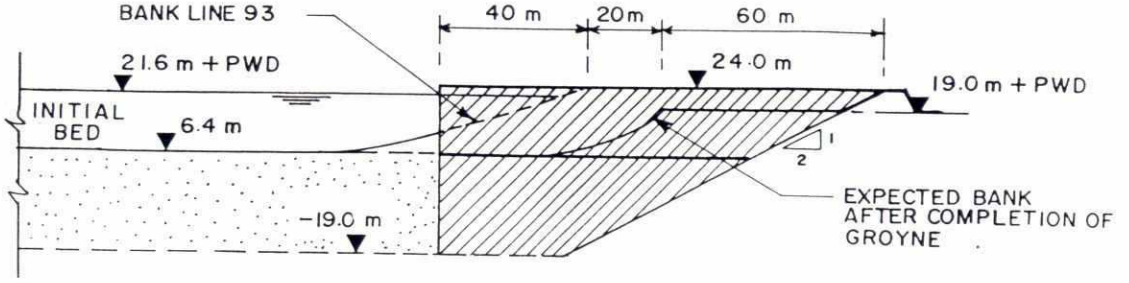
KAMARJANI MODEL TEST T 3 DEEPEST POINT OF SCOUR HOLE	FAP – 21/22 BANK PROTECTION AND RIVER TRAINING / (AFPM) PILOT PROJECT	
	FINAL REPORT	FIG. A.14-20



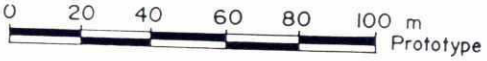
KAMARJANI MODEL
TEST T 5

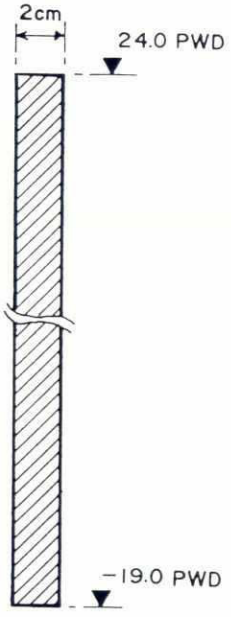
FAP – 21/22
BANK PROTECTION AND RIVER TRAINING / (AFPM) PILOT PROJECT

FINAL REPORT | FIG. A.14 - 21



SECTION A-A



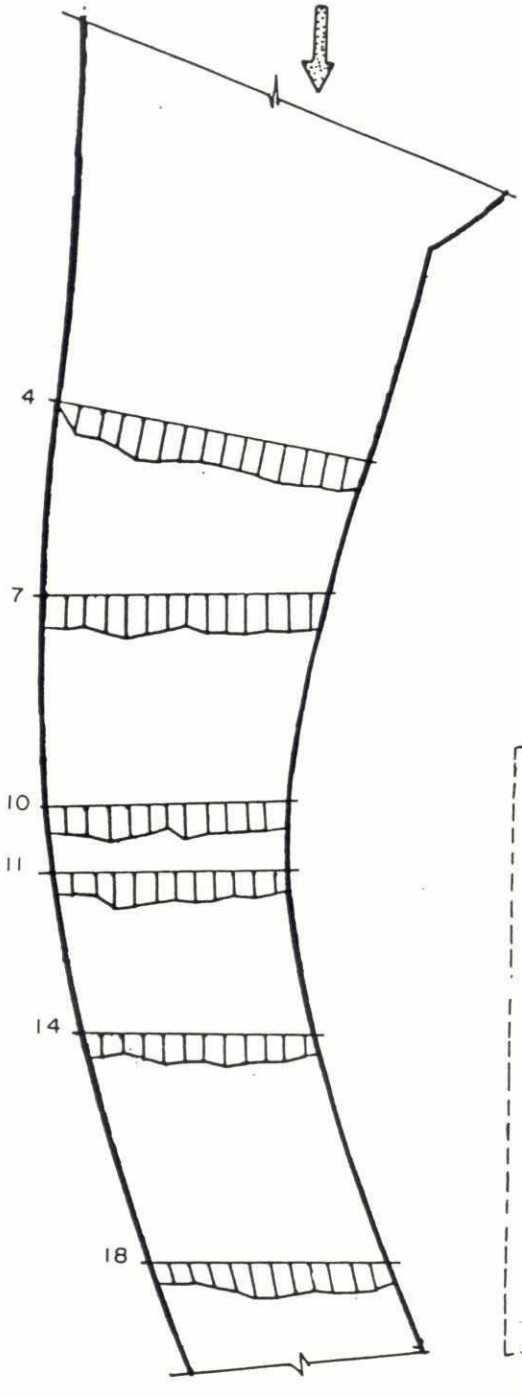


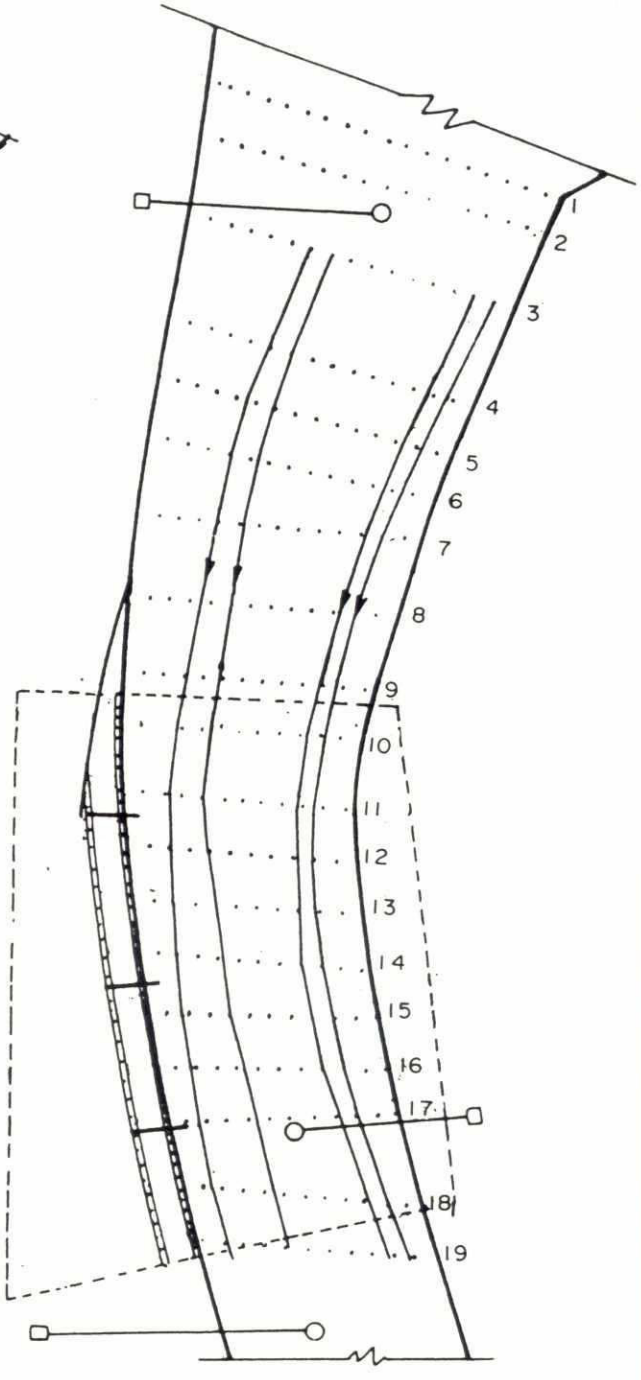
SECTION K-K

KAMARJANI MODEL
TEST T 5

FAP – 21/22
BANK PROTECTION AND RIVER TRAINING / (AFPM) PILOT PROJECT

FINAL REPORT | FIG. A.14-22





Q = 240 l/s

Q = 240 l/s

LEGEND

0 4 6m/s

Flow line

Movable bed.

Point gauge

m500 400 300 200 100 0 500m PROTO TYPE

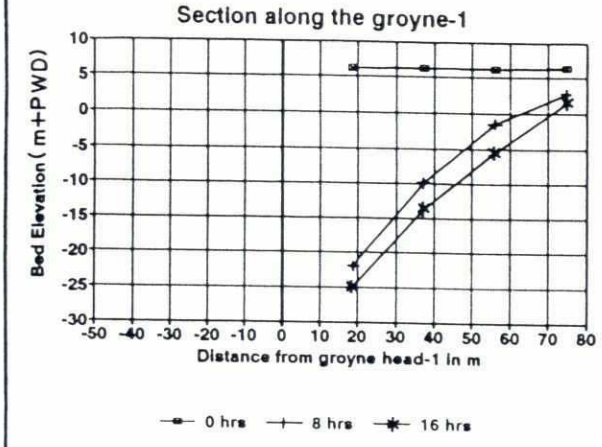
KAMARJANI MODEL
TEST T 5
FLOW LINE & VELOCITY PROFILE

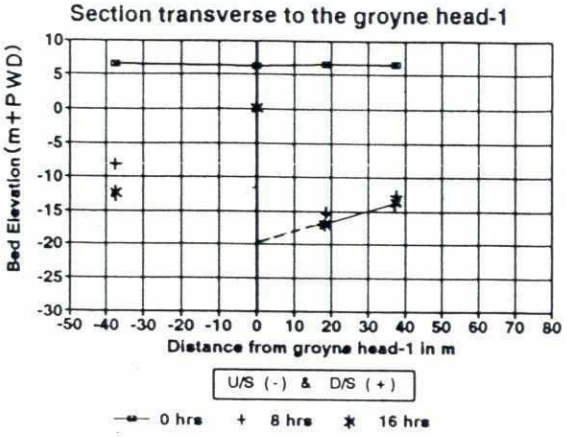
FAP – 21/22

BANK PROTECTION AND RIVER TRAINING / (AFPM) PILOT PROJECT

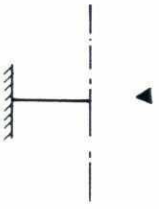
FINAL REPORT

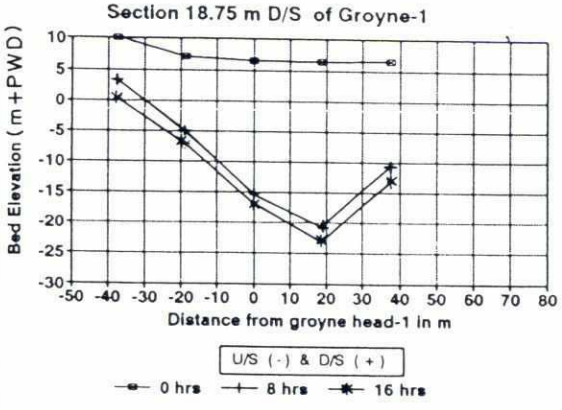
FIG. A. 14-23

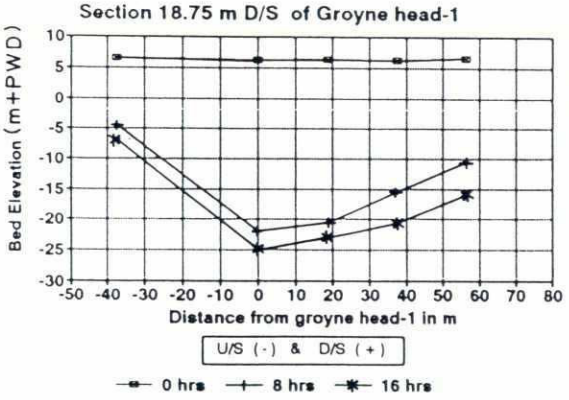












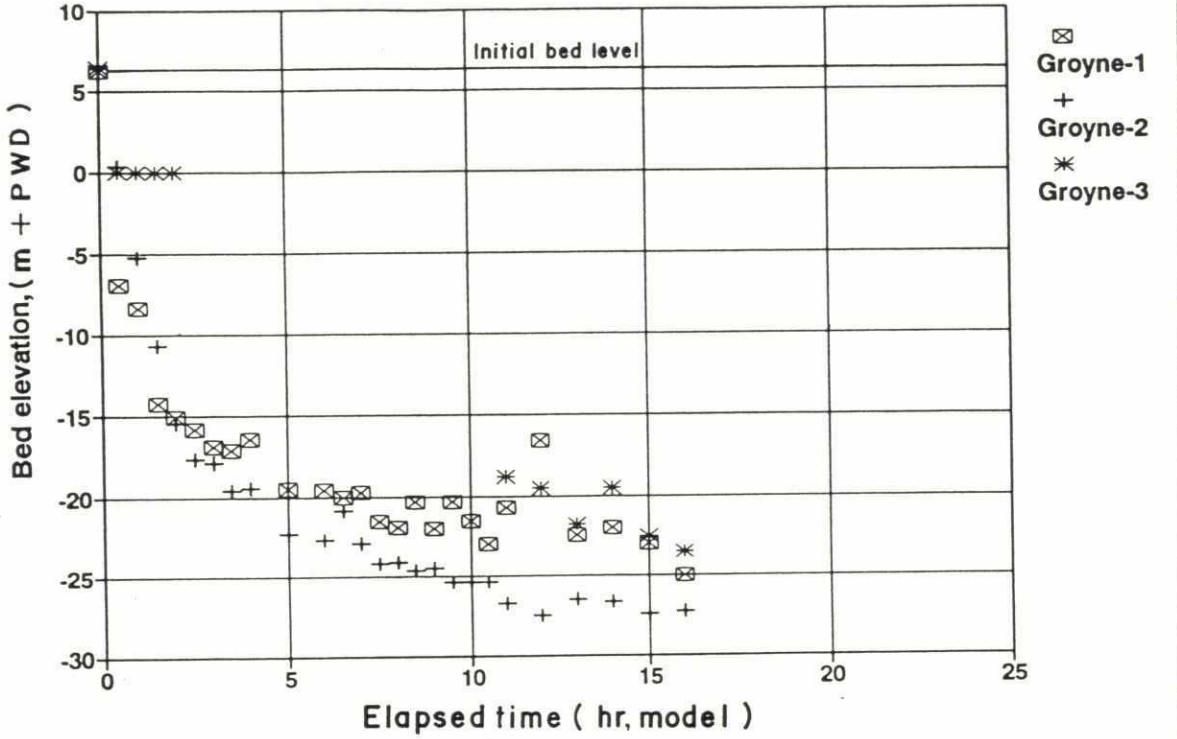




LEGEND

1. LOCATION OF DEEPEST POINT ..... ▲

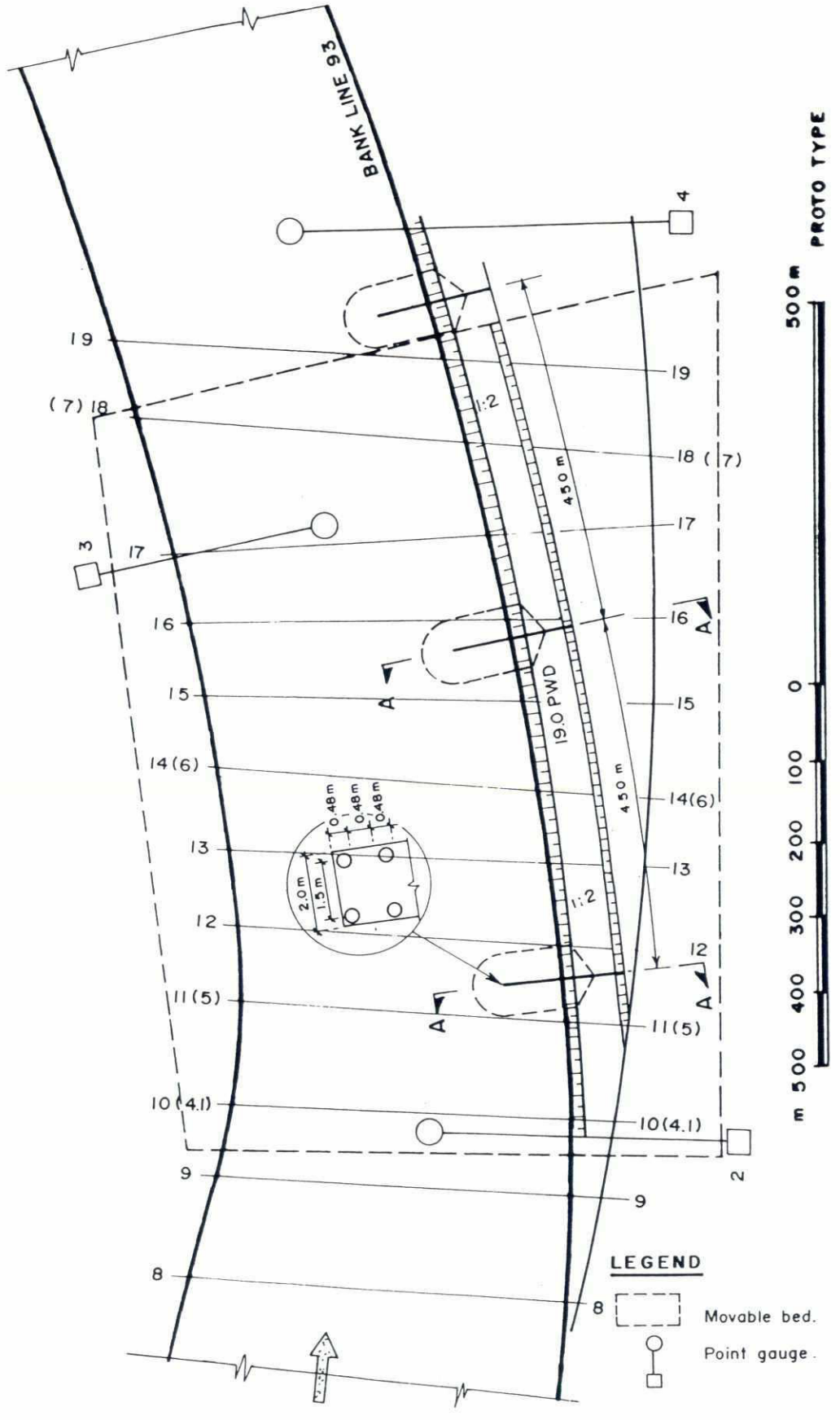
KAMARJANI MODEL **TEST : T 5** GROYNE - 1 PROFILES OF DEEPEST SCOURHOLES	**FAP - 21/22** BANK PROTECTION AND RIVER TRAINING / (AFPM) PILOT PROJECT
	FINAL REPORT | FIG. A.14-24



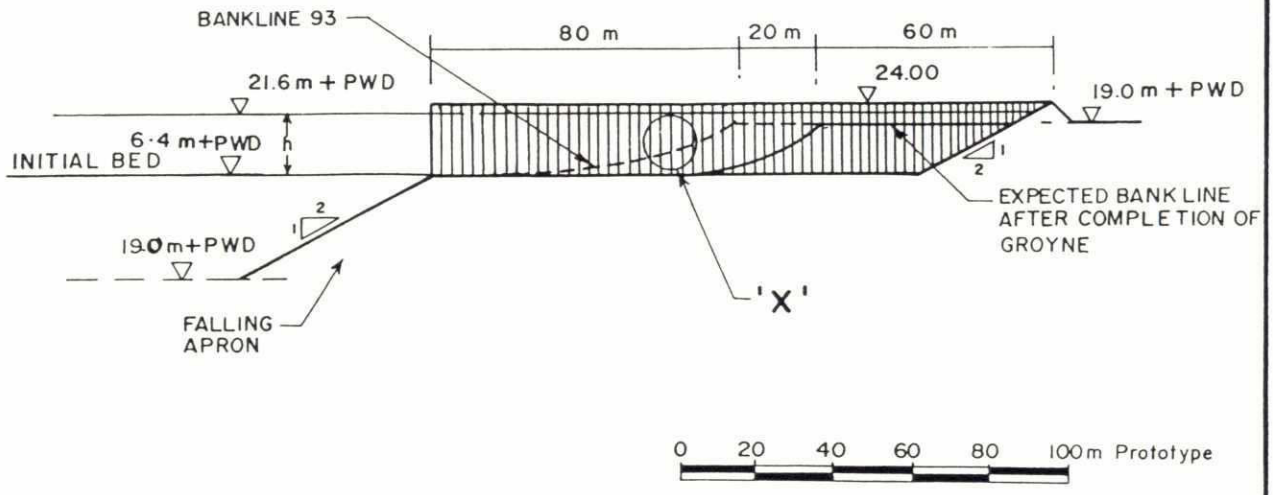
18.75 m D/S of Each Groyne Head in m

W.A.R.P.O. LIBRARY. DHAKA

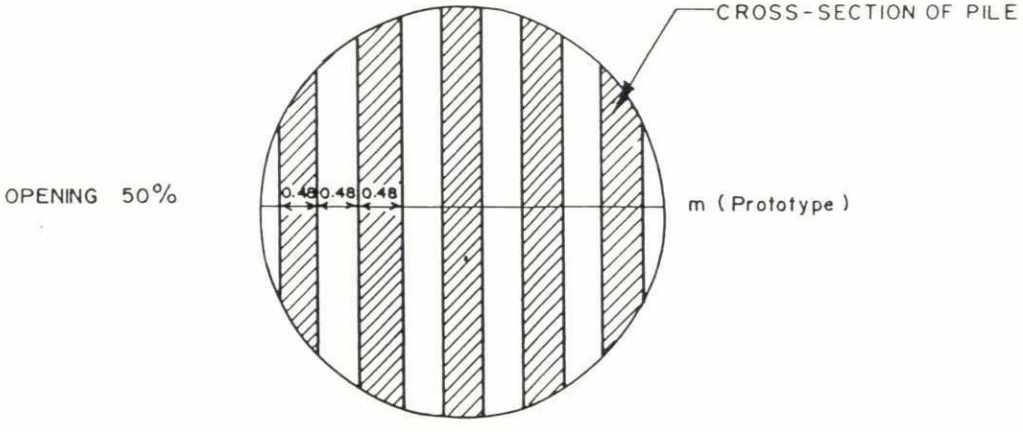
KAMARJANI MODEL TEST T 5 DEEPEST POINT OF SCOUR HOLE	FAP – 21/22 BANK PROTECTION AND RIVER TRAINING / (AFPM) PILOT PROJECT	
	FINAL REPORT	FIG. A. 14-25



KAMARJANI MODEL PLAN OF PERMEABLE GROYNE TEST T 7	FAP – 21/22 BANK PROTECTION AND RIVER TRAINING / (AFPM) PILOT PROJECT	
	FINAL REPORT	FIG. A.14–26

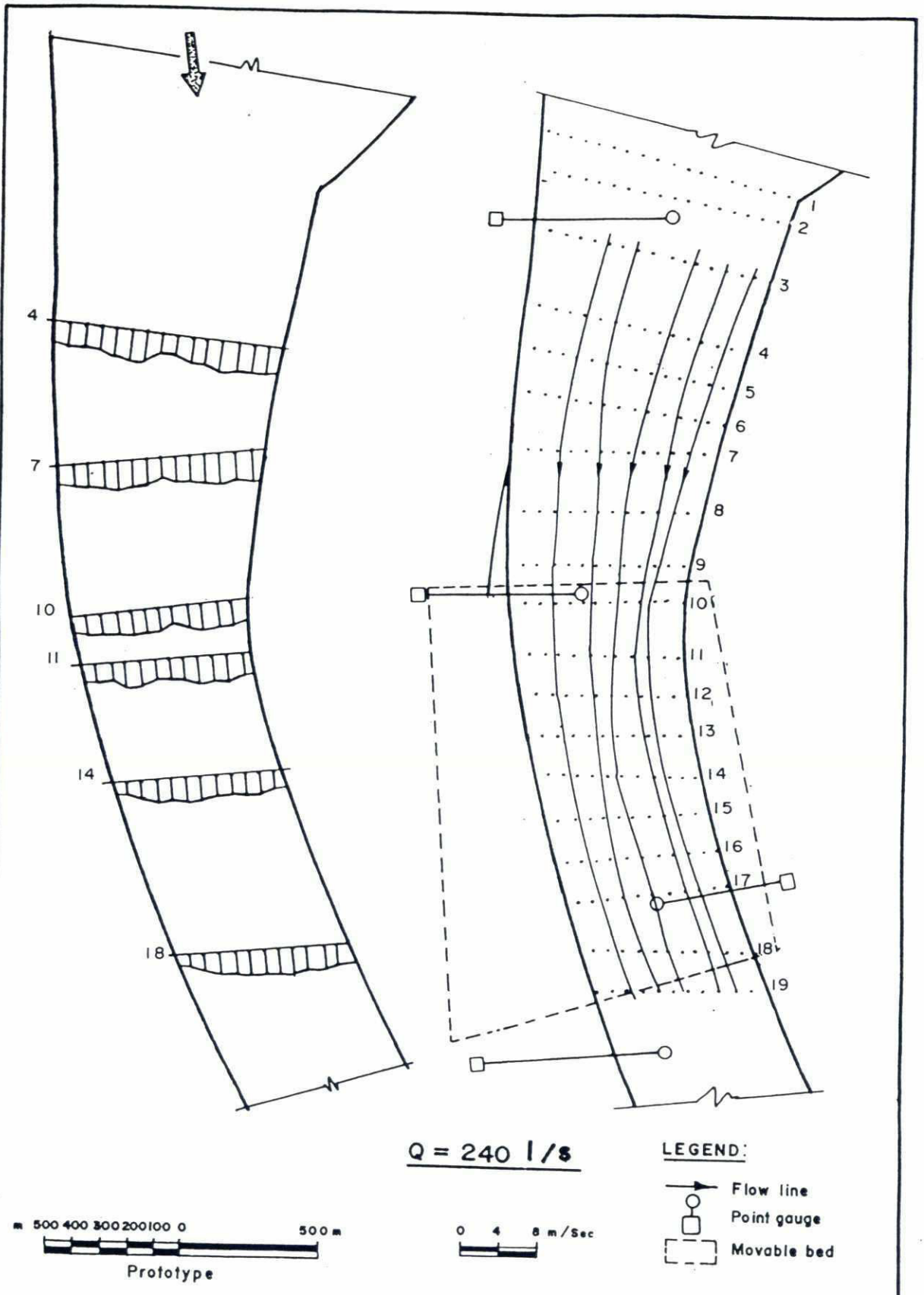


SECTION A-A



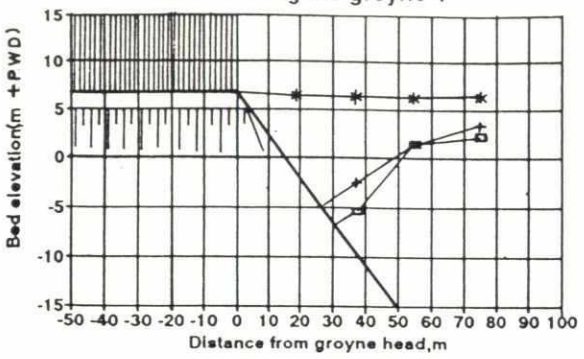
DETAIL OF 'X'

KAMARJANI MODEL TEST T 7	FAP - 21/22 BANK PROTECTION AND RIVER TRAINING / (AFPM) PILOT PROJECT	
	FINAL REPORT	FIG. A. 14 - 27

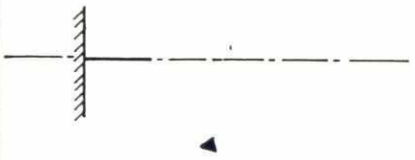


KAMARJANI MODEL TEST T 7 FLOW LINE & VELOCITY PROFILE	FAP – 21/22 BANK PROTECTION AND RIVER TRAINING / (AFPM) PILOT PROJECT FINAL REPORT | FIG. A.14-28

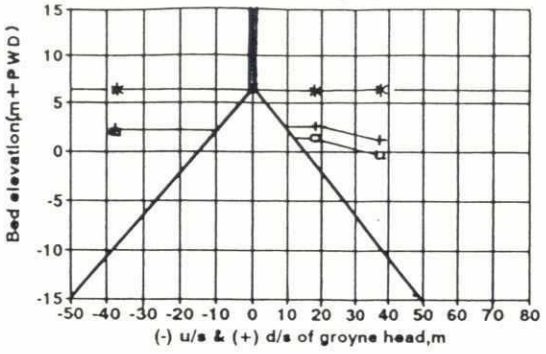
Section along the groyne-1



0 hrs 8 hrs 16 hrs



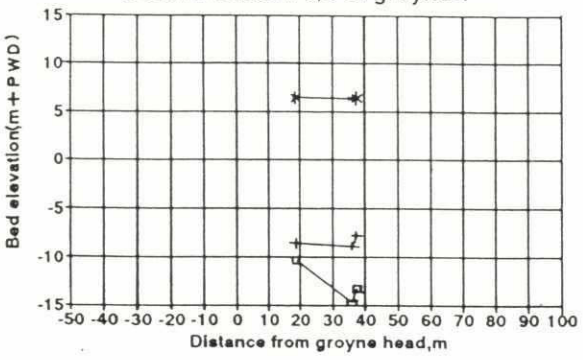
Transverse section through groyne head



0 hrs 8 hrs 16 hrs



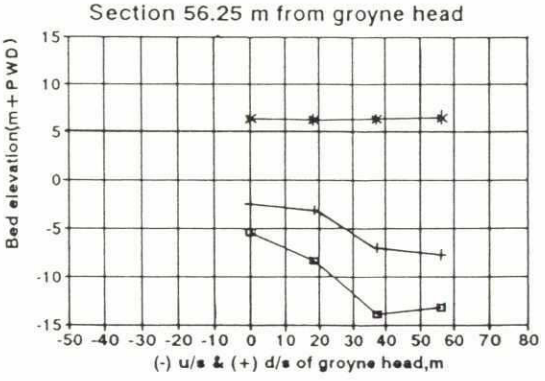
Section 56.25 m d/s of groyne-1



0 hrs 8 hrs 16 hrs



Section 56.25 m from groyne head



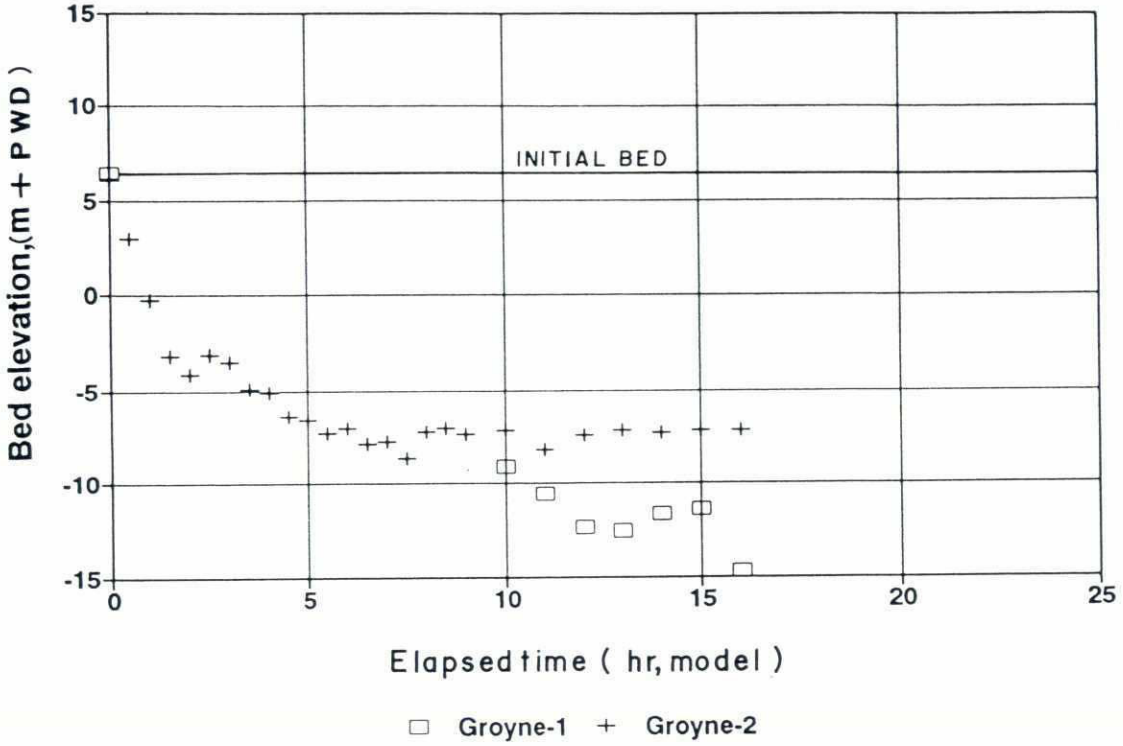
0 hrs 8 hrs 16 hrs

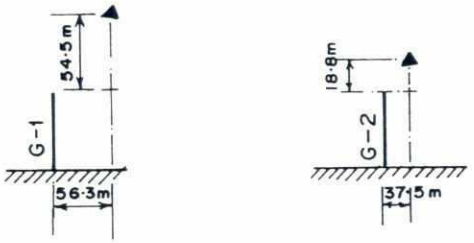


LEGEND

1. LOCATION OF DEEPEST POINT ▲

KAMARJANI MODEL TEST T 7 GROYNE NO. 1 PROFILE OF DEEPEST SCOURHOLE	FAP – 21/22 BANK PROTECTION AND RIVER TRAINING / (AFPM) PILOT PROJECT
	FINAL REPORT | FIG. A.14-29

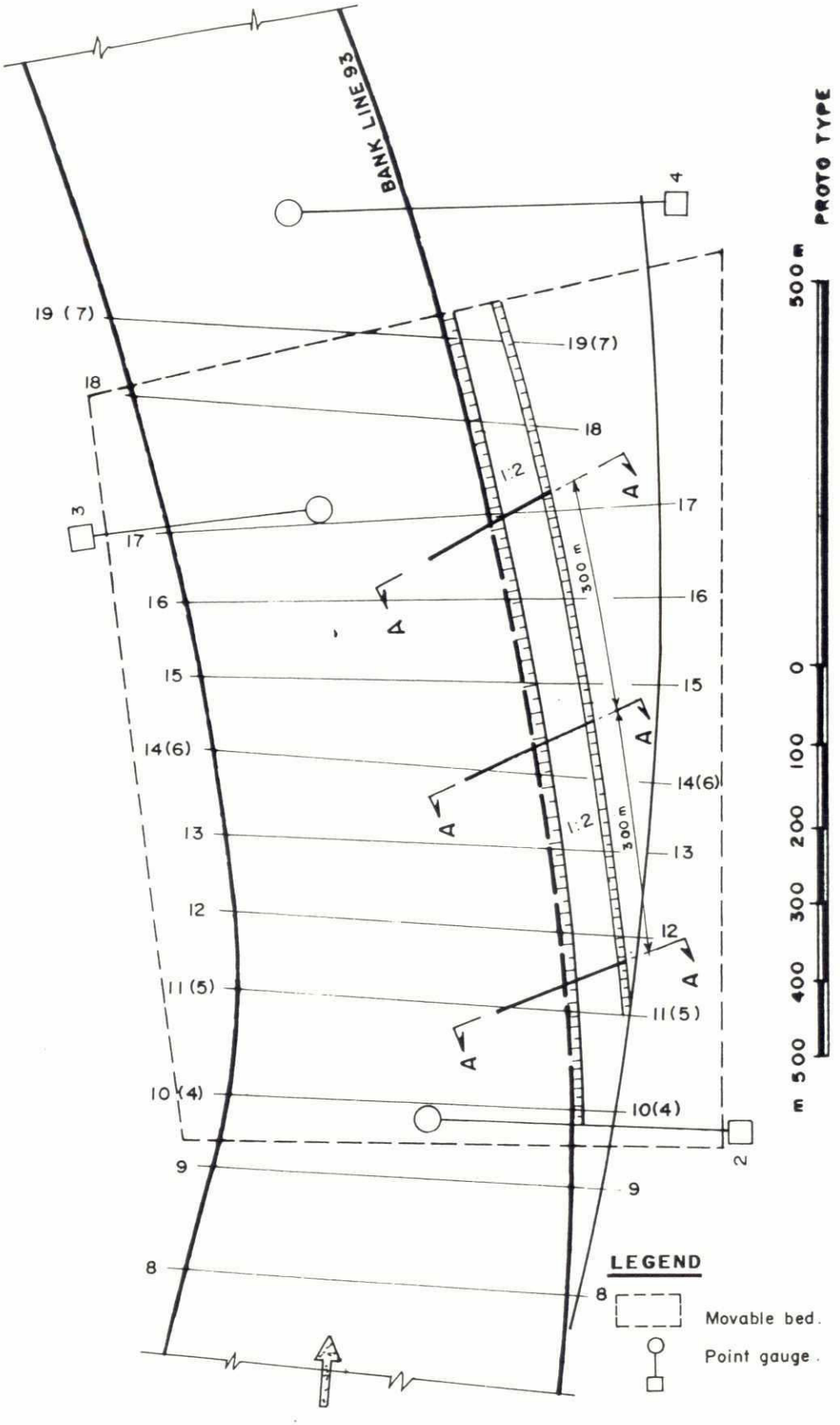




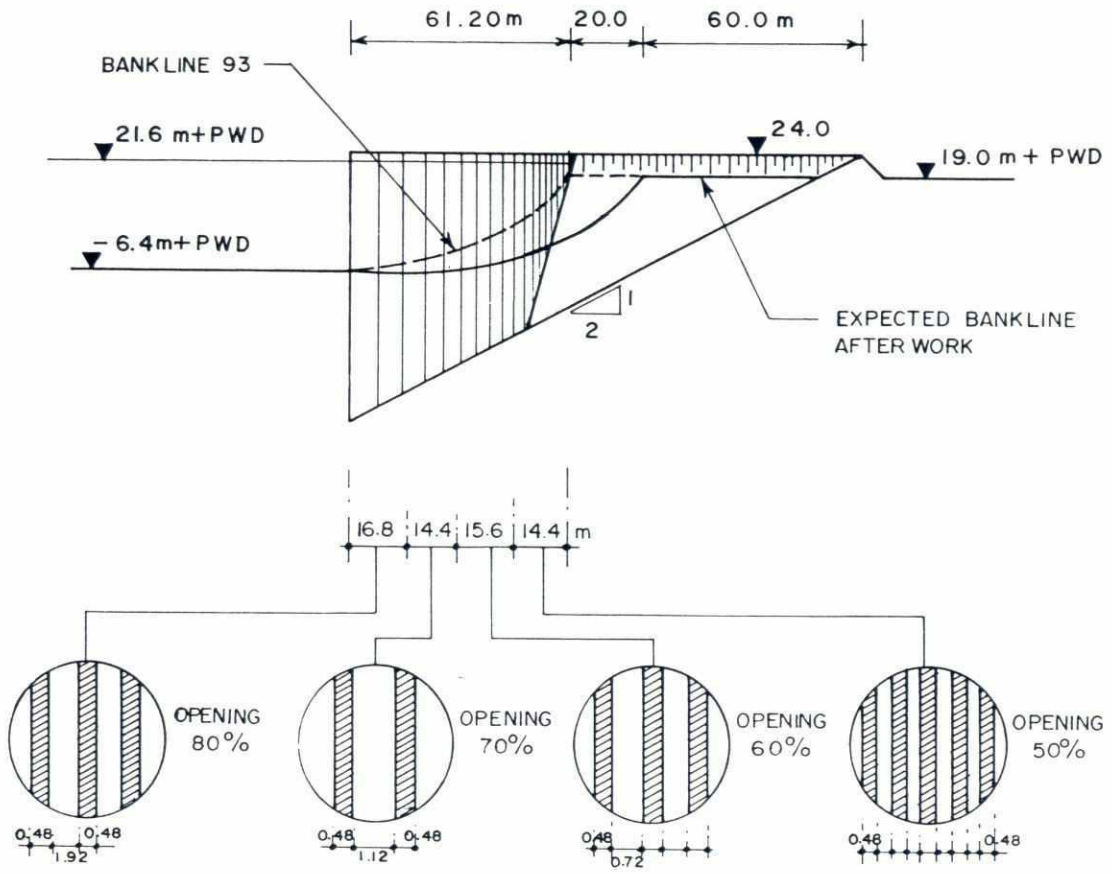
LEGEND

1. LOCATION OF DEEPEST POINT ····· ◀

KAMARJANI MODEL DEEPEST POINT OF SCOUR HOLE TEST : T 7	FAP – 21/22 BANK PROTECTION AND RIVER TRAINING / (AFPM) PILOT PROJECT
	FINAL REPORT | FIG. A.14-30



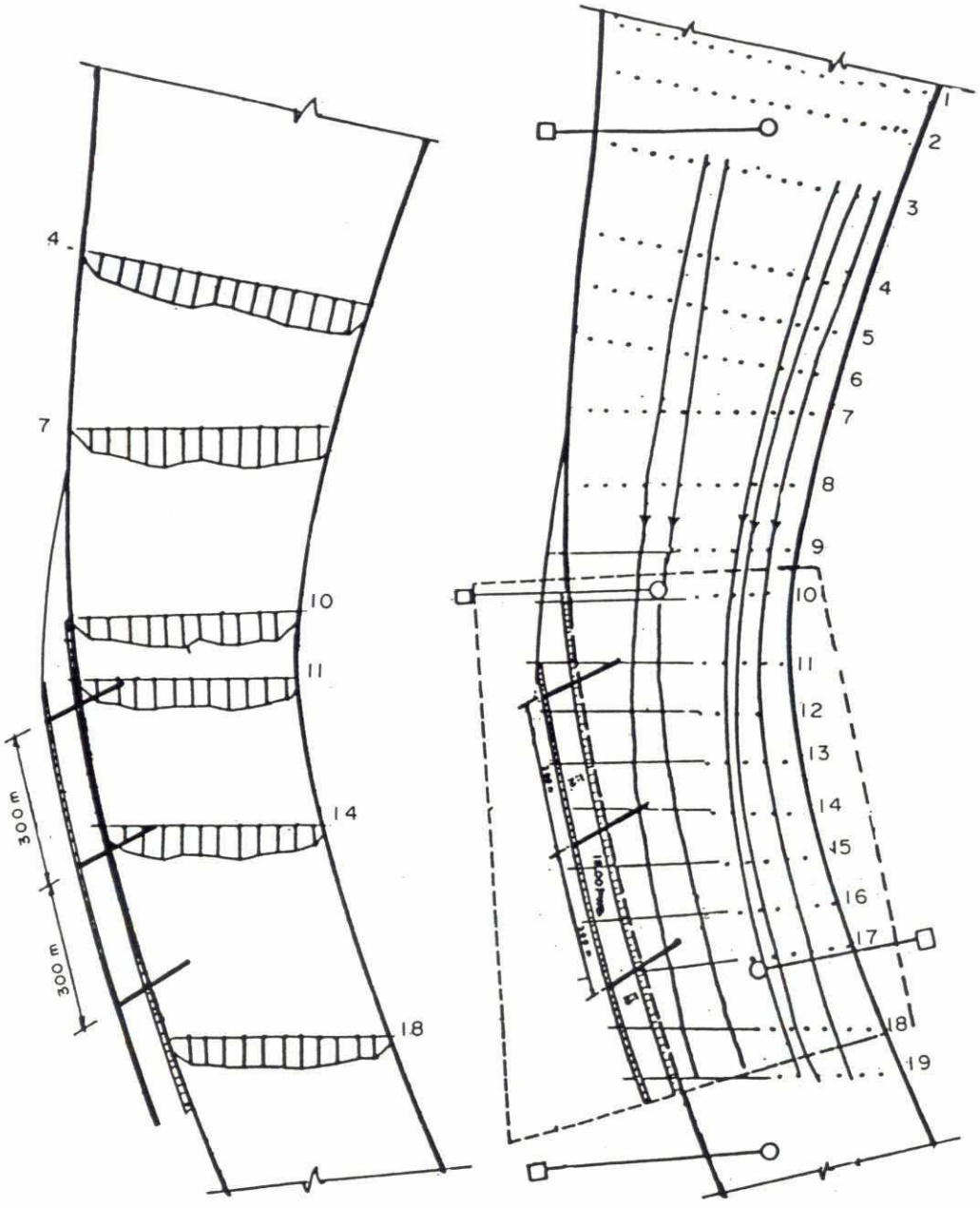
KAMARJANI MODEL TEST T 10	FAP – 21/22 BANK PROTECTION AND RIVER TRAINING / (AFPM) PILOT PROJECT	
	FINAL REPORT	FIG. A.14-31



SECTION A-A



KAMARJANI MODEL TEST T 10	FAP – 21/22 BANK PROTECTION AND RIVER TRAINING / (AFPM) PILOT PROJECT	
	FINAL REPORT	FIG. A.14–32



Q = 240 l/s

0 4 8 m/Sec

m 500 400 300 200 100 0 500 m

Prototype

LEGEND:

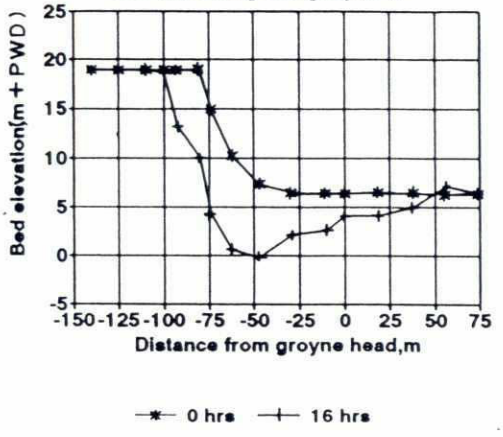
Flow line

Point gauge

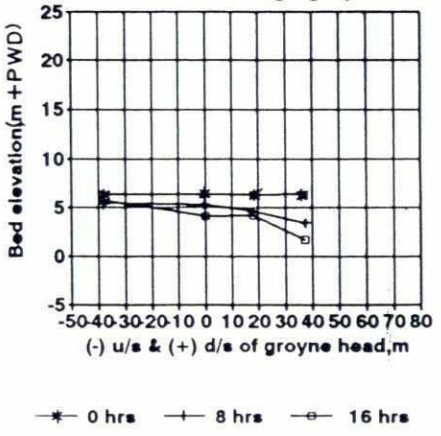
Movable bed

KAMARJANI MODEL TEST T 10 FLOW LINE & VELOCITY PROFILE	FAP – 21/22 BANK PROTECTION AND RIVER TRAINING/ (AFPM) PILOT PROJECT	
	FINAL REPORT	FIG. A.14 - 33

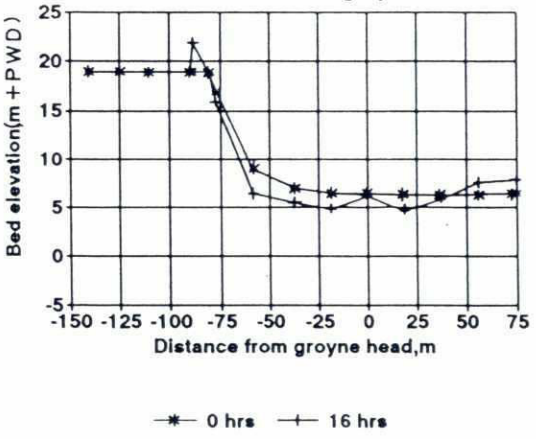
Section along the groyne-1



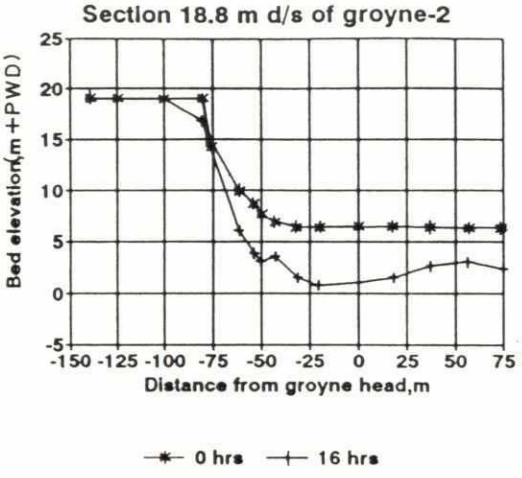
Transverse section through groyne head

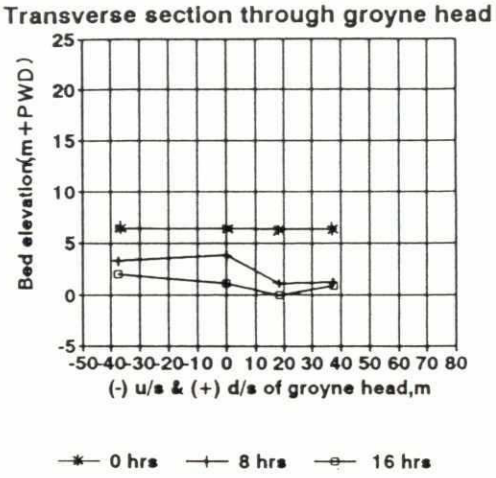


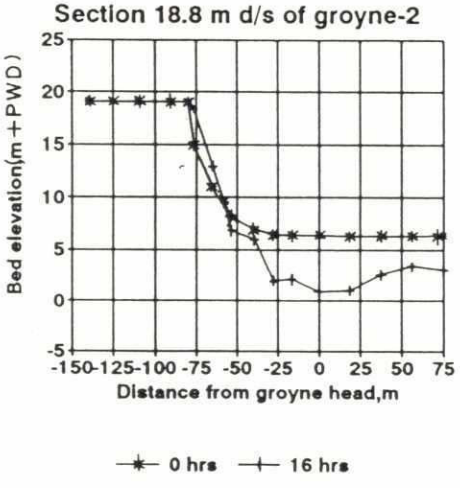
Section 18.8 m d/s of groyne-1



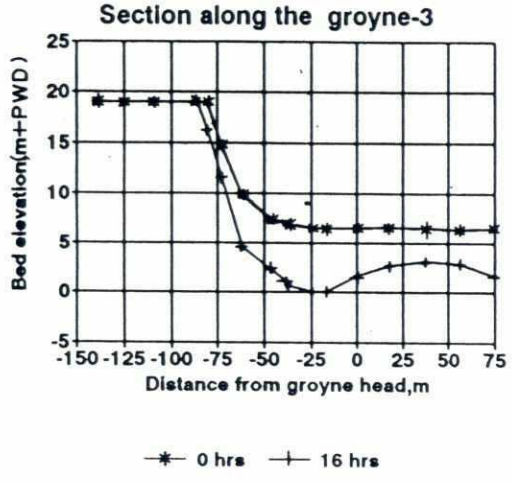
KAMARJANI MODEL TEST T 10 GROYNE NO. 1 LONGITUDINAL AND CROSS SECTION	FAP – 21/22 BANK PROTECTION AND RIVER TRAINING / (AFPM) PILOT PROJECT FINAL REPORT | FIG. A.14-34

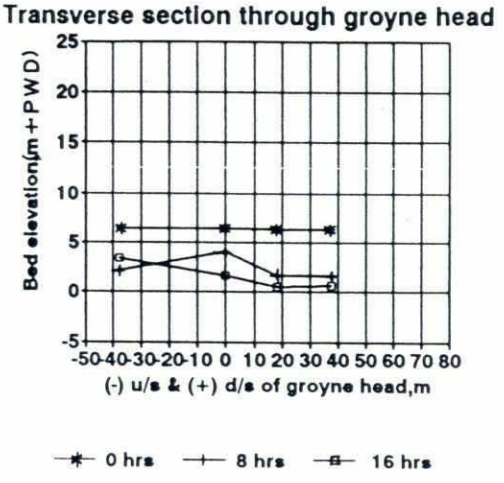


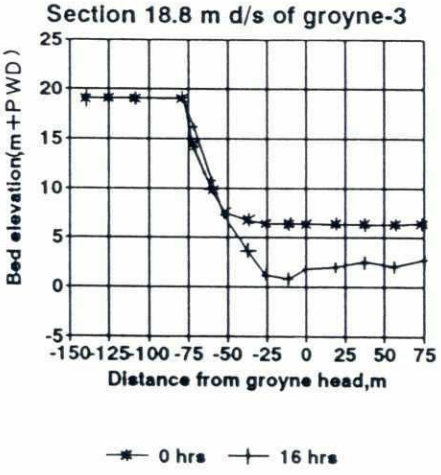




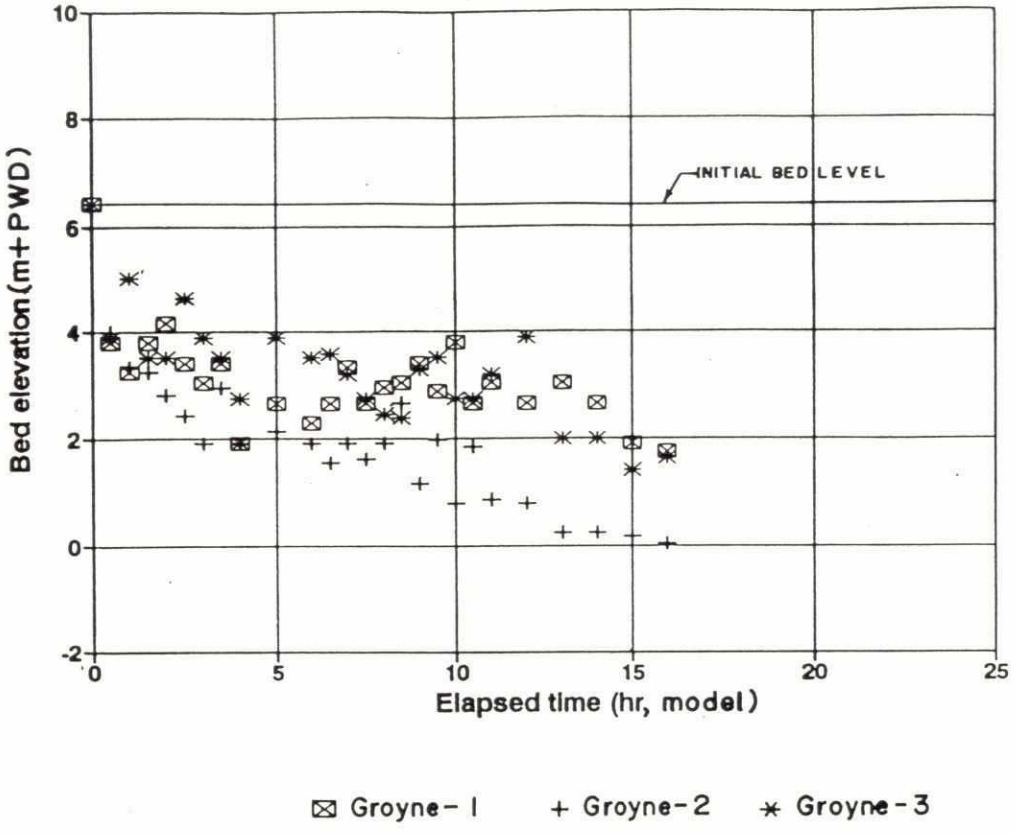
KAMARJANI MODEL **TEST T 10** GROYNE NO. 2 LONGITUDINAL AND CROSS SECTION	**FAP – 21/22** BANK PROTECTION AND RIVER TRAINING / (AFPM) PILOT PROJECT FINAL REPORT | FIG. A.14-35

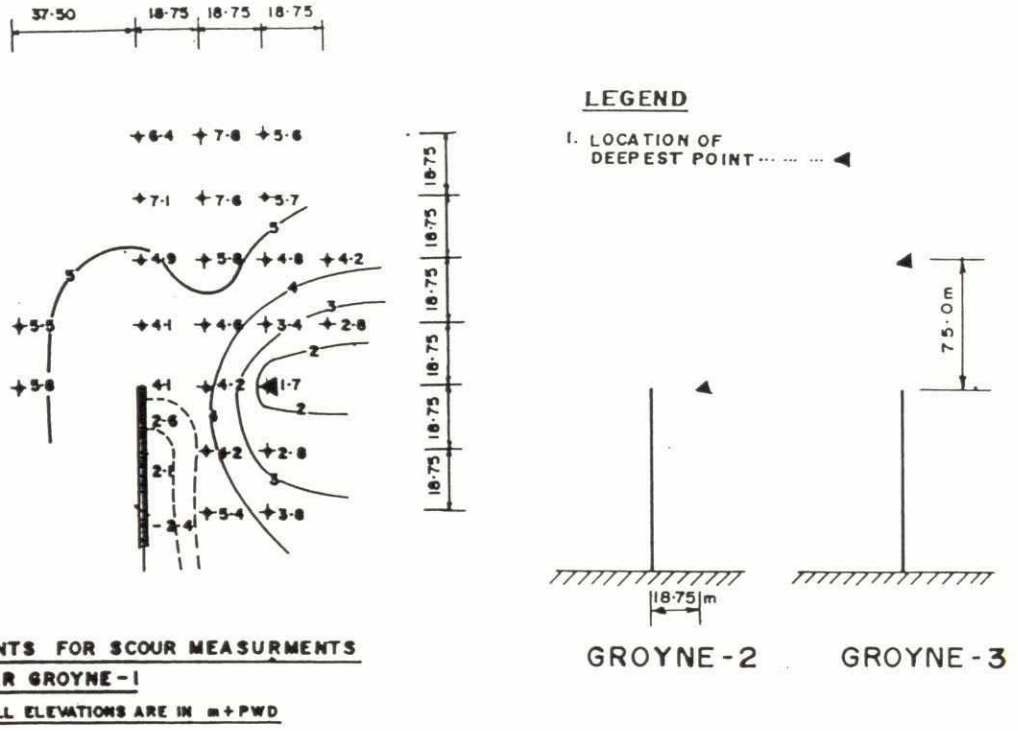




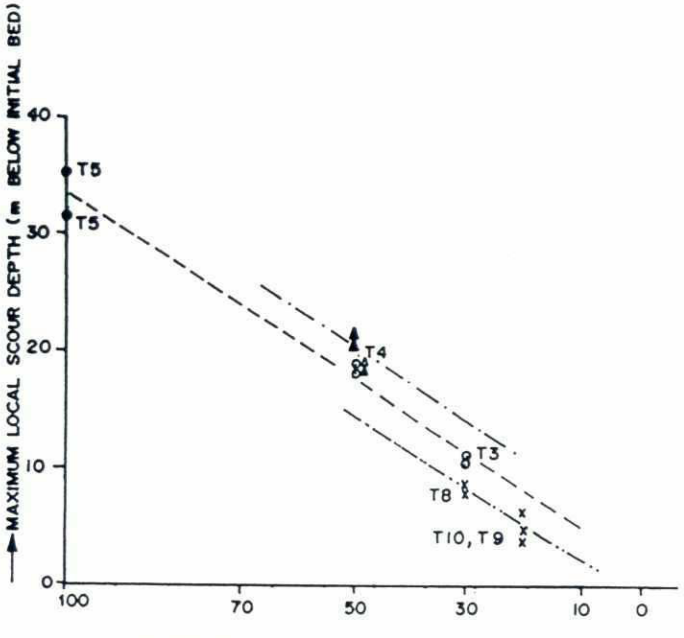


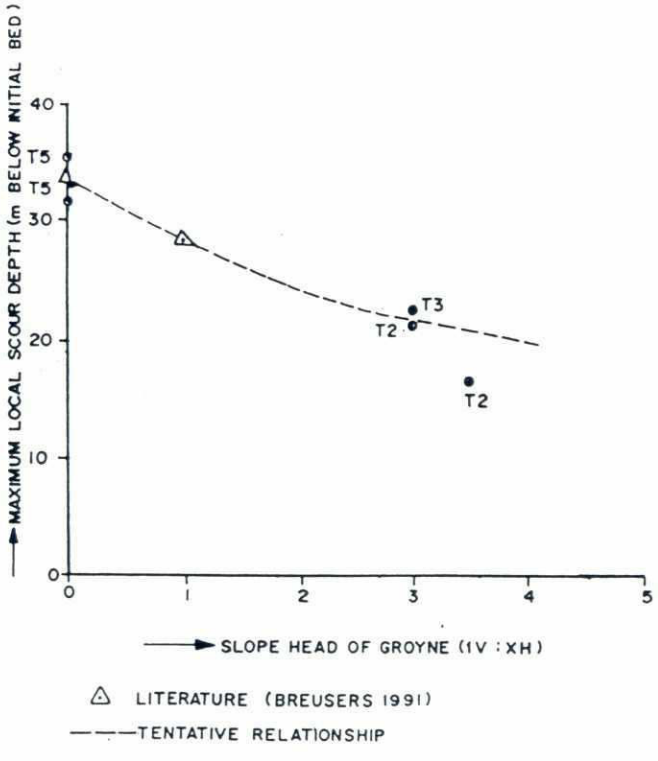
KAMARJANI MODEL TEST T 10 GROYNE NO. 3 LONGITUDINAL AND CROSS SECTION	FAP – 21/22 BANK PROTECTION AND RIVER TRAINING / (AFPM) PILOT PROJECT	
	FINAL REPORT	FIG. A.14-36



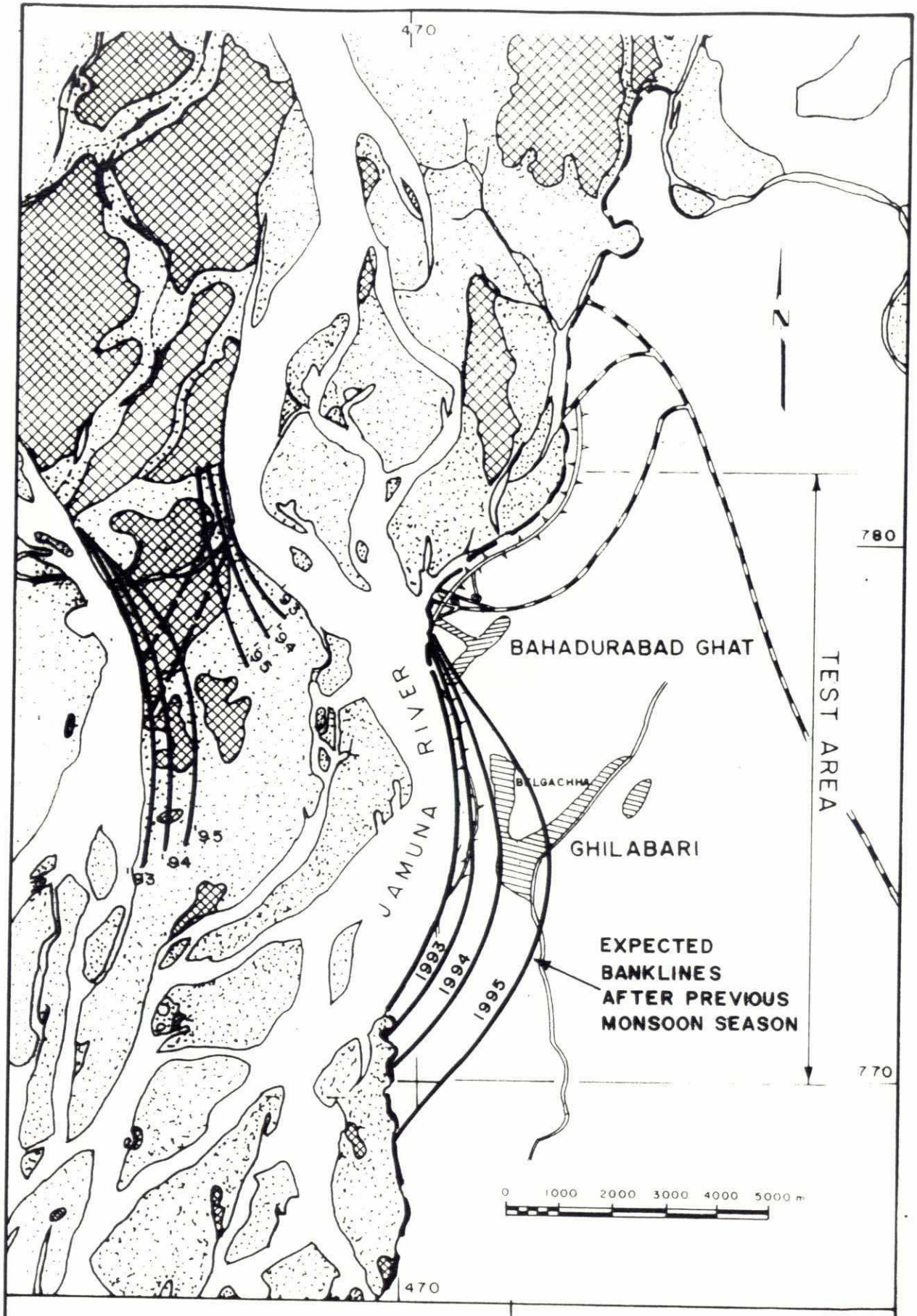


KAMARJANI MODEL **DEEPEST POINT OF SCOUR HOLE** **TEST : T 10**	**FAP – 21/22** BANK PROTECTION AND RIVER TRAINING / (AFPM) PILOT PROJECT FINAL REPORT | FIG. A.14 – 37





KAMARJANI MODEL SCOUR DEPTH AS A FUNCTION OF BLOCKAGE AND SLOPE	FAP – 21/22 BANK PROTECTION AND RIVER TRAINING/ (AFPM) PILOT PROJECT	
	FINAL REPORT	FIG. A.14–38



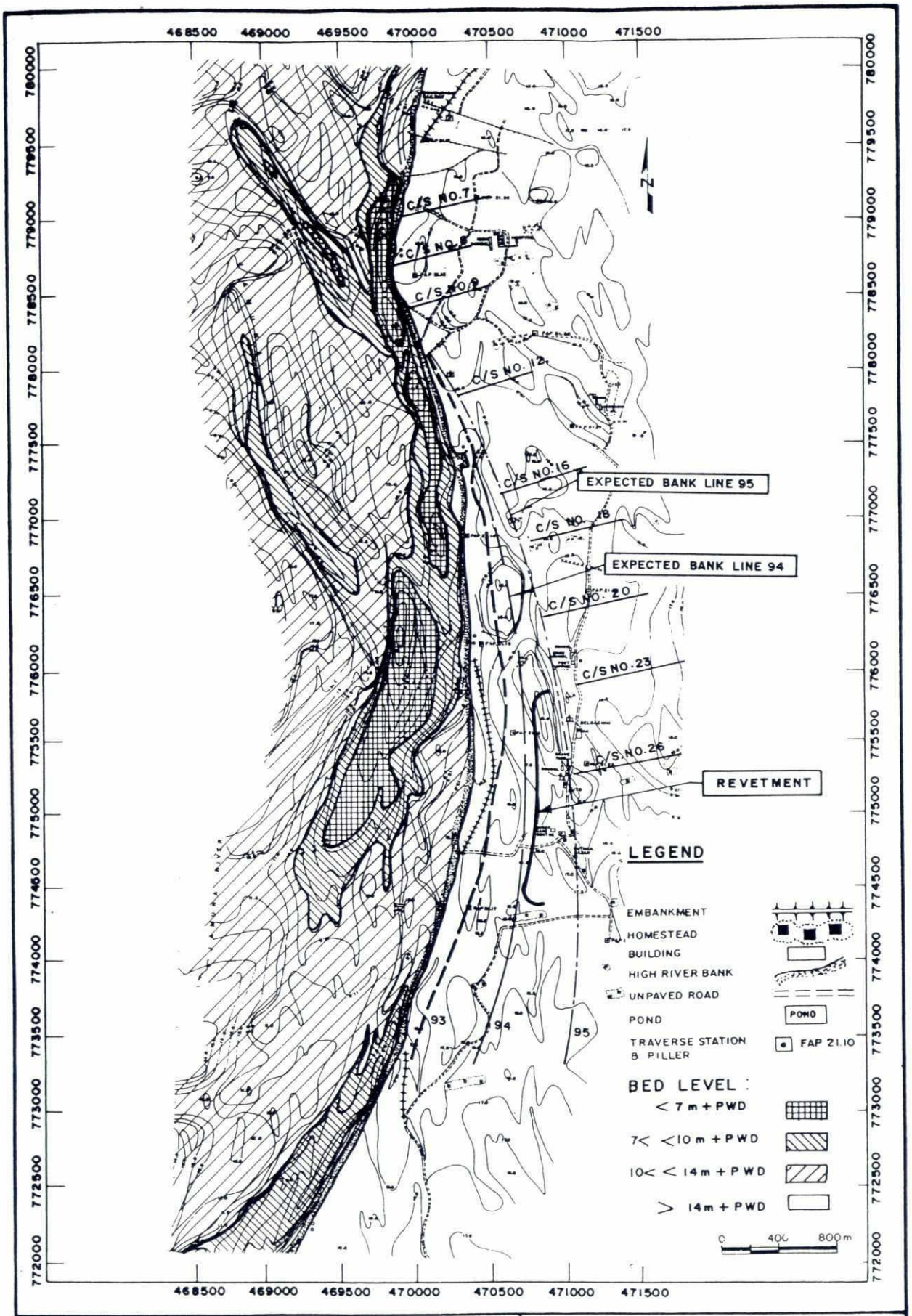
LOCATION OF BAHADURABAD AND EXPECTED BANK EROSION

FAP - 21/22

BANK PROTECTION AND RIVER TRAINING/ (AFPM) PILOT PROJECT

FINAL REPORT

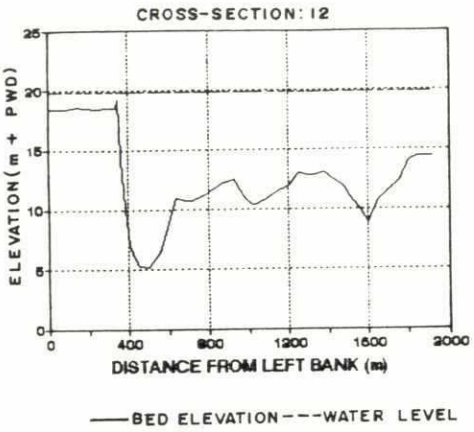
FIG. A.14-39

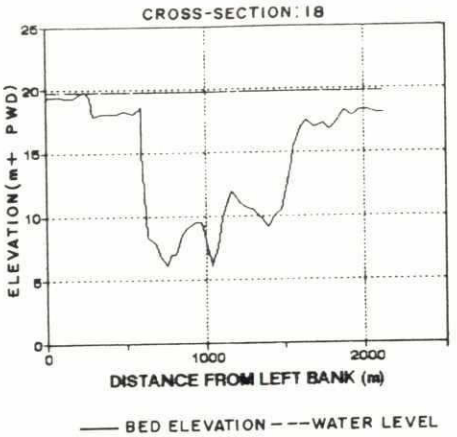


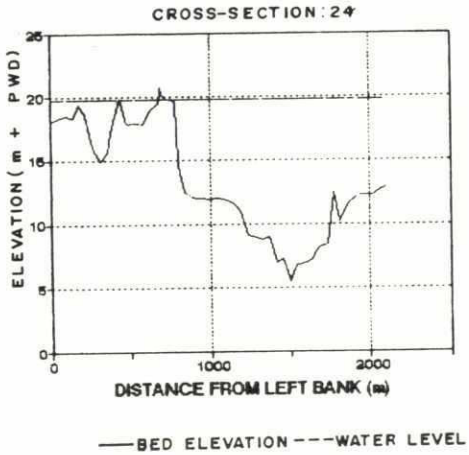
BAHADURABAD SITE SURVEY
(MARCH 1992)

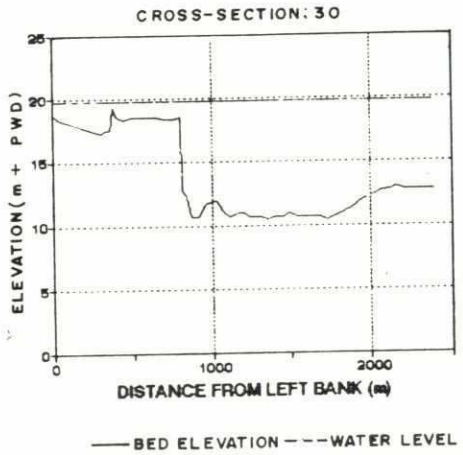
FAP -- 21/22
BANK PROTECTION AND RIVER TRAINING / (AFPM) PILOT PROJECT

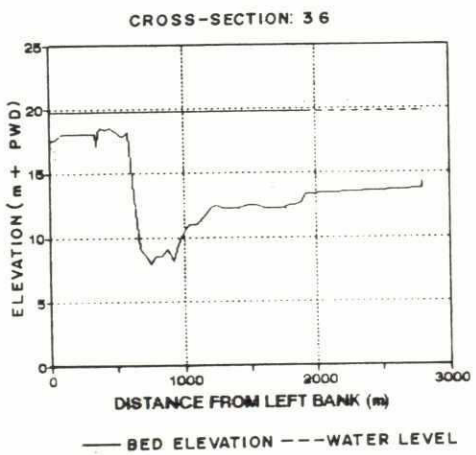
FINAL REPORT | FIG. A.14-40

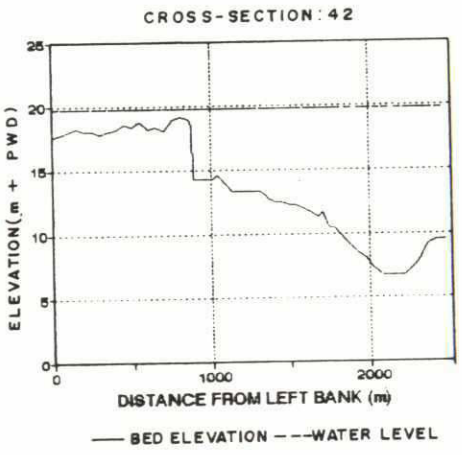








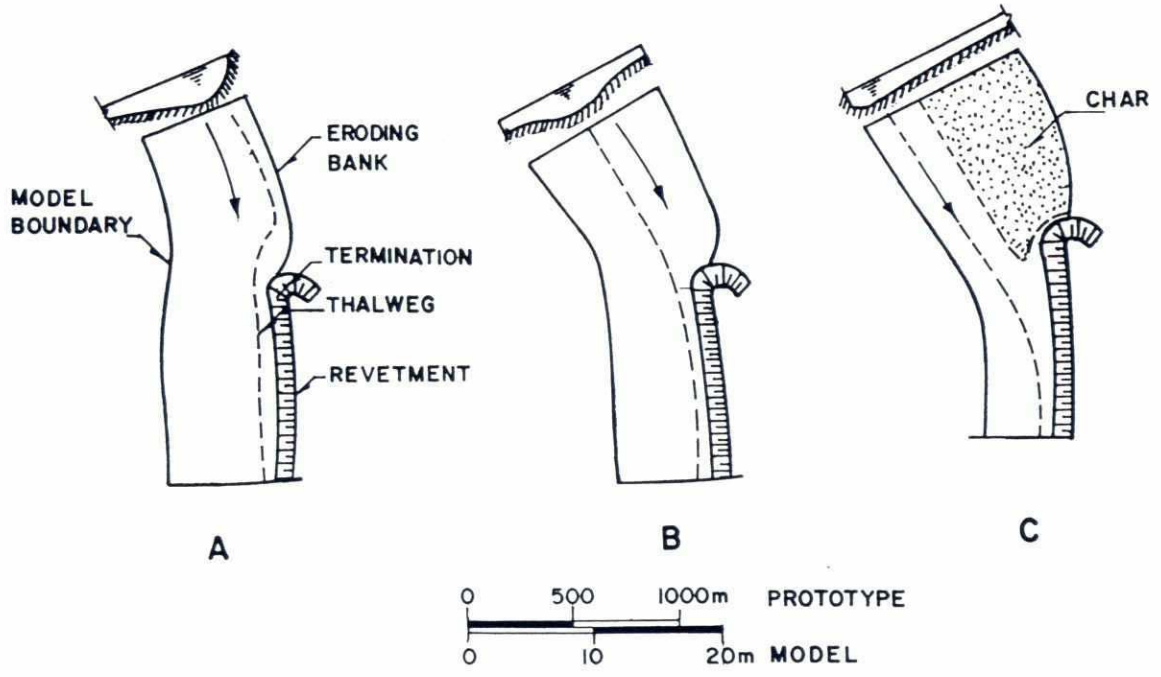




BAHADURABAD
CROSS SECTIONS

FAP – 21/22
BANK PROTECTION AND RIVER TRAINING / (AFPM) PILOT PROJECT

FINAL REPORT | FIG. A.14-41

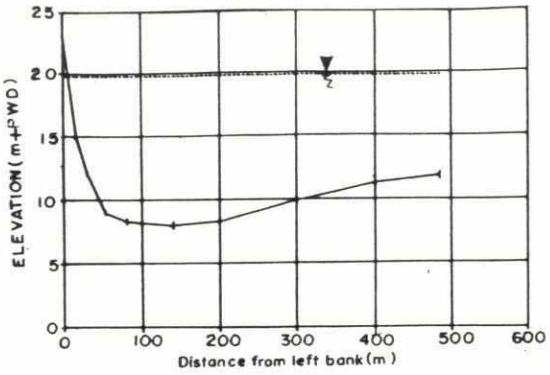


LEGEND

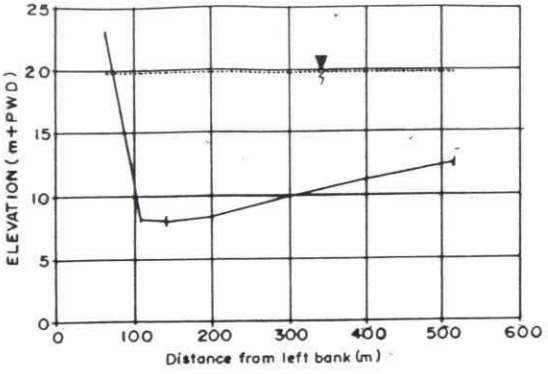
A, B, C – EXTREME ALIGNMENT OF APPROACH CHANNEL

BAHADURABAD MODEL DIFFERENT APPROCH CHANNELS	FAP – 21/22 BANK PROTECTION AND RIVER TRAINING / (AFPM) PILOT PROJECT	
	FINAL REPORT	FIG. A. 14– 42

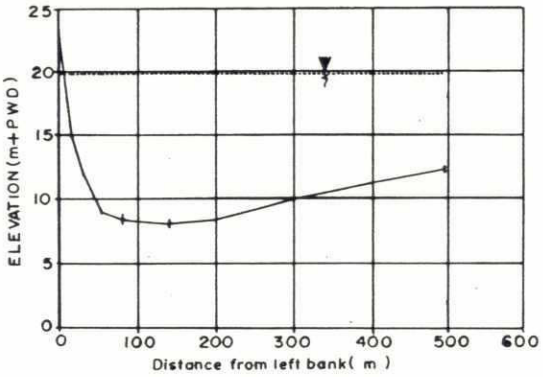
C.S. 1



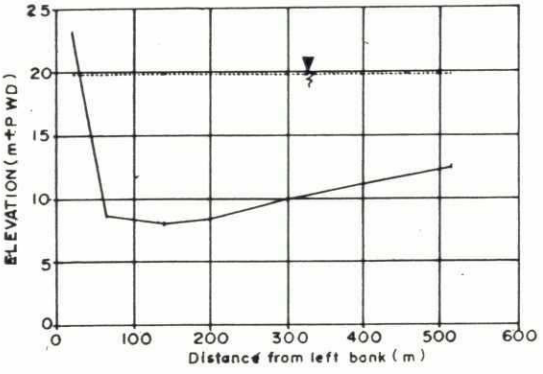
C.S. 9



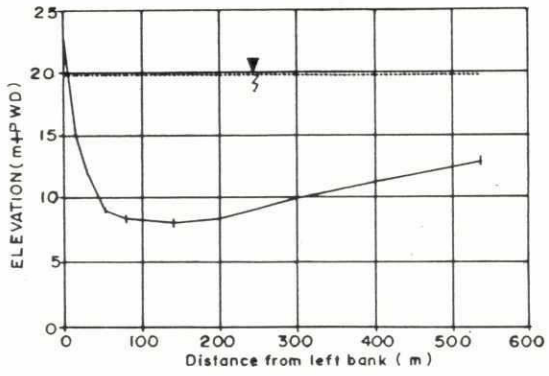
C.S. 3



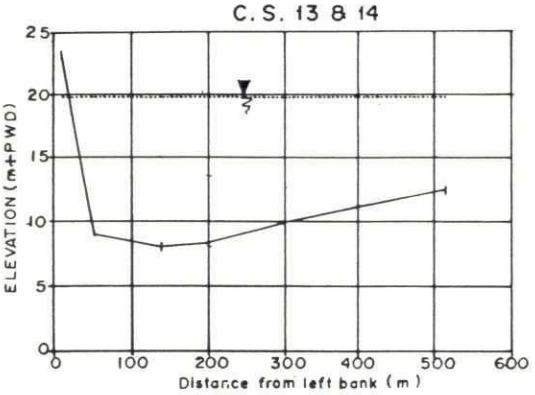
C.S. 11



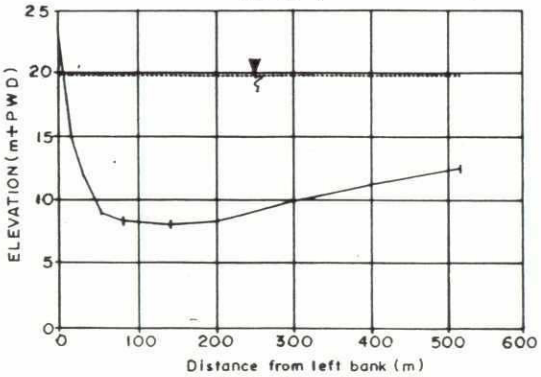
C.S. 5



C.S. 13 & 14



C.S. 7



BAHADURABAD MODEL

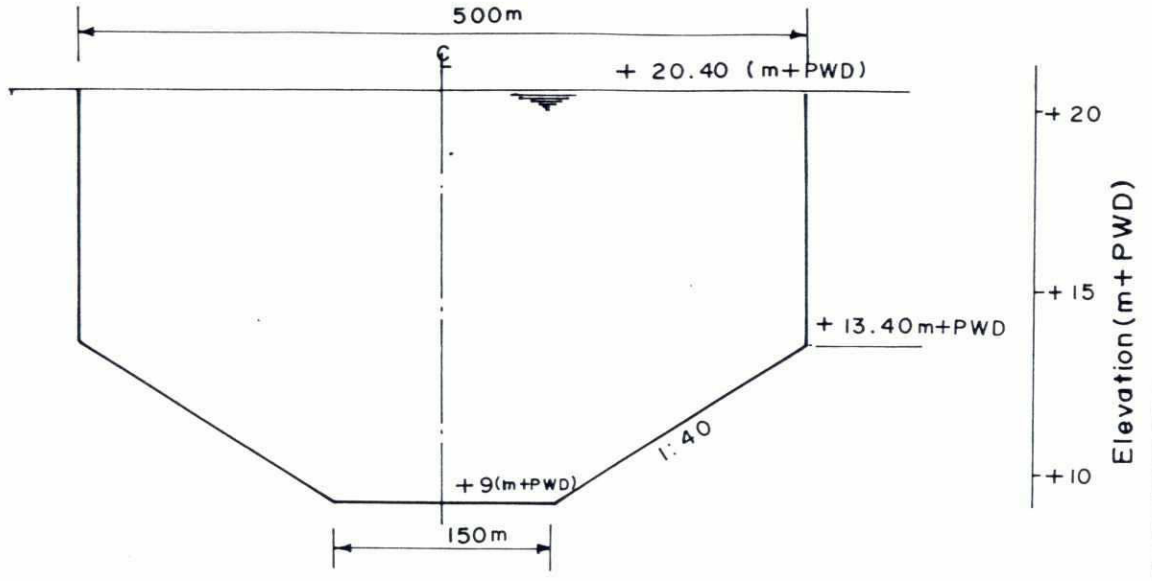
CROSS SECTIONS

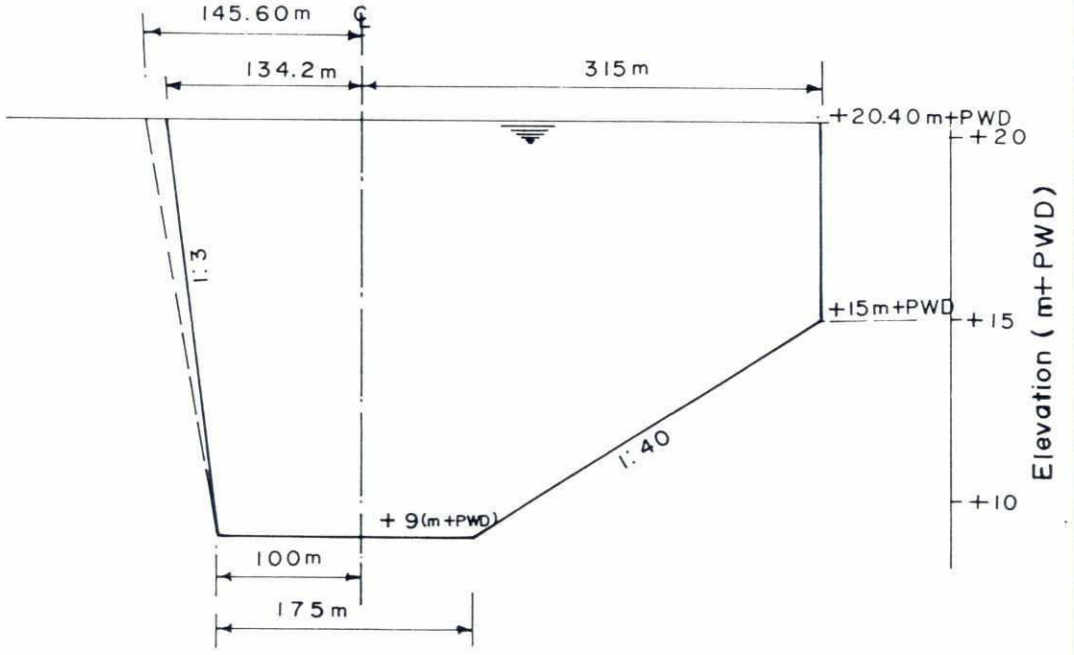
TYPE A

FAP – 21/22

BANK PROTECTION AND RIVER TRAINING / (AFPM) PILOT PROJECT

FINAL REPORT | FIG. A.14-43

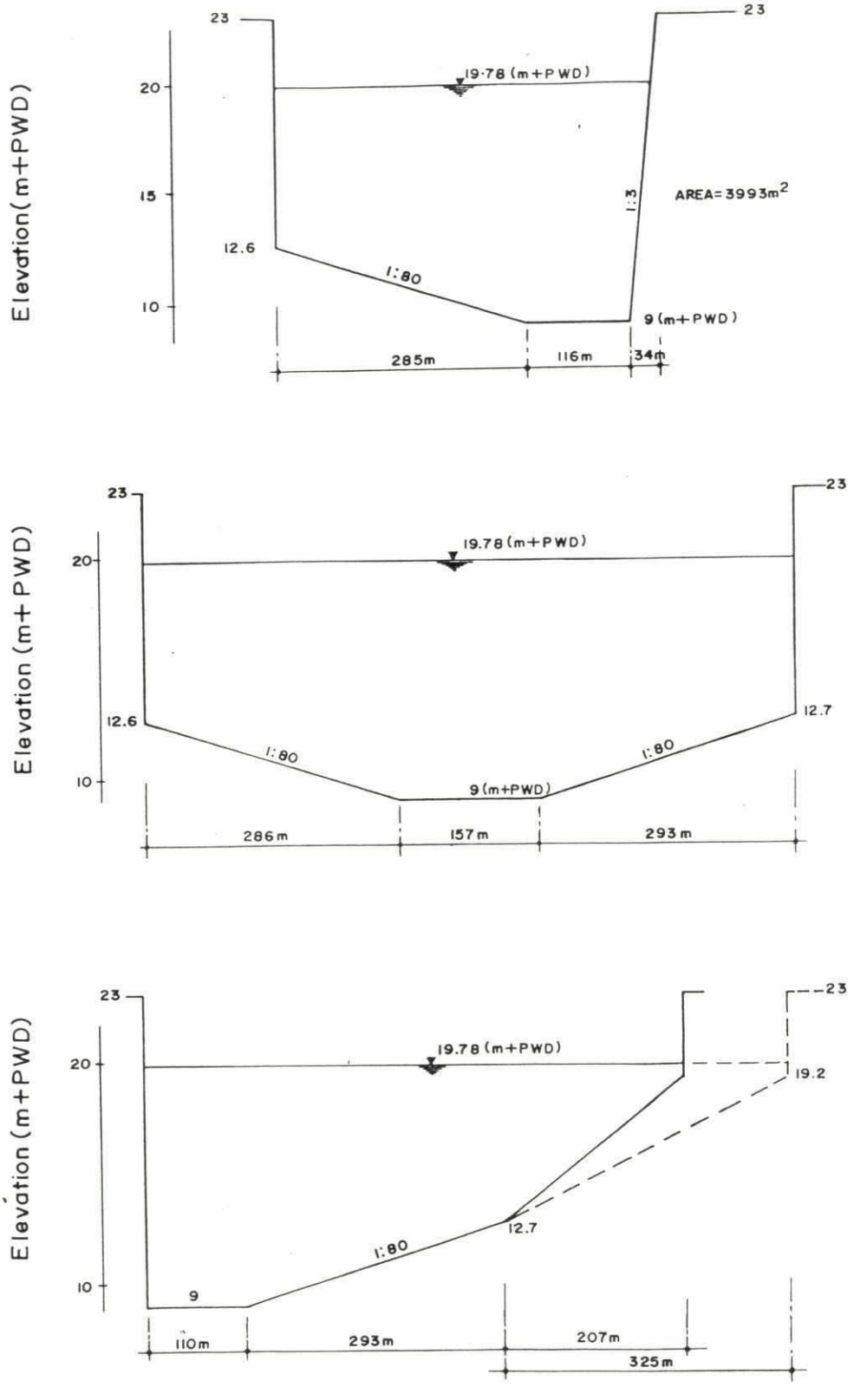




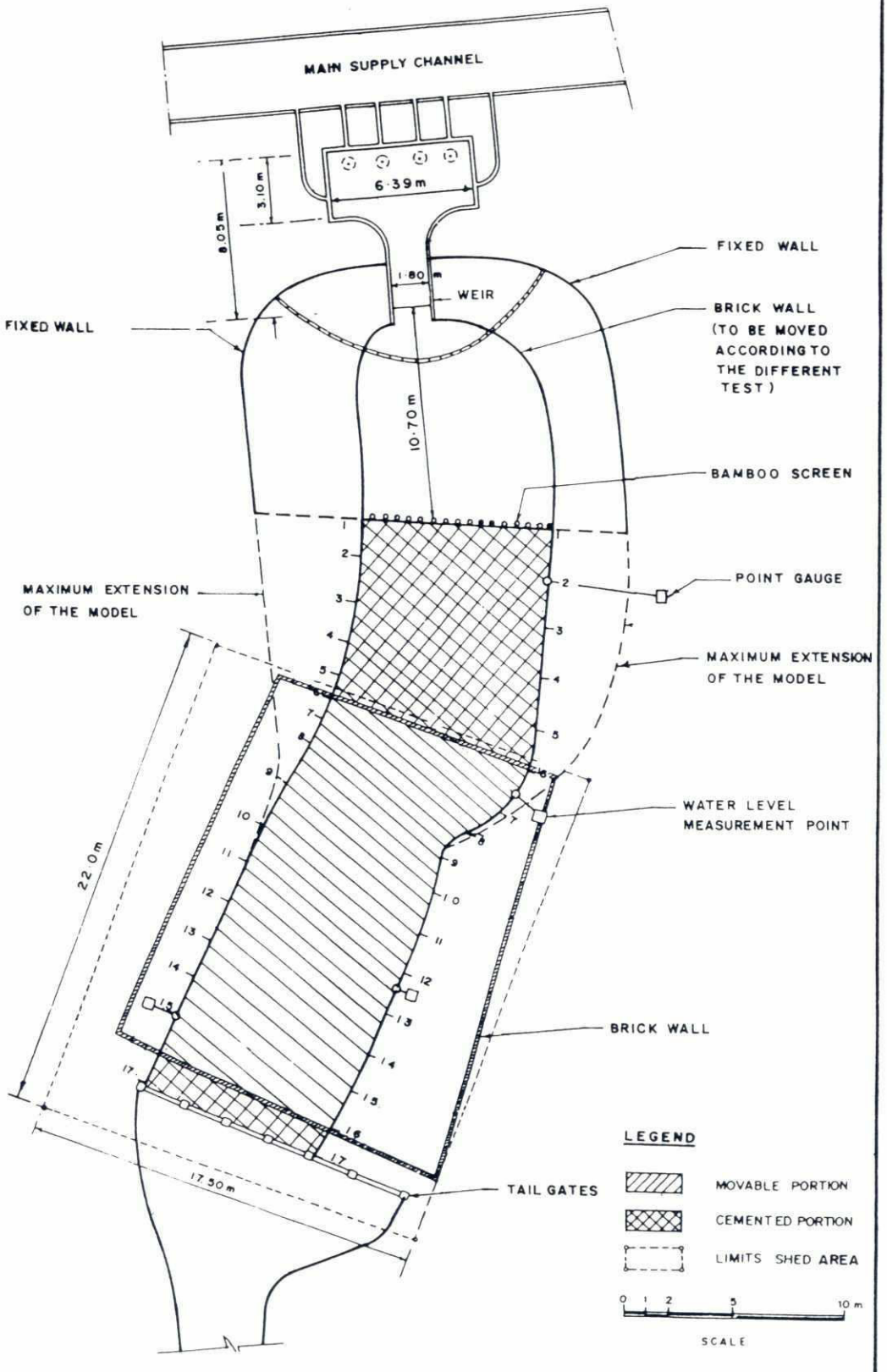
BAHADURABAD MODEL
CROSS SECTIONS
TYPE B

FAP – 21/22
BANK PROTECTION AND RIVER TRAINING / (AFPM) PILOT PROJECT

FINAL REPORT | FIG. A. 14–44



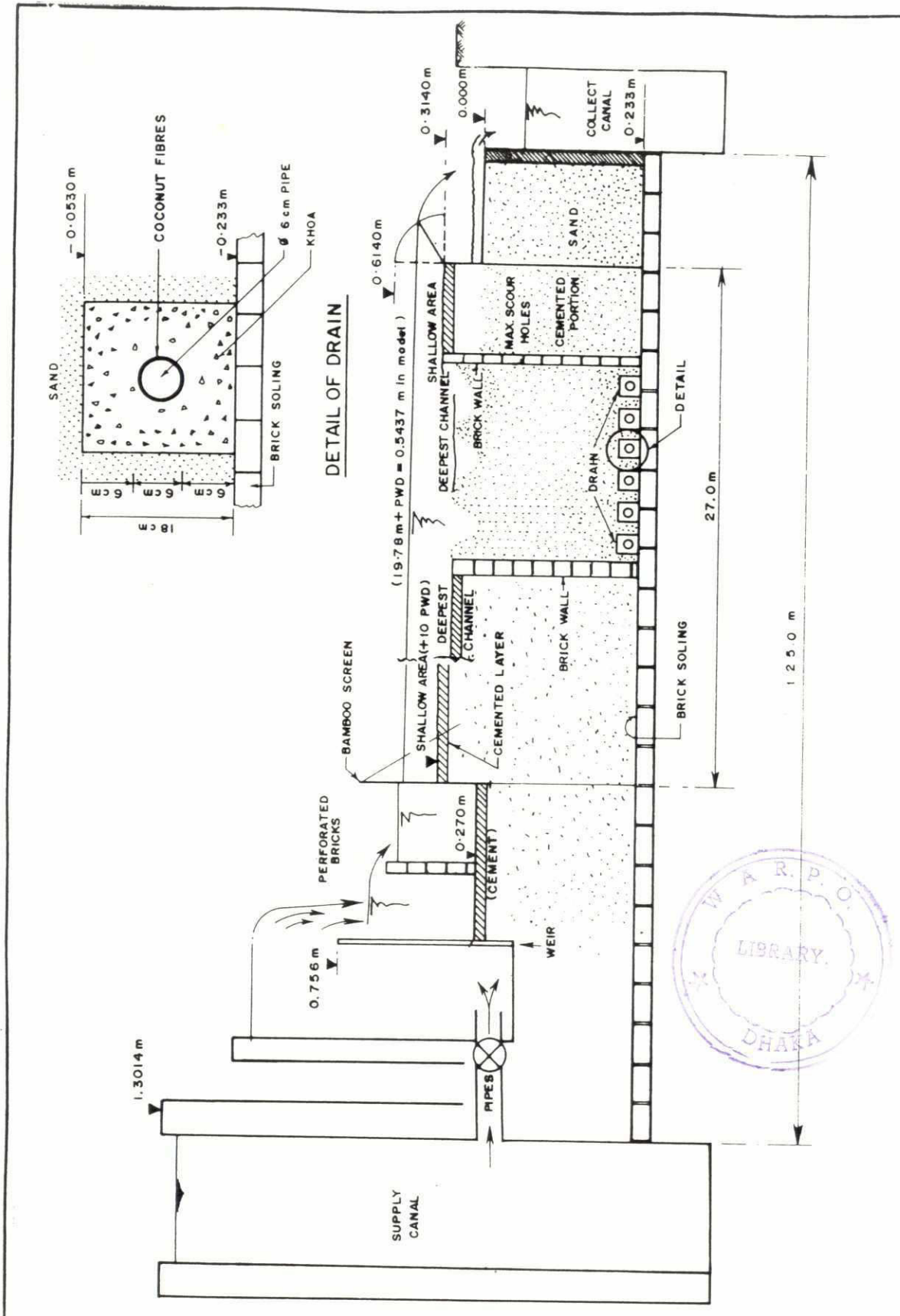
BAHADURABAD MODEL CROSS SECTIONS TYPE C	FAP – 21/22 BANK PROTECTION AND RIVER TRAINING / (AFPM) PILOT PROJECT	
	FINAL REPORT	FIG. A.14–45



LAY-OUT OF BAHADURABAD MODEL
(SCALE OF THE MODEL: 1/60)

FAP – 21/22
BANK PROTECTION AND RIVER TRAINING / (AFPM) PILOT PROJECT

FINAL REPORT | FIG. A.14-46



W A R P O
LIBRARY
DHAKA

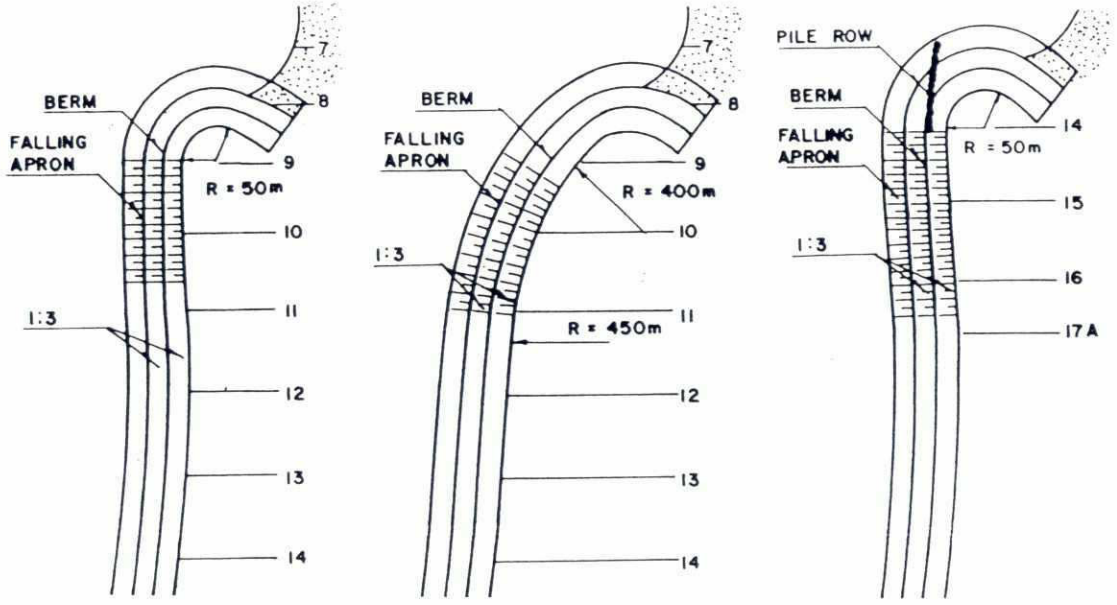
BAHADURABAD SCALE MODLE

(LONGITUDINAL SECTION)

FAP – 21/22

BANK PROTECTION AND RIVER TRAINING / (AFPM) PILOT PROJECT

FINAL REPORT | FIG. A.14– 47

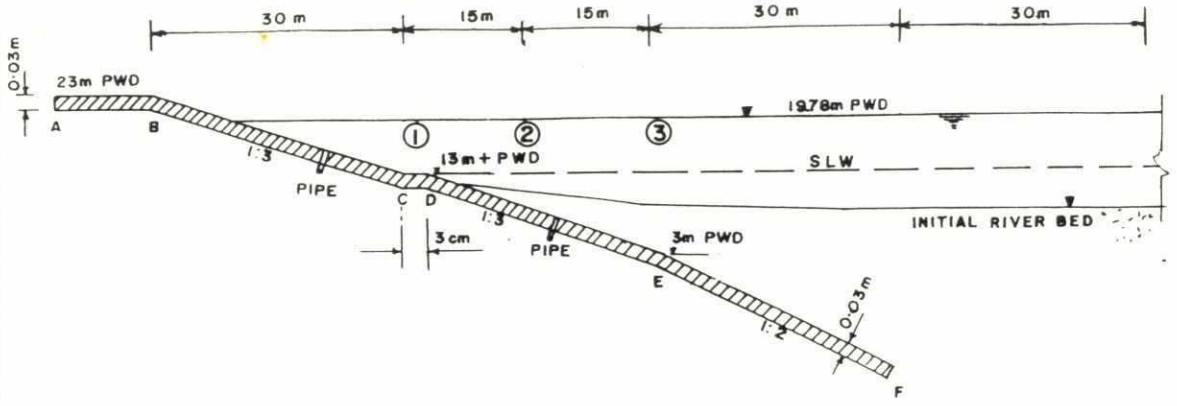


LEGEND

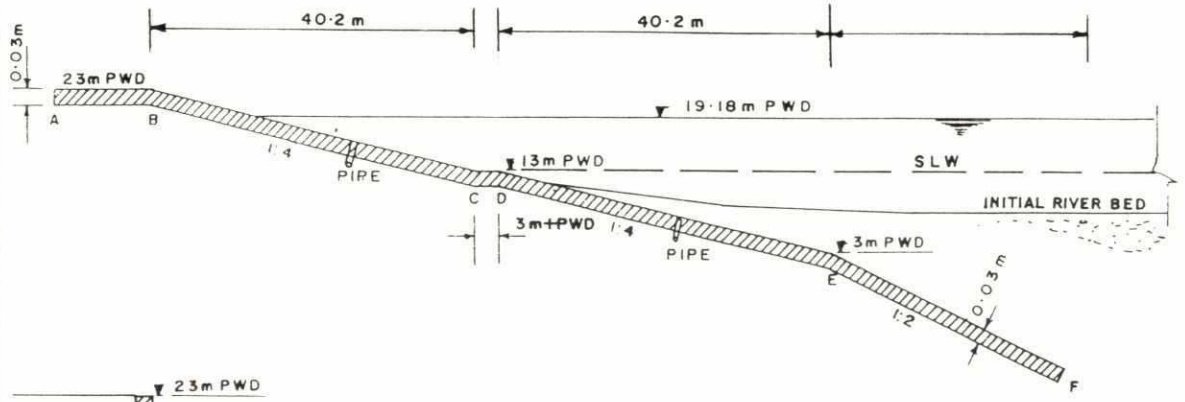
I ..... TERMINETION I WITH R = 50 m.

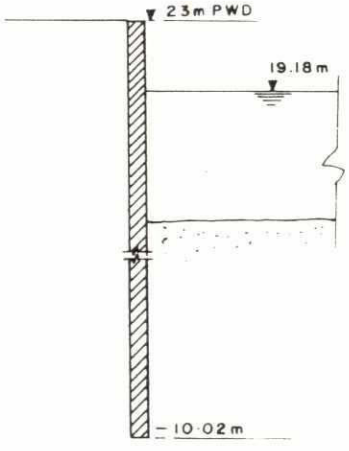
BAHADURABAD MODEL LAY OUT OF THREE UPSTREAM TERMINATION	FAP – 21/22 BANK PROTECTION AND RIVER TRAINING / (AFPM) PILOT PROJECT	
	FINAL REPORT	FIG. A.14-48

G&Q



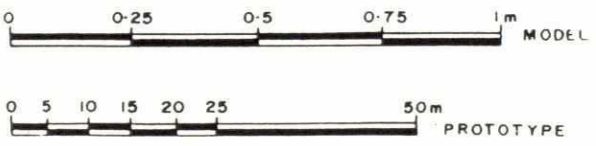
CROSS SECTION
SLOPE 1:3



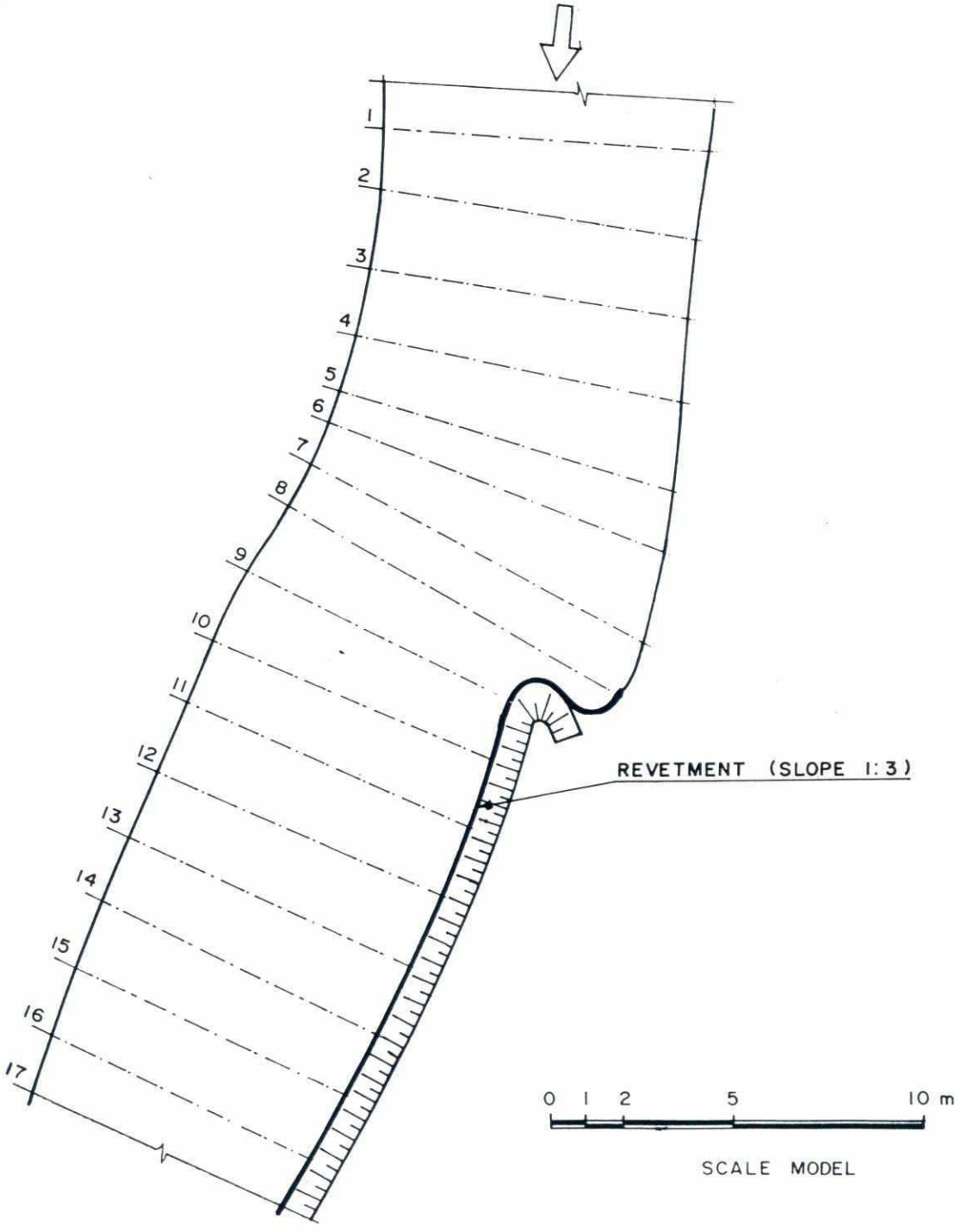


SHEET PILE

CROSS SECTION
SLOPE 1:4



BAHADURABAD REVETMENT SLOPE 1:3 & 1:4 AND VERTICAL SHEET PILE	**FAP – 21/22** BANK PROTECTION AND RIVER TRAINING / (AFPM) PILOT PROJECT
	FINAL REPORT | FIG. A.14-49



BAHADURABAD MODEL

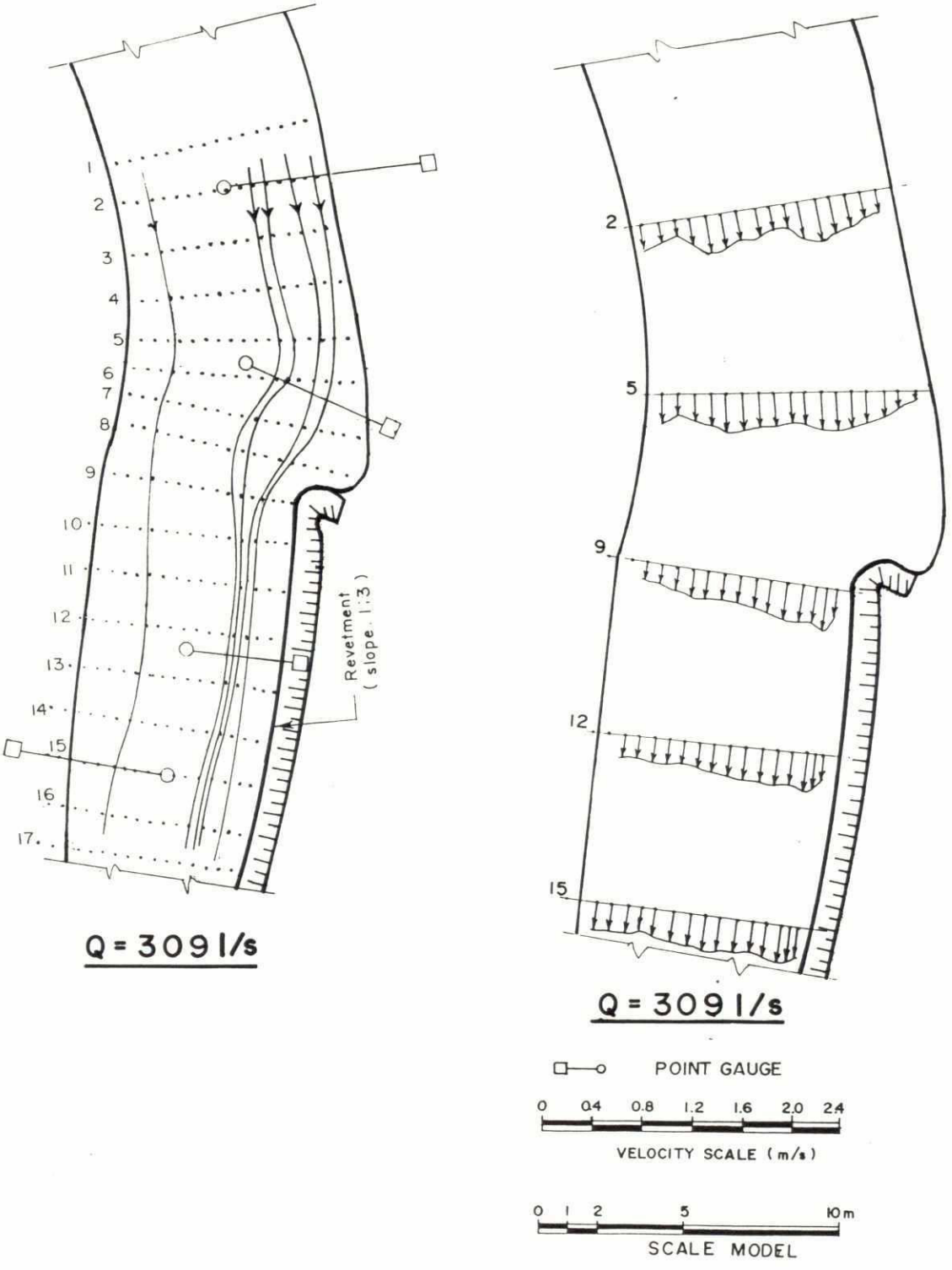
LAYOUT PLAN OF

TEST T 2

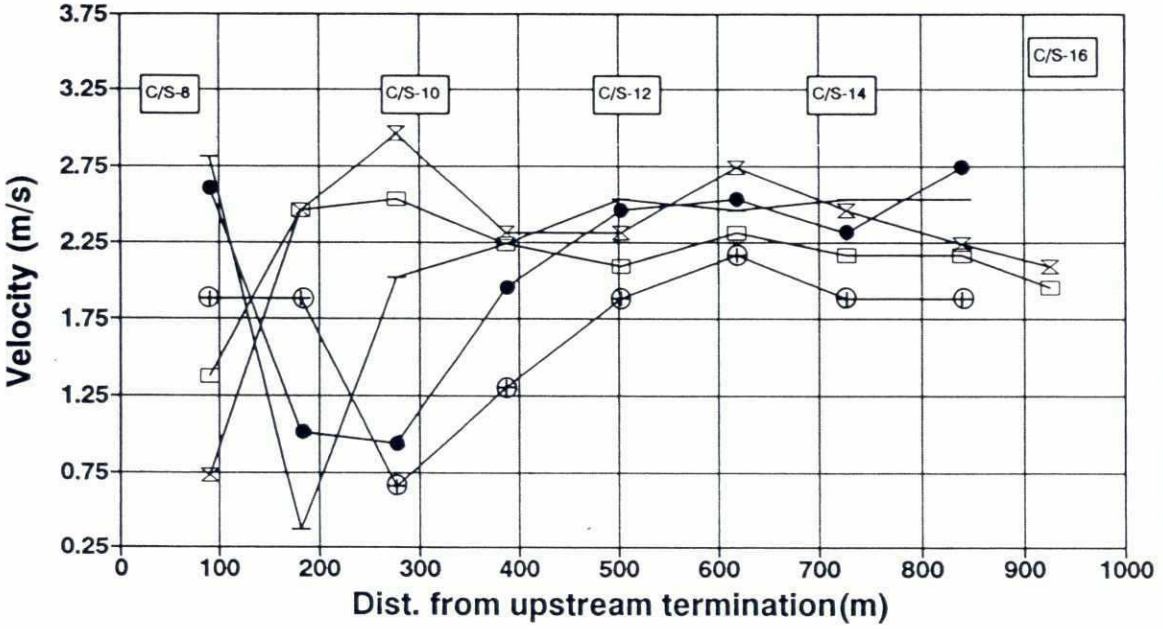
FAP – 21/22

BANK PROTECTION AND RIVER TRAINING / (AFPM) PILOT PROJECT

FINAL REPORT | FIG. A.14-50



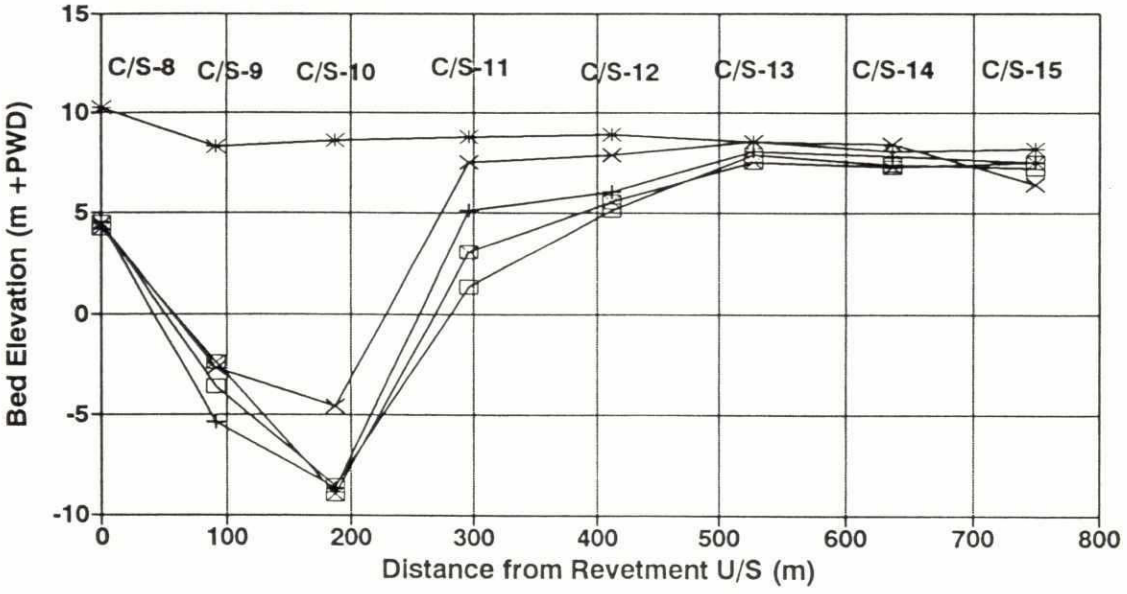
BAHADURABAD MODEL **TEST T 2** FLOW LINE & VELOCITY PROFILE	**FAP – 21/22** BANK PROTECTION AND RIVER TRAINING / (AFPM) PILOT PROJECT
	FINAL REPORT | FIG. A.14 – 51



LEGEND

- 30 m from L.B.
- 45 m from L.B.
- 60m from L.B.
- 90m from L.B.
- 120.0m from L.B.

BAHADURABAD MODEL VELOCITY ALONG THE REVETMENT TEST T 2	FAP – 21/22 BANK PROTECTION AND RIVER TRAINING / (AFPM) PILOT PROJECT
	FINAL REPORT | FIG. A.14–52



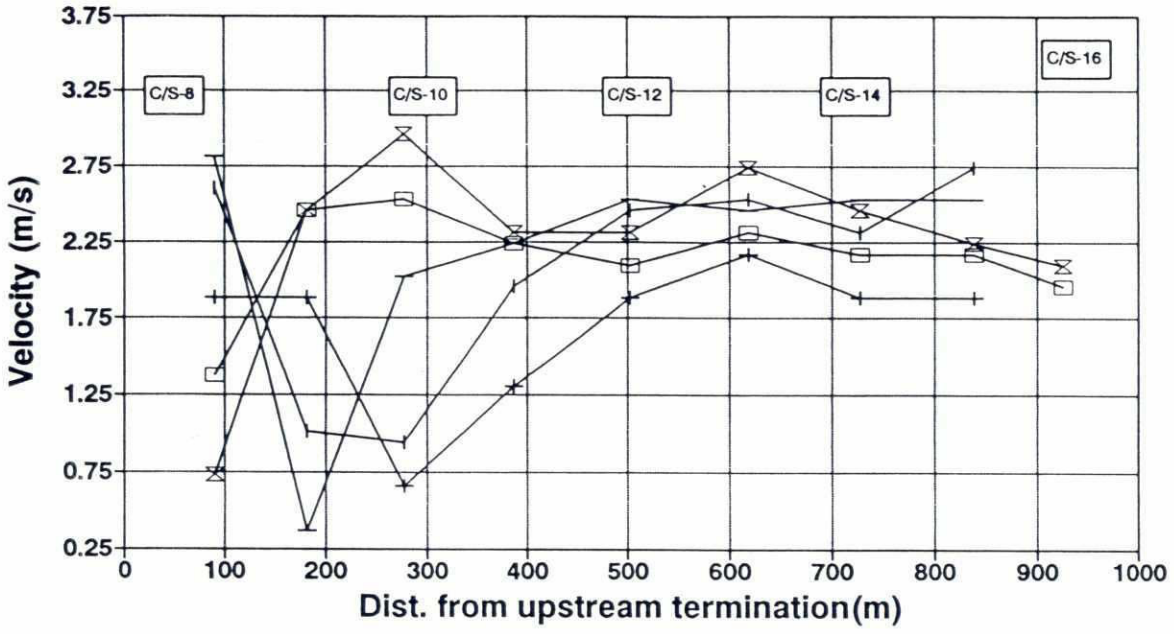
LEGEND

- After 0 hours
- After 4 hours
- After 8 hours
- After 12 hours
- After 16 hours

BAHADURABAD MODEL
LONG SECTIONS OF SCOUR HOLE
TEST T 2

FAP – 21/22
BANK PROTECTION AND RIVER TRAINING/
(AFPM) PILOT PROJECT

FINAL REPORT | FIG. A.14 – 53



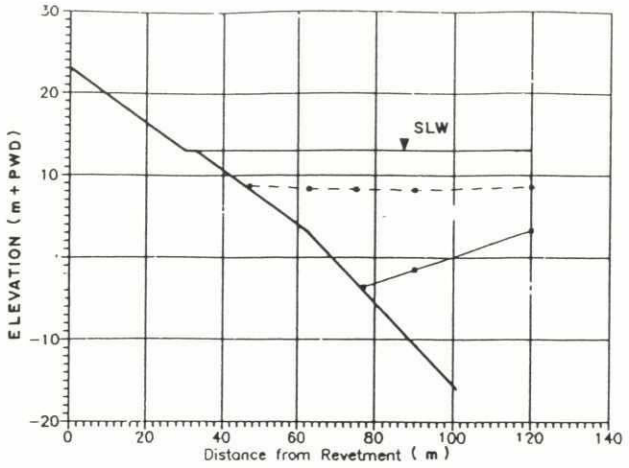
LEGEND

- 30 m from L.B.
- 45 m from L.B.
- 60m from L.B.
- 90m from L.B.
- 120.0m from L.B.

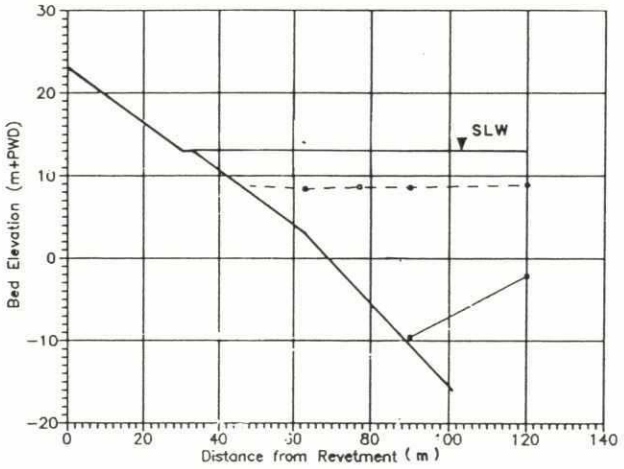
BAHADURABAD MODEL
VELOCITY ALONG THE REVETMENT
TEST T 2

FAP – 21/22
BANK PROTECTION AND RIVER TRAINING / (AFPM) PILOT PROJECT

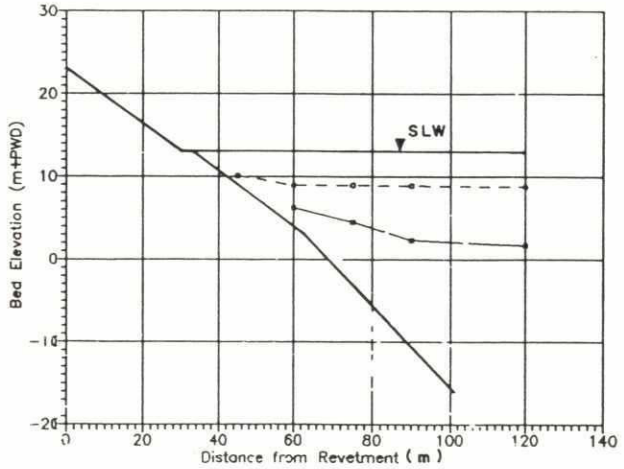
FINAL REPORT | FIG. A.14-54



CROSS SECTION: 9



CROSS SECTION: 10



CROSS SECTION: 11

LEGEND

——— REVETMENT

INITIAL BED LEVEL

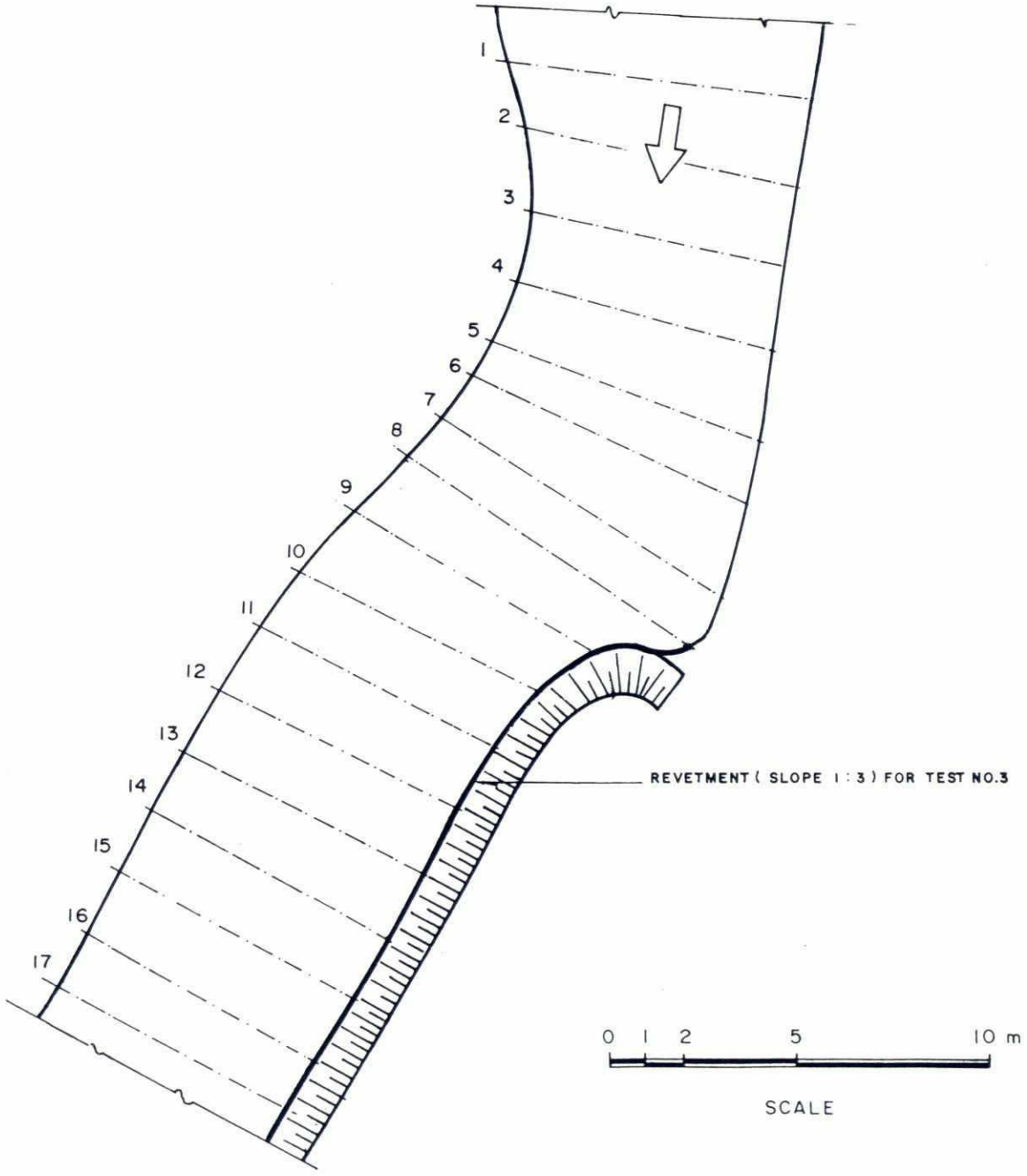
FINAL BED LEVEL

SLW STANDARD LOW WATER

BAHADURABAD MODEL
CROSS SECTION OF SCOUR HOLES
TEST T 2

FAP – 21/22
BANK PROTECTION AND RIVER TRAINING / (AFPM) PILOT PROJECT

FINAL REPORT | FIG. A.14-55



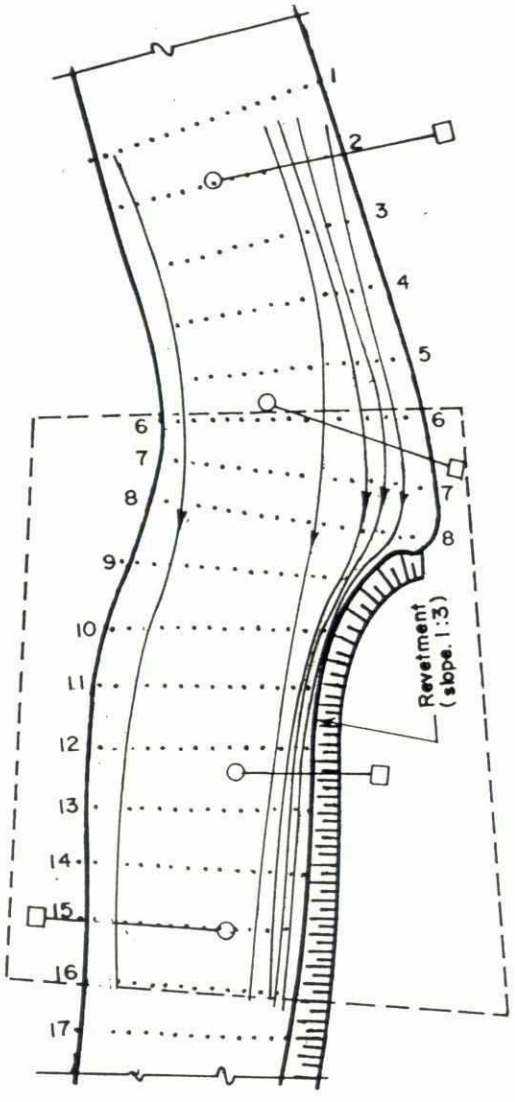
BAHADURABAD MODEL

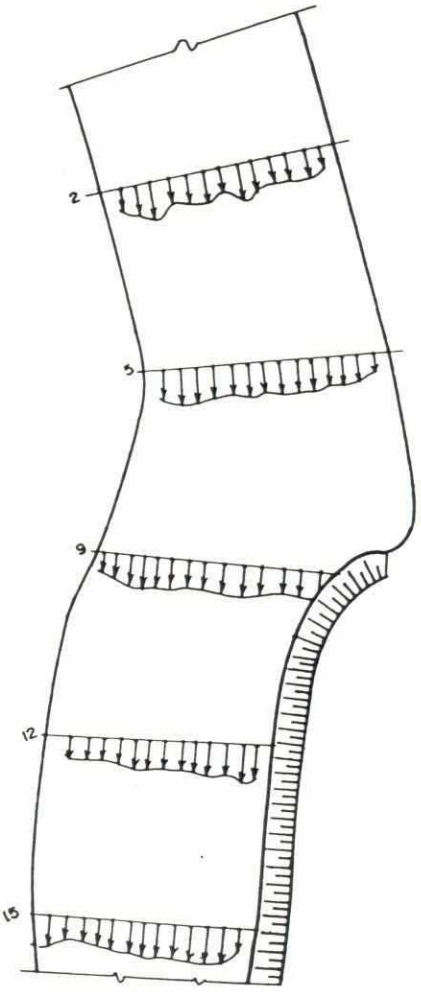
LAYOUT PLAN OF TEST T 3

FAP – 21/22

BANK PROTECTION AND RIVER TRAINING / (AFPM) PILOT PROJECT

FINAL REPORT | FIG. A.14–56





Q = 280 l/s

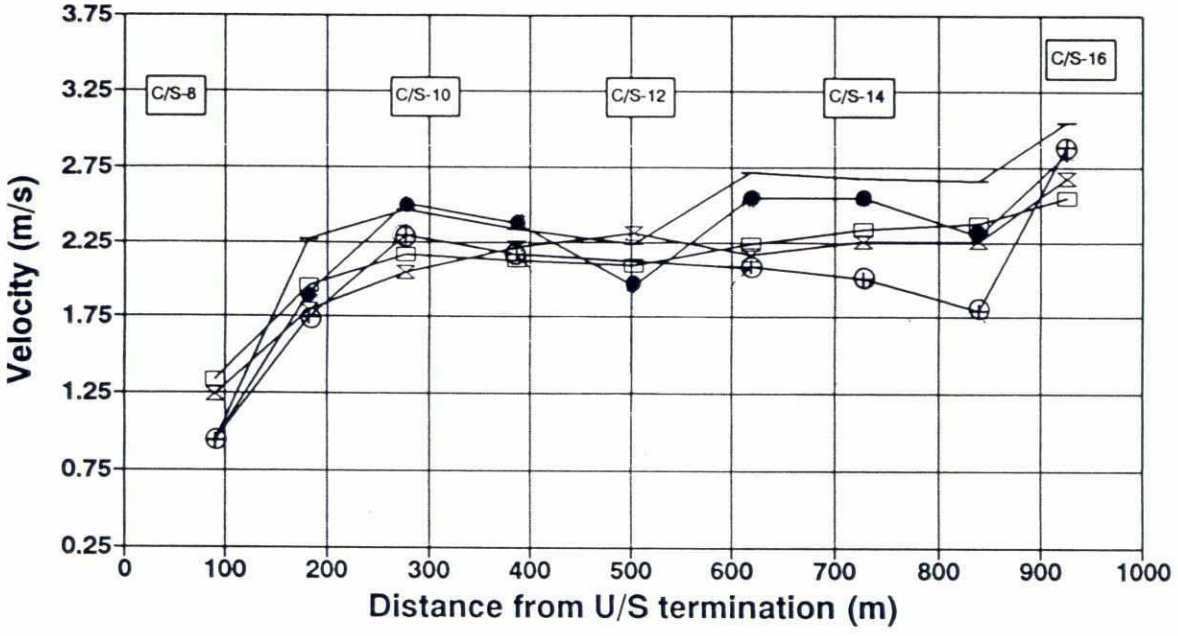
0 0.4 0.8 1.2 1.6 2.0 2.4
VELOCITY SCALE (m/s)

0 1 2 5 10 m
MODEL SCALE

LEGEND:

Flow line
Point gauge
Movable bed

BAHADURABAD MODEL TEST T 3 FLOW LINE & VELOCITY PROFILE	FAP – 21/22 BANK PROTECTION AND RIVER TRAINING / (AFPM) PILOT PROJECT	
	FINAL REPORT	FIG. A. 14–57



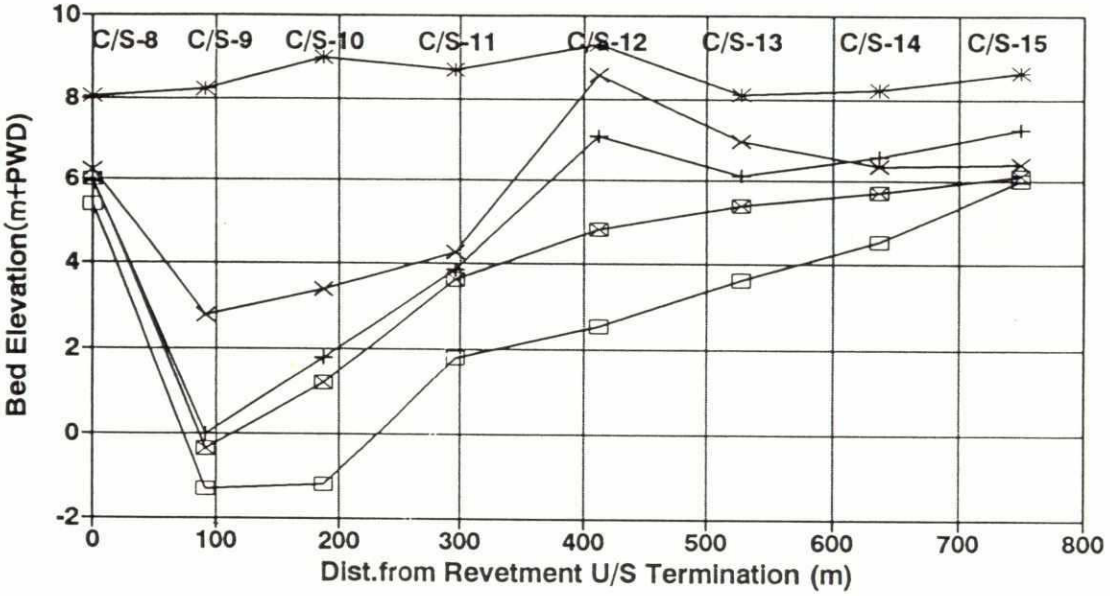
LEGEND

- 30 m from L.B.
- 45 m from L.B.
- 60m from L.B.
- 90m from L.B.
- 120.0m from L.B.

BAHADURABAD MODEL
VELOCITY ALONG THE REVETMENT
TEST T 3

FAP – 21/22
BANK PROTECTION AND RIVER TRAINING / (AFPM) PILOT PROJECT

FINAL REPORT | FIG. A.14–58



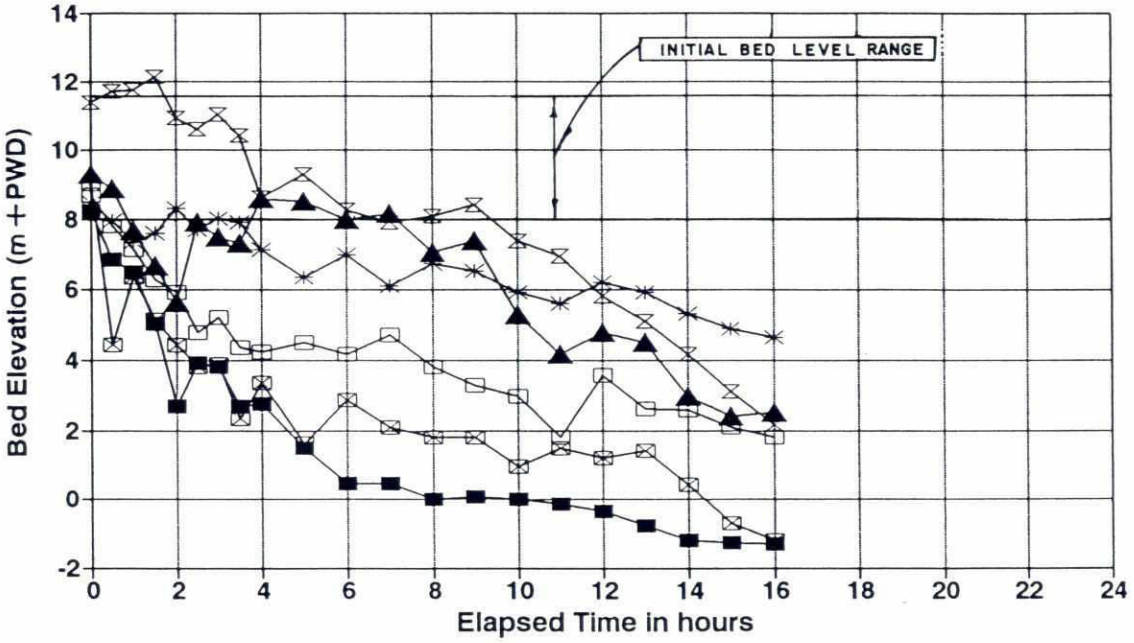
LEGEND

- After 0 hours
- After 4 hours
- After 8 hours
- After 12 hours
- After 16 hours

BAHADURABAD MODEL
LONG SECTIONS OF SCOUR HOLE
TEST T 3

FAP – 21/22
BANK PROTECTION AND RIVER TRAINING / (AFPM) PILOT PROJECT

FINAL REPORT | FIG. A.14–59



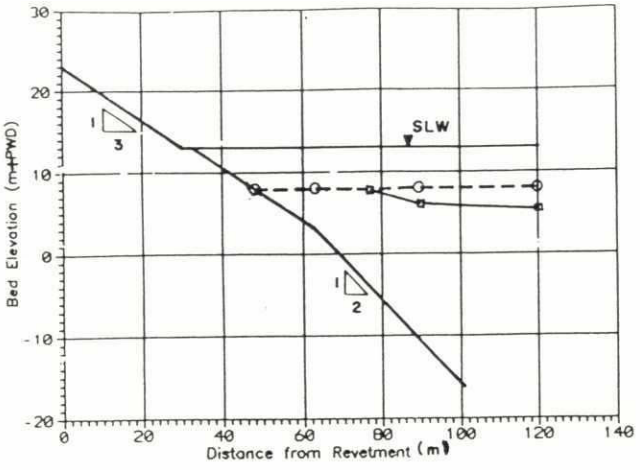
LEGEND

- C/S-6 (210m - L/B)
- C/S-7 (210m - L/B)
- C/S-9 (0m - L/B)
- C/S-10 (0m - L/B)
- C/S-11 (0m - L/B)
- C/S-12 (210m - L/B)

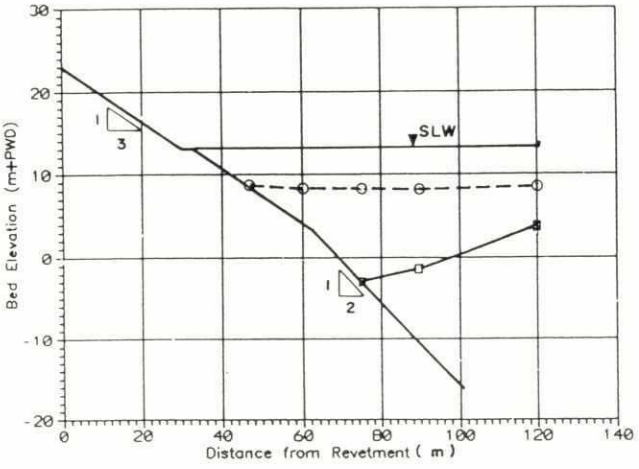
BAHADURABAD MODEL
MEASURMENT OF BED EROSION
TEST T 3

FAP – 21/22
BANK PROTECTION AND RIVER TRAINING / (AFPM) PILOT PROJECT

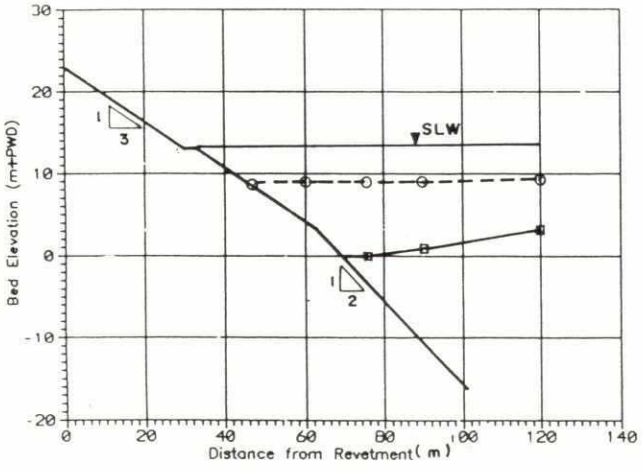
FINAL REPORT | FIG. A.14 – 60



CROSS SECTION : 8



CROSS SECTION : 9



LEGEND

REVETMENT

INITIAL BED LEVEL

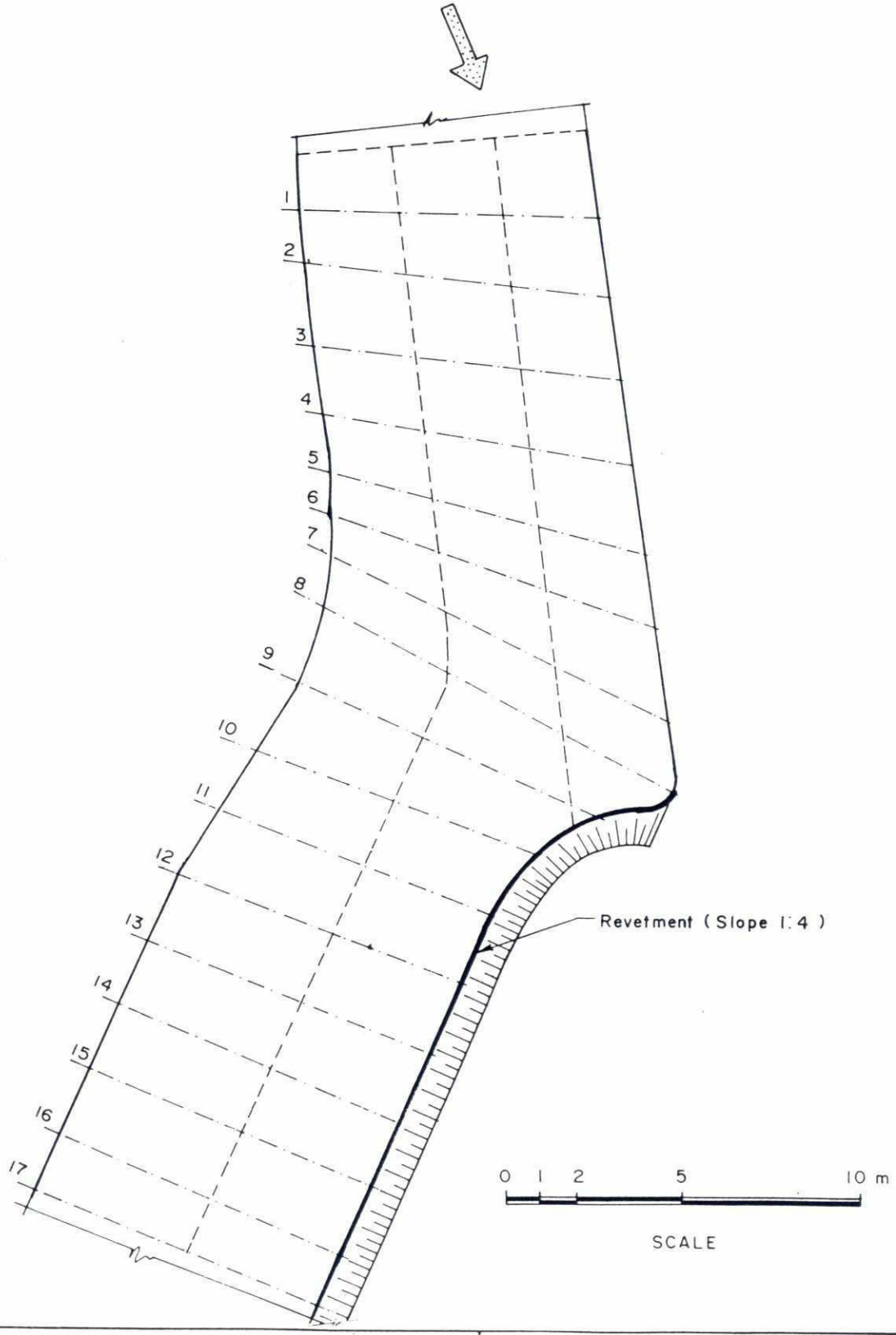
FINAL BED LEVEL

CROSS SECTION : 10

BAHADURABAD MODEL
CROSS SECTION OF SCOUR HOLES
TEST T 3

FAP – 21/22
BANK PROTECTION AND RIVER TRAINING / (AFPM) PILOT PROJECT

FINAL REPORT | FIG. A.14 – 61



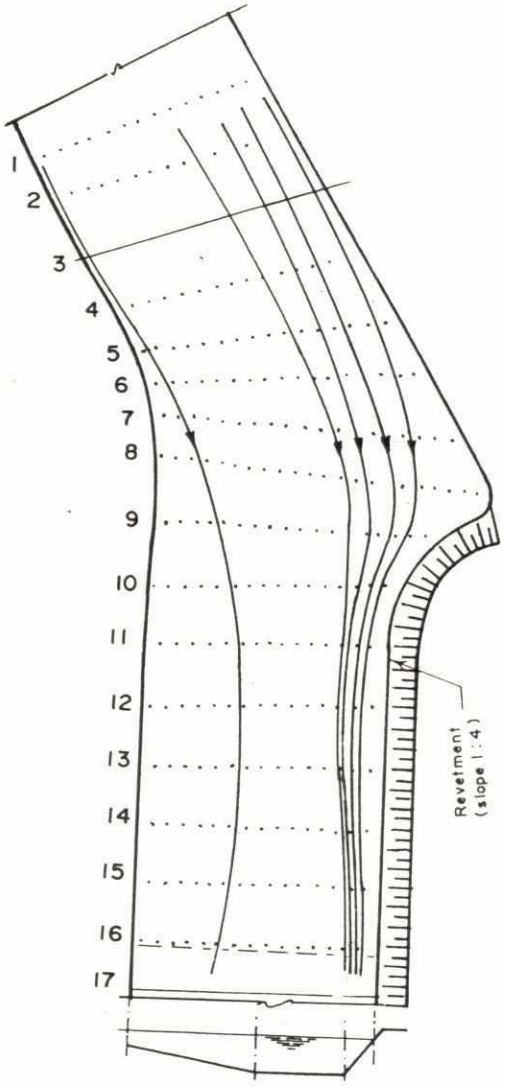
BAHADURABAD MODEL

LAYOUT PLAN OF
TEST : T 5

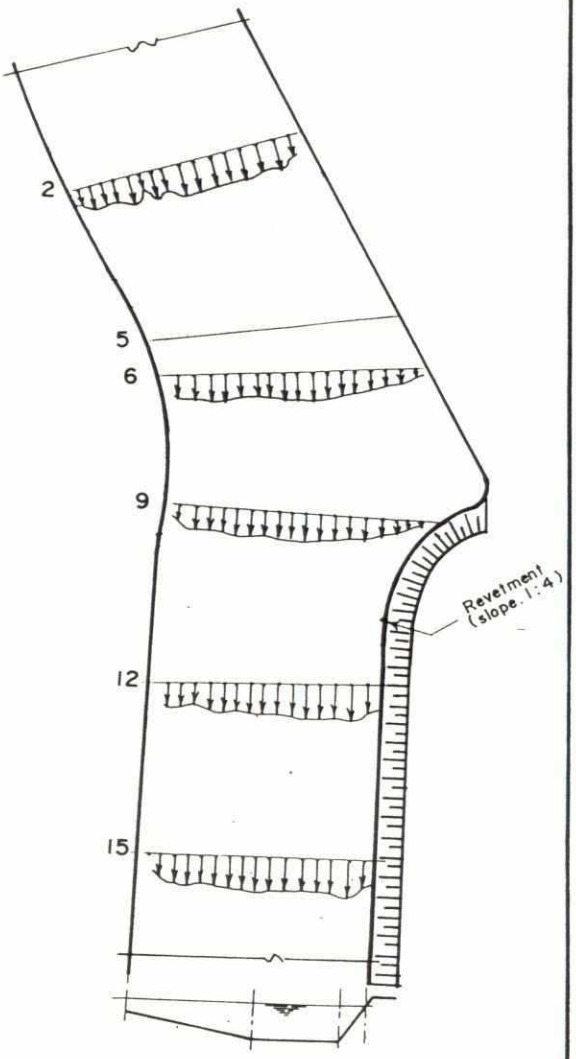
FAP – 21/22

BANK PROTECTION AND RIVER TRAINING / (AFPM) PILOT PROJECT

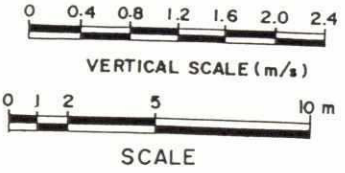
FINAL REPORT | FIG. A.14–62



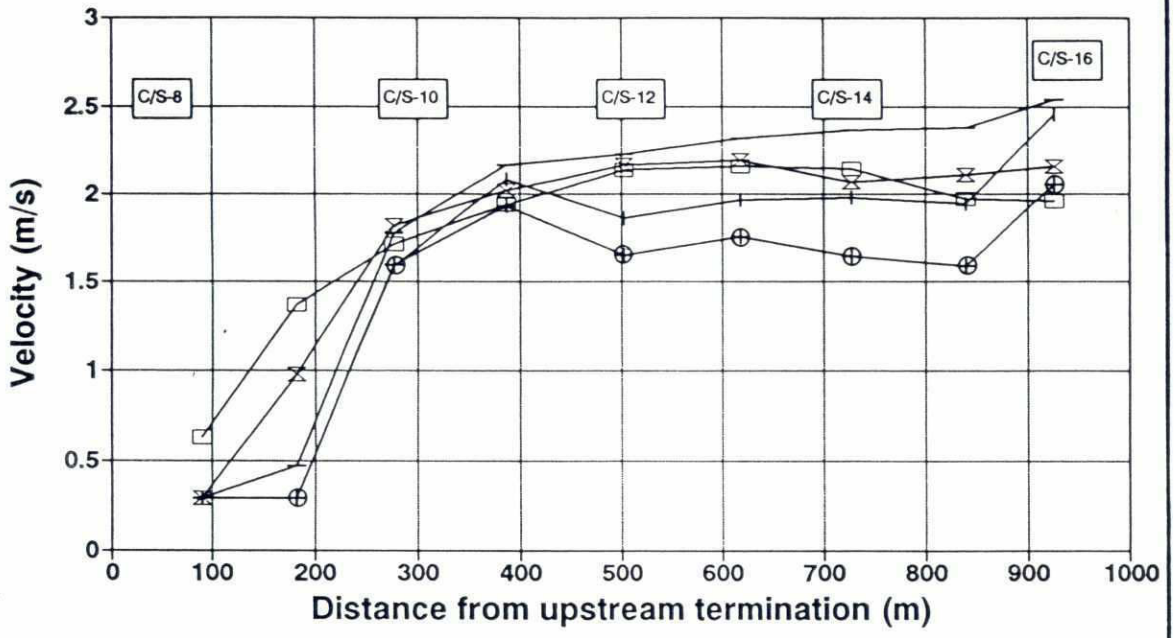
Q = 268 l/S



Q = 268 l/S



BAHADURABAD MODEL TEST T 5 FLOW LINE & VELOCITY PROFILE	FAP – 21/22 BANK PROTECTION AND RIVER TRAINING / (AFPM) PILOT PROJECT FINAL REPORT | FIG. A.14–63



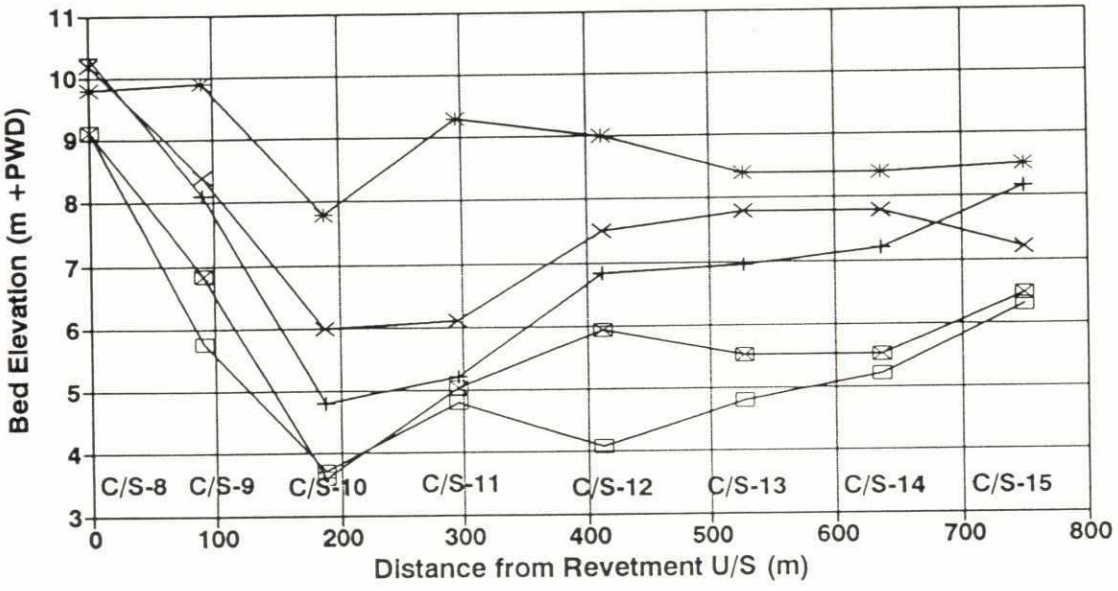
LEGEND

- 30 m from L.B.
- 45 m from L.B.
- 60m from L.B.
- 90m from L.B.
- 120.0m from L.B.

BAHADURABAD MODEL
VELOCITY ALONG THE REVETMENT
TEST T 5

FAP – 21/22
BANK PROTECTION AND RIVER TRAINING / (AFPM) PILOT PROJECT

FINAL REPORT | FIG. A.14-64



W.A.R.P.O. LIBRARY. LAHORE

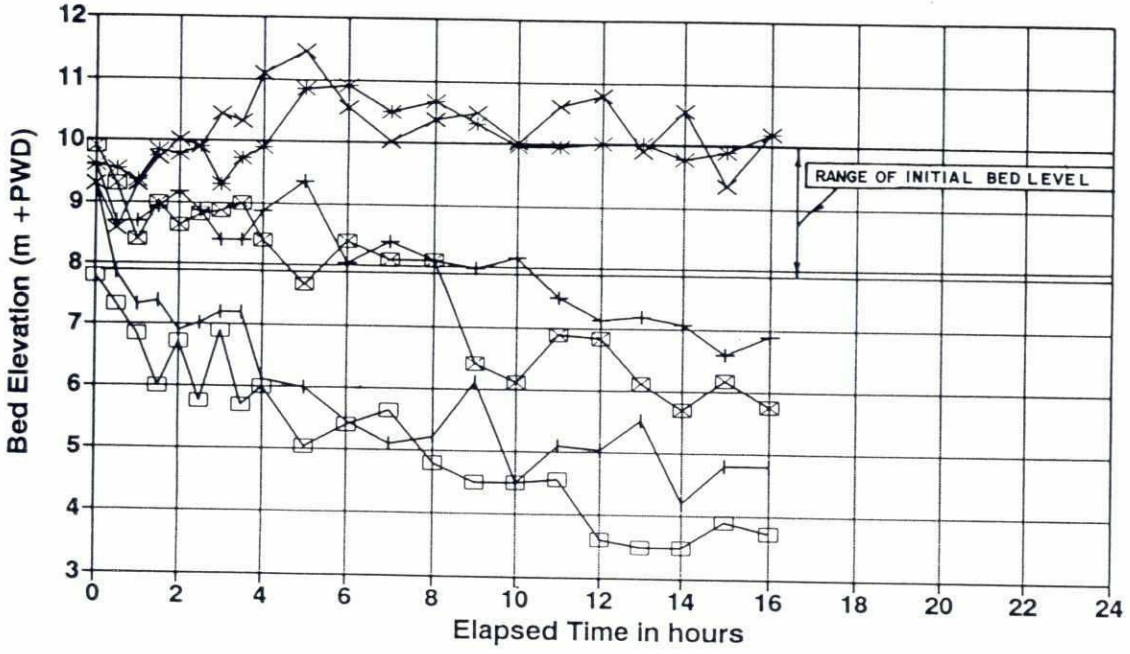
LEGEND

- After 0 hours
- After 4 hours
- After 8 hours
- After 12 hours
- After 16 hours

BAHADURABAD MODEL
LONG. SECTIONS OF SCOUR HOLE
TEST T-5

FAP – 21/22
BANK PROTECTION AND RIVER TRAINING / (AFPM) PILOT PROJECT

FINAL REPORT | FIG. A.14–65



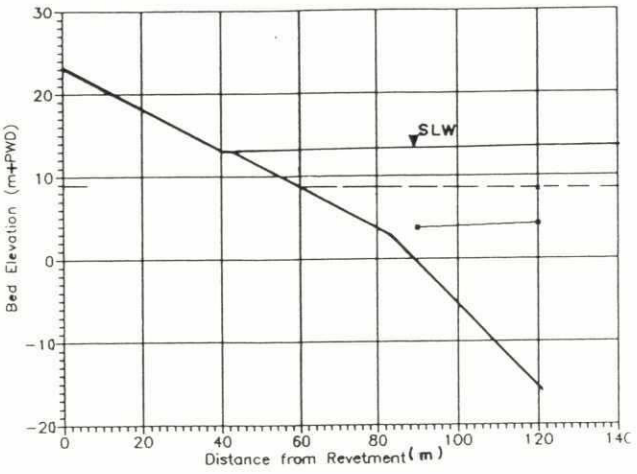
LEGEND

- C/S-6 (210m - L/B)
- C/S-7 (210m - L/B)
- C/S-9 (0m - L/B)
- C/S-10 (0m - L/B)
- C/S-11 (0m - L/B)
- C/S-12 (210m - L/B)

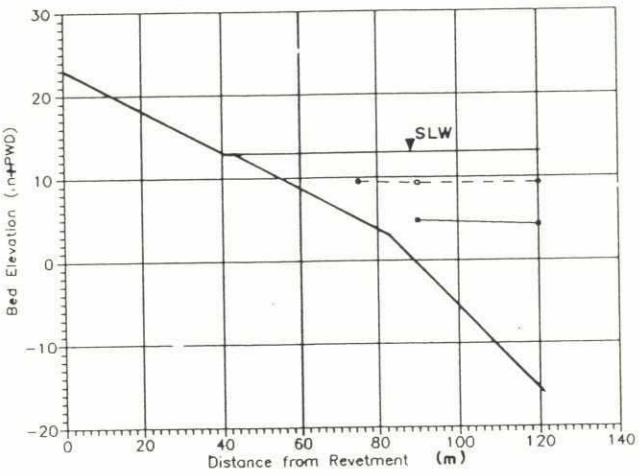
BAHADURABAD MODEL
MEASURMENT OF BED EROSION
TEST T 5

FAP – 21/22
BANK PROTECTION AND RIVER TRAINING / (AFPM) PILOT PROJECT

FINAL REPORT | FIG. A.14-66



CROSS SECTION : 10



CROSS SECTION : 11

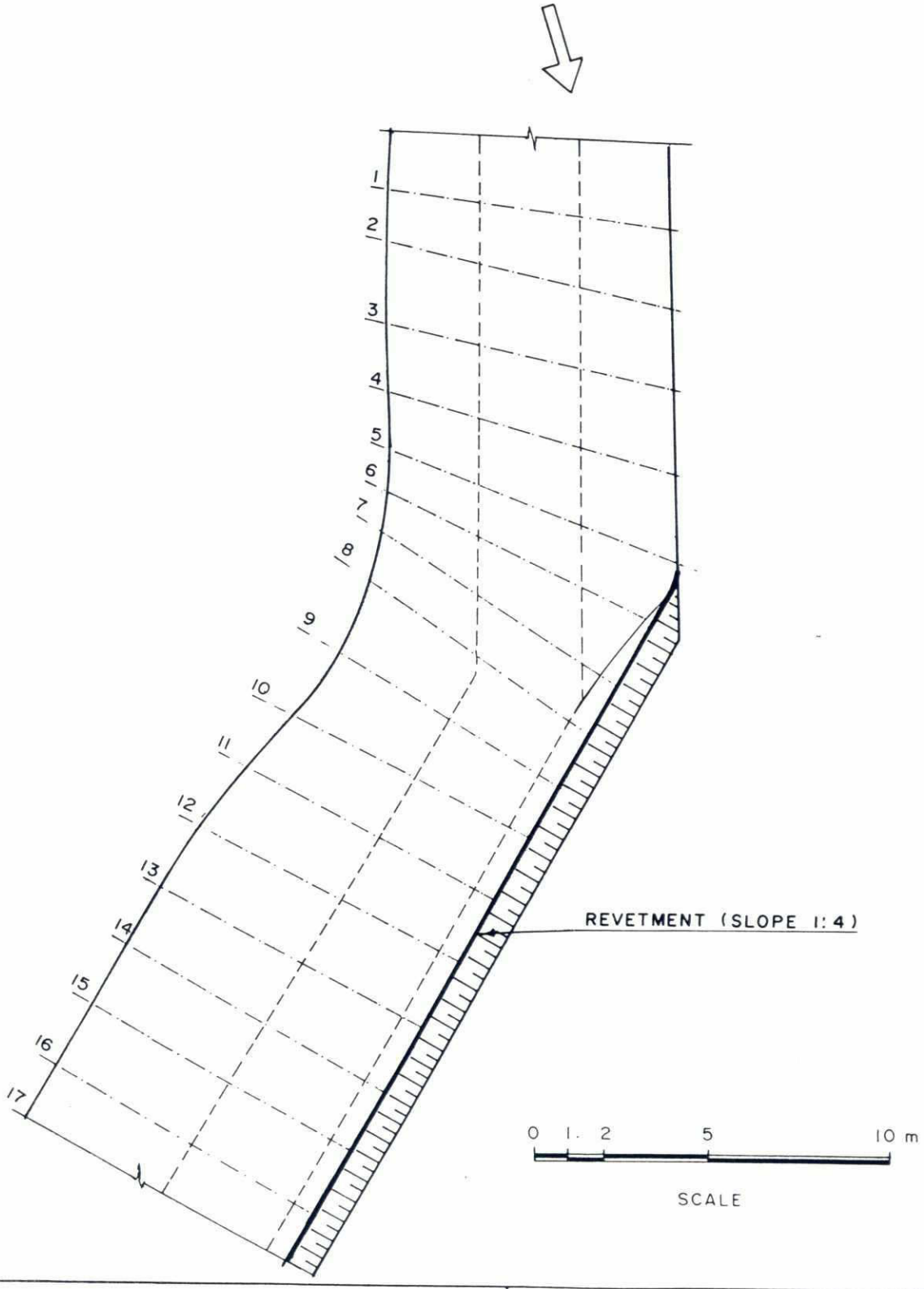
LEGEND

REVETMENT

INITIAL BED LEVEL

FINAL BED LEVEL

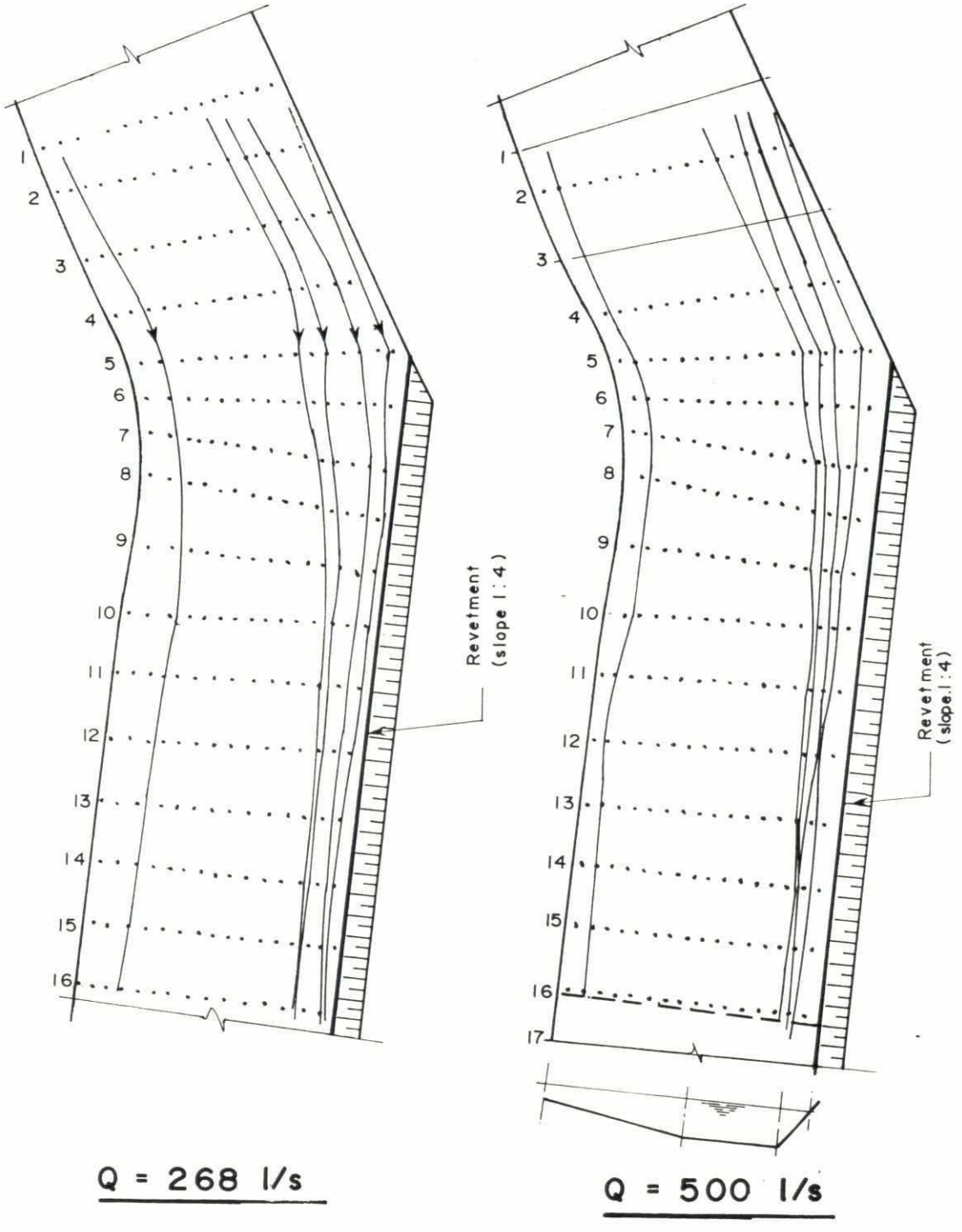
BAHADURABAD MODEL CROSS SECTION OF SCOUR HOLES TEST T 5	FAP – 21/22 BANK PROTECTION AND RIVER TRAINING/ (AFPM) PILOT PROJECT
	FINAL REPORT | FIG. A. 14 – 67



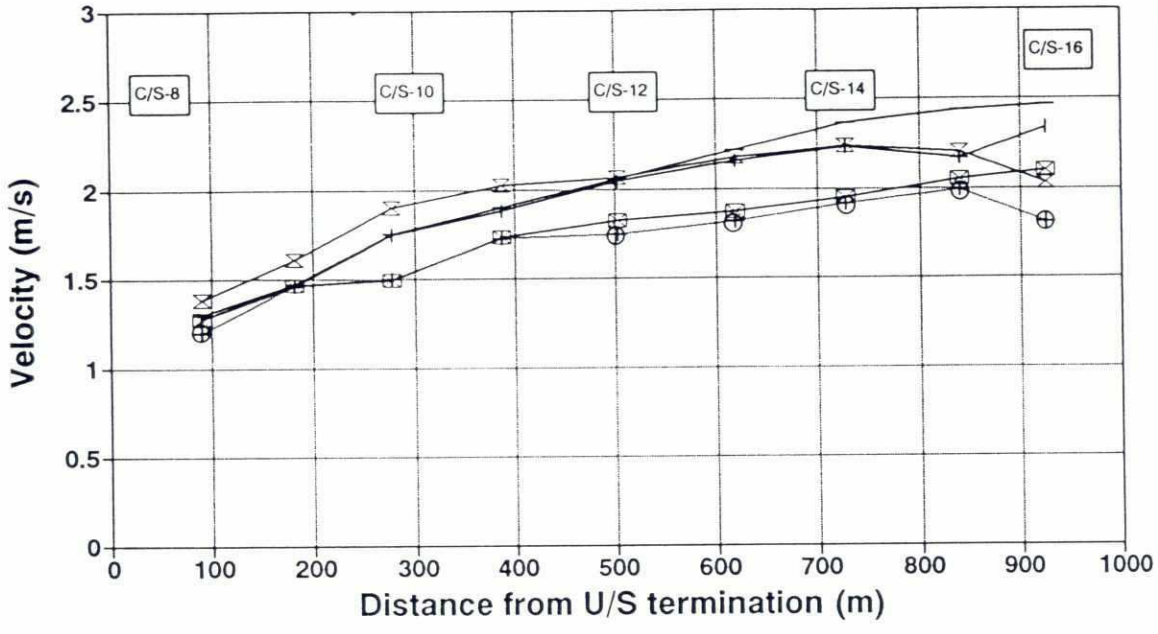
BAHADURABAD MODEL
LAYOUT PLAN OF
TEST T 7

FAP – 21/22
BANK PROTECTION AND RIVER TRAINING / (AFPM) PILOT PROJECT

FINAL REPORT | FIG. A.14-68



BAHADURABAD MODEL TEST T 7 FLOW LINE	FAP – 21/22 BANK PROTECTION AND RIVER TRAINING / (AFPM) PILOT PROJECT	
	FINAL REPORT	FIG. A.14–69



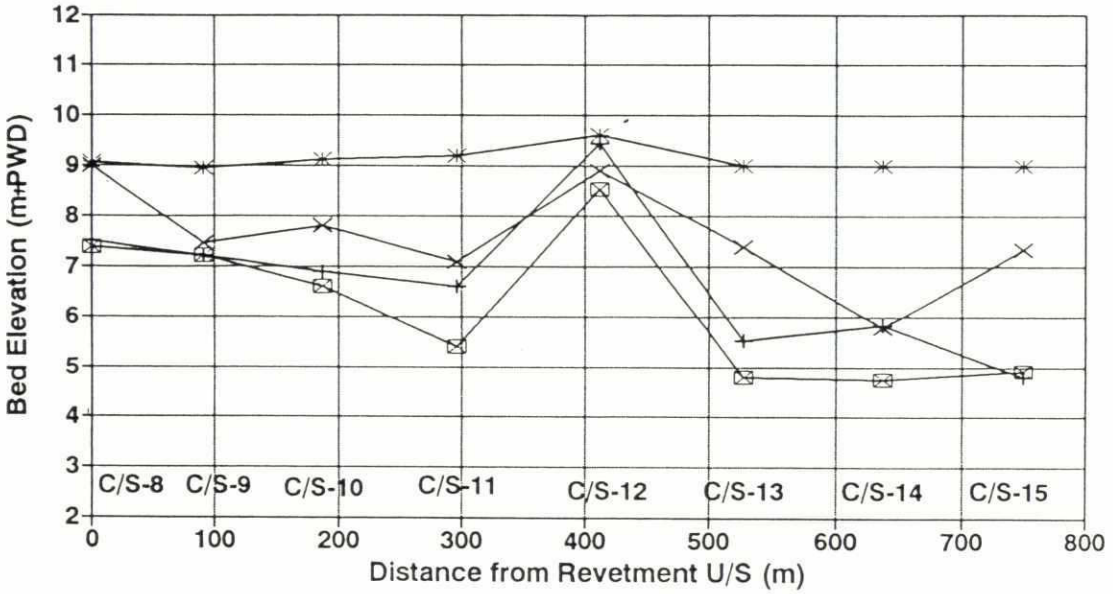
LEGEND

- 30 m from L.B.
- 45 m from L.B.
- 60m from L.B.
- 90m from L.B.
- 120.0m from L.B.

BAHADURABAD MODEL
VELOCITY ALONG THE REVETMENT
TEST T 7

FAP – 21/22
BANK PROTECTION AND RIVER TRAINING / (AFPM) PILOT PROJECT

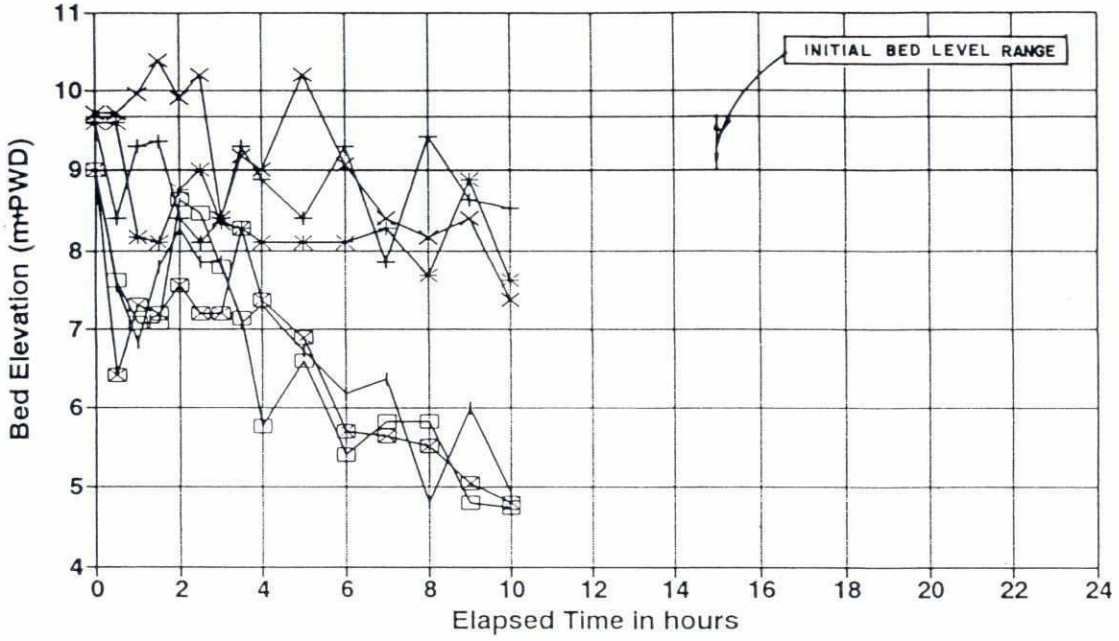
FINAL REPORT | FIG. A.14–70



LEGEND

- Initial
- After 4 hours
- After 8 hours
- After 10 hours
- After 16 hours

BAHADURABAD MODEL LONG SECTIONS OF SCOUR HOLE TEST T 7	FAP – 21/22 BANK PROTECTION AND RIVER TRAINING / (AFPM) PILOT PROJECT FINAL REPORT | FIG. A.14 – 71



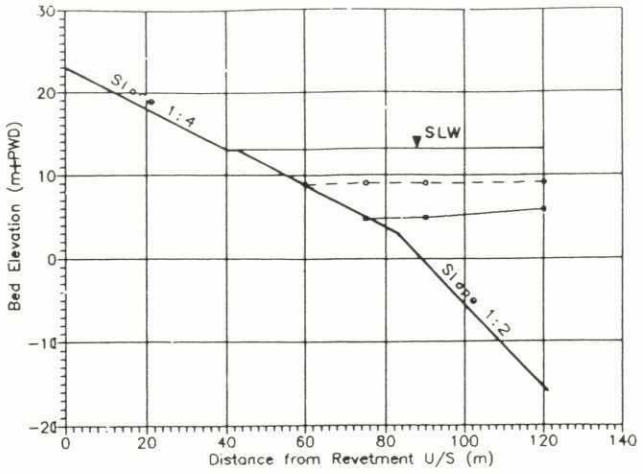
LEGEND

- C/S-6 (210m - L/B)
- C/S-7 (210m - L/B)
- C/S-12 (210m - L/B)
- C/S-13 (75m - L/B)
- C/S-14 (75m - L/B)
- C/S-15 (90m - L/B)

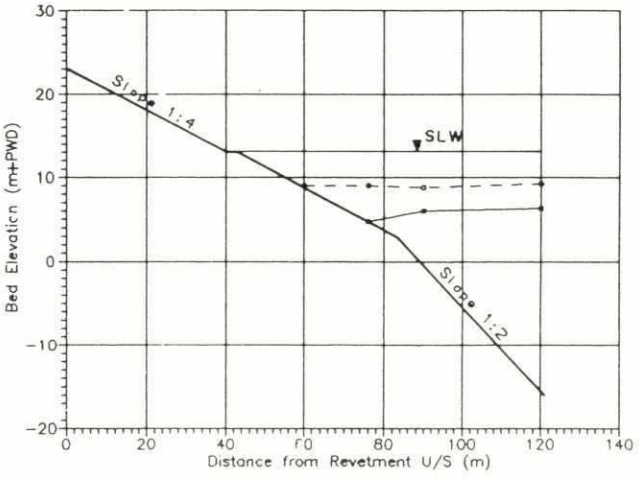
BAHADURABAD MODEL
MEASURMENT OF BED EROSION
TEST T 7

FAP – 21/22
BANK PROTECTION AND RIVER TRAINING / (AFPM) PILOT PROJECT

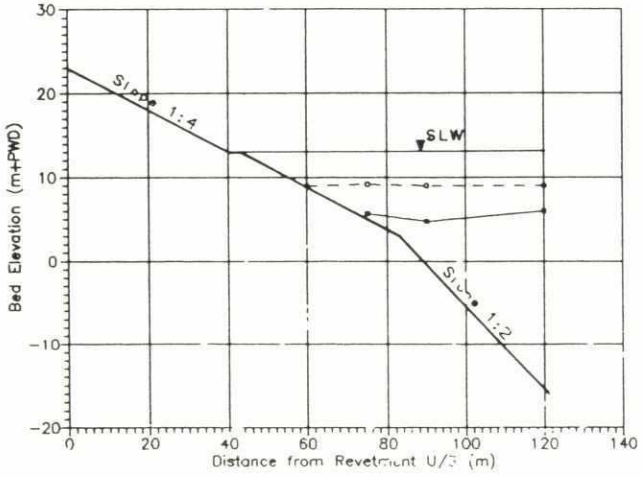
FINAL REPORT | FIG. A.14-72



CROSS SECTION : 13



CROSS SECTION : 14



CROSS SECTION : 15

LEGEND

REVETMENT

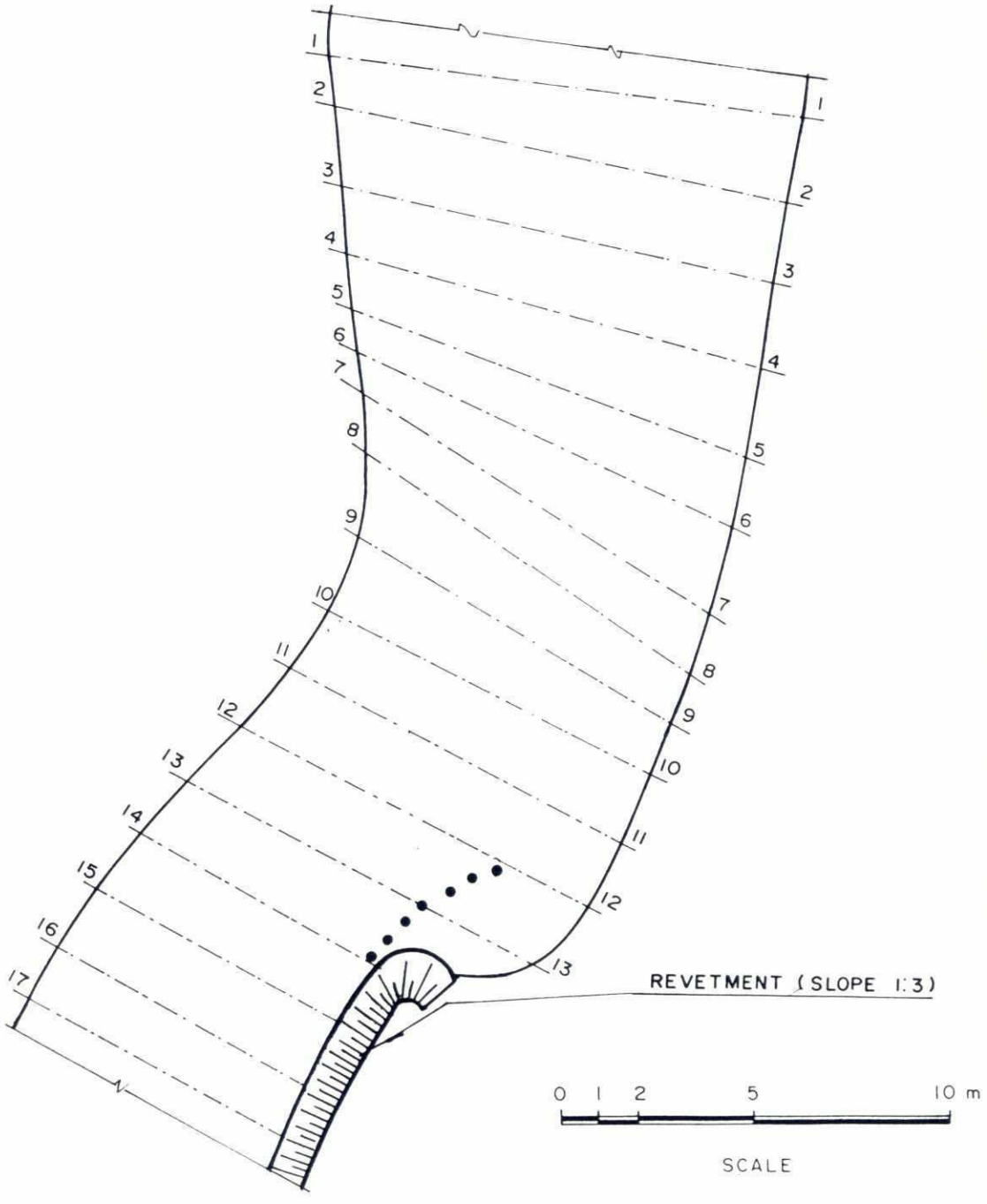
INITIAL BED LEVEL

FINAL BED LEVEL

BAHADURABAD MODEL
CROSS SECTION OF SCOUR HOLES
TEST T 7

FAP – 21/22
BANK PROTECTION AND RIVER TRAINING / (AFPM) PILOT PROJECT

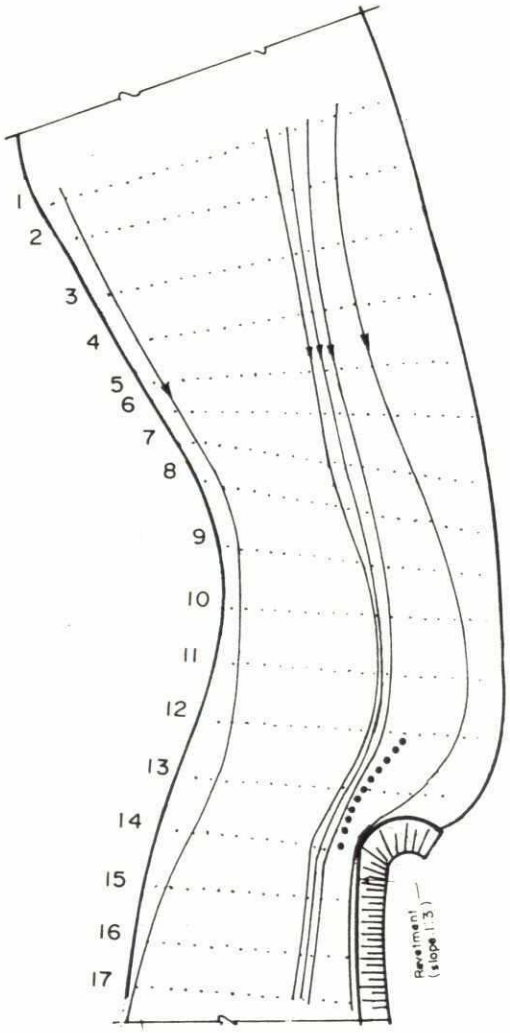
FINAL REPORT | FIG. A.14-73



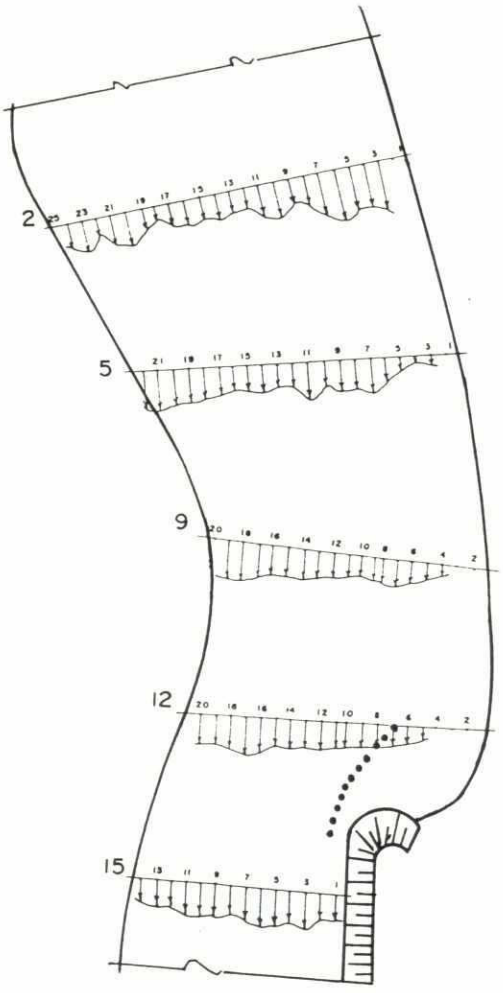
BAHADURABAD MODEL
LAY OUT PLAN OF
TEST T 10

FAP – 21/22
BANK PROTECTION AND RIVER TRAINING / (AFPM) PILOT PROJECT

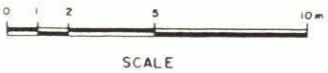
FINAL REPORT | FIG. A.14-74



Q = 274 l/S

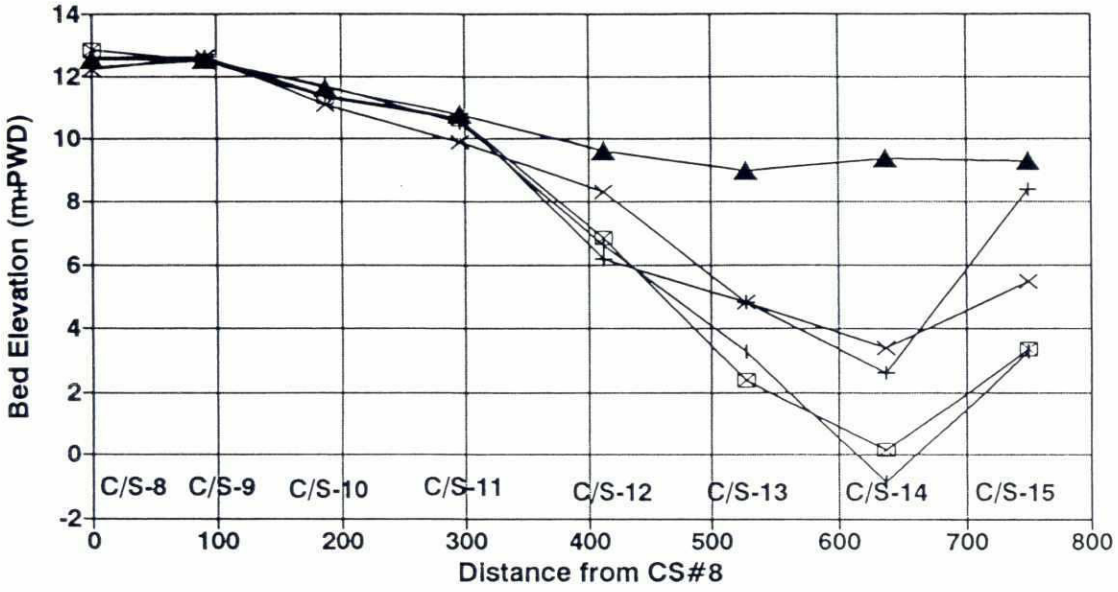


Q = 274 l/S



SCALE

BAHADURABAD MODEL TEST T 10 FLOW LINE & VELOCITY PROFILE	FAP – 21/22 BANK PROTECTION AND RIVER TRAINING / (AFPM) PILOT PROJECT FINAL REPORT | FIG. A.14- 75



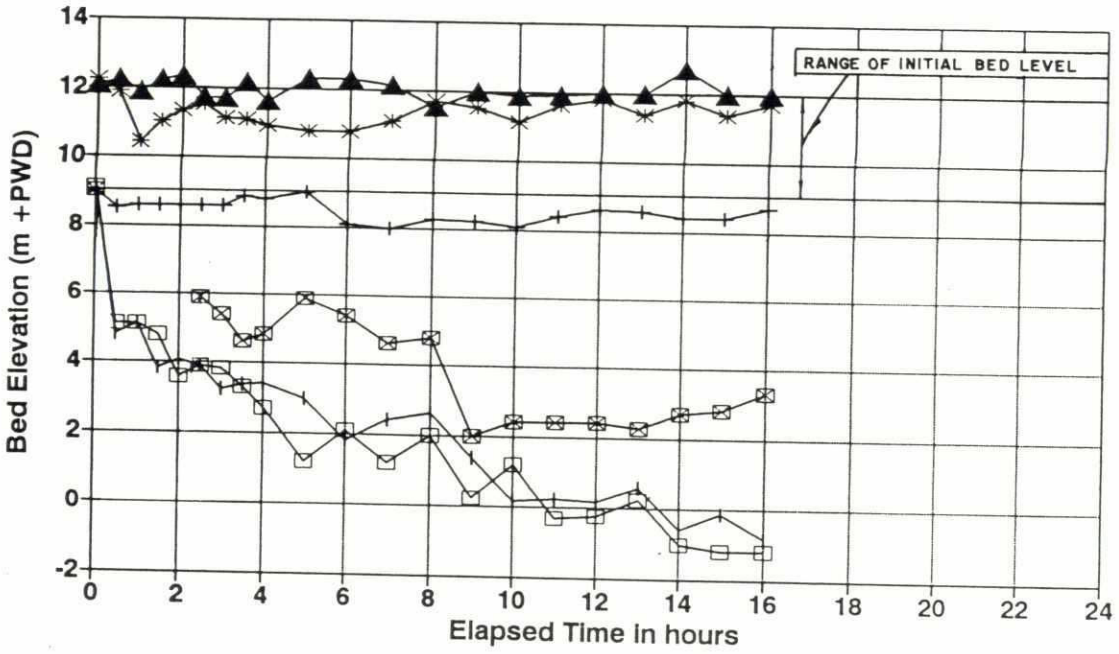
LEGEND

- Initial
- After 12 hours
- After 4 hours
- After 16 hours
- After 8 hours

BAHADURABAD MODEL
LONG SECTIONS OF SCOUR HOLES
TEST T 10

FAP – 21/22
BANK PROTECTION AND RIVER TRAINING / (AFPM) PILOT PROJECT

FINAL REPORT | FIG. A.14-76

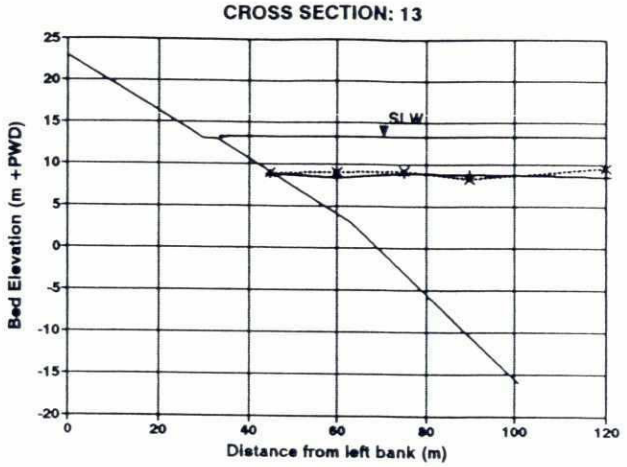


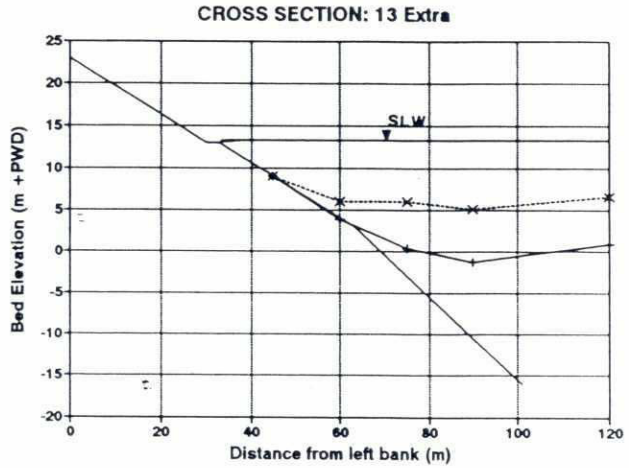
LEGEND

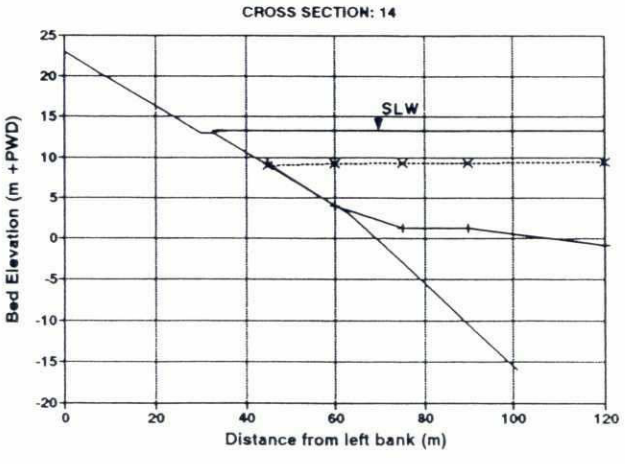
- C/S-6 (210m - L/B)
- C/S-13)
- C/S-7 (210m - L/B)
- C/S-13(a)
- C/S-12 (210m - L/B)
- C/S-14

W A R P O
LIBRARY
DHAKA

BAHADURABAD MODEL BED EROSION TEST T 10	FAP – 21/22 BANK PROTECTION AND RIVER TRAINING / (AFPM) PILOT PROJECT	
	FINAL REPORT	FIG. A.14-77







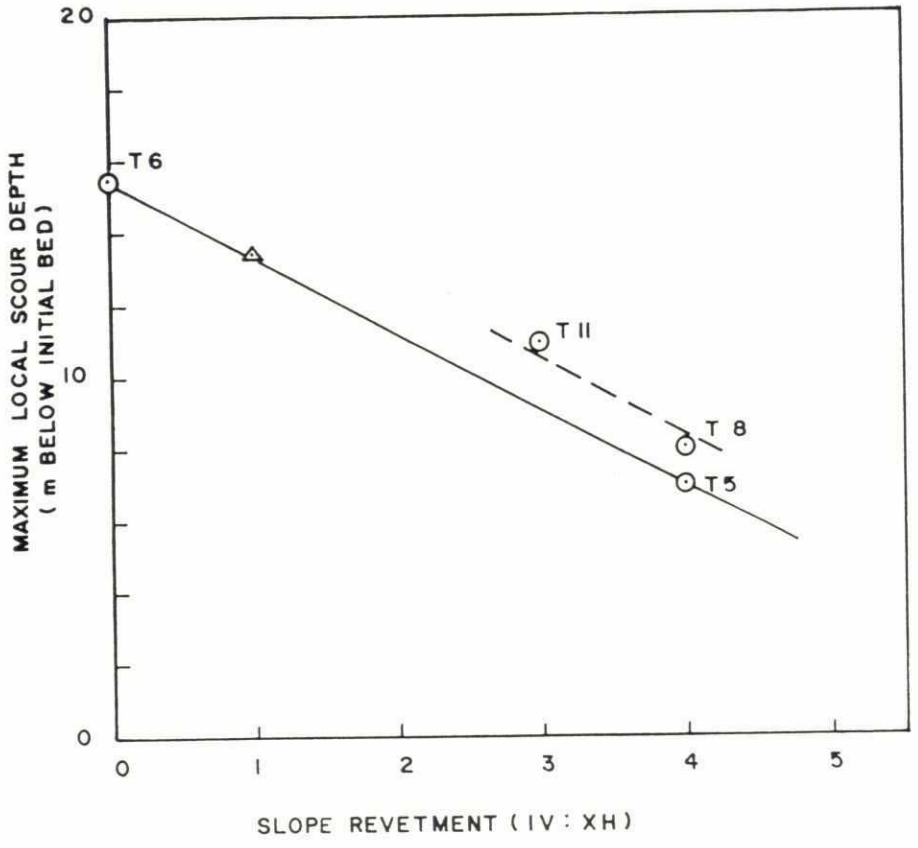
LEGEND

- Revetment (1:3)
- Initial bed
- Final bed
- SLW

BAHADURABAD MODEL
CROSS SECTIONS OF SCOUR HOLES
TEST T 10

FAP – 21/22
BANK PROTECTION AND RIVER TRAINING / (AFPM) PILOT PROJECT

FINAL REPORT | FIG. A.14 – 78

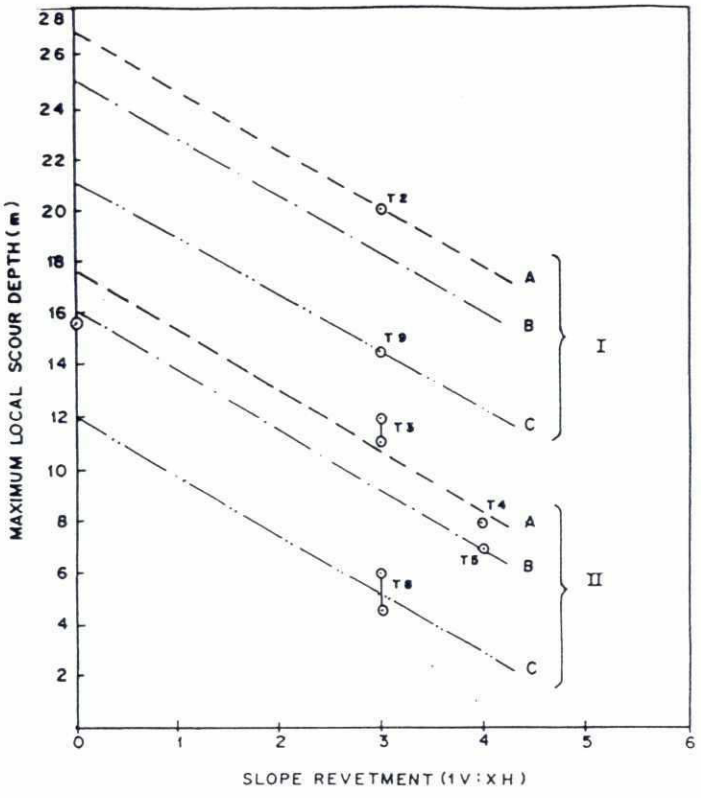


BAHADURABAD MODEL
LOCAL SCOUR DEPTH AS
A FUNCTION OF REVETMENT SLOPE

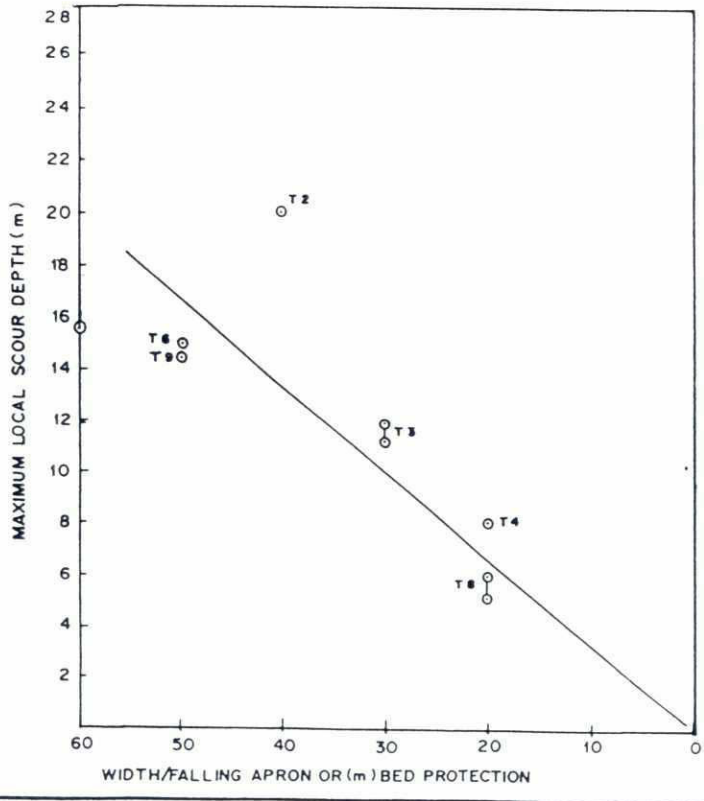
FAP – 21/22
BANK PROTECTION AND RIVER TRAINING / (AFPM) PILOT PROJECT

FINAL REPORT | FIG. A.14-79

I TERMINATION WITH R= 50m
II TERMINATION WITH R= 450m



A, B AND C-DIFFERENT CHANNEL ALIGNMENT



BAHADURABAD MODEL

LOCAL SCOUR DEPTH AS A FUNCTION OF REVETMENT SLOPE AND CHANNEL ALIGNMENT

FAP - 21/22

BANK PROTECTION AND RIVER TRAINING / (AFPM) PILOT PROJECT

FINAL REPORT | FIG. A.14 - 80

PHOTOS

690



Photo - 1: Test T2

Deepest point of scour hole near upstream groyne

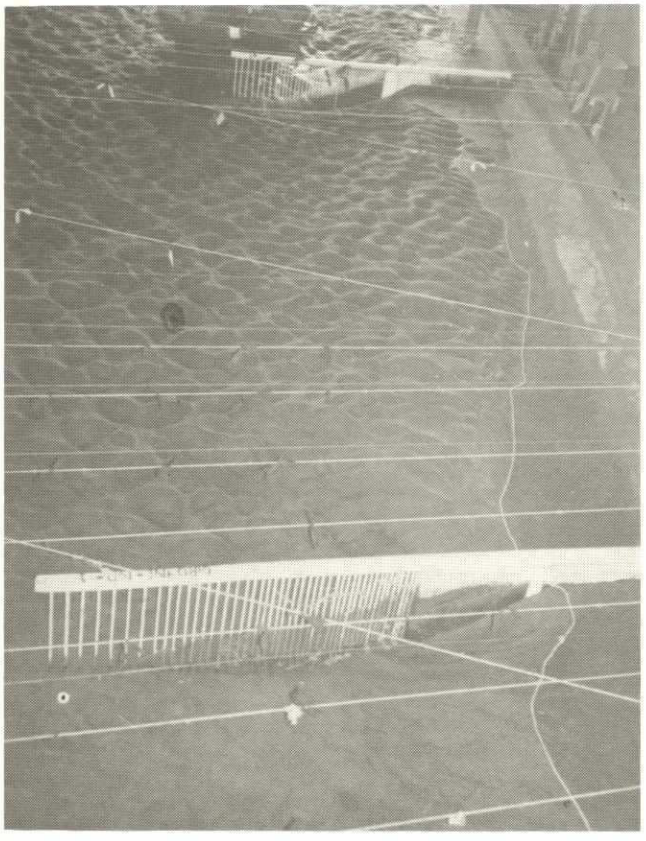


Photo - 2: Test T9

Upstream groyne



Photo - 3: Test T4

Upstream groyne with bed protection

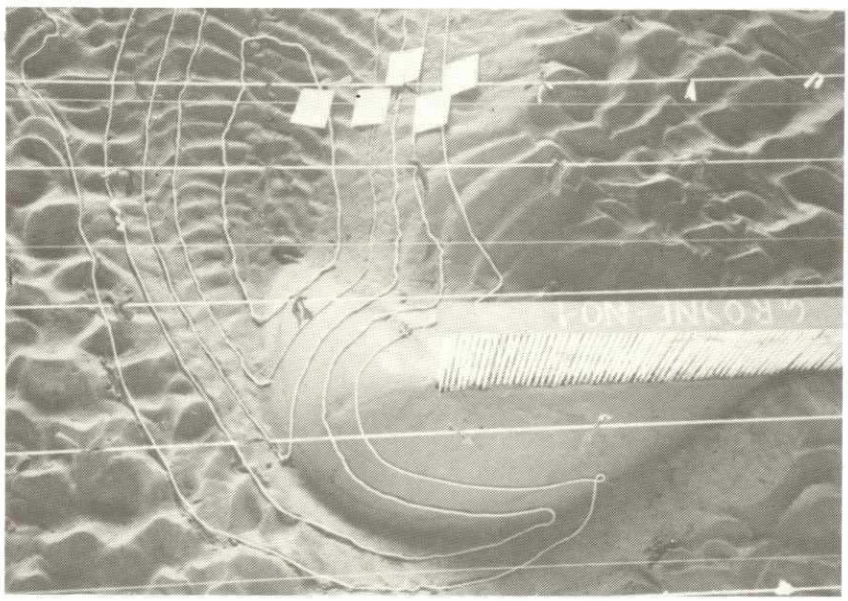


Photo - 4: Test T6

Upstream groyne head with bed protection



Photo - 5: Test T5

Deepest point of scour hole of upstream groyne without bed protection



Photo - 6: Test T9

Upstream termination of revetment with radius 50 m



Photo - 7: Test T4

Upstream termination of revetment with radius 450 m



Photo - 8: Test T2

Upstream termination of revetment with radius 50 m

694

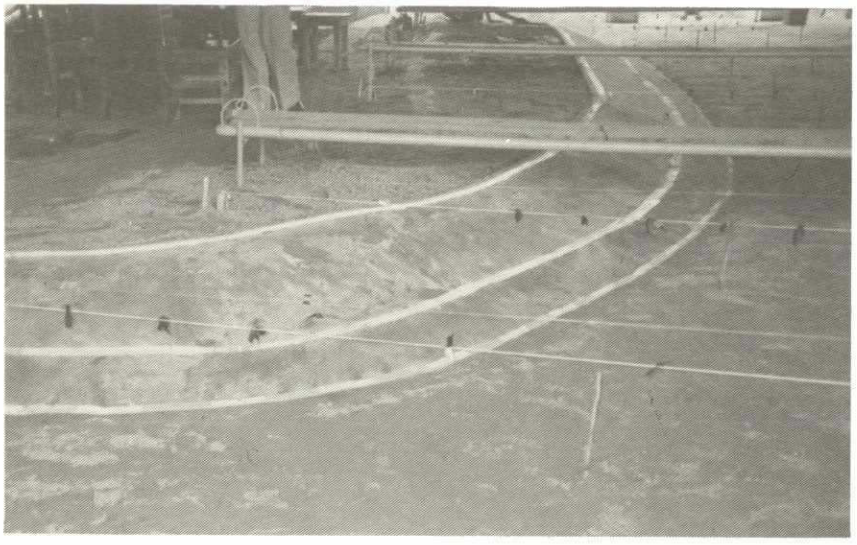


Photo - 9: Test T3

Upstream termination of revetment with radius 450 m and initial bed

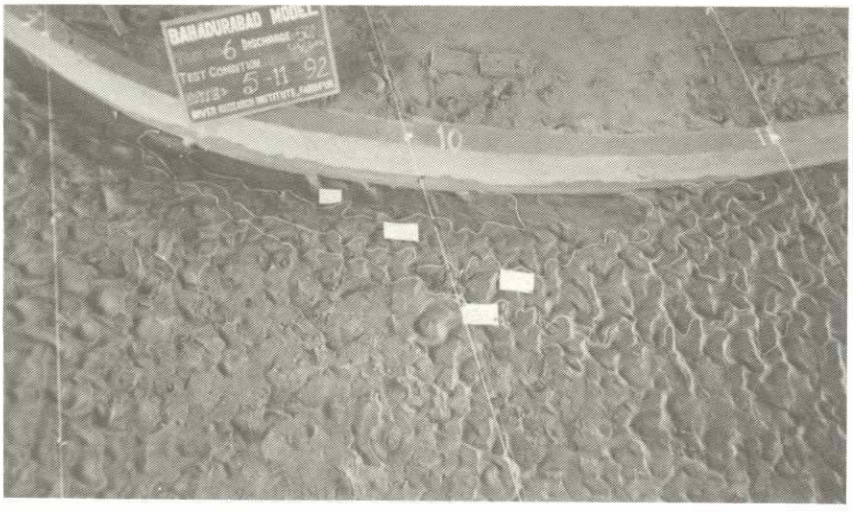
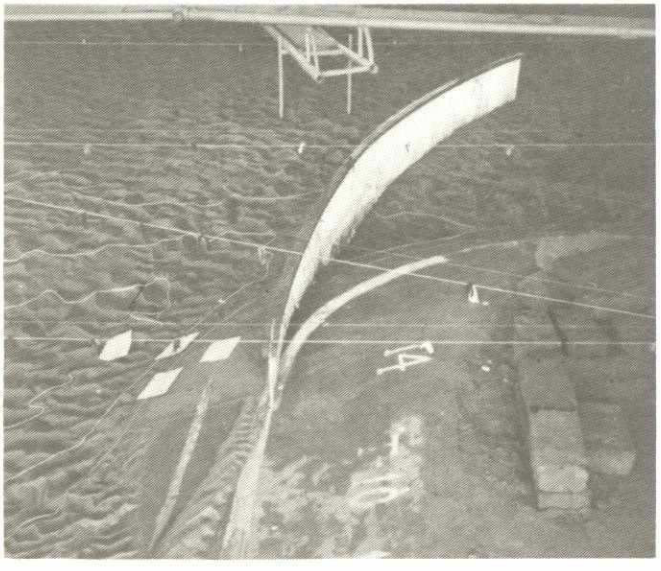


Photo - 10: Test T6

Upstream termination of a vertical wall, radius 450 m



W.A.R.P.O.
LIBRARY.

Photo - 11: Test T10

Upstream termination of revetment with a row of piles